

Topics in Stereochemistry, Volume 19

Editors
Ernest L. Eliel
Samuel H. Wilen

JOHN WILEY & SONS

**TOPICS IN
STEREOCHEMISTRY**

VOLUME 19

ADVISORY BOARD

STEPHEN J. ANGYAL, *University of New South Wales, Sydney,
Australia*

ALAN R. BATTERSBY, *Cambridge University, Cambridge, England*

GIANCARLO BERTI, *University of Pisa, Pisa, Italy*

F. ALBERT COTTON, *Texas A & M University, College Station, Texas*

JOHANNES DALE, *University of Oslo, Oslo, Norway*

DAVID A. EVANS, *Harvard University, Cambridge, Massachusetts*

MEIR LAHAV, *The Weizmann Institute of Science, Rehovoth, Israel*

JEAN-MARIE LEHN, *Collège de France, Paris, France*

JAN MICHALSKI, *Centre of Molecular and Macromolecular Studies,
Polish Academy of Sciences, Lodz, Poland*

KURT MISLOW, *Princeton University, Princeton, New Jersey*

MICHINORI ŌKI, *Okayama University of Science, Okayama, Japan*

VLADIMIR PRELOG, *Eidgenössische Technische Hochschule, Zurich,
Switzerland*

GÜNTHER SNATZKE, *Ruhruniversität, Bochum, Federal Republic of
Germany*

JOHN B. STOTHERS, *University of Western Ontario, London, Ontario,
Canada*

HANS WYNBERG, *University of Groningen, Groningen, The Netherlands*

TOPICS IN

STEREOCHEMISTRY

EDITORS

ERNEST L. ELIEL

Professor of Chemistry

*University of North Carolina
Chapel Hill, North Carolina*

SAMUEL H. WILEN

Professor of Chemistry

*City College, City University of New York
New York, New York*

VOLUME 19



AN INTERSCIENCE ® PUBLICATION

JOHN WILEY & SONS

New York • Chichester • Brisbane • Toronto • Singapore

An Interscience® Publication
Copyright © 1989 by John Wiley and Sons, Inc.

All rights reserved. Published simultaneously in Canada.

Reproduction or translation of any part of this work
beyond that permitted by Section 107 or 108 of the
1976 United States Copyright Act without the permission
of the copyright owner is unlawful. Requests for
permission or further information should be addressed to
the Permissions Department, John Wiley & Sons, Inc.

Library of Congress Catalog Card Number 67-13943

ISBN 0-471-50752-0

Printed in the United States of America
10 9 8 7 6 5 4 3 2 1

To the memory of

David Ginsburg

INTRODUCTION TO THE SERIES

It is patently impossible for any individual to read enough of the journal literature so as to be aware of all significant developments that may impinge on his or her work, particularly in an area such as stereochemistry, which knows no topical boundaries. Stereochemical investigations may have relevance to an understanding of a wide range of phenomena and findings irrespective of their provenance. Because stereochemistry is important in many areas of chemistry, comprehensive reviews of high quality play a special role in educating and alerting the chemical community to new stereochemical developments.

The above considerations were reason enough for initiating a series such as this. In addition to updating information found in such standard monographs as *Stereochemistry of Carbon Compounds* (Eliel, McGraw-Hill, 1962) and *Conformational Analysis* (Eliel, Allinger, Angyal, and Morrison, Interscience, 1965; reprinted by American Chemical Society, 1981) as well as others published more recently, the series is intended also to deal in greater detail with some of the topics summarized in such texts. It is for this reason that we have selected the title *Topics in Stereochemistry* for this series.

The series is intended for the advanced student, the teacher, and the active researcher. A background of the basic knowledge in the field of stereochemistry is assumed. Each chapter is written by an expert in the field and, hopefully, covers its subject in depth. We have tried to choose topics of fundamental importance aimed primarily at an audience of inorganic and organic chemists. Yet, many of these topics are concerned with basic principles of physical chemistry and some deal with stereochemical aspects of biochemistry as well.

It is our intention to produce future volumes at intervals of one to two years. The editors will welcome suggestions as to suitable topics.

We are fortunate in having been able to secure the help of an international board of editorial advisors who have been of great assistance by suggesting topics and authors for several chapters and by helping us avoid, in so far as possible, duplication of topics appearing in other, related monograph series. We are grateful to the editorial advisors for this assistance, but the editors and authors alone must assume the responsibility for any shortcomings of *Topics in Stereochemistry*.

E. L. ELIEL
S. H. WILEN

PREFACE

In this, the nineteenth volume of the series *Topics in Stereochemistry*, we are pleased to be able to present five chapters with a wide spread of interest, ranging from stereochemical aspects of solid-state nuclear magnetic resonance to the bearing of enzyme stereospecificity on the understanding of processes of evolution.

The first chapter, "Molecular Structure and Carbon-13 Chemical Shielding Tensors Obtained from Nuclear Magnetic Resonance" by Julio C. Facelli and David M. Grant of the University of Utah, deals with the additional chemical and nmr information that can be obtained by measurement of the anisotropic chemical shifts in solids as compared to the isotropic shifts in liquids and solutions. In the opinion of the editors, the authors have presented the complex subject of shielding tensors, their relation to anisotropic chemical shifts, and the meaning of such shifts in remarkably lucid fashion. We hope and trust that the chapter will enable our readers to obtain a better understanding of solid state nmr and the information that can be derived from it.

The second chapter, "Resolution of Enantiomers via Biocatalysis" by Charles J. Sih and Shih-Hsiung Wu of the University of Wisconsin, deals with kinetic resolution, principally of alcohols, acids, and esters, making use of the generally high substrate stereoselectivity of enzymes. The emphasis is on hydrolytic enzymes: esterases and lipases. The chapter includes a general treatment of the efficacy of enzymatic kinetic resolution in terms of fundamental kinetic parameters.

The third chapter, "Stereospecificity in Enzymology: Its Place in Evolution" by Steven A. Benner, Arthur Glasfeld, and Joseph A. Piccirilli of the Swiss Federal Institute of Technology, Zurich, Switzerland, is quite different in content from most of the other chapters published in this Series. It relates the substrate and product stereoselectivity of enzymes from a variety of different organisms to the evolutionary relationship, if any, between these organisms. It is pointed out that enzyme stereospecificity, considered as an evolutionary trait, may be adaptive, nonadaptive and drifting, or nonadaptive but preserved through "structural coupling" to an adaptive trait, and that comparison of the stereochemistry of functionally related enzymes from different species can be used to establish hypotheses as to which of the three modes above is the one actually operating.

The fourth chapter, "Enantioselective Synthesis of Non-racemic Chiral

Molecules on an Industrial Scale" by John W. Scott of Hoffman-La Roche, Inc., draws attention to the fact that, to an increasing extent, the pharmaceutical industry in particular is interested in synthesizing chiral substances in enantiomerically pure form. This can be done in three ways: by resolution, by synthesis from readily available optically active precursors, and by enantioselective synthesis. The author presents in detail six quite variegated examples of enantioselective syntheses that are practiced commercially and for which experimental procedures are available.

The last chapter, "Stereochemistry of the Base-Promoted Michael Addition Reaction" by David A. Oare and Clayton H. Heathcock of the University of California at Berkeley, presents an exhaustive—and as far as we are aware the first—summary of the stereochemical aspects of 1,4-addition of carbanionic and similar species to α,β -unsaturated carbonyl and related compounds. In addition to presenting an enormous amount of empirical information painstakingly collected from the literature, the authors have undertaken a classification of the stereochemical aspects of various addition schemes, similar to analogous classifications previously used by Heathcock and others for the aldol condensation. A sequel to this chapter by the same authors, dealing with uncatalyzed Michael reactions of enamines and Lewis acid catalyzed reactions of enol ethers with α,β -unsaturated carbonyl compounds, will appear in the next volume of this Series.

This volume is dedicated to the memory of David A. Ginsburg who passed away, after a long illness, on March 9, 1988. Dave Ginsburg had been an advisor to this Series since its inception in 1967 and, among all our advisors, excelled in the number of constructive suggestions for major topics and authors that he made. Not just one or two, but several chapters that have appeared in this Series resulted from his suggestions. We shall miss him both as one of our most helpful advisors and as a personal friend.

ERNEST L. ELIEL
SAMUEL H. WILEN

Chapel Hill, North Carolina

New York, New York

May 1989

CONTENTS

MOLECULAR STRUCTURE AND CARBON-13 CHEMICAL SHIELDING TENSORS OBTAINED FROM NUCLEAR MAGNETIC RESONANCE	1
<i>by Julio C. Facelli and David M. Grant</i>	
<i>Chemistry Department</i>	
<i>University of Utah</i>	
<i>Salt Lake City, Utah</i>	
RESOLUTION OF ENANTIOMERS VIA BIOCATALYSIS	63
<i>by Charles J. Sih and Shih-Hsiung Wu</i>	
<i>School of Pharmacy</i>	
<i>University of Wisconsin</i>	
<i>Madison, Wisconsin</i>	
STEREOSPECIFICITY IN ENZYMOLOGY: ITS PLACE IN EVOLUTION	127
<i>by Steven A. Benner, Arthur Glasfeld, and Joseph A. Piccirilli</i>	
<i>Laboratory for Organic Chemistry</i>	
<i>Swiss Federal Institute of Technology</i>	
<i>Zurich, Switzerland</i>	
ENANTIOSELECTIVE SYNTHESIS OF NON-RACEMIC CHIRAL MOLECULES ON AN INDUSTRIAL SCALE	209
<i>by John W. Scott</i>	
<i>Chemical Development Department</i>	
<i>Hoffman-La Roche, Inc.</i>	
<i>Nutley, New Jersey</i>	
STEREOCHEMISTRY OF THE BASE-PROMOTED MICHAEL ADDITION REACTION	227
<i>by David A. Oare and Clayton H. Heathcock</i>	
<i>Department of Chemistry</i>	
<i>University of California</i>	
<i>Berkeley, California</i>	
SUBJECT INDEX	409
CUMULATIVE INDEX, VOLUMES 1-19	419

**TOPICS IN
STEREOCHEMISTRY**

VOLUME 19

Molecular Structure and Carbon-13 Chemical Shielding Tensors Obtained from Nuclear Magnetic Resonance

JULIO C. FACELLI* AND DAVID M. GRANT

Chemistry Department, University of Utah, Salt Lake City, Utah

- I. Introduction
- II. Theoretical Background
 - A. The Shielding Tensor
 - B. Quantum Mechanical Formulation of the Chemical Shielding
 - C. Ab Initio Methods for the Calculation of the Chemical Shielding
 - 1. The GIAO Formulation
 - 2. IGLO Method
 - 3. The LORG method
- III. Experimental Techniques
 - A. The CP/MAS Experiment
 - B. ^{13}C Shift Tensors from Single Crystal Experiments
 - C. ^{13}C Shift Tensors in Disordered Materials
 - D. Other Methods for Determining ^{13}C Shift Tensors
- IV. Conformational Effects in Solids
 - A. CP/MAS Examples in Organic Molecules
 - B. ^{13}C Shielding Tensors and Molecular Structure
 - 1. The γ -Effect and ^{13}C Shielding Tensors in *cis*- and *trans*-2-Butenes
 - 2. The $^{13}\text{CH}_2$ Shielding in Cycloalkanes, Cycloalkenes, and Heterocycles
 - 3. Tautomerism of Valence Structures in Cyclobutadiene
 - 4. ^{13}C Shielding Tensors in Hydroxybenzenes
 - 5. Effects of Side Chain Conformation in Substituted Benzenes
 - 6. Conformational Effects of Carbonyl Carbons in Polypeptides
 - 7. ^{13}C Shielding Tensors in Retinal Derivatives
 - C. Crystal Packing Effects on Chemical Shielding Tensors
- V. Theoretical Calculations of the Angular Dependence of the ^{13}C Shielding Tensors in Model Compounds
- VI. Conclusions
- Acknowledgments
- References

*Also Departamento de Física, Facultad de Ciencias Exactas y Naturales, Universidad de Buenos Aires, Ciudad Universitaria, 1428 Buenos Aires, Argentina

I. INTRODUCTION

One of the most important observations in the early days of NMR spectroscopy was the dependence of the magnetic resonance frequency upon the chemical or electronic environment of the nucleus. These experimental results were followed rather quickly by Ramsey's theoretical formulation (1) of chemical shielding which recognized the tensorial character of the interaction. The physical basis of chemical shielding may be visualized from an idealized experiment in which the transition frequency of a nuclear spin is considered for an isolated molecule at various orientations relative to an external magnetic field. The local magnetic field at the nucleus depends upon the orientation of the molecule with respect to the external magnetic field as a consequence of differential shielding resulting from anisotropy in the electron distribution in the vicinity of the nucleus. Thus, the reorientation of such an idealized molecule would be accompanied by a shift in the NMR frequency of the nucleus. A similar but realizable experiment, to be discussed later, can be performed by reorienting a single crystal in a magnetic field while following the orientational dependence of the resonance frequency. These data determine the ^{13}C shielding tensors and provide insight into the three dimensional distribution of molecular electrons.

For many years, owing to experimental limitations, NMR spectra of organic compounds were studied to any appreciable extent only in the liquid phase, where the rapid molecular tumbling prevented the observation of the tensorial features of chemical shielding. Only average or 'isotropic' shifts can be determined from liquid phase data. Even so, early isotropic ^{13}C chemical shifts were found to depend significantly upon molecular conformations. Work from this laboratory on simple hydrocarbons (2, 3) expressed the shielding in terms of additivity parameters, many of which depend on conformational coiling and folding. The importance of conformational effects found in the cyclic alkanes (4, 5) firmly established ^{13}C resonance methods as a powerful tool in the field of conformational analysis. Reference 2 on a variety of flexible alkanes and ref. 4 on conformational dependence in methylcyclohexanes provided an introduction to much of the early work on which structural and conformational analysis by NMR methods was based, and both have been cited extensively. The studies of methyl-methyl interactions in methylbenzenes, (6) and more recently the study of the highly flexible conformations observed in hydroaromatics (7) are further examples from this laboratory that illustrate the use of liquid phase ^{13}C NMR in conformational analysis. These representative publications from our laboratory along with an immense amount of work from many other sources provide the basis for the use of NMR in the liquid phase in conformational analysis.

When one records only the isotropic chemical shifts obtained from liquids, a great deal of information on the shielding tensor is left unmeasured. Molecular rotation, rapid on the NMR time scale, averages the components of the shielding tensor to its isotropic value and eliminates the three-dimensional information available in the full tensor. Furthermore, quenching of the molecular motion in the solid state often provides interesting additional information which is absent in both liquids and gases. The immobilization of molecules in a solid is usually associated with a freezing of the conformational structure as observed (8) in a number of solid samples. The rigidity imposed by the crystal lattice may destroy the effective symmetry found in rapidly equilibrating molecules. Such a break in symmetry can give rise to more lines in a magic angle spinning (MAS) spectrum than are found in the corresponding liquid phase spectrum. Conformational splitting of MAS lines has been observed in a variety of organic compounds as well as in natural and synthetic polymers (8). In section IV a brief description of some relevant results, obtained using cross polarization (CP) and MAS methods in organic molecules, is given as a background for the results obtained from tensor information. CP/MAS can not only be used to understand conformational changes in solids, but at times becomes the best tool for conformational analysis of materials (e.g. amorphous substances) that are unsuitable for X-ray studies. The CP/MAS method is also useful for relatively insoluble materials (e.g. intracitable polymers) or molecules for which conformational information cannot be obtained by NMR in solution. It is apparent that a great deal of information on molecular electronic structure can be obtained if the ^{13}C chemical shift tensors, or at least their principal values, are measured and properly rationalized. These techniques have been applied to several types of solids including single crystals, polycrystalline and amorphous powders, frozen liquids and gases, and matrix isolated compounds, using rather elaborate instrumental techniques, complicated data reduction schemes, and extensive theoretical methods to correlate the molecular structural information with the experimental results. Isolation of organic compounds at cryogenic temperatures in glasses and matrices deserves special comment because in many cases it is the only accessible method for studying highly reactive compounds using NMR.

In Section II the necessary theoretical background is developed. Special attention is given to the current quantum mechanical methods used to calculate ^{13}C chemical shielding because of their importance in the interpretation of experimental results. Even if a large number of shielding tensors had been available in the literature during previous decades, the full potential of these tensorial data would have been appreciated only in the last 4-5 years, when powerful computers and new theoretical formulations have become available to provide the relatively reliable calculations for molecules of interest to the experimentalist.

In Section III the experimental techniques used to measure ^{13}C shift tensors are described in some detail and appropriate references are given for further study.

Section IV includes a brief account of illustrative conformational studies using MAS followed by an extensive review of relevant work in which ^{13}C shielding tensors have been related to the molecular structure.

In Section V theoretical predictions of potentially important conformational features are presented along with their consequences for shielding tensors. These examples illustrate ways in which theoretical work can be used to direct the design of future experiments in this relatively new area of conformational analysis.

II. THEORETICAL BACKGROUND

A. The Shielding Tensor

Shielding concepts may be formulated, using tensor mathematics and quantum mechanical perturbation theory, with expressions that can be used to calculate the ^{13}C shielding tensors at different levels of approximation. Lack of space precludes giving more than a cursory description of the tensor algebra, but the reader unfamiliar with the subject is referred to a standard text (9) on this subject. The shielding tensor of the nucleus is defined by the differential change in the electronic energy, E , of the molecule caused by both the external magnetic field, \mathbf{H} , and the magnetic field of the A^{th} nuclear moment, μ_A (10). Expressed in mathematical terms this becomes:

$$\sigma_{\alpha\beta} = \left(\frac{\partial^2 E(\mathbf{H}, \mu_A)}{\partial \mathbf{H}_\alpha \partial \mu_{A\beta}} \right)_{\mu_A = \mathbf{H} = 0} \quad [1]$$

where the Cartesian coordinates are given by α and β .

The $\sigma_{\alpha\beta}$ is found, empirically, to be a correct mathematical description of the screening phenomena, and furthermore the tensorial character of $\sigma_{\alpha\beta}$ is evident from eq. [1]. The $\sigma_{\alpha\beta}$ is a real tensor of second rank, and its non-symmetric properties follow from,

$$\sigma_{\alpha\beta} = \frac{\partial^2 E}{\partial \mathbf{H}_\alpha \partial \mu_\beta} \neq \frac{\partial^2 E}{\partial \mathbf{H}_\beta \partial \mu_\alpha} = \sigma_{\beta\alpha} \quad [2]$$

The interested reader is referred to Robert and Wiesenfeld (11) for a detailed discussion of the characteristics of the antisymmetric part of the shielding tensor. Quantum chemical calculations of the antisymmetric components of the shielding tensors have been published for a large variety of compounds (12). For the purposes here, it is sufficient to indicate that the shielding tensor

$\sigma_{\alpha\beta}$ can be separated into its symmetric and antisymmetric parts as defined by

$$\sigma_{\alpha\beta}^S = \frac{1}{2} (\sigma_{\alpha\beta} + \sigma_{\beta\alpha}) \quad [3]$$

$$\sigma_{\alpha\beta}^A = \frac{1}{2} (\sigma_{\alpha\beta} - \sigma_{\beta\alpha}) \quad [4]$$

For available external magnetic fields, the NMR spectrum depends only on the symmetric part of the tensor (13). Therefore, it is sufficient to concentrate on $\sigma_{\alpha\beta}^S$ and its properties. The symmetric part of a real, second rank tensor is specified in any arbitrary reference frame by six independent numbers; alternatively, the tensor can be diagonalized by an orthogonal transformation and expressed by the three principal values and the corresponding principal axes. In its diagonal form, the tensor may also be expressed in irreducible form using the isotropic shielding, σ_{iso} , the anisotropy of the shielding, δ , and the asymmetry parameter, η , given by

$$\sigma_{\text{iso}} = \frac{1}{3} (\sigma_{zz} + \sigma_{xx} + \sigma_{yy}) = \frac{1}{3} \text{tr } \boldsymbol{\sigma} \quad [5]$$

$$\delta = \sigma_{zz} - \sigma_{\text{iso}} \quad [6]$$

$$\eta = \frac{\sigma_{yy} - \sigma_{xx}}{\delta} \quad [7]$$

where it is assumed that $|\sigma_{xx} - \sigma_{\text{iso}}| \leq |\sigma_{yy} - \sigma_{\text{iso}}| \leq |\sigma_{zz} - \sigma_{\text{iso}}|$. These three parameters are closely related to the spherical representation of the shielding tensor (14). One third of the trace of σ , $\text{tr } \sigma$, is the isotropic value of the shielding which is the quantity measured by typical NMR methods in solution, in the gas phase, or in the solid state using the MAS method. Note that $(1/3)\text{tr } \sigma$ is not the quantity which is available from the NMR experiment, as one can measure only a chemical shift difference between the resonance frequency of the nucleus and some arbitrary standard. Very intricate procedures have been developed to determine absolute shieldings in selected compounds (15) and an updated list of absolute shielding references has been given recently by Jameson and Mason (16).

B. Quantum Mechanical Formulation of the Chemical Shielding

The electronic Hamiltonian of a molecule in the presence of a time independent magnetic field, in atomic units, is given by

$$\mathcal{H} = \frac{1}{2} \sum_k \left[\frac{1}{i} \nabla_k - \frac{1}{c} \mathbf{A}_k(\mathbf{r}) \right]^2 + V(\mathbf{r}) \quad [8]$$

where standard notation (10) is followed and $\mathbf{A}_k(\mathbf{r})$ is the vector potential at the position of the electron k . In the Coulomb gauge, the vector potential for the superposition of an homogeneous magnetic field and the dipolar field from the magnetic moment of the nucleus is given by

$$\mathbf{A}_k(\mathbf{r}) = \frac{1}{2} \mathbf{H} \times (\mathbf{r}_k - \mathbf{r}_0) + (\boldsymbol{\mu} \times \mathbf{r}_k)/r_k^3 \quad [9]$$

where \mathbf{r}_k is the position of the k^{th} electron measured from the coordinate origin, $\boldsymbol{\mu}$ is the magnetic moment of the nucleus and \mathbf{r}_0 is the origin of the vector potential. Equations [8] and [9] can be expanded as

$$\mathcal{H} = \mathcal{H}_0 + \mathcal{H}_1 + \mathcal{H}_2 + \mathcal{H}_3 \quad [10]$$

where

$$\mathcal{H}_0 = \frac{1}{2} \sum_k \nabla_k^2 + V(\mathbf{r}) \quad [11]$$

$$\mathcal{H}_1 = \frac{1}{c} \sum_k \mathbf{H} \cdot \mathbf{L}_k \quad [12]$$

$$\mathcal{H}_2 = \frac{1}{c} \sum_k \boldsymbol{\mu} \cdot \frac{\mathbf{L}_k}{r_k^3} \quad [13]$$

$$\mathcal{H}_3 = \frac{1}{2c^2} \sum_{\alpha, \beta}^3 \left[\boldsymbol{\mu}_\alpha \left(\sum_k \frac{r_k^2 \delta_{\alpha\beta} - r_{k\alpha} r_{k\beta}}{r_k^3} \right) \mathbf{H}_\beta \right] \quad [14]$$

In eqs. [11–14] the gauge origin has been selected at the nucleus for which the shielding tensor is calculated. \mathcal{H}_0 is the electronic Hamiltonian for the molecule in the absence of both the external and dipolar magnetic fields. \mathcal{H}_1 , \mathcal{H}_2 and \mathcal{H}_3 are much smaller than \mathcal{H}_0 and their contributions to the electronic energy of the system can be calculated using perturbation theory. In accordance with eq. [1] only the terms bilinear in the external magnetic field and the nuclear dipolar moment have to be considered in the calculation of the shielding tensors. In first order perturbation theory \mathcal{H}_3 makes a contribution to the energy, the so-called diamagnetic term, which is bilinear in $\boldsymbol{\mu}$ and \mathbf{H} . For a real electronic wave function in a Σ state (i.e. nonparamagnetic), \mathcal{H}_1 and \mathcal{H}_2 make no contribution to the shielding in first order perturbation theory, but at second order they provide a bilinear contribution in $\boldsymbol{\mu}$ and \mathbf{H} through a cross term which is referred to as the paramagnetic contribution. When the origin of the gauge is selected at the nucleus at which the shielding is calculated, the chemical shifts and the anisotropy of the ^{13}C shielding ten-

sors are dominated by the paramagnetic contribution (10). Third order effects are considered of minor importance for ^{13}C shielding, but there is some indication that their contribution could be important in molecules containing heavy nuclei (17). Thus, up through second order perturbation theory only \mathcal{H}_3 and the product of \mathcal{H}_2 and \mathcal{H}_1 make contributions to the ^{13}C shielding; when the origin of the gauge is selected at the nucleus under consideration the diamagnetic and paramagnetic terms are given respectively by:

$$\sigma_{\alpha\beta}^{(d)} = \frac{1}{2c^2} \left\langle \psi_0 \left| \sum_k (r_k^2 \delta_{\alpha\beta} - r_{k\alpha} r_{k\beta}) r_k^{-3} \right| \psi_0 \right\rangle \quad [15]$$

$$\sigma_{\alpha\beta}^{(p)} = \frac{-1}{2c^2} \sum_{n \neq 0} \frac{\left\langle \psi_0 \left| \sum_k \frac{L_{k\alpha}}{r_k^3} \right| \psi_n \right\rangle \langle \psi_n | L_{k\beta} | \psi_0 \rangle + \text{C.C.}}{(E_n - E_0)} \quad [16]$$

where C.C. is the complex conjugate of the previous term, $|\psi_0\rangle$ is the electronic wave function of the ground state with eigenvalue E_0 and $|\psi_n\rangle$ are the wave functions of the excited states of \mathcal{H}_0 with eigenvalues E_n .

In paramagnetic molecules the chemical shifts are dominated by the large Fermi contact interaction between the unpaired electrons and the nuclear magnetic moment (18). In this review we are going to discuss only nonparamagnetic species, even though a great deal of information can be obtained from paramagnetic compounds.

One of the difficult problems encountered in the computation of eqs. [15] and [16] is associated with the selection of the gauge, which in these two equations was done by placing its origin at the nucleus under consideration. Other choices are equally valid, and while the diamagnetic and paramagnetic contributions depend upon the selection of the gauge origin, the total shielding given by

$$\sigma = \sigma^{(d)} + \sigma^{(p)} \quad [17]$$

does not depend on that choice providing that the exact electronic wave functions are used in the calculations. Therefore extreme care has to be exercised in the selection of the perturbation scheme used in the calculation of shielding tensors. Note that an exact calculation is not possible for any molecule because the exact wavefunctions and energies for all the eigenstates of \mathcal{H}_0 are unavailable for use in eqs. [15] and [16]. Epstein (19) has demonstrated that the CHF (Coupled Hartree Fock) perturbation theory or any other variational method is gauge invariant for a complete basis set. Unfortunately, the use of a truncated basis set can introduce significant inaccuracies into the calculation of shielding constants, and therefore the selection of gauge is always a serious

problem in shielding calculations. A numerical example of the gauge problems has been illustrated in recent calculations by Holler and Lischka (20).

C. Ab Initio Methods for the Calculation of the Chemical Shielding

The methods for the calculation of the chemical shielding using either *ab initio* or semiempirical methods have been reviewed by Ebraheem and Webb (10). Since the publication of their review new advances have been reported annually in the Specialist Periodical Reports on NMR Spectroscopy (21). A short account of the more effective *ab initio* methods for the calculation of chemical shielding is included here for the benefit of the readers.

Three of the more effective *ab initio* methods currently used for the calculation of chemical shieldings are the GIAO (Gauge Invariant Atomic Orbitals) method of Ditchfield (22), the IGLO (Individual Gauge for Localized Orbitals) method of Kutzelnigg (23) and the LORG (Localized Orbital/Local Origin) method of Hansen and Bouman (24). Regular CHF methods can also be applied to the calculation of chemical shielding but their application is limited to very small molecules or molecules with high symmetry owing to the need for very large basis sets to achieve gauge invariance in the results (20, 25, 26). The GIAO, IGLO and LORG methods alleviate gauge problems by using different schemes to avoid the spurious gauge effects that arise in the calculation of the paramagnetic term using incomplete basis sets in the expansion of the electronic wave function (19). A similar scheme of local gauge origins was also proposed by Levy and Ridard (27), using the so-called orbital pair theory of shielding, but only a few applications of this method have been reported in the literature.

1. The GIAO Formulation

The GIAO method (22) expands the electronic wave function in a linear combination of functions centered at the different nuclei in the molecule given by:

$$\psi_\nu(\mathbf{H}) = \exp\left(-\frac{i}{c} \mathbf{A}_\nu \cdot \mathbf{r}\right) \phi_\nu \quad [18]$$

where ϕ_ν is any kind of real atomic orbital (AO), normally gaussian functions. The vector potential, \mathbf{A}_ν , is chosen as

$$\mathbf{A}_\nu = \frac{1}{2} \mathbf{H} \times \mathbf{R}_\nu \quad [19]$$

where \mathbf{R}_ν is the position of the ν nucleus measured from the origin. Unfortu-

nately, these functions, ψ_v , are called gauge invariant atomic orbitals, GIAO, even though they explicitly depend on the gauge origin. Pople (28) has proposed to call them "gauge dependent atomic orbitals". The insertion of these AO in the expressions for the wave function leads to expressions of the shielding that are formally independent of the gauge selection, but the consequences of the approximation are incompletely understood. For instance, Epstein (19) mentions that the GIAO method leads to wave functions in which $\nabla \cdot \mathbf{J} \neq 0$. Ditchfield implementation of the GIAO theory uses the FPT (Finite Perturbation Theory) as the scheme to calculate the paramagnetic contribution to the shielding (22). Several *ab initio* and semiempirical implementations of the GIAO method have been reported (10, 22).

In a recent publication, Ditchfield and his co-workers (29) have used the method to analyze the effects of hydrogen bonding and of temperature on the shielding in small molecules. Other important applications of this method come from a group (30) who applied the method to calculate properties in molecules of biological interest.

In general, good results can be obtained with this method even when basis sets of double ζ quality are used. An extensive comparison of the GIAO method with the IGLO for different basis sets has been published (31), and the reader is referred to this source for a more complete account of relevant references on the GIAO method and the quality of its results.

2. IGLO Method

The two basic ideas introduced into the standard CHF perturbation theory in order to develop the IGLO theory (23) of chemical shielding are:

1. The CHF equations are solved in a localized basis set of molecular orbitals (MO).
2. For each localized molecular orbital the gauge origin is chosen at the centroid of charge of the MO.

Obviously the method becomes formally gauge invariant, because after imposing both conditions 1) and 2) no freedom to choose any gauge origin remains.

Within the Hartree-Fock (32) approximation the canonical MO's $|\varphi_i\rangle$ satisfy the equation:

$$F|\varphi_i\rangle = \epsilon_i|\varphi_i\rangle \quad [20]$$

where F is the Fock operator and ϵ_i the orbital energies. The total electronic energy does not change by intrashell mixing (i.e. linear combinations of MO's within the occupied or vacant sets do not change the total electronic energy of

the system); it is therefore possible to choose those occupied orbitals, given by linear combinations of the canonical MO's, which satisfy certain properties. For instance, Boys' localization criterion (33) is used in the IGLO approach to obtain the localized orbitals used in the perturbation calculation. As the expressions for the CHF theory are usually derived assuming canonical orbitals, the use of localized orbitals, which do not diagonalize the Fock operator in eq. [20], requires a new set of expressions for the CHF theory (23, 34, 35). They are not repeated here, but they are included in the final expressions for the shielding given below.

The second feature of the IGLO method invokes the use of different gauge origins for each of the localized orbitals. This is accomplished by introducing a new set of orbitals, $|\psi_k\rangle$, defined by

$$|\varphi_k\rangle = e^{i\Delta_k} |\psi_k\rangle \quad [21]$$

where,

$$\Delta_k = \frac{1}{2c} (\mathbf{R}_k \times \mathbf{H}) \cdot \mathbf{r} \quad [22]$$

and \mathbf{R}_k is chosen at the center of gravity of the orbital $|\varphi_{k0}\rangle$. In this way the CHF equations become

$$\{\tilde{F}_{k1} - \tilde{P}_{k1}F_0\}|\psi_{k0}\rangle + F_0|\psi_{k1}\rangle = 0 \quad [23]$$

where the notation of refs. 23, 34, and 35 is used. The shielding tensor is given by

$$\sigma = 2 \sum_{k=0}^{occ} \{ \langle \psi_{k0} | \tilde{h}'_{k2} | \psi_{k0} \rangle - 2 \langle \psi_{k0} | h'_1 | \psi_{k1} \rangle \} \quad [24]$$

where the diamagnetic and paramagnetic bond contributions (36) are defined by

$$\sigma_d^{\text{xy}} = \langle \psi_{(x-y)_0} | \tilde{h}'_{k2} | \psi_{(x-y)_0} \rangle \quad [25]$$

$$\sigma_p^{\text{xy}} = \langle \psi_{(x-y)_0} | h'_1 | \psi_{(x-y)_1} \rangle \quad [26]$$

The \tilde{h}'_{k2} and h'_1 operators are given by

$$h'_1 = -\frac{i}{c} \frac{\mu \times (\mathbf{r} - \rho)}{|\mathbf{r} - \rho|^3} \cdot \mathbf{p} \quad [27]$$

$$\tilde{h}'_{k_2} = \frac{1}{2c^2} \frac{\{\mathbf{H} \times (\mathbf{r} - \mathbf{R}_k)\}\{\boldsymbol{\mu} \times (\mathbf{r} - \boldsymbol{\rho})\}}{|\mathbf{r} - \boldsymbol{\rho}|^3} \quad [28]$$

where $\boldsymbol{\rho}$ is the position of the nucleus under consideration. These expressions have been used (36) to provide a physical interpretation of the chemical shift in terms of individual bond contributions.

The IGLO method has been used with great success not only to predict ^{13}C isotropic shifts (34, 35) in a large number of molecules but also to assign the tensor components of ^{13}C shift tensors measured at low temperature in this laboratory (37-42). One of the big advantages of the IGLO method is its ability to predict the shielding principal values reasonably well even when moderately small basis sets (double ζ) are used in the calculations. This makes calculations of ^{13}C shifts possible in fairly large molecules which do not possess high symmetry.

3. The LORG Method

The LORG approach recently proposed by Hansen and Bouman (24), is similar to the IGLO approach. The main differences are encountered in the computer implementation and in the use of the random phase approximation (43) (RPA) as the perturbation scheme. A detailed comparison between the IGLO and LORG methods is to be presented elsewhere (44).

Using the notation of ref 24, the LORG formulas for the chemical shielding of a nucleus located at the origin of coordinates are given by:

$$\sigma = \sum_{\alpha} \sigma^d(\alpha, \alpha) + \sum_{\alpha, \beta} \sigma^d(\alpha, \beta) + \sum_{\alpha} \sigma^p(\alpha, \alpha) \sum_{\alpha \beta} \sigma^p(\alpha, \beta) \quad [29]$$

where

$$\sigma_{ij}^d(\alpha, \alpha) = c^{-2} \langle \alpha | \{(\mathbf{r} - \mathbf{R}_{\alpha}) \cdot \mathbf{r} \delta_{ij} - [\epsilon_i \cdot (\mathbf{r} - \mathbf{R}_{\alpha})] [\epsilon_j \cdot \mathbf{r}] \} / r^3 | \alpha \rangle \quad [30]$$

$$\sigma_{ij}^d(\alpha, \beta) = ic^{-2} \left[\epsilon_i \cdot \left\langle \alpha \left| \frac{\mathbf{L}}{r^3} \right| \beta \right\rangle \right] [\epsilon_j \cdot \{(\mathbf{R}_{\alpha} - \mathbf{R}_{\beta}) \times \langle \beta | \mathbf{r} | \alpha \rangle\}] \quad [31]$$

$$\sigma_{ij}^p(\alpha, \alpha) = -2c^{-2} \sum_{m,n} \left[\epsilon_i \cdot \left\langle \alpha \left| \frac{\mathbf{L}}{r^3} \right| m \right\rangle \right] (A - B)^{-1}_{\alpha m, \alpha n} [\epsilon_j \cdot \langle n | \mathbf{L}^{(\alpha)} | \alpha \rangle] \quad [32]$$

$$\sigma_{ij}^p(\alpha, \beta) = -2c^{-2} \sum_{m,n} \epsilon_i \left\langle \alpha \left| \frac{\mathbf{L}}{r^3} \right| m \right\rangle (A - B)^{-1}_{\alpha m, \beta n} [\epsilon_j \cdot \langle n | \mathbf{L}^{(\alpha)} | \beta \rangle] \quad [33]$$

Note that if the iterative formulation is used (45), it is no longer possible to

separate the $\sigma^p(\alpha, \alpha)$ and the $\sigma^p(\alpha, \beta)$ contributions. In eqs. [29-33] $|\alpha\rangle$ and $|\beta\rangle$ represent localized MO's and $(A - B)^{-1}$ is the first order polarization propagator for a complex perturbation, which depends on the ground state and the excited states of the molecules (43). Depending upon the selection of \mathbf{R}_α different theoretical estimates of the chemical shielding are obtained.

If one sets $\mathbf{R}_\alpha = 0$ (i.e. a common gauge origin for all the localized orbitals), then the standard CHF scheme is recovered and none of the computational advantages of using local gauges is realized. To take advantage of the use of local gauges two selections of \mathbf{R}_α have been proposed (24):

- i) FULL LORG uses $\mathbf{R}_\alpha = \langle \alpha | \mathbf{r} | \alpha \rangle$, i.e. \mathbf{R}_α is taken at the center of charge for all localized orbitals, $|\alpha\rangle$. This selection is similar to the selection used for the IGLO method.
- ii) LORG uses $\mathbf{R}_\alpha = 0$ for all localized orbitals, $|\alpha\rangle$, directly bonded to the nucleus under consideration. For all other orbitals in the molecule \mathbf{R}_α is taken at the center of charge of the orbital, that is, $\mathbf{R}_\alpha = \langle \alpha | \mathbf{r} | \alpha \rangle$.

Empirically it has been found (24, 45) that the second choice produces better results for a variety of basis sets. The results for the calculation of shielding using the LORG method are similar, in quality, to those obtained with the IGLO method, and calculations using double ζ quality basis sets produce results that are in reasonable agreement with the experimental values.

The use of the GIAO, IGLO and LORG methods has had a significant impact in the calculation of shielding tensors making it possible, with currently available computational resources, to calculate ^{13}C chemical shieldings in molecules with up to 8-9 atoms excluding hydrogens. The size of molecules that can be handled should double in the near future, as new improvements in the software and hardware become available.

III. EXPERIMENTAL TECHNIQUES

In this section the relevant techniques used in solid state NMR are briefly described and their relationship with the measurements of ^{13}C shift tensors is discussed in detail.

A. The CP/MAS Experiment

In solid organic materials it is necessary to decouple the abundant spins, usually ^1H , in order to observe the high resolution spectra of dilute spins like ^{13}C . This can be accomplished in a relatively easy way by the use of high power

decoupling (46) ($\gamma H_1 \approx 40$ to 100 kHz) at the ^1H resonance frequency. In absence of shielding anisotropies this double resonance experiment produces reasonable ^{13}C linewidths of 10–50 Hz in typical organic solids. The high power proton irradiation can also improve the signal to noise ratio, S/N, by meeting the Hartmann-Hahn (47) condition

$$\gamma_{^{13}\text{C}} \mathbf{H}_{1\text{C}} = \gamma_{^1\text{H}} \mathbf{H}_{1\text{H}} \quad [34]$$

The magnetization of the highly sensitive protons can be transferred to the non-abundant species with a theoretical improvement in the S/N which approaches the 4-fold ratio of $\gamma_{^1\text{H}}/\gamma_{^{13}\text{C}}$. The pulse sequences of several CP experiments are shown in Figure 1 for the three most popular variations of the experiment. The spin lock with multiple contact times is of particular importance for samples with very long relaxation times ($T_{1\rho}$), but this requires the high power ^1H decoupler to be on for an extended period of time. Owing to equipment limitations, this requirement may not always be feasible. The dipolar dephasing experiment (48) can be used to separate protonated carbons (CH and CH_2) from quaternary and methyl carbons, and therefore is useful in spectral assignments. It may also be convenient to add a 90° flip-back pulse in the proton channel at the end of the CP sequence to alleviate relaxation problems (49). When the CP technique is used, the limiting factor in the repetition time usually becomes the proton relaxation time and not the typically longer ^{13}C relaxation time. This constitutes another advantage of the CP experiments over the typical Fourier transform (FT) experiments which are usually limited by ^{13}C relaxation. It may be noted that in samples with large amounts of paramagnetic centers the limiting factor can be the duty cycle of the high power electronics.

Even under high power ^1H irradiation, solid state ^{13}C NMR lines may be extraordinarily broad because of anisotropy in the shielding interactions (see the Section below on powder patterns). In order to suppress this broadening the sample must be rotated about an axis at the magic angle (54.73°) with respect to the external magnetic field (14, 46). Spinning speeds of the order of several KHz are required to completely average the shielding interactions. The resulting ^{13}C spectra recorded under CP/MAS conditions are liquid-like with linewidths in the range of 2–40 Hz depending on the sample and the magnitude of the external magnetic field. As a consequence of spinning the sample, all of the information on the shift tensors, except for the trace of the tensor, is lost in a MAS experiment providing the spinning speed is much larger than the line width caused by the chemical shift anisotropy.

The capabilities described above are available as standard features on most NMR commercial spectrometers used for solid state and as optional accessories on some liquid phase NMR spectrometers.

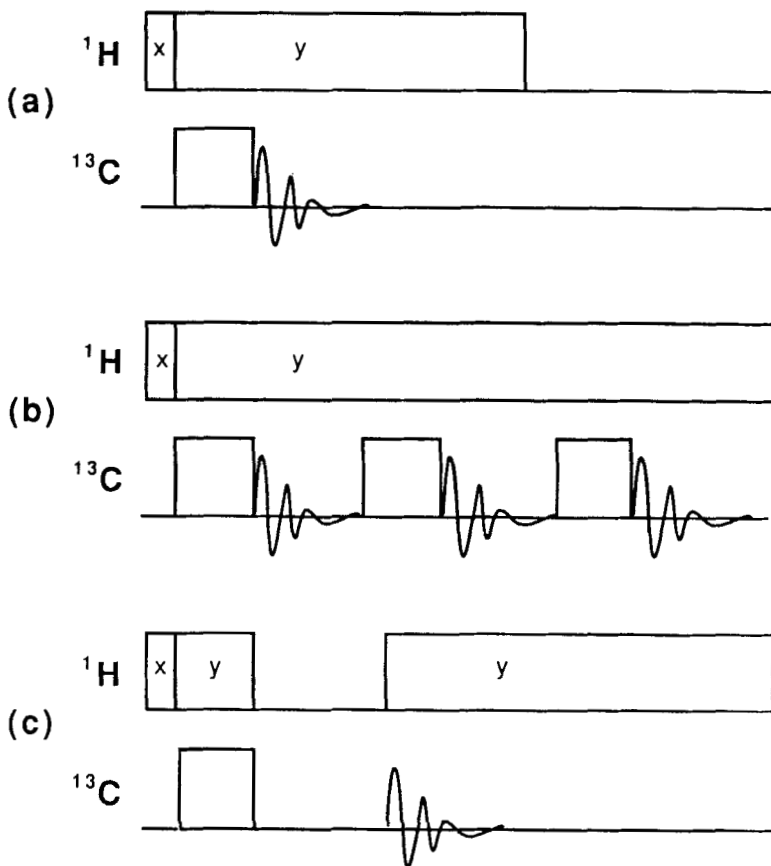


Figure 1. Pulse sequences commonly used in the CP experiment; a) single contact experiment; b) spin lock with multiple contact times; c) dipolar dephasing.

B. ^{13}C Shift Tensors from Single Crystal Experiments

Solid state NMR measurements on single crystals provide the maximum information available concerning ^{13}C chemical shift tensors. These experiments can provide the principal values of the chemical shift tensor and the orientation of their respective principal directions. In some cases, owing to the inversion symmetry of the NMR experiments and the symmetries of some unit cells, ambiguities remain as to the orientation of the principal axes system

(PAS) in the molecular frame. These difficulties can often be resolved using chemical arguments, or theoretical considerations or both (50).

The major limitation of single crystal techniques is the availability of suitable single crystals of adequate size for the NMR experiment. The low sensitivity of NMR experiments makes it necessary to use reasonably large crystals (~ 10 to 30 mm^3), which are difficult to obtain. Moreover, prismatic type crystals are preferable to needles or plates, which usually are inappropriate for NMR studies. The experiments on single crystals require a mechanical device to change the orientation of the crystal relative to the magnetic field in a prescribed way while, at the same time, they use the common solid state NMR techniques such as CP and high power ^1H decoupling.

The resonance frequency for a nucleus is given by (51)

$$\delta_{\text{lab}} = \sigma_{xx}^{\text{sam}} \sin^2 \theta \cos^2 \phi + \sigma_{yy}^{\text{sam}} \sin^2 \theta \sin^2 \phi + \sigma_{zz}^{\text{sam}} \cos^2 \theta \\ + \sigma_{yx}^{\text{sam}} \sin^2 \theta \sin^2 2\phi + \sigma_{zx}^{\text{sam}} \sin 2\theta \cos \phi + \sigma_{zy}^{\text{sam}} \sin 2\theta \sin \phi \quad [35]$$

where σ_{ij}^{sam} are the elements of the symmetric part of shift tensor and the polar angles, θ and ϕ , describe the orientation of the magnetic field in the sample frame. The single crystal spectrum will contain a resonant line at frequency δ_{lab} for each nonmagnetically equivalent nucleus in the unit cell. To obtain the tensorial information contained in the σ_{ij}^{sam} terms, the orientation of the crystal is changed while monitoring the resonance frequencies as a function of the orientational angles θ and ϕ . Equation [35] is used to obtain the coefficients, σ_{ij}^{sam} , from the data acquired on the orientational dependence of the resonance frequencies. These coefficients, σ_{ij}^{sam} , are the components of the symmetric part of the shift tensor in the sample frame, and a separate set of components exists for each magnetically nonequivalent nucleus in the unit cell. For each carbon, the six σ_{ij}^{sam} constitute a symmetric matrix that can be diagonalized to obtain the principal values and their respective principal directions (PAS) in the crystal frame. These principal values of the shift tensor differ from those of the shielding tensor only by the shift selected as a reference.

To obtain information on the relationship between the molecular structure and the shift tensors, it is necessary to obtain the principal axes of the shift tensors in the molecular frame, because the orientation of the PAS in the sample frame is of limited chemical utility. The transformation from the sample frame to the molecular frame can be achieved using a variety of methods:

1. Appropriate chemical assumptions may be made about the orientation of the principal components of the shielding tensors based on previous experience in similar compounds, or theoretical considerations, or both;

2. Morphological characteristics of the NMR sample may be used to determine crystal cleavage planes or axes. Literature information on the orientation of the unit cell with respect to the planes and/or axes may be used to transform the PAS from the sample frame to the unit cell frame; using X-ray data it is then straightforward to transform into the molecular frame;
3. X-ray and/or optical measurements may be made to determine the crystallographic axes of the actual crystal used in the NMR experiments;
4. Crystals with sufficient symmetry may exhibit enough redundancy in the NMR data to obtain the orthogonal transformation from the sample frame to the molecular frame from the NMR data directly.

All of these methods have been used by different research groups to obtain the orientation of the PAS in the molecular frame and, depending on the system, offer different advantages and drawbacks. It is always helpful when two or more methods agree with each other in the assignment of the shielding tensors of the various nuclei because of the possibility for ambiguities in the several individual approaches.

There are basically two ways in which the orientational dependence of the shielding, given by eq. [35] can be explored. The traditional way, described in detail in several monographs (14, 46, 51) consists of performing small step rotations around three orthogonal axes following the lines during the rotations. A typical rotational pattern obtained by these techniques is shown in Figure 2. As can be seen from the figure, there are areas in which severe overlaps and crossings of the lines occur making the identification of the resonance lines difficult if not at times impossible. With the increase of the number of magnetically nonequivalent carbons in the unit cell, the increasing complexity of the rotational pattern seriously limits the use of this traditional method for obtaining the ^{13}C chemical shielding tensors in single crystals. Until now most of the single crystal results reported have been obtained using this technique, and therefore the upper molecular size that may be studied by this method is in the range of 15–20 magnetically nonequivalent carbons per unit cell.

Very recently, in this laboratory, a new two-dimensional technique (52, 53, 54) has been introduced that replaces the small angular displacements by large amplitude rotations. This technique spreads the NMR signal in two dimensions allowing one to obtain the correlation of the shielding at two very different orientations. The method improves the determination of the shielding tensor components and makes the assignment of the resonance lines straightforward. An example of a two-dimensional spectrum is given in Figure 3. The use of these techniques has the potential of extending the single

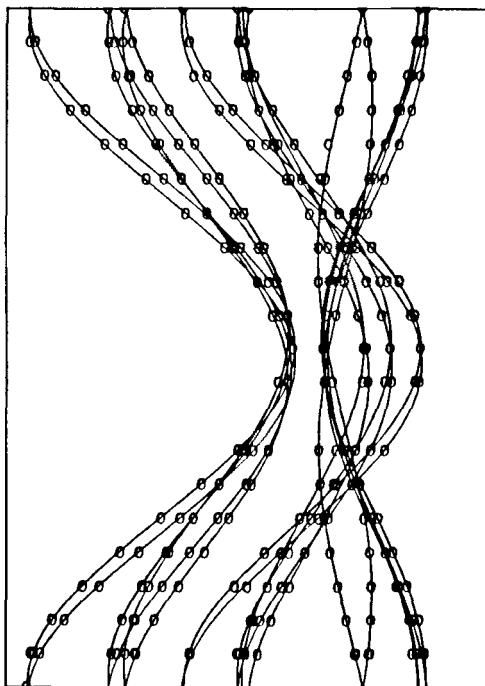


Figure 2. Rotational pattern of a single crystal: Least squares fit of a single rotation of 1,3,5-trimethoxybenzene.

crystal methodology to molecules with up to 50–100 magnetically nonequivalent nuclei per unit cell. A limitation of the technique is associated with the need for relatively long carbon $T_{1\rho}$'s in order for the magnetization to be preserved during the mechanical rotation of the sample. This could create a serious problem in some crystals that contain paramagnetic impurities, free electrons, or quadrupolar nuclei. The larger number of scans required in 2D experiments at the present time precludes the use of this approach in molecules with ^1H relaxation times longer than a few seconds.

C. ^{13}C Shift Tensors in Disordered Materials

When single crystals are not available, it is still possible to obtain valuable though incomplete information concerning the ^{13}C shielding tensors. In most cases this information is limited to the principal values of the shift tensor, whereas the orientation of the PAS can at times be inferred in molecules with high symmetry (a C_3 or higher symmetry axis) or be determined using dipolar spectroscopy. Until now these experimental techniques, because of their rela-

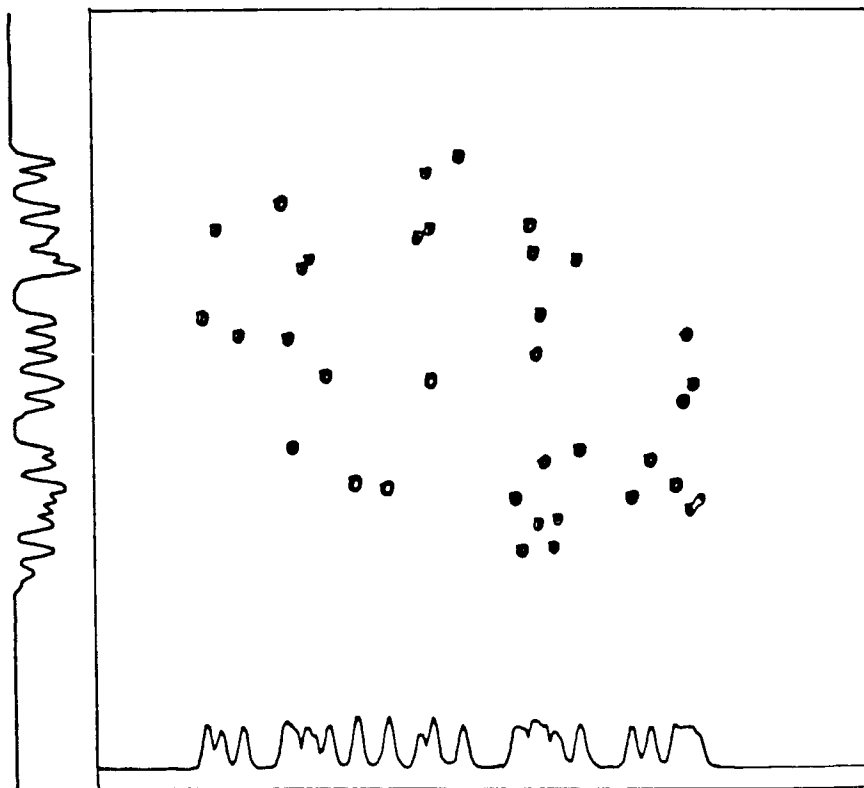


Figure 3. Two-dimensional NMR spectrum of a single crystal of 1,2,3-trimethoxybenzene showing the resolution of all 36 lines.

tive simplicity, have produced the main body of data on chemical shielding (55). Of particular importance has been the application of powder methods, especially at cryogenic temperatures, to molecules which are gases or liquids at ambient temperatures. The main limitation of powder spectra is the serious overlap of the resonance bands which limits the measurement of shielding tensors to no more than 3 to 5 chemically nonequivalent nuclei per molecule. While these limitations can be overcome by selective isotope enrichment, this approach is quite costly and provides an option that can be exercised only as a last resort.

The spectral response of a polycrystalline material or truly amorphous materials is given by (14, 46)

$$I(\omega) = \begin{cases} \pi^{-1}[(\omega_3 - \omega)(\omega_2 - \omega_1)]^{-1/2} F\left\{\left(\frac{(\omega_3 - \omega_2)(\omega - \omega_1)}{(\omega_3 - \omega)(\omega_2 - \omega_1)}\right)^{1/2}, \frac{\pi}{2}\right\} & \text{for } \omega_1 < \omega < \omega_2 \\ \pi^{-1}[(\omega_3 - \omega_2)(\omega - \omega_1)]^{-1/2} F\left\{\left(\frac{(\omega_3 - \omega)(\omega_2 - \omega_1)}{(\omega_3 - \omega_2)(\omega - \omega_1)}\right)^{1/2}, \frac{\pi}{2}\right\} & \text{for } \omega_2 < \omega < \omega_3 \\ 0 & \text{for } \omega < \omega_1 \text{ and } \omega > \omega_3 \end{cases} \quad [36]$$

where ω_1 , ω_2 and ω_3 are the principal values of the shift tensor given in rank order, and $F(k, \phi)$ is the incomplete elliptic integral of the first kind. For the simplest case in which two of the principal value of the shift tensor are degenerate, the line shape is given by

$$I(\omega) = \begin{cases} \frac{1}{\sqrt{3} \omega_0 \delta} \frac{1}{\sqrt{1 + (2\omega/\omega_0 \delta)}} & \text{for } \frac{\omega_0 \delta}{2} < \omega < \omega_0 \delta \\ 0 & \text{for } \omega < \frac{\omega_0 \delta}{2} \text{ and } \omega > \omega_0 \delta \end{cases} \quad [37]$$

where $\omega_0 = (1/3)(2\omega_1 + \omega_3)$ and δ is given by eq. [6].

In Figure 4 the corresponding powder patterns from the eqs. [36] and [37] are shown; the break points that correspond to the principal values of the shift tensors are clearly indicated. There is a very important difference between the axially symmetric and asymmetric cases because only in the first case is it possible to assign the principal axes of the shift tensor to the corresponding principal values from a powder pattern. The degeneracy of two of the principal values of the shift tensor is usually accompanied by the existence of a C_3 or higher symmetry axis in the molecule, and simple group theory arguments can be used to identify the unique principal value corresponding to the symmetry axis. The principal directions associated with the other two degenerate tensor values lie in the plane perpendicular to the symmetry axes. In the more general case, of an asymmetric pattern, even if the orientation of the principal axes are known from symmetry considerations, there are actually $3!$ possible ways to assign the three measured principal values to the three principal axes. In the most general case in which the molecule has no symmetry, the orientations of the principal axes in the molecule are unknown from the experimental data. Assignments have been made by using theoretical pre-

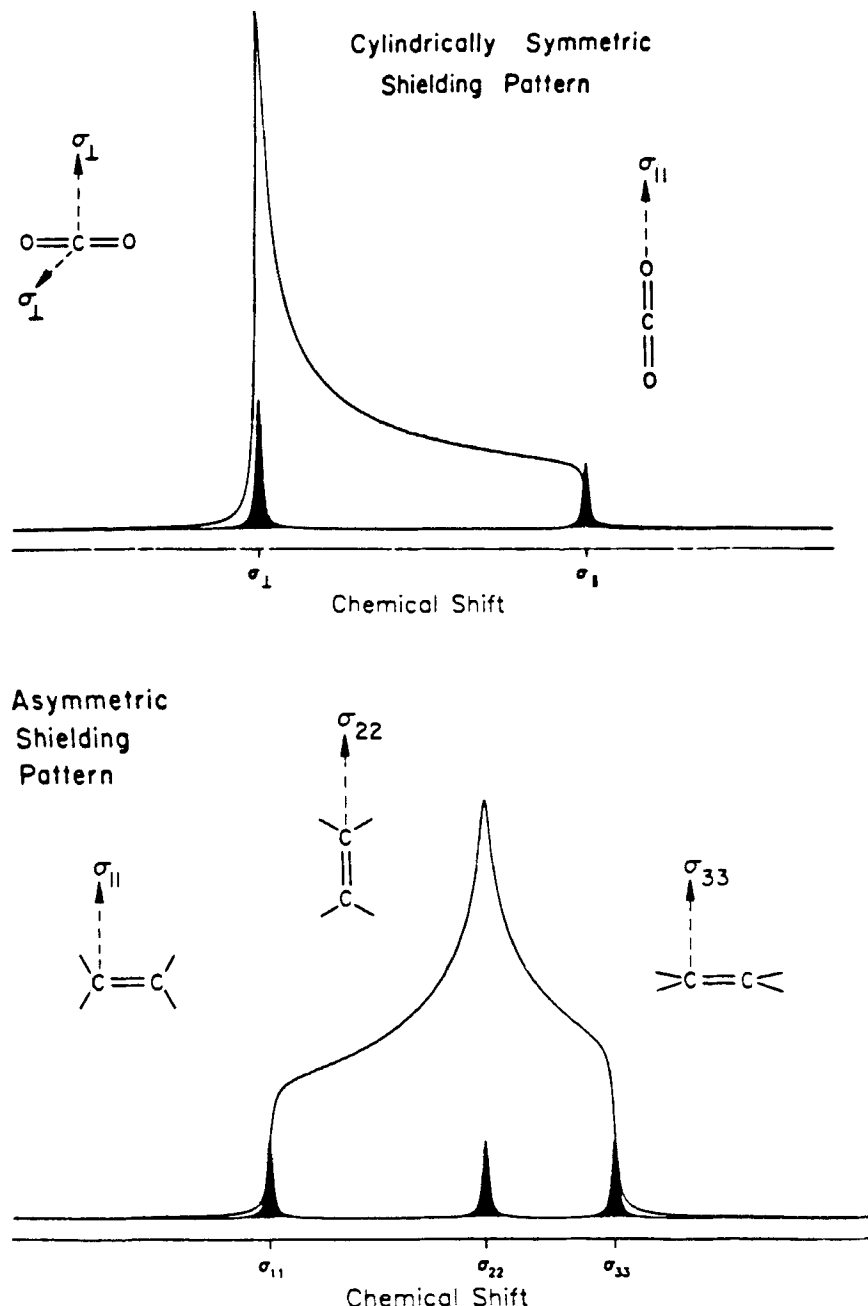


Figure 4. Powder pattern for an axially symmetric (top) on non axially symmetric (bottom) shielding tensor. The position of the principal values is indicated in the spectra.

dictions, by analogy with similar molecules or by dipolar spectroscopic measurements (56-58).

In very simple cases it is possible to obtain the principal values of the shift tensors by simple inspection of the spectra because they are given by the break points in the powder pattern as indicated in Figure 4. This can be done only when the spectrum has isolated and well characterized tensorial bands. An obvious problem with this method is the lack of any objective criteria to determine the error associated with the measurement. To overcome these problems fitting techniques using a SIMPLEX method have been used in our laboratory (59). With starting values usually estimated from the inspection of the experimental spectra, a spectrum can be simulated and compared with the experimental one. The merit function given by the sum of the squares of the deviation between the experimental and simulated spectra is minimized in terms of the spectral parameters: the principal values of the various shift tensors and appropriate line broadening functions. After convergence an error analysis is performed and the standard deviations and the correlation matrix for the parameters are obtained. This procedure allows the determination of the principal shift components in molecules with up to 3 or 4 chemically non-equivalent carbon atoms with standard deviations usually not exceeding 1 ppm. The fitting procedure can take several hours on a micro VAX depending upon the spectral complexity and the number of tensorial bands which are fitted.

Several other methods (60-65) have been proposed to measure the principal components of the shift tensors in powders. All of them involve moving the sample in the magnetic field and they are not always suitable for studies of matrix isolated compounds at low temperature.

Herzfeld and Berger (60) have proposed the analysis of the sidebands in a slow speed MAS spectrum to obtain the principal shift values. When a sample is spun at the magic angle at slow speeds compared with the anisotropy of the chemical shift, the spectrum consists of a central band positioned at the isotropic frequency of chemical shift, ν_0 , and side bands at frequencies ($\nu_0 \pm n\nu_r$), where n is an integer and ν_r is the spinning frequency of the sample. In practice only a few side bands can be observed in the spectrum because their intensity rapidly decreases when $n\nu_r$ exceeds the width of the anisotropy. The intensity of these sidebands is a function of the anisotropy of the chemical shift and can be calculated using Bessel functions. By inverting the processes it is possible to obtain the principal values of the shift tensor from the measurement of the intensities of a finite number of side bands. A major problem with this method is the need for precise intensity measurements that usually are less accurate than frequency or line position measurements in NMR experiments. A similar approach using second and third moments, which requires intensity measurements for all the side bands, has also been proposed (61).

Recently variable-angle sample spinning (VASS) has been proposed (62) as a method to obtain the principal values of shift tensors. In the fast motional regime (i.e., $\nu_r \gg \Delta\sigma$) the intensity distribution of the central band of the spectrum is given by

$$I(\theta, \alpha, \beta) = I_0 \left\{ \sigma_i + \frac{1}{2} (3 \cos^2 \theta - 1) \left[\frac{1}{2} (3 \cos^2 \beta - 1)(\sigma_{33} - \sigma_i) \right. \right. \\ \left. \left. + \frac{1}{2} \sin^2 \beta \cos 2\alpha (\sigma_{11} - \sigma_{22}) \right] \right\} \quad [38]$$

where σ_i is the isotropic shift, σ_{11} , σ_{22} and σ_{33} are the principal components of the shift tensor given in order of increasing field, θ is the angle between the spinner axis and the external magnetic field, and α and β are the Euler angles that relate the PAS of the shielding to the spinner frame (i.e. for a disordered sample they are the powder averaging angles). If the experiment is performed in the high speed regime, all the intensity will be concentrated at the central band described by eq. [38]. If θ is the magic angle the resonance will occur at σ_i , and eq. [38] designates the MAS condition. If θ is different from the magic angle, the spectral pattern will be given by the powder average over α and β of expression [38] making it possible to obtain different powder patterns for different θ angles. These patterns can be simulated using the techniques (59) described above for static powder patterns. The availability of additional spectra with different patterns of break points, which actually can even cross over one another when θ is changed, make this method superior to fitting strongly overlapping bands. A typical series of recorded spectra is shown in Figure 5.

Several two-dimensional experiments have been proposed to obtain the principal components of the shift tensor in disordered materials. Terao et al. (63) and Maciel et al. (64) have used two-dimensional methods to spread the powder patterns of each chemically nonequivalent carbon in the F_2 direction. Depending upon their respective isotropic shifts, overlapping in these 2D experiments is either eliminated or at least alleviated when compared with one-dimensional spectra. The dispersion of spectra into two dimensions is accomplished by changing the orientation of the spinning axes during the evolution period of a typical 2D experiment. This technique requires samples with long relaxation times in the rotating frame, $T_{1\rho}$, to preserve the magnetization during the mechanical reorientation of the sample, which may take from 300 ms to 2 s. Very few applications of these techniques have been reported in the literature, but as these features become available in commercial solid state probes, it is expected that an increase in the number of applications might materialize.

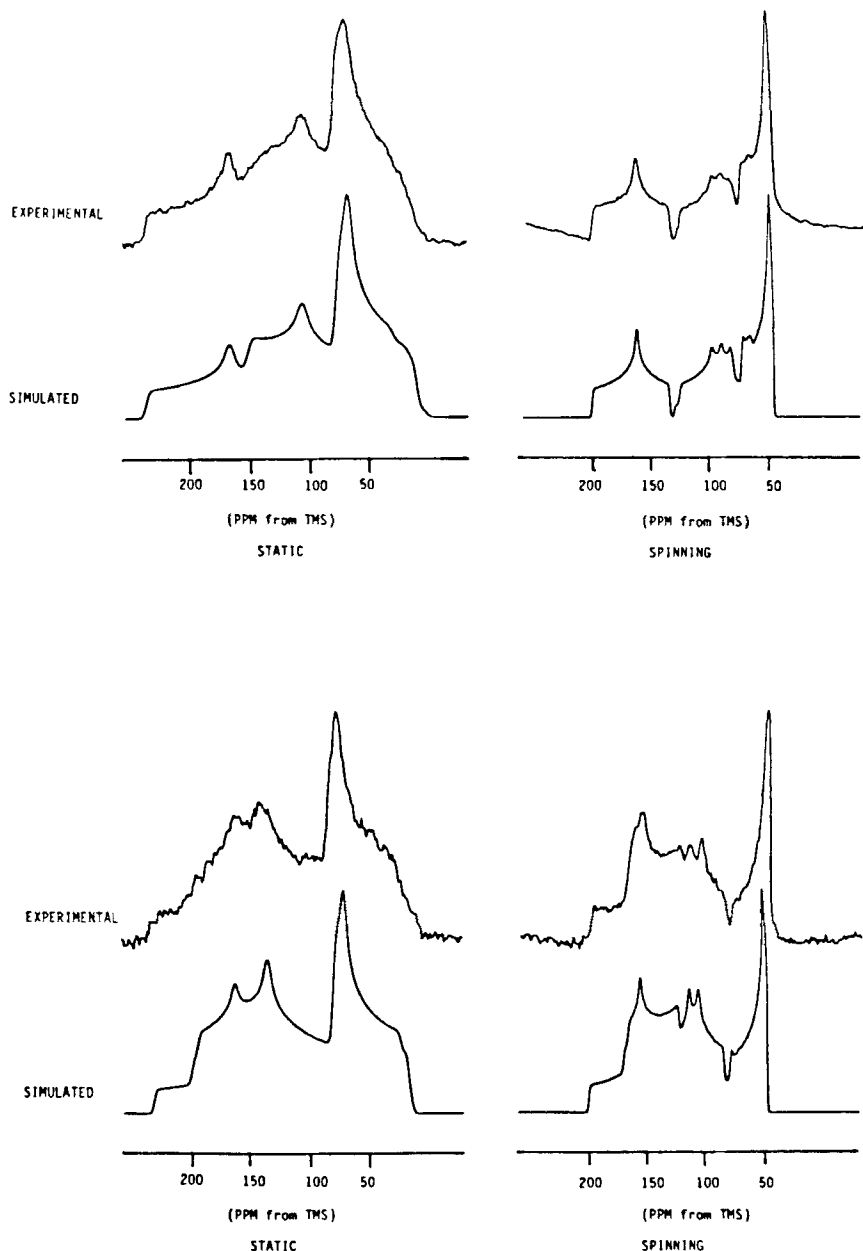


Figure 5. Simulated and experimental spectra of 1,3,5-trimethoxybenzene (top) and *p*-dimethoxybenzene (bottom). Comparison of the static spectra and the off-magic angle spinning spectra.

A two-dimensional experiment separating the side bands originating from different carbons has been proposed by Aue et al. (65). These investigators accomplished the separation by synchronizing the data acquisition with the rotational echoes of the slow MAS spectra; in this way the side band patterns of different carbons are sorted in the F_1 direction by their respective isotropic chemical shifts.

Dipolar spectroscopy (56, 57, 58) can be used to obtain information on the orientation of the principal components of the shielding tensor by studying the coupling between an abundant spin (e.g. ^{19}F , ^{14}N , etc.) with ^{13}C at natural abundance or between ^{13}C - ^{13}C in dilabeled compounds. The labeling with ^{13}C further serves to increase the S/N of the spectrum. These methods, however, tend to require higher quality spectra in order to achieve the desired accuracy in the fitting procedures. The use of dilabeled ^{13}C materials (56, 58) allows the shielding principal axes to be specified with respect to the ^{13}C - ^{13}C dipolar axis. Dilution of the compound in an inert matrix reduces intermolecular ^{13}C - ^{13}C interactions and helps to sharpen the spectra. High quality spectra assist in obtaining better information on the orientation of the shielding tensors. When possible it is convenient to obtain the principal shift values in an independent way by using either singly labelled or natural abundance materials. As in the case of simple shielding powder patterns the spectra parameters: shift components, relative orientation in the dipolar frame, dipolar constant, and broadening functions, can be obtained by fitting the experimental spectra using techniques similar to those described above (59).

A two-dimensional technique using the ^{13}C - ^1H dipolar coupling has been proposed (66) to measure the orientation of the ^{13}C shift tensor relative to the ^{13}C - ^1H dipolar axes. This experiment uses a standard CP preparation sequence to polarize the ^{13}C spins followed by an evolution time with the ^1H decoupler off-resonance such that the effective field in the rotating frame is at a magic angle with the external magnetic field. This eliminates the ^1H - ^1H dipolar interactions during the evolution periods, and the detection is done under ^1H high power decoupling. In this experiment, the dipolar coupling is projected on the F_1 axes (i.e. cuts at constant ω_2 give Pake doublets for different shielding values), and the shielding powder pattern is obtained by the projection on the F_2 axis. Examples in the case of benzene at 148°K are given in Figure 6. By simulation and comparison with the experiment it is possible to obtain the relative orientation of the shielding tensor in the C-H dipolar frame. The information content of the 2D spectra is the same as in the one dimensional dipolar spectra, but the 2D case is more sensitive for determining the relative orientations of the PAS for the various interactions affecting the spectrum.

Unfortunately, fitting dipolar spectra can be complicated by deviations from an ideal spectral response arising from molecular librations (57, 67, 68)

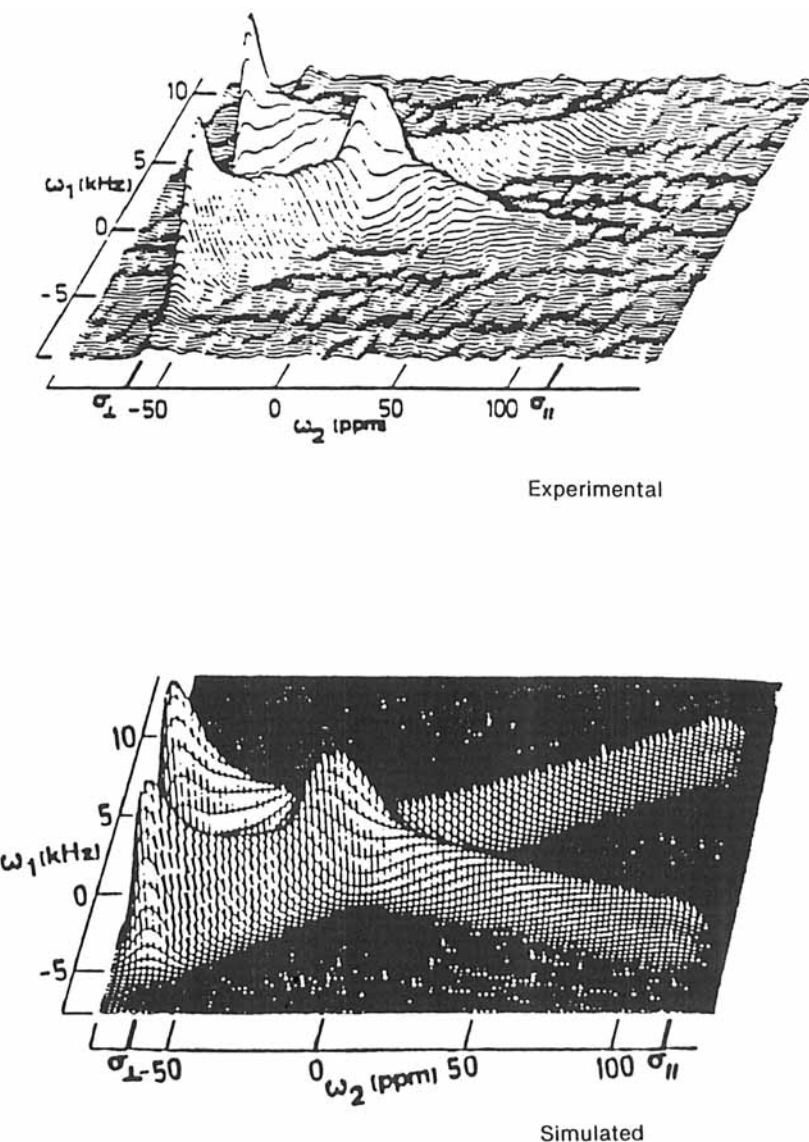


Figure 6. 2D dipolar spectra of benzene at 148 K. The ω_2 axes represent the chemical shielding and the ω_1 the dipolar interaction. Upper figure: Experimental spectrum. Lower figure: Simulated spectrum. The simulated spectrum has been generated using $\sigma_{\perp} = -63$ ppm, $\sigma_{\parallel} = 117$ ppm, $D_{\parallel}(C-H) = 11,660$ Hz and $D_{\parallel}(C-C-H) = 1520$ Hz. From ref. 66 with permission.

and from non-secular contributions to the relaxation (69). These phenomena add to the complexity of the dipolar patterns, and care must be taken to account properly for their perturbation of the spectral response before extracting a set of spectral parameters. Motional breaking of the dipolar symmetry (57, 67, 68) requires more complex physical models to interpret the spectral patterns, and these additional fitting parameters may reduce the accuracy in the determination of the shielding values and the orientation of PAS in the molecular frame.

D. Other Methods for Determining ^{13}C Shift Tensors

The use of liquid crystals for determining chemical shift anisotropies provides an alternative to solid state NMR techniques. Molecules dissolved in a liquid crystal solution are preferentially oriented, and this allows one to extract some information on the anisotropy of the shift tensor. This technique was reviewed (70) in 1982 and some improvements and applications to ^{13}C shielding tensors were provided in later work (71). Serious variations in the chemical shift arising from solvent and susceptibility effects preclude this method from achieving universal acceptance. The serious discrepancies found between the liquid crystal results and those obtained by solid state NMR are also an indication of difficulties encountered in liquid crystal experiments (72).

Finally we should note that the measurement of the paramagnetic contribution to the shielding anisotropy in the molecule's center of mass can be effected in small, highly symmetric molecules using molecular beam techniques (73). These results relate NMR and molecular beams in a very interesting manner, but such an approach is unlikely to provide extensive information on the chemical shift anisotropy in more than a very limited number of molecular systems.

IV. CONFORMATIONAL EFFECTS IN SOLIDS

A. CP/MAS Examples in Organic Molecules

As discussed in the introduction, MAS spectra may at times contain more structural information than found in liquid or solution NMR spectra. This is a consequence of freezing the molecular conformations in the solid state. In this section we discuss briefly several relevant conformational studies which use MAS techniques, and appropriate references of comprehensive reviews on the subject are cited.

Extensive reviews on the application of CP/MAS to conformational studies have been published recently (8, 74). The topics covered by the Saito review

(8) focus on CP/MAS applications to polymeric systems including polysaccharides, polypeptides, proteins, and synthetic polymers. The difficulty in obtaining either single crystals or solutions for these polymeric materials explains in part the attractiveness of the CP/MAS approach. The review by Terao and Inashiro (74) focuses on smaller organic molecules and also includes conformational applications of relaxation measurements in the solid state. Unfortunately, CP/MAS applications using model organic compounds have been limited in scope and as yet do not provide much of a framework for this type of study. Thus, researchers often have to depend on theoretical formulations as a way to develop a basis for interpreting the conformational information found in the limited amount of chemical shielding data and for directing future experimental efforts. A series of calculations of conformational effects in some structural moieties will be presented in the next section.

Another significant difference between CP/MAS and solution spectra originates in intermolecular interactions arising from crystal packing forces which break the symmetry of chemically equivalent groups in the unit cell. For example, in 2,4-dinitrotoluene (49) a doublet with a 3 ppm splitting is found in the CP/MAS spectra of two otherwise chemically equivalent methyl groups which are crystallographically non-equivalent in the unit cell. Packing effects in several anti-inflammatory steroids have been reported in a recent thesis (75). Unfortunately, the interpretation of these splittings is only partially understood.

It is important to alert the reader that rather severe assignment problems are routinely encountered in solids. In many cases the assignments may be made by comparing the solid state shifts with assigned liquid phase shifts, but this approach may encounter problems. For example, it is well documented in the case of glucose (76) that isotropic chemical shifts exhibit different rank orderings in the solid and liquid phases. In some cases only specific isotope labeling can resolve the assignment problems in the solid state.

A classical example of conformational freezing in the solid state studied by CP/MAS relates to a study of a series of *p*-alkoxybenzoic acids (77). In Figure 7 the CP/MAS spectra of several *p*-alkoxybenzoic acids are shown, and the chemical shifts for their ring carbons are given in Table 1. A difference of 6 to 9 ppm between the chemical shifts of C₃ and C₅, the carbons *ortho* to the alkoxy group, is observed for the three compounds because the alkoxy group is frozen in one of two possible planar conformations. In solution the alkoxy groups flip back and forth between the two planar conformations rapidly on the NMR time scale, and the C₃ and C₅ peaks average into a single signal with a shift value that is very close to the average of the shift of the two *ortho* carbons in the solid. In the case of *p*-butoxybenzoic acid there are more splittings than those described above, and the additional break in symmetry has

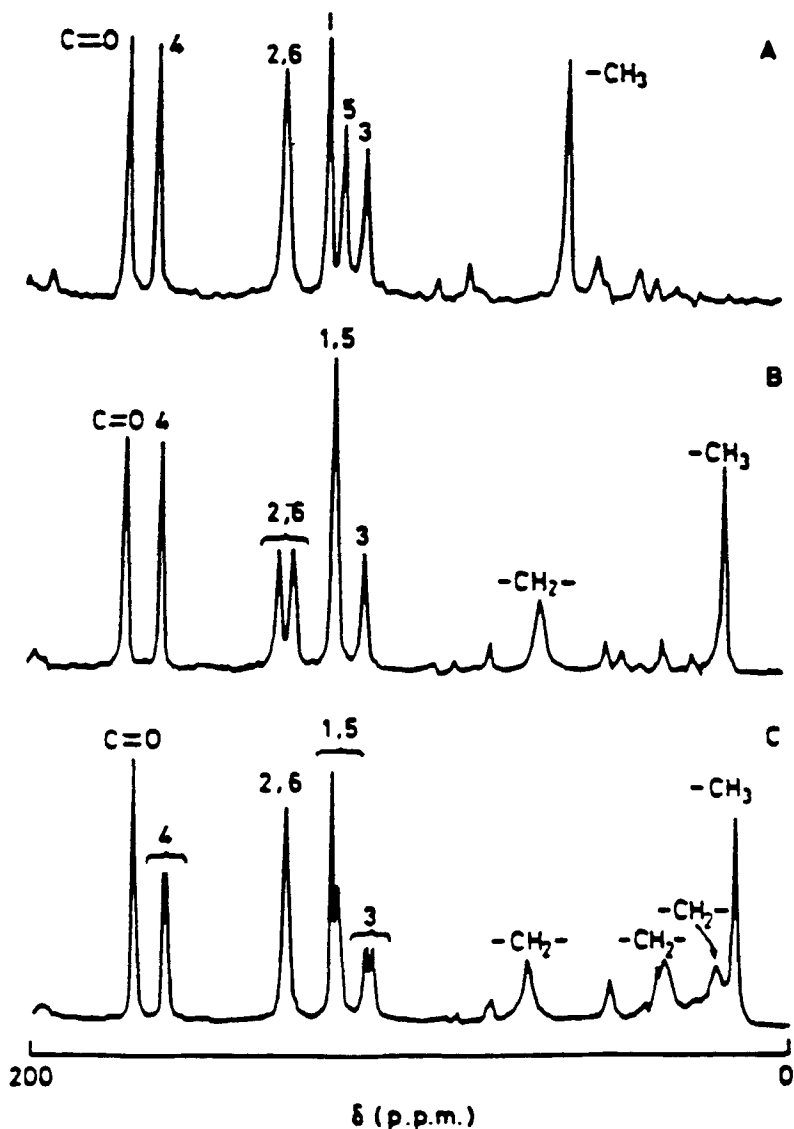


Figure 7. ^{13}C solid-state NMR spectra of *p*-alkoxybenzoic acids. For assignments see Table 1. Smaller unidentified peaks are spinning side bands. A) *p*-methoxybenzoic acid; B) *p*-ethoxybenzoic acid; C) *p*-butoxybenzoic acid. From ref. 77 with permission.

Table 1
¹³C Chemical Shift of the Aromatic Carbons in *p*-Alkoxybenzoic Acids^a

Substituent	C ₁	C ₂	C ₆	C ₃	C ₅	C ₄	
Me	120.4 (124.5)		131.9 (133.3)		110.7 (115.4)	116.2	165.4 (164.2)
Et		119.2 (124.1)	133.9 (132.6)	130.1	112.2 (115.5)	119.2	164.7 (163.1)
Bu		121.1 (123.8)		133.3 (132.3)	112.0 110.3 (115.1)	121.1 119.4	165.5 164.4 (163.3)

^aValues from ref. 77. All values in ppm from TMS; values in parentheses correspond to measurements in solution. Note that recent work in single crystals of polysubstituted methoxybenzenes (54) and in *ortho*-substituted benzenes (78) suggests that the assignments of the *ortho* carbons should be reversed.

been attributed to the crystallographic packing of molecules in the unit cell. However, the assignments of C₃ and C₅ given in the early work (77) may be in error in view of recent results on methoxybenzenes (54, 78). A doubling of the resonance lines is observed for the C₂ resonance in *p*-ethoxybenzoic acid, and this has been explained (77) by the presence of two conformers caused by a rotation of 180° about the C_{ipso}-CO₂H bond. These features, known from X-ray studies, are supported by the NMR results which confirm the existence of a disordered phase. A more complete discussion of the effect of the methoxy groups on the chemical shift of the *ortho* carbons is given below where the ¹³C shielding tensors of methoxybenzenes are discussed.

B. ¹³C Shielding Tensors and Molecular Structure

The use of chemical shielding tensors in conformational analysis is a field which is in its infancy. Only a handful of papers by a few researchers have been devoted to this topic. It is clear from these limited results, however, that NMR is an extremely powerful technique for studying conformational features in solid materials, especially those for which single crystals are not available to provide X-ray data.

One of the disadvantages of MAS techniques is that conformational effects upon the isotropic shifts, usually in the order of 3–10 ppm, are not easily determined by MAS owing to low resolution of solid state NMR signals (79). In this section we will show that the conformational effects can often be amplified in the tensor shielding components, and, even more important, that the conformational perturbations affect specific shielding components in

quite different ways. As mentioned above it is quite difficult to make assignments of some CP/MAS spectra where the shift tensors exhibit very similar isotropic values. Even peaks with similar principal tensor values but different orientations in the unit cell cannot be resolved in a CP/MAS spectrum, but they will separate nicely in a single crystal experiment. Therefore, the use of the full tensor not only can provide better information on the relationship between shielding and molecular structure, but also can alleviate the assignment problems encountered in solid state NMR. Several examples of the relationship between molecular structure and shielding tensors are presented in the following subsections. Examples from our laboratory along with others from the literature represent an extensive review of the subject through the summer of 1988. We emphasize the importance of theoretical considerations which in this early phase can be also very helpful as a method for assigning ^{13}C shielding tensors and for giving a conceptual basis to this emerging field.

1. *The γ -Effect and ^{13}C Shielding Tensors in cis- and trans-2-Butenes*

Until now the most common conformational effects observed in both liquids and solids are those originating from the proximity of γ structural groups (2-5). This effect in liquids has been rationalized with a steric model (3), but until recently no detailed information on the tensor basis of this γ effect has been available with which to discuss the phenomenon. The γ effect on the liquid phase ^{13}C chemical shift of *cis*- and *trans*-butenes has been known for many years, but the ^{13}C powder spectra of *cis*- and *trans*-butenes have been obtained (37, 80) only recently, at low temperature ($< 20\text{K}$). The experimental and calculated principal shift values for the methyl groups are shown with their respective calculated orientations in Figure 8. The LORG (24) calculation of the ^{13}C shift tensors have been done using the D95* basis set (81), which includes polarization functions on the carbon atoms. Experimental geometries (82, 83) were used in the calculations. It is important to note that the theoretical calculations played a critical role in these studies as the spatial assignments shown in Figure 8 are based solely on the theoretical predictions, in as much as there is no information on the orientation of the principal axes of the shift tensor from the powder spectra. The theoretical assignment of the components in the molecular frame is felt to be justified by the excellent agreement found between the measured and calculated principal shift values.

The ^{13}C shielding components depend in a striking manner upon the positions of the methyl groups in the two isomeric butenes. While the isotropic values of the methyl shielding change only 6-7 ppm from the *trans* to the *cis* conformation, the component perpendicular to the molecular plane of these butenes changes by 21 ppm; the inplane components are almost identical within experimental error. This is perhaps one of the most dramatic examples

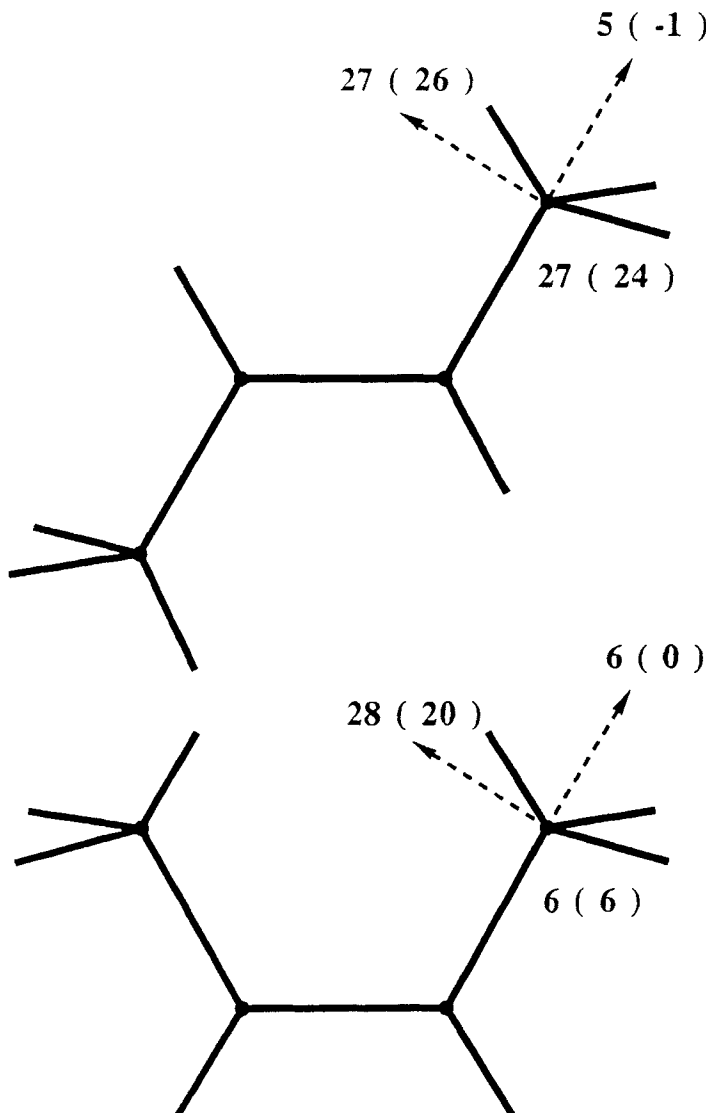


Figure 8. ^{13}C principal shift values placed in the molecular frame according to the LORG calculated results in *cis*- and *trans*-butene. There is one component perpendicular to the plane of the paper in each molecule. The calculated values are given between parenthesis. Calculated values referenced to CH_4 , experimental ones to TMS.

of a specific three-dimensional steric interaction and therefore illustrates the informational importance of shielding tensor components compared with isotropic shift values.

2. *The $^{13}\text{CH}_2$ Shielding in Cycloalkanes, Cycloalkenes, and Heterocycles*

The effect of the CCX angle on $^{13}\text{CH}_2$ shielding tensors in a large number of cycloalkanes, cycloalkenes, and heterocyclic compounds has been reported (41). The directions of the principal components of the shielding tensors for $^{13}\text{CH}_2$ groups is basically dictated by the local symmetry of the $^{13}\text{CH}_2$ group and is affected only to a minor degree by remote or non-local groups. The orientation of the principal axes for the $^{13}\text{CH}_2$ shift tensors is given in Figure 9.

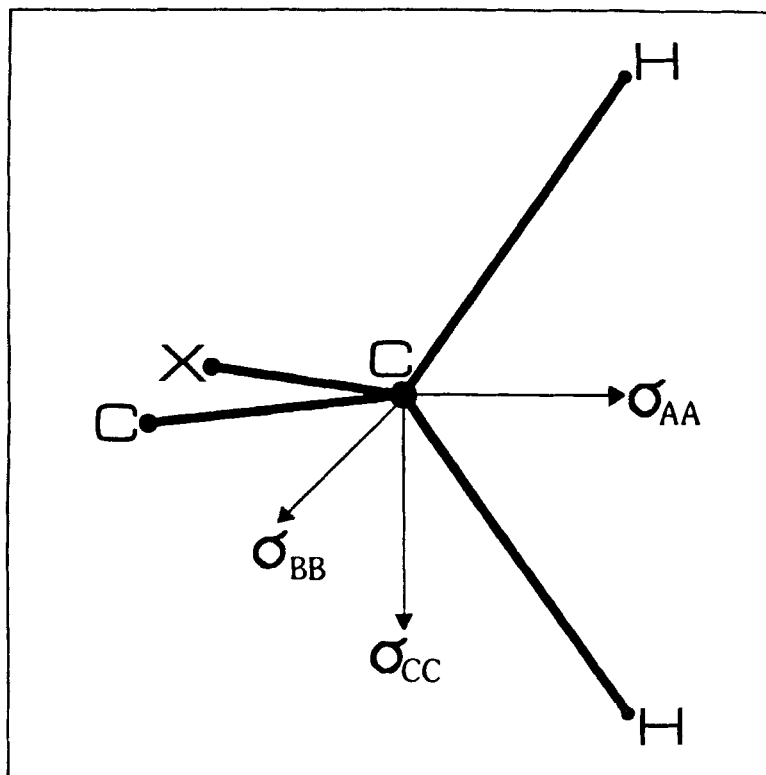


Figure 9. Local symmetry axes for the CH_2 group shielding tensors.

It was found (41) that the σ_{AA} and σ_{BB} components are dominated by electronic effects and show minimal correlation with the CCX angle, but this is not the case for σ_{CC} , the component which aligns approximately perpendicular to the CCX plane. The value of σ_{CC} exhibits a strong dependence on the CCX angle. This component is the most upfield in three-membered ring compounds and the most downfield in four- and five-membered ring compounds as may be observed in Figure 10 for the principal components of the $^{13}\text{CH}_2$ shielding tensors in cyclopropane, cyclobutane, and cyclopentane. In these cases the electronic perturbations are small, and it is observed that σ_{AA} and σ_{BB} are almost constant, with ranges of 2 ppm and 10 ppm, respectively. Conversely, the range for σ_{CC} is 85 ppm, changing from -36 ppm in cyclopropane to +49 ppm in cyclopentane. From this example it is apparent that the sensitivity of the different shielding components upon the conformational structure is much larger than the sensitivity exhibited by the isotropic shifts. The downfield shift of 31 ppm in the isotropic shift values observed in this series of compounds almost entirely resides in σ_{CC} which lies perpendicular to the CCC plane. This example illustrates how a shielding component can be used to characterize molecular geometry in compounds not easily studied by other techniques. Highly reactive compounds, isolated in an inert gas matrix, can be studied by these methods where the more traditional techniques such as X-ray or neutron diffraction may be impractical.

3. Tautomerism of Valence Structures in Cyclobutadiene

Recently a combination of the shielding tensor measurements with dipolar spectroscopy and theoretical calculations has been used to establish the structure of cyclobutadiene at low temperature (42). This application of low temperature NMR solid state techniques to structural analysis in highly reactive compounds deserves attention because the method promises to be one of the premier tools for structural and conformational analysis in such compounds.

The interconversion between valence tautomers of cyclobutadiene has been the subject of several studies (84, 85, 86) but previous experiments have failed to resolve all of the critical issues. In a recent letter Orendt et al. (42) have reported the NMR spectra of 1,2-[$^{13}\text{C}_2$]-cyclobutadiene, which is stable only when isolated at low temperatures (84), in an inert matrix such as solid argon. The NMR results provided definite evidence of the interconversion between equivalent tautomers. In Figure 11 the experimental spectrum is compared with simulations using ^{13}C shift values obtained from IGLO (23) calculations employing an optimized geometry for cyclobutadiene (87). It is clear from this figure that the simulation labeled C, which corresponds to a molecule which is non-rotating and rapidly interconverting between 1A and 1B (see Fig. 12), is the closest to the experimental spectrum. The combination of

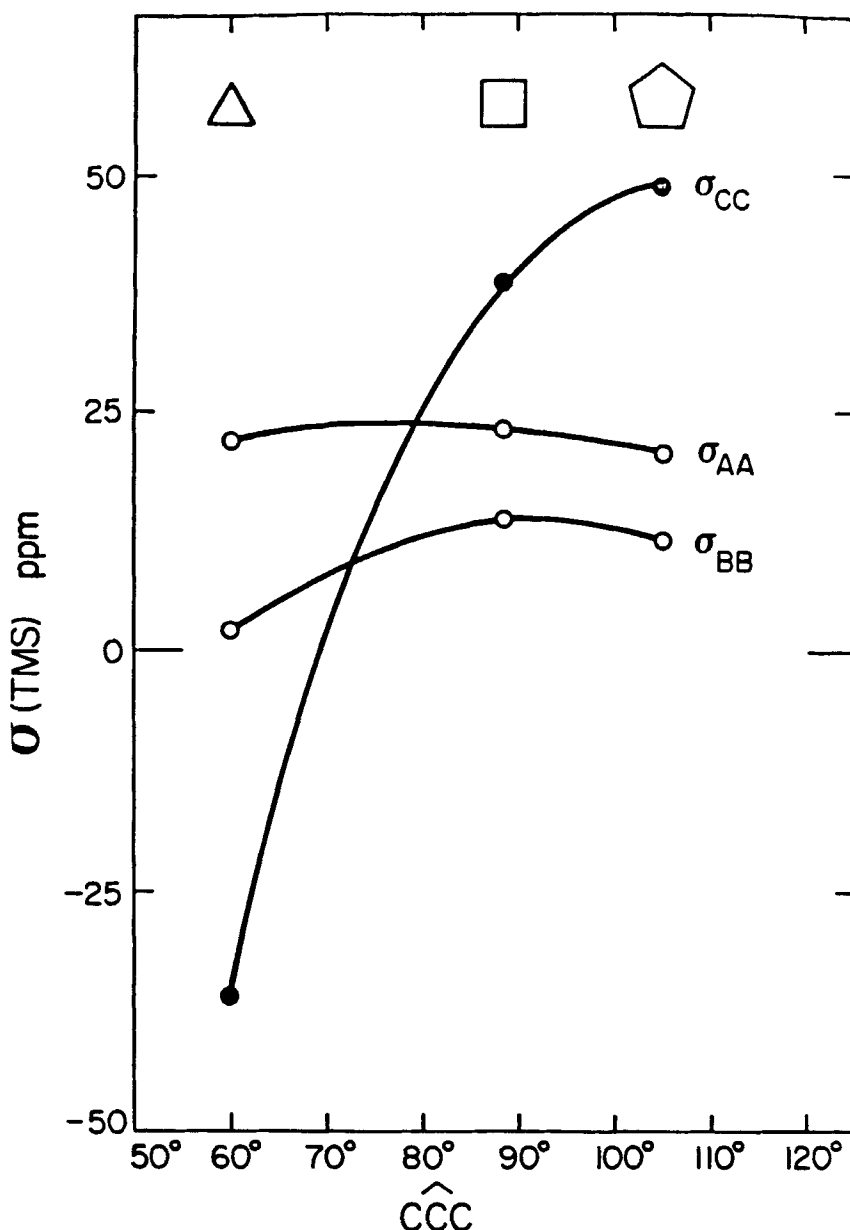


Figure 10. ^{13}C shielding components shown as a function of the CCC angle in cyclopropane, cyclobutane and cyclopentane. The orientation of σ_{AA} , σ_{BB} , and σ_{CC} is shown in Figure 9.

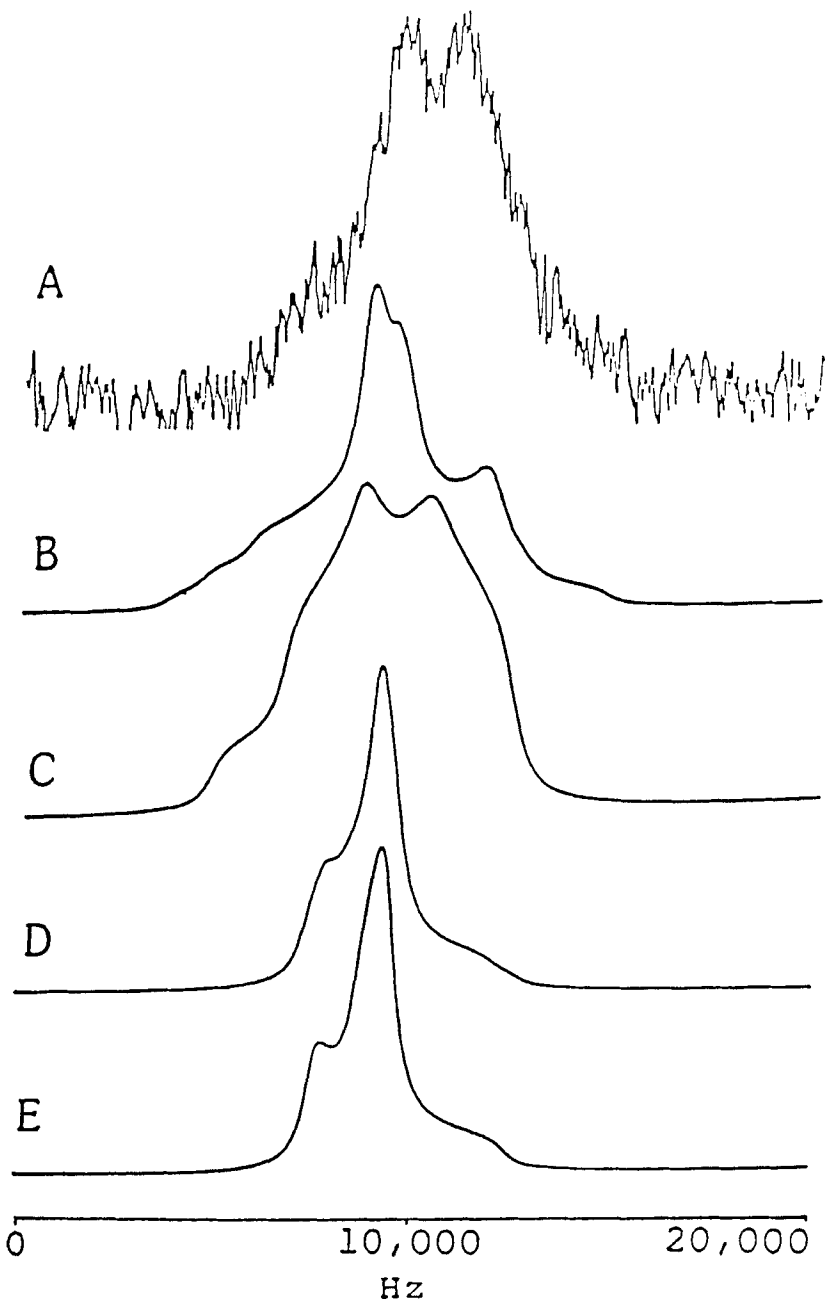


Figure 11. (A) Observed ^{13}C NMR spectrum of 1,2-[$^{13}\text{C}_2$]-cyclobutadiene. (B) Simulated spectrum for a static 1:1 mixture of 1A and 1B (Fig. 12). (C) Non-rotating species, rapidly interconverting between 1A and 1B. (D) 1:1 Mixture, rapidly rotating species, noninterconverting between 1A and 1B. (E) Rapidly rotating species rapidly interconverting between 1A and 1B.

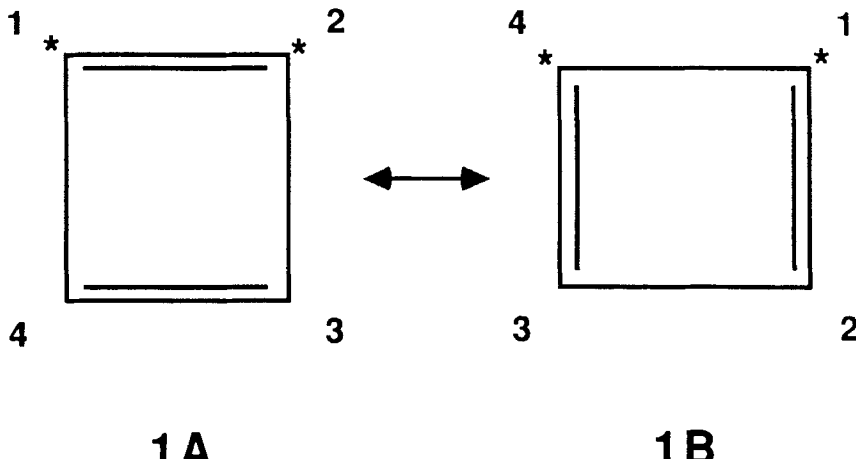


Figure 12. Valence tautomers of 1,2-[$^{13}\text{C}_2$] cyclobutadiene.

theoretical methods used for the calculation of the ^{13}C shielding tensors, and of NMR solid state data for a low temperature matrix allows one to solve a significant structural problem. This kind of methodology, which is just emerging, should have tremendous impact on the study of conformational structures of highly reactive species.

4. ^{13}C Shielding Tensors in Hydroxybenzenes

The conformational effect of an OH group on the aromatic shift tensors in β -quinol (1,4-dihydroxybenzene) have been reported by two groups (88, 89) using both the single crystal technique and the slow MAS method. In Table 2 the average results for the shieldings of the carbons *ortho* to the OH group are compared with the IGLO calculated values for dihydroxybenzene. There are no consistent trends that can be observed in Table 2 and the agreement with theory is poor when compared with the results obtained in studies on substituted methoxybenzenes (54). This lack of consistency in the experimental values may be attributed to the polymorphism of the substance as well as to varying conformations of the OH group, arising from the number of nonequivalent molecules in the unit cell. Different molecules in the unit cell are involved in different hydrogen bond situations, and this may, owing to averaging, make the values entered in Table 2 unrepresentative of a single structure. The theoretical results indicate that changes in the conformation of the OH group can have a large effect (up to 20 ppm) on the shielding components of the *ortho* carbons. These preliminary results portend high promise

Table 2
Comparison of Experimental and Theoretical Values of the ^{13}C Shift Principal
Values of the *ortho* carbons in β -quinol

	σ_{11}	σ_{22}	σ_{33}
C_2 (cis to OH)	196 ^a	131 ^a	19 ^a
	199 ^b	131 ^b	25 ^b
	219 ^c	123 ^c	15 ^c
C_3 (trans to OH)	200 ^a	134 ^a	20 ^a
	191 ^b	136 ^b	19 ^b
	206 ^c	143 ^c	-1 ^c

^aAverage values from ref. 88; in the α -form, referenced to TMS.

^bAverage values from ref. 89; in the β -form, referenced to TMS.

^cIGLO calculated values in OH-benzene using a double ξ basis set. As the second substituent in β -quinol is in the *meta* position, it will have a very small substituent effect and it is reasonable to compare these values to the experimental ones. Standard geometry was used in the calculations. Calculated values are referenced to CH_4 .

for more detailed studies on the conformational effect of the OH group on the ^{13}C shielding tensors of the *ortho* carbons. Careful studies in molecular systems in which hydrogen bond interactions are carefully taken into account are necessary to establish rules on the influence of the ^{13}C shielding in neighboring *ortho* carbon atoms.

5. Effects of Side Chain Conformation in Substituted Benzenes

Deviations from local symmetry in the aromatic and carboxyl carbon shift tensors in pyromellitic acid dihydrate (PMDH) have been reported (90). The principal values of the shift tensor are given in Table 3 along with the relevant angles which determine the orientation of the principal axes in the molecular frame. The large deviation, 5.2° , from the normal of the benzene ring for the principal axis corresponding to the upfield shielding component of C_1 is much larger than any other deviation measured in substituted benzenes. This has been attributed to the non-coplanarity of the carboxylic groups with the benzene ring (see Figure 13). It is noted in Table 3 that the deviation of the principal axis for the upfield component from the normal to the benzene ring is only 1.9° for the protonated carbons, C_3 , $\text{C}_{3'}$, and 2.2° for C_2 and $\text{C}_{2'}$. Large deviations from the normals to the carbonyl plane are also observed in the σ_{33} axis of the carboxylic carbon shielding tensors. It is apparent from Table 3 that the orientation of the upfield, σ_{33} , shielding components of both the aromatic and the carboxylic carbons are sensitive to the orientation of the

Table 3
Principal Shift Values and Their Orientation in Pyromellitic Acid Dihydrate^a

	Principal Value	Angle	With direction
C ₁	30.6	5.2°	Ring normal
	155.6		
	221.6	5.2°	C(1)-C(4)
C ₂	29.4	2.2°	Ring normal
	163.2		
	232.6	4.2°	C(2)-C(5)
C ₃	11.5	1.9°	Ring normal
	171.2		
	216.7	3.5°	C(3)-H(1)
C ₄	106.6	4.3°	Carboxyl group normal
	162.4	4.8°	C(4)-O(2)
	247.0		
C ₅	105.0	4.9°	Carboxyl group normal
	168.5	4.4°	C(5)-O(4)
	263.0		

^aShift values in ppm from TMS taken from ref. 90. Numbering according to Figure 13.

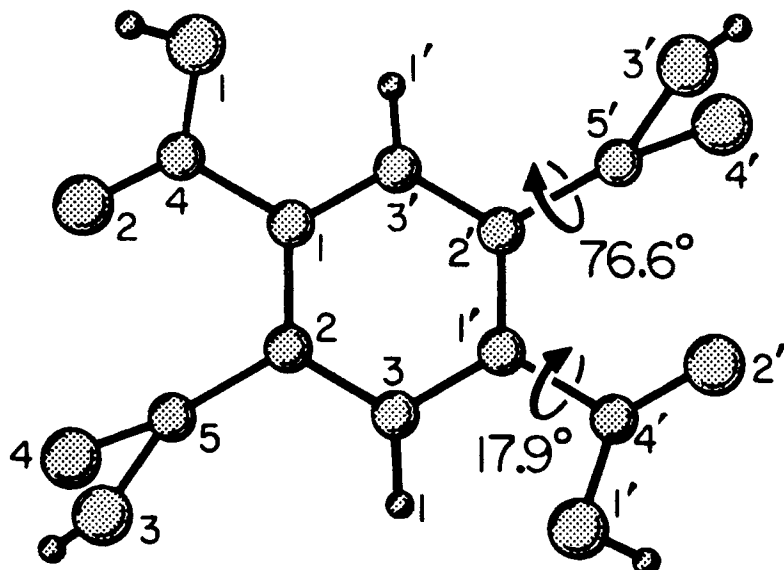


Figure 13. Numbering of carbons in pyromellitic acid dihydrate. From ref. 90, with permission.

carboxylic group with respect to the benzene plane in this type of molecule. Systematic studies in comparable molecules as well as theoretical calculations are needed in order to establish quantitative relationships which can be used to correlate NMR tensorial information with the conformational angle between two sp^2 carbons directly bonded to each other.

Side chain conformational effects on the aromatic chemical shift tensors in acetophenone (see Figure 14) have been studied using single crystal methods (91) at -170°C , and Table 4 contains the principal values of the ^{13}C shift tensors for the aromatic carbons. There are several conformational effects that are apparent from the data in Table 4. At such low temperatures the

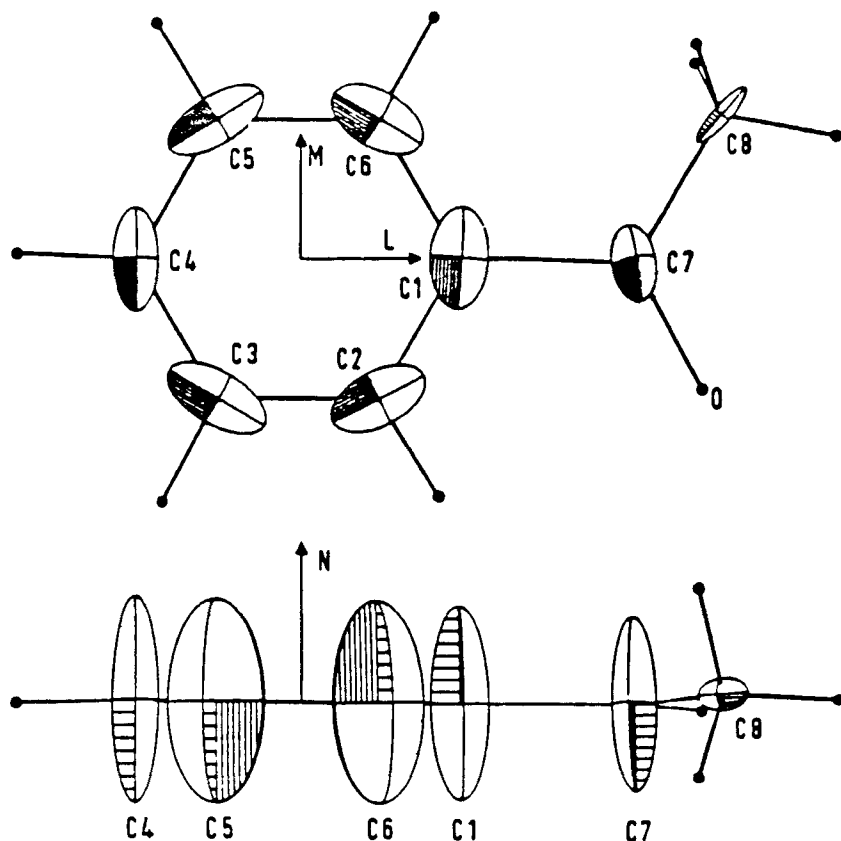


Figure 14. Representation of the ^{13}C chemical shielding tensors in acetophenone. The length of each ellipsoid axis is proportional to the shielding in that direction relative to a reference which is different for every type of carbon atom and it is defined by $\sigma_{ref} = \sigma_{11} - 1/3(\sigma_{33} - \sigma_{11})$. The size of each ellipsoid is a measure of the anisotropy of the corresponding tensor. The methyl tensor is magnified by a factor of 2. Reproduced with permission from ref. 91.

Table 4
 ^{13}C Chemical Shift Principal Values of the Aromatic Carbons in Acetophenone^a

	σ_{11}	σ_{22}	σ_{33}	$\langle\sigma\rangle$	σ_{liq}
C ₁	223.1	157.8	20.0	133.6	136.3
C ₂	227.6	156.6	-2.3	127.3	128.1
C ₃	229.9	144.8	7.7	127.5	128.1
C ₄	240.4	155.5	3.7	133.2	131.3
C ₅	234.6	145.7	6.5	128.9	128.1
C ₆	222.9	157.3	7.0	129.1	128.1

^aAll values in ppm referenced to TMS from ref. 91. Carbon numbering is given in Figure 14.

conformation of the methyl ketone group is frozen and the two *ortho* and the two *meta* carbons lack the equivalence found in the liquid phase spectrum. Modest changes are observed in their isotropic values: thus, C₂ is 1.8 ppm more shielded than C₆ and C₃ is 1.4 ppm more shielded than C₅. In the tensor principal components of the *ortho* carbons, conformational effects as large as 9 ppm are found for σ_{33} , the component perpendicular to the aromatic plane, and -4.7 ppm for σ_{11} , the component which lies approximately along the C-H bond in the *ortho* carbons. The other in-plane component, σ_{22} , perpendicular to the C-H bond shows only a modest 0.7 ppm difference. The small effect on the isotropic value, 1.8 ppm, is clearly explained by a cancellation between the effects on σ_{11} and σ_{33} . When individual shift components exhibit opposite shifts, then significant conformational information is lost in the isotropic shift observed by MAS. The conformational effects on the isotropic value of the *meta* carbons are small; C₃ is 1.4 ppm upfield from C₅. In this case the major contribution arises from σ_{11} , which is displaced by 4.7 ppm upfield from C₅. The steric effect on σ_{33} is, as expected, very small.

A complete study of the conformational effects on the shielding tensors in polysubstituted methoxybenzenes has been published (54). Single crystal studies at room temperature have been reported for 1,4-dimethoxybenzene, (1,4-DMB), 1,3,5-trimethoxybenzene (1,3,5-TMB) and 1,2,3-trimethoxybenzene (1,2,3-TMB). The molecular conformations found in these crystals are shown in Figure 15. The results have been analyzed using substituent effect concepts and *ab initio* calculations of the shielding tensor in the anisole parent. The measured principal values of the shift tensors are given in Table 5, and the multiple linear regression analysis of these experimental data is presented in Table 6, along with the quantum mechanical predictions calcu-

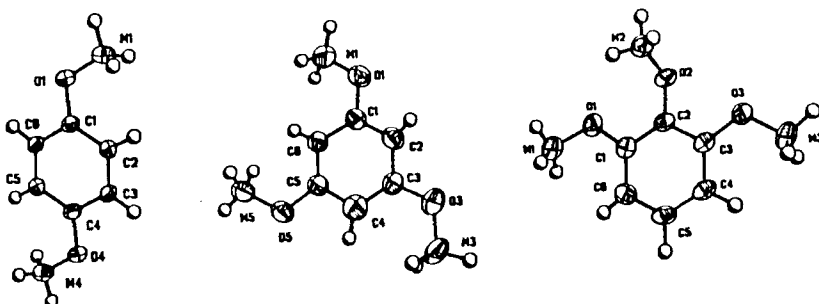


Figure 15. Numbering of carbons in 1,4-dimethoxybenzene, 1,3,5-trimethoxybenzene and 1,2,3-trimethoxybenzene.

lated with the IGLO (23) and LORG (24) methods. From the conformational view point it is important to notice that the so called steric factors have to be included in the correlations in order to take into account the non-equivalence of the two carbons *ortho* to the methoxy group. A -5.9 ppm steric effect is observed in the isotropic value which is in reasonable agreement with the value of -7.55 ppm obtained, by liquid phase NMR, in *ortho* substituted benzenes (78) and values of -9.7 ppm and -10.0 ppm are calculated using the IGLO and LORG methods, respectively. The richness of tensor data is apparent from Table 6, where, as in the case of acetophenone, the steric effect on the shielding of the *ortho* carbons is by no means uniformly distributed among the various principal shielding components. *Ortho* effects range from -11.4 ppm for σ_{33} to -1.9 for σ_{22} . In this case the effect on σ_{11} is of the same sign as for σ_{33} , unlike the trend observed in acetophenone. It is also very important to note, in Table 6, that the electronic substituent effects are not isotropic; for instance, the electronic effect of the methoxy group on the *ipso* carbon varies from -11.3 ppm for σ_{11} to 58.3 ppm for σ_{33} . The mechanisms of the electronic effects on the different components of the shielding tensor have been rationalized using standard arguments based on the theory of electronic substituent effects (54).

The other important conformational feature in the methoxybenzenes which deserves special consideration is found in the shielding tensor of the methyl group at C₂ in 1,2,3-TMB. Though the data in Table 5 for most of the methyl shifts do not exhibit any unusual variations, the C₂ methyl shielding in 1,2,3-TMB is atypical as the result of the two *ortho* methyls at C₁ and C₃ which force the middle CH₃ out of the plane of the benzene ring. The dihedral angle for the C-C-O-CH₃ group is almost perpendicular (75.9°) to the ring whereas most methoxy groups lie in the plane of the aromatic ring and are perturbed only by the *ortho* proton *cis* to the methoxy group. The respective ¹³C shift tensor of Me-2 has principal components of 88 ppm, 88 ppm, and 10

Table 5
**Principal Values of the ^{13}C Chemical Shift Tensors in Polysubstituted
 Methoxybenzenes^a**

Assignment	σ_{11}	σ_{22}	σ_{33}	σ Average
1,4-Dimethoxybenzene				
M1	80	72	13	55
C1	232	159	70	154
C2	200	131	22	118
C3	193	137	6	112
1,3,5-Trimethoxybenzene				
M1	80	69	11	53
M3	80	70	11	54
M5	80	69	9	53
C2	155	108	29	97
C4	152	105	17	91
C6	151	107	1	86
C1	240	168	73	161
C3	238	169	73	160
C5	240	169	74	161
1,2,3-Trimethoxybenzene				
M1	83	71	9	54
M2	88	83	10	60
M3	82	70	13	55
C1	218	172	73	154
C2	179	164	71	138
C3	217	172	72	153
C4	187	123	7	106
C5	227	136	10	124
C6	186	121	8	105

^aAll values in ppm referenced to TMS from ref. 54. Each reported value is average from all the molecules in the unit cell. Numbering according to Figure 15.

ppm. The first two are 8 and 14 ppm downfield, respectively, from those observed in the other methoxy groups in Table 5. The 10 ppm value of σ_{33} is within the experimental range observed in the other compounds. Once again one may see a very specific conformational effect on the components of the shift tensors. While σ_{33} , the shielding component which lies along the O-CH₃

Table 6
Multiple Regressional Substituent Parameters for the Principal Values of the ^{13}C
Chemical Shift Tensors in Methoxybenzenes^{a,b}

Structural Parameters	σ_{11}	σ_{22}	σ_{33}	σ_{iso}
Ipsos	11.3 ± 2.4 (13,13)	30.0 ± 3.3 (23,24)	58.3 ± 3.6 (55,52)	33.2 (30,30)
Ortho	-31.6 ± 1.7 (-30,-27)	-7.7 ± 1.9 (-13,-9)	8.1 ± 2.6 (13,14)	-10.4 (-10,-7)
Meta	-0.2 ± 6 (1,-1)	0.0 ± 2.0 (-2,0)	-4.4 ± 2.4 (+4,2)	-1.5 (1,0)
Para	-9.6 ± 2.6 (-18,-15)	-14.3 ± 3.2 (-11,-8)	-4.2 ± 3.7 (-1,0)	-9.4 (-10,-8)
Steric (ortho-methyl)	-4.5 ± 2.1 (-12,-13)	-1.9 ± 2.9 (-6,-6)	-11.4 ± 3.2 (-11,-11)	-5.9 (-10,-10)

^aAll values in ppm, from ref. 54.

^bTheoretical predictions of the substituent parameters appear in parenthesis below the fitting parameters (IGLO, LORG, respectively). The theoretical parameters have been calculated from work on anisole and benzene.

bond, is unaffected by the out-of-plane conformation of the methoxy group at C_2 , large downfield shifts are observed in the components perpendicular to the $\text{C}-\text{O}$ bond. This anisotropic effect may be explained with the same arguments used for the α -substituent effect in the methyl groups (37).

In Table 7 the $\text{C}-\text{H}$ and $\text{C}-\text{O}$ paramagnetic bond contributions, in the local bond frame (36, 54), are given for the $\text{O}-^{13}\text{CH}_3$ shielding tensors in two types of configurations. A planar and an out-of-plane methyl in anisole are compared with each other and with those of dimethyl ether. Several observations can be made based on these results. In the planar configuration, the relatively large value of $\sigma_{ii}^{\text{CH}} = 5$ ppm for the $\text{C}-\text{H}_{2,3}$ bond indicates a compression of these bonds caused by the *ortho* proton. Also interesting to note is the large value of $\sigma_{ii}^{\text{CH}} = -27$ ppm for the $\text{C}-\text{H}_{2,3}$ bonds, while $\sigma_{ii}^{\text{CH}} = -19$ ppm for the CH_1 bond which is free from steric interactions. This last paramagnetic bond contribution agrees well with those obtained for the out-of-plane methyl at C_2 in 1,2,3-TMB and with those in dimethyl ether. Very small variations are

Table 7
Paramagnetic Bond Contributions to the Methyl Shielding Tensor for Two Conformations of Anisole and Dimethyl Ether^a

	σ_{ii}	σ_{jj}	σ_{kk}
Planar Anisole			
C-H ₁	0.1	-19	-45
C-H _{2,3}	5.0	-27	-38
C-O	0.0	-17	-24
Out-of-Plane Anisole			
C-H ₁	0.1	-18	-52
C-H _{2,3}	0.2	-16	-47
C-O	0.1	-19	-26
Dimethyl ether			
C-H ₁	0.1	-19	-47
C-H _{2,3}	0.2	-17	-41
C-O	0.0	-24	-30

^ai, j, and k are the directions, respectively, along the designated bond, perpendicular to the designated bond in the O-C-H plane, and perpendicular to the O-C-H plane. H₁ is the proton in the C-O-C- plane and H_{2,3} are those out of that plane. All values in ppm. A negative sign in the paramagnetic bond contributions indicates a downfield shift.

observed in the IGLO bond contribution from the C-O bond whether in the in-plane or out-of-plane conformation. The σ_{kk}^{CH} components in the planar form compare well with those calculated for dimethyl ether and other methoxy groups (37), but significant downfield shifts are observed for the σ_{kk}^{CH} contribution calculated for the out-of-plane conformation. This can be rationalized as follows: when the methoxy group is forced out of the plane, the C-O bond is destabilized by the absence of the conjugative interactions between the oxygen lone pairs and the π -electronic structure (92), and the antibonding C-O orbital will have a lower energy in the out-of-plane configuration. As the antibonding orbital has the proper symmetry to be mixed with the occupied C-H orbitals through the angular momentum operator, a downfield shift in σ_{kk}^{CH} is produced in much the same way as noted for more electronegative substituents (37).

6. Conformational Effects of Carbonyl Carbons in Polypeptides

The conformational dependence of carbonyl principal shift values in ^{13}C enriched glycine (Gly^*) has been studied in $(\text{Gly}^*)_n\text{I}$, $(\text{Gly}^*)_n\text{II}$, $(\text{Gly}^*)_5$ and in several co-polymers with Ala, Leu, Glu(OBzl), Asp(OBzl), and Val (93). Standard notation (94) is used for the oligomer structures. The various structures into which the (Gly^*) residue is incorporated induce different conformational and hydrogen bond features in the residue.

The effect of the secondary structure on the principal shift values is a combination of strictly conformational effects (i.e. the change in the torsion angles) and change in the hydrogen bond distances and angles for the different secondary protein structures (94). Experimentally it is not possible to separate these individual effects on the shielding tensors. It is observed in Figure 16 that σ_{11} , the component perpendicular to the $\text{C}=\text{O}$ bond in the $\text{C}-\text{C}=\text{O}$ plane, is not affected by the secondary structure whereas σ_{22} and σ_{33} are markedly affected by the secondary structure of the protein. The values of σ_{22} are dramatically different for the helix conformations relative to the β -sheet conformations. Very few variations are observed for the helix conformations; moreover the value in $(\text{Gly})_n\text{II}$, which has a 3_1 helix, is within experimental error of the σ_{22} values in several α and ω helices. In the case of the polypeptides in the β -sheet conformation a 3 ppm difference, that is outside of the experimental error, is observed between the $(\text{Gly})_n\text{I}$ and $(\text{Val},\text{Gly})_n$. This 3 ppm effect is a consequence of different β -sheet conformations. The component which is perpendicular to the carbonyl plane is also sensitive to the secondary structure. It moves by 6 ppm from $(\text{Gly})_n\text{I}$ to $(\text{Gly})_n\text{II}$. For the compounds with α -helix conformations the σ_{33} value is within experimental error of the value in $(\text{Gly})_n\text{II}$. The value for $(\text{Asp(OBzl}),\text{Gly})_n$, which presents an ω -helix, is also within the experimental error of the value in $(\text{Gly})_n\text{II}$. In this case it is noteworthy that the σ_{33} value in $(\text{Val},\text{Gly})_n$, which is a β -sheet, is not close to the value for $(\text{Gly})_n\text{I}$, the other β -sheet in Figure 16.

While no clear physical interpretation of the changes noted in the shielding tensor principal values in terms of either electronic or structural changes has been given, it is clear that the effects correlate with the changes in the secondary structure. Additional theoretical work may be needed to clarify in detail the electronic mechanisms that produce the experimental results reported above. The same researchers have presented a theoretical analysis of the conformational and hydrogen bond dependence of the isotropic ^{13}C chemical shieldings using the tight-binding MO theory within the CNDO approximation (95) for polypeptides and for model compounds (96) using the FPT-INDO approach. Calculations have not been reported on the behavior of the principal components of the shift tensors.

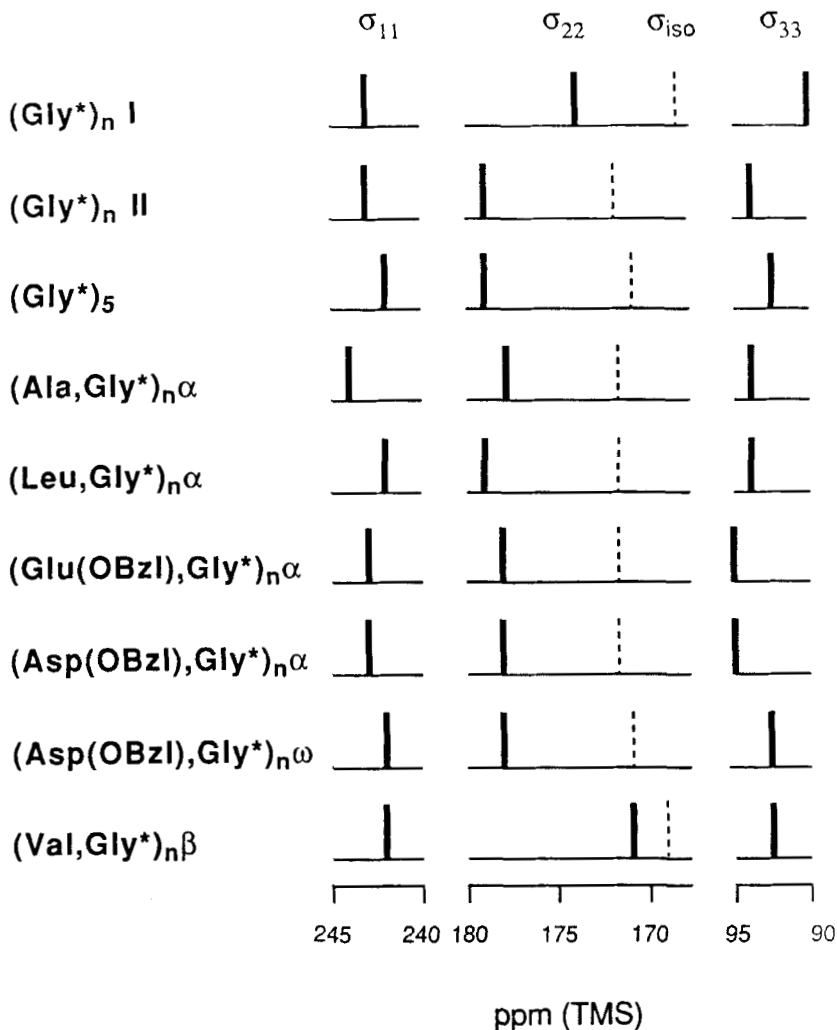


Figure 16. Observed stick spectra of ^{13}C NMR isotropic chemical shifts and tensor principal components of glycine carbonyl carbons of poly [$1-^{13}\text{C}$]-glycine and [$1-^{13}\text{C}$] glycine-containing polypeptide. From ref. (93).

Large conformational effects have been also observed by CP/MAS solid state NMR, for the isotropic shieldings tensor of C_α and C_β in polypeptides (8), but the authors are unaware of any systematic studies—which could prove to be very rewarding—of the conformational behavior of the principal values of shielding tensors for such polypeptides.

7. ^{13}C Shielding Tensors in Retinal Derivatives

Several papers (97–100) have been published on the ^{13}C shift tensors of retinal derivatives and their relationship to the molecular conformation in synthetic materials as well as in membranes. In Figure 17 the ^{13}C principal shift elements of the protonated olefinic carbons of *all-trans*-retinal are shown. The tensors of the olefinic carbons can be divided into two categories, the even-numbered C_8 , C_{10} , C_{12} , and C_{14} with $\sigma_{33} \sim 50\text{--}65$ ppm from TMS and the odd-numbered C_7 and C_{11} with σ_{33} upfield at 30–40 ppm from TMS. The σ_{33} components are of aliphatic character and lie in the direction perpendicular to the plane of the double bond. These odd-even effects on σ_{33} have also been reported in *6-s-trans-all-trans*-retinoic acid and in unprotonated retinal Schiff bases, but they are not observed in *N*-butyl-2,4,6-octatrienylidine-imine. Therefore, the odd-even effect has been attributed to the methyl substitution of the polyene chain and reported to be independent of the functional group at C_{15} . Harbison and coworkers (98) have attributed these alternations to the γ effect of the proximate methyl groups. The ^{13}C shift tensors of several retinal derivatives and related compounds are shown in Table 8. It is apparent that the variations in the individual components are much larger than those in the isotropic values. Theoretical and additional experimental work on model compounds would still be beneficial for a full understanding of the relationship between the ^{13}C shift principal components and the molecular structure.

The effect of the *cis-trans* isomerization of the carbonyl group in retinal is shown in Figure 18, where the principal shift values are compared at C-12 for *all-trans* and for *13-cis* retinal. It is observed that the in-plane components, σ_{11} and σ_{22} , are barely affected by the change in conformation while σ_{33} is moved upfield by 16.2 ppm in the *cis* compound. The change of 6 ppm in the isotropic values, therefore, originates almost totally in the component perpendicular to the double bond. Similar results have been reported for *cis*- and *trans*-polyacetylenes (101). This steric effect is usually observed in the shielding component perpendicular to the plane in which there is high molecular strain owing to the steric repulsion of the hydrogens.

In Figure 19 the ^{13}C principal chemical shift values for C_5 in *6-s-trans* and *6-s-cis* retinoic acid are presented. In these molecules all of the changes upon isomerization are observed in σ_{11} , the component that lies approximately perpendicular to the double bond in the CCC plane. The change in one of the in-plane components of the shielding has been attributed to the disruption of the conjugative effects between the $\text{C}_5\text{-C}_6$ double bond and the rest of the chain, making the $\text{C}_5\text{-C}_6$ bond a rather more isolated double bond and reducing, in part, the delocalization of its π electrons into the polyene chain. This argument is supported by the large angle, $40\text{--}65^\circ$, found in the *6-s-cis* conforma-

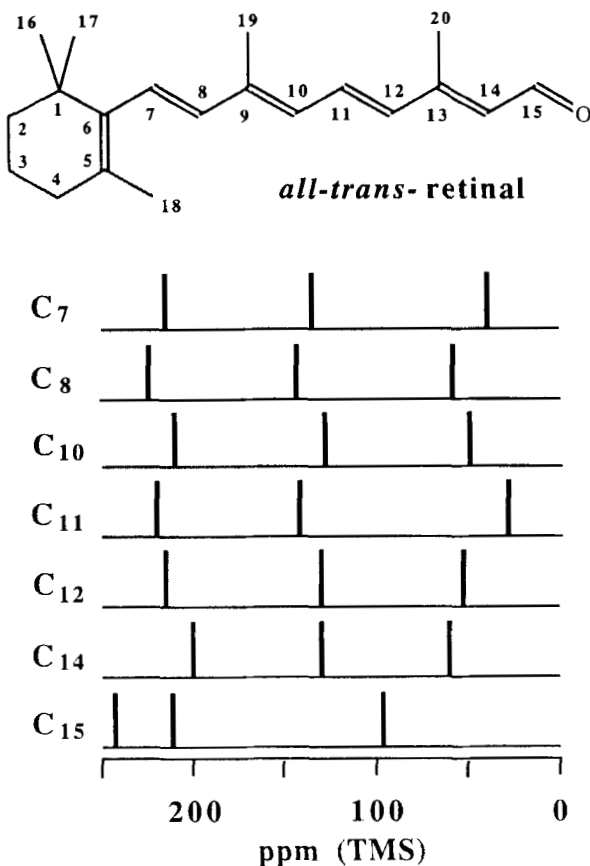


Figure 17. ^{13}C chemical shift tensor principal values for the protonated olefinic carbons of *all-trans*-retinal obtained from the sideband intensities of spectra of labeled and unlabeled retinal by the method of Herzfeld and Berger (60). From ref. 98.

tion, between the cyclohexane ring and the conjugated chain. In the *s-trans* structure the conformation is almost planar owing to the high degree of conjugation between the C₅-C₆ bond and the side chain. The conformational dependence of the principal shift values in retinal derivatives and related compounds have been used to analyze the results in ^{13}C -5-bacteriorhodopsin (bR) in membranes (97). Also in Fig. 19, the principal shift values in ^{13}C -5-bR are compared with those of 6-*s-trans* and 6-*s-cis*-retinoic acids. It is apparent that

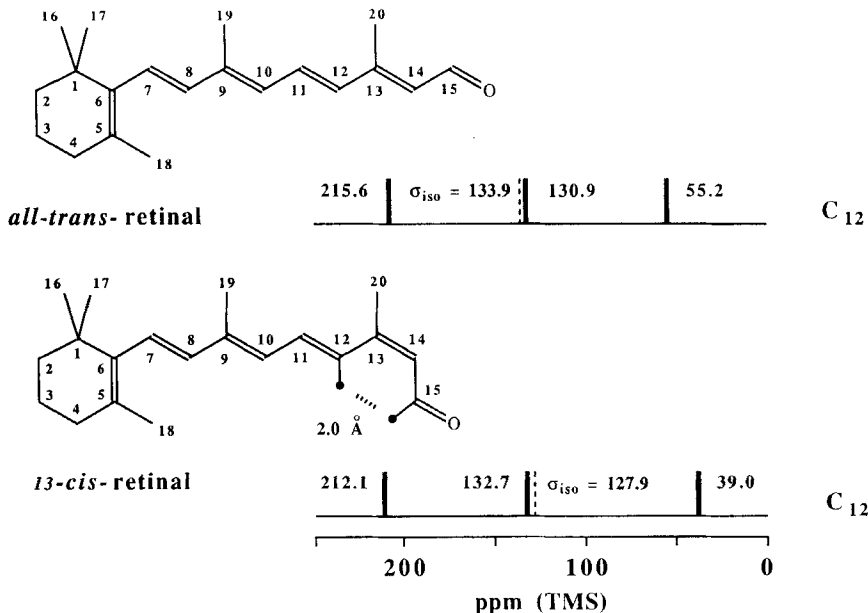


Figure 18. Chemical shift tensor principal values for the C-12 resonance of *all-trans* and 13-*cis* retinal showing the effect of the steric interaction on σ_{33} . From ref. 98. The nomenclature of the principal values has been changed to follow the rank order notation used in this review.

bacteriorhodopsin is found in a *trans* conformation as revealed by the large downfield shift of σ_{11} with respect to the *cis* compound. The large downfield shift observed in σ_{22} has been attributed to the presence of an adjacent negative charge. The authors (97) reinforce their arguments for the *trans* conformation in ^{13}C -S-5-bR by using other supporting information such as the isotropic shielding of other carbons in the polyene chain. This is a clear example of the importance of using the full tensorial information to elucidate the detailed conformations which are found in very complex molecular systems. Certainly the difficulty of using labeled materials is compensated in large measure by the rich return in information. This study also points out the need for considerable additional work on model compounds in order to establish appropriate relationship between the shielding tensor elements and molecular conformation.

C. Crystal Packing Effects on Chemical Shielding Tensors

Very little is known about the crystal packing effects on the ^{13}C shielding tensors. The two kinds of perturbations arising from crystal packing forces

Table 8
Chemical Shift Tensors in Olefinic Carbons of Retinal Derivatives and Related Compounds^a

Position	σ_{11}	σ_{22}	σ_{33}	$\langle \sigma_{iso} \rangle$
<i>all-trans</i> -Retinal				
5	215.9	141.1	30.9	129.3
6	230.4	141.5	51.0	141.0
7	213.8	134.5	38.8	129.0
8	224.2	144.4	59.2	142.6
9	228.0	168.5	32.7	143.1
10	211.2	129.7	50.2	130.4
11	220.0	142.2	29.3	130.5
12	215.6	130.9	55.2	133.9
13	249.9	187.6	31.2	156.2
14	200.7	131.0	60.9	130.9
Unprotonated Retinal Schiff Bases				
5	202.2	143.2	33.0	126.1
6	235.5	134.6	41.7	137.3
7	214.9	131.6	30.3	125.6
8	224.1	132.2	62.7	139.7
9	221.7	155.4	30.3	135.8
10	207.6	127.3	61.4	132.1
11	213.3	136.6	28.8	126.2
12	210.1	130.1	67.0	135.7
13	237.0	165.8	28.7	143.8
14	204.9	124.7	63.9	131.2
<i>6-s-trans-all-trans</i> -Retinoic Acid				
5	234.9	143.1	28.1	135.4
7	225.6	132.8	34.3	130.9
9	235.2	159.7	24.3	139.7
13	257.0	183.3	25.9	155.4
14	211.8	104.3	51.2	122.4

Table 8 (cont.)

N-Butyl-2,4,6-octatrienylidineimine

1	245.9	168.9	78.8	164.5
2	207.6	128.2	61.8	132.5
3	230.9	131.1	61.6	141.2
4	202.9	141.2	54.8	133.0
5	217.4	132.2	65.0	138.2
6	209.3	134.9	57.8	134.0
7	225.0	131.6	49.2	135.3

^aAll values in ppm from TMS. Numbering according to Figure 17. Values from refs. 97-100.

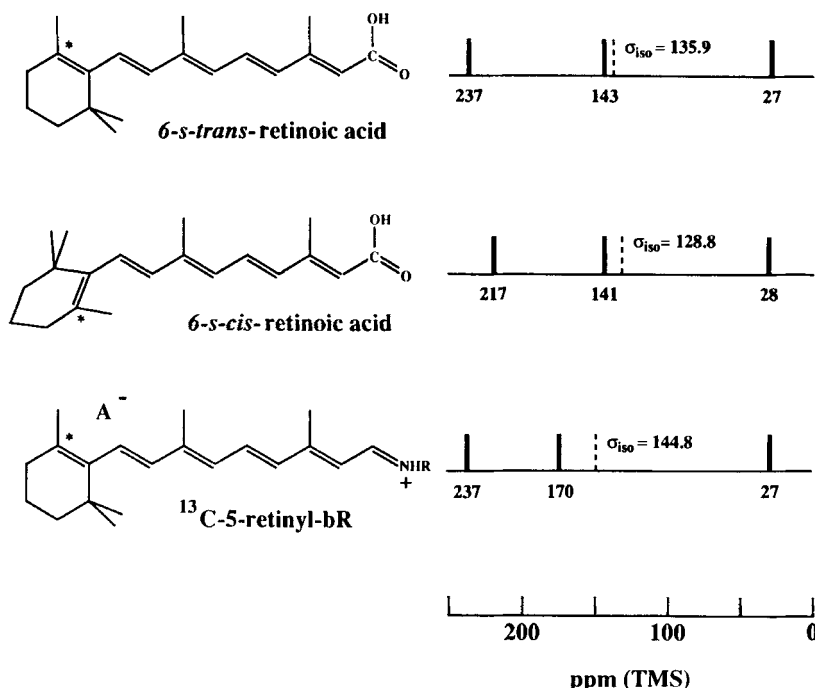


Figure 19. Chemical shielding tensors of hydrated ¹³C-5-labeled retinyl-bR compared with those of ¹³C-5 carbons in 6-s-cis (triclinic) and 6-s-trans (monoclinic) retinoic acid. The position of A⁻ is arbitrary. The 6-s-cis conformer is shown in a skewed conformation. From ref. 99.

which could affect the shielding are: first, changes in the electronic structure caused by the proximity of other molecules, and second, deformations of the molecular geometry from intermolecular crystal packing forces. The first effect is basically a van der Waals polarization of the electronic cloud and to a first approximation would be comparable to the solvent effects observed by NMR on liquids or gases. The second possible effect arises from changes in the molecular geometry in the crystalline environment which may be significantly different from the geometry in the gas phase as a result of packing interactions. In some cases, even the molecular symmetry in the crystal can be altered and the ^{13}C shift tensors affected accordingly. From the experimental perspective, it is not possible to discriminate between the two types of effects because they are indistinguishable in the solid state NMR data. Fortunately, these question can be addressed using theoretical calculations on molecules with distorted geometries and on clusters of molecules. This last approach has been used to study solvent effects on shielding, but it is complicated by counter point effect of the superposition of the basis sets (102). It is expected that the direct electronic effects would be of the same order of magnitude as the solvent effects in liquids and therefore less than 1 ppm. Under this circumstance it is likely that changes caused by proximate molecules may be less than the resolution of the solid state measurements.

The indirect effect arising from structural deformations has been detected in the isotropic shift in several cases (49, 75, 103). The packing effects on the shielding tensors of naphthalene have been studied recently in this laboratory (104). The intermolecular interactions reduce the number of symmetry planes and leave an inversion center as the only symmetry element for the naphthalene molecule in the crystalline phase. This break in the symmetry of the molecule, observed from single crystal work, has not been noticed in the MAS spectrum of the compound presumably owing to the reduced resolution and the elimination of tensorial information. In Table 9, the principal values of the five non-equivalent carbons in a single crystal of naphthalene are entered along with their averages and the solution values. It is apparent that the intermolecular effects on the isotropic values of the chemical shift are fairly small, all of them below 2 ppm. The effect of the change in symmetry in the crystalline environment on the isotropic values ^{13}C shielding tensors is also very small. The difference of the isotropic values of C_1 and C_8 is only 0.7 ppm and that between C_2 and C_7 , 0.6 ppm. These values are probably below the resolution of an MAS spectrum. The effect of the broken symmetry on the shielding components is however much larger. While relatively small changes are observed in σ_{33} and σ_{11} , σ_{22} varies from 145.5 ppm in C_1 to 140.3 ppm in C_8 . The changes in the individual components have been attributed to the close proximity of a hydrogen to a neighboring molecule in the vicinity of C_1 (105). More theoretical and experimental work is needed to fully understand the importance and the generality of such effects.

Table 9
Principal Values of the ^{13}C Shift Tensors in Naphthalene^a

	σ_{11}	σ_{22}	σ_{33}	$\langle\sigma\rangle_{\text{iso}}$	δ_{lig}
C ₁	223.8	145.5	20.1	129.8	127.7
C ₂	227.6	138.3	10.1	125.3	125.3
C _{4a}	208.7	202.1	-6.3	134.8	133.3
C ₇	227.6	139.3	10.8	125.9	125.3
C ₈	224.5	140.3	22.6	129.1	127.7

^aAll values in ppm from TMS taken from ref. 104.

V. THEORETICAL CALCULATIONS OF THE ANGULAR DEPENDENCE OF THE ^{13}C SHIELDING TENSORS IN MODEL COMPOUNDS

With current computational means it is now possible to perform accurate calculations of the ^{13}C shielding tensors. In this section calculations are presented on the dihedral angular dependence of the principal ^{13}C shielding components in 1,3-butadiene and *n*-butane. The LORG (24) calculations have been performed using the D95* basis set (81), which includes polarization functions for the carbon atoms, and the standard geometrical model was used. The CCCC dihedral angles were varied from 0° (*cis*) to 180° (*trans*) in 20° steps. All values are referenced to methane, using an absolute shielding value of 183.12 ppm.

In Figure 20 the calculated values for the $^{13}\text{CH}_3$ and $^{13}\text{CH}_2$ tensors of *n*-butane are presented. For the $^{13}\text{CH}_3$ shielding tensor it is observed that while σ_{iso} has a range of only 5–6 ppm, $\sigma_{\perp_{\text{ccc}}}$, the component which lies approximately perpendicular to the CCC plane, has a range of ca. 20 ppm and $\sigma_{\parallel_{\text{C}_1-\text{C}_2}}$, which lies approximately parallel to the C₁–C₂ bond, changes by ca. 15 ppm from the *cis* to the *trans* conformation. Minor variations are observed for the third principal component, which is approximately perpendicular to the C₁–C₂ bond and in the CCC plane. It is interesting to observe that while $\sigma_{\perp_{\text{ccc}}}$ moves upfield with the steric strain, $\sigma_{\parallel_{\text{C}_1-\text{C}_2}}$ moves downfield. The values of the three principal components for the *trans* conformation are characteristic of the CH₃ groups (37), but interesting crossovers are observed for the *cis* conformation, where the $\sigma_{\parallel_{\text{C}_1-\text{C}_2}}$ component becomes the furthest downfield. The shielding components of the $^{13}\text{CH}_2$ group are also shown in Fig. 20. As is characteristic of the $^{13}\text{CH}_2$ shielding components (39), σ_{AA} and σ_{BB} , the com-

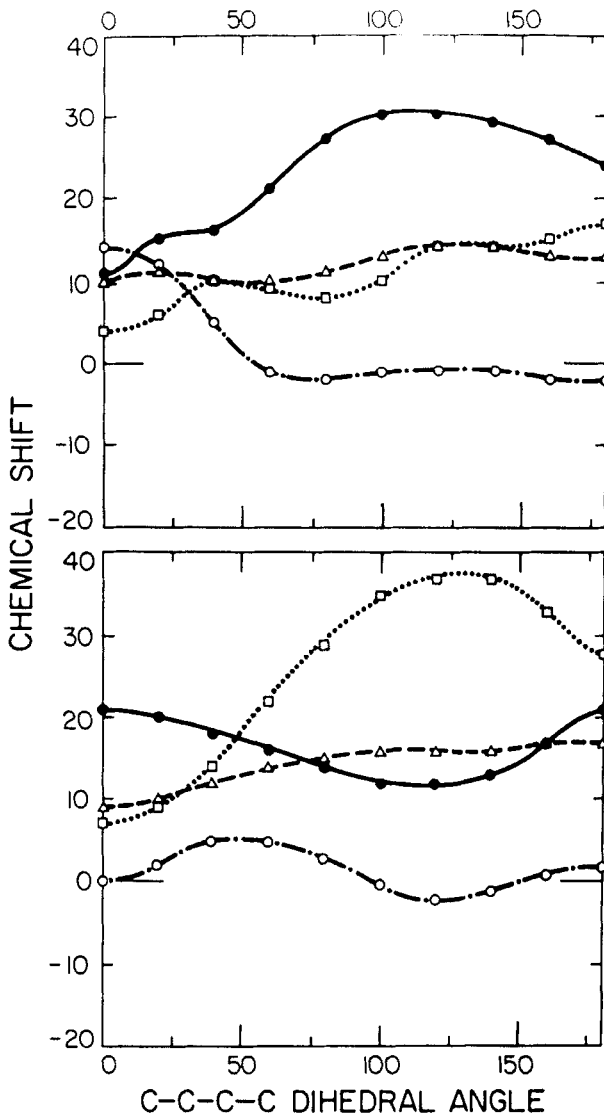


Figure 20. Angular dependence of the ^{13}C shielding principal components in *n*-butane. $^{13}\text{CH}_3$ (top) and $^{13}\text{CH}_2$ (bottom). Values in ppm referenced to methane. The *cis* configuration corresponds to a CCCC dihedral angle of 0° . For the $^{13}\text{CH}_3$ shielding tensor, (○) component along the C-C bond; (□) component perpendicular to the C-C bond and to the C-C-C plane; (●) component perpendicular to the C-C bond in the C-C-C plane. (Δ) isotropic value. For the $^{13}\text{CH}_2$ shielding tensor (○) σ_{BB} ; (●) σ_{AA} ; (□) σ_{CC} ; (Δ) isotropic value. For the definition of σ_{AA} , σ_{BB} and σ_{CC} see Figure 9.

ponents in the CCC plane show little variation with molecular structure; the changes in the σ_{iso} are also fairly small. This is not the case for σ_{CC} , the component approximately perpendicular to the CCC plane, which moves upfield for molecular conformations with a high degree of strain. This behavior is similar to that observed in cycloalkanes (39).

In Figs. 21 and 22 the dependence of the principal components on the dihedral angle in the ^{13}CH and $^{13}\text{CH}_2$ shielding tensors in 1,3-butadiene is shown. In both cases the σ_{33} components, which lie approximately perpendicular to the CCC plane, show the very characteristic upfield shift for the strained *cis* conformation. This component is about 15 ppm upfield in the *cis* with respect to the *trans* conformer, but in spite of this common trend, the σ_{33} components for the ^{13}CH and the $^{13}\text{CH}_2$ shielding tensors exhibit a fairly different angular dependence. Similar ranges of ca. 20 ppm are observed for the other shielding components except for the σ_{22} component of the $^{13}\text{CH}_2$ group which has a modest range of about 7 ppm. The relative extremes observed in the angular dependence of σ_{11} for the CH_2 and σ_{22} for the CH shieldings are situated at the positions of the relative extremes observed in the angular dependence of the calculated total energy, which is dominated by the resonance effects between the two double bonds. It is interesting to observe the inverse behavior of these two components with the CCCC dihedral angle. A more complete mechanistic study of these features is deferred to further investigation, but it is apparent that conjugative effects play an important role in the determination of the angular dependence of these two shielding components.

The isotropic shieldings exhibit a smaller range, about 10 ppm, as a consequence of cancellation of effects between the different components. Moreover, as the different components are influenced by different electronic effects, (i.e. steric forces for σ_{33} , conjugative effects for σ_{11} and σ_{22}). Thus it may not be possible to correlate the angular dependence of σ_{iso} with particular electronic effects whereas it may be possible to do with the individual components.

It is apparent from these theoretical studies on *n*-butane and 1,3-butadiene that there is much more information in the individual components of the ^{13}C shielding tensors than in the isotropic shifts. The theoretical results presented in this section also exemplify the advantages of using tensor components for conformational analysis instead of the characteristic isotropic values. The tensor principal components exhibit a larger range of values and therefore they can contribute more accurate conformational information. Also it is apparent that these values have a more intimate relationship with the three-dimensional electronic structure of a molecule than do the isotropic values, in which the effect is an average.

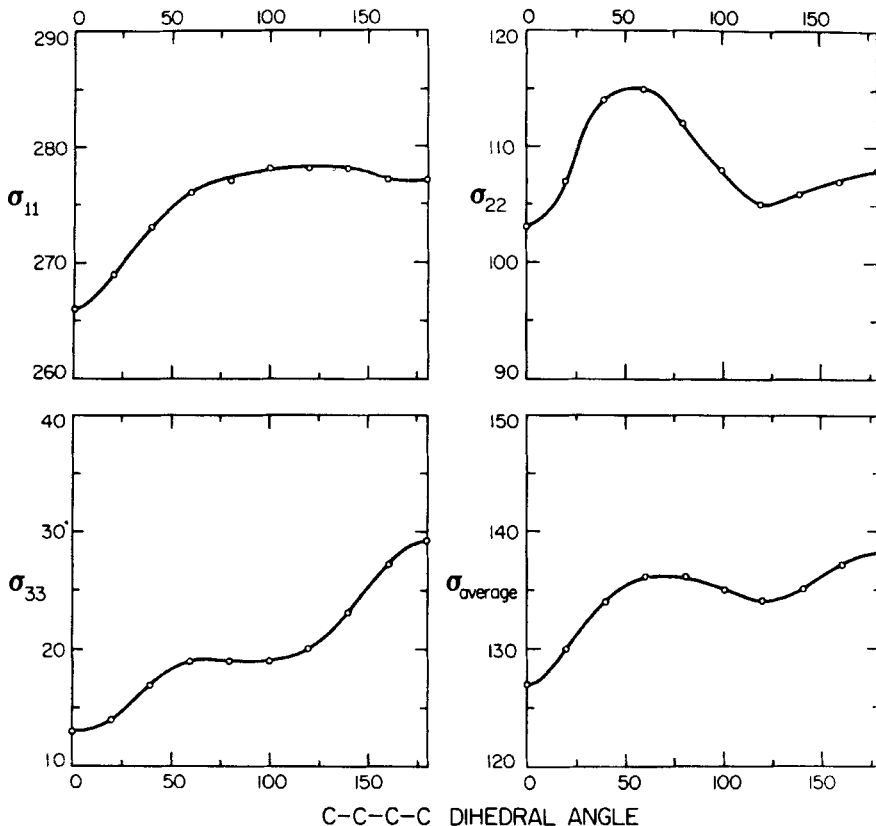


Figure 21. Angular dependence of the ^{13}CH shielding components in 1,3-butadiene. Values in ppm referenced to methane. The *cis* configuration corresponds to a CCCC dihedral angle of 0° .

VI. CONCLUSIONS

From the results presented and discussed herein it is apparent that the determination of ^{13}C chemical shielding tensors can have a tremendous impact in the elucidation of chemical structural problems. The current experimental capabilities allows the determination of ^{13}C shielding tensors, or at least their principal values, in almost all types of molecular systems. While the experimental techniques required for these measurements are certainly much more complicated than those required for NMR in liquids or even for the CP/MAS experiments used to determine isotropic shieldings in solids, the examples

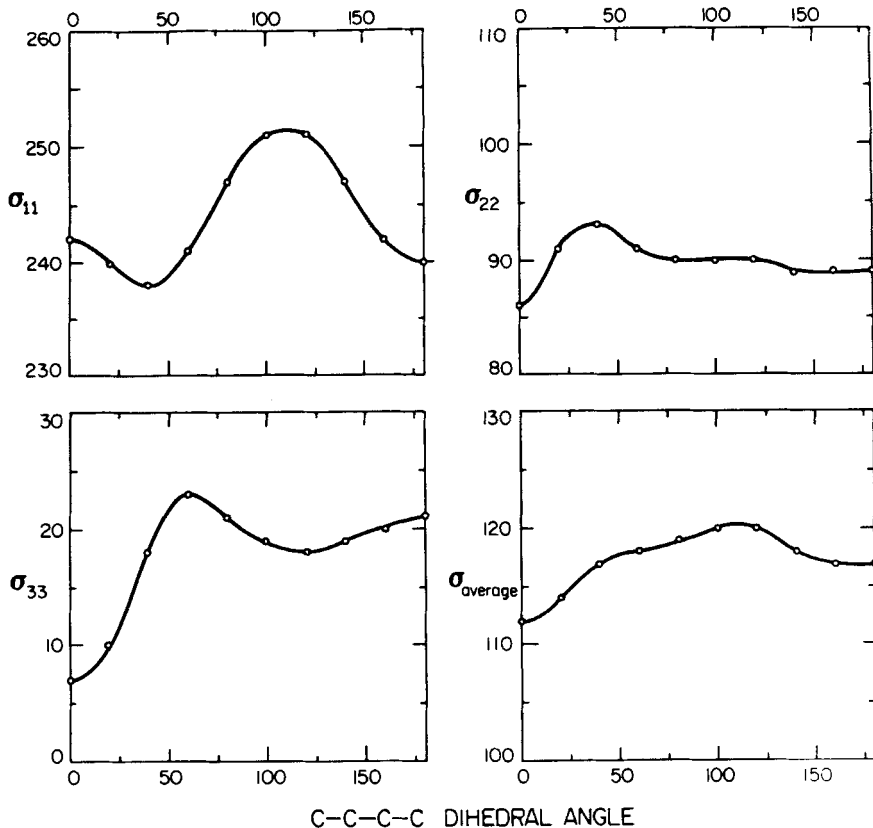


Figure 22. Angular dependence of the shielding components of the $^{13}\text{CH}_2$ in 1,3-butadiene. Values in ppm, referenced to methane. The *cis* configuration corresponds to a CCCC dihedral angle of 0° .

provided here should encourage the measurement of ^{13}C shielding tensors in view of the much greater information available in these data.

There is still a need to determine ^{13}C shielding tensors and/or their principal values in a larger number of compounds than heretofore studied in order to provide the necessary basis to make the technique a practical tool for conformational analysis. This has been done very successfully in the past using isotropic chemical shieldings and J coupling constants, which are used routinely in conformational analysis of molecules in solution.

The powerful computational techniques described here also can be used, as shown in Section V, to guide the researchers to series of compounds for which well designed experiments have the potential to provide relevant structural information.

ACKNOWLEDGMENTS

The ^{13}C shielding tensor work at Utah has been supported by NSF grant # CHE-8310109, NIH grant # 5 RO1 GM 08521-27 and DOE grant #DE-FG02-86ER13510. The San Diego Supercomputer Center (SDSC) is thanked for a generous allocation of computer time. The authors express their gratitude to their many colleagues at Utah, who over the years have made this work possible and to Drs. W. Kutzelnigg, M. Schindler, T.D. Bouman and A.E. Hansen for copies of their IGLO and LORG programs. Special thanks are given to Mrs. Louise Trapier for typing the manuscript.

REFERENCES

1. Ramsey, N. F. *Phys. Rev.* **1950**, *78*, 699-703.
2. Grant, D. M.; Paul, E. G. *J. Am. Chem. Soc.* **1964**, *86*, 2984-2990.
3. (a) Paul, E. G.; Grant, D. M. *J. Am. Chem. Soc.* **1963**, *85*, 1701. (b) Grant, D. M.; Cheney, B. V. *J. Am. Chem. Soc.* **1967**, *89*, 5315-5318. (c) Cheney, B. V.; Grant, D. M. *J. Am. Chem. Soc.* **1967**, *89*, 5319-5327. (d) Strong, A. B.; Ikenberry, D.; Grant, D. M. *J. Magn. Reson.* **1973**, *9*, 145-156; Errata **1976**, *21*, 157-165.
4. Dalling, D. K.; Grant, D. M. *J. Am. Chem. Soc.* **1967**, *89*, 6612-6622; Duddeck, H. *Topics in Stereochem.* **1986**, *16*, 219-324.
5. (a) Dalling, D. K.; Grant, D. M.; Johnson, L. F. *J. Am. Chem. Soc.* **1971**, *93*, 3678-3682. (b) Dalling, D. K.; Grant, D. M. *J. Am. Chem. Soc.* **1972**, *94*, 5318-5324. (c) Dalling, D. K.; Grant, D. M.; Paul, E. G. *J. Am. Chem. Soc.* **1973**, *95*, 3718-3724. (d) Dalling, D. K.; Grant, D. M. *J. Am. Chem. Soc.* **1974**, *96*, 1827-1834.
6. (a) Woolfenden, W. R.; Grant, D. M. *J. Am. Chem. Soc.* **1966**, *88*, 1496-1502. (b) Dalling, D. K.; Ladner, K. H.; Grant, D. M.; Woolfenden, W. R. *J. Am. Chem. Soc.* **1977**, *99*, 7142-7150.
7. (a) Dalling, D. K.; Zilm, K. W.; Grant, D. M.; Heeschen, W. A.; Horton, W. J.; Pugmire, R. J. *J. Am. Chem. Soc.* **1981**, *103*, 4817-4824. (b) Morin, F. G.; Horton, W. J.; Grant, D. M.; Dalling, D. K.; Pugmire, R. J. *J. Am. Chem. Soc.* **1983**, *105*, 3992-3998. (c) Morin, F. G.; Horton, W. J.; Grant, D. M.; Pugmire, R. J.; Dalling, D. K. *J. Org. Chem.* **1985**, *50*, 3380-3388.
8. Saito, H. *J. Magn. Reson. Chem.* **1986**, *24*, 835-852, and references therein.
9. Rose, M. E. *Elementary Theory of Angular Momentum*; John Wiley: NY, 1967.
10. Ebraheem, K. A. K.; Webb, G. A. *Progress in NMR Spectroscopy* **1977**, *11*, 149-181.
11. Robert, J. B.; Wiesenfeld, L. *Phys. Reports* **1982**, *86*, 363-401.
12. Facelli, J. C.; Orendt, A. M.; Grant, D. M.; Michl, J. *Chem. Phys. Lett.* **1984**, *112*, 147-149.
13. (a) Schneider, R. F. *J. Chem. Phys.* **1968**, *48*, 4905-4909. (b) Griffin, R. G.; Ellet, J. D.; Mehring, M.; Bullitt, J. G.; Waugh, J. S. *J. Chem. Phys.* **1972**, *57*, 2147-2155.
14. U. Haeberlen, "High Resolution NMR in Solids, Selective Averaging"; *Adv. in Magnetic Resonance Supplement 1*, Academic: NY 1976.
15. Jameson, C. J. *Bull. Magn. Reson.* **1981**, *3*, 1-28.

16. Jameson, C. J.; Mason J. In *Multinuclear NMR*; Mason, J., Ed.; Plenum: NY, 1987.
17. Cherenisin, A. A.; Schastnev, P. V. *J. Magn. Reson.* **1984**, *40*, 459-468.
18. LaMar, G. N.; Horrocks, W. De W.; Holm, R. H., Eds.; *NMR of Paramagnetic Molecules*; Academic: NY, 1973.
19. Epstein, S. T. *Isr. J. Chem.* **1980**, *19*, 154-158.
20. Holler, R.; Lischka, H. *Mol. Phys.* **1980**, *41*, 1017-1040.
21. Jameson, C. J. In *Specialist Periodical Reports on NMR Spectroscopy*; Webb, G. A., Ed.; The Chemical Society: London, 1987.
22. Ditchfield, R. *Mol. Phys.* **1974**, *27*, 789-807.
23. Kutzelnigg, W. *Isr. J. Chem.* **1980**, *19*, 193-200.
24. Hansen, A. E.; Bouman, T. D. *J. Chem. Phys.* **1985**, *82*, 5035-5047.
25. Lazzaretti, P.; Zanasi, R. *J. Chem. Phys.* **1981**, *75*, 5019-5027.
26. Lazzaretti, P.; Rossi, E.; Zanasi, R. *J. Am. Chem. Soc.* **1983**, *105*, 12-15.
27. Levy, B.; Ridard, J. *Mol. Phys.* **1982**, *44*, 1099-1107.
28. Pople, J. A. *Discuss. Faraday Soc.* **1962**, *34*, 7-14.
29. McMichael-Rohlfing, C.; Allen, L. C.; Ditchfield, R. *Chem. Phys. Lett.* **1982**, *86*, 380-383.
30. Ribas Prado, F.; Griessner-Prettre, C. *J. Magn. Reson.* **1982**, *47*, 103-117.
31. Chestnut, D. B.; Foley, C. K. *Chem. Phys. Lett.* **1985**, *118*, 316-321.
32. Szabo, A.; Ostlund, N. S., *Modern Quantum Chemistry*. Macmillan: NY, 1982.
33. Boys, S. F. *Rev. Modern Phys.* **1960**, *32*, 296-299.
34. Schindler, M.; Kutzelnigg, W. *J. Am. Chem. Soc.* **1983**, *105*, 1360-1370.
35. Schindler, M.; Kutzelnigg, W. *J. Chem. Phys.* **1982**, *76*, 1919-1933.
36. Facelli, J. C.; Grant, D. M.; Michl, J. *Int. J. Quantum Chem.* **1987**, *31*, 45-55.
37. Solum, M. S.; Facelli, J. C.; Michl, J.; Grant, D. M. *J. Am. Chem. Soc.* **1986**, *108*, 6464-6470.
38. Beeler, A. J.; Orendt, A. M.; Grant, D. M.; Cutts, P. W.; Michl, J.; Zilm, K. W.; Downing, J. W.; Facelli, J. C.; Schindler, M. S.; Kutzelnigg, W. *J. Am. Chem. Soc.* **1984**, *106*, 7672-7676.
39. Facelli, J. C.; Orendt, A. M.; Beeler, A. J.; Solum, M. S.; Grant, D. M.; Michl, J.; Depke, G.; Malsch, K. D.; Murthy, P. *J. Am. Chem. Soc.* **1985**, *107*, 6749-6754.
40. Orendt, A. M.; Facelli, J. C.; Grant, D. M.; Michl, J.; Walker, F. H.; Dailey, W. P.; Waddell, S. T.; Wiber, K. B.; Schindler, M.; Kutzelnigg, W. *Theor. Chim. Acta* **1985**, *68*, 421-430.
41. Facelli, J. C.; Orendt, A. M.; Solum, M. S.; Depke, G.; Grant, D. M.; Michl, J. *J. Am. Chem. Soc.* **1986**, *108*, 4268-4272.
42. Orendt, A. M.; Arnold, B. R.; Radziszewski, J. G.; Facelli, J. C.; Malsch, K. D.; Strub, H.; Grant, D. M.; Michl, J. *J. Am. Chem. Soc.* **1988**, *110*, 2648-2650.
43. Jorgensen, P.; Simons, J. *Second Quantization-Based Methods in Quantum Chemistry*. Academic: NY, 1981.
44. Facelli, J. C.; Grant, D. M.; Bouman, T. D.; Hansen, A. E., submitted for publication.
45. Bouman, T. D.; Hansen, A. E. *Chem. Phys. Lett.* **1988**, *149*, 510-515.
46. Mehring, M. *High Resolution NMR Spectroscopy in Solids*; Springer-Verlag: NY, 1976.
47. Hartmann, S. R.; Hahn, E. L. *Phys. Rev.* **1962**, *128*, 2042-2053.
48. Opella, S. J.; Frey, M. H. *J. Am. Chem. Soc.* **1979**, *101*, 5854-5856.

49. Balimann, G. E.; Groombridge, C. J.; Harris, R. K.; Packer, K. J.; Say, B. J.; Tanner, S. F. *Phil. Trans. Royal Society: London*, **1981**, *A* 299, 643-663.
50. Carter, C. M.; Alderman, D. W.; Facelli, J. C.; Grant, D. M. *J. Am. Chem. Soc.* **1987**, *109*, 2639-2644.
51. Veeman, W. S. *Progress in NMR Spectroscopy* **1984**, *16*, 193-235.
52. Carter, C. M.; Alderman, D. W.; Grant, D. M. *J. Magn. Reson.* **1985**, *65*, 183-186.
53. Sherwood, M. H.; Alderman, D. W.; Grant, D. M. manuscript in preparation.
54. Carter, C. M.; Facelli, J. C.; Alderman, D. W.; Grant, D. M.; Dalley, N. K.; Wilson, B. E. *J. Chem. Soc., Faraday Trans. I.* **1988**, *84*, 3673-3690.
55. Duncan, T. M. *J. Phys. Chem. Ref. Data*, **1987**, *16*, 125-151.
56. Zilm, K. W.; Grant, D. M. *J. Am. Chem. Soc.* **1981**, *103*, 2913-2922.
57. Solum, M. S.; Facelli, J. C.; Gan, Zh.; Grant, D. M. *Mol. Phys.* **1988**, *64*, 1031-1040.
58. Zilm, K. W.; Beeler, A. J.; Grant, D. M.; Michl, J.; Chou, T. C.; Allred, E. L. *J. Am. Chem. Soc.* **1981**, *103*, 2119-2120.
59. Alderman, D. W.; Solum, M. S.; Grant, D. M. *J. Chem. Phys.* **1986**, *84*, 3717-3725.
60. Herzfeld, J.; Berger, A. E. *J. Chem. Phys.* **1980**, *73*, 6021-6030.
61. Maricq, M. M.; Waugh, J. S. *J. Chem. Phys.* **1979**, *70*, 3300-3316.
62. Sethi, N. K.; Grant, D. M.; Pugmire, R. J. *J. Magn. Reson.* **1987**, *71*, 476-479.
63. Terao, T.; Fuji, T.; Onodera, T.; Saika, A. *Chem. Phys. Lett.* **1984**, *107*, 145-148.
64. Maciel, G. E.; Szeverenyi, N. M.; Sardashti, M. *J. Magn. Reson.* **1985**, *64*, 365-374.
65. (a) Aue, W. P.; Ruben, D. J.; Griffin, R. G. *J. Magn. Reson.* **1981**, *43*, 472-477. (b) Yarim-Agaev, Y.; Tutunjian, P. N.; Waugh, J. S. *J. Magn. Reson.* **1982**, *47*, 51-60.
66. Linder, M.; Hohener, A.; Ernst, R. R. *J. Chem. Phys.* **1980**, *73*, 4959-4970.
67. Tritt-Goc, J.; Pislewski, N.; Haeberlen, U. *J. Chem. Phys.* **1986**, *102*, 133-140.
68. Millar, J. M.; Thayer, A. M.; Zax, D. B.; Pines, A. *J. Am. Chem. Soc.* **1986**, *108*, 5113-5116.
69. Gan, Zh.; Facelli, J. C.; Grant, D. M. *J. Chem. Phys.* **1988**, *89*, 5542-5546.
70. Lounila, J.; Jokisaari, J. *Prog. Nucl. Magn. Reson. Spectroscopy* **1982**, *15*, 249-290.
71. Parhami, P.; Fung, B. M. *J. Am. Chem. Soc.* **1985**, *107*, 7304-7306.
72. Hiltunen, Y. *Mol. Phys.* **1987**, *62*, 1187-1194.
73. Flygare, W. H. *Chem. Rev.* **1974**, *74*, 653-687.
74. Terao, T.; Inashiro, F., In *Applications of NMR Spectroscopy to Problems in Stereochemistry and Conformational Analysis*; Takeuchi, Y.; Marchand, A. P., Eds.; VCH: Deerfield Beach, 1986.
75. Sutton, P. A. "Crystal packing effects on the photochemical oxidation and solid state ¹³C NMR chemical shifts of several anti-inflammatory steroids." Purdue University: West Lafayette, IN 1984.
76. Pfeffer, P. E.; Hicks, K. B.; Frey, M. H.; Opella, S. J.; Earl, W. L. *J. Carbohydr. Res.* **1984**, *3*, 197-217.
77. Hays, G. R. *J. Chem. Soc., Perkin II*, **1983**, 1049-1052.
78. Biekofsky, R. R.; Pomilio, A. B.; Contreras, R. H.; de Kowalewski, D. G.; Facelli, J. C. *Magn. Reson. Chem.*, in press.
79. VanDerHart, D. L.; Earl, W. L.; Garraway, A. N. *J. Magn. Reson.* **1981**, *44*, 361-401.
80. Zilm, K. W.; Conlin, R. T.; Grant, D. M.; Michl, J. *J. Am. Chem. Soc.* **1980**, *102*, 6672-6676.

81. Dunning, T. H.; Hay, P. J. In *Methods in Electronic Structure Theory*; Schaefer, H. F., Ed.; Plenum: NY, 1977.
82. Kondo, S.; Sakurai, Y.; Hirota, E.; Morino, Y. *J. Mol. Spectrosc.* **1970**, *34*, 231-244.
83. Almenningen, A.; Anfinsen, I. M.; Haaland, A. *Acta Chem. Scand.* **1970**, *24*, 43-49.
84. Bally, T.; Masmune, S. *Tetrahedron*, **1980**, *36*, 343-370.
85. Carpenter, B. K. *J. Am. Chem. Soc.* **1983**, *105*, 1700-1701.
86. Dewar, M. J. S.; Merz, K. M. Jr.; Stewart, J. J. P. *J. Am. Chem. Soc.* **1984**, *106*, 4040-4041.
87. Borden, W. T.; Davidson, E. R.; Hart, P. *J. Am. Chem. Soc.* **1978**, *100*, 388-392.
88. Matsui, S.; Terao, T.; Saika, A. *J. Chem. Phys.* **1982**, *77*, 1788-1799.
89. Burgar, M. I. *J. Phys. Chem.* **1984**, *88*, 4920-4930.
90. Tegenfeldt, J.; Feucht, H.; Ruschitzka, G.; Haeberlen, U. *J. Magn. Reson.* **1980**, *39*, 509-520.
91. van Dongen Torman, J.; Veeman, W. S.; deBoer, E. *J. Magn. Reson.* **1978**, *32*, 49-55.
92. Natiello, M. A.; Contreras, R. H.; Facelli, J. C. de Kowalewski, D. G. *J. Phys. Chem.* **1983**, *87*, 2603-2607.
93. Ando, S.; Yamanobe, T.; Ando, I.; Shoji, A.; Ozaki, T.; Tabeta, R.; Saito, H. *J. Am. Chem. Soc.* **1985**, *107*, 7648-7652.
94. Walton, A. G. *Polypeptides and Protein Structure*; Elsevier: Amsterdam, **1981**.
95. Yamanobe, T.; Ando, I.; Saito, H.; Rabeta, R.; Shoji, A.; Ozaki, T. *Bull. Chem. Soc. Jpn.* **1985**, *58*, 23-29.
96. Ando, I.; Saito, H.; Tabeta, R.; Shoji, A.; Ozaki, T. *Macromolecules* **1984**, *17*, 457-461.
97. Harbison, G. S.; Smith, S. O.; Pardoën, J. A.; Courtin, J. M.; Lugtenburg, J.; Herzfeld, J.; Mathies, R. A.; Griffin, R. G. *Biochemistry* **1985**, *24*, 6955-6962.
98. Harbison, G. S.; Mulder, P. P. J.; Pardoën, J. A.; Lugtenburg, J.; Herzfeld, J.; Griffin, R. G. *J. Am. Chem. Soc.* **1985**, *107*, 4809-4819.
99. Harbison, G. S.; Smith, S. O.; Pardoën, J. A.; Mulder, P. P. J.; Lugtenburg, J.; Herzfeld, J.; Mathies, R.; Griffin, R. G. *Biochemistry* **1984**, *23*, 2662-2667.
100. Harbison, G. S.; Smith, S. O.; Pardoën, H.; Winkel, C.; Lugtenburg, J.; Herzfeld, J.; Mathies, R.; Griffin, R. G. *Proc. Nat. Acad. Sci. USA*, **1984**, *81*, 1706-1709.
101. Mehring, M.; Weber, T.; Muller, W.; Wegner, G. *Solid State Comm.* **1983**, *45*, 1079-1082.
102. Ferchiou, S.; Giessner-Prettre, C. *Chem. Phys. Lett.* **1983**, *103*, 156-160.
103. Terao, T.; Maeda, S.; Yamabe, T.; Akagi, K.; Shirakawa, H. *Chem. Phys. Lett.* **1984**, *103*, 347-351.
104. Sherwood, M. H., Facelli, J. C.; Alderman, D. W.; Grant, D. M., manuscript in preparation.
105. Pawley, G. S.; Yeats, E. A. *Acta Crystallogr.* **1969**, *B25*, 2009-2013.

Resolution of Enantiomers via Biocatalysis

CHARLES J. SIH AND SHIH-HSIUNG WU

School of Pharmacy, University of Wisconsin, Madison, Wisconsin

- I. Introduction
- II. General Mechanistic Principles
 - A. Irreversible Case
 - 1. Kinetic Control
 - 2. Thermodynamic Control
 - 3. Quantitative Treatment of Kinetic Resolution Data
 - B. Reversible Case
- III. Strategies for Improving Enantioselectivity
 - A. Search for Different Biocatalytic Systems
 - B. Recycling of the Product
 - C. Modification of the Substrate
 - D. Sequential and Competitive Kinetic Resolutions
 - E. Biocatalytic Resolutions in Biphasic Aqueous-organic Media
- IV. Second-order Asymmetric Transformations
- V. Selected Examples of Kinetic Resolutions
 - A. Acyclic Alcohols
 - B. Cyclic Alcohols
 - C. Cyclic Allylic Alcohols
 - D. Acyclic α,β -Unsaturated Alcohols
 - E. Carboxylic Acids
 - F. Resolutions in Apolar Solvents
- VI. Conclusions
- References

I. INTRODUCTION

Although many impressive advances have been made in the field of asymmetric catalysis (1) in recent years, resolution methods [enzymic and nonenzymic (classical) (2)] continue to play a dominant role in the preparation of enantiomerically pure organic compounds. This is because both optical antipodes are frequently required for pharmacokinetic (3) and drug-receptor interaction studies (4). Moreover, it is often more economical to carry out the total synthesis on racemic material and perform a resolution at the end of the synthetic sequence.

Biocatalytic resolution procedures are receiving increasing attention largely because of the newer developments in molecular biology and enzyme technology. Genetic engineering has paved the way for the preparation of altered enzymes with improved physical and chemical properties. Further, the catalytic efficiency of enzymes can be enhanced considerably via the use of continuous-flow enzyme reactors or immobilization techniques. However, while biochemical (enzymic and microbial) resolution procedures have been extensively used since the beginning of the century, little attention has been paid to the mechanistic principles that determine enantioselectivity. Consequently, much of the literature data has not been organized in a format that allows a direct comparison of the relative enantioselectivity of biocatalytic systems.

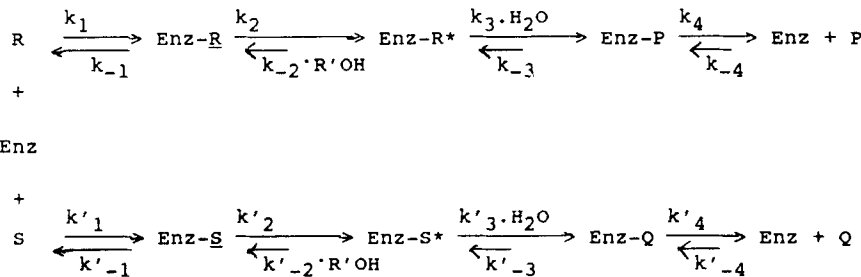
In this chapter, we first consider the kinetic and mechanistic features of enzymes that govern enantioselective processes and describe a method for the systematic treatment of biochemical kinetic resolution data. We then extend our discussion to strategies for improving the enantioselectivity of biocatalytic systems and finally look at some selected biochemical resolutions to provide a brief overview of the more recent developments in the field. Our coverage is focused on esterases and lipases because of space limitations. It is hoped that this article will serve as a platform from which chemists can arrange past and future kinetic resolution data into a unifying framework and provide impetus for further experimentation to unravel the stereochemical complexity of biocatalytic systems.

II. GENERAL MECHANISTIC PRINCIPLES

A. Irreversible Case

1. Kinetic Control

Let us consider an enzyme such as an esterase, which binds with each enantiomer (*R* or *S*) of a racemic mixture to form two diastereomeric complexes Enz-*R* and Enz-*S*. In the Enz-*R* complex, the non-covalent bonding interactions are optimal, so that the *R*-enantiomer is poised for efficient catalysis to give the product, *P* [maximization of k_{cat}/K_m]. In contrast, the non-covalent bonding interactions of the *S*-enantiomer with the enzyme are not as favorable, and inefficient or slow catalysis of the Enz-*S* complex to *Q* follows. A simplified enzymatic mechanism of ester hydrolysis is shown below.



Scheme 1

According to Scheme I, the *R* and *S* enantiomers compete for free enzyme, Enz, to form the complexes Enz-*R* and Enz-*S*; they then undergo catalysis to give their respective acyl-enzymes, Enz-*R** and Enz-*S**. In turn, hydrolysis of the acyl-enzyme intermediates yields the enzyme-product complexes, Enz-*P* and Enz-*Q*, that dissociate to afford free enzyme, Enz, and the products, *P* and *Q*.

There are several steps in this mechanism, but the ones that are important in determining enantioselectivity are those steps leading up to and including the first irreversible step (k_{cat}/K_m). In the above scheme, when the concentration of *R'OH* is low, the conversions of Enz-*R* \rightarrow Enz-*R** and Enz-*S* \rightarrow Enz-*S** become virtually irreversible. Thus, k_{cat}/K_m is the apparent second order rate constant for the reaction of the enzyme and the substrate at infinitely low substrate concentration (Sub \rightarrow 0) to give product(s), and k_{cat} and K_m denote turnover number and Michaelis constant, respectively. Hence, the relative rates of these two parallel steps are [$k_2(\text{Enz-}R)$] and [$k'_2(\text{Enz-}S)$].

For enzyme systems that obey Michaelis-Menten kinetics (5) (Figure 1A) (that is, $k_{-1} \gg k_2$ and $k'_{-1} \gg k'_2$), the enantiomer ratio, *E*, is governed by the relative rate constants of binding and catalysis as predicted by eq. [1]. *R* and *S* denote the concentrations of the competing enantiomers; *R*₀ and *S*₀ are the initial concentrations.

$$E = \frac{\ln\left(\frac{R}{R_0}\right)}{\ln\left(\frac{S}{S_0}\right)} = \frac{\left(\frac{k_{\text{cat}}}{K_m}\right)_R}{\left(\frac{k_{\text{cat}}}{K_m}\right)_S} = \frac{k_2(k_1/k_{-1})}{k'_2(k'_1/k'_{-1})} \quad [1]$$

On the other hand, when enzyme systems follow Van Slyke kinetics (5) (Figure 1B) (that is, $k_{-1} \ll k_2$ and $k'_{-1} \ll k'_2$), the enantiomer ratio, *E*, is

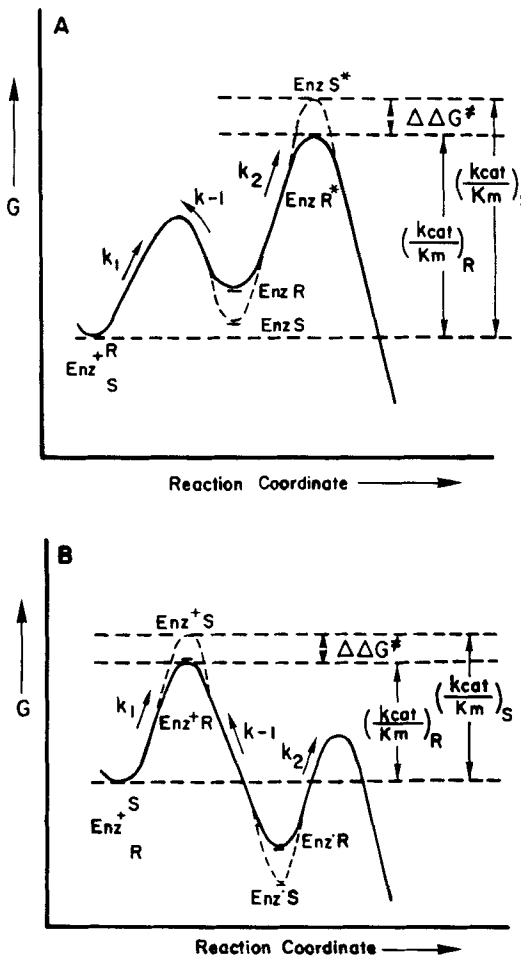


Figure 1. Free energy profiles illustrating a hypothetical biocatalytic kinetic resolution reaction that follows: (A) Michaelis-Menten or (B) Van Slyke kinetics.

dictated solely by the relative rate constants of formation of Enz-*R* and Enz-*S* (eq. [2]).

$$E = \frac{k_1}{k'_1} \quad [2]$$

According to transition state theory (6), the enantiomer ratio, *E*, is related to the thermodynamic term $\Delta\Delta G^\ddagger$ (free energy difference of the diastereomeric transition states) by the following relationship (eq. [3]).

$$\Delta\Delta G^\ddagger = -RT \ln E \quad [3]$$

It is readily apparent that an *E* value of 100 corresponds to a $\Delta\Delta G^\ddagger$ value at 25°C of approximately 3 kcal mole⁻¹.

These principles of kinetic resolution are essentially the same as the competitive reaction between any two compounds (7a) (that is, kinetic isotope effects, alternate substrates, asymmetric catalysis, etc.), and Kagan (7b) has recently reviewed the general mechanistic aspects of this subject. However, it should be noted that k_1 is not a simple diffusion constant but includes binding and conformational effects. In kinetic isotope effect studies, it is generally accepted that $k_1 = k'_1$, but in enantiomer selection processes the difference in the values of k_1 and k'_1 can be very significant. Therefore, one cannot make the tacit assumption that enzyme systems having low k_{cat}/K_m values (slower reaction rate at low substrate concentration) are more enantioselective. The derivation of eq. [1] is based on the assumption that the reaction is irreversible and is devoid of substrate or product inhibition. The enantiomer ratio, *E*, is not affected when the free enzyme, Enz, forms non-productive complexes with either the substrate or the product (i.e., alcohol or acid). However, if the *R*-enantiomer or the product, *P*, or the alcohol component inhibits the reaction of Enz-*S* and the *S*-enantiomer or *Q* inhibits the reaction of Enz-*R* (Scheme 1), the treatment becomes very complex, and *E* will not only vary with changes in the substrate concentration, but also with the extent of conversion, *c*. An example of the effect of substrate concentration on the stereochemical specificity of human liver esterase was recorded by Bamann (8) as early as 1929. He observed that the stereochemical preference of this enzyme was changed by varying the concentration of substrate. However, the presence of interfering enzyme(s) of opposite chirality was not excluded.

2. Thermodynamic Control

Let us envisage that the *R* enantiomer of a racemic mixture is again a good substrate because its non-covalent bonding interaction with the complemen-

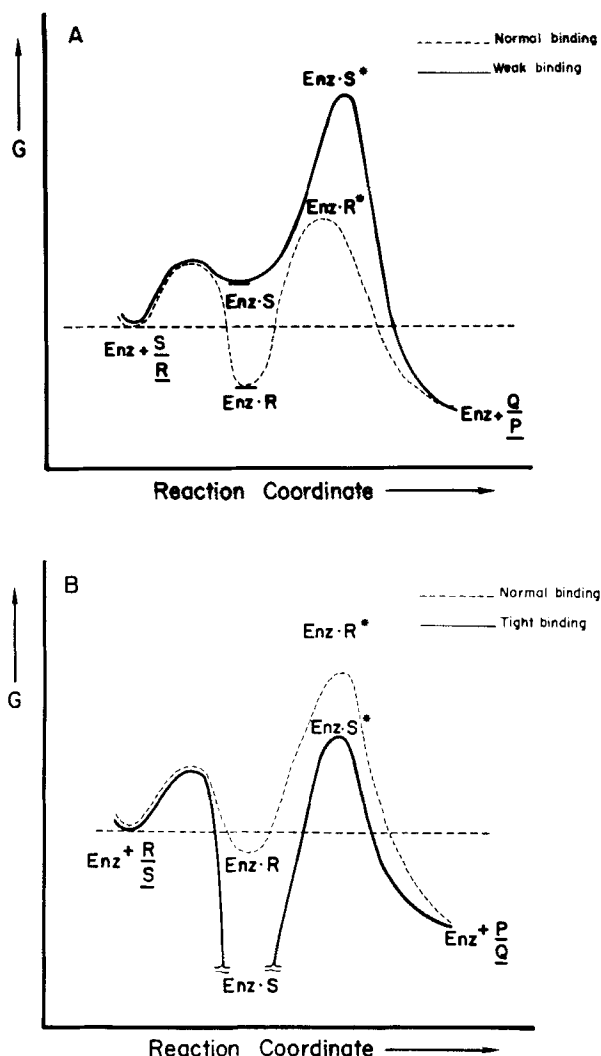
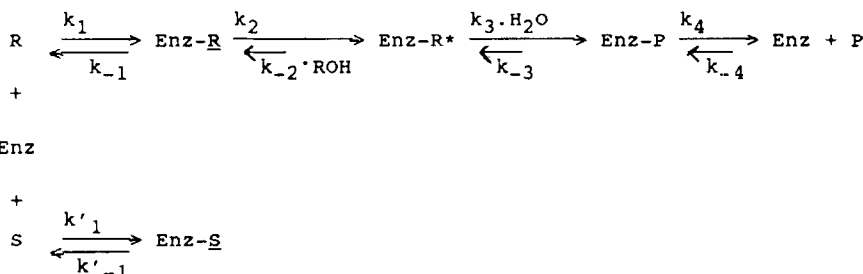


Figure 2. Free energy profiles depicting a hypothetical biocatalytic resolution wherein the *S*-enantiomer binds (A) weakly and (B) tightly to the enzyme.

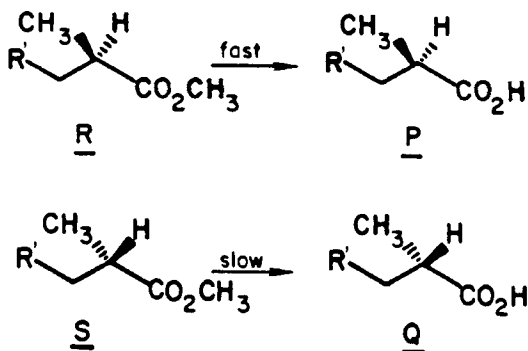
tary active site binding area of the enzyme is highly favorable. This ensures that the Enz-*R* complex will undergo rapid catalysis to *P*. In contrast, the *S*-enantiomer binds poorly (Figure 2A) or not at all to the enzyme, or it may form a non-productive dead-end complex with the enzyme (Figure 2B). As a consequence, the reaction is allowed to proceed to equilibrium because the enzyme is unable to convert the *S* enantiomer to form *Q*, as illustrated schematically below (Scheme 2).



All processes that belong to this category are completely stereospecific. In the most desirable situation, the *S* enantiomer binds very poorly to the enzyme (Figure 2A) (i.e., $k'_{-1} \gg k'_1$), *R* is transformed entirely into *P* and the remaining substrate consists solely of enantiomerically pure *S*. Such systems are ideally suited for the preparation of both optical antipodes in very high chemical yield and enantiomeric purity. Conversely, when the *S* enantiomer binds tightly to the enzyme (Figure 2B) ($k'_1 \gg k'_{-1}$), the *S* enantiomer behaves as a competitive inhibitor and *R* is only incompletely transformed into *P*, because, as the reaction progresses and *R* diminishes, more and more of the free enzyme is competitively bound as the inactive Enz-*S* complex. The remaining substrate fraction consists of an enantiomeric mixture partly enriched in the *S* enantiomer.

3. Quantitative Treatment of Kinetic Resolution Data

Although numerous enzymatic kinetic resolution experiments have been conducted, the resulting data, with very few exceptions, have not been quantitatively analyzed to allow comparison of enantioselectivity. Consider a typical kinetic resolution experiment using two different ester hydrolases, where one of the enantiomers is preferentially hydrolyzed as shown (Scheme 3):



Scheme 3

Let us assume that, for enzyme 1, the reaction is terminated at 69% conversion ($c = 0.69$) and the enantiomeric excess of the product fraction ($ee_p = (P-Q)/(P+Q)$), and that of the remaining substrate ($ee_s = (S-R)/(R+S)$) were determined to be $ee_p = 0.40$ and $ee_s = 0.90$. For enzyme 2, the reaction is terminated at 35% conversion ($c = 0.35$) with $ee_p = 0.85$ and $ee_s = 0.45$. The question now arises: Which of the two enzymes is the more enantioselective one? One obvious way to compare enantioselectivity would be to terminate both enzymatic reactions at the same conversion, c . However, this is tedious to achieve experimentally, because the kinetics of hydrolysis must be continuously and carefully monitored. Even then, it would be difficult to terminate both reactions exactly at the same conversion. Consequently, there is a clear need to express enantioselectivity in terms of an index that is independent of the variable c . The enantiomer ratio, E , is a biochemical constant that is independent of time and substrate concentration (9). Equation 1 can be easily converted into a form (eq. [4]) that relates E to c and ee_s and is suitable for graphical representation (9).

$$\frac{\ln([1 - c][1 - ee_s])}{\ln([1 - c][1 + ee_s])} = E \quad [4]$$

Thus, substituting the values of ee_s and c for the two enzymes, the E values for enzymes 1 and 2 are calculated to be 6 and 19, respectively. A theoretical plot of ee_s (enantiomer excess of the residual substrate) as a function of c for various values of E is shown in Figure 3A. As can be seen, the value of ee_s increases with extent of conversion, c . Hence, highly enantiomerically enriched remaining substrate may be obtained with enzymes of low E value by

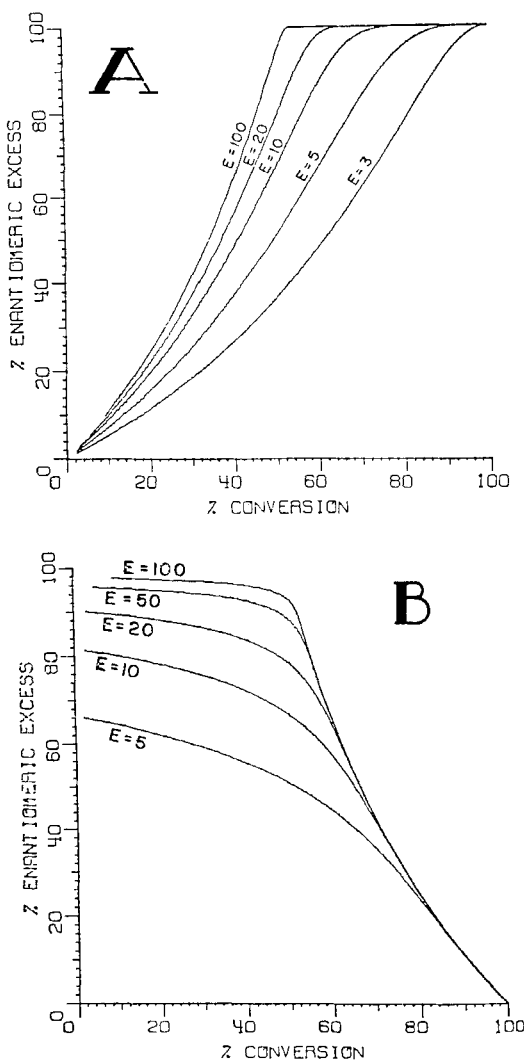


Figure 3. Plot of percent enantiomer excess (*ee*) vs. the percent conversion for various enantioselectivity ratios (*E*). (A) Substrate-remaining fraction, $ee_S = (S - R)/(R + S)$. (B) Product fraction, $ee_P = (P - Q)/(P + Q)$. (Reprinted with permission from *J. Am. Chem. Soc.* **104**:7294–7299 (1982). Copyright 1982 American Chemical Society.)

simply extending reaction times but at the expense of chemical yield. A similar expression may be derived to relate ee_p (enantiomeric excess of the product), c , and E (eq. [5]):

$$\frac{\ln[1 - c(1 + ee_p)]}{\ln[1 - c(1 - ee_p)]} = E \quad [5]$$

The corresponding graph (Figure 3B) shows an abrupt decrease in ee_p for values of c beyond 0.5. Therefore, if the product fraction is of interest, the conversion (c) should be terminated prior to a value of 0.5 irrespective of the value of E .

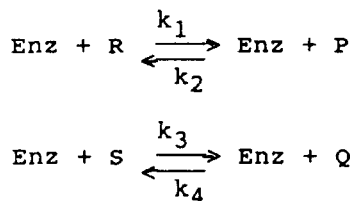
Although the value of c is usually determined experimentally by methods such as GC or HPLC, it is more accurate and convenient to calculate c by taking advantage of the following relationship (eq. [6]).

$$c = \frac{ee_s}{ee_s + ee_p} \quad [6]$$

Hence, in kinetic resolution experiments, if the values of ee_s and ee_p are defined, the values of c and E may be calculated accurately from eqs. [6] and [4], or [5] respectively.

B. Reversible Case

For enzyme-catalyzed condensation reactions in biphasic systems (water plus water immiscible organic solvent), the reactions are reversible. Hence, the rate constants for both the forward and the reverse reactions must be considered. In the presence of an excess quantity of acyl donor or acceptor ($> 10 K_m$), the scheme for either esterification or transesterification (ester interchange) may be envisaged as follows:



where R , S and P , Q are pairs of enantiomers; k_1 , k_2 and k_3 , k_4 denote the apparent second order rate constants (k_{cat}/K_m) for the forward and reverse reactions, respectively. As the enzyme only speeds up the attainment of equilibrium but does not change the position of equilibrium, the equilibrium con-

stant (K) depends only on the initial and final states and is independent of the reaction pathway. Therefore, the equilibrium constants for the pair of enantiomers in achiral solvent media should be equal (eq. [7]). It is readily apparent from eq [7] that when $k_2 > k_4$, $k_1 > k_3$.

$$K = \frac{k_2}{k_1} = \frac{k_4}{k_3} = \frac{R}{P} = \frac{S}{Q} \quad [7]$$

This relationship reveals that *the sense of preferred chirality for the forward (esterification) and reverse (hydrolytic) reactions is retained*. That is, if R is the fast reacting enantiomer in the forward reaction, P must be the fast reacting enantiomer in the reverse reaction.

For reversible biocatalytic systems, a new expression, which incorporates the thermodynamic parameter K , is required for the calculation of the enantiomer ratio, E (eq. [8]) (10).

$$\frac{\ln\left[1 - (1 + K)\left(1 - \frac{R}{R_0}\right)\right]}{\ln\left[1 - (1 + K)\left(1 - \frac{S}{S_0}\right)\right]} = E \quad [8]$$

where

$$E = k_1/k_3; \quad K = k_2/k_1 = k_4/k_3$$

When k_2 and $k_4 = 0$, eq. [8] is reduced to the familiar homocompetitive eq. [9] for the irreversible case (9).

$$\frac{\ln\left[\frac{R}{R_0}\right]}{\ln\left[\frac{S}{S_0}\right]} = E \quad [9]$$

According to the principle of microscopic reversibility (11), reversible reactions must proceed through the same transition state(s) in both directions. Consequently, *if the reaction conditions for the forward and reverse reactions are identical, the enantiomer ratios or E values for the forward reaction (k_1/k_3) and the reverse reaction (k_2/k_4) must be the same, in accordance with the predictions of Eq. 7*. It is noteworthy that E is a kinetic parameter whose value will vary with different catalysts, whereas K is a thermodynamic function that is independent of the properties of enzymes. However, both E and K

are sensitive to environmental changes such as the water content of the medium, species of acyl donor and acceptor, pH, temperature, etc. Because the enantioselectivity of enzyme-catalyzed synthesis depends on the complex interaction of both kinetic and thermodynamic functions, it is difficult to predict the stereochemical behavior of such systems.

To correlate the extent of conversion (c) with the enantiomer excess of substrate (ee_s) and the product (ee_p) fractions, eq. [8] was transformed into the following equations

$$\frac{\ln[1 - (1 + K)(c + ee_s\{1 - c\})]}{\ln[1 - (1 + K)(c - ee_s\{1 - c\})]} = E \quad [10]$$

$$\frac{\ln[1 - (1 + K)c(1 + ee_p)]}{\ln[1 - (1 + K)c(1 - ee_p)]} = E \quad [11]$$

The theoretical curves (Figure 4), generated from eqs. [10] and [11] provide a useful overview of the interrelationships between the variables c , ee_s , and ee_p for fixed values of E and K . These computer-generated graphs show that a small increase in the value of K has a very pronounced effect on the enantiomeric purity of the substrate and product fractions even for a system with a very high E value. For example, for a biochemical system with an E

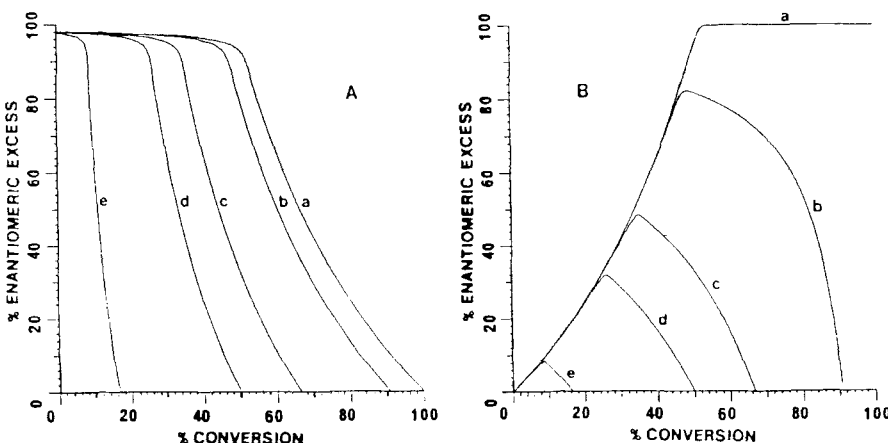


Figure 4. Expression of the percentage enantiomeric excess (ee) of product (A) and substrate-remaining fractions (B) as a function of the percentage conversion at different values of E and K . These curves were computer generated from Eqs. (10) and (11) for an E value of 100. The values of K were (a) 0, (b) 0.1, (c) 0.5, (d) 1, and (e) 5. (Reprinted with permission from *J. Am. Chem. Soc.* 109:2812-2817 (1987). Copyright 1987 American Chemical Society.)

value of 100 and K values ranging from 0 to 1 (Figure 4, A, B), the ee_S and ee_P at 50% conversion are as follows: 0.95 ($K = 0$); 0.81 ($K = 0.1$); 0.33 ($K = 0.5$); and 0 ($K = 1$). It is evident that the enantiomeric purity of both fractions is inversely related to the magnitude of K .

For the reversible systems, the kinetics of enzymic resolution may be visualized to occur as follows: at the initial stages of the reaction, the enzyme preferentially attacks the fast reacting enantiomer R and transforms it to P . The high enantioselectivity results from a large difference in the net rates of the two competing reactions. As the reaction for the fast reacting enantiomer approaches equilibrium, the net rate ($R \rightleftharpoons P$) gradually diminishes, while the concentration of the slow reacting enantiomer, S , is still largely unchanged. When the equilibrium of the fast reacting enantiomer is established (net rate = 0), the enantiomeric purity of the substrate (ee_S) and the product (ee_P) fractions begin to fall owing to the concentration changes of the slow-reacting enantiomer.

III. STRATEGIES FOR IMPROVING ENANTIOSELECTIVITY

The biocatalysts used for the separation of enantiomers are usually either commercially available enzymes or intact microorganisms. In many instances, the reaction is only partially enantioselective ($E = 1-10$), which may be interpreted in two ways. Either the preparation contains a single enzyme that is only partially enantioselective, or the preparation may contain more than one enzyme of opposite stereochemical preference.

In asymmetric catalysis, the presence of competing enzymes of opposite chirality can be readily uncovered because the enantiomer excess of the product (ee_P) is affected by changes in substrate concentration (pseudo-first order becomes zero order) (1b). However, changes in substrate concentration cannot be used as a diagnostic indicator in kinetic resolutions because they are always k_{cat}/K_m processes. The E value of each competing enzyme for a specified substrate is manifested in the experimentally determined E_{app} value (eq. [12]), where the α 's are proportionality constants to take care of the different concentrations of each type (R or S) of enzyme present (9)

$$E_{app} = \frac{\sum \alpha_1 \left(\frac{k_{cat}}{K_m} \right)_{R_1} + \alpha_2 \left(\frac{k_{cat}}{K_m} \right)_{R_2} \dots \alpha_i \left(\frac{k_{cat}}{K_m} \right)_{R_{n-1}}}{\sum \alpha_1 \left(\frac{k_{cat}}{K_m} \right)_{S_1} + \alpha_2 \left(\frac{k_{cat}}{K_m} \right)_{S_2} \dots \alpha_i \left(\frac{k_{cat}}{K_m} \right)_{S_{n-1}}} \quad [12]$$

Consequently, the presence of two or more competing enzymes attuned to substrates of opposite chirality in biocatalytic resolution systems cannot be

easily identified. Instead, a series of experiments must be conducted to establish whether the activity of one competing enzyme has been selectively decreased by the use of inhibitors, changes in pH or temperature, or by fractionation of the enzyme preparation. However, it is important to keep in mind that any agent that changes the protein conformation will also alter the *E* value of that biocatalyst. The following approaches may be used to improve the enantioselectivity of biocatalytic systems.

A. Search for Different Biocatalytic Systems

Because of a lack of rational criteria for the design or selection of new biocatalysts, a time-consuming examination of a large number of different biocatalytic systems is often required before a suitable biocatalyst is found. Consequently, rapid detection methods that provide a preliminary indication of enantioselectivity are used first before a rigorous quantitative analysis (*E* determination) of a biocatalytic system is made. Two procedures are generally followed. In the competitive method, a racemic substrate is exposed to biocatalytic systems (enzymes or microorganisms) and samples are withdrawn at appropriate time intervals (that is, 24 and 72 h) for analyses (TLC, GLC, HPLC). Those biocatalysts that give an approximately 1:1 substrate to product ratio after prolonged incubation are selected for further evaluation. When both enantiomers are available, a non-competitive procedure may be employed. Each enantiomer is separately incubated with a biocatalyst and the relative rate of catalysis is compared. Thus the stereochemical preference of the biocatalyst is readily established (for instance, by visual inspection of a TLC plate). While each procedure has its own merit in terms of reliability or simplicity, these two sets of kinetic data sometimes yield apparently contradicting stereochemical results because they have different connotations. This is best illustrated by the following published example. In 1927, Rona and Ammon (12) investigated the action of hog liver esterase on the pure enantiomers of methyl mandelate. They found that the levorotatory isomer was more rapidly hydrolyzed. However, this result was in direct contrast to that obtained with the racemate, in which the dextrorotatory ester was split more efficiently. It is to be noted that the discrimination of two competing enantiomers by biocatalysts is *always* dictated by the enantiomer ratio, *E* (eq. [1]), the ratio of the specificity constants $[(k_{\text{cat}}/K_m)_{(-)} / (k_{\text{cat}}/K_m)_{(+)}]$, and this ratio is independent of substrate concentration and time. On the other hand, in the non-competitive experiments described above, it is the velocity of the reaction of the (-)-enantiomer at one substrate (*S*) concentration, $v_{(-)} = [V_{\text{max}}S_{(-)}] / [K_m + S_{(-)}]$, that is compared to the velocity of the (+)-enantiomer at the same concentration, $v_{(+)} = [V_{\text{max}}S_{(+)}] / [K_m + S_{(+)}]$. When $S \gg K_m$, $v = V_{\text{max}} (V_{\text{max}} = K_{\text{cat}} \text{Enz})$ and the ratio becomes $k_{\text{cat}(-)} / k_{\text{cat}(+)}$. There-

fore, the E value of a biocatalyst can be obtained from non-competitive kinetics only if the k_{cat}/K_m is determined separately for each enantiomer.

B. Recycling of the Product

An interesting feature of kinetic resolution processes is that the residual substrate fraction can be obtained in high enantiomeric purity even for biocatalytic systems that possess low E values. That is, the optical yield can be enhanced at the expense of chemical yield (9). For example, for a biocatalyst with an E value of 5 (Figure 3A), the optical purity of the remaining substrate (ee_S) at 60% conversion is 0.64, whereas at 80% conversion ee_S is elevated to 0.99. On the other hand, the reaction must be terminated prior to 50% conversion to maximize the optical yield of the product fraction (Figure 3B). For biocatalysts with moderate E values ($E = 5-10$), the product may be recycled to enhance the optical purity (ee_P), that is, for hydrolytic enzymes the product may be easily reesterified and again incubated with the same biocatalyst. For these recycling studies, a new expression is needed to relate the variables c , E , ee_0 (initial ee), and ee' (final desired ee).

If we consider one mole of an antipodal mixture with an initial ee of ee_0 , this would contain $(1 + ee_0)/2$ mole of R_0 (fast reacting) and $(1 - ee_0)/2$ mole of S_0 (slow reacting). It follows that $R = (1 + ee_0)/2 - c[(1 + ee')/2]$ and $S = (1 - ee_0)/2 - c[(1 - ee')/2]$. Substitution of these terms into eq. 9 affords eq. [13].

$$\left[1 - c\left(\frac{1 + ee'}{1 + ee_0}\right)\right] = \left[1 - c\left(\frac{1 - ee'}{1 - ee_0}\right)\right]^E \quad [13]$$

This equation allows one to generate a useful graph (Figure 5) for the estimation of the relationship between ee' and c at various fixed values of E and ee_0 . For example, starting with an antipodal mixture with an ee_0 of 0.67 and an E of 10, the ee' obtainable after 80% conversion is 0.91. In principle, the product could be recycled an infinite number of times to achieve the ultimate goal of absolute enantiomeric purity (100%). In reality, to prepare enantiomers with ee' values of >0.98 , it would be more convenient to select biocatalytic systems with E values of ≥ 10 and subject the product to recycling not more than two times. Several successful applications of this recycling technique have been reported (13).

C. Modification of the Substrate

The enantioselectivity of a biocatalytic system can frequently be improved by manipulating the structural feature(s) of the substrate molecule, an approach

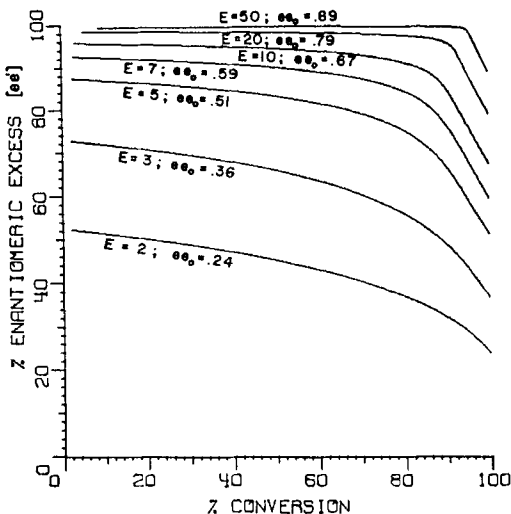


Figure 5. Expression of the final percent enantiomer excess function of the percent conversion for various values of initial enantiomer excess (ee_0) and enantiomer ratio (E). (Reprinted with permission from *J. Am. Chem. Soc.* **104**:7294-7299 (1982). Copyright 1982 American Chemical Society.)

that is most suited to the background of synthetic chemists. For hydrolytic enzymes, it is convenient to re-design the ester grouping with a view to maximizing the difference between $(k_{cat}/K_m)_R$ and $(k_{cat}/K_m)_S$. The gist of this approach is illustrated by some selected examples.

Ladner and Whitesides (14) were successful in preparing optically active epoxy alcohols using a crude preparation of porcine pancreatic lipase (PPL). Although the enzyme responsible for catalyzing the hydrolyses of glycidol esters has yet to be defined, the preparation has an *S*-stereochemical preference and better enantioselectivity was observed with longer *n*-alkyl esters (i.e., *n*-butyryl vs. acetyl) (**1a-1e**) (Table 1).

Tabushi et al. (15), investigated the hydrolysis of (\pm) -methyl phenyllactate derivatives (**2a-2h**) catalyzed by chymotrypsin (α -chT). The results showed that the *S*-enantiomer was preferentially cleaved and the acyloxyl group on the α -carbon, $\text{PhCH}_2\overset{\underset{\text{R}}{\text{CH}}}{\text{CH}}-\text{COOCH}_3$ (**2a-2h**) had a pronounced influence on

the enantioselectivity of the biocatalyst. The enantiomer ratio, E , was raised from 16 for $\text{R}=\text{OH}$ (**2a**) to a value of 26 for $\text{R}=\text{CH}_3\text{CO}_2\text{CH}_2\text{CO}_2$ (**2e**) (Table 2).

Pig liver esterase (PLE) has been shown to hydrolyze the *R* enantiomer of several 3-hydroxy-3-methylalkanoic acid esters (**3a-3f**) of the form $\text{R}_1\text{C}-(\text{Me})(\text{OH})\text{CH}_2\text{COOR}_2$ (16) enantioselectively (Table 3).

Table 1
Hydrolysis of Glycidol Esters Catalyzed by PPL

		<u>R</u>	<u>S</u>
(+)-1	<u>R</u>	Conversion (%) (6 h)	<u>E</u>
1a	CH ₃	60	4
1b	C ₂ H ₅	60	11
1c	C ₃ H ₇	60	13
1d	C ₄ H ₉	60	16
1e	C ₅ H ₁₁	60	16

Table 2
Hydrolysis of PhCH₂CH(R)-COOCH₃ Catalyzed by Chymotrypsin

<u>R</u>	<u>E</u>
2a OH	16
2b CH ₃ CO ₂	7
2c HOCH ₂ CO ₂	16
2d HOCH ₂ CH ₂ CO ₂	15
2e CH ₃ CO ₂ CH ₂ CO ₂	26
2f CH ₃ CO ₂ CH ₂ CH ₂ CO ₂	15
2g n-C ₄ H ₉ CO ₂	15
2h t-C ₄ H ₉ CO ₂	4

Table 3
Hydrolysis of $R_1C(Me)(OH)CH_2COOR_2$ Catalyzed by PLE

	<u>R_1</u>	<u>R_2</u>	<u>Conversion (%)</u>	<u>E</u>
3a	$(CH_3O)_2CHCH_2$	CH ₃	67 (24 h)	9
3b	$(CH_3O)_2CHCH_2$	C ₂ H ₅	75 (72 h)	6
3c	PhCH ₂ OCH ₂ CH ₂	CH ₃	40 (72 h)	2
3d	PhCH ₂ OCH ₂ CH ₂	C ₂ H ₅	52 (72 h)	6
3e	CH ₂ =CHCH ₂	CH ₃	84 (5 h)	4
3f	CH ₂ =CHCH ₂	C ₂ H ₅	50 (2 h)	5

These compounds are valuable chiral intermediates for the synthesis of analogs of Compactin (17) and Mevinolin (18), potent inhibitors of 3-hydroxy-3-methylglutaryl coenzyme A (HMG-CoA) reductase, the key regulatory enzyme in sterol biosynthesis (19).

It is noteworthy that changing from a methyl to an ethyl ester leads to different results with different compounds. When the R_1 group is 2,2-dimethoxyethyl (**3a** and **3b**), the *E* value drops from 9 for the methyl ester to 6 for the ethyl ester. However, when the R_1 group is 2-(benzyloxy)ethyl (**3c** and **3d**), the *E* value of the ethyl ester is 6 whereas for the methyl ester it drops to 2. Finally, if R_1 is allyl (**3a** and **3f**), the effect of changing from a methyl to an ethyl ester is small.

The hydrolysis of methyl (*RS*)-3-arylothio-2-methylpropionate (**4a-4d**) by *Mucor miehei* lipase (20) was examined because the *S*-enantiomer is a key intermediate for the preparation of Captopril, 1-[*(2S*)-3-mercaptop-2-methylpropionyl]-L-proline, a potent antihypertensive agent (21). The addition of methoxy substituents on the arylthio moiety of the molecule markedly improved the enantioselectivity as depicted below (Table 4).

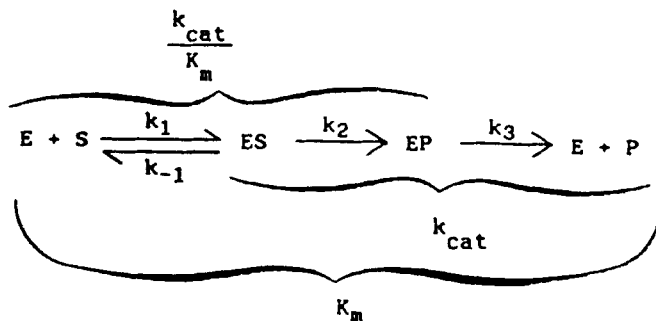
The above examples show that the *E* value of a biocatalytic system can be improved by making structural changes in the substrate molecule. However, to gain a better insight into the enantioselectivity of enzymes, it is desirable to collect more systematic data correlating changes in structural features of each enantiomer with the kinetic parameters k_{cat}/K_m and k_{cat} . This information allows one to dissect out the rate constants of the individual steps of the overall reaction that is affected by structural modifications as illustrated below.

Table 4
Enzymatic Hydrolysis of (\pm)-3-Aroylthio-2-methylpropionate

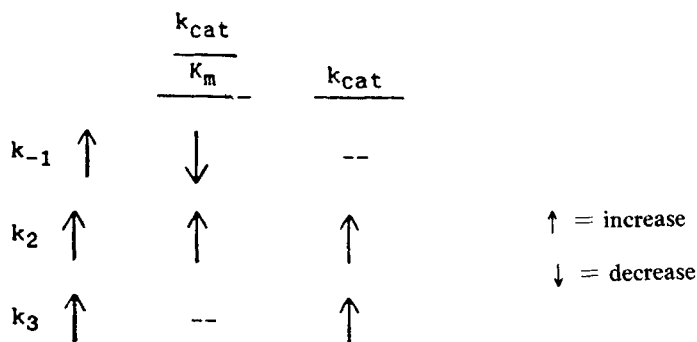
(\pm) -4		$M. miehei$ lipase H_2O	S
<u>R</u>	Conversion (%) (44-96 h)	<u>E</u>	
4a		37	3
4b		55	2
4c		47	8
4d		47	10

For example, a decrease in (k_{cat}/K_m) suggests that the binding step is affected (an increase in k_{-1} —the rate constant of dissociation of ES). When (k_{cat}/K_m) and k_{cat} both increase, it is the catalytic step (k_2) that is enhanced. Finally when only k_{cat} is increased, it is the rate constant of dissociation (k_3) of the enzyme-product (EP) complex that is altered. This more refined analysis could lead to some useful predictions relating substrate structures to stereospecificity of biocatalysts (Scheme 4).

A quantitative analysis of the contribution of steric, electrical, and polarizability effects to the enantiomer ratio, E , in the hydrolysis of esters of the general formula ArCH(X)OAc by *Rhizopus nigricans* was recently reported (22). The results showed that in this series the E value decreases with increasing size and electron withdrawing ability of X and with increasing polarizability of Ar. The calculated E values coincided reasonably well with those observed experimentally (Table 5).



$$K_m = \frac{k_3(k_{-1} + k_2)}{k_1(k_2 + k_3)} ; \quad k_{cat} = \frac{k_2 k_3}{k_2 + k_3} ; \quad \frac{k_{cat}}{K_m} = \frac{k_1 k_2}{k_{-1} + k_2}$$



Scheme 4 A simplified irreversible three-step mechanism of enzyme catalysis

It would be interesting to determine whether the intermolecular force (IMF) equation (see footnote *a* to Table 5) could be also extended to other biocatalytic systems for the prediction of enantioselectivity.

D. Sequential and Competitive Kinetic Resolutions

In the enzymatic hydrolysis of racemic axially-disymmetric diacetates (A and B, Scheme 5), two kinetic resolution steps are operating in tandem.

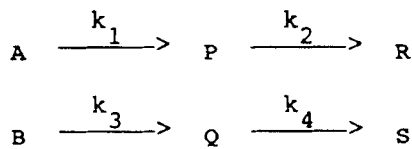


Table 5
Comparison of Experimental and Calculated Enantiomer Ratios (E)

<u>ArCH(X)OAc</u>			<u>E(obs)</u>	<u>E(calcd)^a</u>
<u>Ar</u>	<u>X</u>			
Ph	Me		16	10
Ph	CH ₂ Cl		4	5
Ph	C=CMe		7	4
Ph	Et		4	9
Ph	Pr		9	6
Ph	i-Pr		3	5
Ph	t-Bu		1	1
Ph	CF ₃		1	1
Ph	CO ₂ Me		5	5
Ph	CH ₂ Ph		8	6
1-naphthyl	Me		320	96
2-naphthyl	Me		72	102
2-furyl	Me		2	6
2-thienyl	Me		4	6
2-pyridyl	Me		3	4
3-pyridyl	Me		37	4

^aSee Charton, M.; Charton, B. I. *J. Theor. Biol.* **1982**, *99*, 629 for a discussion as to how these values are calculated.

The enantiomeric monoacetates (P and Q) are formed at varying rates; in turn, they are further hydrolyzed to the diols (R and S) as shown. The enantiomeric purity of each fraction is dependent on the magnitude of the four relative second order rate constants (k_{cat}/K_m), k_1 , k_2 , k_3 , and k_4 . When the enzyme retains the same stereochemical preference ($k_1 > k_3$ and $k_2 > k_4$) and the rate constants of the second parallel steps are greater than or equal to those of the first ($k_2 \geq k_1$ and/or $k_4 \geq k_3$), B and R accumulate in enantiomerically pure forms. This type of kinetic behavior has been observed during the hydrolysis of 2,2'-diacetoxy-1,1'-binaphthyl (**5**) by the fungus, *Absidia glauca* (23).

Quantitative expressions have been derived for this consecutive kinetic resolution system. These equations [14–20] allow the calculation of the concentration of *A*, *B*, *P*, *Q*, and *R*, *S* for any degree of conversion and the relative rate constants.

$$P = \frac{A_0}{1 - E_2} \left[\left(\frac{A}{A_0} \right)^{E_2} - \left(\frac{A}{A_0} \right) \right] \quad [14]$$

$$R = A_0 - A - P \quad [15]$$

$$Q = \frac{B_0}{1 - E_3} \left[\left(\frac{B}{B_0} \right)^{E_3} - \left(\frac{B}{B_0} \right) \right] \quad [16]$$

$$S = B_0 - B - Q \quad [17]$$

where

$$E_1 = \frac{k_1}{k_3} = \frac{\ln\left(\frac{A}{A_0}\right)}{\ln\left(\frac{B}{B_0}\right)} \quad [18]$$

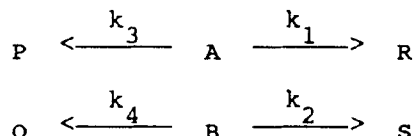
$$E_2 = \frac{k_2}{k_1} = 1 - \frac{A_0}{P} \left[\left(\frac{A}{A_0} \right)^{E_2} - \left(\frac{A}{A_0} \right) \right] \quad [19]$$

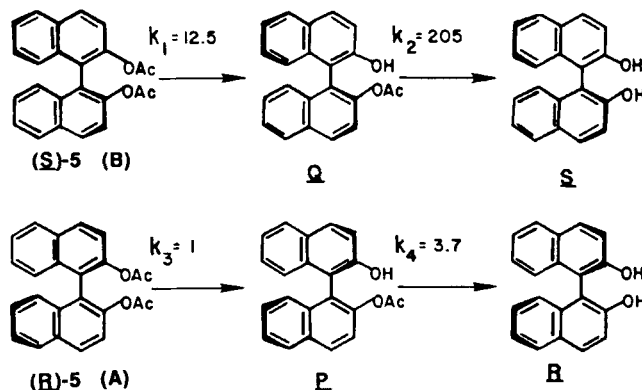
$$E_3 = \frac{k_4}{k_3} = 1 - \frac{B_0}{Q} \left[\left(\frac{B}{B_0} \right)^{E_3} - \left(\frac{B}{B_0} \right) \right] \quad [20]$$

The relative rate constants for the *A. glauca* system, which has *S*-stereochemical preference, were calculated from the experimental kinetic data (*ee* and *c*).

This apparent amplification of enzymic enantioselectivity is a consequence of the favorable interaction of the relative rate constants as shown (Scheme 5). A different kinetic pattern was observed for the hydrolysis of (\pm)-*trans*-4-cyclopentene-1,3-diol diacetates and (\pm)-*trans*-cycloalkane-1,2-diol diacetates catalyzed by pig liver esterase (PLE) (24).

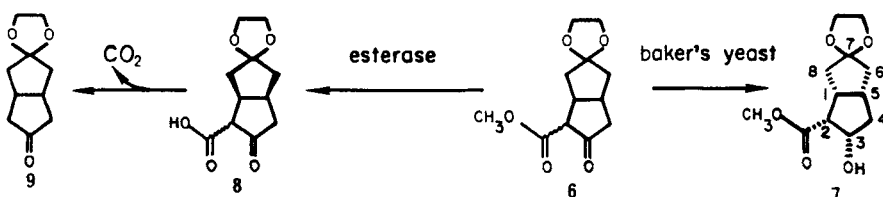
A different type of kinetic resolution process that conforms to the following kinetic pattern has recently been observed with an intact microorganism.





Scheme 5 Enzymatic kinetic resolution of axially-disymmetric (\pm)-2,2'-diacetoxy-1,1'-binaphthyl

It is noteworthy that the system becomes apparently more enantioselective when $k_1 > k_2$ and $k_4 > k_3$. Brooks (25) noted that the (racemic) *1R**, *5S** isomer of methyl (*2RS*)-3-oxo-7,7-(ethylenedioxy)bicyclo[3.3.0]octane-2-carboxylate (**6**) is reduced by a dehydrogenase enzyme present in baker's yeast to the single enantiomer methyl (+)-(i*R*,*2R*,*3S*,*5S*)-3-hydroxy-7,7-(ethylenedioxy)bicyclo[3.3.0]octane-2-carboxylate (**7**) in a combination of enantioselective synthesis and kinetic resolution. The unreduced *1S*,*5R* enantiomer is selectively hydrolyzed by an esterase in the same yeast via a kinetic resolution process operating at a slightly slower rate than the reduction reaction, to provide a proposed β -keto acid intermediate (**8**). Subsequent non-enzymic decarboxylation leads to the observed achiral product, 7,7-(ethylenedioxy)bicyclo[3.3.0]-octan-3-one (**9**). The above process is an example of a competitive kinetic resolution of a racemate by two different enzyme catalyzed reactions (Scheme 6).



Scheme 6 Competitive kinetic resolution of a racemate catalyzed by yeast enzymes

E. Biocatalytic Resolutions in Biphasic Aqueous-organic Media

In a normal hydrolytic reaction, water is also a substrate. Its high relative concentration (55.5 M) drives the reaction toward completion at equilibrium. By replacing water with a biphasic aqueous-organic solvent reaction medium, the water activity is lowered and the thermodynamic equilibrium of the reaction is now shifted toward the synthetic direction (26). Moreover, if the product(s) has good solubility in the organic phase and poor solubility in the aqueous phase while the reactants have the opposite solubility behavior, the reaction is shifted even further toward esterification (27).

Several types of hydrolytic enzymes (proteases (28), amidases (29), lipases (30)) have been shown to catalyze stereospecific condensation reactions in such organic biphasic milieus. In particular, microbial lipases (EC 3.1.1.3) have been widely used for the resolution of racemic alcohols and carboxylic acids through esterification. These enzymes are relatively stable to non-polar organic media and catalyze reactions efficiently at the lipid/water interface.

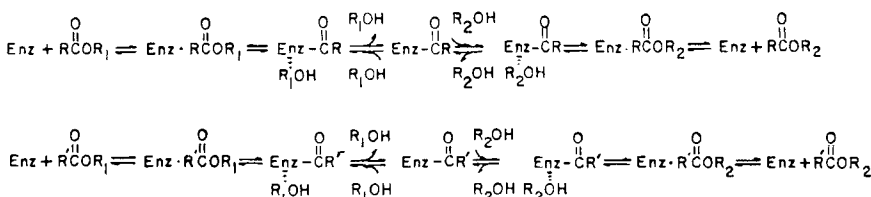
As shown in the previous section, the enantiomer ratio, E , may be calculated from the values of ee_S and ee_P using the homocompetitive eq. [4] for irreversible systems (9). This relationship also holds for lipases even though these enzymes do not behave according to classical Michaelis-Menten kinetics. As the surface active properties of enantiomers are identical, the net penetration rate of the enzyme into the interface is not affected by the changes in the relative concentrations of the enantiomers (31).

On the other hand, when hydrolases are used for kinetic resolutions via esterifications in aqueous-organic biphasic media, the reactions are reversible. Hence, a new expression which incorporates the important thermodynamic parameter K is required for the calculation of E (eq. [8]). The equilibrium constant, K , is directly related to the water content of the medium and determines the maximum obtainable chemical yield [$c = 1/(1 + K)$]. Although there is a general tendency to assume that if no exogenous water is added to the organic phase, reverse hydrolysis becomes negligible, in reality, the small quantity of residual water normally present in the enzymic protein and the water generated as the product of esterification are sufficient to serve as reagent for reverse hydrolysis (30b).

Several approaches may be used to minimize the reverse biocatalyzed hydrolysis. In principle, the addition of an excess amount of achiral acyl donor or acceptor to the medium could drive the reaction to completion, provided that the enzyme is not denatured under these conditions. However, it is more advantageous to select a particular acyl donor or acceptor, such that the product ester cannot be hydrolyzed efficiently by the enzyme. In such a case, there is a large difference in the specificity constants (k_{cat}/K_m) for the forward and reverse reactions, resulting in an equilibrium constant, $K = [(k_{cat}/K_m)_{reverse}]/$

$[(k_{\text{cat}}/K_m)_{\text{forward}}]$, that favors esterification. For example, in the lipase-catalyzed esterification of (\pm) -2-(*p*-chlorophenoxy)propionic acid with either *n*-butanol or cyclohexanol as the acyl acceptor, a much lower *K* value was observed for the cyclohexyl ester system (0.02 vs. 0.15). Apparently, the ester of a secondary alcohol is more resistant to enzymic hydrolysis than that of a primary alcohol (10).

The reaction mechanism and the enzymatic complexes in the kinetic resolution of racemic carboxylic acids or esters for an ordered mechanism via esterification may be envisaged as shown (Scheme 7) (R' = mirror image of R).



Scheme 7

Inherent in this reaction mechanism is the presence of two covalent bond-breaking and forming steps. It is to be noted that $\Delta\Delta G^\ddagger$ is the sum of the energy differences between all of the corresponding diastereomeric transition states ($\Delta\Delta G^\ddagger = \Delta\Delta G_1^\ddagger + \Delta\Delta G_2^\ddagger + \dots + \Delta\Delta G_{n-1}^\ddagger$). However, for the purpose of this illustration (Figure 6A), we have made the presumption that the energy differences between the transition states of the covalent bond-forming and breaking steps are the dominant ones ($\Delta\Delta G^\ddagger = \Delta\Delta G_1^\ddagger + \Delta\Delta G_2^\ddagger$). In reality, this need not be the case (see Figure 1B).

It is readily apparent from Scheme 7, that either the acid ($R_1=H$) or its corresponding ester ($R_1=CH_2R$) may be used as the acyl donor in enzyme-catalyzed esterification or transesterification reactions. Mechanistically, these two types of reactions proceed via different transition states for all the steps leading to and including the formation of the acyl-enzyme intermediates

($\text{Enz}-\overset{\text{O}}{\underset{\parallel}{\text{C}}}-\text{R}$ and $\text{Enz}-\overset{\text{O}}{\underset{\parallel}{\text{C}}}-\text{R}'$). Furthermore, the subsequent reaction of the

achiral alcohol, $R_2\text{OH}$, with $\text{Enz}-\overset{\text{O}}{\underset{\parallel}{\text{C}}}-\text{R}$ and $\text{Enz}-\overset{\text{O}}{\underset{\parallel}{\text{C}}}-\text{R}'$ to form the chiral

products $\overset{\text{O}}{\underset{\parallel}{\text{C}}}-\text{R}-\text{OR}_2$ and $\overset{\text{O}}{\underset{\parallel}{\text{C}}}-\text{R}'-\text{OR}_2$ also proceed via different transition states (Figure 6A). Hence, despite the apparent similarity, the *E* and *K* values for esterification and transesterification will be different and will be

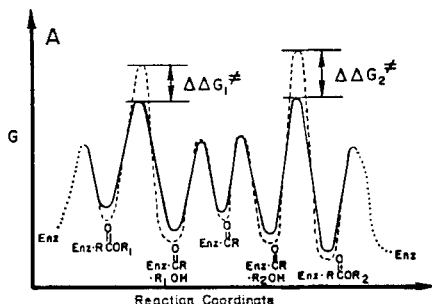
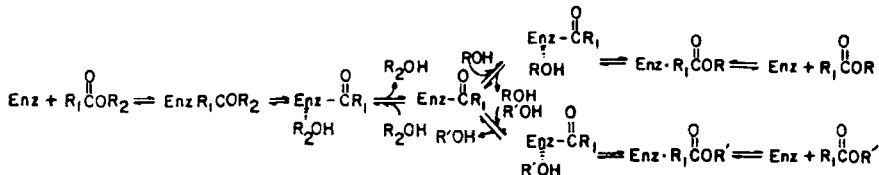


Figure 6A. Free energy profile depicting a hypothetical kinetic resolution of a carboxylic acid or ester via esterification or transesterification.

markedly influenced by the nature of the achiral alcohol (R_2OH). Moreover, by raising the concentration of the achiral alcohol, the reaction becomes virtually irreversible.

The reaction pathways for the kinetic resolution of two enantiomeric chiral alcohols (ROH and $R'OH$) (assuming an ordered mechanism) via esterification ($R_2=H$) or transesterification ($R_2=CH_2R$) is outlined in Scheme 8.



Scheme 8

In this case, the achiral acid ($R_2=H$) or the ester ($R_2=CH_2R$) forms the



same acyl-enzyme intermediate, $\text{Enz}-\text{C}-\text{R}_1$, which then reacts with the enantiomeric chiral alcohols to form the two energetically different transition states that determine the E value ($\Delta\Delta G^\ddagger$) (Fig. 6B). Consequently, the E value will be the same for esterification and transesterification reactions and will not be affected by changes in the concentration of the achiral acid, but the value of K will be different.

The physical state of the substrate has a pronounced effect on the enzymatic catalytic rate. For example, in a nonpolar organic medium, the ester substrate is fully dispersed and is less susceptible to enzymic lipolysis owing to

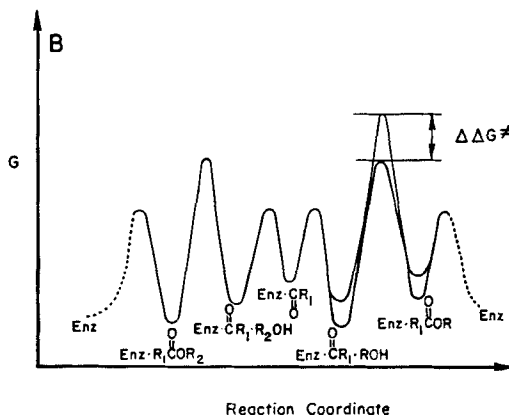


Figure 6B. Free energy profile illustrating a hypothetical kinetic resolution of a chiral alcohol via esterification.

the lack of a lipid-water interface. On the other hand, the acid substrate forms micelles or emulsions, which are readily attacked by the lipase. However, if the acid is insoluble in the organic medium, the reaction rate is markedly reduced because of the sluggish enzymatic action on a solid substrate.

Esterification takes place even in aqueous media. Therefore during the lipase-catalyzed hydrolysis of esters containing long-chain acids such as methyl laurate, reverse enzyme-catalyzed equilibration becomes prominent, and low optical and chemical yields are obtained (30a). A useful diagnostic indicator of a reversible biocatalytic kinetic resolution system is that the enantiomeric purity of the remaining substrate (ee_s) decreases when the conversion is extended beyond 50%. In contrast, in the irreversible case, ee_s increases as the conversion is extended.

All available experimental data appear to support the above theoretical considerations (IIB) in that the preferred sense of chirality for the forward and reverse reactions is usually maintained. For example, the ester of the $(-)-1R,2S,5R$ enantiomer of menthol was preferentially formed and hydrolyzed by the lipase of *Candida cylindracea*; likewise the $(+)-R$ enantiomer of 2-(*p*-chlorophenoxy)propionic acid and its ester were preferentially esterified and hydrolyzed respectively by the same lipase (10). However, in some organic solvents, the conformation of the enzyme protein may be drastically altered and a reversal of the preferred sense of chirality may be observed.

As far as the enantioselectivity for the forward and reverse reactions is concerned, the theory predicts that if the reaction conditions are identical, the E value for the forward and reverse reactions should be the same. However, in practice the E values are always different because the hydrolytic (water) and

the esterification (water-organic) reactions proceed through different transition states under different reaction conditions.

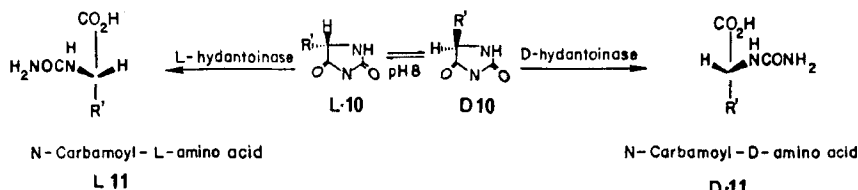
There are several inherent disadvantages associated with the esterification method. The enzyme has lower catalytic efficiency in biphasic media and a larger quantity of enzyme is required for the reaction. Also, the enzyme is unstable in polar organic media, so that only nonpolar solvents (such as *iso*-octane, hexane, cyclohexane) can be used. In addition, it is seldom possible to obtain the remaining substrate fraction in high enantiomeric purity ($ee \geq 0.98$) because of the problem of reversible biocatalysis. On the other hand, by selecting a suitable acyl donor or acceptor, enzyme-catalyzed esterification in biphasic media can be highly enantioselective. In many instances, the E values of esterification are higher than those of the corresponding enzymic hydrolysis of racemic esters. For example, in the *C. cylindracea* lipase-catalyzed hydrolysis of the butyl and cyclohexyl esters of (\pm) -2-(*p*-chlorophenoxy)propionic acid, the E values are 6 and 22, respectively, whereas the E values for the corresponding esterification are 12 and 80. Moreover, the experimental protocol is simple to execute because the acid and alcohol are added directly to the reaction mixture without prior chemical manipulation(s). Finally, substrate and product inhibition can often be alleviated in biphasic media. This method thus provides a useful alternative to the classical hydrolytic resolution procedure for the laboratory preparation of optically active compounds.

IV. SECOND-ORDER ASYMMETRIC TRANSFORMATIONS

As in all conventional resolution processes, enzymic or nonenzymic, the maximum obtainable yield of one pure enantiomer is 50%. However, if a reaction could be conducted under conditions wherein the substrate may be racemized *in situ*, it should then be possible to transform the substrate completely to the desired enantiomeric pure product. This approach not only obviates the tedious recycling steps of the undesired remaining enantiomer, but more importantly, the enantiomer excess of the product (ee_P) is now independent of the extent of conversion, c , and the process becomes apparently more enantioselective. For example, the ee_P at 50% conversion of a conventional enzymatic kinetic resolution with an E value of 10 is 0.67. Under *in situ* racemization conditions, the ee_P will remain at 0.82 throughout the conversion. This type of enzymatic second-order asymmetric transformation (32) has thus far been achieved only in a very limited number of cases.

The classic examples are the enzymatic synthesis of *L*- and *D*-amino acids from racemic 5-substituted hydantoins (33-35). Hydantoins (**10**) are readily racemized in dilute alkaline solution; for example, 5-phenyl-*D*-hydantoin is spontaneously racemized between pH 7.6 and 9.6 where the enzymatic hydro-

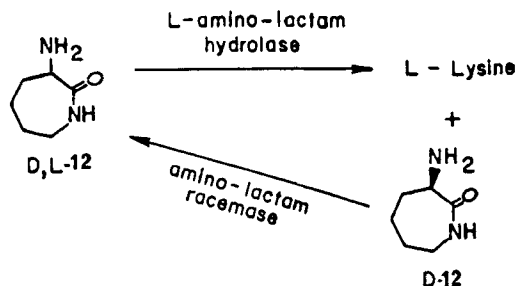
lysis occurs effectively. Consequently, if the *D*-isomer of hydantoins (*D*-10) is not hydrolyzed by the enzyme, a complete conversion of *DL*-hydantoin to *N*-carbamoyl-*L*-amino acid (*L*-10) is possible. Conversely, it is possible to prepare *N*-carbamoyl-*D*-amino acid (*D*-11) if the enzyme is specific for the *D*-isomer of hydantoins (Scheme 9).



Scheme 9 Enzymatic resolution of hydantoins

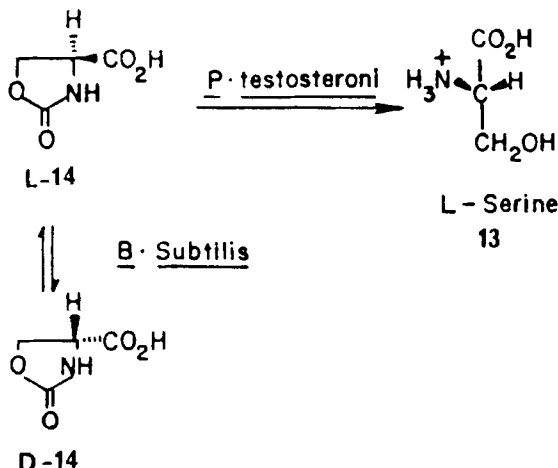
The enzyme dihydropyrimidinase (EC 5.3.2.2) catalyzes the hydrolytic ring-opening reaction of dihydropyrimidines to *N*-carbamoyl- β -amino acids. This enzyme also hydrolyzes several 5'-monosubstituted hydantoins to produce *N*-carbamoyl amino acids and is identical with hydantoinase (36). Because *L*- and *D*-hydantoinases are widely distributed among microorganisms, this approach has been used for the industrial synthesis of several *D*- and *L*-amino acids (33).

A combination of chemical and microbiological methods is used for the synthesis of *L*-lysine. *DL*- α -amino- ϵ -caprolactam (12) is obtained from cyclohexene in three chemical steps. Hydrolysis of the *L*-isomer by cells of *Candida humicola* containing *L*-specific α -amino- ϵ -caprolactamase produces *L*-lysine (*ee* = 0.96–1.0). The *D*- α -amino- ϵ -caprolactam (*D*-12) is racemized by a racemase from *Alkaligenes faecalis* (37) (Scheme 10).



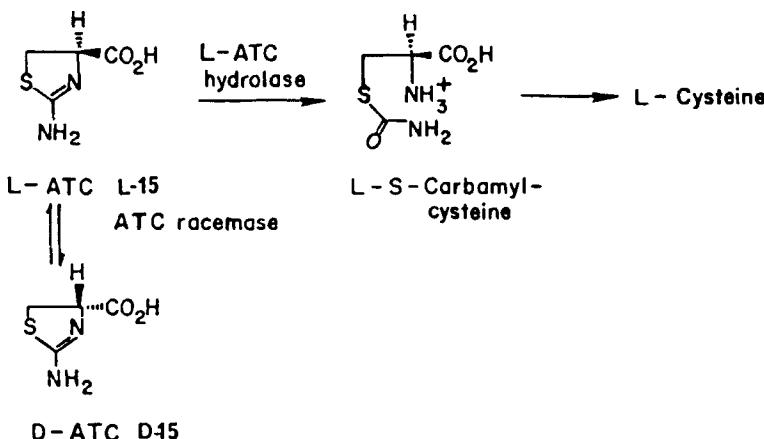
Scheme 10 Chemoenzymatic synthesis of *L*-lysine

A simple biochemical method for the production of *L*-serine (**13**) from *DL*-2-oxazolidine-4-carboxylic acid (**14**), an intermediate in the chemical synthesis of *DL*-serine has recently been reported. This procedure entails the hydrolysis of *L*-**14** to *L*-serine (**13**) by the microbe *Pseudomonas testosteroni* and the racemization of *D*-**14** to *DL*-**14** by *Bacillus subtilis* (38) (Scheme 11).



Scheme 11 Enzymatic synthesis of *L*-serine

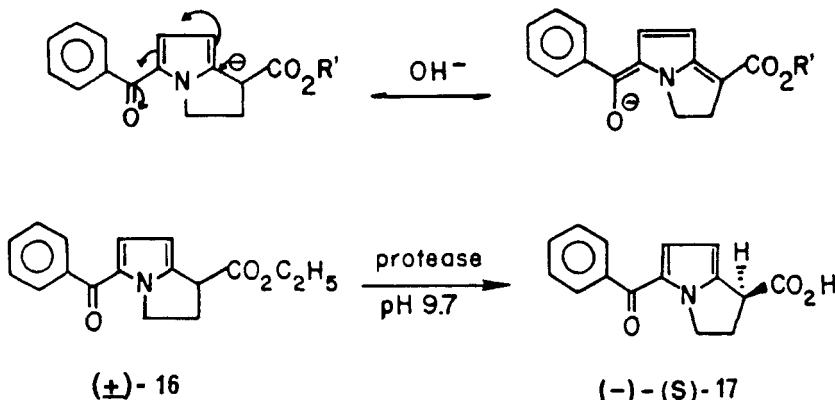
A similar enzymatic process has been developed for the industrial production of *L*-cysteine from *DL*-2-aminothiazoline-4-carboxylic acid (*DL*-ATC) (**15**), an intermediate in the chemical synthesis of *DL*-cysteine. In this case, both the *L*-ATC hydrolase and ATC racemase reside in the same microorganism, *Pseudomonas thiazolinophilum* (39) (Scheme 12).



Scheme 12 Enzymatic synthesis of *L*-cysteine

An example of enzymatic second order asymmetric hydrolysis of carboxylic esters (40) is the preparation of (-)-ketorolac (17), a potent antiinflammatory and analgesic agent (41). Because the chiral center in the ketorolac ester can be easily racemized under mildly basic conditions as a consequence of the resonance stabilization of the anion, it is a suitable substrate for *in situ* racemization followed by enantioselective enzymatic hydrolysis. The protease of *Streptomyces griseus* was found to be highly enantioselective in cleaving the ethyl ester grouping of the *S*-16 ($E = > 100$). By carrying out the enzymatic hydrolysis at pH 9.7, *in situ* racemization occurred and a 92% yield of the *S*-17 was obtained with an *ee* of 0.85.

One crystallization afforded the *S*-17 with *ee* = 0.94 (Scheme 13).



Scheme 13 Enzymatic preparation of (-)-ketorolac (17)

It is evident that when the chiral center of a racemic substrate can be racemized under either mildly acidic or mildly basic conditions or by a racemase, enzymatic enantio-convergent transformation may be used to convert a racemic substrate entirely into an enantiomerically pure product.

V. SELECTED EXAMPLES OF KINETIC RESOLUTIONS

In this section we describe some selected published examples to illustrate the usefulness of biochemical kinetic resolutions. Our focus here is on recent work pertaining to the preparation of optically active chirons that are of interest to synthetic chemists.

A. Acyclic Alcohols

In recent years, there has been increasing interest in the synthesis of small optically active fragments that can be incorporated into compounds of syn-

thetic and medicinal interest with retention of chirality. Optically active epichlorohydrin is a typical example; it is used for the synthesis of β -adrenergic blocking agents, insect pheromones, *L*-carnitine, etc. It is apparent that the ready availability of epichlorohydrin in enantiomerically pure forms would have wide applications in organic chiral syntheses. Although *R*- and *S*-epichlorohydrin had been successfully synthesized from the common intermediate, *R*-3-tosyloxy-1,2-propanediol, which in turn is obtained from *D*-mannitol, the overall synthesis requires many steps (42). Hence, many research groups have attempted the use of enzymatic methods for the preparation of this chlorohydrin.

A variety of enzymes and microorganisms were examined for the hydrolysis of (\pm)-1-acetoxy-2,3-dichloropropane (**18**), whose hydrolysis product is convertible to epichlorohydrin (43). All of the preparations showed *R*-stereochemical preference but low enantioselectivity (Table 6).

Several 3-substituted 1,2-diacetoxypropane derivatives (**19a**-**19c**) were subjected to enantioselective hydrolysis by many commercial lipase preparations (44). The most selective of these was found to be the lipoprotein lipase (Amano 40) (Table 7).

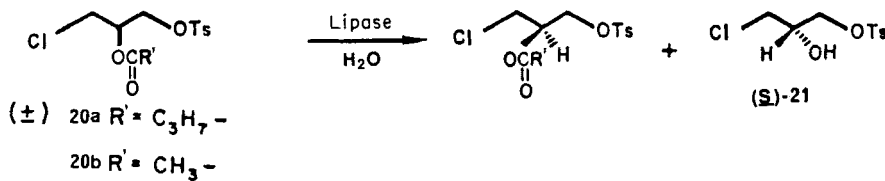
Table 6
Lipase-Catalyzed Hydrolysis of (\pm)-1-Acetoxy-2,3-dichloropropane (**18**)

$\begin{array}{c} \text{CH}_2\text{OAc} \\ \\ \text{CHCl} \end{array}$	$\xrightarrow{\text{H}_2\text{O}}$	$\begin{array}{c} \text{CH}_2\text{OH} \\ \\ \text{Cl}-\text{C}-\text{H} \\ \\ \text{CH}_2\text{Cl} \end{array}$	+	$\begin{array}{c} \text{CH}_2\text{OAc} \\ \\ \text{H}-\text{C}-\text{Cl} \\ \\ \text{CH}_2\text{Cl} \end{array}$
(\pm) - 18		(<i>R</i>) - 18		(<i>S</i>) - 18

Enzyme source	Conversion (%)	E
Porcine pancreatic lipase (Amano)	80 (17 h)	4
Mucor mucedo lipase (Amano)	87 (17 h)	2
Mucor angulisporus (IAM)	91 (96 h)	2
Equine pancreas acetone powder	81 (17 h)	4
Rabbit pancreas acetone powder	83 (17 h)	2

Evidently, structural variations at C-3 have a marked influence on enantioselectivity.

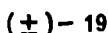
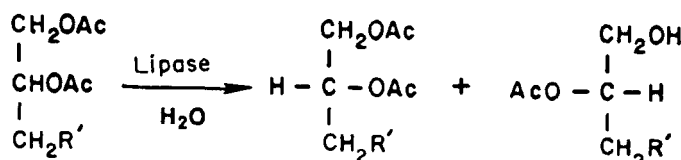
On the other hand, many commercial lipase preparations were found to catalyze the hydrolysis of (\pm)-2-acyloxy-3-chloropropyl *p*-toluenesulfonate (**20a,b**) to (*S*)-2-hydroxy-3-chloropropyl *p*-toluenesulfonate (**21**) with a



high degree of enantioselectivity (45). When both the *R*- and *S*-chirons of high optical purity are required, it is necessary to find a biocatalytic system with a high catalytic rate and high enantioselectivity (*E* = >100), so that a small amount of enzyme catalyzes the rapid turnover of a large amount of substrate to yield virtually a 1:1 substrate to product ratio (thermodynamic control, $k'_- \gg k'_+$). Although the lipases from *Aspergillus niger*, *Mucor sp.*, *Rhizopus delemar* and *Rhizopus japonicus* were all highly stereospecific, their hydrolytic rates were relatively slow resulting in incomplete hydrolysis and hence low enantiomeric purity of the residual starting ester.

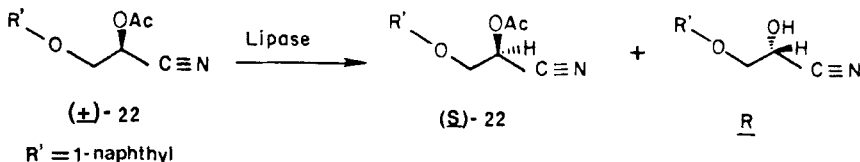
On the other hand, the lipoprotein lipase Amano 3 (LPL; *Pseudomonas aeruginosa*) was found to be uniquely suited for this resolution. In a typical experiment, 0.1 g of LPL was incubated with 10 g of (\pm) -2-butanoyloxy-3-chloropropyl *p*-toluenesulfonate (**20a**) in 90 ml of 0.1 M phosphate buffer, pH 7.25, at 33°C. The reaction was completed within 4 h to yield an approximately 1:1 ratio of substrate to product with an *E* value of >100. The acetyl ester (**20b**) was found to be a less suitable substrate because of its insolubility which resulted in slower conversion. The LPL biocatalytic system provides a facile method for the preparation of *R*- and *S*-epichlorohydrins.

Table 7
Hydrolysis of 3-Substituted 1,2-Diacetoxypropane Derivatives



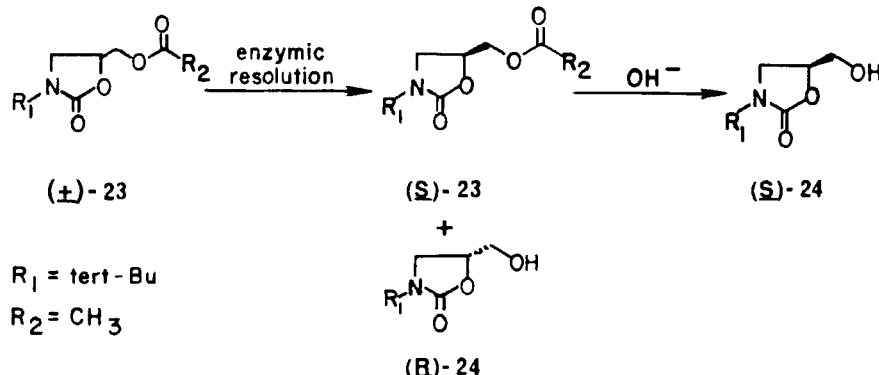
<u>R'</u>	<u>Stereochemical preference</u>	Conversion (%) (17 h)	E	
			19a	19b
Cl	R	75		5
Br	R	70		4
Ø	S	50		14

Cyanohydrins are versatile synthons because they can be readily converted to α -hydroxycarboxylic acids, α -hydroxyaldehydes, and ethanolamine derivatives, which include many pharmacologically active compounds. However, they are known to be rather unstable because they are in rapid equilibrium with the corresponding aldehydes and hydrogen cyanide (46). Hence, biochemical transformations have been used to prepare optically active cyanohydrins. A facile synthesis of (*S*)-(-)-propranolol was thus developed (47). The key intermediate, (*S*)-2-acetoxy-3- α -naphthoxypropionitrile (*S*-22), was



obtained via kinetic resolution using a lipase derived from *Pseudomonas sp.* ($E = 10$) at pH 5.0. A *Bacillus sp.* also preferentially cleaved the *R*-22 and the enantioselectivity was improved by altering the R' group (48) (Table 8).

Since (*S*)-5-hydroxymethyl-3-alkyloxazolin-2-one (*S*-24) is a valuable intermediate for the synthesis of optically active (*S*) beta-blockers, a number of enzymes and microorganisms were evaluated for the enantioselective hydrolysis of (\pm) -5-acetoxymethyl-3-*tert*-butyl-oxazolidin-2-one (23) (Scheme 14).



Scheme 14 Biocatalytic resolution of (\pm) -5-acetoxymethyl-3-*tert*-butyl-oxazolidin-2-one (23)

Among the commercially available lipases examined, all exhibited *R* stereochemical preference (for *R*-24) and catalyzed the hydrolysis with a moderate degree of enantioselectivity. The best one was the lipase PL 266, derived from *Alcaligenes sp.* which showed an E value of 7 (49) (Table 9).

Of about 600 species of microorganisms (bacteria yeast and molds) that were examined, the *Enterobacter* and *Klebsiella* species were found to cata-

Table 8
Microbial Preparation of Optically Active Cyanohydrins

	<u>R'</u>	<u>Conversion (%)</u>	<u>E</u>
22a	C ₆ H ₅	55 (12 h)	29
22b	p-MeC ₆ H ₄	59 (12 h)	17
22c	m-MeC ₆ H ₄	48 (48 h)	75

lyze this kinetic resolution with modest enantioselectivity—*E* values ranging from 4–8 depending on the strain used. However, the rates of hydrolysis were rather low (49) (Table 10).

In an attempt to improve the enantioselectivity of this resolution, the substituents *R*₁ and *R*₂ on the oxazolidinone nucleus (23a–23f) were varied (50). The redesigned substrates were exposed to the lipoprotein lipase (LPL) of *P. aeruginosa* (Amano 3) (Table 11).

It is apparent that LPL is more specific towards substrates with a longer saturated aliphatic ester (23b, 23c, 23e, 23f)—the *E* value improved from 7 to 16. Moreover, the hydrolytic rate was also enhanced 3–6 fold.

Optically active 3-chloro-2-methyl-1-propanol is an important intermediate in the synthesis of the psychotropic drug Nozidan. Several commercial lipases were evaluated for their abilities to catalyze the hydrolysis (±)-3-chloro-2-methylpropyl propionate. Lipases derived from *Candida cylindra-*

Table 9
Lipase-Catalyzed Hydrolysis of (±)-5-Acetoxymethyl-3-*tert*-butyl-oxazolidin-2-one (23)

<u>Enzyme</u>	<u>Conversion (%)</u>	<u>E</u>
Lipoprotein lipase (LPL, Amano 3)	70 (6 h)	7
Lipase PL 266 (<i>Alcaligenes sp.</i>)	71 (10 h)	7
Lipase AL (<i>A. chromobacter sp.</i>)	65 (24 h)	2
Pancreatin	86 (24 h)	2

Table 10
Microbial Hydrolysis of (\pm)-5-Acetoxymethyl-3-*tert*-butyl-oxazolidin-2-one (23)

<u>Microorganism</u>	Conversion (%) (6 h)	<u>E</u>
<i>Enterobacter aerogenes</i> IFO 13534	78	5
<i>Enterobacter cloacae</i> IFO 3320	80	4
<i>Klebsiella pneumoniae</i> IFO 3512	80	6
<i>Klebsiella pneumoniae</i> IFO 12059	74	7
<i>Klebsiella pneumoniae</i> IFO 12932	81	6
<i>Klebsiella pneumoniae</i> IFO 13541	70	8

Table 11
Improvement of Enantioselectivity by Changing Substituents on the
Oxazolidinone Nucleus

<u>Substrate (23)</u>	Conversion (%) (18 h)	<u>E</u>
R ₁ = <u>tert</u> -Bu		
23a R ₂ = (CH ₃) ₂ CH	83	5
23b R ₂ = n-C ₅ H ₁₁	65	16
23c R ₂ = n-C ₇ H ₁₇	65	16
R ₁ = <u>iso</u> -Pro		
23d R ₂ = (CH ₃) ₂ CH	75	8
23e R ₂ = n-C ₅ H ₁₁	65	16
23f R ₂ = n-C ₇ H ₁₇	64	17

Table 12
Lipase-Catalyzed Hydrolysis of (\pm)-3-chloro-2-methylpropyl Propionate

<u>Lipase</u>	<u>Conversion (%)</u>	<u>E</u>
Porcine pancreas (PPL)	20	11
	38	7
	81	3
<i>Rhizopus arrhizus</i>	7	5
	13	4
<i>Rhizopus delemar</i>	11	3
	45	2
	76	3

cea, *Penicillium camemberti*, and *Geotrichum candidum* were found to be completely nonenantioselective whereas lipases from porcine pancreas and *Rhizopus sp.* preferentially cleaved the levorotatory enantiomer but showed low to moderate enantioselectivity (51) (Table 12).

In the case of PPL, the *E* value decreased from 11 to 3 as the reaction proceeded to higher conversion. This observation suggests the presence of competing enzymes of opposite stereochemical preference in the crude porcine pancreatic preparation. The length of the fatty acid moiety has an influence on the enantioselectivity. The *E* value decreased from 6 for the acetyl and propionyl esters, to 2 for the lauryl and oleyl esters.

In connection with the synthesis of erythronolide A, a number of (\pm)-methyl *syn* and *anti*-2-methyl-3-acetoxy-propionate derivatives (25) were exposed to the lipase preparations (Amano A and A-6) from *Aspergillus niger* (52) (Tables 13 and 14).

The data clearly show that both commercial lipase preparations were effective in catalyzing the kinetic resolution of the (\pm)-*syn* and *anti*-propionate derivatives to yield valuable building blocks containing two chiral centers of high stereochemical homogeneity. With one exception (25*i*), the 3*S* acetates were hydrolyzed more rapidly than the 3*R* acetates and far more rapidly than the methyl ester group. The configuration of the methyl group at C-2 did not appear to affect the enantioselectivity.

The absolute configurations of the optically active 2-, 3-, and 2,5-alkylcyclohexanols were assigned using this stereochemical behavior.

All of the above data are consistent with the notion that lipase-catalyzed enantioselective hydrolyses of primary esters proceed with low to moderate enantioselectivity. High *E* values are obtained in hydrolytic resolutions only when the ester group is attached directly to the asymmetric carbon.

Table 13
Lipase-Catalyzed Kinetic Resolution (\pm)syn-25

			Lipase	Conversion (%)	E
25a		A	53 (5 h)	28	
		A-6	47 (3 h)	23	
25b		A	57 (8 h)	19	
		A-6	34 (8 h)	12	
25c		A	40 (24 h)	8	
		A-6	57 (24 h)	11	
25d		A	61 (27 h)	23	
		A-6	72 (27 h)	10	
25e		A	55 (24 h)	17	
		A-6	46 (8 h)	18	

Table 14
Lipase-Catalyzed Kinetic Resolution (\pm)anti-25

			$\xrightarrow[\text{H}_2\text{O}]{\text{Lipase}}$	
		(\pm) Anti (2S,3R)-25 (2R,3S)-25		
25f			A	57 (6.5 h) 31
			A-6	60 (6 h) 20
25g			A	54 (8 h) 64
			A-6	55 (8 h) 46
25h			A	42 (28 h) >100
			A-6	56 (28 h) 44
			$\xrightarrow[\text{H}_2\text{O}]{\text{Lipase}}$	
		(\pm) Anti (2S,3R)-25 (2R,3S)-25		
25i			A	36 (24 h) 70
			A-6	47 (24 h) 47

B. Cyclic Alcohols

Oritani and Yamashita (53) have conducted extensive studies on the microbial resolutions of racemic cyclic terpene alcohols. They observed that microorganisms generally cleave equatorial acetates. Thus, acetates of conformationally stable axial cyclohexanols are not hydrolyzed whereas axial acetates that can be ring-inverted to equatorial conformations are readily cleaved. The authors divided the six-member ring terpene alcohols into two types, type A and type B (the enantiomer of type A). The acetates of optically active alco-

Table 15
Microbial Resolution of Alkylcyclohexyl Acetates

Compound	R ₁	R ₂	R ₃	R ₄	Configuration at Carbinol Center	
					Type A	Type B
<u>trans</u> -2-Methylcyclohexanol	H	H	H	CH ₃	R	S
<u>cis</u> -2-Methylcyclohexanol	H	H	CH ₃	H	S	R
Carvomenthol	CH(CH ₃) ₂	H	H	CH ₃	R	S
Isocarvomenthol	H	CH(CH ₃) ₂	H	CH ₃	R	S
Neoisocarvomenthol	CH(CH ₃) ₂	H	CH ₃	H	S	R
Menthol	CH ₃	H	H	CH(CH ₃) ₂	R	S
Isomenthol	H	CH ₃	H	CH(CH ₃) ₂	R	S
Neoisomenthol	CH ₃	H	CH(CH ₃) ₂	H	S	R
Isopulegol	CH ₃	H	H	C(=CH ₂)CH ₃	R	S
Iso-isopulegol	H	CH ₃	H	C(=CH ₂)CH ₃	R	S
Neoiso-isopulegol	CH ₃	H	C(=CH ₂)CH ₃	H	S	R
<u>cis</u> -3-Methylcyclohexanol	CH ₃	H	H	H	R	S
<u>trans</u> -3-Methylcyclohexanol	H	CH ₃	H	H	S	R

The absolute configuration of the optically active 2-, 3-, and 2,5-alkylcyclohexanols were assigned using this stereochemical behavior.

holts belonging to type A are easily hydrolyzed but their antipodes belonging to type B are not easily hydrolyzed by the enzyme (Table 15).

(-)-Menthol [(-)26] is one of the most important terpene alcohols and is used extensively in the perfumery, pharmaceutical, and flavoring industries. As chemical synthesis leads to racemic 26 (undesirable flavor), optical resolution methods have been used to obtain (-)-26 on an industrial scale (54). Biochemists have conducted extensive studies using microbial esterases to resolve kinetically various (\pm)-menthyl esters (27). Numerous microorganisms were shown to cleave various esters of (\pm)-menthol, such as formates, acetates, propionates, caproates, and esters of higher fatty acids (27a-e) enantioselectively. The best microorganism was the yeast *Rhodotorula mucilaginosa* AHu 3243 which was highly selective towards the (-)-isomer ($E = > 100$). However, the E value decreased as the size of the ester increased (55) (Table 16).

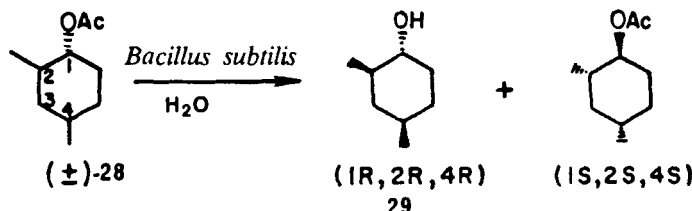
The reaction velocity could be enhanced by the use of α -haloacid esters of menthol (55); (\pm)-menthyl succinate was used as substrate to facilitate product recovery (57). (\pm)-Isopulegyl acetate or chloroacetate was hydrolyzed by *Pseudomonas sp.* NOF-5 to (-)-isopulegol in 40–45% yield in 3 days with an E value of > 100 (58).

Bacillus subtilis var. *niger* catalyzed the enantioselective hydrolysis of the acetate of (\pm)-*t*-2, *t*-4-dimethyl-*r*-1-cyclohexanol (28) to give (-)-(1*R*,2*R*,4*R*)-

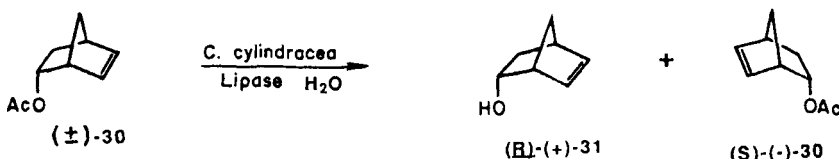
Table 16
Microbial Hydrolysis of (\pm)-Menthyl Esters (27)

(\pm) -27	R'	(-)-Menthol (-)-26	
		Conversion (%) (48 h)	E
27a	CH ₃	42	> 100
27b	C ₅ H ₁₁	20	33
27c	C ₉ H ₁₉	16	11
27d	C ₁₃ H ₂₇	17	4
27e	C ₁₇ H ₃₃	19	3

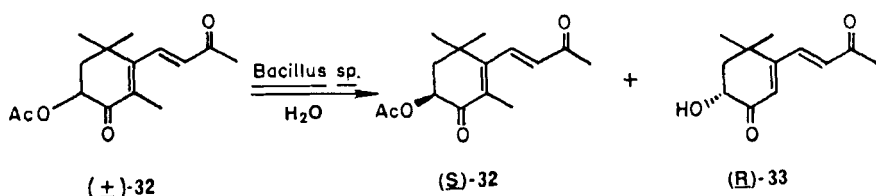
2,4-dimethyl-1-cyclohexanol (**29**) in 49.5% yield in 2 days ($E = >100$), which was chemically converted into the ketone for the synthesis of the anti-fungal antibiotic cycloheximide (**59**).



A multigram preparation of (+)-endo-norbornenol (**31**) and (-)-endo-norbornenyl acetate (*S*-**30**) with optical purities of 90% and 95% respectively was accomplished by hydrolysis of (\pm)-5-endo-norbornen-2-yl acetate (**30**) using the lipase of *Candida cylindracea* (60). Although the E value was moderate ($E = 35$), reasonable chemical and optical yields for both (*R*)-(+)-**31** and (*S*)-(−)-**30** were obtained by using the following recycling strategy. Enzymatic hydrolysis was terminated at 40% conversion; this furnished (+)-**31** with $ee_P = 0.90$. The recovered enriched (*S*)-**30** was again subjected to enzymatic hydrolysis until an additional conversion of 20% was obtained (60% of the starting (\pm)-**30** had then been consumed); the remaining (*S*)-(−)-**30** was shown to have $ee_S = 0.96$.



For the synthesis of astaxanthin, a carotenoid pigment prepared from β -ionone, a microbiological resolution of (\pm)-3-acetoxy-4-oxo- β -ionone (**32**) was developed. A bacterium soil isolate, identified as a *Bacillus* sp., showed exceptionally high enantioselectivity. This strain cleaved (*R*)-**32** to yield the enantiomerically pure 3-hydroxy-4-oxo- β -ionone (**33**); (*S*)-**32** of the racemate (\pm)-**32** was not hydrolyzed ($E = >100$) (54, 61).

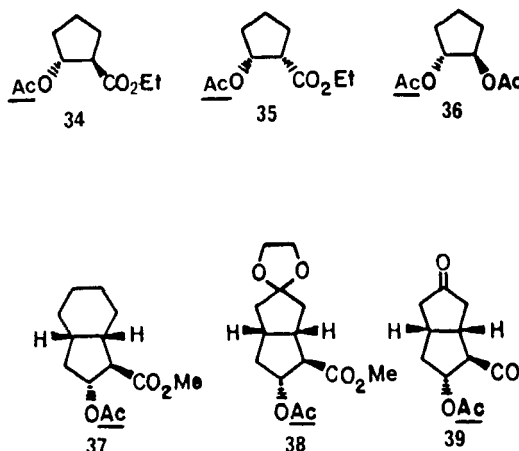


Recently, Schneider (24b) reported the enzymatic hydrolysis of (\pm)-*trans*-1-hydroxy-2-acetoxycyclohexane with pig liver esterase (PLE), but the reaction proceeded with low enantioselectivity ($E = 2$). On the other hand, the lipase of *Pseudomonas fluorescens* (Amano) catalyzed the acetate hydrolysis of several (\pm)-acetoxycyclopentanes (**34–39**) to give the corresponding alcohols of high enantiomeric purities. The lipase hydrolyzed acetates of the *R* configuration (62) (Table 17).

C. Cyclic Allylic Alcohols

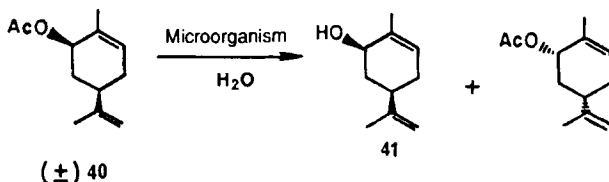
The acetate of (\pm)-2-cyclohexenol, the basic ring structure of (\pm)- β,γ -unsaturated cyclic terpene alcohols, is hydrolyzed by microorganisms or enzymes to

Table 17
Hydrolysis of (\pm)-Acetoxycyclopentanes Catalyzed by *Pseudomonas* Lipase



<u>Substrate</u>	<u>Conversion (%)</u>	<u>E</u>
34	32 (6 h)	>100
35	46 (1.5 h)	>100
36	49 (8 h)	>100
37	48 (24 h)	>100
38	15 (56 h)	3
39	13 (27 h)	9

yield (\pm)-2-cyclohexenol ($E = 1$) (65). It appears that a β -substituent on the ring of (\pm)-2-cyclohexenyl acetate is required to attain high enantioselectivity. Thus, the acetate of (\pm)-*cis*-carveol (**40**) was hydrolyzed by several microorganisms to yield (2*R*)-(–)-*cis*-carveol (**41**) of high enantiomeric purity (63) (Scheme 15).

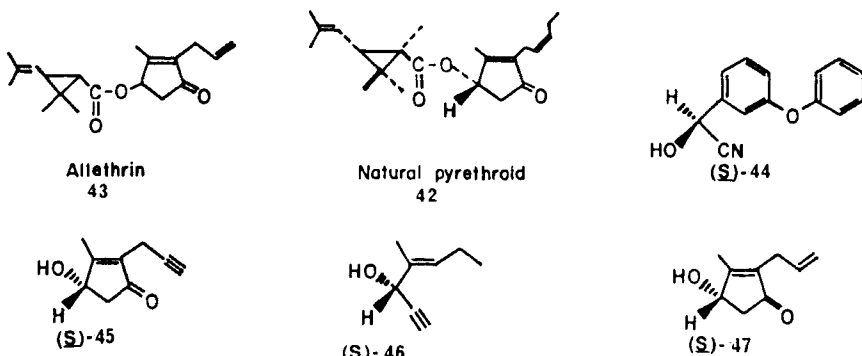


	Conversion (%) (48 h)	<i>E</i>
<i>Bacillus subtilis</i> var. <i>niger</i>	33	67
<i>Candida cylindracea</i>	37	25
<i>Trichoderma</i> sp.	30	>100

Scheme 15 Microbial hydrolysis of (\pm)-40

In the field of fine chemicals, optically active hydroxycyclopentenones are important intermediates for the synthesis of insecticides, perfumes, and pharmaceuticals (i.e., allethrin, *cis*-jasmone, prostaglandins, etc.).

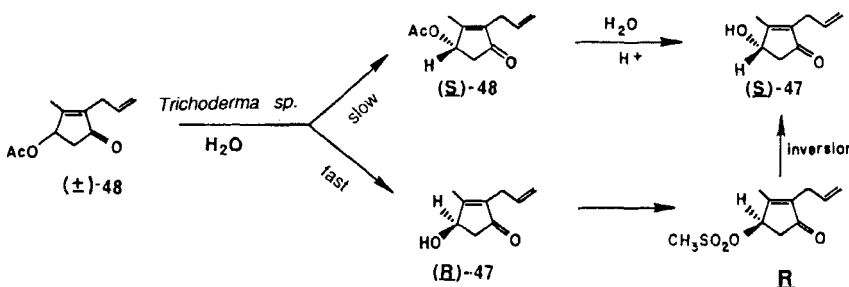
Synthetic pyrethroids are a group of esters with potent insecticidal activities (64). Allethrin (**43**), a synthetic analog of natural pyrethrin-I (**42**), is a typical member of this family. The insecticidal activity of allethrin (**43**) depends on the configuration of the alcohol moiety, allethrolone (**47**). The (+)-



S-allethrolone [(+)-(S)-47] ester has stronger insecticidal activity than the ester of its enantiomer.

Through structural modification of the pyrethroid alcohol moiety, a variety of improved synthetic pyrethroid insecticides was developed (65). These industrially important chiral secondary alcohol moieties besides allethrolone are: 4-hydroxy-3-methyl-2-propargyl-2-cyclopentenone (**45**), α -cyano-3-phenoxybenzyl alcohol (**44**), and 1-ethynyl-2-methyl-2-penten-1-ol (**46**). In all these cases, the *S*-alcohols are insecticidally dominant over their respective enantiomers.

An important resolution process for the preparation of (+)-(S)-47 was achieved via the hydrolysis of (\pm)-O-acetylallethrolone (**48**) catalyzed by the esterase of *Trichoderma sp.* (66). In this procedure, (*R*)-47 is produced and (*S*)-48 remains.



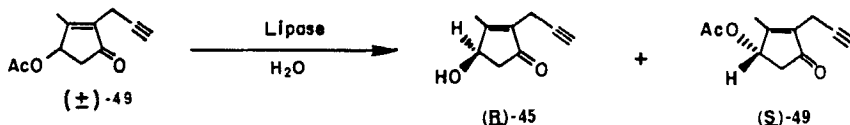
Hence, chemical hydrolysis of (*S*)-48 and inversion of (*R*)-47 via the mesylate are required. The *E* value of this system was calculated to be 40. When (\pm)-O-formyl-allethrolone was used as the substrate, the *E* value dropped to 3.

Through the screening of several hundred microorganisms, a large number of microbes were found to hydrolyze (\pm)-49 (p. 108) asymmetrically. With the exception of *Saccharomyces fragilis* which has an *S*-stereochemical preference, all the other microorganisms examined hydrolyzed (*R*)-49 preferentially. The *E* values ranged from 3 to 22.

The behavior of commercial microbial lipases was examined for the resolution of (\pm)-49. Several of these afforded (*R*)-45 and (*S*)-49 of high enantiomeric purity (67).

Lipases from *Arthrobacter sp.*, *Pseudomonas sp.*, and *Alcaligenes sp.* gave remarkably high enantiomeric purities at around 50% conversion. This suggested that these enzymes are highly enantioselective towards (*R*)-49 whereas (*S*)-49 binds very poorly or not at all to the enzyme. The *Arthrobacter* lipase catalyzed hydrolysis proceeded even at a substrate concentration of as high as 80% in H_2O and this particular reaction stopped practically at 50% conversion where (*R*)-49 was consumed completely. With respect to the

Lipase	Conversion (%) (23 h)	E
<i>Arthrobacter sp.</i> SNK	50	>100
<i>Pseudomonas sp.</i> Amano "P"	47	100
<i>Alcaligenes sp.</i> Meito "PL"	47	>100
<i>Chromobacterium sp.</i> Toyo "LP"	55	>100
<i>Humicola sp.</i> Amano "CE"	47	15



chain length of the acid moiety, the enantioselectivity of the hydrolysis with this lipase was not influenced by the chain length at all. These results imply that this enzymatic process could be used for the optical resolution of (\pm) -49 on an industrial scale. Advantages are the high enantiomeric purity of the products and the high substrate concentration; in addition, the process is catalytic. Moreover, the reaction is easily controlled by starting or stopping vigorous stirring. Finally, no organic solvents were included in the reaction mixtures which consist of two liquid phases. This makes the product recovery easy.

It is interesting to note that the enantioselective hydrolyses of (\pm) -48 by various microorganisms and lipases were similar to those of (\pm) -49. The highest enantiomeric purity of the liberated (R) -47 was obtained with the *Arthrobacter* lipase as for (R) -45. However, the reaction rates of (\pm) -48 were about one-third to two-thirds of those for (\pm) -49, depending on the particular lipase. Kinetic analysis revealed that this was due to a decrease in V_{max} for (\pm) -48 whereas the difference in the K_m for the two acetates was small. This indicates that the change of the propynyl to a propenyl group at the C-2 position retards the cleavage of the ester bond but does not affect the binding of the substrates to the enzyme (67).

A new synthetic route for 2-substituted-4-hydroxycyclopentenones (**51**) via molecular rearrangement of 2-furylcarbinols (**50**) has been reported (68). Because optically active **51** is needed, the tertiary alcohol precursor was acetylated to yield **52** (Table 18), which is subjected to enzymatic resolution.

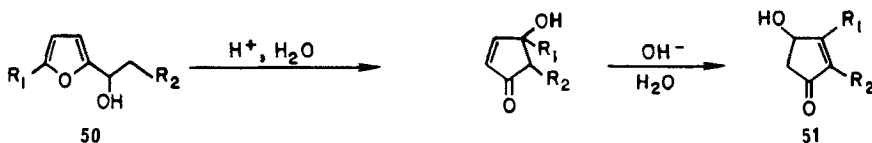


Table 18
PLE-catalyzed Hydrolysis of (\pm)-52

 $(4R, 5S)$ -52 $(4S, 5R)$ -52	$\xrightarrow[\text{H}_2\text{O}]{\text{PLE}}$	
	<u>R'</u>	<u>Conversion (%)</u>
52a	CH ₃	31 (24 h)
52b	n-C ₅ H ₁₂	43 (20 h)
52c	1-Pentenyl	43 (24 h)
52d	1-Butynyl	46 (20 h)
		<u>E</u>
52a	CH ₃	34
52b	n-C ₅ H ₁₂	>100
52c	1-Pentenyl	>100
52d	1-Butynyl	>100

While it is generally perceived that tertiary esters are difficult to hydrolyze enzymically, pig liver esterase (PLE) was found to hydrolyze (\pm)-(4*R*^{*},5*S*)-4-acetoxy-4-methyl-5-substituted-2-cyclopenten-1-one (52) with a high degree of enantioselectivity to yield (4*S*,5*R*)-53 and (4*R*,5*S*)-52 (67). The enantioselectivity improved as *R'* increased in size.

A variety of microorganisms were also found to catalyze the hydrolysis of (\pm)-(4*R*^{*},5*S*)-4-acetoxy-4-methyl-5-allyl-2-cyclopenten-1-one (54) with varying degrees of enantioselectivity (69). All of them have the same stereochemical preference as PLE; the notable exception being *Pseudomonas fragi* which afforded the 4*R*,5*S*-isomer of 55 (Table 19).

The optically pure (4*S*,5*R*)-55 can be readily and stereospecifically isomerized to yield (*S*)-2-allyl-3-methyl-4-hydroxy-cyclopenten-1-one (56) (*ee* = 0.97) (70).

For the 4-normethyl series (57), different microorganisms were required to catalyze the enantioselective hydrolysis. The most suitable one was a *Pseudomonas sp.* which was highly selective for the 4*R*-acetate (*E* = >100) (71).

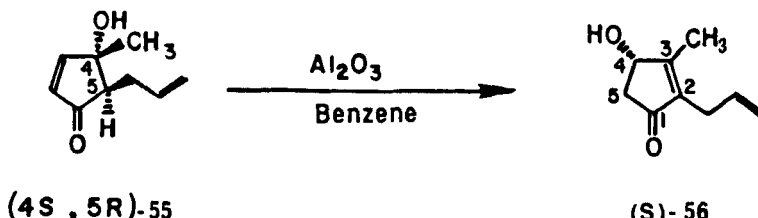


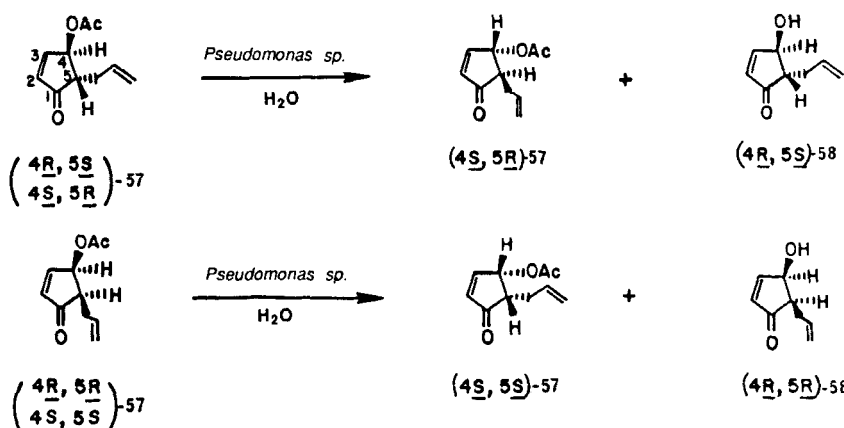
Table 19
Microbial Hydrolysis of (\pm)-4-Acetoxy-4-methyl-5-allyl-2-cyclopenten-1-one (54)

Microorganism	Stereochemical Preference	Conversion (%) (48 h)	E
<i>Hansenula anomala</i> var. <i>ciferrii</i>	4S,5R	39	>100
<i>Pleurotus ostreatus</i>	4S,5R	31	39
<i>Metschnikowia pulcherrima</i>	4S,5R	40	95
<i>Candida krusei</i>	4S,5R	41	>100
<i>Pseudomonas fragi</i>	4R,5S	24	48

Apparently, the enzyme is not affected by the sense of chirality at C-5. Since both (4*R*,5*S*)- and (4*R*,5*R*)-58 can be easily isomerized to 4*R*-hydroxy-2-allylcyclopentenone, this synthetic route can be easily adapted for the preparation of optically active prostaglandins.

D. Acyclic α,β -Unsaturated Alcohols

α -Cyano-3-phenoxybenzyl alcohol (44) is the alcohol moiety of the highly potent insecticides, fenvalerate (α -cyano-3-phenoxybenzyl 2-(4-chlorophenyl)-



3-methylbutyrate) (**60**) (72) and cypermethrin (α -cyano-3-phenoxybenzyl chrysanthemate) (73). The results of the enantioselective hydrolysis of (\pm)-**59** acetate by commercial lipases are tabulated below (67) (Table 20).

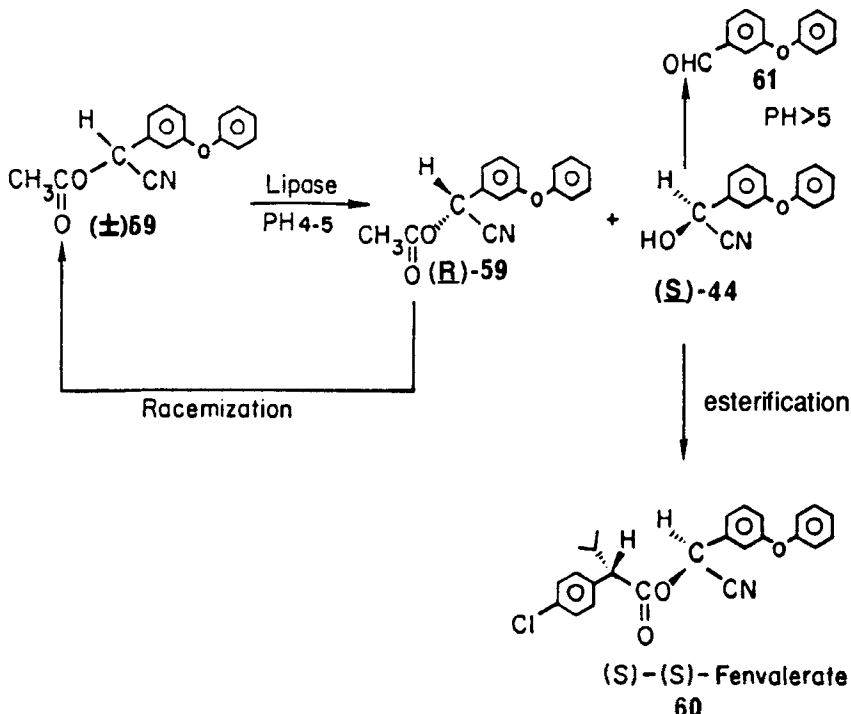
Table 20
Enzymatic Preparation of α -Cyano-3-phenoxybenzyl Alcohol (**44**)

<u>Lipase</u>	<u>Stereochemical Preference</u>	<u>Conversion (%)</u>	<u>E</u>
<i>Arthrobacter sp.</i> SNK	<u>S</u>	49 (7 h)	>100
<i>Pseudomonas sp.</i> Amano "P"	<u>S</u>	50 (23 h)	88
<i>Alcaligenes sp.</i> Meito "PL"	<u>S</u>	50 (23 h)	98
<i>Chromobacter sp.</i> Toyo "LP"	<u>S</u>	50 (23 h)	>100
<i>Achromobacter sp.</i> Meito "AL"	<u>S</u>	48 (23 h)	79
<i>Candida cylindracea</i> Meito "MY"	<u>R</u>	51 (23 h)	12

Most of the lipases tested preferentially cleaved (*S*)-**59** to give the insecticidally active (*S*)-**44**, the stereochemistry being different from the case of **45** or **47**. The highest enantioselectivity and particularly spontaneous termination of the reaction at 50% conversion was observed with the *Arthrobacter* lipase as it was for **49** and **48**. Although the activity of the lipase was not significantly changed in the range of pH 4 to 7, phenoxybenzaldehyde (**61**) is liberated from (*S*)-**44** in an undesirable side reaction especially at a pH higher than 5. Hence, the reaction is carried out at a pH between 4 and 5. Esterification of (*S*)-**44** with (*S*)-2-(4-chlorophenyl)-3-methylbutyryl chloride produced the most potent stereoisomer of fenvalerate (**60**). The compound (*R*)-**59** is easily racemized by organic base without producing the aldehyde and can thus be recycled (Scheme 16).

Finally, it is interesting to consider why the (*S*)-**59** was enantioselectively cleaved, in contrast to the case of (*R*)-**49**. The actual bulkiness of the groups attached to the asymmetric carbon follows the order of

| |
-C(CH₃)=C-CH₂C≡CH > -CH₂-C=O in **45** and - ϕ -o- ϕ > -C≡N in **44**.
Thus, the binding of (*S*)-**59** to the active site of the enzyme and the positioning of the carbonyl group are similar to those of (*R*)-**49**. The *R* and *S* designations are simply due to a change in the sequence rule. As far as the physiologically active enantiomer is concerned, the stereochemistry of the (*S*)-**44** is opposite to that of (*S*)-**45** when one considers the hydrogen and hydroxyl groups attached to the respective asymmetric carbon atoms.



Scheme 16 Chemoenzymatic synthesis of *(S)-(S)*-fenvaleterate

1-Ethynyl-2-methyl-2-penten-1-ol (**46**) is the α -ethynyl type of secondary alcohol moiety of empenthrin (1-ethynyl-2-methyl-2-pentenyl (*1R*)-chrysanthemate) (74). In studies of the resolution of the acetate of (\pm) -**46** using commercial lipases, *(R)*-**46** of high optical purity was obtained with the lipases from *Arthrobacter sp.* and *Pseudomonas sp.* However, the reaction rate and the enantioselectivity were lower than those for **49**.

A number of (\pm) -acetylenic acetates were subjected to *Bacillus subtilis* var. *niger* for kinetic resolution. In every case, the same sense of chirality was observed (Table 21) (75). Substrates with aliphatic and phenoxyphenyl side chains gave moderate *E* values ($= 2-20$). Among the regioisomers of 1-(allylphenyl)-1-(3-propyn)-1-ols, only the acetate of the *p*-isomer was hydrolyzed with high enantioselectivity ($E = 47$).

E. (\pm) -Carboxylic Acids

Several synthetically useful bifunctional chiral synthons were prepared via hydrolysis of their racemic carboxylic esters (13a) (Table 22). These optically

Table 21
Enantioselective Hydrolyses of (\pm)-Acetylenic Acetates by *Bacillus subtilis* var. *niger*

$\begin{array}{c} \text{R}_1 \\ \\ \text{C}\equiv\text{C}-\text{CH}_2-\text{OAc} \end{array}$ (\pm)	$\begin{array}{c} \text{R}_1 \\ \\ \text{C}\equiv\text{C}-\text{CH}(\text{H}, \text{OH})-\text{OAc} \end{array}$	E
C ₂ H ₅	57 (72 h)	7
n-C ₃ H ₇	57 (72 h)	16
n-C ₄ H ₉	53 (72 h)	2
n-C ₈ H ₁₇	30 (72 h)	2
(CH ₃) ₂ C=CH(CH ₂) ₂	46 (72 h)	3
$\begin{array}{c} \text{CH}_3 \\ \diagdown \\ \equiv-\text{CH}_2-\text{CH}=\text{C}(\text{CH}_3) \\ \diagup \quad \text{Y} \end{array}$	60 (96 h)	20
$\begin{array}{c} \text{CH}_3 \\ \diagdown \\ \text{CH}_3\text{CH}_2\text{CH}=\text{CH}(\text{CH}_3) \\ \diagup \quad \text{Y} \end{array}$	48 (23 h)	13
$\begin{array}{c} \text{C}_6\text{H}_5-\text{O}-\text{C}_6\text{H}_5 \\ \diagdown \quad \diagup \\ \text{Y} \end{array}$	65 (19 h)	11
$\begin{array}{c} \text{C}_6\text{H}_5-\text{CH}_2-\text{CH}_2-\text{CH}_2-\text{CH}_2-\text{CH}_2-\text{CH}_2-\text{C}_6\text{H}_5 \\ \diagdown \quad \diagup \\ \text{Y} \end{array}$	47 (5 h)	2
$\begin{array}{c} \text{C}_6\text{H}_5-\text{CH}_2-\text{CH}_2-\text{CH}_2-\text{CH}_2-\text{CH}_2-\text{CH}_2-\text{C}_6\text{H}_5 \\ \diagdown \quad \diagup \\ \text{Y} \end{array}$	67 (19 h)	9
$\begin{array}{c} \text{C}_6\text{H}_5-\text{CH}_2-\text{CH}_2-\text{CH}_2-\text{CH}_2-\text{CH}_2-\text{CH}_2-\text{C}_6\text{H}_5 \\ \diagdown \quad \diagup \\ \text{Y} \end{array}$	52 (10 h)	47
$\begin{array}{c} \text{F} \\ \\ \text{Br}-\text{C}_6\text{H}_3-\text{CH}_2-\text{CH}_2-\text{CH}_2-\text{C}_6\text{H}_3-\text{Br} \\ \diagdown \quad \diagup \\ \text{Y} \end{array}$	43 (24 h)	1

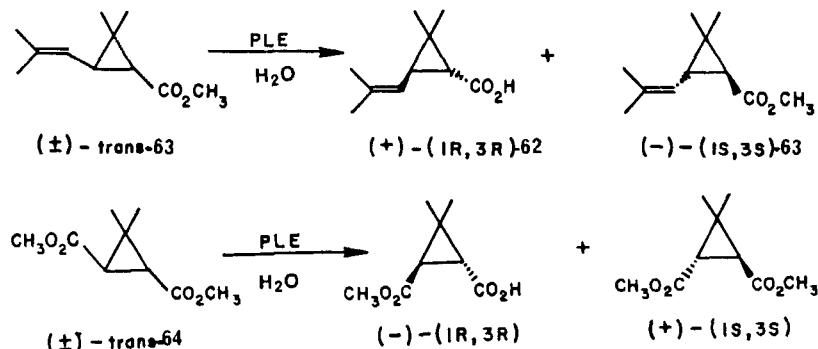
active building blocks possess the desired stereochemical and functional features of macrolide antibiotics.

The physiological activities of pyrethroid insecticides are intimately associated with the stereochemical features (*1R,3R*) of the chrysanthemic acid moiety (**62**) (76). Hence, enzymatic methods were developed for the resolution of

Table 22
Bifunctional Chiral Synthons

<u>Substrate</u>	<u>Microorganism/ Enzyme</u>	<u>Enantiomer Preferentially Cleaved</u>	<u>E</u>
	<i>Gliocladium roseum</i>	2R,4R	11
	<i>Gliocladium roseum</i>	2S,3S	20
	Pig liver esterase	2S,3R	10
	<i>Enterobacter cloacae</i>	R	>100
	<i>Bacillus sp.</i>	R	14

(\pm)-chrysanthemic acids. While the *cis*-methyl esters of chrysanthemic acid were very slowly attacked by pig liver esterase (PLE), the *R* enantiomer of (\pm)-methyl *trans*-chrysanthemate (**63**) was readily hydrolyzed by the enzyme but with low enantioselectivity (*E* = 4). Similarly, the carolic acid derivatives (**64**), important chiral building blocks of pyrethroids, were cleaved with low enantioselectivity (*E* = 7) (77) (Scheme 17).



Scheme 17 PLE-catalyzed hydrolysis of (\pm)-63 and 64

Pig liver esterase (PLE) was found to catalyze the hydrolyses of a number of (\pm)-allenic esters with low to moderate enantioselectivity (78). When the C-4 substituents are relatively small or acyclic, the enzyme was consistently *S*-ester selective; in contrast, PLE exhibited *R*-ester selectivity when the C-4 substituents were relatively large or cyclic. The *E* values were largest when the degrees of substitution at the C-2 and C-4 positions were greatest (Table 23).

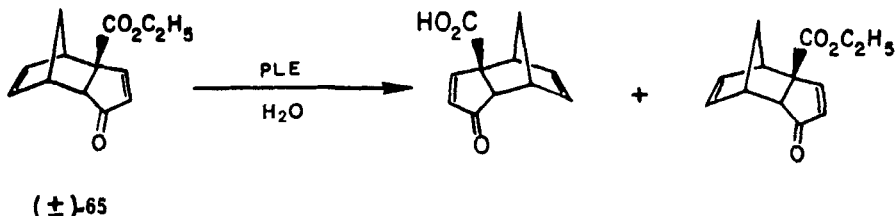
Generally, the more highly substituted the allene, the slower the rate of PLE-catalyzed hydrolysis. Also ethyl esters are hydrolyzed more slowly than methyl esters.

Access to optically active *endo*-tricyclodecadienones has been achieved by PLE-catalyzed kinetic resolution of the tricyclic ester (65). This tricyclic system can be easily transformed into a functionalized cyclopentenone. A very

Table 23
PLE-catalyzed Hydrolyses of (\pm)-Allenic Esters

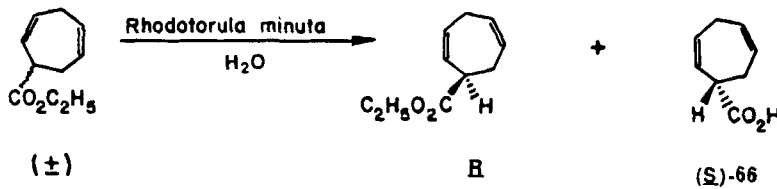
R_1	R_2	R_3	Conversion (%)	<i>E</i>
a) C_6H_{13}	H	H	31 (24 h)	3
b) C_6H_{13}	H	H	38 (96 h)	2
c) C_2H_5	H	CH_3	50 (13 h)	1
d) C_2H_5	CH_3	H	50 (1.5 h)	1
e) C_2H_5	CH_3	CH_3	50 (22 h)	2
f) Ph	H	H	18 (6 h)	1
g) Ph	H	CH_3	10 (6 h)	1
h) Ph	C_2H_5	H	50 (22 h)	3
i) Ph	CH_3	CH_3	50 (29 h)	58
j) Ph	C_2H_5	CH_3	44 (96 h)	32
k) Ph	CH_3	C_2H_5	54 (72 h)	26
l) Ph	C_2H_5	C_2H_5	35 (48 h)	>100
m) cyclohexyl	CH_3	CH_3	51 (72 h)	3

significant improvement in both enantioselectivity and reaction rate was attained by replacing acetone with acetonitrile as the co-solvent. However, this effect of acetonitrile appears to be highly substrate dependent (79).



<u>Reaction conditions</u>	<u>Conversion (%)</u>	<u>E</u>
10% acetone, 20°C, 7 h	23	63
0.2 M acetonitrile, 20°C, 4.5 h	45	>100

Ectocarpene [*(S)*-*(+)*-6-(*Z*-but-1'-enyl)-cyclohepta-1,4-diene] is the male-gamete attractant of marine brown algae (80). It was synthesized from the key chiral intermediate (*S*)-*(+)*-2,5-cycloheptadienecarboxylic acid (*S*-66), which in turn was obtained via microbial enantioselective hydrolysis of its (±)-ethyl ester. Among the organisms examined, the yeast, *Rhodotorula minuta* var. *texensis* IFO 1102 was found to be most suitable (*E* = 20) for this transformation (81).



α -Methylarylacetic acids are an important class of non-steroidal antiinflammatory drugs. [Among the best known are ibuprofen, flurbiprofen, ketoprofen, and suprofen (all of which are substituted α -methylbenzeneacetic acids), and naproxen (a substituted α -methylnaphthaleneacetic acid) (82).] The antiinflammatory activity of these drugs is generally associated with the *S* enantiomer, which is obtained via chemical resolution methods. Recently, an enzymatic resolution process was developed for the preparation of optically active α -methylarylacetic acids using the lipase of *Candida cylindracea* (Ta-

Table 24
Kinetic Resolution of (\pm)-Arylpropionic Esters

	<u>Substrate structure</u>	<u>Conversion (%)</u>	<u>E</u>
2-Phenylpropionate		37	10
Ibuprofen		42	84
Flurbiprofen		27	14
Suprofen		49	>100
Ketoprofen		28	4
Naproxen		39	>100

ble 24). The enzyme has *S* enantioselectivity and can tolerate high substrate and product concentrations (83).

F. Resolution in Apolar Solvents

As many organic solvents are known to inactivate or denature biocatalysts, the selection of a suitable organic solvent for a biphasic biocatalytic resolution is of paramount importance. Some rules were formulated for the optimization of biocatalytic systems in organic media using the logarithms of the partition coefficient, $\log P$, as a quantitative measure of solvent polarity (84). Biocata-

lytic activity is low in polar solvents having a $\log P < 2$, is moderate in solvents having a $\log P$ between 2 and 4, and is high in apolar solvents having a $\log P > 4$. An account of the state of the art of medium engineering for bioorganic reactions has recently been described by Laane (85).

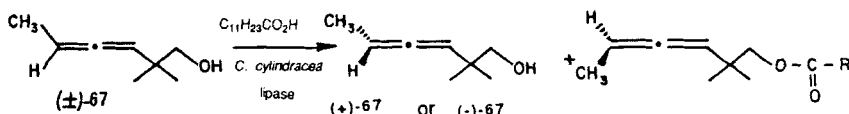
Langrand et al. (30b) conducted a systematic preparative resolution of α -substituted cyclohexanols using the lipase of *Candida cylindracea* (Table 25). This enzyme is selective for *R* alcohols and the α -*trans* compounds are esterified.

Table 25
Resolution of α -Substituted Cyclohexanols

Alcohol	T°C (time)	Configuration of the reacting enantiomer	c (%)	E
(\pm)- <u>trans</u> -2-Methylcyclohexanol	40°C (5.5 h)	(-)	45	>100
(\pm)- <u>cis</u> -2-Methylcyclohexanol	40°C (10.5 h)	(-)	52	25
(\pm)- <u>trans</u> -2-Ethylcyclohexanol	40°C (8 h)	(-)	48	>100
(\pm)- <u>trans</u> -2-Isopropylcyclohexanol	35°C (11 h)	(-)	40	>100
(\pm)- <u>cis</u> -2-Isopropylcyclohexanol	40°C (192 h)	(-)	30	23
(\pm)- <u>trans</u> -2-tert-Butylcyclohexanol	40°C (95 h)	(-)	34	>100
(\pm)-Menthol	45°C (8 h) 40°C (88 h)	(-)	45	92
(\pm)-Isomenthol	40°C (17 h)	(-)	56	15
(\pm)-Neomenthol	40°C (88 h)	(-)	45	31
			36	84

fied more rapidly than the α -*cis* ones. The difference in the *E* value at 45 and 56% conversion for (\pm)-menthol is due to reversibility of the reaction (30b). Several research groups used the lipase of *Candida cylindracea* for the resolution of (\pm)-menthol via enantioselective esterification. The *E* value varied widely depending on the acyl donors used (30c). Highly enantioselective esterification was achieved with 5-phenylvaleric acid (*E* = > 100). Moreover, the *E* value varied markedly depending on the experimental conditions used (30a).

The resolution of allenic alcohols via enantioselective esterification with lauric acid was examined. The reactions were carried out in hexane and *C. cylindracea* lipase as the biocatalyst. No enantioselectivity was observed for most of the substrates examined except **67** (86).



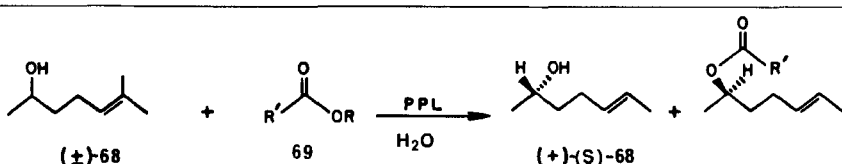
The *E* value was calculated to be 8 (31% conversion). The reversibility of the reaction was indicated by the drop of the *E* value to 2 at 85% conversion.

Commercial mass trapping of the pest, *Gnathotrichus retusus* requires an efficient method for the synthesis of (+)-(S)-sulcatol (**68**) (87). The preparative resolution of (\pm)-sulcatol was examined via transesterification using lipases of *Candida cylindracea* and porcine pancreas (PPL). The lipase of *Candida cylindracea* preferentially esterified the (+)-(S) enantiomer in anhydrous ether, but the enantioselectivity was low (*E* = 3). On the other hand, PPL exhibited a moderate preference (*E* = 10) for the (-)-(R) enantiomer. However, when the commercial Sigma PPL preparation was dehydrated to constant weight under vacuum, a three-fold enhancement in the *E* value was observed:

Ester	<i>E</i> (PPL)	
	Untreated	Dehydrated
Tributyrin	9	24
Trifluoroethyl laurate	34	100

The enantioselective transesterification of (\pm)-sulcatol (**68**) catalyzed by PPL was unaffected by changes in the leaving group (-OR) of the acylating ester (**69**). Increases in the chain length of the acid moiety of the acylating ester from C_4 to C_8 had little effect on the enantiomer ratio, *E*. However, use of the activated ester, trifluoroethyl laurate, resulted in a four-fold increase in the *E* value (Table 26). This example demonstrates that enantioselectivity can

Table 26
Effect of Acylating Ester on Enantioselectivity



Ester, $\text{R}'\text{-C}(\text{O})\text{-OR}$

$\text{R}'\text{-}$	-OR	Relative rate	E
$\text{C}_3\text{H}_7\text{-}$	$\text{H}_2\text{C}(\text{O}_2\text{CR}')\text{HC}(\text{O}_2\text{CR}')\text{H}_2\text{CO}-$	1	24
$\text{C}_3\text{H}_7\text{-}$	$\text{Cl}_3\text{CCH}_2\text{O-}$	2	24
$\text{C}_3\text{H}_7\text{-}$	$\text{F}_3\text{CCH}_2\text{O-}$	3	22
$\text{C}_7\text{H}_{15}\text{-}$	$\text{Cl}_3\text{CCH}_2\text{O-}$	4	24
$\text{C}_7\text{H}_{15}\text{-}$	$\text{F}_3\text{CCH}_2\text{O-}$	4	19
$\text{C}_{11}\text{H}_{23}\text{-}$	$\text{Cl}_3\text{CCH}_2\text{O-}$	3	27
$\text{C}_{11}\text{H}_{23}\text{-}$	$\text{F}_3\text{CCH}_2\text{O-}$	3	100

be dramatically increased by modifying the reaction conditions. A combination of enzyme dehydration and ester selection increased the E value ten-fold.

The resolution of several racemic aliphatic secondary alcohols was accomplished via esterification in hexane using the lipase derived from *Mucor miehei* and hexanoic acid (88). The results show that this biocatalytic system has a preference for the *R* enantiomer.

The esterification of (\pm) -2-octanol was found to be markedly influenced by the chain length of the acid. Acetic acid was unreactive. The E value increased to >50 for C_6 and C_8 fatty acids and declines beyond C_8 to rise again to >50 for C_{16} . Similar observations were made for 2-hexanol and 2-decanol (Table 27).

The results of the esterification of several other (\pm) -alcohols with octanoic acid and the above lipase are listed in Table 27. Cyclohexylmethylcarbinol, phenylmethylcarbinol, and 3-dodecyn-2-ol were all esterified with a strong preference for the *R*-enantiomer. The reduced enantioselectivity exhibited by *M. miehei* lipase for 3-octanol, citronellol, and for α -branched 2-carbinols such as 3-methyl-2-butanol indicates that high enantioselectivity requires that the carbinol carbon be the asymmetric center and that larger alkyl groups preferably be unbranched in the immediate vicinity of that carbon.

Table 27
Resolution of (\pm)-Carbinols by *M. miehei* Lipase

Alcohol	E (k_R/k_S)
3-Methyl-2-butanol	2
2-Pentanol	2
2-Hexanol	10
2-Octanol	>50
2-Decanol	8
2-Dodecanol	15
Cyclohexylmethylcarbinol	>50
Phenylmethylcarbinol	42
3-Dodecyn-2-ol	>50
3-Octanol	1
2-Methyl-1-decanol	1
2-Methyl-1-dodecanol	1
2-Phenyl-1-propanol	<1
1,2-Isoipropylideneglycerol	1
Citronellol	1
4-Methyl-2-pentanol	24

VI. CONCLUSIONS

The usefulness of biocatalytic procedures for the separation of optical antipodes has long been recognized (89) and their use in preparative resolutions will continue to grow in momentum. Despite its many promising features, the biocatalytic approach is still in its formative stage. A major limitation of the method is the lack of an arsenal of biocatalysts with well-defined enantioselectivities to enable the chemist to resolve enantiomers with predictability.

Up to now, most of the biocatalytic resolutions have been conducted using hydrolytic enzymes. Many of these (i.e., microbial lipases) have flexible active-site pockets and thus can assume a variety of conformations for the accommodation of a broad range of substrates (induced-fit). Consequently, it is not surprising to find that the enantioselectivity of these biocatalytic systems can vary markedly with different substrates. In fact, the enantioselectivity can often be reversed by altering a substituent quite remote from the chiral center. Conversely, enzymes that possess rigid (lock-key) active-site pockets exhibit high enantioselectivities but can accept only a very narrow spectrum of substrates.

However, these shortcomings are likely to be overcome by a methodical search for new biocatalysts with improved chiral catalytic properties (90) and

by more systematic investigations of the relationship between changes in substrate structure and the stereochemical behavior of known enzymes (22). Computer graphics have been used for the modeling of enzyme-substrate interactions to predict specificity and stereospecificity of enzymes (91) whose conformations (native or complexed) have been defined by X-ray crystallography. Moreover, more general methods of improving the enantioselectivity of biocatalysts may be developed possibly via noncovalent modification of the protein conformation (92) to further extend their usefulness.

We hope this chapter will stimulate further systematic studies of biocatalytic systems so that the sense of chirality and the enantiomer ratio (E) may soon be predictable for biocatalytic resolutions of several classes of racemic compounds at a level of accuracy akin to those of *L*- and *D*-acylases for the resolution of racemic amino acids. We are cautiously optimistic that biocatalytic procedures will be considered in the near future as an alternative rather than a supplement to nonenzymic procedures.

REFERENCES

1. (a) Bosnich, B. In *Asymmetric Catalysis*; Bosnich, B., Ed.; Martinus Nijhoff: Dordrecht, 1986; NATO ASI Series No. 103, pp 4-18. (b) Sih, C. J.; Shieh, W. R.; Chen, C. S.; Wu, S. H.; Girdaukas, G. In *Intern. Sympos. on Bioorganic Chemistry*; Breslow, R., Ed.; *Ann. N.Y. Acad. Sci.* **1986**, *471*, 293-254.
2. Wilen, S. H.; Collet, A.; J. Jacques, J. *Tetrahedron* **1977**, *33*, 2725-2736.
3. Williams, K.; Lee, E. *Drugs* **1985**, *30*, 333-354.
4. Ariens, E. J. In *Stereochemistry and Biological Activity of Drugs*; Ariens, E. J.; Soudijn, W.; Timmermans, P. B. M. W. M., Eds.; Blackwell: Oxford, 1983, pp 11-32.
5. Segel, I. H. *Enzyme Kinetics*; John Wiley & Sons: New York, 1975; pp 19, 25.
6. Eyring, H. *Chem. Rev.* **1935**, *17*, 65-77.
7. (a) Russell, G. A. In *Techniques of Organic Chemistry*; Weissberger, A., Ed.; John Wiley Interscience: New York, 1961; Vol. VIII, Pt. 1, 2nd Ed., pp 343-388. (b) Kagan, H.; Fiaud, J. C. In *Topics in Stereochemistry*; Eliel, E. L.; Wilen, S. H., Eds.; John Wiley Interscience: N.Y.; 1988; Vol. 18, pp 249-330.
8. Bamann, E. *Ber.* **1929**, *62*, 1538-1548.
9. Chen, C. S.; Fujimoto, Y.; Girdaukas, G.; Sih, C. J. *J. Am. Chem. Soc.* **1982**, *104*, 7294-7299.
10. Chen, C. S.; Wu, S. H.; Girdaukas, G.; Sih, C. J. *J. Am. Chem. Soc.* **1987**, *109*, 2812-2817.
11. Burwell, R. L., Jr.; Pearson, R. G. *J. Phys. Chem.* **1966**, *70*, 300-302.
12. Rona, P.; Ammon, R. *Biochem. Z.* **1927**, *181*, 49-79.
13. (a) Sih, C. J.; Chen, C. S.; Girdaukas, G.; Zhou, B. N. In *Basic Biology of New Developments in Biotechnology*; Hollaender, A.; Laskin, A. L.; Rogers, P., Eds.; Plenum: New York, 1983; pp 215-230. (b) VanMiddlesworth, F.; Wang, Y. F.; Zhou, B. N.; DiTullio, D.; Sih, C. J. *Tetrahedron Lett.* **1985**, 961-964.

14. Ladner, W. E.; Whitesides, G. *J. Am. Chem. Soc.* **1984**, *106*, 7250-7251.
15. Tabushi, I.; Yamada, H.; Sato, H. *Tetrahedron Lett.* **1975**, 309-312.
16. Wilson, W. K.; Baca, S. B.; Barber, Y. J.; Scallen, T. J.; Morrow, C. J. *J. Org. Chem.* **1983**, *48*, 3960-3969.
17. (a) Brown, A. G.; Smale, T. C.; Kling, T. J.; Hasenkamp, R.; Thompson, R. H. *J. Chem. Soc. Perkin Trans. I.* **1976**, 1165-1170. (b) Endo, A.; Kuroda, M.; Tsujita, Y. *J. Antibiot.* **1976**, *29*, 1346-1348.
18. Alberts, A. W.; Chen, J.; Kuron, G.; et al. *Proc. Natl. Acad. Sci. USA* **1980**, *77*, 3957-3961.
19. Sato, A.; Ogiso, A.; Noguchi, H.; Mitsai, S.; Kankeko, I.; Shimada, Y. *Chem. Pharm. Bull.* **1980**, *28*, 1509-1525.
20. Gu, Q. M.; Reddy, D. R.; Sih, C. J. *Tetrahedron Lett.* **1986**, 5203-5206.
21. Ondetti, M. A.; Rubin, B.; Cushman, D. W. *Science* **1977**, *196*, 441-444.
22. Charton, M.; Ziffer, H. *J. Org. Chem.* **1987**, *52*, 2400-2403.
23. (a) Wu, S. H.; Zhang, L. Q.; Chen, C. S.; Girdaukas, G.; Sih, C. J. *Tetrahedron Lett.* **1985**, 4323-4326. (b) Fujimoto, Y.; Iwadate, H.; Ikekawa, N. *J. Chem. Soc., Chem. Commun.* **1985**, 1333-1334. (c) Miyano, S.; Kawahara, K.; Inoue, Y.; Hashimoto, H. *Tetrahedron Lett.* **1987**, 355-356.
24. (a) Sih, C. J.; Wu, S. H.; Fujimoto, Y. In *Perspectives in Biotechnology*; Duarte, J. M. C.; Archer, L. J.; Bull, A. T.; Holt, G., Eds.; Plenum: New York, 1987; NATO ASI Series A, Life Sci., Vol. 128, pp 43-53. (b) Crout, D. H. G.; Gaudet, U. S. B.; Laumen, K.; Schneider, M. P. *J. Chem. Soc., Chem. Commun.* **1986**, 808-810.
25. Brooks, D. W.; Wilson, M.; Webb, M. *J. Org. Chem.* **1987**, *52*, 2244-2248.
26. (a) Kasche, V. *Enzyme Microb. Technol.* **1986**, *8*, 4-16. (b) Brink, L. E. S.; Tramper, J. *Biotechnol. Bioeng.* **1985**, *27*, 1258-1269. (c) Halling, P. J. *Enzyme Microb. Technol.* **1984**, *6*, 513-516. (d) Carrea, G. *Trends Biotechnol.* **1984**, *2*, 102-106.
27. Martinek, K.; Semenov, A. N.; Berezin, I. V. *Biochim. Biophys. Acta* **1981**, *658*, 76-89.
28. (a) Fruton, J. S. *Adv. Enzymol. Rel. Areas Mol. Biol.* **1982**, *53*, 239-306. (b) Oyama, K.; Irino, S.; Harada, T.; Hagi, N. *Ann. N. Y. Acad. Sci.* **1984**, *434*, 95-98. (c) Markussen, J.; Velund, A. In *Enzymes in Organic Synthesis*; Pitman: London, 1985; pp 188-203.
29. Kasche, V.; Haufler, U.; Riechmann, L. *Ann. N. Y. Acad. Sci.* **1984**, *434*, 99-105.
30. (a) Langrand, G.; Baratti, J.; Buono, G.; Triantaphylides, C. *Tetrahedron Lett.* **1986**, *27*, 29-32. (b) Langrand, G.; Secci, M.; Buono, G.; Baratti, J.; Triantaphylides, C. *Tetrahedron Lett.* **1985**, *26*, 1857-1860. (c) Koshiro, S.; Sonomoto, K.; Tanaka, A.; Fukui, S. J. *Biotechnol.* **1985**, *2*, 47-57. (d) Kirchner, G.; Scollar, M. P.; Klibanov, A. M. *J. Am. Chem. Soc.* **1985**, *107*, 7072-7076.
31. Verger, R.; Mieras, M. C. E.; DeHaas, G. H. *J. Biol. Chem.* **1973**, *248*, 4023-4034.
32. Morrison, J. D. In *Asymmetric Synthesis*; Morrison, J. D., Ed.; Academic: New York, 1983; Vol. 1, pp 3-6.
33. Esaki, N.; Soda, K.; Kumagai, H.; Yamada, H. *Biotechnol. Bioeng.* **1980**, *22* (Suppl. 1, Ferment.: Sci. Technol. Future), 127-141; CA 93:91246u.
34. Cecere, F.; Gallic, G.; Morisi, F. *FEBS Lett.* **1975**, *57*, 192-195.
35. Yokozeki, K.; Nakamori, S.; Eguchi, C.; Yamada, K.; Mitsugi, K. *Agric. Biol. Chem.* **1987**, *51*, 355-362; Yokozeki, K.; Sano, K.; Eguchi, C.; Yamada, K.; Mitsugi, K. *ibid.* **1987**, *51*, 363-369.
36. Wallach, D. P.; Grisolia, S. J. *Biol. Chem.* **1957**, *226*, 277-288.

37. Fukumura, T. *Agric. Biol. Chem.* **1977**, *41*, 1321-1325, 1327-1330.
38. Yokozeki, K.; Majima, E.; Izawa, K.; Kubota, K. *Agric. Biol. Chem.* **1987**, *51*, 963-964.
39. Sano, K.; Eguchi, C.; Yasuda, N.; Mitsugi, K. *Agric. Biol. Chem.* **1979**, *43*, 2373-2374.
40. Fülling, G.; Sih, C. J. *J. Am. Chem. Soc.* **1987**, *109*, 2845-2846.
41. Guzman, A.; Yuste, F.; Toscano, R. A.; Young, J. M.; Van Horn, A. R.; Muchowski, J. M. *J. Med. Chem.* **1986**, *29*, 589-591.
42. Baldwin, J. J.; Raab, A. W.; Mensler, K.; Arison, B. H.; McClure, D. E. *J. Org. Chem.* **1978**, *43*, 4876-4878.
43. Iriuchijima, S.; Keiyu, A.; Kojima, N. *Agric. Biol. Chem.* **1982**, *46*, 1593-1597.
44. Iriuchijima, S.; Kojima, N. *Agric. Biol. Chem.* **1982**, *46*, 1153-1157.
45. Hamaguchi, S.; Ohashi, T.; Watanabe, K. *Agric. Biol. Chem.* **1986**, *50*, 375-380, 1926-1632.
46. Tennant, G. In *Comprehensive Organic Chemistry*; Sutherland, I. O., Ed.; Pergamon: Oxford, 1979; Vol. 2, pp 385-590.
47. Matsuo, N.; Ohno, N. *Tetrahedron Lett.* **1985**, 5533-5534.
48. Ohta, H.; Miyamae, Y.; Tsuchihashi, G. *Agric. Biol. Chem.* **1986**, *50*, 3181-3184.
49. Hamaguchi, S.; Hasegawa, J.; Kawaharada, H.; Watanabe, K. *Agric. Biol. Chem.* **1984**, *48*, 2055-2059.
50. Hamaguchi, S.; Asada, M.; Hasegawa, J.; Watanabe, K. *Agric. Biol. Chem.* **1984**, *48*, 2331-2337.
51. Lavayre, J.; Verrier, J.; Baratti, J. *Biotechnol. Bioeng.* **1982**, *24*, 2175-2187.
52. Akita, H.; Matsukura, H.; Oishi, T. *Tetrahedron Lett.* **1986**, 5241-5244.
53. Oritani, T.; Yamashita, K. *Agric. Biol. Chem.* **1973**, *37*, 1687-1689, 1691-1694, 1695-1700; **1974**, *38*, 1961-1964, 1965-1971.
54. Krasnobajew, V. In *Biotechnology*; Kieslich, K., Ed.; Verlag Chemie: Weinheim, 1984; Vol. 6a, pp 98-125.
55. Yamaguchi, Y.; Oritani, T.; Tajima, N.; Komatsu, A.; Moroe, T. *J. Agr. Chem. Soc. (Japan)* **1976**, *50*, 475-480.
56. Takasago Perfumery K. K. Japanese Patent, 106, 767, 1974.
57. Omata, T.; Iwamoto, N.; Kimura, T.; Tanaka, A.; Fukui, S. *Eur. J. Microbiol. Biotechnol.* **1981**, *11*, 199-204.
58. Inagaki, T.; Ueda, H. *J. Agr. Chem. Soc. (Japan)* **1987**, *61*, 227-232.
59. Oritani, T.; Kudo, S.; Yamashita, K. *Agric. Biol. Chem.* **1982**, *46*, 757-760.
60. Eichberger, G.; Penn, G.; Faber, K.; Griengl, H. *Tetrahedron Lett.* **1986**, 2843-2844.
61. Becher, E.; Albrecht, R.; Bernhard, K.; Leuenberger, H. G. W.; Mayer, H.; Müller, R. K.; Schüep, W.; Wagner, H. P. *Helv. Chim. Acta* **1981**, *64*, 2419-2435.
62. Xie, Z. F.; Suemune, H.; Sakai, K. *J. Chem. Soc., Chem. Commun.* **1987**, 838-839.
63. Oritani, T.; Yamashita, K. *Agric. Biol. Chem.* **1980**, *44*, 2637-2642.
64. Elliot, M. *Environmental Health Perspectives* **1976**, *13*, 3-13.
65. Matsuo, T.; Nishioka, T.; Hirano, M.; Suzuki, Y.; Tsushima, K.; Itaya, N.; Yoshioka, H. *Pesticide Sci.* **1980**, *11*, 202-218.
66. Oritani, T.; Yamashita, K. *Agric. Biol. Chem.* **1975**, *39*, 89-96.
67. Hirohara, H.; Mitsuda, S.; Ando, E.; Komaki, R. In *Biocatalysts in Organic Syntheses*; Tramper, J.; Van der Plas, H. C.; Linko, P., Eds.; Elsevier: Amsterdam, 1985; pp 119-134.

68. Piancatelli, G. *Heterocycles* **1982**, *19*, 1735-1744.
69. Minai, M.; Katsura, T. Eur. Patent, 80671, 1984.
70. Minai, M.; Katsura, T. Japanese Patent Appl., 144729, 1984.
71. Minai, M.; Katsura, T. Japanese Patent Appl., 204357, 1984.
72. Sumitomo Chemical Co. Japanese patent, 49-26425, 1974.
73. Matsuo, T.; Itaya, N.; Mizutani, T.; Ohno, N.; Fujimoto, K.; Okuno, Y.; Yoshioka, H. *Agric. Biol. Chem.* **1976**, *40*, 247-249.
74. Sumitomo Chemical Co. Ger. Offen., Patent 2,418,950, 1974.
75. (a) Sugai, T.; Kuwahara, S.; Hoshino, C.; Matsuo, N.; Mori, K. *Agric. Biol. Chem.* **1982**, *46*, 2579-2585. (b) Mori, K.; Akao, H. *Tetrahedron* **1980**, *36*, 91-96.
76. Arlt, D.; Jautelat, M.; Lantzsch, R. *Angew. Chem. Int. Ed. Engl.* **1981**, *20*, 703-722.
77. Schneider, M.; Engel, N.; Boensmann, H. *Angew. Chem. Int. Engl.* **1984**, *23*, 64-66.
78. Ramaswamy, S.; Hui, R. A. H. F.; Jones, J. B. *J. Chem. Soc., Chem. Commun.* **1986**, 1545-1546.
79. Eichberger, G.; Faber, G. P. K.; Griengl, H. *Tetrahedron Lett.* **1986**, 2843-2844.
80. Müller, D. G.; Jaenicke, L.; Donike, M.; Akintobi, T. *Science* **1971**, *171*, 815-817.
81. Kajiwara, T.; Sasaki, Y.; Kimura, F.; Hatanaka, A. *Agric. Biol. Chem.* **1981**, *45*, 1461-1466.
82. Lombardino, J. G. *Nonsteroidal Antiinflammatory Drugs*; John Wiley & Sons: New York, 1985; pp 254-398.
83. (a) Gu, Q. M.; Chen, C. S.; Sih, C. J. *Tetrahedron Lett.* **1986**, 1763-1766. (b) Sih, C. J.; Gu, Q. M.; Fülling, G.; Wu, S. H.; Reddy, D. R. *Developments in Industrial Microbiology.* **1988**, *29*, 221-229.
84. Laane, C.; Boeren, S.; Vos, K.; Veeger, C. *Biotechnol. Bioeng.* **1987**, *30* 81-87.
85. Laane, C. *Biocatalysis* **1987**, *1*, 17-22.
86. Gil, G.; Ferre, E.; Meou, A.; Le Petit, J.; Triantaphylides, C. *Tetrahedron Lett.* **1987**, 1647-1648.
87. Stokes, T. M.; Oehlschlager, A. C. *Tetrahedron Lett.* **1987**, 2091-2094.
88. Sonnet, P. E. *J. Org. Chem.* **1987**, *52*, 3477-3479.
89. Pasteur, L. *Compt. Rend.* **1858**, *46*, 615-618.
90. Cheetham, P. S. *J. Enzyme Microb. Technol.* **1987**, *9*, 194-213.
91. Björkling, F.; Norin, T.; Szmulik, P.; Boutelje, J.; Hult, K.; Kraulis, P. *Biocatalysis* **1987**, *1*, 87-98.
92. Ammon, R.; Fischgold, H. *Biochem. Z.* **1931**, *234*, 54-61.

Stereospecificity in Enzymology: Its Place in Evolution

STEVEN A. BENNER, ARTHUR GLASFELD, and
JOSEPH A. PICCIRILLI

*Laboratory for Organic Chemistry, Swiss Federal Institute of Technology
Zurich, Switzerland*

Glossary

- I. Introduction
- II. Interpretations
 - A. Historical and Functional Models
 - B. Classes of Enzymes
- III. Classes Showing Stereochemical Homogeneity
 - A. Amino Acid Decarboxylases
 - B. Conclusions
- IV. Classes Showing Stereochemical Heterogeneity
 - A. Phosphoryl Transfers
 - B. Beta-Ketoacid Decarboxylases
 - C. Dehydrogenases Dependent on Nicotinamide Cofactors
 - 1. Correlations
 - 2. Historical Models
 - 3. Functional Models
 - 4. Controversy
 - 5. Distinguishing Functional and Historical Cases
 - 6. The Simplest Historical Model
 - 7. Further Tests
 - 8. Extension of the Functional Model
 - D. Addition-Elimination Reactions
- V. Fatty Acid Synthesis: Many Steps, Many Stereochemical Distinctions
- VI. Enzymes Displaying Stereochemical Infidelity
- VII. Conclusions
 - Note added in proof
 - Acknowledgment
 - References

Glossary

Adaptive trait: A behavior in a protein that arises in response to natural selection searching for behaviors that contribute optimally to the survival of a host organism

Conserved trait: If two homologous proteins share a common trait, the trait is said to be conserved

Convergent evolution: If two non-homologous proteins share a common trait, that trait is said to be the result of convergent evolution

Cryptic stereospecificity: A stereochemical distinction that can be detected experimentally only through the use of isotopic substitution

Divergent evolution: If two homologous proteins differ in a trait, the difference is said to have arisen by divergent evolution

Functional model: An explanation for biochemical behavior that considers primarily the influence of natural selection on the behavior of biological macromolecules

Functional trait: A trait that is interpreted in terms of biological function; as natural selection is the only mechanism for obtaining functional behavior in living organisms, functional traits must also be adaptive traits

Historical model: An explanation for biochemical behavior that considers primarily the history and pedigree of biological macromolecules

Homology: A relationship between two proteins such that they share a common ancestor

Neutral drift: Changes in structure and behavior in biological macromolecules that are not adaptive but rather reflect the accumulation of random mutations that are neither favored nor disfavored by natural selection.

I. INTRODUCTION

Four decades have passed since it became generally recognized that enzymes can distinguish between enantiotopic groups of their substrates (1-4). This recognition marked the beginning of a major evolution in our understanding of enzymatic reactions. Scarcely a decade earlier, a role for citric acid in the citric acid cycle had been “disproven” by an analysis that assumed that groups in a molecule related by a mirror plane were indistinguishable (5-7). Today, the stereospecificity of enzymatic reactions is intensely investigated; the field is now represented by over 10,000 scholarly papers.

Discrimination between enantiotopic and diastereotopic groups is a special case of the selectivity that enzymes display generally. However, unlike substrate specificity (including distinctions between enantiomers and diastereomers), discrimination between the enantiotopic groups presents special experimental and interpretive problems. The distinction is “cryptic” (Figure 1) (8); only through the judicious use of isotopic substitution is it possible to tell that a distinction is made at all. Further, as biological systems generally disregard isotopic substitution, the distinction cannot have direct biological significance.

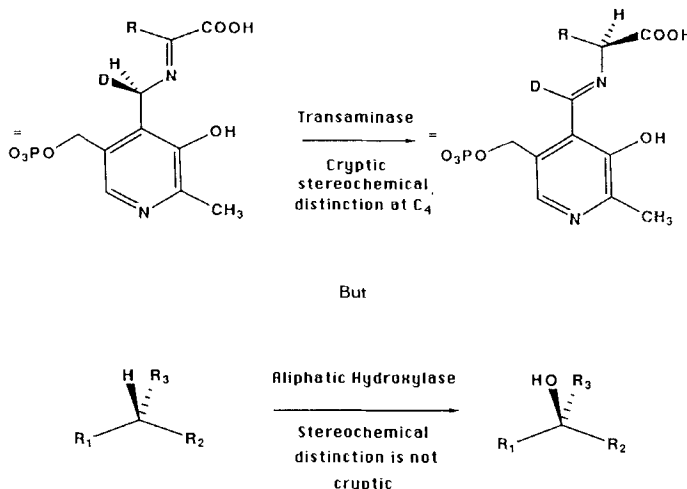


Figure 1. Cryptic stereospecificity.

This second point is central to the interpretive problem presented by cryptic stereospecificity. One can, if one wishes, study a Picasso with an electron microscope. Data will be collected, and papers based on the collected data might well be accepted by professional journals. However, studies at such high level of resolution will reveal nothing significant about the painting, which was neither designed with this detail in mind, nor executed with the precision necessary to convey information at this level of resolution.

Chemists studying the cryptic stereospecificities of enzymes are faced with a similar problem. Enzymes and their stereospecificities were not designed. Rather, they are the products of evolutionary processes, and an appreciation of this fact and its implications is a necessary first step if we are to understand enzymatic behavior (9, 10). Evolution produces two categories of traits in biological systems. A trait can be adaptive, meaning that it influences the survival of the host organism and therefore is the target of natural selection. A trait can be non-adaptive, meaning that, were it different, the survival of the host would be unaffected.

These traits behave differently in evolution and are interpreted differently in terms of biology. Normally, non-adaptive traits drift rapidly upon the accumulation of random "neutral" mutations in a gene (11, 12). Neutral drift is non-functional and non-deterministic. Alternatively, the non-adaptive trait

can (in principle) be structurally coupled to another (adaptive) trait. If this coupling is tight, the non-adaptive trait cannot drift without altering the adaptive trait at the same time. Such non-adaptive traits will not drift, but rather will be conserved over significant evolutionary time.

It is impossible to interpret enzymatic behavior without knowing whether it is adaptive, non-adaptive/conserved, or drifting. As natural selection is the only mechanism for obtaining functional behavior in enzymes, only adaptive traits can reflect biological function and underlying chemical principles (9, 13–15). Non-adaptive/conserved traits reflect ancient historical accidents. While not interpretable in terms of chemical principles, they may be useful in reconstructing the biochemical details of ancient organisms and interrelating the pedigrees of modern organisms (15). Drifting traits reflect recent historical accidents. They are the random blots of painting on Picasso's canvas, the trivia of biochemistry, and reflect neither history, pedigree, nor chemistry.

Surprisingly little concern has been given to these issues in enzyme stereochemistry, and little tolerance is displayed by the biochemical community when these issues are raised. In enzyme stereochemistry, discussions focus almost exclusively on the technology needed to determine the stereochemical course of enzymatic reactions, and stereochemical results are generally interpreted only at the level of chemical mechanism. For example, if a methyl group is enzymatically transferred with inversion of configuration, this is viewed only as evidence for a one step mechanism. In contrast, transfer with retention is viewed as evidence for a reaction proceeding via an enzyme-methyl intermediate; in the two-step mechanism, inversion at each step produces overall net retention (16).

While such views are sound, they cannot "explain" stereospecificity in any fundamental sense and do not permit conclusions to be drawn regarding the chemical or biological significance of cryptic stereospecificity. Nor can they answer the underlying question: "So what?" Even if stereochemical diversity (for example, inversion versus retention in the example above) is correlated with mechanistic diversity (for example, one- or two-step mechanism), we still cannot say whether the choice of a particular mechanism is adaptive or not, or whether the mechanistic choices displayed by natural enzymes reveal something fundamental about biochemical behavior, reflect ancient historical accident, or are simply random.

Unfortunately, similar statements can be made about most bio-organic data. However, evolutionary interpretations that can be found in the literature remain, with only a few notable exceptions, casual. Most referees accept only the most cautious statements of the evolutionary significance of the data collected. Only rarely is evolutionary understanding the goal of the research.

Thus, as a result of intensive experimental effort we now know that a particular alkaline phosphatase from *E. coli* operates via a two-step mechanism

(17), a particular chorismate mutase catalyzes a reaction via a chair transition state (18), and that the elimination of water from fumarate catalyzed by a particular fumarase is not concerted (19). However, we cannot say whether such behaviors are adaptive, conserved, or drifting; thus, we cannot say whether they have any chemical or biological significance.

This review seeks to fill this gap for cryptic stereospecificity. Other types of enzymatic behavior are discussed elsewhere (9, 13-15). The discussion of cryptic stereochemical distinctions made by enzymes will be directed towards developing competing "functional" and "historical" models as explanations for the stereochemical results observed for each case (9).

II. INTERPRETATIONS

Like any biological trait, enzymatic stereospecificity is a product of two competing evolutionary processes, natural selection and neutral drift. To be selected, the trait must influence the ability of the host organism to survive and reproduce.

In principle, adaptive and non-adaptive stereospecificity might be distinguished by examining the stereospecificities of enzymes that are homologous (related by a common ancestor) and analogous (performing similar functions in different organisms). In homologous enzymes, non-adaptive stereospecificity is expected to drift during divergent evolution (11). In contrast, stereospecificity that performs a selected function should be conserved during divergent evolution.

In non-homologous enzymes, non-adaptive stereospecificity is expected to be similar only to the extent anticipated by random statistics. Conversely, if a set of non-homologous enzymes catalyzing the same reaction have all convergently evolved to have the same stereospecificity, this is a strong argument that the stereochemical distinction is functionally adaptive.

In practice, several factors complicate this analysis. First, enzymes catalyzing analogous reactions from different organisms are far more likely to be homologous than non-homologous. Thus, the number of non-homologous enzymes catalyzing analogous chemical processes is often insufficient to permit a statistically significant comparison for a variable (such as stereospecificity) that can adopt only two values.

Second, methods for determining homology may fail to detect distant homology that might be relevant to an understanding of the stereochemical behavior of a class of enzymes. Homology between two proteins is generally identified by sequence comparisons or immunological cross-reactivities; other approaches are demonstrably inadequate. However, the similarity between two highly divergent sequences may be insufficient to provide a statistically

convincing case for homology. This creates problems, especially since tertiary structure is more highly conserved than either sequence or immunological cross-reactivity in proteins (20). To the extent that cryptic stereospecificity depends on tertiary structure, similar stereospecificities in distantly homologous proteins would properly be explained as a result of homology (not adaptation). Because sequence similarities are inadequate to prove homology, however, the identical stereospecificities would be misinterpreted as convergent evolution, leading to the opposite conclusion that they are adaptive.

Third, non-functional traits can be constrained from drifting simply by being coupled structurally to selected traits (*vide supra*) (9). Thus, a cryptic stereochemical distinction might be highly conserved in divergent evolution, even though it itself is not adaptive, simply because it is tightly coupled to another adaptive trait. Thus, not all conserved traits need be directly functional.

Fourth, when enzymes catalyzing analogous reactions in two different organisms have opposite stereospecificities, it is possible that this divergence does *not* mean that the stereospecificity is neutral but rather may reflect functional adaptation in the two proteins for two different environments.

These reservations make single items of stereochemical data difficult enough to interpret. However, another obstacle to the development of an understanding of the evolutionary significance of cryptic stereospecificity is the attitude of biological chemists themselves. To some, cryptic stereochemical distinctions appear to be too "subtle" to influence the survival of a host organism. To others, the fact that stereochemical diversity correlates with mechanistic diversity, and the presumption that mechanistic diversity must be important are sufficient to conclude that such stereochemical diversity must be adaptive.

For example, cryptic stereospecificity is often the same in homologous enzymes. Its subtlety prompts the belief that it is not adaptive. Thus, the dogma in some quarters is that cryptic stereospecificity is more highly conserved than almost any other enzymatic behavior because it is tightly coupled to tertiary structure in a protein (21). Stereospecificity presumably cannot be reversed without altering tertiary structure and, presumably, destroying catalytic activity or some other selected behavior.

There is remarkably little basis in fact for this opinion. First, as a special example of substrate specificity, stereospecificity is expected to diverge at a rate similar to that for the divergence of substrate specificity in general (9). This rate is rapid, although some of the rate can undoubtedly be ascribed to positive selection for new functions.

Further, there are several examples where a modest change in substrate structure or enzyme structure changes the stereospecificity of an enzymatic reaction. For example, the cryptic stereospecificity of citrate synthase from

Clostridium acidi-urici is reportedly reversed upon exposure of the enzyme to oxidizing conditions (Figure 2) (22). Data are inadequate to rule out other explanations for the observation; in particular, it is possible that this organism has two isozymes of the enzyme with opposite stereospecificity, and that the more abundant enzyme is more sensitive to destruction by oxygen. The clear implication, however, is that enzymatic stereospecificity can be reversed with only small changes in the structure of the protein.

Stereospecificity in an enzymatic reaction can certainly be altered by small changes in substrate structure. The stereochemical orientation of substrate and cofactor in dihydrofolate reductase is reversed upon binding of methotrexate, a close structural analog of dihydrofolate (Figure 3) (23). Likewise, acetoacetate decarboxylase from *Clostridium acetobutylicum* decarboxylates 2-methylacetoacetate with 98% retention of configuration (Figure 4, top) (24). In contrast, decarboxylation of acetoacetate proceeds essentially with racemization (25). The stereospecificity of chymotrypsin with respect to the chirality of the substrate is largely reversed by the substitution of an oxygen for a nitrogen (Figure 4, bottom) (26). Orcinol hydroxylase transfers the 4'-*pro-R* hydrogen of NADH with "natural" substrates. With substrate analogs, the 4'-*pro-S* hydrogen is reportedly removed in several cases (27).

If small changes in the structure of substrates can reverse stereospecificity in an enzyme, it seems possible that a small number of amino acid replacements in the protein will also reverse stereochemistry. However, there are few pertinent data. Although several examples are now known where distantly homologous proteins have opposite stereospecificity, there are no cases where proteins with greater than 50% sequence identity have opposite stereospecificity.

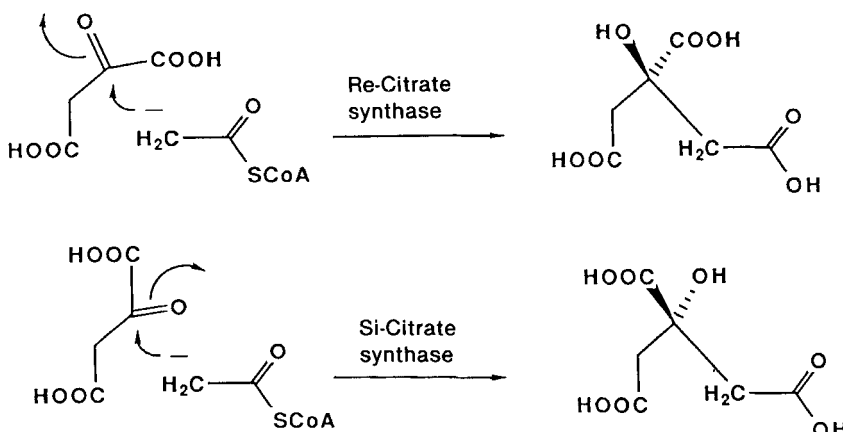


Figure 2. Alteration of stereospecificity in citrate synthase.

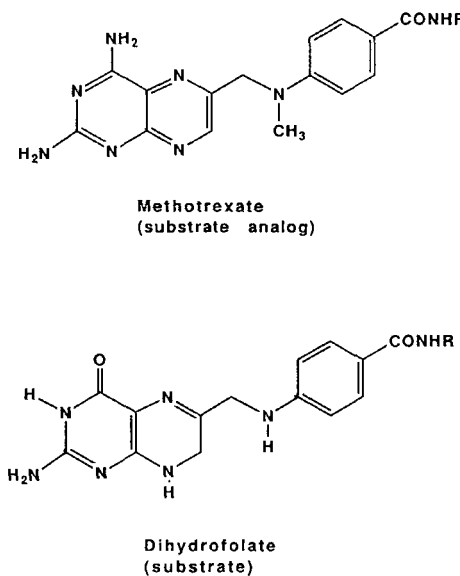


Figure 3. Alteration of stereospecificity in dihydrofolate reductase.

A. Historical and Functional Models

It is a theme of this review that conclusions about adaptation and molecular evolution based on intuition or casual analysis are largely suspect. Further, it is clear that in practice, models are never either proven or disproven. In the face of contradicting experimental data, models generally are modified in an *ad hoc* fashion to accommodate the new experimental result. While multiple *ad hoc* modification of a model at some point makes it unacceptable, taste, more than logic, determines when that point arrives.

Thus, to assess the likelihood that cryptic stereospecificity is adaptive or non-adaptive, an intellectual method is needed for systematically collecting and analyzing biochemical data. The approach that we have developed involves constructing contrasting historical and functional models (9). Experiments that are relevant to the models are then done and the models modified to accommodate the new results as they appear. The predictive and experimental value of each of the modified models becomes increasingly limited with further modification. After successive rounds of experiment and modification, the contrasting models are compared and evaluated relative to each other.

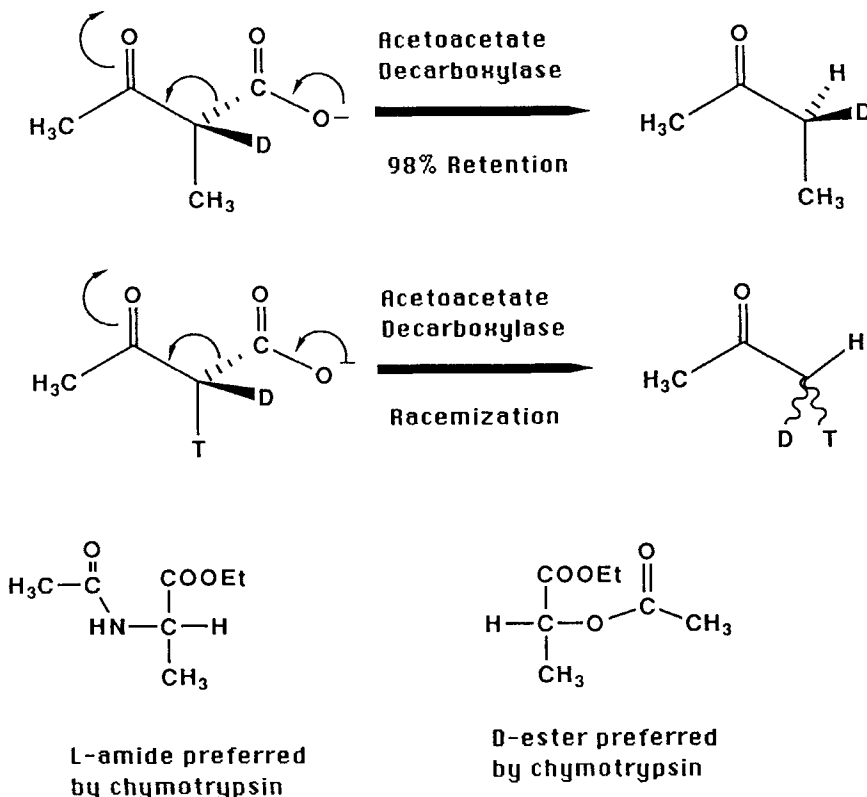


Figure 4. Alteration of stereospecificity by minor alteration in substrate structure.

The cryptic stereochemical outcome of an enzymatic reaction cannot in itself be a selectable trait. Thus, functional models begin with the assumption that the stereochemical distinction reflects an evolutionarily selectable mechanistic distinction in the enzymatic reaction. Identifying this distinction and explaining the basis for its selection then become the foci of the model. In many cases, functional models predict the convergence of stereospecificity in analogous, non-homologous enzymes. In cases where different stereospecificities are found in analogous enzymes from different organisms, a functional model must provide and defend arguments that explain how this behavioral difference reflects adaptation to different environments.

Historical models deny a selectable role for the stereochemical distinction. Rather, historical models explain the distribution of stereospecificities in terms of the pedigree of the enzymes involved. Historical models generally

make no predictions about the relative behaviors of non-homologous enzymes. They generally predict, however, that closely homologous enzymes display the same behavior. For more distantly related enzymes displaying similar stereospecificity, historical models must provide and defend arguments that explain why this non-functional behavior has been conserved during divergent evolution. These "conservation principles" generally must refer to functional traits that are coupled to stereospecificity, or they argue that reversal of stereospecificity requires complicated alteration of the active site.

Each model supports its own type of experimental test. The chemical basis of functional models can be examined experimentally in non-enzymatic systems. Historical models rely on assumptions regarding pedigree in modern enzymes. As the enzymes from extinct organisms generally cannot be retrieved (but see reference 28 for an exception), such assumptions are difficult to test in the laboratory. However, these assumptions can often be examined by sequencing enzymes.

In contrast with kinetic behavior in enzymes (13), where functional models are most appropriate, and the structures of cofactors, where historical models are strongest (15), neither functional nor historical models for cryptic stereospecificity enjoy a dominant position. Indeed, they both can be quite controversial. Thus, cryptic stereospecificity in enzymology is an excellent topic to illustrate the development and testing of functional and historical models in enzymology, and is proving to be valuable for defining the boundary between selected and non-selected behaviors in biological macromolecules.

B. Classes of Enzymes

Enzymes can be divided into classes based on the reaction type that they formally catalyze. In some classes, cryptic stereospecificity is different in different enzymes in the class (8). Some oxidoreductases transfer the 4'-*pro-R* hydrogen from NADH, while others transfer the 4'-*pro-S* hydrogen. Some decarboxylases, replacing a carboxylate group on their substrate with a hydrogen, retain stereochemistry at the reacting center; others invert stereochemistry at that center. Some phosphotransferases produce inversion of stereochemistry at the transferred phosphorus, while others produce retention.

In other classes, cryptic stereochemical distinctions are the same for each enzyme in the class. As far as is known, all microscopic steps in which methyl groups are transferred proceed with inversion (16). All transaminases so far studied abstract the *pro-S* hydrogen of pyridoxamine (8). All enzymatic condensations of acetyl CoA with electrophilic substrates proceed with inversion at the carbanionic center (8).

The process of model building is different for these two classes, and we discuss them separately below.

III. CLASSES SHOWING STEREOCHEMICAL HOMOGENEITY

In many cases, classes of enzymes catalyzing similar reactions have the same stereospecificities. As discussed nearly 15 years ago by Rose and Hanson (8, 29), this generalization is consistent with two alternative models.

A historical model explains stereochemical uniformity within a class of enzymes by assuming that all of the enzymes are descendants of a common ancestor with an arbitrary stereoselectivity, with stereoselectivity highly conserved in the divergent evolution of these proteins. Functional models explain the uniformity by arguing that a particular stereospecificity is needed for optimal catalysis of the reaction in question. Therefore, either by convergent evolution or by functional conservation during divergent evolution, enzymes catalyzing the mechanistically similar reactions should have the same stereospecificity.

It is extremely difficult to distinguish experimentally between these two models. Naively, the historical and the functional models make the same predictions: both predict that the “next” enzyme of the class to be studied will have the same stereospecificity as those already examined. For enzymes outside this class, historical models cannot make predictions unless pedigrees and conservation principles are clearly defined. Further, functional models are predictive only to the extent that the functional model can be applied to different reaction types.

Of course, certain experimental results might contradict either model. For example, if a functional model is constructed to be “universal” (i.e., applying to all enzymes in the class), one might examine many different enzymes in the hope of encountering one that does not conform in stereospecificity. This is conceptually simple. Most scientists (and most funding agencies), however, would find quite uninteresting a research proposal to examine 100 pyridoxal-dependent enzymes in the hope of finding one with an “aberrant” stereospecificity.

Further, a non-conforming enzyme weakens historical models as well. The historical model that accommodates a non-conforming stereospecificity must be modified *ad hoc* to include postulates that there existed more than one ancestral enzyme for the reaction, or must weaken its conservation principles to allow stereospecificity to drift during divergent evolution. Either *ad hoc* modification weakens the predictive power and testability of the model.

A. Amino Acid Decarboxylases

Models explaining the stereospecificity of enzymes catalyzing the decarboxylation of amino acids illustrate these points. These decarboxylases are known in two mechanistic classes (Figure 5). In one class, the amino acid forms a

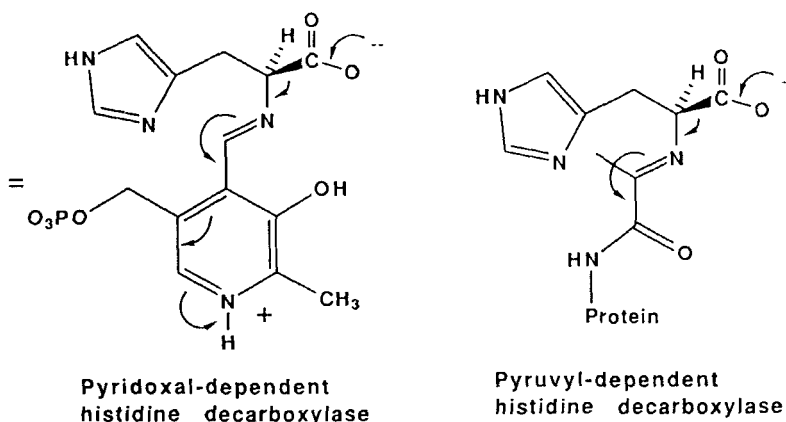


Figure 5. Cryptic stereospecificity of decarboxylases dependent on pyridoxal cofactors.

Schiff's base with a pyridoxal phosphate cofactor in the active site. In the other, the amino acid forms a Schiff's base with a pyruvyl residue covalently embedded in the enzyme's polypeptide chain. In both cases, electrons move from the carboxylate to an electron withdrawing group, and the carboxylate is replaced by a proton that ultimately comes from the solvent.

By 1979, several decarboxylases from both mechanistic classes had been examined. All were reported to catalyze decarboxylation with retention of configuration (Figure 6) (29); the proton replacing the carboxyl group was added to the same side of the molecule as the carbon dioxide departed. Enzymes from the first mechanistic class included tyrosine decarboxylase (30), glutamate decarboxylase (31), and the analogous pyridoxal-dependent serine hydroxymethylase (32). Enzymes from the second mechanistic class included the histidine decarboxylases from *Lactobacillus*, *Clostridium*, and mammals (33, 34).

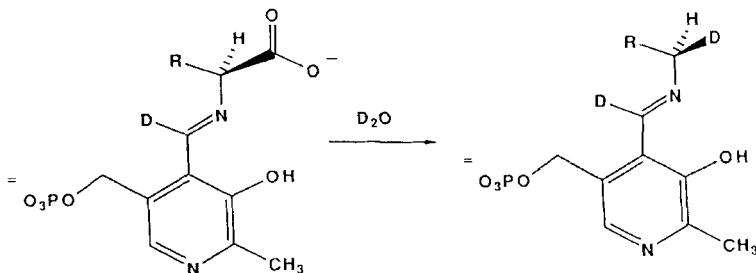


Figure 6. Decarboxylation of an L-amino acid with retention.

This uniformity was widely noted (8, 29), and discussed in terms of the stereoelectronic hypotheses of Dunathan (35). Dunathan argued that breaking of a carbon–carbon bond can occur only when the substrate is in a conformation where the bond overlaps with the pi orbitals of the Schiff's base. This argument is a functional one. It assumes that organisms containing decarboxylases that do not obey this stereoelectronic principle are less fit to survive (14).

Stereoelectronic considerations are not, however, directly relevant to the problem of explaining the choice between retention or inversion. The removal of carbon dioxide and the addition of a proton occur in separate reaction steps. The stereoelectronic argument addresses only the geometric requirements for these individual steps. In contrast, "retention" or "inversion" are overall stereochemical outcomes that depend on the relative geometries of the two steps. Reaction paths that produce either retention or inversion can be constructed so as to be equally satisfactory from a stereoelectronic point of view. Thus, whether Dunathan's hypothesis is affirmed or denied has no impact on any conclusion as to whether decarboxylation is "retentive" or "inertive" for functional or historical reasons.

In enzymes that catalyze the decarboxylation of *beta*-ketoacids, both "retentive" and "inertive" modes are known. Rose argued that this fact makes functional explanations of the stereochemical homogeneity observed in *amino acid* decarboxylases less satisfactory (29). The argument assumes that both classes of decarboxylases (those acting on beta ketoacids and those acting on amino acids) are subject to the same functional constraints, and that stereochemical heterogeneity among beta-ketoacid decarboxylases indicates that there are no functional constraints governing stereochemistry in this class of decarboxylases.

Arguments for either premise are not compelling. It is not clear why enzymes decarboxylating beta-ketoacids should be subject to the same functional constraints as enzymes decarboxylating amino acids, as the reactions proceed via rather different mechanisms. Nor is it certain that the mechanistic heterogeneity observed in beta-ketoacid decarboxylases is not itself functional.

Most authors choose not to distinguish among these possibilities, even though this choice precludes a biological interpretation of the data. For example, in their discussion of the apparent uniform stereospecificities in amino acid decarboxylases, Allen and Klinman simply listed possible interpretations without adopting one preferentially (36).

"The possibility exists that the observed conservation is mechanism based. Alternatively, both classes of amino acid decarboxylases may have risen from a common progenitor. The final possibility is that the choice of retention versus inversion occurred once, in a random manner, for each class of enzymes."

Given stereochemical uniformity in a class of enzymes, none of the alternatives is obviously preferred. However, depending on which is correct, the significance of the data is considerably different. If the uniformity is "mechanism based," this means that the survival of the host organism is influenced by this rather subtle stereochemical distinction. If both classes of enzymes arose from a common ancestor, then drift in stereospecificity must be extremely difficult, as it has been conserved during the same divergent evolution that has seen pyridoxal replaced by pyruvyl as a cofactor. Finally, if the choice is truly random, stereoselectivity cannot be informative about either function or history, suggesting that the trait is not particularly interesting to study.

Without explicit functional or historical models, the only experimental option is to examine more enzymes. This was done in many laboratories. For example, Orr and Gould (37) examined decarboxylases for ornithine, lysine, and arginine from *E. coli*, and for lysine from *Bacillus cadaveris*. All enzymes produced retention. Allen and Klinman (36) examined the stereochemical fate of substrates in S-adenosylmethionine decarboxylase, an enzyme dependent on an active-site pyruvyl residue. The enzyme catalyzed decarboxylation with retention.

Unfortunately, enzymes were not selected for study with the goal of resolving contrasting functional and historical explanations for the uniform stereochemical behavior of these decarboxylases. First, the enzymes examined all came from eubacteria (from the genera *Escherichia*, *Bacillus*, *Streptococcus*, *Lactobacillus*, and *Clostridium*). Though many examples of divergent behavior in proteins can be found within eubacteria, eubacteria are only one of the three kingdoms of life (archaeabacteria, eubacteria, and eukaryotes) available for bio-organic study (38). If the goal is to find examples of non-uniform stereospecificity within a class of enzymes, one is advised to examine organisms from different kingdoms and, if possible, from all three kingdoms.

Further, all of the decarboxylases studied act on the L-enantiomer of the amino acid. Several simple functional models would predict that the preferred stereochemical mode (retention or inversion) should be the same for both D- and L-amino acid. Yet enzymes acting on opposite enantiomers of a substrate are more likely to be non-homologous, or if homologous, likely to have diverged more, and therefore are more likely to have altered stereoselectivities than enzymes acting on the same enantiomers.

In this light, studies of D-amino acid decarboxylases became interesting. Soda and his coworkers examined an enzyme that decarboxylates a D-amino acid, a diaminopimelate decarboxylase from *Bacillus sphaericus*. The enzyme produces decarboxylation with *inversion* of configuration (Figure 7) (39).

We must pause for a moment to consider how this result constrains the logical form of historical or functional models that might be used to explain

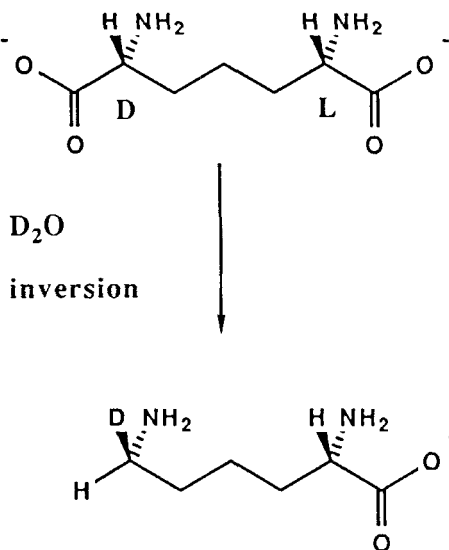


Figure 7. Decarboxylation of a D-amino acid with inversion.

it. These constraints in turn have an impact on the predictions that the models can make, and the experiments that one might do to test the models. We begin with a discussion of functional models.

The products of the enzymatic decarboxylation are the same whether the reaction proceeds with inversion or retention. Thus, the cryptic stereochemical outcome of the reaction cannot in itself be a selectable trait. Further, intermediates in the two reactions, the Schiff's base of a D-amino acid and the Schiff's base of an L-amino acid, are formally enantiomeric, if we ignore the chirality of the enzyme. (Although perhaps offensive to a stereochemical purist, we use the term "locally enantiomeric" to describe two enantiomeric species in a chiral environment where, for convenience in discussion, we overlook the surrounding chirality and the possibility of conformational diastereomerism). Thus, a functional explanation must identify a behavioral difference between the two locally enantiomeric transition states, and then correlate this with an explanation as to why retention is better for one, and inversion is better for the other. As enantiomeric species are energetically identical in an achiral environment, such a model must identify another chiral center in the environment and explain how this chiral center creates a functional difference.

First, and most obviously, the enzymic active site is "globally" chiral; this chirality might certainly be the basis of distinguishing between the two enan-

tiomeric transition states. But the fact that a chiral active site can make this distinction is not (by itself) a satisfactory functional explanation for the opposite stereospecificities. The global chirality of an active site is a variable over evolutionary time. It could have been different, and it could evolve.

Of course, the amino acid components of the proteins themselves are “intrinsically” chiral, meaning that their chirality is not an evolutionary variable. (Indeed, the use of L- instead of D-amino acids might be a prominent example of a non-adaptive trait that is nevertheless highly conserved). It is possible that inversion is functionally optimal for the decarboxylation of D-amino acids because L-amino acids are the building blocks of the polypeptide catalyst. Conversely, retention might be functionally optimal for L-amino acids because of the intrinsic chirality the L-amino acids used in the catalyst. This explanation would be the first to invoke the chirality of the amino acids building blocks of a protein to explain functionally a stereochemical course of enzymatic reactions.

Further, diaminopimelate itself has a second chiral center, and interaction with this center may (at least in principle) be the basis for a distinction between the two transition states. Possibly relevant to this notion is the fact that LL- and DD-diaminopimelates are neither substrates nor inhibitors of the enzyme, implying that the second center has some interaction with the enzyme (40).

Finally, a functional explanation might be constructed that incorporates some historical assumptions. One mode of decarboxylation (let us say, retention) might in fact be optimal for both D- and L-amino acids. However, for historical reasons, one set of amino acid decarboxylases (let us say the D-amino acid decarboxylases) may not have had the opportunity yet to evolve to produce the catalytically optimal retention. Perhaps D-amino acid decarboxylases arose only recently from L-amino acid decarboxylases and have not had time to accumulate the mutations required to become a superior retentive enzyme.

Thus, the stereochemical data from diaminopimelate decarboxylase logically constrain functional models. They must either:

- a. Assume that the second chiral center in diaminopimelate is responsible for the stereochemical distinction; this center is more remote than any center so far suggested to be important in determining stereospecificity in an enzymatic reaction;
- b. Assume that the chirality of the amino acids in an enzyme (the fact that, in the modern world, proteins must be made from L-amino acids) provides a functional basis for different stereospecificities in decarboxylases acting on D- and L-centers (this explanation is unprecedented);

- c. Assume that a stereochemical imperative exists (for either retention or inversion), but that one of the sets of enzymes (either the D- or the L-amino acid decarboxylases) has not evolved to attain it (perhaps because not enough evolutionary time has passed); or
- d. Be abandoned.

None of these options is especially attractive. Several examples are known where pairs of enzymes catalyze identical reactions via enantiomeric transition states. For example, citrate synthases are known that have opposite stereospecificities, a *Re*-citrate synthase from *Clostridium acidi-urici* (41, 42), and *Si*-citrate synthases from other organisms (43). The transition states in these two enzymes are locally enantiomeric (ignoring possible conformational differences in the transition states). Likewise, ethanol dehydrogenases from yeast and *Drosophila* have been recently shown to catalyze reactions via transition states that, except for the chirality of the NADH cofactor, appear to be locally enantiomeric (44). Thus, assumption (b) is known not to apply universally, making it less likely that it applies here.

Thus, at least in some cases, it is not obvious that the chirality intrinsic in proteins by virtue of the fact that their constituent amino acids are chiral selects for one enantiomeric transition state over another. One must note, however, that the citrate synthases mentioned above have different mechanisms, and different properties. The *Re*-specific enzyme requires Mn^{2+} and has a V_{max} of 5.5 I.U./mg, in contrast with the *Si*-enzyme, with a V_{max} of 150 and no metal requirement. Likewise, ethanol dehydrogenase from yeast requires a metal and is much faster than ethanol dehydrogenase from *Drosophila*, which requires no metal ion for catalysis. One cannot absolutely rule out the possibility that these behavioral differences are the result of a sub-optimal selection of a transition state with the incorrect chirality.

Assumption (a) might be evaluated if crystallographic data were available for the enzyme-substrate complex. Such data are almost certainly not immediately forthcoming. However, one might find support for such a hypothesis in the stereospecificities of other decarboxylases that act on substrates with two chiral centers (for example, threonine or isoleucine decarboxylases).

Assumption (c) appears to us to be the most plausible. However, a functional model that is modified to incorporate the possibility that some enzymes have not yet evolved to meet the functional "imperative" is not predictive unless an independent measure of optimality is available.

Such independent measures of optimality are conceivable. For example, one might argue that optimal enzymes have high k_{cat}/K_M values (13), and that D-amino acid decarboxylases are sub-optimal, both stereochemically and kinetically. Indeed, diaminopimelate decarboxylases appear to be kinetically rather slow. Kinetic parameters are shown in Table 1 for a number of amino

Table 1
Kinetic Parameters of Amino Acid Decarboxylases from Microorganisms

Substrate	Source	k_{cat} (sec ⁻¹)	K_M (mM)	$\left(\frac{k_{cat}}{K_M} \right) \text{ mM}^{-1} \text{ sec}^{-1}$	Ref.
L-AMINO ACID DECARBOXYLASES USING PYRIDOXAL					
Lysine	<i>B. cadaveris</i>	86	.37	250	a
Arginine	<i>E. coli</i>	400	.65	600	b
Glutamate	<i>E. coli</i>	115	.5	230	c
D-AMINO ACID DECARBOXYLASES USING PYRIDOXAL					
Diaminopimelate	<i>E. coli</i>	7.5	1.7	4	d
Diaminopimelate	<i>B. sphaericus</i>	28	1.7	17	38
L-AMINO ACID DECARBOXYLASES USING PYRUVYL RESIDUES					
S-Aden.Met	<i>E. coli</i>	40	0.1	400	e
Histidine	<i>Lactobacillus</i>	69	0.9	75	f

^aSoda, K.; Moriguchi, M. *Method. Enzymol.* 1971, 17B, 677. ^bBoeker, E. A.; Snell, E. E. *Meth. Enzymol.* 1971, 17B, 657. ^cHager, L. P. *Method. Enzymol.* 1971, 17A, 857. ^dWhite, P. J. *Method. Enzymol.* 1971, 17B, 142. ^eWickner, R. B.; Tabor, C. W.; Tabor, H. *Method. Enzymol.* 1971, 17B, 647. ^fRosenthaler, J.; Guirard, B. M.; Chang, G. E.; Snell, E. E.; *Proc. Nat. Acad. Sci.* 1965, 54, 152.

acid decarboxylases; the D-amino acid decarboxylases producing inversion have considerably lower k_{cat}/K_M values than L-amino acid decarboxylases producing retention, for enzymes involving both pyridoxal and pyruvyl groups. This is consistent with the notion that amino acid decarboxylases that produce inversion have not yet evolved enough to have the catalytically favored stereospecificity.

Again, the caveat must be stated that specific activities are preferable to turnover numbers or k_{cat} as a measure of optimality in an enzyme, as the former number reflects the size of the enzyme and, presumably, its biosynthetic "cost" to the organism (13). Further, one must remain aware of the fact that differences in kinetic parameters measured *in vitro* need not reflect differences *in vivo* (13).

Thus, a single result can greatly constrain the form of a model, in this case a functional one. New experiments are suggested by these constraints. However, the same result also constrains historical models with the same productive result. In historical models, a functional role for stereospecificity is denied. The historical model must consider two possibilities: The first is that D- and L-decarboxylases are homologous, the second is that they are not.

If the enzymes are not homologous, the historical model postulates that stereospecificity arose randomly in several unrelated ancestral decarboxylases. The model builder may argue that there were three ancestral enzymes, one using pyridoxal acting on L-amino acids, the second using pyridoxal acting on D-amino acids, and the third using pyruvyl acting on L-amino acids. The first and third randomly evolved to decarboxylate with retention, the second with inversion. Again, there must be a conservation principle; once the stereochemical mode is chosen in the ancestral enzyme, it must be conserved during subsequent divergent evolution.

Alternatively, the historical model might postulate that the pyridoxal enzymes producing retention are homologous with the pyruvyl enzymes. Here, stereospecificity is presumed to diverge less rapidly than mechanism. This presumption seems implausible if the stereospecificity is assumed to serve no functional role, as replacing a pyruvyl residue by a pyridoxal residue (or *vice versa*) would seem to require more than enough rearrangement in the active site to permit stereospecificity to drift. Thus, the similar stereospecificities of the two mechanistic classes of decarboxylases probably must again be viewed as the result of accident.

Historical models that assume that "retentive" and "invertive" enzymes are homologous also deny function. The strongest conservation hypotheses then is that stereoselectivity is conserved within a class and that the kinetically most accessible path for evolving a D-decarboxylase from an L-decarboxylase will convert a "retentive" enzyme" into an "invertive" enzyme. A less restrictive conservation hypothesis argues that stereoselectivity is randomized in a divergence that leads to enzymes accepting enantiomeric substrates.

Evaluations of both historical and "historically modified" functional models (for example, models that presume that evolution towards functionally optimal stereospecificity is currently in progress) must ultimately be based on comparisons of sequence data. For example, aspartate aminotransferases from mitochondria and cytoplasm from several organisms are clearly homologous. Other enzymes dependent on pyridoxal, including transaminases, D-serine dehydratase, and the B subunit of tryptophan synthetase, may also share this pedigree (45). The similarities in sequence that support such models are few, so homology must be distant and remains somewhat speculative. Nevertheless, homology among all retentive decarboxylases supports historical arguments explaining the common stereospecificity in terms of a shared pedigree.

However, even the amino acid sequence of diaminopimelate decarboxylase from *E. coli* (46) shows limited similarities with those of other pyridoxal enzymes (47). This suggests (again weakly) that these enzymes with *opposite* stereospecificities are also homologous, a suggestion that supports the "historically modified" functional model (where retention is assumed to be opti-

mal, but that D-amino acid decarboxylases have not yet evolved to this optimum), and weakens the conservation principle (stereospecificity in pyridoxal-dependent enzymes is highly conserved) needed by historical models.

Conversely, more recent studies have shown that the diaminopimelate decarboxylase from wheat germ also produces inversion (48). This result probably argues *against* the historically modified functional model, as it implies that D- and L-amino acid decarboxylases diverged before the divergence of bacteria and plant enzymes. This implies that the D-amino acid decarboxylases should have had enough time to be optimized. The alternative interpretation, that the diaminopimelate decarboxylase evolved independently in plants and bacteria, seems less likely, although the notion could be tested with sequence data.

More data relevant to this discussion were collected in 1979 by Gerdes and Leistner (49). These authors investigated the stereochemical course of lysine decarboxylation in *Bacillus cadaveris* and in *Sedum* plants. They demonstrated that decarboxylation of L-lysine by *B. cadaveris* proceeded with retention, but that the decarboxylation of L-lysine by *Sedum* proceeded with inversion.

Regrettably, the lysine decarboxylase was not purified, and it is not known whether this enzyme contains pyridoxal phosphate, a pyruvyl residue, or neither. Nor are kinetic parameters available. However, if a *bona fide* L-lysine decarboxylase from *Sedum* proceeds with inversion, historical and functional models must be further constrained.

We consider the functional model first and assume that the new enzyme uses pyridoxal as a cofactor. A functional model that explains inversion in L-lysine decarboxylase must identify some functionally relevant difference between the environments of this enzyme and the analogous enzyme from animals and bacteria. This must then form the basis of an argument that inversion is the optimal mode of catalysis in some environments and retention in others. The enzymes might operate in opposite directions physiologically (not likely in this case, but possible in others). Different stereochemical modes might be preferred at different ambient temperatures or pH optima.

Alternatively, a historically modified functional model might be constructed. The enzyme from *Sedum* may be presumed to have evolved from optimized retentive decarboxylases, but itself is not optimized. The prediction would be that the lysine decarboxylase from *Sedum* has a poor k_{cat}/K_M value in contrast to the analogous enzyme from other sources. Alternatively, historical models must propose yet another ancestral decarboxylase, perhaps one unique to plants. The amino acid sequence of the decarboxylase from *Sedum* is then needed as a test of the theory. There should be no homology. Further, L-amino acid decarboxylases from plants should all produce inversion.

A historical model so modified becomes unpredictive except in uninteresting cases, those where high (>50%) sequence similarity is already known. Not only can stereospecificity not make any statement about biological function and chemistry in this case, but it also cannot make statements about very ancient history. It may, however, serve as a tool for understanding evolution within biological kingdoms.

B. Conclusions

Stereospecificity in amino acid decarboxylases appears not to be a selected trait. However, sequence data currently available are insufficient to estimate whether the stereochemical diversity in this class of enzymes arises from drift or multiple ancestry.

While this discussion may seem hopelessly pedantic, it is important. The exercise of constructing formally precise models and the experimental pursuit of their logical implications illustrate the methods that must be applied to elucidate the biological significance of any enzymatic behavior. At the very least, the process forces the experimenter to examine his prejudices concerning the validity of historical and functional pictures of enzymatic behavior. At best, the process suggests new experiments.

Those studying cryptic stereospecificity in enzymes should chose systems with these issues in mind. In pyridoxal enzymes, further studies of enzymes from eubacteria seem to be of little value. However, fungi might contain homologous amino acid decarboxylases that have different stereospecificities. Further, it is interesting to determine whether enzymes catalyzing reactions other than decarboxylations, but dependent on pyridoxal cofactors, act differently on D-amino acids and on L-amino acids. For example, all amino acid transaminases so far studied abstract the *pro-S* hydrogen from pyridoxamine. It is important to determine whether this is true as well in transaminases acting on D-amino acids.

IV. CLASSES SHOWING STEREOCHEMICAL HETEROGENEITY

If members of a class of enzymes catalyzing similar reactions have different stereospecificities, functional models that ascribe a selectable function to stereospecificity must provide a chemical basis for the heterogeneity. Contrasting historical models must either argue that the trait is drifting, or that members of the class arose from two (or more) non-homologous ancestors. Four important classes of enzymes display stereochemical heterogeneity: phosphoryl transferases, beta-ketoacid decarboxylases, dehydrogenases dependent on nicotinamide cofactors, and enzymes catalyzing additions to olefins.

A. Phosphoryl Transfers

Methods for determining the absolute chirality of phosphates substituted with isotopes of oxygen (50) have been used to examine the stereospecificities of many phosphoryl transferases (51-57). Transfer is found in all cases to occur either with retention or with inversion of configuration at the phosphate center, and these results are generally interpreted in terms of two mechanistic alternatives. Inversion of configuration is interpreted as evidence for direct transfer of phosphorus from donor to acceptor in a single-step sequence involving no intermediate. Retention of configuration is interpreted as evidence for a two-step reaction with a phosphoryl-enzyme intermediate. While overall inversion is also consistent with more complicated mechanisms involving an odd number of displacement reactions at phosphorus, and retention is consistent as well with mechanisms postulating an even number of displacements, little evidence supports these more complicated mechanisms. Thus, discussion of the stereospecificity of phosphoryl transferases can move directly to a discussion of why intermediates are functionally better for some phosphoryl transfer reactions than for others.

Table 2 comprises the stereospecificities of a variety of phosphotransferases. It reveals an interesting distribution. Enzymes formally transferring phosphorus within a single molecule produce retention of configuration. Enzymes transferring phosphate from ATP to an alcohol or amine produce inversion. Enzymes transferring phosphorus from an alcohol to water, ATPases, and enzymes transferring phosphorus from phosphate to phosphate show stereochemical heterogeneity.

Table 2
Stereospecificity of Phosphotransferases

TRANSFERRING PHOSPHORUS WITHIN A SINGLE MOLECULE	
Phosphoglucomutase	retention
Phosphoglycerate mutase (rabbit)	retention
Phosphoglycerate mutase (wheat)	retention
TRANSFERRING PHOSPHORUS FROM DONOR TO ACCEPTOR MOLECULES OF EQUAL SIZE	
Nucleoside diphosphate kinase	retention
Nucleoside phosphotransferase	retention
TRANSFERRING PHOSPHORUS FROM DONOR TO ACCEPTORS OF DIFFERENT SIZE	
Acetate kinase	inversion
Acetyl CoA synthetase	inversion
Adenosine kinase	inversion

Table 2
(Continued)

TRANSFERRING PHOSPHORUS FROM DONOR TO ACCEPTORS OF DIFFERENT SIZE	
Adenylate kinase	inversion
Adenylosuccinate synthetase	inversion
Aminoacyl tRNA synthetases	inversion
Creatine kinase	inversion
DNA-dependent RNA polymerase (initiation) (elongation)	inversion
Galactose-1-phosphate uridylyltransferase	retention
Glycerol kinase	inversion
Hexokinase	inversion
Phosphofructokinase	inversion
Phosphoglycerate kinase	inversion
Polynucleotide kinase	inversion
Polynucleotide phosphorylase (exchange) (elongation)	retention
Pyruvate kinase	inversion
tRNA nucleotidyl transferase	inversion
UDP-glucose pyrophosphorylase	inversion
TRANSFERRING PHOSPHORUS TO WATER	
Acid phosphatase (bovine)	retention
Alkaline phosphatase (coli)	retention
Cyclic AMP phosphodiesterase	inversion
Exonuclease (bovine spleen)	retention
Non-specific phosphohydrolase	inversion
5'-Nucleotidase	inversion
Nucleotide pyrophosphatase	retention
Phosphodiesterase (snake venom)	retention
Phosphodiesterase (bovine intestine)	retention
Phosphohydrolase (Enterobacter)	inversion
Phospholipase D (cabbage)	retention
Ribonuclease (pancreatic)	inversion, inversion
Ribonuclease T ₁	inversion
Ribonuclease T ₂	inversion
Staph nuclease	inversion
ATPASES	
Mitochondrial ATPase	inversion
Myosin ATPase	inversion
Ribosome-dependent GTPase	inversion
Sarcoplasma reticulum ATPase	retention
Elongation factor G GTPase	inversion
Elongation factor T GTPase	inversion

Only in the first case is there a simple explanation. On geometric grounds, transfer of a phosphate group in a 1,2-diol can occur only via either an enzyme-phosphoryl (or cofactor-phosphoryl) intermediate, or via a cyclic intermediate that must undergo pseudorotation (Figure 8). In both cases, the stereochemical outcome is retentive (58).

In the other cases, more discussion is necessary. Frey has proposed a fascinating functional explanation for the last subclass of phosphoryl transferases, those that transfer phosphoryl groups between nucleotides. The transfer of phosphate from a nucleoside triphosphate (NTP) to a nucleoside diphosphate (NDP) proceeds via an enzyme-phosphoryl intermediate, but transfer from NTP to a nucleoside monophosphate (NMP) is direct. Frey noted that in the first case the phosphoryl donor and acceptor are approximately the same size (Figure 9) (59). Therefore, a single binding site can accommodate each, the enzyme holding the phosphoryl group while the donor (minus the phosphate) leaves the active site and the acceptor enters. In contrast, with donor and acceptor molecules of different size, the same binding site would not accom-

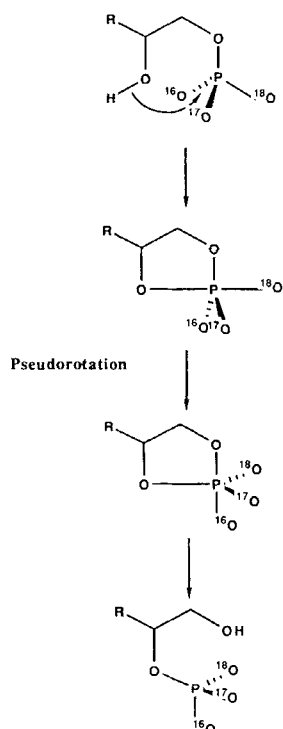


Figure 8. Phosphate transfer involving pseudorotation.

Acceptor and Donor groups the same size

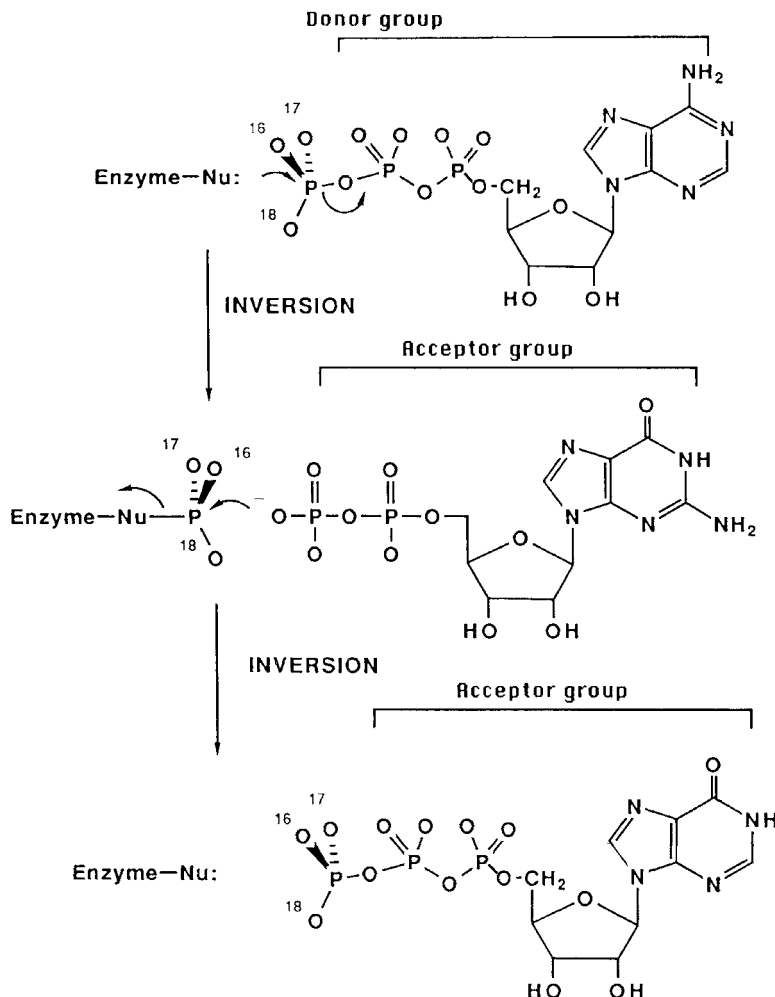


Figure 9. Retention of configuration in enzymes transferring phosphate between molecules with similar structure.

moderate both (Figure 10). Two binding sites must be built into the enzyme, and the transfer is direct from phosphoryl donor in one site to acceptor in the second.

Frey's model has several implications. First, it implies that there is a "cost" associated with evolving an enzyme with an extra binding site. This cost could be either "thermodynamic" (two identical organisms, one with an "inexpensive" NTP-NDP transferase having a single binding site, the other with an "expensive" enzyme with two binding sites, have different survival abilities) or "kinetic" (proteins with one binding site evolve more rapidly). Further, it implies that there is a smaller "cost" for enzymes using two binding sites for donor and acceptor with different sizes than for enzymes using one site (where, for example, a conformational change occurs to accommodate two substrates with different steric requirements). Finally, it suggests that once an enzyme has two binding sites, direct transfer is preferable over a phosphoryl-enzyme intermediate.

These implications have broader impact. If the expense of synthesizing large proteins is sufficiently great to influence the survival of a host organism in phosphoryl transferases, minimizing the size of proteins should be a goal of natural selection with other proteins as well. It is conceivable that such selective pressures might create trade-offs between size and other behaviors. These

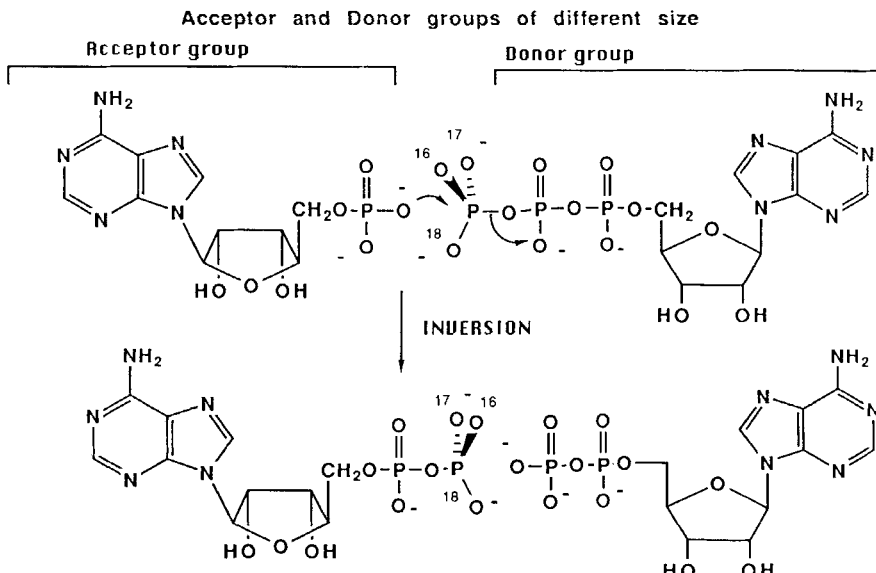


Figure 10. Inversion of configuration in enzymes transferring phosphate between molecules with different structure.

considerations are discussed at length elsewhere (9, 13-15). Finally, it implies that the large size of some enzymes confers selective advantage.

Isolated examples from other classes of enzymes suggest that Frey's hypothesis is not general. For example, two classes of enzymes catalyze the transfer of hydrogen from NAD⁺ and NADP⁺. One class catalyzes direct transfer in an active site with *two* binding sites, the other proceeds via an "enzyme-hydride" intermediate where the reducing equivalent is bound to flavin (60). The existence of these two classes suggests that the cost of constructing additional binding sites may not in fact have a significant impact on survival.

Functional theories can be constructed for the other classes of phosphoryl-transferases. Frey's model would predict that transfer from ATP to an alcohol or amine should proceed with inversion. The donor and acceptor are sufficiently different as to require two binding sites and, once two binding sites are needed, direct transfer is presumed to be optimal. Inversion is observed in these enzymes.

Given this theoretical context, the phosphotransferases that appear to have functionally anomalous stereospecificities are those that transfer phosphoryl groups to water. A functional model based on principles of chemical reactivity can be constructed that suggests that these enzymes should proceed via enzyme-phosphoryl intermediates (and hence with retention) when the enzyme has evolved to have low substrate specificity. The argument is based on the fact that for catalysis to occur an enzyme must bind to the transition state of a reaction more tightly than it binds to the ground state (61).

There are several ways of stating this argument. Drawing on the language of Jencks (62) (which, although theoretically problematical (63), might be the most familiar to the reader), it is difficult for an enzyme to bind and activate small nucleophiles such as water. Thus, in phosphoryl transfers to water, catalysis must be achieved by interactions between the enzyme and the phosphoryl donor.

If the phosphatase has evolved to be non-specific, the enzyme does not have many strong interactions with the phosphoryl donor; thus, the enzyme has few opportunities to "activate" the phosphate donor to achieve catalysis. In these cases, nucleophilic catalysis by a residue in the active site is the only mechanism remaining for catalyzing the transfer of the phosphoryl group. Hence, transfers to water are likely to involve an enzyme-phosphoryl intermediate, especially if the enzyme has low substrate specificity. For an enzyme with high substrate specificity, direct transfer to water from an activated phosphate donor is preferred for the reasons outlined above. In this case, the "binding energy utilized" for catalysis is obtained by interactions between the enzyme and the phosphoryl donor.

This notion is consistent with the fact that many nonspecific phosphatases

produce retention (Table 2). For example, glucose-6-phosphatase, an enzyme with broad substrate specificity, produces retention, consistent with an enzyme-phosphoryl intermediate and the notion that neither the nucleophilic substrate nor the phosphate donor can be activated in an enzyme where water is the nucleophile and the enzyme must accept phosphate donors with a range of structures. In contrast, phosphatases that have narrow substrate specificity (for instance, staphylococcal nuclease and cyclic phosphodiesterases, the second acting on a substrate that is already somewhat reactive), produce inversion. This model is predictive, although the scale that describes the "narrowness" of substrate specificity is only semi-quantitative.

The divergent stereospecificities of ATPases remain a significant problem. These enzymes all catalyze (apparently) chemically identical reactions. While inversion occurs most often when phosphate is transferred from nucleoside triphosphates to water (as expected by the functional model), the ATPase from sarcoplasmic reticulum operates with retention (54). Though one might dismiss this stereochemical difference as the result of random origin or neutral drift, functional models can be constructed.

Most ATPases participate in specific physiological processes (64-69). Normally, the hydrolysis of ATP is coupled to muscle contraction, Ca^{2+} transport, or other metabolic processes. In other cases, "ATPases" are, in fact, ATP synthetases under physiological conditions. Only rarely is the destruction of ATP likely to be the physiological role for an ATPase.

Enzyme-phosphoryl intermediates have different values depending on how the energy of ATP hydrolysis is used. Clearly, enzyme phosphoryl intermediates are kinetically more stable than intermediates where this energy is stored in a high-energy conformation of the enzyme or in a tightly bound enzyme-ADP complex. The increased kinetic stability is advantageous if the high-energy intermediate must undergo conformational contortions, or must survive for periods of time (for example, to permit an ion to diffuse to or from it). It is presumably disadvantageous in other cases, as the need for a second step (the hydrolysis of the covalent enzyme-phosphorus bond) slows down the turnover rate.

These considerations offer a rationalization for the fact that enzyme-phosphoryl intermediates are used uniformly for ion transport, where considerable conformational change must take place in the activated intermediate. It also suggests an explanation for the lack of such a covalent intermediate in myosin ATPases, where the conformational change is presumably itself the work that is physiologically intended, occurs immediately upon the hydrolysis of ATP, and where slowing turnover numbers would be distinctly disadvantageous in muscle tissue, because power per unit volume is extremely important. Finally, ATPases that act physiologically as phosphoryl donors to water should produce inversion unless they are relatively nonspecific for substrate, following the rationale outlined above.

These hypotheses are generated *post hoc*, given the information that ATPases involved in ion transport do indeed catalyze reactions via an enzyme-phosphoryl intermediate, though other ATPases do not. Their value comes, again, in their predictive utility.

Sequence data are rapidly becoming available that make interesting comments on historical views of the stereospecificity of ATPases. Sequences suggest that major classes of phosphoryl transferases with the same stereospecificities are homologous (69, 70). However, there also appear to be sequence similarities in the active site of ATPases that produce retention and those that produce inversion (69), especially around the aspartate that is phosphorylated in the first class (Figure 11). Remarkably, the aspartate that is phosphorylated in the first class is found as a threonine in the second class. Further, the conserved sequence is found between the two nucleotide binding domains predicted in the second class based on structural homologies with adenylate kinase and near Tyr 311, believed to interact with certain inhibitors of ATPase. Thus, the short sequence similarities appear to be significant and suggest that some invertive and retentive ATPases are homologous.

If this suggestion is correct, it again indicates that reaction mechanisms (and therefore stereospecificity) are remarkably adaptable in the face of different functional demands. Aside from suggesting that stereospecificity is a poor indicator of homology in this case, such an indication raises doubts about historical explanations for stereospecificity in general in the presence of alternative functional models.

A final stereochemical point should be noted. Cleland and his coworkers have pioneered the use of chiral complexes between ATP and chromium as stereochemical probes of the active sites of phosphatases (71). Two stereochemical classes of enzymes have been identified; certain members of both classes produce inversion. This may indicate independent origin of two inver-

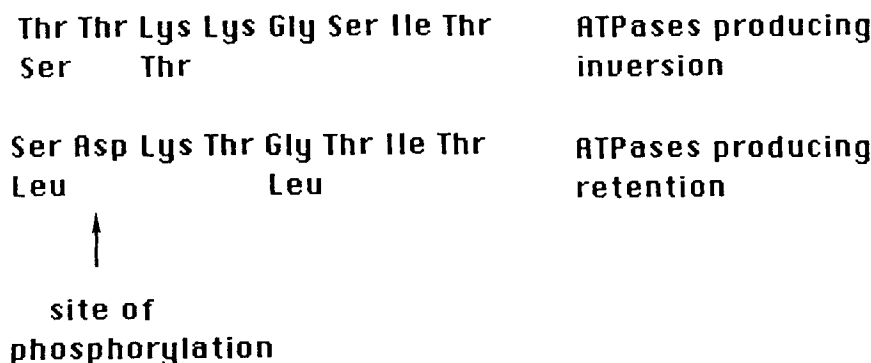


Figure 11. ATPases producing retention and inversion, respectively.

tive classes of enzymes. Alternatively, it may indicate that specificity for the chirality of the conformation in which ATP binds may drift.

B. Beta-Ketoacid Decarboxylases

Decarboxylases acting on beta-ketoacids constitute another class of enzymes that displays stereochemically heterogeneous activity. In 1973, Rose and Hanson noted that of five decarboxylases studied, three decarboxylated substrate with retention of configuration and two with inversion (29). Rose interpreted this as evidence that stereospecificity is selectively "neutral" in these enzymes, arguing that it makes no difference to the survival of the host organism which stereochemical mode was followed. Thus, the stereospecificity of each individual enzyme evolved randomly. A sixth enzyme, acetolactate decarboxylase, has subsequently been examined; it produces inversion (72).

As with pyridoxal-dependent decarboxylases, stereospecificity in decarboxylases acting on beta-ketoacids does not reflect a stereochemical choice in a single transition state but rather the relative stereochemical choices in two separate transition states. The first involves the removal of a carbon dioxide to give an intermediate enol or enol equivalent. The second leads to the protonation of the intermediate to yield the product ketone.

Two mechanisms for catalyzing beta-decarboxylations are well documented by model studies (Figure 12). In the first, metal ions chelated to an alpha ketoacid unit act as an "electron sink," facilitating decarboxylation (73). The decarboxylation of oxaloacetate catalyzed by divalent manganese apparently proceeds via such a mechanism. Alternatively, decarboxylation can be catalyzed by amines. Here, the amine reacts with the keto group to form a Schiff's base. Presumably, the protonated Schiff's base acts as an "electron sink" (24).

Both forms of catalysis are apparently exploited by enzymes, depending on the structure of the substrate (Table 3). For the six enzymes listed in the table, enzymes acting on substrates that possesses an alpha-ketoacid moiety

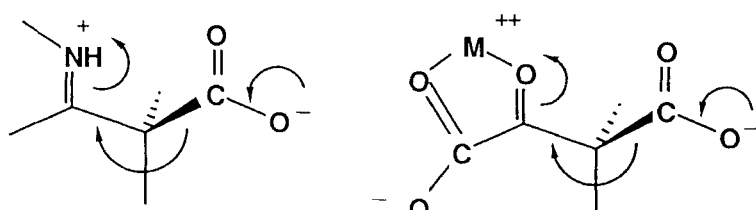


Figure 12. Schiff's base and metal-dependent decarboxylation of beta-ketoacids.

Table 3
Substrates, Stereospecificities, and Requirements for Metal Ions
in Beta-ketoacid Decarboxylases

Enzyme	alpha-Keto acid as substrate?	Stereo-selectivity	Metal ion?
Isocitrate dehydrogenase (NAD^+)	yes	retention	yes
Isocitrate dehydrogenase (NADP^+)	yes	retention	yes
Malic enzyme	yes	retention	yes
Phosphogluconate dehydrogenase	no	inversion	no
UDP-glucuronate decarboxylase	no	inversion	no
Acetolactate decarboxylase	no	inversion	no

capable of coordinating a metal ion require a metal ion catalytic activity. Those that act on substrates lacking this moiety do not require a metal ion.

This observation permits a correlation to be drawn connecting substrate structure, mechanism, and stereospecificity (25, 74). Whenever a metal ion is required for catalysis, the decarboxylation proceeds with retention of configuration; whenever a metal ion is not required, decarboxylation proceeds with inversion of configuration. The two stereochemical modes observed in beta decarboxylases appear to reflect the existence of two mechanisms for enzyme-catalyzed decarboxylations. As a working hypothesis, this correlation predicts the stereochemical preference of any beta decarboxylase whose substrate is known.

The model makes predictions. For example, the biosynthesis of 5-amino-levulinic involves two stereochemically significant steps, the condensation of glycine with succinyl-CoA to yield 2-amino-3-ketoadipate and the decarboxylation of this intermediate to yield 5-aminolevulinic acid (Figure 13) (75). The functional model predicts that the condensation step proceeds with retention, and the decarboxylation with inversion. Consistent with this, the reaction of succinyl CoA and glycine to form aminolevulinic acid was found to proceed via overall inversion (75), requiring that one of the steps is invertive and the other retentive. Further work is necessary to determine whether the model has correctly predicted which step is which.

The functional model was recently scrutinized by a study of the stereochemical course of decarboxylations catalyzed by acetoacetate decarboxylase (25). This enzyme, predicted to produce inversion, surprisingly was found to produce retention and inversion with roughly equal frequencies. This appeared to reflect stereo-nonspecific protonation of an intermediate enamine, not racemization of starting material or equilibration of label in product or Schiff's base between product and enzyme (Figure 14). This interpretation was confirmed by a series of control experiments.

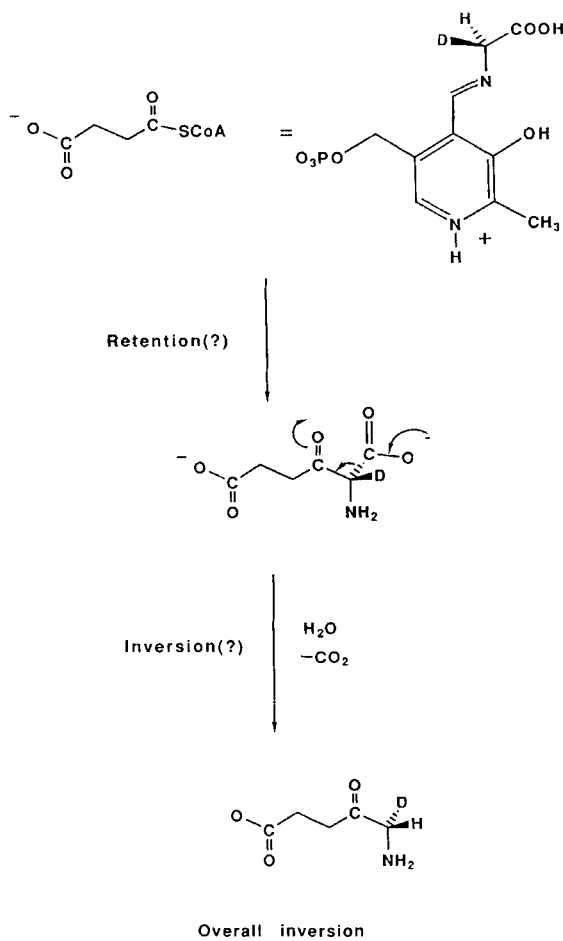


Figure 13. Cryptic stereospecificity in aminolevulinate synthase.

The functional model predicted that acetoacetate decarboxylase would produce inversion; retention would have been considered a contradictory result. The observed result neither confirmed or contradicted the model cleanly. To explain this result functionally, an *ad hoc* hypothesis was introduced. Noting that the rate of protonation of the enamine of acetone in solution at the physiological pH (*pH* 6) was on the same order of magnitude as the steady state turnover rate of the enzyme, the argument was made that protonation from the solvent would be kinetically competent to carry the flux through the active site. Thus, there appears to be little need for enzymatic catalysis of the protonation of the enamine. Protonation directly from solvent

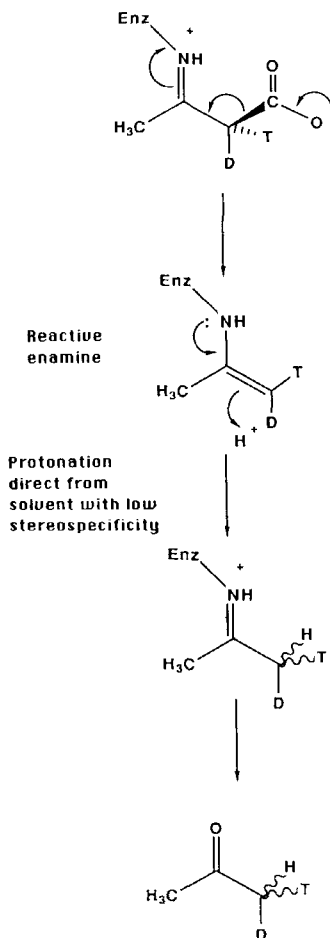


Figure 14. Reactive intermediate proposed to explain racemization in the decarboxylation of acetoacetate.

plausibly would proceed with lower stereoselectivity than protonation by a general acid provided from the active site. Thus, when the intermediate is extremely reactive, one might expect low cryptic stereospecificity.

While the introduction of *ad hoc* arguments might be excused for a theory at an early stage of development, the *ad hoc* modification could be tested, as a similar argument should apply to other unsubstituted enamines that are intermediates in enzymatic reactions. For example, a similar enamine (here, of pyruvate) is an intermediate in the conversion of aspartate to alanine catalyzed by aspartate beta-decarboxylase (Figure 15). As the enamine of pyru-

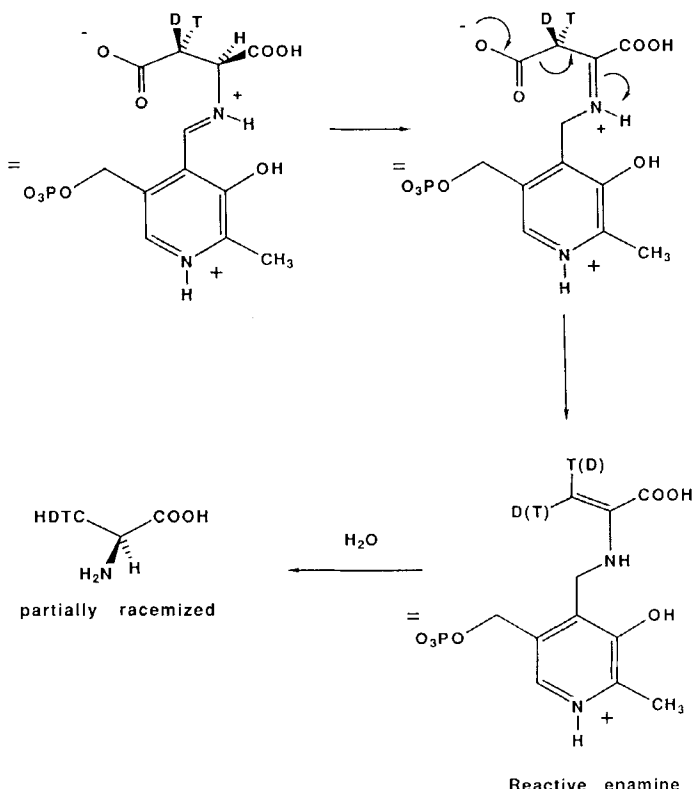


Figure 15. Reactive intermediate proposed to explain partial racemization in the decarboxylation of aspartate.

vate with pyridoxamine should have a chemical reactivity similar to that of the intermediate in the reaction catalyzed by acetoacetate decarboxylase, the enamine might also be protonated directly from solvent with incomplete stereospecificity.

Indeed, alanine formed as a product of aspartate beta-decarboxylase was found to be substantially racemized (76). This is consistent with the modified hypothesis. Unfortunately, control experiments have not yet been done to distinguish between racemization as a result of partial stereospecificity in the

decarboxylation step (consistent with the *ad hoc* explanation) and racemization resulting from subsequent enzyme-catalyzed exchange of the protons on the product.

Recently, the stereospecificity of oxaloacetate decarboxylase (OAD) from *Pseudomonas putida* was examined as a further test of the model. The OAD requires a divalent metal cation; the metal presumably chelates the alpha-ketoacid moiety of the substrate providing an electron sink for decarboxylation (Figure 12) (25). The natural substrate is presumably oxaloacetate. Thus, on mechanistic considerations, OAD from *Pseudomonas* is expected to catalyze the decarboxylation of oxaloacetate with retention, as do other metal-dependent OAD's.

In fact, OAD from *Pseudomonas* produces inversion (77). This stereochemical result violates the correlation in Table 3. Indeed, the result is inconsistent with any simple functional explanation for stereospecificity in decarboxylases based on a property intrinsic in the substrate, as OAD from *Klebsiella aerogenes* (biotin dependent) (78, 79), pyruvate carboxylase (biotin dependent) (80), and malic enzyme all produce retention (81). In the last case, the enzyme producing retention appears to operate via the same mechanism as the OAD from *Pseudomonas*. The inescapable conclusion is that mechanistic diversity in beta-decarboxylases does not always correlate with stereochemical diversity. However, the result is also inconsistent with "historical" explanations that presume common ancestry for beta-decarboxylases, with stereospecificity highly conserved during divergent evolution.

Thus, beta-ketoacid decarboxylases display a full range of stereochemical diversity: retention, inversion, and racemization. Three explanations must be considered for these results: (a) there exist several independent pedigrees of decarboxylases descended from several ancestral decarboxylases, where stereospecificity is non-functional but highly conserved; (b) stereospecificity is a non-functional trait capable of facile neutral "drift" as homologous enzymes diverge; or (c) stereospecificity is a functional trait, where a mechanistic imperative is different in different decarboxylases because the enzymes perform subtly different roles in subtly different environments.

Data are insufficient to distinguish between these three alternatives, although possibilities (a) and (b) seem to be the most likely. It is important to collect sequence data to distinguish between these two possibilities, as the outcome here will influence our view of functional and historical models for stereospecificity in general. In particular, if stereospecificity in decarboxylases can easily drift, this would suggest that other stereochemical behaviors of enzymes can drift as well.

C. Dehydrogenases Dependent on Nicotinamide Cofactors

Of the dehydrogenases dependent on nicotinamide cofactors that have been studied, about half transfer the *pro-R* hydrogen of NAD(P)H, while half transfer the *pro-S* hydrogen (Table 4, Figure 16) (21). This stereochemical choice does not obviously correspond to a mechanistic choice. Rather, stereospecificity appears to be determined only by the relative orientation of the substrate and the cofactor in the active site, an orientation that in turn is determined by the relative positions of active site residues. These positions seem to be arbitrary. Therefore, historical explanations for stereospecificity in dehydrogenases have been predominant in the literature.

Table 4a
Stereospecificity of Dehydrogenases Arranged by E.C. Number

E.C.	Name	Stereochemistry
1.1.1.1	Alcohol dehydrogenase (yeast)	<i>pro-R</i>
1.1.1.3	Homoserine dehydrogenase	<i>pro-R</i>
1.1.1.6	Glycerol 2-dehydrogenase	<i>pro-R</i>
1.1.1.8	Glycerol-3-phosphate dehydrogenase	<i>pro-S</i>
1.1.1.26	Glyoxylate reductase	<i>pro-R</i>
1.1.1.27	L-Lactate dehydrogenase	<i>pro-R</i>
1.1.1.28	D-Lactate dehydrogenase	<i>pro-R</i>
1.1.1.29	Glycerate dehydrogenase	<i>pro-R</i>
1.1.1.30	3-Hydroxybutyrate dehydrogenase	<i>pro-S</i>
1.1.1.35	3-Hydroxyacyl CoA dehydrogenase	<i>pro-S</i>
1.1.1.37	Malate dehydrogenase	<i>pro-R</i>
1.1.1.38	Malic enzyme	<i>pro-R</i>
1.1.1.40	Malic enzyme (NADP)	<i>pro-R</i>
1.1.1.50	3-Hydroxysteroid dehydrogenase (P. test.)	<i>pro-S</i>
1.1.1.51	beta-Hydroxysteroid dehydrogenase	<i>pro-S</i>
1.1.1.60	Tartronate semialdehyde reductase	<i>pro-R</i>
1.1.1.62	Estradiol 17-beta-dehydrogenase	<i>pro-S</i>
1.1.1.64	Testosterone beta-dehydrogenase	<i>pro-S</i>
1.1.1.72	Glycerol dehydrogenase (NADP)	<i>pro-R</i>
1.1.1.79	Glyoxylate reductase (NADP)	<i>pro-R</i>
1.1.1.81	Hydroxypyruvate reductase	<i>pro-R</i>
1.1.1.82	Malate dehydrogenase (NADP)	<i>pro-R</i>
1.1.1.100	3-Oxoacyl ACP reductase	<i>pro-S</i>
1.1.1.108	Carnitine dehydrogenase	<i>pro-S</i>

Table 4b
Stereospecificity of Dehydrogenases Arranged by the pK_{eq}
for their Physiological Reaction

E.C.	Name	pK_{eq}	Stereochemistry
1.1.1.26	Glyoxylate reductase	17.5	<i>pro-R</i>
1.1.1.79	Glyoxylate reductase (NADP)	17.5	<i>pro-R</i>
1.1.1.60	Tartronate semialdehyde reductase	13.3	<i>pro-R</i>
1.1.1.29	Glycerate dehydrogenase	13.3	<i>pro-R</i>
1.1.1.72	Glycerol dehydrogenase (NADP)	12.8	<i>pro-R</i>
1.1.1.81	Hydroxypyruvate reductase	12.4	<i>pro-R</i>
1.1.1.82	Malate dehydrogenase (NADP)	12.1	<i>pro-R</i>
1.1.1.37	Malate dehydrogenase	12.1	<i>pro-R</i>
1.1.1.38	Malic enzyme	12.1	<i>pro-R</i>
1.1.1.40	Malic enzyme (NADP)	12.1	<i>pro-R</i>
1.1.1.27	L-Lactate dehydrogenase	11.6	<i>pro-R</i>
1.1.1.28	D-Lactate dehydrogenase	11.6	<i>pro-R</i>
1.1.1.1	Alcohol dehydrogenase (yeast)	11.4	<i>pro-R</i>
1.1.1.6	Glycerol 2-dehydrogenase	11.3	<i>pro-R</i>
1.1.1.8	Glycerol-3-phosphate dehydrogenase	11.1	<i>pro-S</i>
1.1.1.3	Homoserine dehydrogenase	10.9	<i>pro-R</i>
1.1.1.108	Carnitine dehydrogenase	10.9	<i>pro-S</i>
1.1.1.35	3-Hydroxyacyl CoA dehydrogenase	10.5	<i>pro-S</i>
1.1.1.30	3-Hydroxybutyrate dehydrogenase	8.9	<i>pro-S</i>
1.1.1.50	3-Hydroxysteroid dehydrogenase	8.0	<i>pro-S</i>
1.1.1.62	Estradiol 17-beta-dehydrogenase	7.7	<i>pro-S</i>
1.1.1.64	Testosterone beta-dehydrogenase	7.6	<i>pro-S</i>
1.1.1.100	3-Oxoacyl ACP reductase	7.6	<i>pro-S</i>
1.1.1.51	beta-Hydroxysteroid dehydrogenase	7.6	<i>pro-S</i>

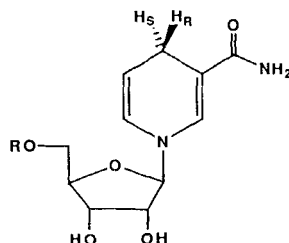


Figure 16. Cryptic stereospecificity at cofactor in dehydrogenases.

1. Correlations

With stereospecificities known for nearly 200 dehydrogenases, empirical correlations with satisfactory statistics are possible. These serve as the starting point for constructing testable models, both historical and functional. Here as above, exceptions to such correlations, and how they are treated, determine the development of the models. Failure to discard a correlation in the face of a significant exception runs the risk of destroying the rigor and predictability of a model. Yet, discarding a poorly understood correlation because of a single exception runs the risk that a valuable model will be overlooked; this risk is especially high in the early stage of model-building, where the significance of the exception may not be understood or where the reported data themselves may be incorrect.

Conservatism is the rule in literature interpreting these correlations. Interesting and experimentally testable correlations have been discarded in the face of a single (and often poorly understood) counterexample. For example, Davies and coworkers suggested that dehydrogenases involved in consecutive steps in a biochemical pathway should have the same stereospecificity at the nicotinamide cofactor (82). Though originally an empirical generalization, the model has clear "historical" basis. If enzymes catalyzing consecutive steps in a metabolic pathway are homologous, and if stereospecificity is highly conserved, this rule follows deductively. These assumptions have received some independent experimental support from work by Ornston and his co-workers (83). Further, Davies' model makes the general statement that reaction type, mechanism, and substrate specificity all diverge faster than stereoselectivity. This may be true or false, but it is interesting, and deserves exploration.

However, exceptions exist to the empirical rule. Nitrate reductase (forming nitrite) and nitrite reductase (forming ammonia) from *Canadida utilis* have opposite stereospecificities at NADH (84). Further, enzymes presumed to act consecutively in the metabolism of cinnamyl alcohol in plants have opposite stereospecificities (85). In light of these two exceptions, the correlation has been dismissed (21), and it appears as if no further investigations of this generalization have been undertaken. This is unfortunate. It is certainly conceivable that *some* pairs of enzymes catalyzing consecutive steps in a metabolic pathway are not homologous. Further, there are independent ways of assessing homology in these cases, sequence comparisons being the most direct. Thus, if sequence data suggest that these pairs of consecutive enzymes with opposite stereospecificities are not homologous, no serious damage is done to the assumptions underlying the historical model. Indeed, it would be interesting to know how often enzymes catalyzing consecutive steps in metabolism are homologous. Conversely, if the consecutive enzymes with opposite ste-

reoselectivities prove to be homologous, the result strongly contradicts a conservation principle that assumes that stereospecificity is highly conserved, and casts doubt on historical models that depend on it. Thus, the model stimulates experimental work that is useful regardless of the results.

What constitutes an unacceptable level of exception to a rule is often a matter of taste. For example, a recent review criticized fourteen generalizations concerning the stereospecificities of enzymes dependent on nicotinamide cofactors (21). Generalizations that had "too many" exceptions were discarded. However, a rule correlating stereospecificity in dehydrogenases with the mode of cofactor binding (where *pro-S* and *pro-R* stereospecificities correlate with a *syn* or *anti* orientation of the nicotinamide ring around the glycosidic bond, Figure 17) with 6 confirming instances and 1 exception (14%) was regarded as "the only mechanistic explanation" for stereospecificity that was "receiving growing acceptance." A rule with some 50 confirming instances and 6 exceptions (12%) was dismissed as having "untenability" that is "overwhelmingly evident."

Here, as above, we believe that a more productive approach evaluates generalizations by their ability to suggest testable functional or historical models. Exceptions are treated as logical constraints on the form of the historical or functional model. Further, exceptions must be critically evaluated with respect to the model they are intended to disprove. If an exception is presumed to challenge a functional model, its evolutionarily relevant function must be known. If an exception is presumed to challenge a historical model, information about its pedigree is relevant.

An important set of empirical generalizations for dehydrogenases was introduced in slightly different forms by Vennesland, Colwick, and Bentley. Often referred to as "Bentley's rules," these generalizations are (86, 87):

1. The stereospecificity of a particular enzyme does not depend on the source of the enzyme.
2. The stereospecificity of a particular reaction is the same in those cases where both NAD⁺ and NADP⁺ can be used as coenzymes.
3. If a single enzyme uses a range of substrates, the stereospecificity with respect to cofactor will be the same with all substrates.

These generalizations have only a few exceptions, and some remarkable confirmations. Lactate dehydrogenases all transfer the *pro-R* hydrogen (21), regardless of whether they are isolated from mammals (bovine, rabbit, and pig), amphibians (frog), fish (halibut), birds (turkey), dogfish, plants (potato), arthropods (horseshoe crab), lower eukaryotes (sea worm, abalone), or bacteria (*E. coli*, *Lactobacillus*) (21). Malate dehydrogenases from many sources also transfer the *pro-R* hydrogen, including those from mammals (pig), plants (potato, wheat germ), birds (chicken), arthropods (*Drosophila*),

fungi (*Neurospora*), bacteria (*B. subtilis*), and archaeabacteria (*Sulfolobus acidocaldarius*, *Thermplasma acidophilum*, *Halobacter halobium*) (88, 89). The 3-hydroxybutyryl-CoA and 3-hydroxybutyryl-acyl carrier protein dehydrogenases transfer the *pro-S* hydrogen, including those from mammal (bovine, rat, pig), bacteria (*Rhodopseudomonas*, *Escherichia*, *Brevibacter*), from birds (pigeon), and from yeast (21, 90). Together, these organisms include several representatives from every kingdom of life on the planet.

2. Historical Models

A historical model stating that stereoselectivity (a) is not functional, (b) is "random," and (c) can drift randomly is inconsistent with the generalizations above. For example, if stereospecificity can drift, the stereospecificities of lactate and malate dehydrogenases would not be as uniform as they are. Thus, a constrained historical model must assume that when cofactor stereospecificity originated in an enzyme, it was random. However, the model must assume that once established, stereospecificity in the dehydrogenases was highly conserved during subsequent divergent evolution. Further, the model must assume that all modern dehydrogenases acting on a particular substrate are homologous.

The range of organisms over which Bentley's first rule applies suggests that stereoselectivity was conserved in the time since the divergence of plants, animals, insects, eubacteria, and archaeabacteria. This is the most ancient divergence that can be identified in modern biology. Thus, a historical model seeking to explain this rule must presume that stereoselectivity with respect to cofactor is very rigorously conserved indeed. Not surprisingly, several arguments can be found in the literature that it is *impossible* for a *pro-R* enzyme to evolve to become a *pro-S* enzyme (91, 92).

Such extreme conservation of stereospecificity is remarkable, as it appears that stereospecificity in a dehydrogenase can be reversed by simply reversing the geometry in which the nicotinamide ring is bound in the active site (Figure 17). Rotating the nicotinamide ring 180° around the glycosidic bond (for example, from a syn conformation to an anti conformation) would present the opposite face of the cofactor to the substrate and therefore produce an enzyme with opposite stereospecificity. Such a rotation leaves all other features of the enzyme-cofactor complex unchanged and appears to take place when dihydrofolate is replaced with methotrexate in complexes with NAD⁺ and dihydrofolate reductase (*vide supra*).

Extreme conservation of the mode of binding (syn versus anti) of the nicotinamide cofactor might be explained by an assumption that reversing the mode of cofactor binding requires simultaneous replacement of a large number of amino acids in the active site. Enzymes with only some of these replace-

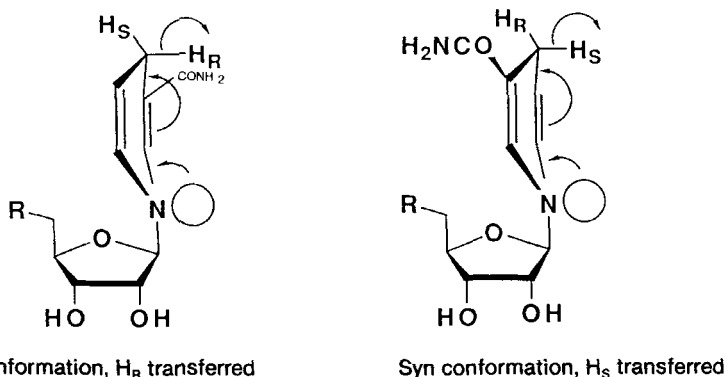


Figure 17. Correlation of stereospecificity with conformation of bound cofactor in dehydrogenases.

ments are presumed to be inactive catalytically. Organisms containing these "intermediate" enzymes would die. In this view, mode of cofactor binding (and hence, stereospecificity) is presumed to be tightly coupled to catalytic activity, tertiary structure, or some other functional trait. Therefore, stereospecificity is conserved, even though it itself serves no selectable function.

Although this model cannot be ruled out *a priori*, it is problematical. Rossmann has argued from structural data that the dinucleotide binding domains of various dehydrogenases are similar; this similarity presumably reflects a common pedigree (93, 94). However, by this argument, the dinucleotide binding domains of glyceraldehyde-3-phosphate dehydrogenase and malate dehydrogenase (dehydrogenases with opposite stereospecificity with respect to nicotinamide cofactor) are homologous. If Rossmann's argument is correct, stereospecificity with respect to cofactor is not absolutely conserved. Indeed, it diverges faster than general tertiary structure in a domain and faster than the divergence of primary sequence, at least of key residues in the dinucleotide binding domain of these proteins.

Similarly, the stereospecificities of ethanol dehydrogenases from yeast and *Drosophila* are opposite (95). Yet the dinucleotide binding domains of the two enzymes appear to be homologous based on sequence analysis (96).

A modified historical model to explain these facts relies on the notion of "domain shuffling" in the evolution of proteins (97). In this model, only the dinucleotide binding domains of glyceraldehyde-3-phosphate dehydrogenase and malate dehydrogenase are homologous. This homology indicates only a very ancient common ancestry. The modern enzymes in each class arose fol-

lowing the appending of two non-homologous catalytic domains to each of the proteins, a process that is presumed to create random stereospecificities in two new proteins with different substrate specificities. In subsequent divergent evolution, both stereospecificity and substrate specificity was conserved.

Such a model is consistent with the fact that the relative positions of the catalytic and dinucleotide binding domains in the polypeptide chains of the ethanol dehydrogenases from yeast and *Drosophila* are reversed. Indeed, there is a possible (but imperfect) correlation between stereospecificity and the relative positions of the two domains.

Simply assuming, however, that stereospecificity with respect to cofactor (and hence, presumably, the mode of cofactor binding, Figure 18) is highly conserved is insufficient to explain Bentley's first rule. We must also presume that enzymes catalyzing analogous reactions in different organisms generally share a common ancestor. This requires the additional assumption that drift in *substrate specificity* is also constrained. Strictly, the general substrate specificity of one primordial enzyme cannot have evolved to encompass substrates within the general substrate specificity of the other. This conservation principle is necessary because divergence in substrate specificity can create stereochemical diversity just as easily as divergence in the mode of cofactor binding.

For example, if a gene for a dehydrogenase is lost by deletion, the lost catalytic function can be replaced by the evolution of substrate specificity of a second dehydrogenase to assume the role of the deleted enzyme. This process is facile in molecular evolution; indeed, it occurs on the laboratory time scale. For example, a new chorismate mutase has evolved from a prephenate binding site in less than 40 years in a strain of *Bacillus subtilis* with the native chorismate mutase deleted (98). In *E. coli* lacking beta-galactosidase, a new beta-galactosidase emerges after another protein (with unknown function) undergoes two point mutations (99).

This process provides a mechanism for creating stereochemical diversity in a class of dehydrogenases, even given the assumption that mode of cofactor binding is rigorously conserved. For example, if the gene for malate dehydrogenase (transferring the *pro-R* hydrogen) is lost, and the activity is replaced by the evolution of a 3-hydroxybutyrate dehydrogenase (*pro-S* specific) with conservation of cofactor stereospecificity, a *pro-S* specific malate dehydrogenase is the result. Because this process is so facile, it is to be expected, certainly over long periods of evolutionary time. The fact that malate dehydrogenase does not display the expected stereochemical diversity indicates, in the historical view, that deletion-replacement events have not occurred in the time separating archaebacteria, eubacteria, and eukaryotes.

The implications of this second conservation principle are quite interesting

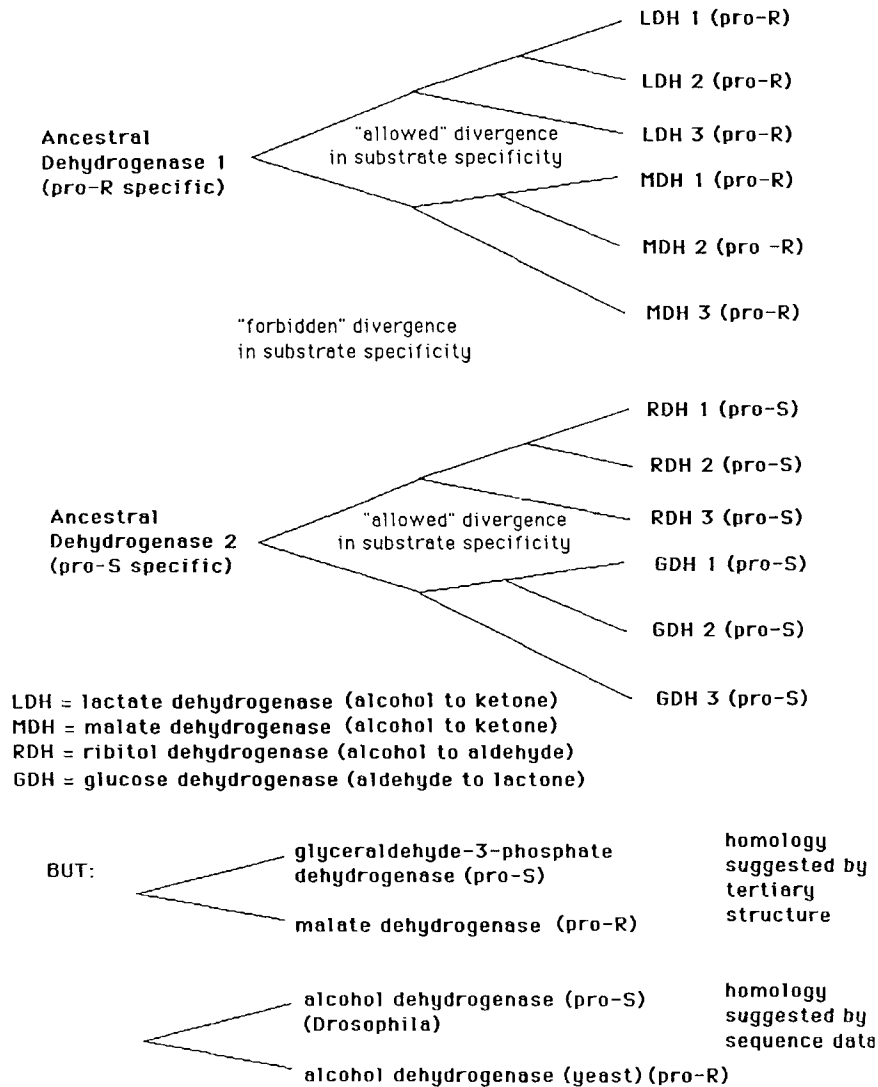


Figure 18. Evolutionary trees used for historical explanation of stereospecificity in dehydrogenases.

and quite general, both in terms of how proteins evolve and how structure and function are related in proteins. If all malate dehydrogenases (*pro-R* specific) are related and had pedigrees independent of 3-hydroxybutyrate dehydrogenases (all *pro-S* specific), the separation of the major subclasses of dehydrogenases must have been quite ancient (Figure 18). Further, if enzymes do

not alter their general substrate specificities in the evolutionary time separating mammals, plants, and archaebacteria, with no malate dehydrogenases becoming 3-hydroxybutyrate dehydrogenases, and *vice versa*, the constraint on substrate specificity is quite remarkable.

This view is significant because it contradicts other data that suggest that substrate specificity can diverge rather easily (9). For example, substrate specificities are quite different in the E (ethanol) and S (steroid) isozymes of horse liver alcohol dehydrogenase; yet amino acids sequences of these two enzymes differ at only 6 positions. Further, rapid divergence of substrate specificity is known in nature. The sequences of dehydrogenases acting on ribitol (from *Klebsiella*) glucose (*B. megaterium*), and ethanol (from *Drosophila*) show that these enzymes are homologous. Further, *pro-R* specific dehydrogenases acting on sorbitol (sheep) and ethanol (yeast) are also homologous (100).

These caveats do not require abandoning the "consensus" historical model. For example, in organisms having both lactate and 3-hydroxybutyrate dehydrogenases, it might be easier ("kinetically") to evolve a new lactate dehydrogenase from an old lactate dehydrogenase than from a 3-hydroxybutyrate dehydrogenase (9). This assumption may then be used to explain an absence of examples of homologous modern lactate and 3-hydroxybutyrate dehydrogenases. Likewise, divergence of substrate specificity might be influenced by positive selection pressures, while divergence in cryptic stereospecificity might occur only via neutral drift. The former might be expected to be faster than the latter, although little evidence supports this expectation.

Further, lactate and malate have considerable structural similarity, and the substrate conservation principle could be modified to allow substrate specificity to evolve within a general structural class. However, malate and 3-hydroxybutyrate also have similar structures (Figure 19). Whether lactate (enzymatically formed by transfer of the *pro-R* hydrogen) is viewed as having a structure more similar to 3-hydroxybutyrate (enzymatically formed by transfer of the *pro-S* hydrogen) or to malate (enzymatically formed by transfer of the *pro-R* hydrogen) is difficult to judge objectively. Further, glyoxylate reductase and L-lactate dehydrogenase might be considered to act on the same class of substrates; thus, their identical cofactor stereospecificity (*pro-R*) could be interpreted as evidence that the two are related. However, the stereospecificities of the two enzymes with respect to small molecule substrate are opposite (101).

Thus, the minimal historical model consistent with the data presented so far must presume: (a) a functionally constrained stereospecificity having random origin and no selectable value, yet rigorously conserved since the divergence of archaebacteria, eubacteria, and eukaryotes; (b) a common ancestor with a defined stereospecificity for enzymes acting on the same substrate from

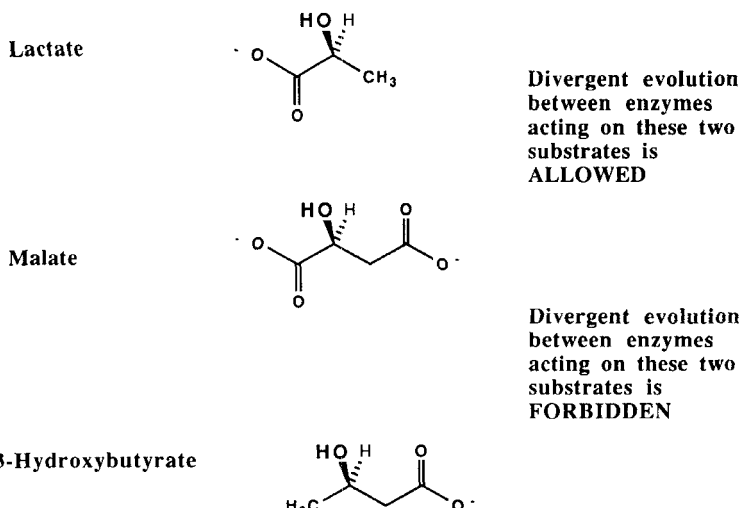


Figure 19. Historical models for stereospecificity in dehydrogenases must assume certain constraints in the divergence of substrate specificity.

plants, animals, and eubacteria (generally), and archaeabacteria in the case of malate dehydrogenase; and (c) a substrate specificity that is highly conserved, with enzymes acting on one general class of substrates unable to evolve from those acting on another. This model, although rarely stated in its complete form, makes up the modern consensus regarding dehydrogenase stereoselectivity.

This consensus historical model has recently been modified by Schneider-Bernloehr and her colleagues, who argued that dehydrogenases related to *Drosophila* ADH (DADH) will transfer the *pro-S* hydrogen and those related to yeast ADH (YADH) will transfer the *pro-R* hydrogen (102). Further, they correlate enzymes in the first class as having low molecular weights (ca. 28,000 Daltons) and require no metal ion for catalysis, while those in the second class as having higher molecular weights (ca. 36,000 Daltons) and requiring Zn^{2+} for catalysis. This correlation was similar to that suggested by Jornvall and his colleagues (96). It has, however, a corresponding functional interpretation (*vide infra*).

The model loses some of its value in view of the homology between DADH and YADH themselves. Given this fact, the model makes no absolute predictions. Rather, it again reduces to the statement that dehydrogenases that are more closely related to DADH are more likely to transfer the *pro-S* hydrogen, while those more closely related to YADH are more likely to transfer the

pro-R hydrogen. This statement is never disputed, either by functional or by historical advocates.

Further, although molecular weight and metal ion requirements might be interpreted as evidence for homology in the absence of sequence data, such evidence is weak. Indeed, the predictive weakness of a historical model based on such evidence is illustrated by a variety of dehydrogenases from mammals. These include (a) a "mevaldate reductase" from rat liver, an enzyme with low molecular weight (27–30,000), apparently requiring no metal, but nevertheless transferring the *pro-R* hydrogen (103); (b) an "aldehyde reductase" from pig kidney, an enzyme with high molecular weight (42,000), transferring the *pro-R* hydrogen, but nevertheless containing no metal ion (104, 105); (c) "aldehyde reductases" from human and rat brain, enzymes with high molecular weight (40,000), transferring the *pro-R* hydrogen, but nevertheless containing no metal ion (106); and (d) several enzymes known under a variety of names, including "carbonyl reductase," "ketoprostaglandin reductase," and "xenobiotic ketone reductase," with molecular weights reported to range from 30,000 to 40,000, mostly transferring the *pro-S* hydrogen (107).

3. Functional Models

The consensus model can be challenged only by an alternative functional model that makes contrasting experimental predictions. Such a functional model was proposed in 1982 by one of us (108). Another model was proposed more recently by Srivastava and Bernhard (109).

The first functional model begins with a stereoelectronic analysis of NADH. In the reduced cofactor, a lone pair of electrons on nitrogen is adjacent to an antibonding orbital associated with the ribose carbon–oxygen bond (Figure 17). Two conformations, syn and anti, permit overlap between these two orbitals. The overlap is expected to distort the nitrogen from planarity; in the original model the dihydronicotinamide ring adopts a boat conformation as a result (108, 110).

Boat conformations in cyclohexadiene systems have some precedent (111), although the extent of the distortion is disputed (112). Recent crystallographic data have provided definitive data in the case of dihydronicotinamide (113). A boat conformation does not exist in simply substituted dihydronicotinamide rings, at least not in the ground state. Stereoelectronic interactions do appear to distort the nitrogen from planarity, however, and structural, spectroscopic, and computational data are consistent with the stereoelectronic model as applied to transition state structures and energies (113, 114).

The prediction from this stereoelectronic argument is that the *pro-R* hydrogen is transferred from the anti conformer of NADH, while the *pro-S* hy-

drogen is from the syn conformer. Thus, the stereoelectronic argument provides a chemical rationale for a correlation (*vide supra*) that was proposed much earlier on empirical grounds (94, 115).

Recently, glutathione reductase has been suggested as an enzyme that violates this correlation (116). The enzyme transfers the *pro-S* hydrogen but has been reported to bind NADH in an "anti" conformation (116). Although the coordinates needed to evaluate this possibility have not yet been published, private communication suggests that this "violation" is an interesting one (117). The crystallographic definition of the "anti" conformation in this case corresponds to a dihedral angle (C(2)-C(1)-N-C(2')) of approximately 74°. This is different from the stereoelectronic definition (where this angle is close to 0°). Indeed, NADH bound in the active site of glutathione reductase appears to have a conformation where the orbital on nitrogen containing the lone pair is orthogonal to the antibonding orbital of the carbon-oxygen bond. This may be related to the fact that glutathione reductase catalyzes a reaction involving flavin, thereby differing from other dehydrogenases that have been crystallized.

The functional model next assumes that enzymes adjust the internal equilibrium constant, defined as the ratio of enzyme-bound substrates to enzyme-bound products at equilibrium, to catalytically optimal values (118). The anti conformation of NADH is presumed to be a weaker reducing agent than the syn conformation. Thus, within a class of analogous reactions (for instance, the reduction of carbonyls to alcohols) enzymes evolved to reduce "easy-to-reduce" carbonyls should have evolved to transfer the *pro-R* hydrogen, while those evolved to reduce "hard-to-reduce" carbonyls should have evolved to transfer the *pro-S* hydrogen (108).

The functional model explains the common stereospecificities of lactate dehydrogenases, malate dehydrogenases, and 3-hydroxybutyryl CoA dehydrogenases as the products either of convergent evolution to, or of functional constraint on drift away from, *pro-R*, *pro-R*, and *pro-S* stereospecificity, respectively. The absolute stereospecificities are predictable based on the redox potentials of lactate, malate, and 3-hydroxybutyrate. As in any functional model, this argument requires no comment about the homology of any of these enzymes.

This model unifies stereochemical data for dehydrogenases interconverting alcohols and carbonyls. A correlation (108) between stereoselectivity and redox potential of natural substrate (Table 4b) divides dehydrogenases into three groups. Those reducing thermodynamically unstable carbonyl groups transfer the *pro-R* hydrogen; those reducing stable carbonyl groups transfer the *pro-S* hydrogen. In regions in between, where the equilibrium constant for the redox reaction is approximately 10^{-11} M, where the functional theory argues that stereoselectivity has little or no selective value, some enzymes transfer the *pro-R* hydrogen, while others transfer the *pro-S* hydrogen.

4. Controversy

A lively controversy has surrounded the functional model. The first challenge argued that three enzymes, 3-hydroxysteroid dehydrogenase from rat liver, 20-hydroxysteroid dehydrogenase from rat ovaries, and 21-hydroxysteroid dehydrogenase from bovine adrenals, all violate the correlation in Table 4b (119). The three "counterexamples" were assumed to "dispel" the correlation, rendering the mechanistic analysis above "not pertinent."

The discussion in the early sections of this review alerts the reader to three issues that must be considered before accepting this critique. First, the functional model makes experimentally testable predictions and has proven valuable in directing experimental work. Second, the three exceptions are advanced to dismiss a correlation that includes some 120 examples (95). Last, the three exceptions are advanced to dismiss a functional model. Therefore, it is relevant to ask whether the selectable functions of the enzymes discussed are correctly identified. As the functional model concerns properties of the substrate that the enzyme has evolved to act upon, the question of physiological substrate becomes central (9).

The literature almost certainly misassigns the physiological substrates of two of the three enzymes discussed (21-hydroxysteroid dehydrogenase and 3-hydroxysteroid dehydrogenase). In the first case, the k_{cat}/K_M for the alleged substrate (dehydrocortisone) is four orders of magnitude smaller than expected based on the k_{cat}/K_M values of enzymes catalyzing similar reactions. Further, dehydrocortisone has never been detected in natural tissues (95). Likewise, the "3-hydroxysteroid dehydrogenase" from liver almost certainly has not evolved to act specifically on 3-hydroxysteroids. The enzyme converts benzene dihydrodiol to catechol, reduces quinones to hydroquinones, and catalyzes redox reactions on phenylglyoxal, a variety of nitrobenzaldehydes and acetophenones, and chloral hydrate (95), all with the same facility with which it oxidizes 3-hydroxysteroids.

The natural substrate of 20-hydroxysteroid dehydrogenase from rat ovaries is also disputed (95). Nevertheless, the third violation of the correlation is the most likely of the three to be an actual challenge of the functional model.

The functional model has been the subject of other less coherent criticism. For example, it has been argued that lactate and malate dehydrogenases should not be included in the correlation as two separate entries, as the two enzymes are homologous (120). Though this may be true, the criticism begs the central question. Malate and lactate dehydrogenases are either homologous or they are not. If they are homologous, the question remains as to whether their common stereospecificity reflects conservation for functional reasons. If they are not homologous, the question remains as to whether their common stereospecificity reflects functional or accidental convergence.

Another criticism is based on the fact that some dehydrogenases act on a

range of carbonyl substrates with a range of redox potentials. For example, lactate dehydrogenase and liver alcohol dehydrogenase act on substrates both with redox potentials in the *pro-R* region of the plot, and with redox potentials in the *pro-S* region (21). The criticism is confused. While the functional model argues that stereospecificity of a dehydrogenase has evolved functionally to reflect the redox potential of a natural substrate, it does not argue that the redox potential of a substrate *per se* determines stereospecificity. Stereospecificity is determined by the placement of amino acids in the active site. This placement has evolved over millions of years; it does not change in the laboratory when the enzyme is challenged with a new substrate with a different redox potential. Only if the enzyme is forced to evolve to accept the new substrate as a natural substrate does one expect stereospecificity to reverse so as to reflect a mechanistic imperative.

Of course, enzymes (such as liver alcohol dehydrogenase) may act naturally on a range of substrates. In these cases, functional theories based on a property of a specific substrate cannot make predictions, and data from such enzymes cannot be used to evaluate a functional theory.

Other criticisms are simply based on chemical misapprehensions. For example, the equilibrium constant for the overall reaction catalyzed by isocitrate dehydrogenase is less than 10^{-11} , and arguments have been made that the enzyme should transfer the *pro-S* hydrogen, not the *pro-R* hydrogen, to be consistent with the correlation in Table 4b (120). Of course, the quoted equilibrium constant for the overall reaction catalyzed by isocitrate dehydrogenase includes a decarboxylation step; the microscopic equilibrium constant for the redox reaction itself is much different. Indeed, based on an estimated equilibrium constant for the redox reaction alone, isocitrate dehydrogenases are expected to transfer the *pro-R* hydrogen. All examined (so far) do.

More extreme error is reflected by the recent direct comparison of the equilibrium constants for the reactions catalyzed by glutamate dehydrogenase, ethanol dehydrogenase, and glyceraldehyde-3-phosphate dehydrogenase. The comparison was used to question the validity of the correlation in Table 4b (120). As the units of the three equilibrium constants are M^2 , M, and unitless, respectively, the significance of a direct comparison of their numerical values is less than clear, and the relevance of such a comparison to an evaluation of the correlation and the functional model is minimal.

A final criticism enjoying currency at the time of this writing is that the functional model is too restricted in its scope, and that enzymes must meet too many criteria to serve as critical tests of the model. For example, a recent paper from Kozarich's laboratory argued that "the number of tests that a dehydrogenase must pass in order for it to be included in [the functional] hypothesis suggests that the NAD-dependent dehydrogenases are a too inherently complex class of enzyme to serve as a paradigm" (121).

The criteria that must be met for an enzyme presumed to serve as a critical

test for the functional model were defined in 1983: the enzymes must have well-defined physiological functions, act on unconjugated substrates (a criterion introduced to avoid enzymes that might operate via radical intermediates), and act on substrates with redox potentials one log unit from the break in the correlation in Table 4b. The first criterion is demanded by the logic of functional models; one cannot evaluate functional models for enzymatic behavior using enzymes whose physiological function is unknown. The second criterion is needed to evaluate any model based on assumptions regarding mechanism. A correlation presumably rooted in mechanism would be most remarkable if it is obeyed by enzymes employing different mechanisms. Finally, a functional model can be critically challenged only if a property that is presumed to be strongly favored by natural selection is not observed by experiment.

Analogous criteria are essential for evaluating *any* functional model; experiments that ignore them can draw no conclusions. They *must* be accepted, regardless of their "complexity." Nevertheless, in the case of alcohol dehydrogenases, these criteria scarcely limit opportunities for experimental test. Over 100 alcohol dehydrogenases fulfill the first requirement; 70 fulfill all three. Further, in the last five years, some 24 new enzymes have been examined as tests of the model. While not all of these enzymes have provided critical tests to distinguish between functional and historical models, several have (*vide infra*).

Based on the criticisms reviewed above, one recent commentator concluded that "the drawbacks [of the functional model] are overwhelming" (21). That criticisms such as these are considered overwhelming might be regarded as an indication of the novelty of functional and historical analysis in general. However, it is unfortunate that these criticisms have led in the literature to the conclusion that "the validity of this new postulate should await the test of time" (21). Time does not test hypotheses. Given two opposing models, a historical model complicated by constraints needed to explain available data, and an untested functional model, experiments that distinguish between the two are needed.

5. *Distinguishing Functional and Historical Cases*

Many data have now been collected for the purpose of evaluating the relative merits of functional and historical explanations for the stereospecificity of dehydrogenases. In some cases (for example, the stereospecificity of "lactaldehyde reductase"), incorrect biochemical identification prevented meaningful interpretation of the data (110, 122-124). However, other data have substantially narrowed the scope of historical models. Other experiments have tested the chemical and kinetic rationales underlying the functional model, includ-

ing the stereoelectronic effects (*vide supra*), and the assumptions made by the functional model regarding internal equilibrium constants (118).

Some of the most interesting tests have examined the functional model purely as a logical formalism. The danger of a formalistic approach to model testing is that the formalism can be mistaken for underlying reality by the not-too-careful scientist. For example (*vide supra*), the direct comparison of equilibrium constants with different units, the confusion over the physiological substrates of dehydrogenases, and the confusion over the mode of cofactor binding by glutathione reductase all reflect problems in identifying formalism. However, once the potential for such confusion is recognized and avoided, logical formality is a most valuable property in a model. In particular, the formalism offers the opportunity for "mechanical" tests of the model, and can be directly applied to new systems as a first step in exploratory research to detect other selected traits.

For example, drift of stereospecificity is expected only in alcohol dehydrogenases where the functional model predicts that stereospecificity is a weakly selected trait. The formalism of the correlation in Table 4b suggests that such enzymes act on substrates near the "break" in the correlation. Stereochemical heterogeneity is therefore expected in enzymes catalyzing the interconversion of $\text{CH}_2\text{-CH}_2\text{-OH}$ and $\text{CH}_2\text{-CHO}$ groups, as the equilibrium constant for this reaction is approximately 10^{-11}M .

Clear examples of such stereochemical diversity were first discovered through efforts to discover stereochemical heterogeneity in such enzymes. Ethanol dehydrogenase from *Drosophila* and hydroxymethylglutaryl-CoA (HMG-CoA) reductase from *Acholeplasma* were found to have stereospecificities opposite to those of analogous enzymes from previously studied organisms (95, 125). To rule out the possibility that the stereospecificities of dehydrogenases in *Drosophila* and *Acholeplasma* are *generally* different from stereospecificities of dehydrogenases found in other organisms, the stereospecificities of many dehydrogenases from the two organisms were determined (Table 5). The only enzymes displaying stereochemical heterogeneity were the two mentioned above (44, 125).

6. *The Simplest Historical Model*

The new data collected from these studies require a re-evaluation of the consensus historical model for dehydrogenase stereospecificity. The following facts are especially important:

Fact 1: Certain enzymes catalyzing analogous reactions appear to be non-homologous but nevertheless have the same stereospecificities. Examples include: glucose-6-phosphate dehydrogenase and glucose dehydrogenase (non-homologous judging by sequence) (126); metal-dependent alcohol dehy-

Table 5

Stereospecificities of Alcohol Dehydrogenases from a Variety of Sources. *pro-R* Stereospecificity is Designated "A", and *pro-S* Stereospecificity is Designated "B"

Prediction of functional theory for: Substrate	Experimentally Determined Stereospecificity of Dehydrogenase from:						
	mammal	insect	plant	fungus	eubac- teria	myco- plasma	archae- bacteria
A							
Malate	A	A	A	A	A	?	A
Lactate	A	A	A	A	A	A	A
A/B							
Ethanol	A	B	B	A	A	A	A
Hydroxymethyl glutaryl CoA	A	?	?	A	?	B	?
B							
Glucose-6-P	B	?	?	B	B	?	?
3-Hydroxybutyryl derivatives	B	?	?	B	B	?	?

drogenase from *Saccharomyces* and *Zymomonas* (127, 128) (non-homologous judging by sequence and metal ion requirement); dihydrofolate reductases (non-homologous judging by sequence and tertiary structure) from two bacterial plasmids (129, 130).

Fact 2: Certain enzymes that appear homologous (at least in one domain) nevertheless have the opposite stereospecificities. Examples include: the dinucleotide binding domains of the ethanol dehydrogenases from yeast (*pro-R* specific) and *Drosophila melanogaster* (*pro-S* specific) (homologous by sequence comparisons, Figure 20) (95, 96); the dinucleotide binding domains of glyceraldehyde-3-phosphate dehydrogenases (*pro-S* specific) and lactate dehydrogenases (*pro-R* specific) (homologous based on comparisons of their crystal structures) (93, 94); mammalian aldehyde dehydrogenase (*pro-R* specific) and aspartate-beta-semialdehyde dehydrogenase from *E. coli* (*pro-S* specific) (possibly homologous based on limited sequence similarities) (131); enoyl CoA reductase from yeast (*pro-S* specific) and from mammal (*pro-R* specific) (possibly homologous based on limited sequence similarities) (132, 133).

Fact 3: Certain enzymes that are clearly homologous act on substrates with quite different structures. Examples include: ethanol and sorbitol dehydrogenases (96); ribitol dehydrogenase, glucose dehydrogenases, and ethanol dehydrogenase from *Drosophila* (96, 126).

Drosophila	Lys Asn Val Ile Phe	Val	Ala	Gly	Leu		Gly	Gly	Ile	Gly	Leu
Horse	Gly Ser Thr Cys	Ala	Val	Phe	Gly	Leu	Gly	Gly	Val	Gly	Leu
Yeast	Gly His Trp Val	Ala	Ile	Ser	Gly	Ala Ala	Gly	Gly	Leu	Gly	Ser
Ribitol dehydrogenase	Gly Lys Val Ala	Ala	Ile	Thr	Gly	Ala Ala	Ser	Gly	Ile	Gly	Leu

Figure 20. Sequence comparisons in alcohol dehydrogenases from four organisms.

Fact 4: Stereospecificity in alcohol dehydrogenases correlates with the redox potential of the natural substrate (Table 4b) (108).

Fact 5: In one case, enzymes with unknown pedigree acting on the same substrate have different stereospecificities: the hydroxymethylglutaryl-CoA (HMG-CoA) reductases from rat and yeast have stereospecificities opposite to that from *Acholeplasma* (134, 135).

Fact 6: Certain enzymes with unknown pedigree acting on analogous substrates with opposite chiralities have the same stereospecificities. Examples include: D- and L-lactate dehydrogenases, both transferring the *pro-R* hydrogen (21, 136); L-fucose dehydrogenase and D-glucose dehydrogenase (stereochemistry at C-1 of the sugars has the opposite absolute sense), both transferring the *pro-S* hydrogen (21, 136).

Fact 7: In general, enzymes from widely divergent sources catalyzing a redox reaction far from the break in the correlation (Table 4b) share a common stereospecificity. These are now best exemplified by the malate dehydrogenases mentioned above, including enzymes from eubacteria, archaebacteria, and eukaryotes (88, 89, 136).

A difficult task faces a historical model builder. The enzymes in group 1 appear to be examples of convergent evolution, suggesting functional adaptation. For the pair of dihydrofolate reductases, the argument for convergence is quite strong. In the other cases, however, an advocate of a historical model for dehydrogenase stereospecificity might argue that a *lack* of sequence similarity is inadequate to *rule out* distant homology, implying that stereospecificity is more highly conserved than virtually every other trait in a protein (21).

However, the enzymes in group 2 contradict this implication. Enzymes with detectable (if small) sequence similarities have opposite stereospecificities, making it difficult to state the level of sequence divergence that is required before stereospecificity can be reversed or, conversely, the level of sequence identity that safely predicts that two enzymes will have identical stereospecificity. In other words, the statement "cofactor stereospecificity is highly conserved" is difficult to define objectively. It appears safe to assume,

however, that a pair of natural dehydrogenases with sequence identities greater than 50% will have the same stereospecificities.

A historical model must account for the fact that in some classes of dehydrogenases, evolutionary processes have not created stereochemical diversity in the time separating archaebacteria, eubacteria, and eukaryotes (even though diversity is known in virtually every other biochemical behavior in this range of organisms), while in other cases, evolutionary processes have produced stereochemical diversity in much less time. Further, it must explain why divergence of substrate specificity appears facile (Fact 3), yet evolution of substrate specificity following deletion events has not created stereochemical diversity in most dehydrogenases. Finally, it must account for Fact 7, that stereospecificity within one subclass of dehydrogenases, those interconverting alcohols and ketones, correlates with the redox potential of the natural substrate. This requires a model with at least six hypotheses (125):

Hypothesis 1: To explain the absolute conservation of stereospecificity of malate dehydrogenases (MDH) (compared to HMG-CoA reductases and ethanol dehydrogenases), the drift of stereospecificity in MDH is presumed to be lower than in other dehydrogenases. Likewise, the model must presume that it is impossible to replace MDH by the evolution of the substrate specificity of a *pro-S* specific enzyme (for example, a 3-hydroxybutyrate dehydrogenase) via a deletion-replacement event (*vide supra*). This prohibition applies also to all other dehydrogenases (with a bit less rigor) except for ethanol dehydrogenases and HMG-CoA reductases (137).

While this hypothesis is arbitrary, it might be justified by assuming that most dehydrogenases (including malate dehydrogenases and lactate dehydrogenases) are more "essential" to the survival of the host organism than ethanol dehydrogenases and HMG-CoA reductases. Thus, structural variation (as a prelude to drift in stereospecificity) and deletion are presumed to be more selectively disadvantageous in malate and lactate dehydrogenases than in ethanol dehydrogenases and HMG-CoA reductases (138).

Hypothesis 2: To explain the divergent stereospecificities of HMG-CoA reductase from *Acholeplasma* versus those from yeast and rat, these two enzymes are presumed to be not homologous. This seems more reasonable than proposing that HMG-CoA reductase is uniquely capable of drifting compared with the other enzymes.

Hypotheses 3: It is difficult to argue that stereospecificity with respect to substrate can drift while stereospecificity with respect to cofactor cannot. Therefore, D- and L-lactate dehydrogenases and D- and L-sugar oxidases each are presumed to have arisen independently, and their common stereospecificities are accidental (25% probability, assuming that stereospecificity serves no selectable function).

Hypothesis 4: The dinucleotide binding domains of the ethanol dehydrogenases from *Drosophila* and yeast are almost certainly homologous. Further, as ethanol dehydrogenase is the only enzyme from *Drosophila* that has "abnormal" stereospecificity (11), all dehydrogenases except ethanol dehydrogenase must be presumed to be homologous in *Drosophila* (44, 95). Either the drift of stereospecificity is more rapid for enzymes acting on ethanol than for other enzymes or ethanol dehydrogenases are more easily replaced by deletion/replacement events than are other dehydrogenases.

Hypothesis 5: To explain the correlation between redox potential and stereospecificity observed in alcohol dehydrogenases (Fact 1) drift in substrate specificity between enzymes must be allowed. To avoid a contradiction with Hypothesis 1 (where crossover of substrate specificity is forbidden except for ethanol dehydrogenases and HMG-CoA reductases), enzymes are allowed to evolve to adopt other substrate specificities only if such crossover does not create an enzyme that oxidizes an alcohol with a K_{eq} for the reaction of less than 10^{-11} M from one oxidizing an alcohol with a K_{eq} greater than 10^{-11} M, and vice versa. Thus, a malate dehydrogenase can evolve to become a lactate dehydrogenase but not a 3-hydroxybutyrate dehydrogenase. The structural similarities of oxaloacetate, pyruvate, and acetoacetate (Figure 19) make it difficult to provide a chemical rationale for this special constraint on the divergence of substrate specificity.

Hypothesis 6: The convergent evolution of the stereospecificities of dihydrofolate reductases, glucose dehydrogenases, and metal-dependent alcohol dehydrogenases (Fact 1) must now be viewed as accidental (12.5% probability, assuming that stereospecificity serves no selectable function).

We develop this historical model not because we necessarily believe that it is attractive in comparison with alternative models, but rather because none of the many advocates of historical models have ever rigorously stated what such models must entail to be consistent with fact. Nevertheless, many members of the biochemical community remain strong advocates of historical models as explanations of stereospecificity in alcohol dehydrogenases and in enzymatic stereospecificity in general.

The fact that a historical model must be so complex to be consistent with known fact does not mean that it is wrong (nor that a contrasting functional model is correct). However, the defenders of the consensus model can be faulted for not constructing a formally clear statement of their position, dismissing without sufficient justification several correlations that suggest experimentally testable historical and functional models, and not examining the logical consequences of these models in a rigorous way. Had these expedients been followed, we believe that the historical consensus would be less dogmatically defended.

7. Further Tests for the Model

Any set of data can be explained by a historical model that assumes an arbitrary number of ancestral enzymes interrelated by an arbitrary pedigree. However, the assumption that stereospecificity is so tightly coupled to catalytic activity that it cannot be reversed without destroying catalytic activity is critical even to the highly modified historical model outlined above. In particular, it is necessary to explain the highly conserved stereospecificities of malate dehydrogenases. This assumption can be examined experimentally.

Inspection of the crystal structures of alcohol dehydrogenase suggests that the mode of cofactor binding (anti in this enzyme) is determined by two interactions (Figure 21) (139). On one side of the nicotinamide ring, the enzyme offers residues that form hydrogen bonds to the carboxamide group of the nicotinamide ring. On the other side, the side chain of residue 203 (corresponding to Leu 182 in yeast alcohol dehydrogenase) sterically blocks the carboxamide group in the syn conformation.

Thus, a point mutation in the active site that replaces the bulky side chain of residue 182 in yeast alcohol dehydrogenase should diminish the stereospecificity of the enzyme. (It would not, of course, destroy the stereospecificity entirely, as the hydrogen bonds favoring the anti conformation would remain, even though the steric bulk obstructing the syn conformation is gone.) The historical model predicts that any loss in stereospecificity should be accompanied by a large loss in catalytic activity. Site-specific mutagenesis techniques allow the deliberate synthesis of proteins carrying amino acid replacements (140), and this prediction was not sustained when the mutant was prepared and examined (139).

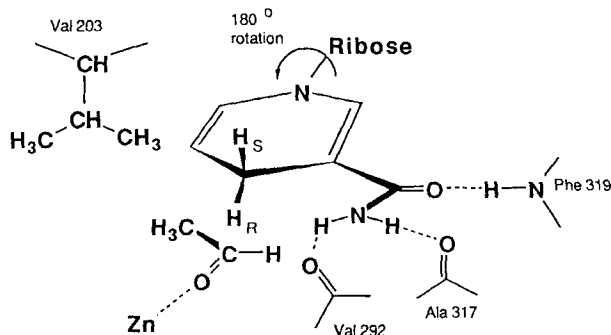


Figure 21. Structural determinants of stereospecificity in alcohol dehydrogenase.

Replacing Leu 182 in yeast alcohol dehydrogenase by Ala leads to a 10,000-fold decrease in the stereospecificity of alcohol dehydrogenase (with respect to cofactor). However, the k_{cat} of the mutant was approximately 40% and 70% (for the oxidation of ethanol and the reduction of acetaldehyde, respectively) of the wild type. Essentially no loss in catalytic activity accompanied the large loss in stereospecificity. Thus, stereospecificity in this dehydrogenase is not tightly coupled to catalytic activity, as historical models normally assume to explain the patterns of stereospecificity observed in dehydrogenases. This suggests that stereospecificity would diverge if it were not directly subject to functional constraints. The fact that stereospecificity has *not* drifted in many dehydrogenases then supports the argument that its drift is directly constrained by function. It remains to be determined whether a complete reversal of stereospecificity can be achieved in this enzyme by the introduction of point mutations.

8. *Extension of the Functional Model*

The discussion above has focused almost exclusively on dehydrogenases interconverting alcohols and the corresponding carbonyl compounds. Enzymes in this subclass of dehydrogenases should have some degree of mechanistic homogeneity and therefore should be directly comparable. However, the formalism of the functional model, especially the relationship between stereospecificity and redox potential, might be extended to other classes of dehydrogenases. For example, the *pro-R* hydrogen might be used to reduce reactive substrates (and the *pro-S* hydrogen to reduce unreactive substrates) in other subclasses of dehydrogenases acting with similar mechanisms on an analogous series of substrates.

In such exploratory research, one recognizes that the formalism is being stretched past the limits of the underlying chemical theory. This simply means that one can neither be too excited if the extension is predictive nor too disappointed if it is not. Conversely, if one is an aggressive critic of the model, one cannot be too excited if the extension is not predictive nor too disappointed if it is.

For example, redox reactions interconverting hemiacetals and their corresponding esters are analogous to redox reactions interconverting simpler alcohols and ketones. The equilibrium constant has the same units for both reactions (permitting direct formal comparison). Further, if the formalism developed for alcohol-ketone interconversions is applied to hemiacetal-lactone interconversions, the prediction is that all enzymes catalyzing the latter transformation will transfer the *pro-S* hydrogen (141).

This happens to be the case (21, 136). At present, over a dozen such enzymes have been studied stereochemically. Some come from widely divergent

organisms, and several are not obviously homologous; all transfer the *pro-S* hydrogen. This is true for L-fucose dehydrogenase and D-glucose dehydrogenase, enzymes that act on substrates of opposite chirality. Historical models that postulate that these enzymes have the same stereospecificity because they are descendants of a common ancestor must explain why stereospecificity is highly conserved with respect to cofactor but not with respect to substrate. In other cases, sequence data argue that homology within this class of dehydrogenases, if it exists at all, must be very distant.

The formalism can also be applied to enzymes catalyzing redox reactions between flavins and nicotinamide cofactors. Often, the redox potential of the enzyme-bound flavin can be measured directly. This avoids the need to correlate stereospecificity with a thermodynamic property of the substrate measured outside the active site—problematical given the acknowledged fact that enzyme-substrate binding interactions could significantly perturb this property. Values for the reduction potential of enzyme-bound flavin range from -465 mV to $+145\text{ mV}$ (10 pK_{eq} units) (142). The formalism again predicts that flavoenzymes transfer the *pro-S* hydrogen to flavins with more negative redox potentials and enzymes transfer the *pro-R* hydrogen to flavins with less negative potentials.

Table 6 shows an apparent trend in this direction. The reader should be cautioned that the reduction potentials reported for enzyme-bound flavins are disappointingly variable from laboratory to laboratory and method to method. Solubilization of membrane-bound flavoenzymes can cause large changes in measured redox potentials. Thus, a selection of the data must be made. While the selection inevitably requires subjective decision and clearly may prejudice conclusions, the data in Table 6 were chosen based on their apparent reliability, consistency, and availability.

Another extension of the formalism explains the fact that all alcohol dehydrogenases that employ a metal ion display *pro-R* stereospecificity (128). The presence of a metal ion as an electrophilic activator is expected to destabilize all carbonyl compounds (with respect to the corresponding hydroxyl compounds) when compared to electrophilic activation by a proton (128). Thus, the break point in the correlation is expected to be shifted down in the correlation (Table 4b); in other words, it should be possible to find enzymes reducing the same substrate where the enzyme employing a metal for electrophilic activation transfers the *pro-R* hydrogen, while the enzyme employing a proton for the same purpose transfers the *pro-S* hydrogen. The recent demonstration that the iron-dependent alcohol dehydrogenase from *Zymomonas mobilis* transfers the *pro-R* hydrogen is consistent with this model (128).

In other areas, the formalism appears to be difficult to apply. For example, both *pro-R* and *pro-S* stereospecificities are known in enzymes catalyzing the oxidation of aldehydes to carboxylic acid derivatives (Table 7) (21,

Table 6
List of Stereospecificities of Flavin-Dependent Dehydrogenases Ordered by Redox Potential

Enzyme Name	Cofactor	A/B ^a	E1	E2	E3	E4 (mv)	Titrant	pH/T(°C)	E _{corr} ^b	Ref
Putidaredoxin Red.	NADH	B		-283			Dithionite	-/-	-283	c
Lipoamide DH	NADH	B		-280		-346	Dithionite	7.0/25	-280	d
NADPH Ox. (Superoxide)	NADPH	A	-304	-258			Dithionite	7.0/25	-280	e
Adrenodoxin Red.	NADPH	B		-291			NADH	7.5/-	-261	f
Thioredoxin Red.	NADPH	B		-243		-260	NADH	7.0/12	-260	g
Cytochrome b ₅ Red.	NADH	A		-258			Dithionite	7.0/25	-258	h
Old Yellow Enzyme	NADPH	A	-245	-215			Dithionite	7.0/25	-230	i
Cytochrome P-450 Red.	NADPH	A	-110	-270	-290	-365	Dithionite	7.0/25	-190	j
FMN Reductase	NADH	A		-200			—	7.0/25	-200	k

^a Reference 136; *pro-R* stereospecificity is designated "A", and *pro-S* stereospecificity is designated "B". ^b Two electron reduction potentials corrected to pH 7.0, 25°C (O'Donnell, M. E.; Williams, C. H. *J. Biol. Chem.* 1983, 258, 13795-805). ^c Marbach, W. J.; Thesis, University of Illinois, 1972. ^d Matthews, R. G.; Williams, C. H. *J. Biol. Chem.* 1976, 251, 3956-64. ^e Kakinuma, K.; Kaneda, M.; Chiba, T.; Ohnishi, T. *J. Biol. Chem.* 1986, 261, 9426-32. ^f Lambeth, J. D.; Karin, H. *J. Biol. Chem.* 1976, 251, 4299-306. ^g O'Donnell, M. E.; Williams, C. H. *J. Biol. Chem.* 1983, 258, 13795-805. ^h Iyanagi, T. *Biochem.* 1977, 16, 2725-2730. ⁱ Stewart, R. C.; Massey, V. *J. Biol. Chem.* 1985, 260, 13639-47. ^j Iyanagi, T.; Makino, N.; Mason, H. S. *Biochem.* 1974, 13, 1701-10. ^k Fisher, J.; Walsh, C. T. *J. Am. Chem. Soc.* 1974, 96, 4345-6.

136). Several mechanistic types of enzymes are involved, including enzymes that presumably oxidize thiohemiacetals between the substrate and a cysteine side chain to yield thioesters covalently bound to the enzyme, enzymes that oxidize thiohemiacetals between two substrates to produce non-covalently bound thioesters, and enzymes that produce mixed anhydrides with phosphoric acid.

Enzymes forming a carboxylic acid as a product generally belong to the first mechanistic class. Five examples transfer the *pro-R* hydrogen, one transfers the *pro-S* hydrogen (21). Enzymes forming acyl phosphates transfer the *pro-S* hydrogen, however; these presumably also proceed via an acyl-enzyme intermediate (although perhaps higher in energy). Chemical intuition suggests that the thiohemiacetal-thioester equilibrium constant is smaller than the hemiacetal-ester equilibrium constant. As all of the latter transfer the *pro-S* hydrogen, the formalism makes no useful prediction regarding the stereospecificities of members of the first class. The best that the functional model at present can do is argue that the thiohemiacetal-thioester equilibrium constant is near the break in the correlation. This suggests possibility for further experiments. Historical models fare little better. Limited sequence similarities exist between the *pro-S* hydrogen and the *pro-R* hydrogen enzymes, suggesting that dehydrogenases with opposite stereospecificities are more closely homologous than enzymes with similar stereospecificities where homology is presumed to be an explanation for this similarity (131).

Amino acid dehydrogenases present another stereochemical problem. Glutamate, leucine, diaminopimelate, and phenylalanine dehydrogenases all transfer the *pro-S* hydrogen, while alanine dehydrogenase transfers the *pro-R* hydrogen (21, 136). There is no obvious difference in redox potentials that might explain this difference (Table 8). Nevertheless, limited data suggest that the stereochemical difference between alanine and other amino acid dehydrogenases is maintained in a range of organisms (21, 136). More data (especially from enzymes that are evolutionarily distant) are necessary before one can decide whether stereospecificity in amino acid dehydrogenases is adaptive or not.

Further, the stereospecificity with respect to cofactor for the reduction of alpha-beta unsaturated thioesters appears to be a non-selected trait. Examples are discussed in detail below.

Less conventional applications of the formalism are also possible. For example, the enzyme NADPH-NAD⁺ transhydrogenase catalyzes the transfer of "hydride" between NAD⁺ and NADP⁺. The *pro-S* hydrogen of NADPH is removed; the *pro-R* hydrogen of NADH is removed (60). The distinction is subtle, and the functional model, combined with the notion of "descending staircase internal thermodynamics" (13), predicts that the choice of hydrogen is determined by the physiological direction of flux through this enzyme. In

Table 7
Stereospecificities and Equilibrium Data of Enzymes Catalyzing the Nicotinamide Cofactor-dependent Oxidation of Aldehydes

Enzyme	E.C.#	Spec. ^a	pK _{eq} ^b	Source
<i>A. Aldehyde dehydrogenases producing carboxylic acids</i>				
UDP-glucose dehydrogenase	1.1.1.22	B	—	Bovine
Histidinol dehydrogenase	1.1.1.23	A	—	<i>Neurospora</i>
Aldehyde dehydrogenase	1.2.1.3	A	—	Yeast, Bovine, Equine
Aminobutyraldehyde dehydrogenase	1.2.1.19	A	—	<i>Pseudomonas</i>
Succinate semialdehyde dehydrogenase	1.2.1.24	A	—	<i>Pseudomonas</i>
Aminopropionaldehyde dehydrogenase	1.2.1.X	A	—	Chicken
<i>B. Aldehyde Dehydrogenases producing phosphate anhydrides</i>				
Aspartate semialdehyde dehydrogenase	1.2.11	B	6.5 ^c	<i>E. coli</i>
Glyceraldehyde-3-phosphate dehydrogenase	1.2.1.12	B	7.3 ^d	<i>E. coli</i> , <i>Acholeplasma</i> , Yeast, Horseshoe crab, Surgeon, Bee, Turkey, Rabbit, Pea
<i>C. Aldehyde Dehydrogenases producing thioesters</i>				
Hydroxymethylglutaryl-coenzyme A reductase	1.1.1.34	A,B	—	<i>Acholeplasma</i> , Yeast, Rat
Aldehyde dehydrogenase (acylating)	1.2.1.10	A	3.9 ^e	<i>Clostridium</i>
Cinnamoyl-coenzyme A reductase	1.2.1.44	B	3.3 ^f	<i>Forsythia</i>
Glyoxylate dehydrogenase	1.2.1.17	B	5.1 ^g	<i>Alcaligenes</i>

^aReference 136; ^bpro-R stereospecificity is designated "A", and pro-S stereospecificity is designated "B". ^cK_{eq} is unitless. ^dK_{eq} is unitless. ^eBlack, S. *Meth. Enz.* 1962, 5, 823. ^fCori, C. F.; Velick, S. F.; Cori, G. T. *Biochim. Biophys. Acta* 1950, 4, 16. ^gStadtman, E. R.; Burton, R. M. *Meth. Enz.* 1955, I, 518. ^hLuderitz, T.; Grisebach, H. *Eur. J. Biochem.* 1981, 119, 115. ⁱQuayle, J. R. *Biochem. J.* 1963, 87, 368.

Table 8
Stereospecificities of Amino Acid Dehydrogenases

Enzyme	E.C. no.	pK_{eq}	Spec.
Alanine dehydrogenase	1.4.1.1	13.2	A
Glutamate dehydrogenase	1.4.1.2	13.3	B
Glutamate dehydrogenase ($NADP^+$)	1.4.1.4	13.3	B
Leucine dehydrogenase	1.4.1.9	13.0	B
Glycine dehydrogenase	1.4.1.10	10.6	
3,5-diaminohexanoate dehydrogenase	1.4.1.11	9.4	
2,4-diaminopentanoate	1.4.1.12	14.0	
Diaminopimelate dehydrogenase	1.4.1.16		B
Phenylalanine dehydrogenase			B

Stereochemical data is from reference 136. *Pro-R* stereospecificity is designated "A" and *pro-S* stereospecificity is designated "B". The equilibrium constant has units M^2 .

the beef heart enzyme that has been studied, the direction of flux (oxidation of NADPH) and the observed stereospecificities are consistent with the functional model. It would be interesting to see if this is true for transhydrogenases from other sources, especially those that catalyze the reverse reaction (the oxidation of NADH) under physiological conditions.

Finally, in elegant studies of model compounds, Ohno and his colleagues have recently discovered that the stereospecificity of "hydride" transfer is dependent on the redox potential driving the reaction (143). This is in a model system; there is no enzyme involved, and the dihydronicotinamide ring has a structure distinctly different from that in the natural cofactor. Yet the apparent control of stereospecificity in solution by a thermodynamic property of the reacting molecules parallels directly the functional model proposed to explain the stereospecificity of dehydrogenases. The parallel between chemistry inside and outside the active site is most remarkable, especially as the analogy appears to be purely formal.

D. Addition-Elimination Reactions

Both "syn" and "anti" transition state geometries are possible for the addition of a proton and a nucleophile (HX) to an olefin and, in the microscopic reverse reaction, the elimination of the elements HX to form an olefin. Intermediary geometries form twisted olefins that presumably are not allowed (14).

Stereoelectronic considerations suggest that the "anti" transition state is slightly preferred in concerted elimination reactions, as the electrons from the bond to the departing electrophile are oriented such that they can move directly into the antibonding orbital of the bond to the departing nucleophile

(144). However, stereoelectronic principles make no explicit statement regarding the preferred stereochemical course of a stepwise addition/elimination reaction.

Many enzymes catalyze addition/elimination reactions, and both syn and anti geometries are known. "Anti" stereoselectivity is found in the addition/elimination reaction catalyzed by fumarase, aspartate ammonia lyase (145-148), arginosuccinase (149), aconitase (150), oleic acid dehydratase from *Pseudomonas* (151), adenylosuccinase (152), malease (153), enolase (154), phenylalanine ammonia lyase (155), and histidine ammonia lyase (156). Other reactions that are analogous in the broadest sense also proceed via "anti" transition states. For example, the decarboxylative elimination of 5-pyrophosphomevalonate (3,5-dihydroxy-3-methylpentanoic acid, 5 pyrophosphate) proceeds with an overall "anti" stereoselectivity (157). The decarboxylation of cis-aconitate to give itaconate also proceeds with "anti" stereochemistry (158).

Enzymes catalyzing "syn" addition/elimination reactions include cis-cis-muconate cycloisomerase (159), enoyl-CoA hydratase (160), dehydroquinate synthase (161), beta-hydroxydecanoylthioester dehydratase (162), yeast fatty acid synthetase (163), methylglutaconyl-CoA hydratase (164), and dehydroquinate dehydratase (165). Methacrylate is converted to beta-hydroxyisobutyrate, presumably via the intermediacy of methacrylyl-CoA, by a "syn" addition (166). The 3-dehydroshikimate is converted to protocatechuate via a "syn" elimination (167). Cyclization of carboxymuconic acid to give beta-carboxymuconolactone is also "syn" (168).

A simple proposal to account for the stereochemical diversity in these cases assumes that the elimination reactions catalyzed by the first class of enzymes are concerted, but that those catalyzed by the second class of enzymes are stepwise. For stepwise reactions, one has a choice of several functional hypotheses that argue that "syn" elimination is the preferred stereochemical course. The simplest is that active sites with a single base are "better" for a stepwise elimination than those with multiple functional groups (8). In a "syn" elimination, the base can act both to abstract a proton in the first step and then, in the protonated form, to assist the departure of the nucleophilic group in the second step.

Simple examination of the structure of the substrates lends support to the hypotheses. In many cases where the elimination is "syn" (and presumably stepwise), the departing proton leaves behind a relatively stable anion (e.g., alpha to a thioester or a ketone). In those cases where the elimination is "anti" (and presumably concerted), however, the proton that is leaving is adjacent to a group that is *not* chemically well suited to stabilize an adjacent carbanion (for instance, a carboxylate group). In the first case, a hypothetical "carbanion" intermediate is relatively stable; the hypothesis of a stepwise re-

action is reasonable. In the second case, the hypothetical "carbanion" is not stable; the hypothesis of a concerted reaction is therefore again reasonable.

This sort of argument has some precedent in the literature. For example, Schwab and Klassen proposed that the stereochemical course of allylic rearrangements likewise is stepwise or concerted, syn or anti, depending on the intrinsic reactivity of the substrate molecule (169). While there are perhaps some exceptions to this proposal (170-172), they are best treated in the manner discussed above. The suggestion remains important as a working hypothesis.

Recent experiments by Cleland and his coworkers, however, argue strongly against this simple interpretation. For example, isotope effect studies argue in several cases (phenylalanine ammonia lyase and fumarase) that the reaction proceeds via a stepwise mechanism (19). Though certain caveats may apply to this conclusion (173), the simplest explanation apparently cannot be correct.

A remarkably simple formal rule can be proposed to explain the stereospecificity of enzymatic elimination reactions. This rule is based on consideration of *both* the stability of the carbanion and the carbocation that would be generated in a fully disassociative mechanism. The stability of the carbanion corresponds to the pK_a value of its conjugate acid. The stability of the carbocation corresponds to its pK_{R^+} (174). Tables of these values for a range of compounds are now available, and values can be estimated for carbanions and carbocations that have not been studied.

Figure 22 shows a selection of enzymes arranged according to these values. Readily apparent is the fact that a syn transition state is found when *either* the carbanion or carbocation is relatively stable. Anti transition states are found in the "box" in the upper left hand side of Figure 22, where neither the cation nor the anion is stable. Indeed, for predictive purposes, the rule can be stated formally: If either the pK_a of the carbanion is less than 20, or the pK_{R^+} of the carbocation is greater than -10, the syn transition state will be preferred. This formalism makes mechanistic sense in terms of the lifetime of the proposed intermediate in a stepwise mechanism (175). As a formalism, it can be tested without recourse to assumptions about the detailed mechanism of the reaction.

One might attempt to apply this rule to three enzymes that catalyze three quite similar reactions. These reactions are: (a) the cyclization of *cis-cis*-muconate to give muconolactone, a "syn" addition reaction; (b) the cyclization of *cis-cis*-carboxymuconate to give beta-carboxymuconolactone, also a "syn" addition reaction; and (c) cyclization of *cis-cis*-carboxymuconate to give gamma-carboxymuconolactone, an "anti" addition (Figure 23) (176). The stereospecificities of these enzymes were examined by Kozarich and his group to test an intriguing hypothesis of Ornston that sequential enzymes in a path-

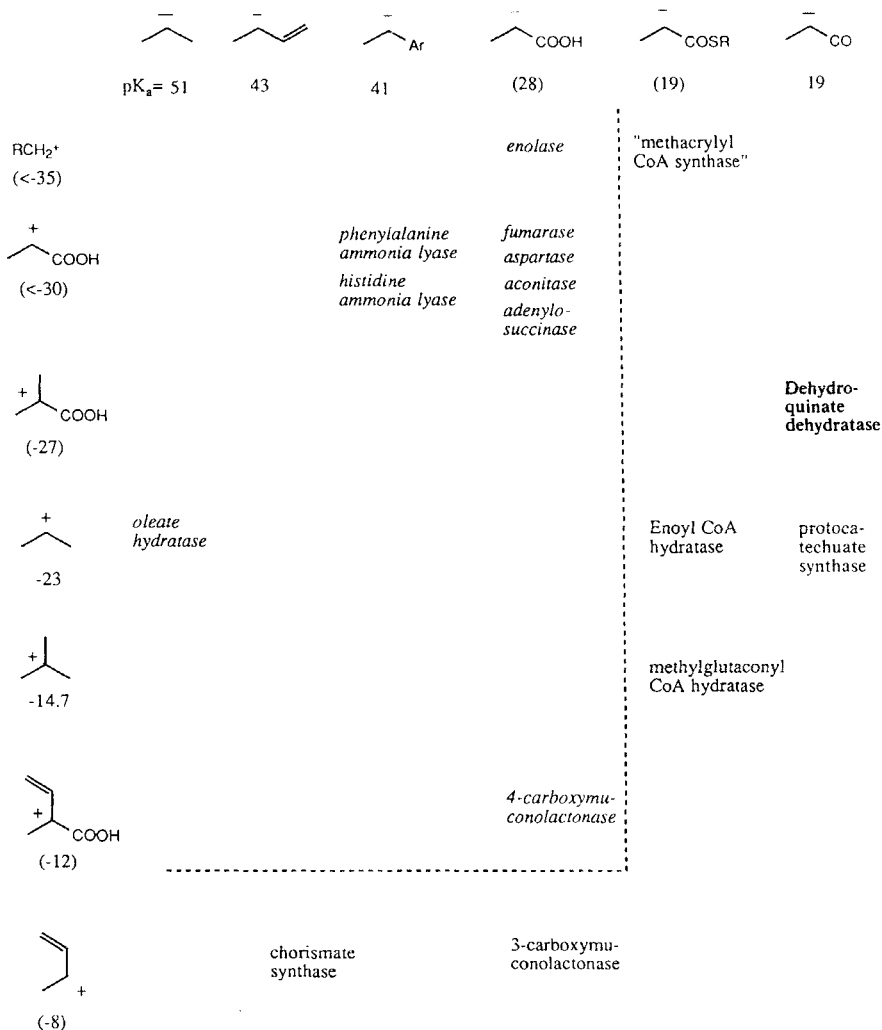


Figure 22. Stereospecificity in dehydratases correlates with substrate structure.

way are related (83). The last enzyme was expected to have the same stereospecificity as the first two.

The fact that the third enzyme catalyzed an "anti" addition/elimination reaction contradicted these expectations. The investigators could propose only that perhaps the "anti" addition to a dicarboxylated double bond proceeded via a transition state or lower energy than a "syn" addition because

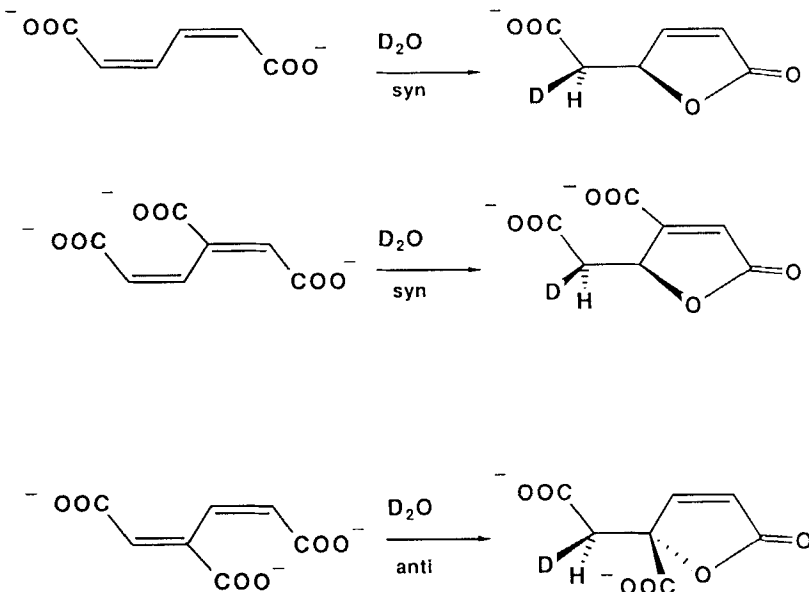


Figure 23. The different stereospecificities of dehydratases catalyzing similar reactions.

the two carboxylate anions are somewhat farther apart in the "anti" transition state than in the "syn" transition state.

This hypothesis is problematic from a theoretical point of view, as there is no evidence that suggests that electrostatic interactions of this type are a major consideration in the evolution of active sites. However, the data are consistent with the rule suggested above. The pK_a for the removal of a hydrogen from all three substrates is expected to be approximately the same; here, we use the value of 24.5 for the pK_a of the protons alpha to the carbonyl function of an ester. Thus, the reaction will be anti except in cases where there is an especially stable carbocation. This is in fact the case for the first two substrates; a secondary allyl carbonium ion has a pK_{R^+} of approximately -8, and a syn transition state is expected.

In the third case, the allyl cation is adjacent to an extra electron withdrawing group, and this is expected to lower the pK_{R^+} by three orders of magnitude. By the formalism proposed above, this carbocation is insufficiently stable to allow the syn transition state.

This formalism is subject to many experimental tests. For example, the conversion of 2,3-dihydroxy-3-methylbutanoate to 2-keto-3-methylbutanoate

in the biosynthesis of valine involves the elimination of water. The formal carbanion (alpha to a carboxylate) has a pK_a value of 28; the formal carbonium ion (tertiary) has a pK_{R^+} value of -14.7 . Thus, the formalism (Figure 22) predicts that the stereospecificity of the elimination be anti.

V. FATTY ACID SYNTHESIS: MANY STEPS, MANY STEREOCHEMICAL DISTINCTIONS

Should the reader by now be convinced that the evolutionary analysis of stereochemical data in enzymology is too complicated to be worth the effort, we must repeat the statement made at the beginning of this review: one cannot interpret stereochemical data (or any other data) in enzymology without such an analysis. This is the primary incentive to examine and test the models developed above. However, a brief discussion of the stereochemical details of fatty acid biosynthesis may provide further encouragement, as it shows how assembling a critical mass of data can provide valuable insight once the task is acknowledged and work begins.

Fatty acids are synthesized in a sequence of reactions catalyzed by a fatty acid synthetase complex (Figure 24) (177). Following a Claisen condensation between a carbanion and a thioester, a 3-ketoacid group is reduced by a nicotinamide-dependent dehydrogenase. The resulting alcohol undergoes elimination to produce an olefin, and the olefin is reduced (again by an enzyme dependent on nicotinamide cofactors) to give a saturated fatty acid thioester.

Many of the cryptic stereospecificities discussed above are exemplified in one or more steps in this sequence, and an interesting pattern has emerged (178–183). With all of the synthetases, the initial Claisen condensation proceeds with *inversion* of configuration. With all of the synthetases, the *pro-S* hydrogen of NADH is used to reduce the 3-ketothioester intermediate. The elimination of water is universally *syn*, and the *trans* olefin is always the product.

So far, the stereospecificities of all enzymatic reactions have been found to be the same in fatty acid synthetases from all of the organisms examined. These results are consistent either with functional models that assume that all of these stereochemical distinctions are adaptive or with the historical view that all of the synthetases are homologous and stereospecificity is highly conserved.

However, in the next step in the pathway, stereochemical uniformity is no longer found. With different synthetases, the addition of hydrogen to the unsaturated thioester occurs with three of the four possible stereochemical courses (3-*Re*/2-*Re*; 3-*Re*/2-*Si*; 3-*Si*/2-*Re*; 3-*Si*/2-*Si*). Further, stereospecificity with respect to *NADH cofactor* for the reduction of the double bond of the enoyl-CoA intermediate in fatty acid synthesis is not the same in different

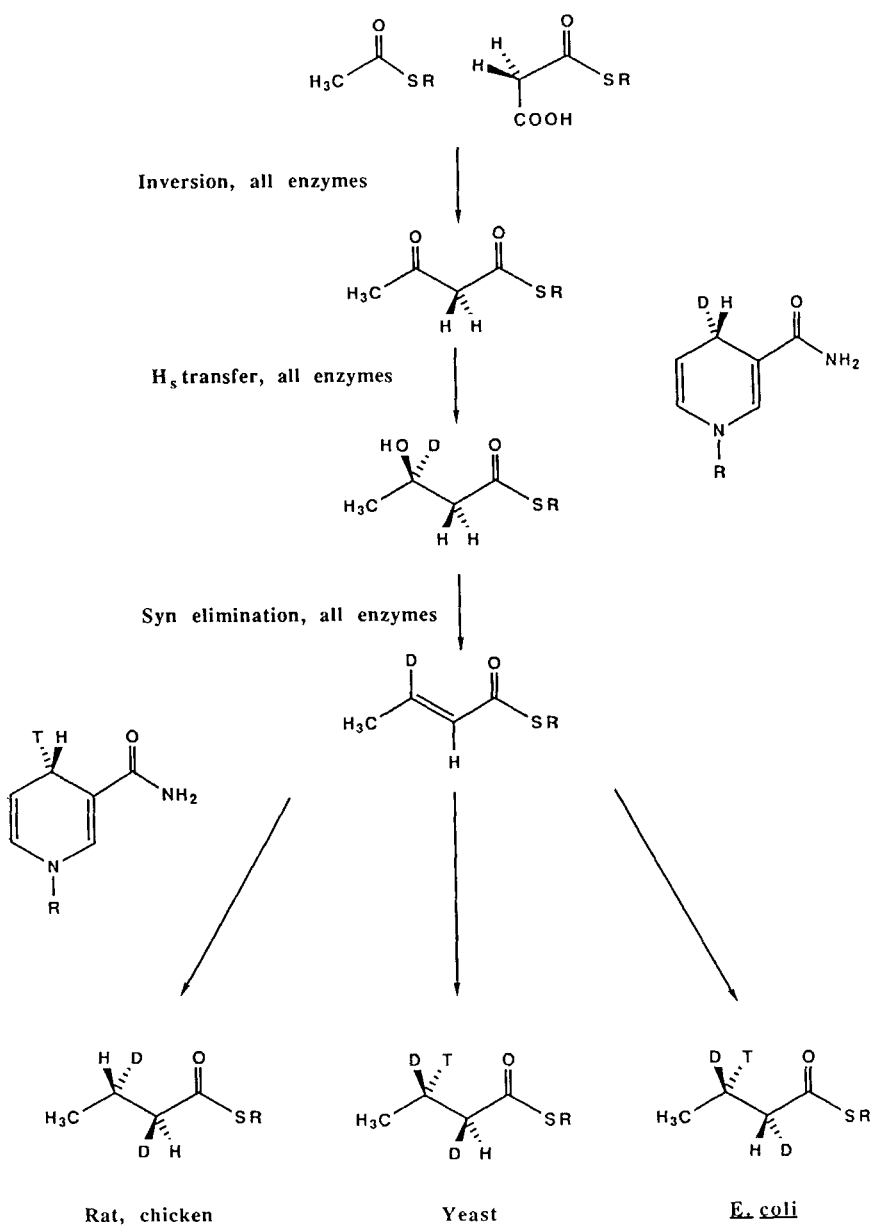


Figure 24. Stereospecificities of fatty acid biosynthesis.

organisms; some enzymes transfer the *pro-R* hydrogen of NAD(P)H and others transfer the *pro-S* hydrogen.

These stereochemical data provide one of the most controlled arguments for and against specific functional and historical models in enzymology. The uniform use of the *pro-S* hydrogen of NADH in the reduction of the 3-keto thioester intermediate is simply explained by the functional model outlined above, as the equilibrium constant for the redox reaction is in the *pro-S* region of Table 4b. The universal use of a syn elimination to form the unsaturated ester intermediate is similarly understood in functional terms. These explanations apply whether the fatty acid synthetases are homologous (in which case stereospecificity has been functionally constrained from drifting) or non-homologous (in which case, stereospecificity has converged). The divergent stereospecificities for the reduction of the carbon–carbon double bond, and the divergence in the choice of hydride of NADH to effect this reduction, are consistent with the notion that stereospecificity in this type of reaction is not a selected trait (or reflects mechanistic divergence), and the diversity reflects either drift or independent pedigree.

Accounting for these data with a historical model is more difficult. Most simply, either the fatty acid synthetase complexes are homologous or they are not. If they are not homologous, a historical model must assume that the common stereospecificities in the first steps arose by convergent evolution, expected only if the stereospecificities are directly adaptive. If they are homologous, historical models must concede that stereospecificity can drift in enzymes catalyzing addition of the elements of molecular hydrogen to a double bond. A concession that stereospecificities of this type can drift in the last steps in fatty acid synthesis makes difficult the assumption that analogous stereospecificities are highly conserved in the first steps.

The asymmetry between functional and historical models in addressing stereochemical problems in fatty acid synthetases arises from the fact that stereochemical imperatives can be different for reactions with different mechanisms, and stereochemical behaviors serving different functions can behave differently during evolution. However, historical models treat stereospecificity as consequences of an arbitrary placement of substrates and functional groups in the active site. As these arrangements serve no selected role in the historical view, the arrangements should behave the same during evolution in different enzyme classes regardless of the function of the enzyme.

Thus, it is conceivable on mechanistic grounds that stereospecificity with respect to cofactor for the reduction of 3-ketoesters is adaptive, while that for the reduction of an enoyl-CoA derivative is not. Conceivably, one stereospecificity can be highly conserved while the other drifts. However, the historical model regards stereospecificity in both cases as the result of an arbitrary arrangement of functional groups in the active site, binding the NADH cofactor

(arbitrarily) in either a syn or an anti conformation. As the orientation of binding serves no functional role (in the historical view), there seems to be no basis for explaining why the orientation drifts when the NADH is used to reduce a carbon–carbon double bond, but does not drift when the NADH is used to reduce a carbonyl group.

Of course, a historical model can explain these data if it is sufficiently complex. Gene fusions have apparently occurred during the evolution of fatty acid synthetase complexes (184–187). One might argue that the enoyl reductase subunits of the various synthetases are non-homologous, while the remaining subunits are homologous. This suggestion might be coupled with the intriguing notion that fatty acid biosynthesis originated relatively recently in evolution (15). Although this historical model is weakly contradicted by sequence data already available (132), specific hypotheses such as the ones proposed here should encourage further investigation.

VI. ENZYMES DISPLAYING STEREOCHEMICAL INFIDELITY

Enzymes need not be completely stereospecific, although the discovery of enzymes with incomplete stereochemical fidelity is undoubtedly hindered by the common prejudice that enzymes are necessarily absolutely stereospecific. Given this prejudice, evidence for incomplete fidelity is in danger of being dismissed as experimental error or artifact.

Careful studies of the intrinsic level of stereochemical error have now been made for a few enzymes. Rétey and his coworkers have studied the stereochemical infidelity of methylmalonyl CoA mutase from *Propionobacterium shermanii*, an infidelity that is quite substantial (188). In contrast, dehydrogenases display little if any stereochemical infidelity. Recent examinations of stereochemical infidelity in lactate and yeast alcohol dehydrogenases suggests that stereochemical error occurs only once in every billion turnovers (139, 189).

Where substantial stereochemical infidelity is observed, it may have both mechanistic and evolutionary implications. As discussed above, decarboxylases operating via an intermediate that is a Schiff's base of a 3-keto-acid proceed with large amounts of racemization. This was explained as a result of the high reactivity of an enamine intermediate in the reaction. Enzymes protonating such reactive intermediates directly from solvent are presumably not selectively disadvantageous compared with enzymes that maintain an active site residue to protonate the intermediate.

A particularly interesting case arises in the biosynthesis of cytidine diphosphate dideoxyhexoses in certain bacteria. In the reduction of the sugar derivative, direct hydrogen transfer from NADH to the substrate can not be dem-

onstrated (190). Further, it appears as if the enzyme catalyzes the release of both the *pro-R* hydrogen and the *pro-S* hydrogen of NADH to solvent (191).

This remarkable lack of stereospecificity with respect to cofactor may have a mechanistic basis. Pyridoxal phosphate is a cofactor for the reaction, and a putative intermediate in the reduction is shown in Figure 25. Remarkably, this intermediate incorporates five conjugated double bonds and two positively charged nitrogens. While single electron transfer is unlikely in most dehydrogenases dependent on nicotinamide cofactors, the intermediate in Figure 25 is exceptional in its ability to accept an electron. Indeed, if any redox enzyme involves NADH radical cations as intermediates, this enzyme should. Thus, on chemical grounds, the absence of stereochemical fidelity in enzymes synthesizing CDP-dideoxyhexoses is consistent with the hypothesis of a radical intermediate in this section.

VII. CONCLUSIONS

The conclusion now is virtually inescapable that the stereospecificities of some enzymatic reactions (decarboxylation of amino acids, decarboxylation of beta-ketoacids, reduction of enoyl thioesters) behave as if they were not the targets of natural selection, while the stereospecificities of others (reduction of keto groups, enzymatic aldol condensations with acetyl CoA, polar elimination reactions, phosphoryl transfer reactions) behave as if they were the targets of natural selection. It remains a challenge to unify this collection of data into a formally simple statement regarding the distinction between selected and non-selected traits in stereochemistry.

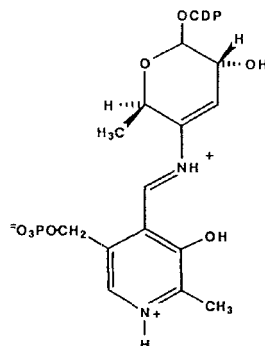


Figure 25. Intermediate in the synthesis of dideoxyhexoses.

A pattern emerges that suggests a set of hypotheses that could serve as the focus for further experimentation and controversy:

- Discrimination between two enantiotopic groups where the distinction determines the chirality of a (non-cryptically) chiral product always reflects selective pressures.
- Discrimination between two enantiotopic groups where the distinction does not determine the chirality of a product, but where the distinction results in the formation of one of two diastereomeric transition states generally reflects selective pressure.
- Discrimination between two enantiomeric transition states, that are made diastereomeric only by virtue of the chirality of the catalyzing enzyme, do not reflect selective pressure (Figure 26).

These rules can be illustrated by a simple example (44). Ethanol dehydrogenases must choose between the *pro-R* and *pro-S* hydrogens of NADH, and between the *pro-R* and *pro-S* hydrogens at carbon-1 of ethanol. As discussed above, natural selection appears to accept either stereochemical outcome at the cofactor, owing to the fortuitous value of the equilibrium constant for the reaction (at the position of the break in the correlation in Table 4b). The ethanol dehydrogenase from *Drosophila melanogaster* transfers the *pro-S* hydrogen from NADH, while the enzyme from *Saccharomyces cerevisiae* transfers the *pro-R* hydrogen (Figure 27) (95).

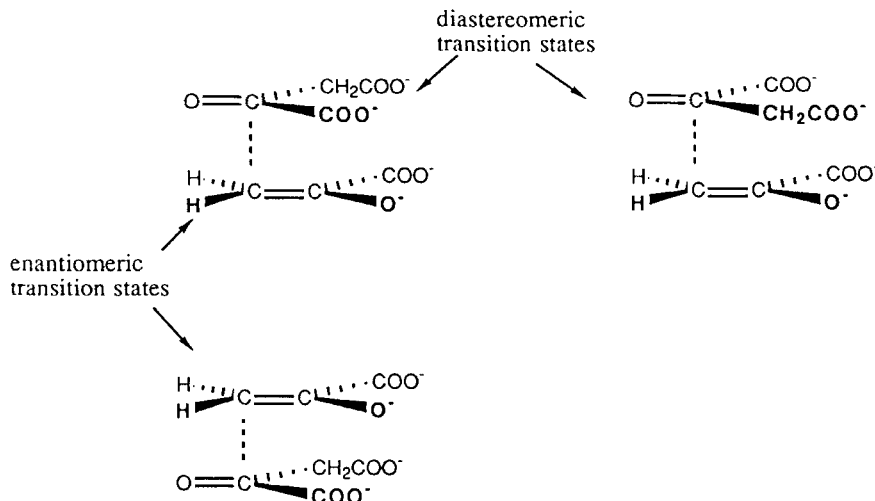


Figure 26. Locally enantiomeric transition states.

Accepting that the distinction between diastereotopic hydrogens of NADH is fortuitously neutral, one might ask whether the second choice, between the *pro-R* and *pro-S* hydrogens at carbon-1 of ethanol, is adaptive or not. Ethanol dehydrogenase from yeast transfers the *pro-R* hydrogen from ethanol to the 4-*Re* face of a nicotinamide ring. The “enantiomeric” transition state (here, considering only atoms directly attached to the reacting centers and ignoring conformation) is the transfer of the *pro-S* hydrogen from ethanol to the 4-*Si* side of nicotinamide ring. A diastereomeric transition state is the transfer of the *pro-R* hydrogen of ethanol to the 4-*Si* face of NAD⁺. If the *pro-R* hydrogen of ethanol is preferred for transfer to the 4-*Re* face of NAD⁺, the *pro-S* hydrogen of ethanol should be preferred for transfer to the 4-*Si* face of NAD⁺. Thus, if this stereochemical distinction is adaptive, alcohol dehydrogenase from *Drosophila* should transfer the *pro-S* hydrogen from ethanol. In fact, they do (44).

This sort of test had been previously proposed by George et al. (191), who attempted to rationalize cofactor stereoselectivity by a hypothesis that enzymes “choose” between diastereomeric transition states so as to minimize steric interactions. Thus, enzymes “match” the face of the substrate to the face of the cofactor so that the bulky groups of the cofactor abut the small groups of the substrate, and vice versa. The authors attempted to test their hypothesis by predicting the stereospecificity of two steroid dehydrogenases, oxidizing respectively an α hydroxyl and a β hydroxyl group. They predicted that the cofactor stereospecificities would be opposite.

Given the functional theory for dehydrogenase stereospecificity, and the discussion above, it can be argued in retrospect that the systems available to the authors were inadequate to test their conjecture. The two steroids had different chiralities, and requirements for metabolic coupling (rule a) dictated the stereospecificity of synthesis of the two compounds. Furthermore, for compounds of this redox potential, the functional model for dehydrogenase stereospecificity suggests that the stereospecificities at cofactor should both be *pro-S* (rule b). In this view, the more subtle diastereomerism (rule c) is expected to be obscured by this functional adaptation.

The general rules formulated here are intended to be the object of experimental test. They do not represent the final word in enzymatic stereospecificity, and additional data could quite easily force their re-evaluation. They do divide selected from non-selected behavior in cryptic stereospecificity and therefore help divide enzymatic traits in general into those controlled by natural selection and those reflecting neutral drift. This division is more than academic. It also marks the line dividing behaviors that are biologically functional from those that are not, behaviors that reflect underlying chemistry from those that do not, and behaviors that are interesting to study from those that are not. To the extent that the division can be made here, it facilitates the division throughout all of bio-organic chemistry.

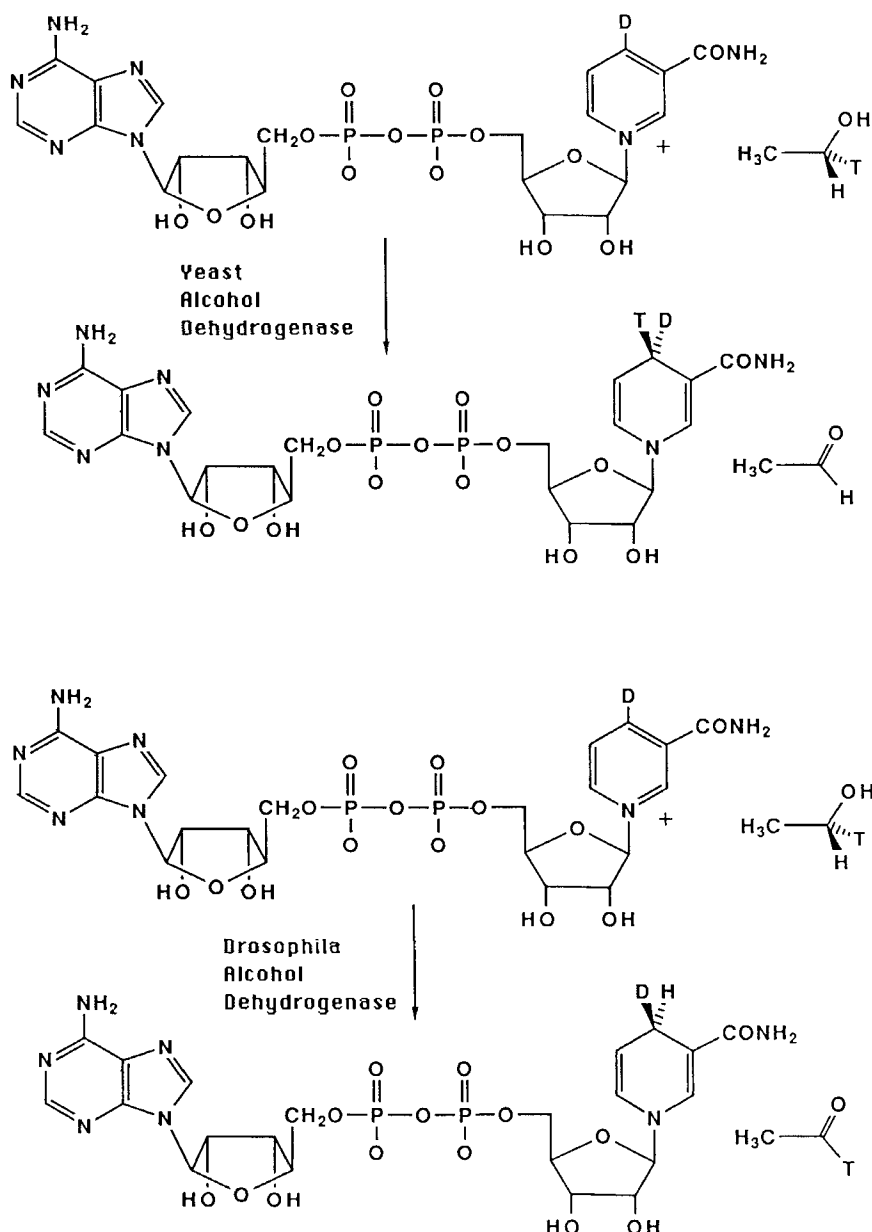


Figure 27. Opposite cryptic stereospecificity in both substrate and cofactor.

Note added in proof

With regard to functional models concerning stereospecificity in dehydrogenases, the original papers presenting the functional model focusing on a correlation between redox potential and stereospecificity (108, 110) excluded enzymes acting on carbonyl groups that were conjugated to olefinic systems. The exclusion was mechanism based: such carbonyls would be the most likely to be reduced via radical anion intermediates instead of via hydride transfer, and the correlation would not be expected to hold with enzymes acting with different mechanisms. Quite recently, Rando and his coworkers (Law, W. C., Kim, S., Rando, R. R. *J. Am. Chem. Soc.* 1989, **111**, 793) reported that the reduction of the carbonyl groups in cis and trans retinal were with the *pro-S* and *pro-R* hydrogens respectively. The first case formally violates the correlation, as the pK_{eq} is ca. 9. As these carbonyl groups are highly conjugated (to a pentaene), radical anion intermediates would be expected to be especially stable in these cases, and it will be interesting to learn the mechanisms of actions of these dehydrogenases.

ACKNOWLEDGMENT

We are indebted to Sandoz, Hoffman-La Roche, Ciba-Geigy, the Swiss National Science Foundation, and the Searle Foundation/Chicago Community Trust for providing support both while this manuscript was being prepared and for much of the research from our laboratory described here. We are also indebted to our colleagues for many interesting discussions and suggestions, and for research results cited throughout the manuscript. Finally, we are indebted to Profs. D. Arigoni, P. A. Frey, K. R. Hanson, J. R. Knowles, and Dr. K. Tanizawa who read and criticized early versions of this manuscript.

REFERENCES

1. Fisher, H. F.; Ofner, P.; Conn, E. E.; Vennesland, B.; Westheimer, F. H. *J. Biol. Chem.* **1953**, *202*, 687.
2. Martius, C.; Schorre, G. *Liebigs Ann. Chem.* **1950**, *570*, 140.
3. Wood, H. G.; Werkman, C. H.; Hemingway, A.; Nier, A. O. *J. Biol. Chem.* **1942**, *142*, 31.
4. Arigoni, D.; Eliel, E. *Topics in Stereochemistry*; John Wiley: New York, 1969; Vol. 4, p 127.
5. Evans, E. A. Jr.; Slotin, L. *J. Biol. Chem.* **1940**, *136*, 301.
6. Benner, S. *Yale Scientific* **1976**, *50*, 4.

7. Ogston, A. G. *Nature* **1948**, *162*, 963.
8. Hanson, K. R.; Rose, I. A. *Acc. Chem. Res.* **1975**, *8*, 1.
9. Benner, S. A.; Ellington, A. D. *CRC Crit. Rev. Biochem.* **1988**, *23*, 369.
10. Dobzhansky, T.; Ayala, F. J.; Stebbins, G. L.; Valentine, J. W. *Evolution*; W. H. Freeman: San Francisco, 1977; p. 19.
11. Kimura, M. *Molecular Evolution, Protein Polymorphism; the Neutral Theory*; Springer-Verlag: Berlin, 1982.
12. Lewontin, R. C. *Sci. Am.* **1979**, *239*, 156.
13. Benner, S. A. *Chem. Rev.* **1989** in press.
14. Benner, S. A. In *Molecular Structure and Energetics*; Lieberman, J.; Greenberg, A., Eds., VCH: New York 1988.
15. Benner, S. A. In *Redesigning the Molecules of Life*; Benner, S. A., Ed.; Springer-Verlag: Berlin, 1988.
16. Zydowsky, T. M.; Courtney, L. F.; Frasca, V.; Kobayashi, K.; Shimizy, H.; Yuen, L.-D.; Matthews, R. G.; Benkovic, S. J.; Floss, H. G. *J. Am. Chem. Soc.* **1986**, *108*, 3152.
17. Jones, S. R.; Kindman, L. A.; Knowles, J. R. *Nature* **1978**, *275*, 564.
18. Copley, S. D.; Knowles, J. R. *J. Am. Chem. Soc.* **1985**, *107*, 5306.
19. Hermes, J. D.; Weiss, P. M.; Cleland, W. W. *Biochemistry* **1985**, *24*, 2959.
20. Lesk, A. M.; Levitt, M.; Chothia, C. *Prot. Engineering* **1986**, *1*, 77.
21. You, K.-S. *CRC Crit. Rev. Biochem.* **1985**, *17*, 313.
22. Stern, J. R.; O'Brien, R. W. *Biochim. Biophys. Acta* **1969**, *185*, 239.
23. Bolin, J. T.; Filman, D. J.; Matthews, D. A.; Hamlin, R. C.; Kraut, J. *J. Biol. Chem.* **1982**, *257*, 13650.
24. Benner, S. A.; Rozzell, J. D.; Jr.; Morton, T. H. *J. Am. Chem. Soc.* **1981**, *103*, 993.
25. Rozzell, J. D. Jr.; Benner, S. A. *J. Am. Chem. Soc.* **1984**, *106*, 4937.
26. Cohen, S. G.; Crossley, J.; Khedouri, E.; Zand, R.; Klee, L. H. *J. Am. Chem. Soc.* **1963**, *85*, 1685.
27. You, K.-S.; Arnold, L. J., Jr.; Kaplan, N. O. *Arch. Biochem. Biophys.* **1977**, *180*, 550.
28. Presnell, S. R. Ph.D. Thesis, Harvard University, 1988.
29. Rose, I. A.; Hanson, K. R. *CRC Crit. Rev. Biochem.* **1972**, *1*, 33.
30. Belleau, B.; Burba, J. *J. Am. Chem. Soc.* **1960**, *82*, 5751.
31. Yamada, H.; O'Leary, M. H. *Biochemistry* **1978**, *17*, 669.
32. Akhtar, M.; Jordan, P. M. *Tetrahedron Lett.* **1969**, 875.
33. Chang, W. C.; Snell, E. E. *Biochemistry* **1968**, *7*, 2005.
34. Battersby, A. R.; Joyeau, R.; Staunton, J. *FEBS Lett.* **1979**, *107*, 231.
35. Dunathan, H. C.; Voet, J. G. *Proc. Natl. Acad. Sci. U.S.A.* **1974**, *71*, 3888.
36. Allen, R. R.; Klinman, J. P. *J. Biol. Chem.* **1981**, *256*, 3233.
37. Orr, G. R.; Gould, S. J. *Tetrahedron Lett.* **1982**, *23*, 319.
38. Woese, C. R. *Microbiol. Rev.* **1987**, *51*, 221-271.
39. Asada, Y.; Tanizawa, K.; Sawada, S.; Suzuki, T.; Misono, H.; Soda, K. *Biochemistry* **1981**, *20*, 6881.
40. Asada, Y.; Tanizawa, K.; Kawabata, Y.; Misono, H.; Soda, K. *Agric. Biol. Chem.* **1981**, *45*, 1513.

41. Gottschalk, G.; Barker, H. A. *Biochemistry* **1966**, *5*, 1125.
42. Gottschalk, G.; Barker, H. A. *Biochemistry* **1967**, *6*, 1027.
43. Falloone, G. R.; Srere, P. *Biochemistry* **1969**, *8*, 4497.
44. Allemann, R.; Hung, R.; Benner, S. A. *J. Am. Chem. Soc.*, **1988**, *110*, 5555.
45. Schiltz, E.; Schmitt, W. *FEBS Lett.* **1981**, *134*, 57.
46. Stragier, P.; Danos, O.; Patte, J.-C. *J. Mol. Biol.* **1983**, *168*, 321.
47. Christen, P.; Metzler, D. E. *Transaminases*; Wiley: New York; 1985.
48. Kelland, J. G.; Palcic, M. M.; Pickard, M. A.; Vederas, J. C. *Biochemistry* **1985**, *24*, 3263.
49. Gerdes, H. J.; Leistner, E. *Phytochem.* **1979**, *18*, 771.
50. Knowles, J. R. *Ann. Rev. Biochemistry* **1980**, *49*, 877-919.
51. Frey, P. A. *Tetrahedron* **1982**, *38*, 1541.
52. Eckstein, F. *Ann. Rev. Biochemistry* **1985**, *54*, 367-402.
53. Gerlt, J. A., In *Phosphorus-31 NMR*; Gorenstein, D. G., Ed.; Academic Press: New York, 1984.
54. Webb, M. R. *Meth. Enzymol.* **1982**, *87*, 301.
55. Buchwald, S. C.; Hansen, D. E.; Hassett, A.; Knowles, J. R. *Meth. Enzymol.* **1982**, *87*, 279-301.
56. van Pelt, J. E.; Iyengar, R.; Frey, P. A. *J. Biol. Chem.* **1986**, *261*, 15995-15999.
57. Hamblin, M. R.; Cummins, J. H.; Potter, B. V. L. *Biochem. J.* **1987**, *241*, 827-833. Cummins, J. H.; Potter, B. V. L. *Eur. J. Biochem.* **1987**, *162*, 123-128.
58. Buchwald, S. L.; Pliura, D. H.; Knowles, J. R. *J. Am. Chem. Soc.* **1982**, *104*, 845.
59. Sheu, K. R.; Richard, J. P.; Frey, P. A. *Biochemistry* **1979**, *18*, 5548. Frey, P. A. *Adv. Enzymol.* **1988**, *62*, in press.
60. Kaplan, N. O. *Methods Enzymol.* **1967**, *10*.
61. Pauling, L. *Chem. Eng. News* **1946**, *10*, 1375.
62. Jencks, W. P. *Adv. Enzymol.* **1975**, *43*, 219.
63. Benner, S. A. *Chimia* **1988**, *42*, 309.
64. Askari, A., Ed.; *Properties and Functions of Na⁺ and K⁺ Activated Adenosinetriphosphatase Ann. N.Y. Acad. Sci.* **1974**, *242*.
65. Carafoli, E.; Scarpa, A., Eds.; *Transport ATPases Ann. N.Y. Acad. Sci.* **1982**, *402*.
66. Cross, R. L. *Ann. Rev. Biochemistry* **1981**, *50*, 681-714.
67. Downie, J. A.; Gibson, F.; Cox, G. B. *Ann. Rev. Biochemistry* **1979**, *48*, 103-31.
68. Walker, J. E.; Saraste, M.; Runswick, M. J.; Gay, N. J.; *EMBO J.* **1982**, *1*, 945.
69. Pederson, P. L.; Carafoli, E. *Trends Biochem. Sci.* **1987**, *12*, 186-188.
70. Hesse, J. E.; Wieczorek, L.; Altendorf, K.; Reicin, A. S.; Dorus, E.; Epstein, W. *Proc. Natl. Acad. Sci. U.S.A.* **1984**, *81*, 4746.
71. Cleland, W. W. *Methods Enzymol.* **1982**, *87*, 159.
72. Hill, R. K.; Sawada, S.; Arfin, S. M. *Bioorg. Chem.* **1979**, *8*, 175-189.
73. (a) Steinberger, R.; Westheimer, F. H. *J. Am. Chem. Soc.* **1949**, *71*, 4158-4159. (b) *Ibid.* **1951**, *73*, 429-435.
74. Vennesland, B. *Top. Curr. Chem.* **1974**, *48*, 39-65.
75. Mueller, W., E.T.H. Dissertation 5507, 1975.

76. Chang, C.-C.; Laghai, A.; O'Leary, M. H.; Floss, H. G.; *J. Biol Chem.* **1982**, *257*, 3564.
77. Piccirilli, J. A.; Benner, S. A. *J. Am. Chem. Soc.* **1987**, *109*, 8084.
78. Dimroth, P. *Eur. J. Biochem.* **1981**, *115*, 353-358.
79. Dimroth, P. *Eur. Biochem.* **1982**, *121*, 443.
80. Dimroth, P. *Eur. Biochem.* **1982**, *121*, 435.
81. Rose, I. A. *J. Biol. Chem.* **1970**, *245*, 6052.
82. Davis, D. D.; Teixeria, A.; Kenworthy, P. *Biol. J.* **1972**, *127*, 335.
83. Yeh, W.-K.; Fletcher, P.; Ornston, L. N. *J. Biol. Chem.* **1980**, *255*, 6342.
84. Davies, D. D.; Kenworthy, P. *Biochem. J.* **1982**, *205*, 581.
85. Mansell, R. L.; Gross, G. G.; Stockigt, J.; Franke, H.; Zenk, M. H. *Phytochem.* **1974**, *13*, 2427.
86. Colwick, S. P.; van Eys, J.; Prk, J. H. In *Comprehensive Biochemistry* 14, 1, Florkin, M.; Stotz, E. H., Eds.; Elsevier: Amsterdam, 1966.
87. Bentley, R. *Molecular Asymmetry in Biology* 2, Academic: New York, 1970.
88. R. Allemann, A. Glasfeld, L. Ge., unpublished.
89. Goerisch, H.; Hartl, T.; Grussebuerer, W.; Stezowski, J. J.; *Biochem. J.* **1985**, *226*, 885.
90. S. A. Benner, unpublished.
91. Garavito, R. M.; Rossmann, M. G.; Argos, P.; Eventoff, W.; *Biochemistry* **1977**, *16*, 5065.
92. Oppenheimer, N. J.; Marschner, T. M.; Malver, O.; Kam, B.; "Proceedings of the Steenbock Symposium," Madison, Wisconsin, July 1985, 15-28, Elsevier: New York, 1986.
93. Rossmann, M. G.; Liljas, A.; Braenden, C.-I.; Banaszak, L. J.; *The Enzymes* **1975**, *11*, 61.
94. Rossmann, M. G.; Moras, D.; Olsen, K. W. *Nature* **1974**, *250*, 194.
95. Benner, S. A.; Nambiar, K. P.; Chambers, G. K. *J. Am. Chem. Soc.* **1985**, *107*, 5513.
96. Jornvall, H.; Persson, M.; Jeffrey, J. *Proc. Nat. Acad. Sci.* **1981**, *78*, 4226.
97. Gilbert, W. A. *Nature* **1978**, *271*, 501.
98. Llewellyn, D. J.; Daday, A.; Smith, G. D. *J. Biol. Chem.* **1980**, 2077.
99. Hall, B. G.; Yokoyama, S.; Calhoun, D. H. *Molec. Biol. Evol.* **1984**, *1*, 109.
100. Joernvall, H.; Bahr-Lindstrom, H. von, Jany, K. D.; Ulmer, W.; Froschle, M. *FEBS Lett.* **1984**, *165*, 190.
101. (a) Krakow, G.; Vennesland, B. *Biochem. Z.* **1963**, *338*, 31. (b) Simon, H.; Kraus, A. *Isotopes in Organic Chemistry* 2 Bunzel, E.; Lee, C. C.; Elsevier: Amsterdam, 1976, p 153.
102. Schneider-Bernloehr, H.; Adolph, H.-W.; Zeppezauer, M. *J. Am. Chem. Soc.* **1986**, *108*, 5573.
103. Beedle, A. S.; Rees, H. H.; Goodwin, T. W. *Biochem. J.* **1974**, *139*, 205.
104. Morpeth, F. F.; Dickinson, F. M. *Biochem. J.* **1980**, *191*, 619.
105. Bosron, W. F.; Prairie, R. L. *Arch. Biochem. Biophys.* **1973**, *154*, 166.
106. Ris, M. M.; von Wartburg, J.-P. *Eur. J. Biochem.* **1973**, *37*, 69.
107. Wermuth, B. *J. Biol. Chem.* **1981**, *256*, 1206.
108. Benner, S. A. *Experientia* **1982**, *38*, 633.
109. Srivastava, D. K.; Bernhard, S. A. *Biochemistry* **1984**, *23*, 4538.

110. Nambiar, K. P.; Stauffer, D. M.; Kolodziej, P. A.; Benner, S. A. *J. Am. Chem. Soc.* **1983**, *105*, 5886.
111. Van der Veen, R. H.; Kellogg, R. M.; Vos, A. *J. Chem. Soc., Chem. Commun.* **1978**, 923.
112. Rabideau, P. W.; Mooney, J. L.; Lipkowitz, K. B. *J. Am. Chem. Soc.* **1986**, *108*, 8130.
113. Glasfeld, A.; Zbinden, P.; Dobler, M.; Benner, S. A.; Dunitz, J. D. *J. Am. Chem. Soc.* **1988**, *110*, 5152.
114. Wu, Y.-D.; Houk, K. N. *J. Am. Chem. Soc.* **1987**, *109*, 2226.
115. Levy, H. R.; Vennesland, B. *J. Biol. Chem.* **1957**, *228*, 85.
116. Pai, E. F.; Schulz, G. E. *J. Biol. Chem.* **1983**, *258*, 1752.
117. Pai, E. F., personal communication to A. G.
118. Ellington, A. D.; Benner S. A. *J. Theor. Biol.* **1987**, *127*, 491.
119. Oppenheimer, N. J. *J. Am. Chem. Soc.* **1984**, *106*, 3032.
120. These criticisms were the basis for the evaluation of a research proposal by the Biophysical Review Group of the National Institutes of Health (NIH), 1982.
121. Chari, R. V. J.; Whitman, C. P.; Kozarich, J. W.; Ngai, K.-L.; Ornston, L. N. *J. Am. Chem. Soc.* **1987**, *109*, 5514.
122. You, K.-S. *Chem. Eng. News* **1986**, *64*, 3.
123. Robinson, W. G. *Methods Enzymol.* **1966**, *9*, 332.
124. Flynn, T. G. *Biochem. Pharmacol.* **1982**, *31*, 2705.
125. Glasfeld, A.; Benner, S. A. *J. Biol. Chem.* **1988**, submitted.
126. Takizawa, T.; Huang, I.-Y.; Ikuta, T.; Yoshida, A. *Proc. Natl. Acad. Sci. U.S.A.* **1986**, *83*, 4157.
127. Williamson, V. M. and Paquin, C. E. *Mol. Gen. Genet.* **1987**, *209*, 374.
128. Glasfeld, A. and Benner, S. A. *Eur. J. Biochem.* **1988**, submitted.
129. Matthews, D. A.; Smith, S. L.; Baccanari, D. P.; Burchall, J. J.; Oatley, S. M.; Kraut, J. *Biochemistry* **1986**, *25*, 4194.
130. The correlation in Table 4 does not apply to dihydrofolate reductase. However, any convergence of behavior is an argument for function; it suggests that stereospecificity is adaptive in these enzymes as well.
131. Hempel, J.; Bahr-Lindstroem, H. von, Joernvall, H. *Eur. J. Biochem.* **1984**, *141*, 21.
132. Schweizer, M.; Roberts, L. M.; Hoeltke, H.-J.; Takabayashi, K.; Hoellerer, E.; Hoffmann, B.; Mueller, G.; Koettig, H.; Schweizer, E. *Mol. Gen. Genet.* **1986**, *203*, 479.
133. In these cases, sequence homologies have been proposed in only small segments of the protein and are of insufficient statistical significant to prove (as opposed to suggest) that the proteins are homologous.
134. Dugan, R. E.; Porter, J. W. *J. Biol. Chem.* **1971**, *246*, 5361.
135. Beedle, A. S.; Munday, K. A.; Wilton, D. C. *Eur. J. Biochem.* **1972**, *28*, 151.
136. You, K.-S. *Meth. Enzymol.* **1982**, *87*, 101.
137. The alternative argument, that the sequence of MDH in archaeabacteria is >50% identical to MDH from eukaryotes and eubacteria, seems less likely (although not impossible) in view of the low structural similarities of other proteins from these two kingdoms. See Hardesty, B.; Kramer, G. *Structure, Function and Genetics of Ribosomes*; Springer-Verlag: Berlin, 1986.
138. This hypothesis might be regarded as demonstrably false; many organisms, including

- Acholeplasma* show no malate dehydrogenase activity. Further, the ethanol dehydrogenases from both *Drosophila* and yeast are evidently under enormous selective pressure. See Kreitman, M. *Nature* 1983, 304, 412.
139. Glasfeld, A.; Thesis, Harvard University, 1988.
 140. Knowles, J. R. *Science* 1987, 236, 1252.
 141. Brink, N. G. *Acta Chem. Scand.* 1953, 7, 1081.
 142. Walsh, C. *Enzymatic Reaction Mechanisms*; W. H. Freeman: San Francisco, 1979.
 143. Ohno, A.; Ohara, M.; Oka, S. *J. Am. Chem. Soc.* 1986, 108, 6438.
 144. March, J. *Advanced Organic Chemistry*, 3rd ed.; Wiley: New York, 1985; p 657.
 145. Anet, F. A. L. *J. Am. Chem. Soc.* 1960, 82, 994.
 146. Englard, S. *J. Biol. Chem.* 1958, 233, 1003.
 147. Jones, V. T.; Lowe, G.; Potter, B. V. L. *Eur. J. Biochem.* 1980, 108, 433.
 148. Takagi, J. S.; Tokushige, M.; Shimura, Y.; Kanehisa, M. *Biochem. Biophys. Res. Commun.* 1986, 138, 568.
 149. Hoberman, H. D.; Havir, E. A.; Rachovansky, O.; Ratner, S. *J. Biol. Chem.* 1964, 239, 3818.
 150. Englard, S. *J. Biol. Chem.* 1960, 235, 1510.
 151. Schroepfer, Jr.; G. L. *J. Biol. Chem.* 1966, 241, 5441.
 152. Miller, R. W.; Buchanan, J. M. *J. Biol. Chem.* 1962, 237, 491.
 153. Englard, S.; Britten, J. S.; Listowsky, I. *J. Biol. Chem.* 1967, 242, 2255.
 154. Cohn, M.; Pearson, J.; O'Connell, E. L.; Rose, I. A. *J. Am. Chem. Soc.* 1970, 92, 4095.
 155. Givot, I. L.; Smith, T. A.; Abeles, R. H. *J. Biol. Chem.* 1969, 244, 6341.
 156. Havir, E. A.; Hanson, K. R. *Biochemistry* 1975, 14, 1620.
 157. Cornforth, J. W.; Cornforth, R. H.; Popjak, G.; Yengoyan, L. *J. Biol. Chem.* 1966, 241, 3970.
 158. Martinoni, B. Q. M. E.T.H. Dissertation 5115, 1973.
 159. Avigad, G.; Englard, S. *Fed. Proc.* 1969, 28, 345.
 160. Willadsen, P.; Eggerer, H. *Eur. J. Biochem.* 1975, 54, 247.
 161. Widlanski, T. S.; Bender, S. L.; Knowles, J. R. In Bartman, W.; Sharpless, K. B., Eds.; *Stereochemistry of Organic and Bioorganic Transformations*, 1987; Workshop Conference, Hoechst, Vol. 17, 275-282.
 162. Schwab, J.; Klassen, J. B.; Habib, A. *J. Chem. Soc. Chem. Comm.* 1986, 357.
 163. Sedwick, B.; Morris, C.; French, S. J. *J. Chem. Soc., Chem. Commun.* 1978, 193.
 164. Messner, B.; Eggerer, H.; Cornforth, J. W.; Mallaby, R. *Eur. J. Biochem.* 1975, 53, 255.
 165. Hanson, K. R.; Rose, I. A. *Proc. Nat. Acad. Sci.* 1963, 50, 981.
 166. Aberhart, J.; Tann, C.-H. *J. Chem. Soc., Perkin Trans. I* 1979, 939.
 167. Scharf, K. H.; Zenk, M. H.; Onderka, D. K.; Carroll, M.; Floss, H. G. *J. Chem. Soc. Chem. Commun.* 1971, 765.
 168. Kirby, G. W.; O'Loughlin, G. J.; Robins, D. J. *J. Chem. Soc. Chem. Commun.* 1975, 402.
 169. Schwab, J.; Klassen, J. B. *J. Am. Chem. Soc.* 1984, 106, 7217.
 170. I am indebted to Prof. J. Schwab for calling these references to my attention.
 171. Caspi, E.; Ramm, P. J. *Tetrahedron Lett.* 1969, 181.
 172. Mortimer, Niehaus *J. Biol. Chem.* 1974, 249, 2833.

173. For example, the kinetic isotope effects were measured on an unnatural substrate.
174. Arnett, E. M.; Hofelich, T. C. *J. Am. Chem. Soc.* **1983**, *105*, 2889.
175. Jencks, W. R. *Acc. Chem. Res.* **1976**, *9*, 425.
176. Kozarich, J. W.; Chari, R. V. J.; Ngai, K.-L.; Ornston, N. L. In *Mechanisms of Enzymatic Reactions: Stereochemistry*, Frey, P. A. Ed., Elsevier: Amsterdam 1986; p 233.
177. Volpe, J. J.; Vagelos, P. R. *Ann. Rev. Biochem.* **1973**, *42*, 21.
178. Singh, N.; Stoops, J. K.; In *Enzyme Mechanisms*, M. I. Page, Ed.; Royal Society: London, 1987.
179. Saito, K.; Kawaguchi, A.; Seyama, Y.; Yamakawa, T.; Okuda, S. *Eur. J. Biochem.* **1981**, *116*, 581.
180. Saito, K.; Kawaguchi, A.; Seyama, Y.; Yamakawa, T.; Okuda, S. *J. Biochem.* **1981**, *90*, 1697.
181. Saito, K.; Kawaguchi, A.; Seyama, Y.; Yamakawa, T.; Okuda, S. *Tennen Yuki Kago-butsu Toronkai Koen Yoshishu*, 24th **1981**, 529.
182. Saito, K.; Kawaguchi, A.; Okuda, S.; Seyama, Y.; Yamakawa, T.; Nakamura, T.; Yamada, M. *Plant Cell. Physiol.* **1980**, *21*, 9.
183. Kikuchi, S.; Kusaka, T. *J. Biochem.* **1984**, *96*, 841.
184. Schweizer, M.; Roberts, L. M.; Hoeltke, H.-J.; Takabayashi, K.; Hoellerer, E.; Hoffman, B.; Mueller, G.; Koettig, H.; Schweizer, E. *Mol. Gen. Genet.* **1986**, *203*, 479.
185. Hardie, D. G.; McCarthy, A. D.; Braddock, M. *Biochem. Soc. Trans.* **1986**, *14*, 568.
186. McCarthy, A. D.; Goldring, J. P. D.; Hardie, D. G. *FEBS Lett.* **1983**, *162*, 300.
187. Chirala, S. S.; Kuziora, M. A.; Spector, D. M.; Wakil, S. J. *J. Biol. Chem.* **1987**, *262*, 4231.
188. Michenfelder, M.; Hull, W. E.; Rétey, J. *Eur. J. Biochem.* **1987**, *168*, 659.
189. Anderson, V. E.; LaReau, R. D. *J. Am. Chem. Soc.* **1988**, *110*, 3695-97.
190. Rubenstein, P. A.; Strominger, J. L. *J. Biol. Chem.* **1974**, *249*, 3782.
191. George, J. M.; Orr, J. C.; Renwick, A. G. C.; Carter, P.; Engel, L. L. *Bioorg. Chem.* **1973**, *2*, 140.

Enantioselective Synthesis of Non-racemic Chiral Molecules on an Industrial Scale

JOHN W. SCOTT

*Chemical Development Department, Hoffmann-La Roche Inc.
Nutley, New Jersey*

- I. Introduction
 - A. The Chemical Process
 - B. Criteria for Enantioselective Synthesis on a Large Scale
- II. Exemplification
 - A. Amino Acids by Enantioselective Hydrogenation
 - B. Enantioselective Cyclopropanation
 - C. Enantioselective Epoxidation of Allylic Alcohols
 - D. Enantioselective Olefin Isomerization
 - E. Enantioselective 2+2 Cycloaddition Reactions
 - F. Enantioselective Hydroboration
- III. Future Trends
 - A. The Problem: Kinetics vs. Enantioselectivity
 - B. Ligand-Accelerated Enantioselective Synthesis
- IV. Conclusion
- References

I. INTRODUCTION

The chemical industry has a need to prepare quantities of chiral non-racemic molecules in enantiomerically homogeneous form. The driving forces for the shift away from racemic compounds are several. The most obvious is that enantiomers are now well known to have, in many cases, entirely different physiological properties (1, 2). The well-known case of thalidomide is the most obvious example. One enantiomer of this racemic mixture is an effective sedative with minimal toxic liability while the other enantiomer is devoid of sedative activity but is one of the most potent teratogens known. Marketing of the racemate in Britain led to an entirely avoidable human tragedy (see, however, 47).

Other less dramatic, but equally significant examples are known. Morphinans of the natural series are potent narcotics while their enantiomers, without narcotic activity, often have very useful (for example, antitussive) activity. Insect pheromone activity is often critically dependent upon en-

antiomeric composition. Cases where the racemate is devoid of activity have been reported (3).

A second major reason for synthesis of non-racemic chiral compounds is economic. If half of the material being manufactured is expensive but inactive "baggage," preparation of the desired homogeneous enantiomer results in a lower production cost (assuming the routes to the enantiomer and racemate are of similar cost) and thus, presumably, in a larger market share and/or profit.

The methodologies available to the industrial chemist for preparation of chiral non-racemic molecules are threefold: classical resolution, use of naturally-occurring enantiomers as starting materials, and asymmetric (enantioselective) synthesis. The choice of the method to be employed in a particular case depends on economic factors as described below.

Traditionally, resolution and the use of the "chiral pool" (4-7) have been the technical bases for obtaining enantiomerically homogeneous compounds. Beginning in the 1970s, enantioselective synthesis reached a level of sophistication where industrial application became feasible and competitive, in the appropriate cases, with the older technologies.

It is the purpose of this article to present the considerations in choosing a chemical process and the criteria that must be met for an enantioselective synthesis to be the process of choice. Several examples of successfully introduced processes will then be given. This latter discussion is limited to chemical enantioselective syntheses; enzymic processes, for example, the large scale immobilized acylase processes used in Japan for the preparation of amino acids (8), while of tremendous economic significance, are outside the scope of this discussion (cf. the chapter by C. J. Sih and S.-H. Wu in this volume).

A. The Chemical Process

In general, the mechanism by which a new chemical reaches commercialization has three phases. After initial identification of the compound, material must be made for testing. At this phase, cost of the material and feasibility of the chemistry employed are of virtually no concern. If the initial evaluation is positive, additional compound is required for further testing. Various synthetic routes to the compound may be devised with an eye towards a facile pilot plant production. The third phase of development, once a compound is projected for commercialization, is an in-depth study to turn the chemistry into a process capable of being run on the desired scale in the most economic manner. Usually, such process research results in several potential routes to the desired compound. Many factors need be considered in reaching a decision as to which route to fully develop and implement. Among the items, many of which are obviously interrelated, to be considered are:

- step yields/overall yield
- linearity of sequence
- throughput
- regulatory impact
- operating costs (labor, materials)
- process reliability
- overheads
- fit with technology practiced in the company
- competition (internal/external)
- robustness of process/degree of control required
- quality of product needed/available
- capital investment
- environmental impact
- raw material and reagent availability
- safety
- technical risk
- patent/trade secret protection

Each of these items brings with it a cost to the final product. Assigning a weighting factor to each item (9) allows the development of fully-loaded costs for the competing processes. It is not unusual, for example, for the fully-loaded cost to show that the highest yield route is not the most economical.

B. Criteria for Enantioselective Synthesis on a Large Scale

Economic analyses of the type described above have led to the conclusion in several cases that enantioselective synthesis provides the lowest cost product; examples are provided in the following section. Here, however, are first indicated some common features of those reactions.

As a general rule, industrial enantioselective syntheses are metal-catalyzed reactions; hence a relatively small amount of (usually expensive) chiral ligand can be parlayed into a large quantity of chiral product. The beneficial effect of catalytic vs. stoichiometric processes on the environment are obvious.

The known metal-catalyzed processes usually proceed in high chemical yield to give products in good-to-excellent enantiomer excess (10, 11). As a result, there is little chemical waste for disposal. Perhaps more importantly, most of the processes contain a step allowing facile further enantiomer enrichment. The products are thus obtained with a very high degree of enantioselectivity.

It is suggested that the features exhibited by those reactions already in

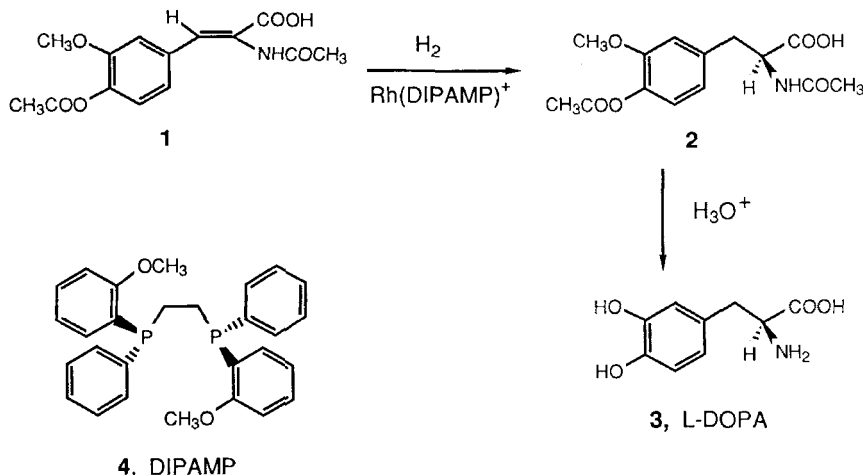
commercialization will be required, except in special cases, for other enantioselective synthesis processes to be economically viable.

II. EXEMPLIFICATION

A. Amino Acids by Enantioselective Hydrogenation

Catalytic hydrogenation is, by its very nature, an efficient and inexpensive technology for which a wealth of industrial experience exists. Many attempts to effect enantioselective catalytic hydrogenations, however, have led to products with disappointingly low enantiomer excesses. This was (and on the whole, still is) undoubtedly caused by the complex nature of heterogeneous catalyst surfaces containing many types of reactive sites. It was not until the advent of the homogeneous Wilkinson's catalyst, $\text{RhCl}[(\text{C}_6\text{H}_5)_3\text{P}]_3$, in 1966 that this situation changed. The realization that substitution of chiral phosphines for triphenylphosphine in this cleanly defined catalyst system might lead to catalysts capable of enantioselective hydrogenation was made by several groups. It was Knowles and co-workers at Monsanto (12) who first moved the technology to the industrial level in their synthesis of L-DOPA (3, Figure 1).

L-DOPA is a drug used in the treatment of Parkinson's disease. It is prepared by hydrogenation of the enamide **1** over a Wilkinson-type catalyst employing the bis(phosphine) ligand DIPAMP (**4**). As in virtually all such hydro-



4, DIPAMP

Figure 1. Synthesis of L-DOPA by asymmetric hydrogenation.

genations, the chemical yield is excellent and the enantiomer excess (94%) is quite good (13). Acidic hydrolysis of the product, protected amino acid **2**, then provides L-DOPA. Although the full details of the Monsanto process have not been revealed, its success appears to rest on three operating parameters. Phosphines such as DIPAMP are usually difficult to synthesize and thus are quite expensive. As a corollary, these phosphines must be used efficiently. In the case at hand, substrate:catalyst ratios as high as 20,000:1 may be employed while still maintaining acceptable hydrogenation times. It appears that these catalysts are not, in general, subject to the types of poisons which deactivate most heterogeneous catalysts. On the other hand, control of certain parameters, such as the oxygen level at the start of the hydrogenations (down to the parts-per-million level), is crucial in maintaining catalyst activity.

The second supposed factor contributing to success of the Monsanto process is that the hydrogenation is run in a solvent system in which the starting material **1** and the product **2** are insoluble, but in which the racemate (conglomerate) corresponding to **2** is soluble. As a result, simple filtration of the reaction mixture at the end of the hydrogenation gives product of high chemical and enantiomeric purity. Finally, the hydrolytic cleavage of the protecting groups from compound **2** is carried out under conditions such that very little, if any, racemization occurs.

It was the Monsanto demonstration of the industrial feasibility of enantioselective hydrogenation which moved enantioselective synthesis, in the minds of many organic chemists, from an exotic curiosity to "real chemistry." The explosive growth, both in breadth and depth, of research in enantioselective synthesis in succeeding years is clearly attributable to this success.

The simpler amino acid, phenylalanine, has also been prepared by enantioselective hydrogenation. According to the available literature (14), the enamide **5** (Figure 2) is hydrogenated over a catalyst system involving the bis(aminophosphine) PNNP (**9**). This hydrogenation is carried out in ethanol at a substrate:catalyst ratio of 15,000:1. A relatively modest 83% enantiomer excess is reported. The hydrogenation product, upon treatment with methanolic hydrogen chloride, is converted to (*S*)-phenylalanine methyl ester (**6**). Crystallization of this material raises the enantiomer excess to 97%. This enriched material, upon reaction with aspartic acid (**7**), is converted to the non-nutritive sweetener aspartame® (**8**). It has been reported (15) that many tons/year of aspartame® are being made by this process.

The use of PNNP in the synthesis of aspartame® on an industrial scale is somewhat surprising in that the obtained enantiomer excess is relatively low. In addition, a very careful control of reaction conditions may be required because of the potential lability of the P-N bond under the reaction conditions, with the attendant loss of catalytic activity.

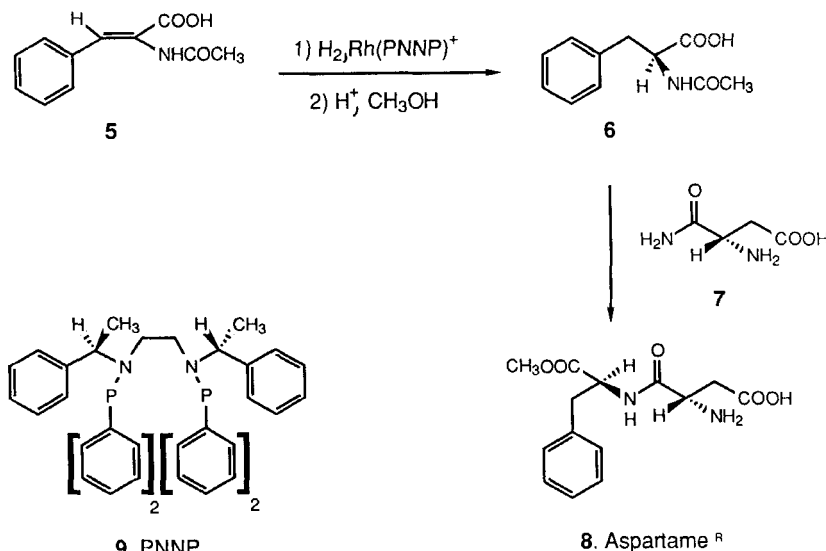


Figure 2. Synthesis of (*S,S*)-aspartylphenylalanine methyl ester by asymmetric hydrogenation.

The chirally-modified Wilkinson's catalyst systems have rather rigid substrate requirements. While aromatic amino acids and (particularly with DIPAMP (16)) aliphatic amino acids are obtained in good enantiomer excesses, few other product types are accessible with an acceptable combination of reaction rate and enantiomer excess. The scope of the reaction, however, has been greatly expanded with the finding (17–19) that ruthenium-based catalysts work effectively with, for instance, allylic alcohols. The successful industrialization of these chiral ruthenium catalysts for products other than amino acids is likely.

B. Enantioselective Cyclopropanation

One of the earliest catalytic enantioselective syntheses to be shown to proceed in very high enantiomer excess was the preparation of cyclopropanes by the reaction of olefins with alkyl diazoacetates in the presence of chirally ligated copper species. Almost 20 years were to pass, however, before industrial application of the reaction was made.

Imipenem (13, Figure 3) is a broad spectrum antibiotic of the thienamycin type. The compound, particularly useful in treatment of urinary tract infections, was found initially to have limited clinical usefulness since it is rapidly degraded by the renal enzyme dehydropeptidase I. An efficient reversible in-

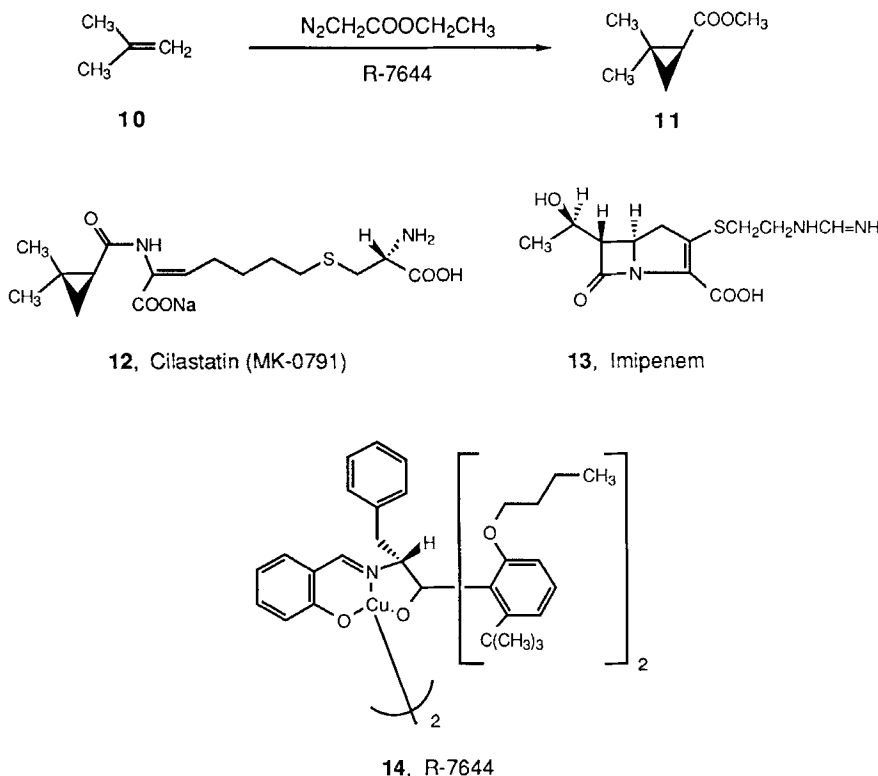


Figure 3. Synthesis of cilastatin by asymmetric cyclopropanation.

Inhibitor of this enzyme is cilastatin (12) and a combination of imipenem and cilastatin is now a very useful pharmaceutical marketed by Merck Sharp and Dohme.

A logical precursor to cilastatin is ethyl (*S*)-2,2-dimethylcyclopropanecarboxylate (11). This compound is prepared (20) by the decomposition of ethyl diazoacetate in isobutylene (10) in the presence of the dimeric chiral copper catalyst R-7644 (14). Few details of the process practiced by the Sumitomo Chemical Co. have been revealed. It is known that a 92% enantiomer excess is obtained. Of particular interest would be the amount of catalyst employed, the method for enantiomer enrichment, and the scale upon which the reaction is run.

Many chiral cyclopropane derivatives are available using this technology. Among the most obvious candidates with economic significance would appear to be analogs of the naturally-occurring pyrethroid insecticides. Al-

though significant synthetic work in this area has been carried out (20), it does not appear as yet to have led to a commercial process.

C. Enantioselective Epoxidation of Allylic Alcohols

The enantioselective epoxidation of allylic alcohols (21) is a very powerful synthetic tool. Over 200 publications describing the use of the method for preparing a wide variety of compounds attest to the usefulness of the technique. Its introduction into industrial practice was delayed for several years by the fact that the reaction usually required at least 50 mole percent of the reactant titanium/tartrate complex. Despite this drawback, a small volume process involving production of a high value-added compound was pursued. The J. T. Baker Co. has taken the Sharpless synthesis (22) of (*7R,8S*)-disparlure (18, Figure 4), the pheromone of the gypsy moth, as basis for production of the compound.

Little has been disclosed about the process employed by J. T. Baker. The initial publication (22) described epoxidation of (*Z*)-2-tridecen-1-ol (15) with tert-butyl hydroperoxide at -40°C for 4 days in the presence of a complex derived from titanium isopropoxide and (*S,S*)-diethyl tartrate. The resultant epoxy alcohol 16, obtained in 80% yield and 91% enantiomer excess, was crystalline, thus presumably allowing for enantiomeric enrichment. A three-step set of conversions, via aldehyde 17, then led to disparlure (18).

The very high activity of disparlure means that, in all likelihood, only a few kilos per year of material are prepared in the indicated manner. The necessity for a four day reaction at -40°C is particularly undesirable from a process viewpoint. It is known that such extreme conditions are not usually required, however. In a number of cases, careful reaction optimization has shown that enantioselective epoxidations can be carried out with as little as 10 mole percent titanium/tartrate complex, at significantly higher temperatures, and/or in much shorter reaction times (23).

Despite the simplifications available by process improvement studies, enantioselective epoxidations tend to become somewhat capricious when lower amounts of titanium/tartrate complex are used. A major breakthrough, and the basis for a truly economical use of enantioselective epoxidation on large scale, came with the finding that addition of molecular sieves to the reaction mixture allows the use of 5 mole percent titanium/tartrate complex in a highly reproducible reaction (24). The ARCO Chemical Company has used this finding as the basis for a facility capable of producing up to 10 tons/year of (*S*)- and (*R*)-glycidol (19, 20, Figure 5) and (*S*)- and (*R*)-methylglycidol (21, 22) (25). The glycidols 19 and 20, obtained in $88 \pm 2\%$ enantiomer excess, are basic building blocks for many highly functionalized chiral molecules (4).

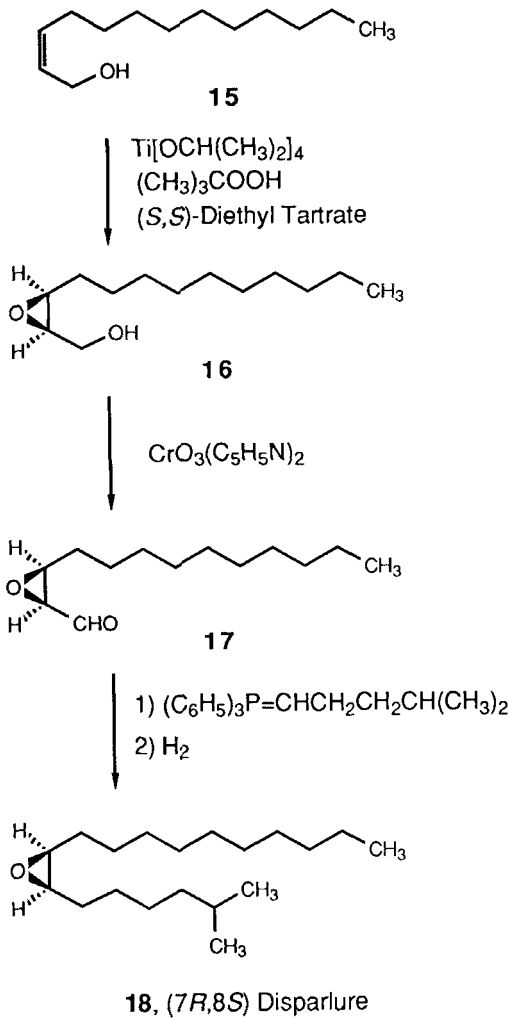


Figure 4. Synthesis of (7*R*,8*S*)-disparlure by asymmetric allylic alcohol epoxidation.

The appearance on the market of significant quantities of the glycidols bodes well for the future of enantioselective epoxidation as an industrial process. Because of their low molecular weights and thus high water solubility, the glycidols are among the most difficult of the epoxy alcohols to make by this technique. Indeed, it was the finding of a proprietary, simplified work-up and product isolation that allowed ARCO to scale up the process in an economically viable fashion. It is now claimed (25) that these advances provide

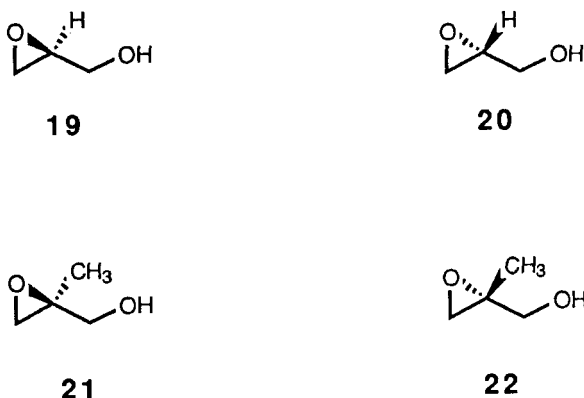


Figure 5. Glycidol derivatives available by asymmetric epoxidation.

an economic advantage over the major competitive route to glycidols, namely the porcine pancreatic lipase-catalyzed hydrolysis of glycidyl butyrate (26). This latter route, currently in development at Genzyme Corp., gives (*R*)-glycidyl butyrate of 92% enantiomer excess (27). Thus, the basis for the further growth of enantioselective epoxidation as an industrial technology is present.

D. Enantioselective Olefin Isomerization

Reactions other than catalytic hydrogenations can be effected with chirally modified Wilkinson's catalysts. A particularly elegant application is found in Takasago Corporation's synthesis of *l*-menthol (29, Figure 6). This process is the most highly developed of all commercial enantioselective syntheses. Since its introduction in 1984, Takasago has captured over 30% of the 3500 ton/year *l*-menthol market (28).

The key, chirality-inducing step in the Takasago synthesis is the isomerization of diethylgeranylamine (25) to the enamine 26 (29,30). This reaction, carried out at 100°C for 15 hr over a rhodium (I) catalyst containing the chiral ligand (*S*)-BINAP (30), gives a 100% conversion to the enamine 26 of 98% enantiomer excess. This reaction is run on a 7 ton batch basis at substrate:catalyst ratios of 8,000–10,000:1. The product is distilled directly from the reaction mixture at low pressure. The residue from this distillation remains catalytically active (28). It can either be used directly for a subsequent reaction or processed for recovery of the rhodium and (*S*)-BINAP.

The six-step Takasago synthesis of *l*-menthol involves initial thermal cracking of β -pinene (23) to myrcene (24). *n*-Butyllithium-catalyzed addition

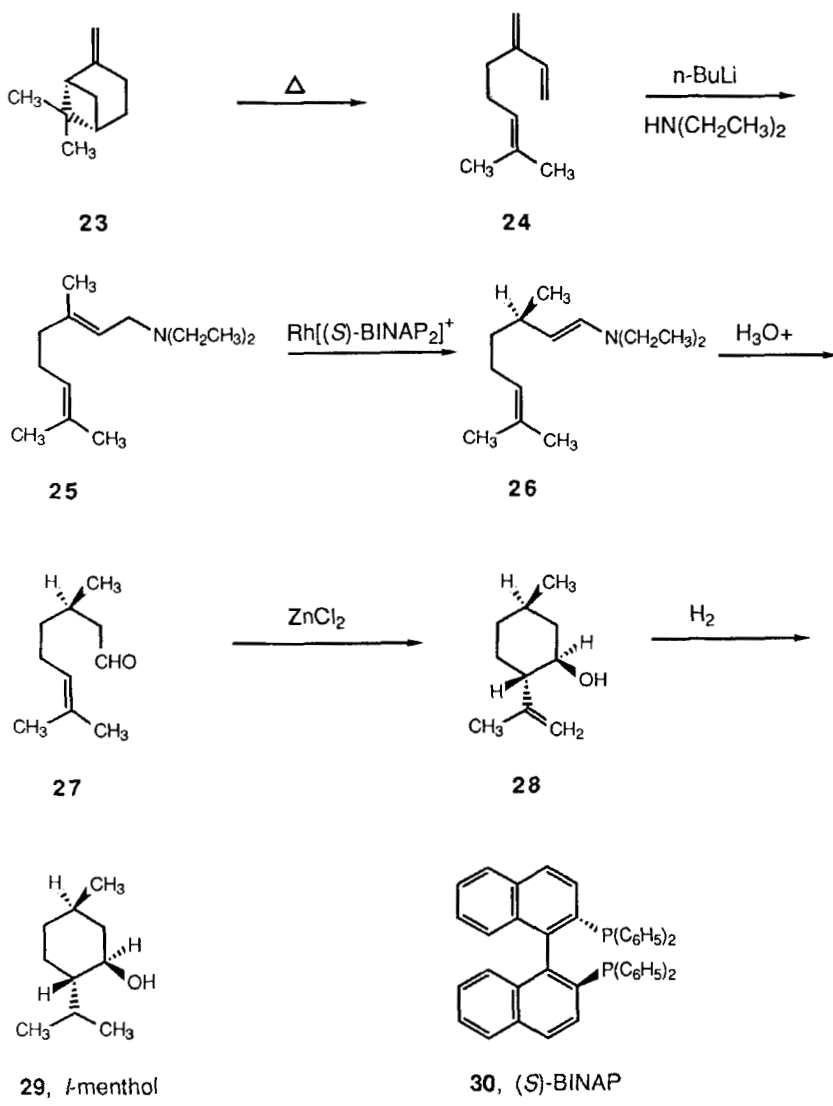


Figure 6. Synthesis of L-menthol involving olefin migration with asymmetric induction.

of diethylamine gives diethylgeranylamine (25) of very high *E*-olefin content. The distilled isomerization product 26 is hydrolyzed to (*R*)-citronellal (27), the Lewis acid-catalyzed cyclization of which gives isopulegol (28). Low temperature crystallization of this molecule provides both chemical and enantio-

meric enrichment. Catalytic reduction of the terminal olefin completes the synthesis.

The olefin isomerization chemistry is also being applied by Takasago, albeit on a significantly smaller scale, to syntheses of hydroxycitronellal, 3,6-dimethyloctanol, and methoxycitronellal. The last compound is reportedly (28) used by the Syntex Corporation in preparation of a juvenile hormone analog.

E. Enantioselective 2 + 2 Cycloaddition Reactions

Non-racemic malic and citramalic acids have significant value as chiral building blocks (4). An efficient synthesis of these compounds was found by Wynberg (31-33). This chemistry, as illustrated in Figure 7 for (*S*)-citramalic acid (37) and (*S*)-malic acid (38), has reached the pilot plant scale at Lonza Ltd., with further scale up anticipated as markets for these compounds develop (34).

As in several other cases examined, the technical details of the industrial process are not available. The published chemistry involves cycloaddition of ketene (31) to trichloroacetone (32) or chloral (33) at -50°C in toluene. Use of 1-2% quinidine (34) as catalyst gives good yields of the (*R*)-oxetanones 35 and 36 in 98 and 94% enantiomer excess, respectively. These materials are brought to enantiomeric homogeneity by crystallization. Mild basic hydrolysis occurs with inversion of configuration to give the product acids 37 and 38.

(*R*)-Citramalic and (*R*)-malic acid are also prepared by this method, using quinine as catalyst. Unfortunately, the enantiomer excesses obtained (85% and 76%) of the (*S*)-oxetanones are somewhat lower than when quinidine is employed.

It has been reported (35) that kilogram quantities of the enantiomeric malic and citramalic acids are being made in this manner.

F. Enantioselective Hydroboration

Enantioselective hydroboration, though a very useful laboratory tool, would normally not be considered an industrial technique as the chiral auxiliary must be employed in a stoichiometric ratio. Nonetheless, Chinoim Pharmaceutical and Chemical Works Ltd. has employed the method (36) to prepare the Corey lactone (44, Figure 8) as well as other, further advanced prostaglandin intermediates.

Once again, knowledge of the industrial process is limited to the original literature. The key, chirality-inducing step is the hydroboration of the substituted cyclopentadiene 40 by diisopinocampheylborane (42), obtained from α -pinene (41). This reaction must be carried out at very low temperatures

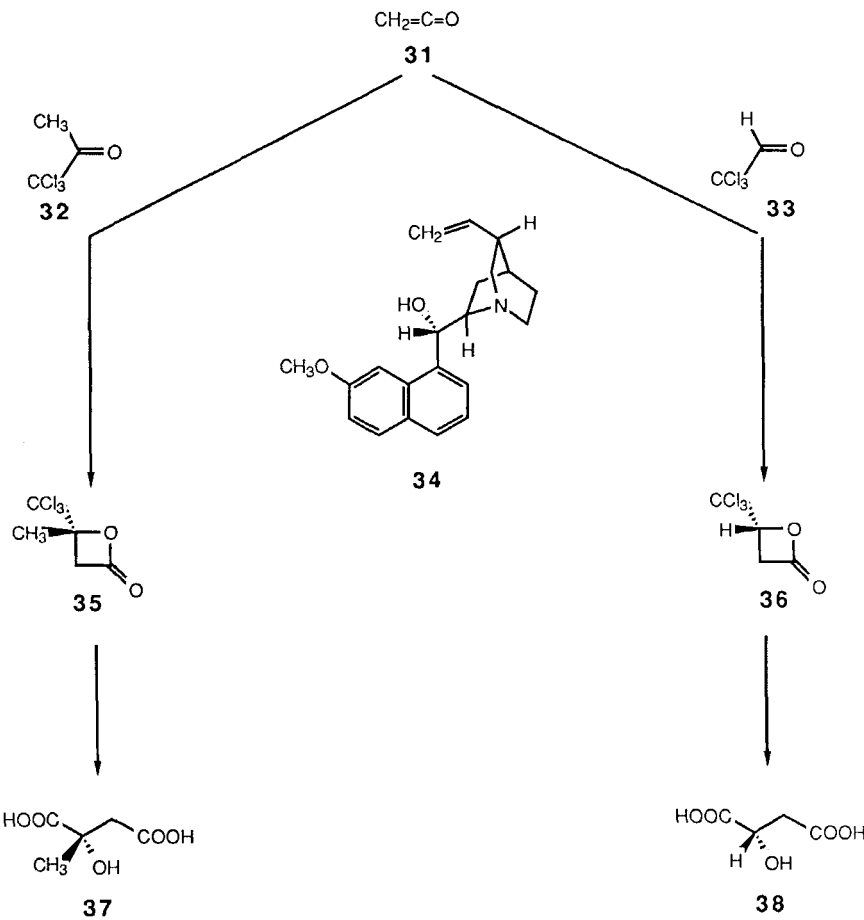


Figure 7. Synthesis of (*S*)-citramalic and -malic acids by asymmetric cycloaddition.

because the diene **40** is prone to olefin rearrangement. The alcohol **43**, obtained in ca. 95% enantiomer excess, is converted, with inversion at the hydroxyl-bearing center, to the Corey lactone in two facile steps.

The enantioselective hydroboration shown in Figure 8 is a technically demanding reaction. Unless significant improvements have been made during process development, reaction control to obtain good yields of product **43** of high enantiomer excess is difficult to achieve consistently. The technical demands of the process, along with the requirement for stoichiometric consumption of the chirality inducing agent can be justified only for a highly valuable compound where competitive synthetic approaches do not exist.

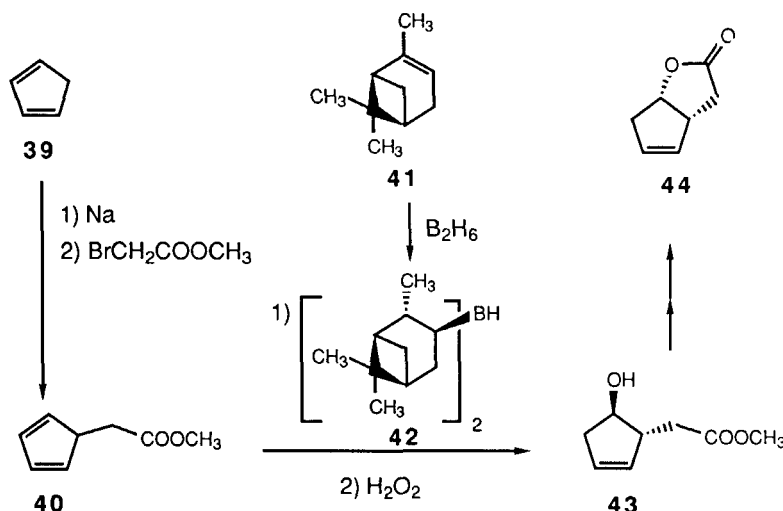


Figure 8. Preparation of the Corey lactone (44) by asymmetric hydroboration.

Examples such as the illustrated Corey lactone synthesis are likely to remain rare and will apply only in very specialized circumstances.

III. FUTURE TRENDS

As described and illustrated above, enantioselective synthesis on the industrial level will be limited, on the whole, to catalytic reactions which offer a very efficient use of the original source of chiral information. Additional examples of the type shown will undoubtedly be brought to technical fruition. A number of well-known synthetic transformations are precluded from implementation, however, since efficient use of the chiral information is not possible.

A. The Problem: Kinetics vs. Enantioselectivity

An illustrative example of the problem is seen in the reduction of an unsymmetrical ketone by lithium aluminum hydride that has been partially decomposed by a chiral alcohol, R*OH (37). A number of species, for example, LiAlH(OR*)₃, LiAlH₂(OR*)₂, LiAlH₃(OR*), and LiAlH₄, are possible, depending upon the amount of chiral alcohol employed. As a general rule, the highest enantiomer excess of the product will be obtained with LiAlH(OR*)₃,

presumably because of the higher steric demands placed on the transition state for reduction by this species. Unfortunately, this species is also generally the slowest reacting of those indicated. For this reason, three moles of R*OH per mole of LiAlH₄ are required to obtain maximum product enantiomer excess.

The problem becomes even more complex with alcohol-modified LiAlH₄ since equilibration, including LiAl(OR*)₄, can occur under the reaction conditions. This allows the presence of more reactive, yet less enantioselective reducing agents in a reaction mixture prepared from one mole of LiAlH₄ and three moles of chiral alcohol. Thus, there is no possibility of carrying out this hydride reduction with a catalytic amount of chiral alcohol.

B. Ligand-Accelerated Enantioselective Synthesis

The lithium aluminum hydride case represents most of the history of enantioselective (asymmetric) synthesis to date: a catalytic, or in this case, stoichiometric reagent is modified with a chiral auxiliary to provide an enantioselective but generally less reactive species. A new type of enantioselective synthesis is beginning to appear. In this chemistry, a reaction which normally does not occur becomes kinetically viable in the presence of a (chiral) ligand. This allows the use of a catalytic amount of the usually expensive chiral ligand in a reaction devoid of the kinetic problems outlined above. While no examples of these "ligand-accelerated enantioselective syntheses" have reached industrial application to date, a very real potential exists. An example of such a reaction is given in Figure 9.

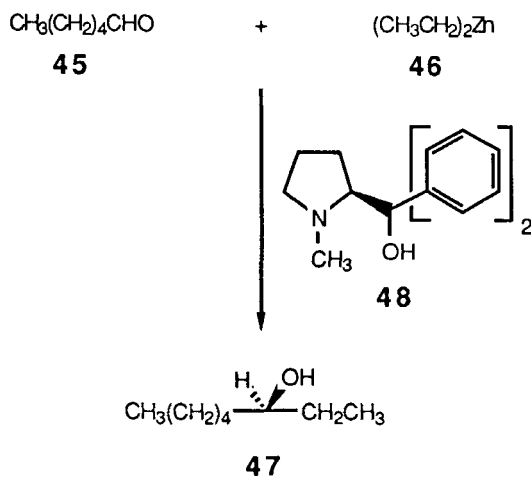


Figure 9. Ligand-accelerated asymmetric synthesis of (S)-3-octanol.

A dialkylzinc does not normally add to an aldehyde to give a secondary alcohol. However, spurred by an initial report in 1984 (38), a number of groups (39–45) have studied the effect of added chiral ligands, usually amino alcohols, on this reaction. One typical result is the reaction of diethylzinc (**46**) with heptanal (**45**) in the presence of 2 mole percent of the amino alcohol **48**, derived from (*S*)-proline (**45**). The (*S*)-alcohol **47** is obtained in 96% yield and 91% enantiomer excess. Not only is this reaction catalytic in the chiral auxiliary but the observed enantioselectivity is significantly greater than that to be expected (46) by reduction of 3-octanone with a chirally modified hydride reagent.

The successfully demonstrated ligand-accelerated enantioselective synthesis of secondary alcohols will surely lead to the search for other such reactions.

IV. CONCLUSION

For obvious reasons, industrial firms are often reluctant to disclose details of their technical processes. Thus, the examples cited above are, in all likelihood, only some of the situations in which enantioselective synthesis is practiced on a large, industrial scale. The processes known to this author clearly demonstrate, however, that chemical enantioselective synthesis has advanced from a laboratory curiosity to a technology providing, under the appropriate circumstances, the cheapest process to produce a number of chiral, non-racemic molecules of economic importance.

REFERENCES

1. Powell, J. R.; Ambre, J. J.; Ruo, T. I. in Wainer, I. W.; Drayer, D. E., Eds.; *Drug Stereochemistry*; Marcel Dekker: New York, 1988; pp 245–270.
2. Ariëns, E. J.; Soudijn, W.; Timmermans, P.B.M.W.M. *Stereochemistry and Biological Activity of Drugs*; Blackwell Scientific: Palo Alto, CA, 1983.
3. Brand, J. M.; Young, J. C.; Silverstein, R. M. in Herz, W. E.; Grisebach, H.; Kirby, G. W., Eds; *Progress in the Chemistry of Organic Natural Products*; Springer-Verlag: New York, 1979; Vol. 37, pp 1–190.
4. Scott, J. W. in Scott, J. W.; Morrison, J. D., Eds.; *Asymmetric Synthesis*; Academic: Orlando, 1984, Vol. 4, pp 1–226.
5. Seebach, D.; Hungerbühler, E. in Scheffold, R., Ed.; *Modern Synthetic Methods 1980*, Otto Salle Verlag, Frankfurt am Main and Verlag Sauerländer, Aarau, 1980.
6. Nógrádi, M. *Stereoselective Synthesis*; VCH Verlagsgesellschaft: Weinheim, 1986, pp 313–314.
7. Coppola, G. M.; Schuster, V. F. *Asymmetric Synthesis: Construction of Chiral Molecules Using Amino Acids*; John Wiley and Sons: New York, 1987.

8. Kaneko, T.; Izumi, Y.; Chibata, I.; Itoh, T., Eds; *Synthetic Production and Utilization of Amino Acids*; John Wiley and Sons: New York, 1974.
9. Berkoff, C. E.; Rivard, D. E.; Kamholz, K.; Wellman, G. R.; Winicov, H. *CHEMTECH* **1986**, *16*, 552-559.
10. Morrison, J. D., Ed.; *Asymmetric Synthesis*; Academic: Orlando, 1985, Vol. 5.
11. Bosnich, B.; Fryzuk, M. D. in Geoffrey, G. L., Ed.; *Topics in Stereochemistry*; John Wiley and Sons: New York, 1981; Vol. 12, pp 119-154.
12. Knowles, W. S. *Acc. Chem. Res.* **1983**, *16*, 106-112.
13. Knowles, W. S.; Sabacky, M. J.; Vineyard, B. D.; Weinkauff, D. J. *J. Am. Chem. Soc.* **1975**, *97*, 2567-2569.
14. ANIC S.p.A., Eur. Patent 77 099, 1983.
15. Sharpless, K. B., Massachusetts Institute of Technology, personal communication, 1986.
16. Scott, J. W.; Keith, D. D.; Nix, Jr., G.; Parrish, D. R.; Remington, S.; Roth, G. P.; Townsend, J. M.; Valentine, Jr., D.; Yang, R. *J. Org. Chem.* **1981**, *46*, 5086-5093.
17. Takaya, H.; Ohta, T.; Sayo, N.; Kumobayashi, H.; Akutagawa, S.; Inoue, S.; Kasahara, I.; Noyori, R. *J. Am. Chem. Soc.* **1987**, *109*, 1596-1597.
18. Noyori, R.; Ohta, M.; Hsiao, Y.; Kitamura, M.; Ohta, T.; Takaya, H. *J. Am. Chem. Soc.* **1986**, *108*, 7117-7119.
19. Kitamura, M.; Hsiao, Y.; Noyori, R.; Takaya, H. *Tetrahedron Lett.* **1987**, *41*, 4829-4832.
20. Aratani, T. *Pure Appl. Chem.* **1985**, *57*, 1839-1844.
21. Rossiter, B. E. in Morrison, J. D., Ed. *Asymmetric Synthesis*, Vol. 5, Academic Press, Orlando, 1985, pp. 193-246.
22. Rossiter, B. E.; Katsuki, T.; Sharpless, K. B. *J. Am. Chem. Soc.* **1981**, *103*, 464-465.
23. Hill, J. G.; Sharpless, K. B.; Exon, C. M.; Regenye, R. *Org. Syn.* **1984**, *63*, 66-78.
24. Gao, Y.; Hanson, R. M.; Klunder, J. M.; Ko, S. Y.; Masamune, H.; Sharpless, K. B. *J. Am. Chem. Soc.* **1987**, *109*, 5765-5780.
25. Coughenour, G., ARCO Chemical Company, personal communication, 1988.
26. Ladner, W. E.; Whitesides, G. M. *J. Am. Chem. Soc.* **1984**, *106*, 7250-7251.
27. Whitesides, G., Harvard Univ., personal communication, 1987.
28. Akutagawa, S., Takasago Corporation, personal communication, 1986.
29. Tani, K. *Pure Appl. Chem.* **1985**, *57*, 1845-1854.
30. Tani, K.; Yamagata, T.; Akutagawa, S.; Kumobayashi, H.; Taketomi, T.; Takaya, H.; Miyashita, A.; Noyori, R.; Otsuka, S. *J. Am. Chem. Soc.* **1984**, *106*, 5208-5217.
31. Wynberg, H.; Staring, E. G. *J. Am. Chem. Soc.* **1982**, *104*, 166-168.
32. Wynberg, H.; Staring, E. G. *J. Org. Chem.* **1985**, *50*, 1977-1979.
33. Staring, E. G. J.; Mooriga, H.; Wynberg, H. *Recl. Trav. Chim. Pays-Bas* **1986**, *105*, 374-375.
34. New, M., Lonza Ltd., personal communication, 1988.
35. Wynberg, H., University of Groningen, personal communication, 1987.
36. Partridge, J. J.; Chadha, N. K.; Uskokovic, M. R. *Org. Syn.* **1984**, *63*, 44-56.
37. Haubenstock, H. in Allinger, N. L.; Eliel, E. L.; Wilen, S. H., Eds.; *Topics in Stereochemistry*; John Wiley and Sons: New York, 1983; Vol. 14, pp 231-300.
38. Oguni, N.; Omi, T. *Tetrahedron Lett.* **1984**, *25*, 2823-2824.
39. Kitamura, M.; Suga, S.; Kawai, K.; Noyori, R. *J. Am. Chem. Soc.* **1986**, *108*, 6071-6072.

40. Soai, K.; Yokoyama, S.; Ebihara, K.; Hayasaka, T. *J. Chem. Soc., Chem. Commun.* **1987**, 1690-1691.
41. Muchow, G.; Vannoorenberghe, Y.; Buono, G. *Tetrahedron Lett.* **1987**, 28, 6163-6166.
42. Soai, K.; Niwa, S.; Yamada, Y.; Inoue, H. *Tetrahedron Lett.* **1987**, 28, 4841-4842.
43. Corey, E. J.; Hannon, F. J. *Tetrahedron Lett.* **1987**, 28, 5233-5236.
44. Corey, E. J.; Hannon, F. J. *Tetrahedron Lett.* **1987**, 28, 5237-5240.
45. Soai, K.; Ookawa, A.; Kaba, T.; Ogawa, K. *J. Am. Chem. Soc.* **1987**, 109, 7111-7115.
46. Grandbois, E. R.; Howard, S. I.; Morrison, J. D. in Morrison, J. D. Ed.; *Asymmetric Synthesis*; Academic: Orlando, 1983; Vol. 2, pp 71-90.
47. DeCamp, W. H. *Chirality* **1989**, 1, 2-6.

Stereochemistry of the Base-Promoted Michael Addition Reaction

DAVID A. OARE and CLAYTON H. HEATHCOCK

Department of Chemistry, University of California, Berkeley, California

I. Introduction

- A. Driving Force and Retro-Michael Addition
- B. 1,2- vs 1,4-Addition
- C. Terms and Nomenclature
- D. Stereoselective Processes
- E. Structural Assignments

II. Intermolecular Addition of Enolates to Various Michael Acceptors

- A. Catalytic Asymmetric Michael Additions
- B. Keto Ester Enolates
 - 1. To α,β -Unsaturated Ketones
 - 2. To α,β -Unsaturated Diesters
- C. Vinylogous Amides
 - 1. To Dianticipated Acceptors
- D. α -Sulfinyl Ketones
 - 1. To α,β -Unsaturated Ketones
- E. Vinylogous Carbamates
 - 1. To Alkylidenemalonates
 - 2. To Methyl Vinyl Ketone and Acrylate Esters
- F. Addition of Diester Anions
 - 1. To Chiral α,β -Unsaturated Imines
 - 2. To α, β -Unsaturated Sulfoxides
 - 3. To α,β -Unsaturated Esters and Nitriles
 - 4. To α,β -Unsaturated Ketones
 - 5. To Dienones
- G. Ester Amide Enolates
 - 1. To α,β -Unsaturated Ketones and Nitroolefins
- H. α -Sulfinyl Esters
 - 1. To α,β -Unsaturated Esters and α,β -Unsaturated Diesters
- I. Dithioester Enethiolates
 - 1. To α,β -Unsaturated Ketones
- J. Ketone and Aldehyde Enolates
 - 1. To Chiral α,β -Unsaturated Sulfoxides
 - 2. To α,β -Unsaturated Ketones
 - 3. Robinson Annulations
 - 4. To α -Sulfinyl Lactones and α -Thiolactones
 - 5. To Nitroolefins

- K. Ester Enolates
 - 1. To α,β -Unsaturated Sulfoxides
 - 2. To α,β -Unsaturated Esters
 - 3. To α,β -Unsaturated α -Sulfinyl Lactones
 - 4. To α,β -Unsaturated Ketones
 - 5. To α,β -Unsaturated α -Sulfinylcycloalkanones
 - 6. To Nitroolefins
- L. Phenylacetonitrile Anion
 - 1. To α,β -Unsaturated Ketones
- M. Vinylous Carbamates
 - 1. To α,β -Unsaturated Esters
- N. Thioamide Enethiolates
 - 1. To α,β -Unsaturated Ketones
- O. Amide Enolates
 - 1. To Crotonamides
 - 2. To Crotonates
- P. Amide Dienolates
 - 1. To α,β -Unsaturated Esters
 - 2. To α,β -Unsaturated Ketones
 - 3. To Nitroolefins
- Q. Metallated Hydrazones and Imines
 - 1. To α,β -Unsaturated Esters
 - 2. To α,β -Unsaturated Diesters
 - 3. To Nitroolefins
 - 4. To α,β -Unsaturated Ketones
 - 4. To α,β -Unsaturated Esters
- R. Carboxylic Acid Dianions
- S. Dithianyldene Anions
 - 1. To α,β -Unsaturated Ketones
- T. Phosphine Oxide Stabilized Allyl Anions
 - 1. To α,β -Unsaturated Ketones
- U. Allyl Sulfoxide Anions
 - 1. To α,β -Unsaturated Lactones
 - 2. To α,β -Unsaturated Ketones
 - 3. To α,β -Unsaturated Keto Esters
- V. Allylmetallanes
 - 1. To Ethylenemalonates
- W. Stereochemical Trends for Intermolecular Michael Additions
- III. Intramolecular Enolate Michael Additions
 - A. Rules for Ring Closure
 - B. Michael Cyclizations
- IV. Sequential Michael Additions
- V. Discussion of Models
- VI. Conclusions
 - Appendix
 - Acknowledgments
 - References

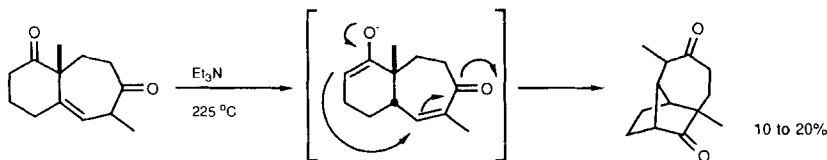
I. INTRODUCTION

The conjugate addition of active methylene compounds to α,β -unsaturated esters and ketones is one of the most widely utilized carbon-carbon bond-forming reactions (1). Although the reaction was first discovered and recognized by Claisen and Komnenos (2), its development was due to Arthur Michael (3, 4).

Beginning in 1887, in a series of papers, Michael described the base-catalyzed coupling of malonates to enones in hydroxylic solvents (5). Today, almost any 1,4-addition of a nucleophile to an activated double bond is referred to as a "Michael addition." In this discussion, we take a somewhat narrower perspective and consider only base-promoted additions of stabilized carbon nucleophiles to activated olefins.

The coupling of carbon acids to α,β -unsaturated esters or ketones under the "traditional" conditions (catalytic amounts of base, protic solvent) is not without limitations (6). Complications caused by regioselectivity of enolate generation, polymerization of the activated olefin, competing 1,2-addition, and instability of the products seriously limit the utility of the process. For this reason, modifications of the Michael addition have been developed wherein stoichiometric amounts of base are used. In these methods, a strong base is generally used to deprotonate the carbon acid irreversibly. The activated olefin is then added, often at low temperatures. Although this method is not completely general, it has greatly extended the scope of the base-promoted Michael addition.

A wide variety of substrates have been employed as donors and acceptors in these procedures. This has led to a multitude of stereoselective versions of the conjugate addition. It is this stereochemical aspect of the Michael addition that is the focus of this review. In particular, we concentrate on the stereoselectivity of the Michael addition in situations where topological considerations do not dictate the stereochemical outcome (as in Scheme 1) (7). Only reactions in which the anionic donor is stabilized by a carbonyl or carbonyl equivalent (imine, hydrazone, olefin, etc.) are considered. This arbitrary distinction excludes some worthy examples (nitroalkanes, dithianes, etc.).



When not discussed explicitly, an effort has been made to provide leading references to closely related processes. Finally, only examples in which the selectivity appears to result from a kinetically controlled process are discussed.

Although some examples are presented, discussion is limited to stereoselective Michael additions where selectivity results from preferential alkylation of one face of an enolate in a ring that contains a stereocenter. The sense of the stereochemical outcome in these cases is often the same as for analogous alkylations with other carbon electrophiles, a topic that has been reviewed recently (8).

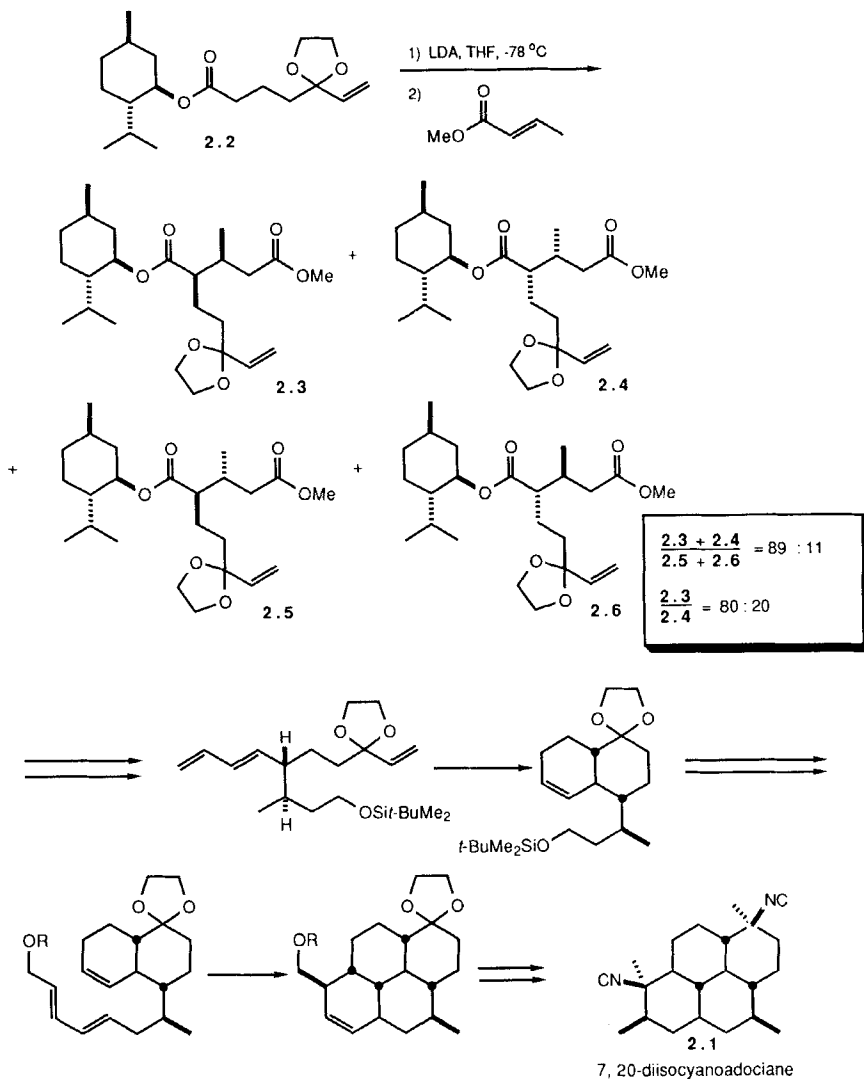
A number of "enolate equivalents" can be induced to undergo conjugate addition through copper catalysis. Notable among these are allyl (9,10) and hydrazone (11) cuprates that, after addition, are readily convertible to carbonyl compounds. In general, the stereochemical behavior of these species is very similar to that observed with simple dialkyl cuprates and will not be discussed.

Although a comprehensive review of the stereochemistry of the Michael addition has not been published, the reader is directed to several reviews that have covered this area, at least in part (12-15). In this review, we have endeavored to discuss the literature of stereoselective Michael additions as completely as possible up to late 1987/early 1988. We apologize in advance to any workers whose contributions we may have inadvertently overlooked in preparing this manuscript.

The Michael addition can be viewed as a vinylogous aldol addition reaction. In contrast to the aldol reaction, however, nature does not appear to make extensive use of the Michael addition in biosynthesis. Hence, the types of products that may be obtained by stereoselective Michael additions are usually not as obviously useful for the synthesis of natural products. Nevertheless, stereoselective carbon-carbon bond formation is an important goal as it expands the number of potential synthetic routes to a given target.

The Michael addition in complex synthesis is nicely illustrated by Corey and Magriotis' synthesis of 7,20-diisocyanoaddociane (**2.I**), illustrated in abbreviated fashion in Scheme 2 (16). One of the key steps of this sequence is the kinetically controlled Michael addition of menthol ester **2.2** to methyl crotonate. With **2.2**, an 89:11 (syn/anti, $(2.3 + 2.4)/(2.5 + 2.6)$) mixture of diastereomer pairs is formed; the major syn diastereomer is formed as a 80:20 (**2.3:2.4**) mixture. Higher selectivity is obtained with the less accessible 8-phenylmenthol analog of ester **2.2**.

If one examines the retrosynthetic strategy employed in this example, one sees that a disconnection was made that requires a stereocenter exocyclic to a six-membered ring. A well-known dictum of retrosynthetic analysis, however,



Scheme 2

is that disconnections that result in appendages carrying stereocenters are to be avoided (17). In this synthesis, then, the stereoselective Michael addition technology has considerably expanded the arsenal of weapons that can be directed at a synthetic problem; a synthetic route that would not previously have been worthy of consideration is now viable.

A. Driving Force and Retro-Michael Addition

In a Michael addition, a carbon–carbon double bond is lost and a carbon–carbon single bond is gained. By using average bond energies one may estimate, all other factors being equal, that this provides about 15–22 kcal/mole of driving force.* If the reaction is carried out under protic conditions with a catalytic amount of base, this is the most important factor. In cases where a preformed enolate is added to an activated olefin, an additional factor must be considered—the relative stabilities of the starting and product enolates. In practice, unless some other rapid pathway intervenes (proton transfer, elimination, etc.) or the reaction is assisted (Lewis acid), the addition of a donor to an acceptor that results in a significant decrease in the stability of the resulting enolate proceeds only with difficulty (18).

Depending on how the reaction is performed, the enolate that results from the conjugate addition can have several fates. For example, if the addition is carried out in the presence of a proton donor, proton transfer can quench the product enolate. If the reaction is performed in the absence of a sufficiently strong electrophile, either external or internal to the substrates, then the formation of a stoichiometric amount of the enolate of the Michael adduct is possible. This latter possibility is often referred to as a “kinetic” Michael addition, although this term is a misnomer.

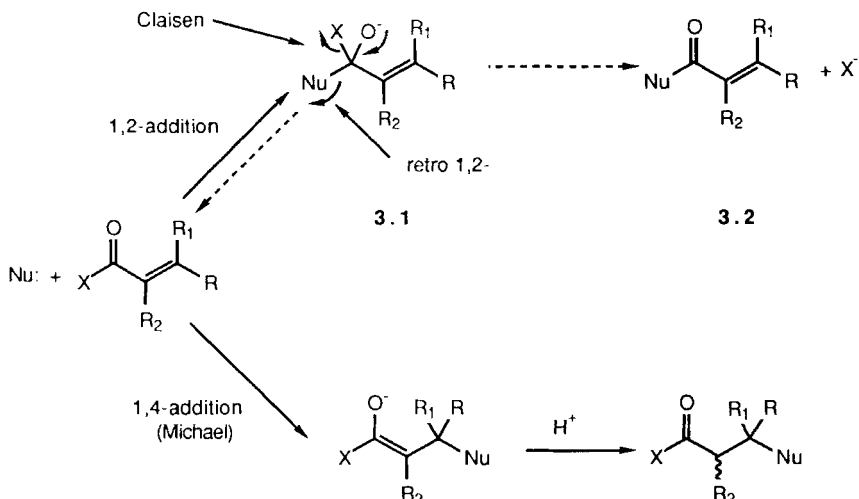
In the presence of excess of the acceptor, poly-Michael addition or polymerization may take place. In particular, polymerization can occur when a very reactive acceptor is used or when the enolate formed in the Michael addition is more reactive than the donor enolate.

Although formally reversible, Michael adducts from donor and acceptor enolates of comparable stabilities or in which a more stable enolate is formed are usually stable to reversal at moderately low temperatures. An important feature is that, under the reaction conditions, 1,2-adducts are often substantially less stable than the 1,4-adducts. This difference in stability can have important consequences (*vide infra*).

B. 1,2- vs 1,4-Addition

In general, Michael acceptors are ambident electrophiles (1,2- and 1,4-addition in Scheme 3). The regiochemistry of nucleophilic addition to activated olefins is an area of both theoretical (19) and experimental (20, 21) interest. Experimentally, it has been determined that a number of factors influence the regiochemical outcome. If a nucleophile adds 1,2, then the fate of

*This is a simplified analysis. Other important factors include the substitution pattern of the acceptor (more substituted olefins are more stable) and potential changes in the σ -bond strengths of the olefin's substituents.



Scheme 3

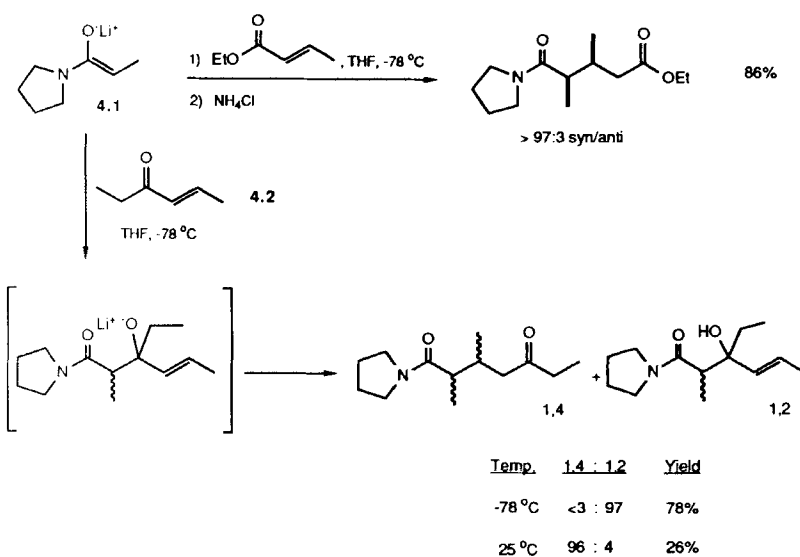
the product depends upon the nature of the carbonyl substituent X . If X^- is a comparable or better leaving group than Nu^- , then intermediate **3.1** can decompose through the Claisen condensation pathway to form **3.2**.

However, if X^- is not a sufficiently good leaving group, the initial 1,2-adducts can reform the starting nucleophile and acceptor. At this point, the nucleophile can once again choose between 1,2- and 1,4-reaction pathways. If the 1,4-adduct is more stable to reversal relative to the 1,2-adduct (a normal condition for most enolates), then the initial 1,2-product is usually siphoned into the conjugate addition manifold.

The regiochemistry of the initial nucleophilic attack is determined by both steric and electronic factors. As would be expected, larger X groups tend to shield the carbonyl carbon and promote 1,4-addition (Scheme 3). On the other hand, if the bulk of R or R_1 is increased, 1,2-addition is more likely.

Electronically, a substituent X on the acceptor capable of donating electron density to the carbonyl carbon favors 1,4-addition. For equally substituted enones (X = alkyl) and enoates (X = alkoxy), nucleophiles are more likely to add 1,4 to enoates. An example of this is shown in Scheme 4. The *N*-propionylpyrrolidine-derived enolate **4.1** adds to ethyl crotonate to give the 1,4-addition product in 86% yield (22). On the other hand, the same amide enolate adds to enone **4.2** to give entirely 1,2-adduct at -78°C and a 96:4 (1,4-/1,2-) mixture of regioisomers after warming to room temperature for several hours (23).

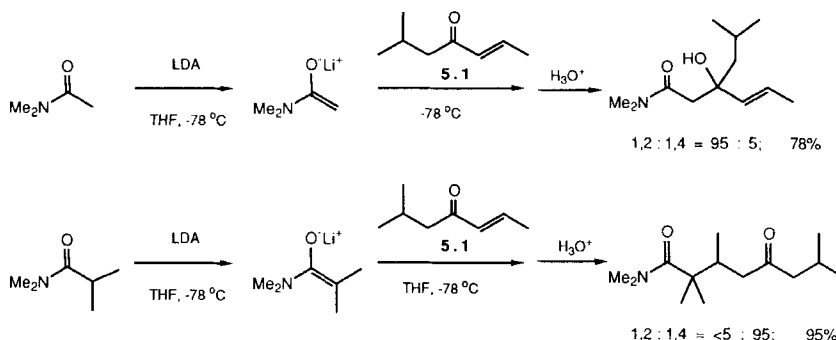
For acceptors in which the carbonyl carbon is more highly substituted than the β -carbon, more bulky nucleophiles have a greater preference for 1,4-addi-



Scheme 4

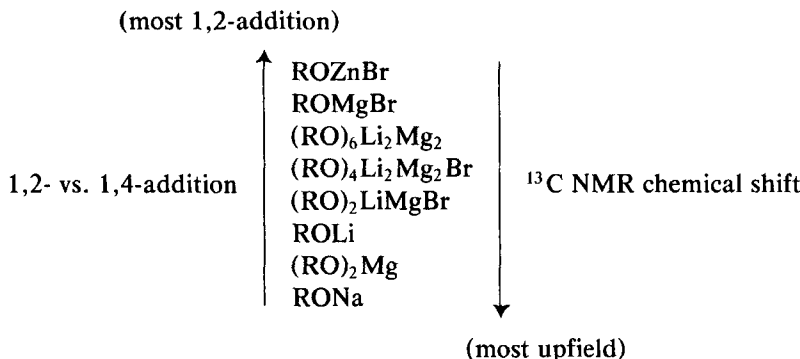
tion. This is illustrated in Scheme 5 for the addition of dimethylacetamide and dimethylisobutyramide enolates to enone **5.1** (24). The dimethylacetamide enolate gives almost entirely 1,2-addition whereas the dimethylisobutyramide enolate gives entirely 1,4-addition.

Other factors that influence the regiochemical outcome are the solvent, the counterion, and the electronic nature of the enolate. The effect of counterion on the regiochemical outcome is illustrated in the low temperature addition of ketone enolates to α,β -unsaturated ketones (25). The regiochemistry of the addition, in this case, correlates with the ^{13}C NMR chemical shift of the reactive carbon of the enolate (26); enolates with more upfield ^{13}C NMR chemical

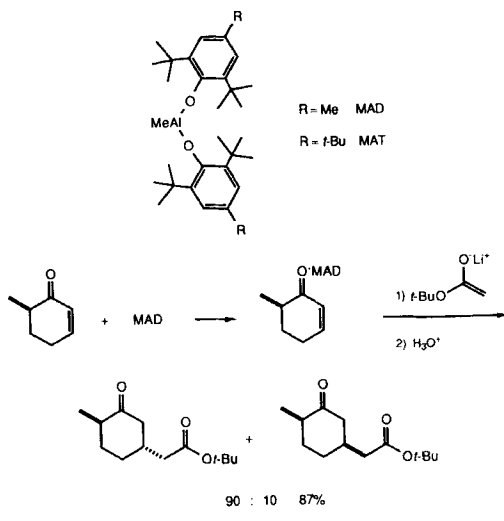


Scheme 5

shifts show a greater proclivity for 1,4-addition. For the addition of the enolate of ethyl *tert*-butyl ketone to chalcone, the following counterion species ($\text{RO} = \text{enolate}$) are ranked in order:



H. Yamamoto and coworkers have developed a scheme that results in the formation of a greater percentage of the 1,4-addition products for the addition of nucleophiles to α,β -unsaturated ketones (27). This strategy involves precomplexation of the α,β -unsaturated ketone with the extremely bulky Lewis acids MAD [methylaluminum bis(2,6-di-*tert*-butyl-4-methylphenoxy)], or MAT [methylaluminum bis(2,4,6-tri-*tert*-butylphenoxide)]. Nucleophiles, including simple alkyllithiums, usually add away from the bulky Lewis acid complex to give 1,4-addition products. Yamamoto and coworkers have reported one example of the addition of a lithium enolate to a MAD-



Scheme 6

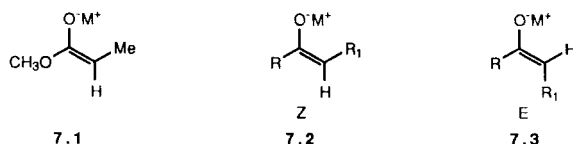
complexed enolate; addition of the lithium enolate of *tert*-butyl acetate to the MAD complex of 5-methyl-2-cyclohexenone gives only 1,4-addition products. The trans and cis isomers were formed in a 90:10 ratio (Scheme 6).

C. Terms and Nomenclature

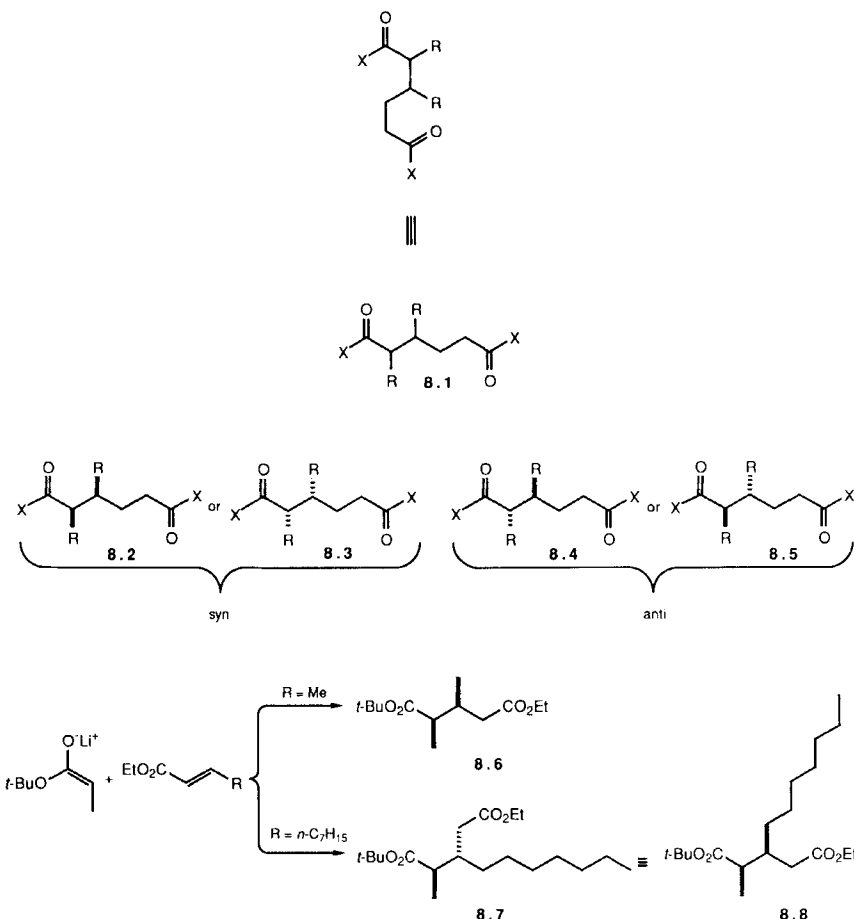
An important factor influencing the stereochemical course of many reactions of acyclic carbonyl compounds is the geometry of the enolate used. Indeed, enolate geometry plays a crucial role in determining the outcome of the Michael addition. The nomenclature system used for enolates is based on the *E/Z* format developed for olefins (28). However, direct application of this system can create confusion. For example enolate 7.1 (Scheme 7) would be termed an *E* enolate when M = Li (OC > OLi in the Cahn-Ingold-Prelog system) while, if M = ZnBr, 7.1 would be called a *Z* enolate (OC < OZn). Despite the change in descriptor, the geometry of these enolates is analogous from the chemical point of view. Hence, a modification where the “OM” is always assigned a higher priority than R (in 7.1) is used (8, 29). Thus, 7.2 is a *Z* enolate while 7.3 is an *E* enolate.

Concerning the relative configuration of stereocenters, the nomenclature used in this review will usually be the syn/anti convention currently used for acyclic aldols and related compounds (29–31). To apply this convention, the carbon backbone is drawn in its longest extended (zig-zag) form such as for 8.1 (Scheme 8). If both of the substituents on the chain project either out of or into the plane of the carbon backbone as in 8.2 or 8.3, then the descriptor is syn. If, instead, one of the substituents extends into the plane of the carbon backbone and the other substituent protrudes out of the plane as in 8.4 or 8.5 the descriptor is anti.

Care must be exercised in using the syn/anti system. For example, 8.6 is called syn, whereas 8.7 would be called anti if the carbon framework were extended in a zig-zag manner along the longest chain. However, both 8.6 and 8.7 are the major stereoisomers obtained from the addition of the *E* lithium enolate derived from *tert*-butyl propionate to the corresponding α,β -unsaturated esters (32). Discussion of the stereochemical outcome in these chemically related cases is obviously complicated by the trivial “switch” in configu-



Scheme 7



Scheme 8

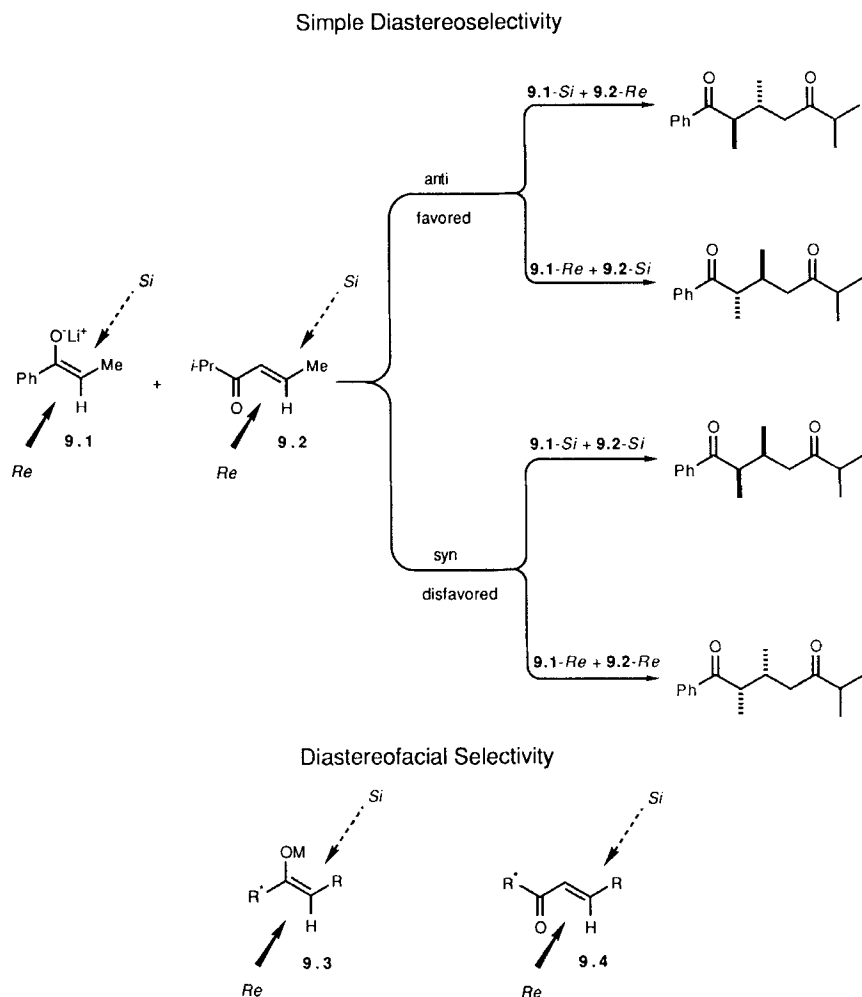
rational assignment caused by uncertainty as to what constitutes the “carbon backbone.” For the purposes of this chapter, the “longest extended form” will be defined as the chain that includes both the anion stabilizing groups of the donor and the acceptor (the carboalkoxy substituents in **8.6** and **8.7**). Using this modification, **8.7** is assigned the syn configuration as depicted in **8.8**, which is the same as for **8.6**.

D. Stereoselective Processes

In any bond-forming reaction, stereochemical differentiation can occur through two fundamental processes. Consider first the bond formation be-

tween two prostereogenic components (33). Stereochemical discrimination can arise if there is an energetic difference in the reactions combining two like faces (*Si, Si* or *Re, Re*) or two unlike faces (*Si, Re* or *Re, Si*). This stereoselective manifold is illustrated in Scheme 9 for the addition of enolate 9.1 to enone 9.2. In this case, the combination of unlike faces (*Se, Re* or *Re, Si*) is favored over combination of like faces (*Si, Si*, or *Re, Re*). This type of stereoselectivity is termed simple diastereoselectivity.

The second fundamental stereoselective process occurs when there is an energetic difference in addition to the two faces of either the donor or accep-



Scheme 9

tor. For example, if addition to either the *Re* or *Si* face of **9.3** is favored as a result of the directing influence of a stereogenic substituent R^* , then what is termed "diastereofacial" selectivity results. Similar considerations apply to addition to the two faces of acceptor **9.4**. Of course, more complicated situations ensue where more than one mode of selectivity is operative. In these instances, combinations of these factors control the stereochemical outcome.

In any bimolecular reaction, four different types of components can be combined in 16 different ways. The four general types of substrates are either (Scheme 10):

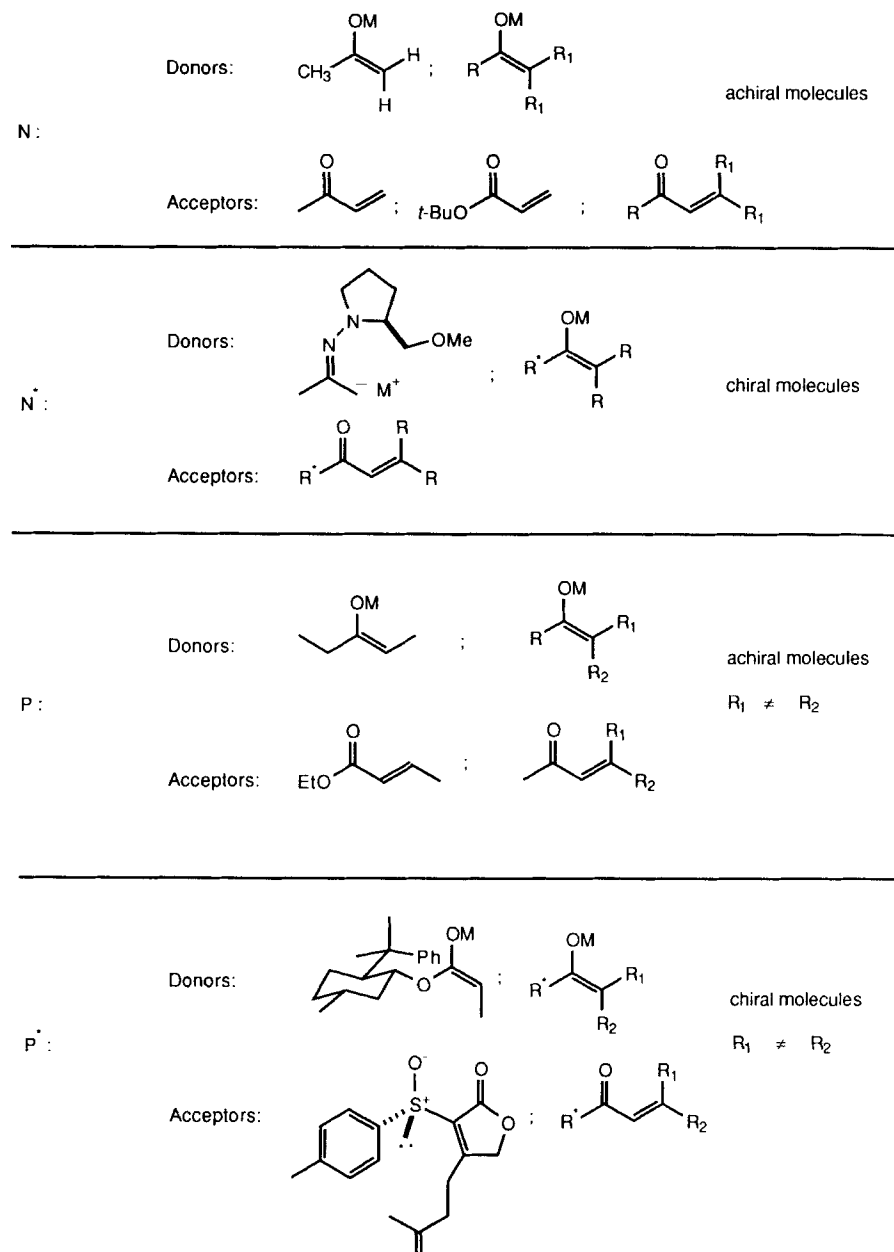
1. An achiral donor or acceptor where reaction occurs at a center that is not prostereogenic (**N**);
2. A chiral donor or acceptor where reaction occurs at a center that is not prostereogenic (**N***);
3. An achiral donor or acceptor where reaction occurs at a center that is prostereogenic (**P**); or
4. A chiral donor or acceptor where reaction occurs at a center that is pro-stereogenic (**P***).

(The designation "chiral" also applies to an achiral donor or acceptor in a chiral, non-racemic medium).

The 16 different combinations of these four components are illustrated in the matrices in Scheme 11. The combinations **N,N** and **N,N*** (or **N*,N**) result in the formation of no new stereocenters and hence diastereoselectivity is not possible. Forming a bond between a prostereogenic center of one component and an achiral component with no prostereogenic center (**N,P** or **P,N**) results in the formation of a new stereocenter with no possibility for stereoselectivity. Creation of a bond between two prostereogenic centers of achiral components (**P,P**) results in the formation of two stereocenters with the possibility of simple diastereoselectivity. Joining **P** and **N*** components (**P,N*** or **N*,P**) results in the formation of a new stereocenter. The factors influencing the stereochemical outcome of this arrangement are the facial preference of the **N*** component along with the relative orientation of the two components in the transition state ("pseudo-simple diastereoselectivity").*

When a bond is formed between the prostereogenic center of a chiral component and an achiral reactant without a prostereogenic center (**P*,N** or **N,P***; Scheme 11), the stereocenter of **P*** influences the relative rates of attack on the diastereotopic faces of the prostereogenic center. Similar considerations apply for bond formation between the prostereogenic center of a chiral reactant and the prostereogenic center of an achiral reactant (**P,P*** or **P*,P**). In this case, the stereocenter of the **P*** component influences the facial

*"Pseudo-simple diastereoselectivity", a term not used heretofore, is explained in detail in the Appendix (p. 391).



Scheme 10

		Acceptor				
		N	P	N*	P*	
Combinations of Components	Donor	N	N,N	N,P	N,N*	N,P*
		P	P,N	P,P	P,N*	P,P*
		N*	N*,N	N*,P	N*,N*	N*,P*
		P*	P*,N	P*,P	P*,N*	P*,P*

		Acceptor				
		N	P	N*	P*	
Factors Influencing the Stereochemical Outcome	Donor	N	O	O	O	F ^a
		P	O	S	F ^a	F ^a ,S
		N*	O	F ^d ,S	O,F ^d ,F ^a ,S	F ^d ,F ^a ,S
		P*	F ^d	F ^d ,S	F ^d ,F ^a ,S	F ^d ,F ^a ,S

O = no possibility of stereoselection
S = simple or "pseudo-simple" diastereoselectivity
F^d = diastereofacial selectivity with respect to donor
F^a = diastereofacial selectivity with respect to acceptor

Scheme 11

preference of addition to its prostereogenic center while simple diastereoselectivity controls the relative orientation observed for the combination of the two prostereogenic centers.

The remaining examples of bond formation between components P* and N*, N* and P*, or P* and P* (Scheme 11) are more complicated examples of the foregoing situations. In these instances, the diastereofacial preference of both the donor and the acceptor determines the stereochemical outcome. In the P*, P* case, the situation is further complicated by the possibility of simple diastereoselectivity.

A further consideration occurs when two chiral components are allowed to react (for example, N*,N*; N*,P*; P*,N*; or P*,P*; Scheme 11). If both reactants are racemic, the possibility exists for mutual kinetic enantioselection (*vide infra*) (31, 34). When only one reactant is racemic, preferential consumption of one enantiomer of the racemic reactant (kinetic resolution) can occur. With enantiomerically pure components, double asymmetric syn-

thesis (or double stereodifferentiation) occurs (34-37). Depending on the chirality of the components used, the facial preferences can either be reinforcing or counteracting. All of the factors described above (simple selectivity and the facial preference of both components) influence selectivity in these cases. Although beyond the scope of this discussion, this is true even if no new stereocenter is formed (N^*, N^*).

E. Structural Assignments

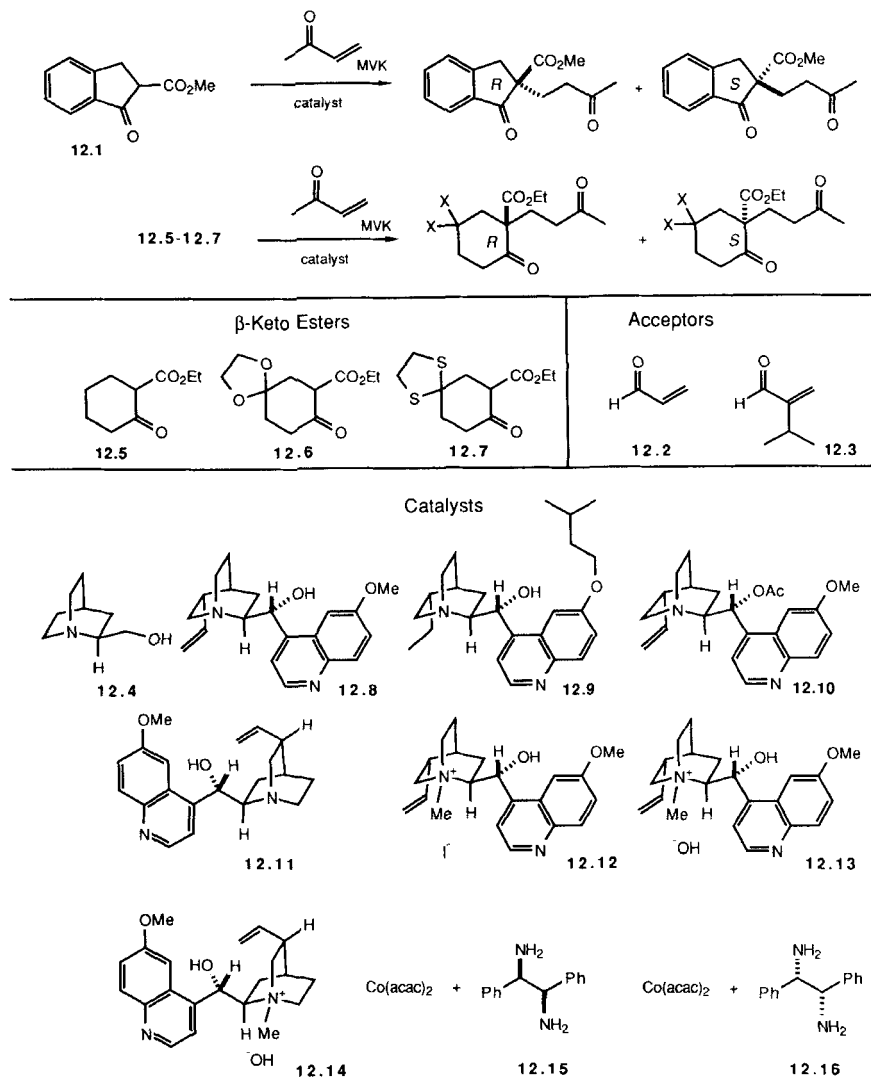
One of the difficulties associated with studying the stereoselectivity of the Michael addition has been determination of the configurations of the products. The wide variety of substrates employed along with the lack of structural rigidity in the products has prevented the development of an all-encompassing NMR correlation. To date, structural assignment has relied heavily on single crystal X-ray structure determination, chemical interconversion, conversion to known compounds, and conversion to compounds for which the structure can be assigned on the basis of NMR.

II. INTERMOLECULAR ADDITION OF ENOLATES TO VARIOUS MICHAEL ACCEPTORS

A. Catalytic Asymmetric Michael Additions

[P^*, N] The classic conditions for performing Michael additions involve the use of a catalytic amount of base in a protic solvent (6). The catalytic role of the base opens the possibility that, by using a chiral, non-racemic base or a base in a chiral, non-racemic environment, the reaction can be catalytic *and* enantioselective. This possibility was first realized by Langstrom and Bergson (38). These workers found that the addition of indanone **12.1** to unsaturated aldehydes **12.2** and **12.3** catalyzed by quinuclidine **12.4** gives products with a non-zero optical rotation (Scheme 12). Although neither the sense or degree of the asymmetric induction was reported, these observations have proved to be the starting point for later investigations that have shown surprising levels of enantioselection. It is interesting to note the homology between **12.4** and the chiral, non-racemic bases used in the more successful efforts (*vide infra*) (39).

Wynberg and coworkers have explored the *cinchona* alkaloid-promoted Michael addition of **12.1** and **12.5-12.7** to methyl vinyl ketone (Scheme 12, Table 1) (40, 41). The catalysts used in the reaction are **12.8-12.14**. Approximately 1 mol% base was employed. The best selectivities were found with indanone **12.1**; under optimal conditions, enantiomeric excesses as high as



Scheme 12

76% were found using free base 12.8 (entry 8, Table 1). The optimal alkaloid for inducing asymmetry depends on the β -keto ester used. For the less acidic 12.5-12.7, methohydroxide 12.13 is necessary to induce conjugate addition. With this base, products with only low levels of asymmetry are produced (entries 5-7 and 11, Table 1).

Table 1
Addition of β -Keto Esters **12.1** and **12.5–12.7** to Methyl Vinyl Ketone Catalyzed by
Optically Active Amines **12.8–12.16** (Scheme 12)

Entry ^a	β -Keto Ester	Catalyst	Solvent	Yield %	Temp. °C	Product Configuration	ee %
1	12.5	12.13	dioxane-2% EtOH	99	25	R	5
2	12.5	12.13	CH ₂ Cl ₂ -2% EtOH	89	25	R	8
3	12.5	12.13	benzene-2% EtOH	99	25	R	10
4	12.5	12.13	toluene-2% EtOH	90	25	R	10
5	12.5	12.13	CCl ₄ -2% EtOH	96	-20	R	22
6	12.6	12.13	CCl ₄ -2% EtOH	100	-21	S	25
7	12.7	12.13	CCl ₄ -2% EtOH	99	-20	S	21
8	<u>12.1</u>	<u>12.8</u>	CCl ₄	99	-21	S	76
9	12.1	12.8	CCl ₄ -2% EtOH	97	25	S	33
10	<u>12.1</u>	<u>12.11</u>	CCl ₄	100	-21	R	69
11	12.1	12.9	CCl ₄	99	25	S	60
11	12.1	12.13	toluene-1% EtOH	100	25	S	15
12	12.1	12.12	toluene	100	25	S	12
13	12.1	12.10	CCl ₄ -2% EtOH	53	25	R	19
14	12.1	12.16	toluene	72	20	R	21
15	12.1	12.16	toluene	83	0	R	28
16	12.1	12.16	toluene	78	-10	R	35
17	12.1	12.16	toluene	74	-20	R	39
18	12.1	12.16	toluene	78	-30	R	49
19	12.1	12.16	toluene	74	-40	R	57
20	12.1	<u>12.16</u>	toluene	50	-50	R	66
21	12.1	12.15	toluene	74	-40	S	58

a. The optimal conditions are underlined in the table.

The enantiomers of the naturally occurring *cinchona* alkaloids are not readily available. However, the diastereomeric alkaloid **12.11** provides access to Michael adducts of opposite configuration to those obtained with **12.8**. The enantioselectivities obtained with **12.11** approach those obtained with **12.8** (entry 10, Table 1).

For achieving the highest levels of asymmetry, optimization of the reaction conditions was crucial. In particular, the presence of ethanol in the reaction mixture results in diminished selectivity. For example, when the solvent is changed from CCl₄ to CCl₄/2% EtOH, the selectivity of the addition drops markedly (entries 8 and 9, Table 1). Lower temperatures, as expected, lead to higher levels of asymmetric induction.

The key role of the alkaloid hydroxy group is seen on comparing the selectivity obtained with **12.8** and **12.10** (entries 9 and 13, Table 1); a decrease in selectivity is found when the ester **12.10** is used. Furthermore, complete removal of the hydroxy from **12.8** leads to products with essentially no enantiomer excess (42).

A disadvantage of using alkaloids to catalyze the asymmetric additions is the necessity of removal of the alkaloid from the products. Three research

groups have reported attempts to eliminate this problem by attaching the alkaloid to a polymer. In the first attempt, Hermann and Wynberg attached the alkaloid to the polymer either through the hydroxy group or through a phenyl ether (43). Although the polymers efficiently catalyzed the reaction, the enantioselectivities obtained were low ($\leq 11\%$ ee with **12.1** and methyl vinyl ketone), consistent with the diminished enantioselectivity seen with **12.10**.

Hodge and coworkers have attached the alkaloid to the polymer through a quaternary ammonium salt linkage to the tertiary amine (44). The counterions examined included hydroxide, bicarbonate, fluoride, and chloride. Of these counterions, fluoride gives the best selectivity; a maximum asymmetric induction of 27% ee is obtained using **12.1** and methyl vinyl ketone.

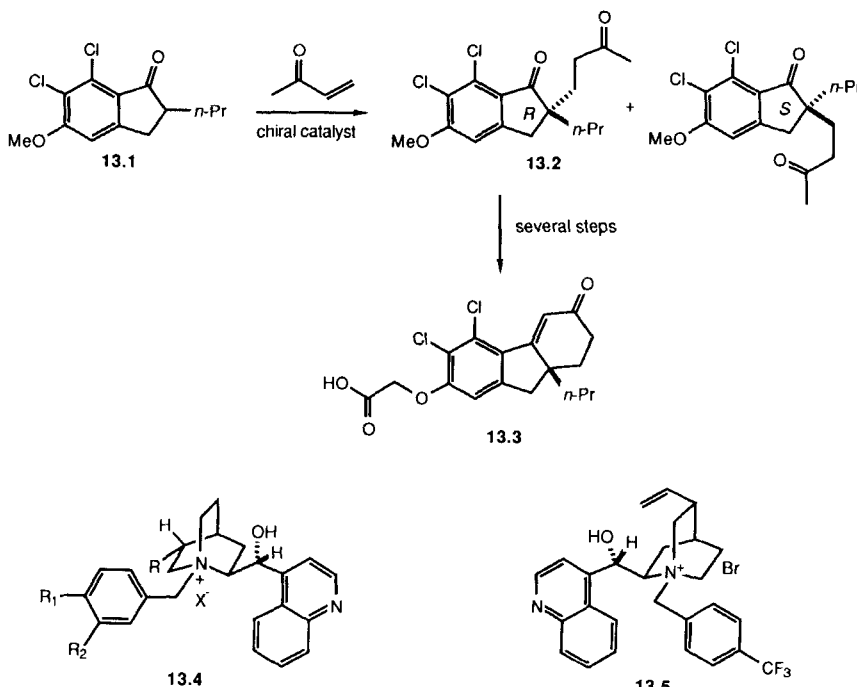
Better success was achieved by Kobayashi and Iwai with a catalyst obtained by copolymerization of the vinyl group of the *cinchona* alkaloids with acrylonitrile (45, 46). Although asymmetric induction was noted with other substrates, enantiomeric excesses were determined only for **12.1** and methyl vinyl ketone; ee's up to 51% were obtained.

As can be seen from the foregoing discussion, selectivity drops with the polymer-bound catalysts. Kobayashi and Iwai have performed further experiments in this area by using catalysts in which the vinyl group of *cinchona* alkaloids was modified (47). Addition of a variety of thiols to the vinyl appendage and subsequent oxidation leads to sulfoxides that, as catalysts, give asymmetric inductions similar to those seen with the polymer-bound alkaloids. Variation of the structure of the thiol resulted in no significant change in the stereochemical outcome of the catalytic process.

An interesting approach to a catalytic, asymmetric Michael addition was reported by Brunner and Hammer (48). The base for this process was obtained from either enantiomer of 1,2-diphenyl-1,2-ethanediamine and Co(acac)₂ (**12.15** and **12.16**, Scheme 12, Table 1). The ratio of indanone **12.1** to the catalyst employed was approximately 20:1. Ethyl 2-methylacetooacetate and indanone **12.1** were used with methyl vinyl ketone for the study. Again, indanone **12.1** is the best Michael donor, as it provides superior selectivities compared to ethyl 2-methylacetooacetate (21–66% ee versus 2–5% ee). Low temperatures were essential for achieving the best selectivities. On decreasing the temperature from 20°C to –50°C, the enantiomeric excess increases from 21 to 66%. At temperatures lower than –50°C, the substrates react torpidly. Control experiments revealed that Co(acac)₂ by itself efficiently promotes the reaction and that the diamine alone only slowly catalyzes the reaction with low asymmetric induction. These factors implicate an asymmetric cobalt species as the active catalyst for the reaction.

All of the foregoing examples were performed with di-stabilized anions. Conn and coworkers at Merck have examined the catalytic, asymmetric Michael addition of **13.1**, which forms a monostabilized anion, to methyl vinyl

ketone (Scheme 13) (49). The initial product (**13.2**) was converted to drug candidate **13.3**. The results of this study are summarized in Table 2 (50). With **13.5**, the *S* enantiomer of **13.2** is obtained in 80% ee. The opposite enantiomer of the product results from the use of the diastereomeric base **13.4**. By optimizing the substituents on the alkaloid, asymmetric induction of no more than 52% ee was obtainable, illustrating the subtle nature of the catalyst involved.

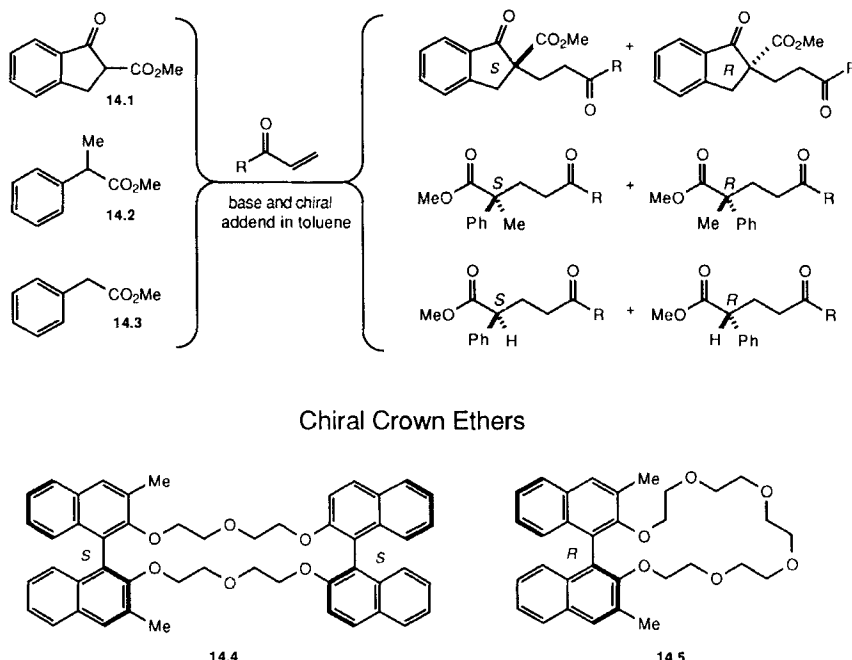


Scheme 13

Table 2
Catalytic Asymmetric Michael Additions of **13.1** to Methyl Vinyl Ketone
(Scheme 13)

Entry	R	Catalyst			Config.	ee %
		R ₁	R ₂	X ⁻		
1	13.5	---	---	---	<i>S</i>	80
2	13.4	CH ₂ =CH	Cl	Cl	<i>R</i>	20
3	13.4	Et	Cl	Cl	<i>R</i>	40
4	13.4	CH ₂ =CH	CF ₃	H	<i>R</i>	40
5	13.4	Et	CF ₃	H	<i>R</i>	52
6	13.4	CH ₂ =CH	CF ₃	H	<i>R</i>	38

Cram and Sogah found that small amounts of base in the presence of chiral, non-racemic crown ethers catalyze asymmetric Michael additions of the active methylene compounds **14.1–14.3** to methyl vinyl ketone and methyl acrylate (Scheme 14, Table 3) (51). The enantiomeric excesses of the products obtained are impressive. One combination (using crown ether **14.4**, keto ester **14.1**, and methyl vinyl ketone) results in essentially complete enantiomeric homogeneity of the product (entry 1). Surprising levels of asymmetric induc-



Scheme 14

Table 3
Catalytic Asymmetric Michael Addition of β -Keto Esters to Methyl Vinyl Ketone (MVK) and Methyl Acrylate (MA) (Scheme 14)

Entry	Chiral Ether	Base	Temp. °C	Enolate	Acceptor	CTN ^a	Yield %	Config.	ee %
1	14.4	<i>t</i> -BuOK	-78	14.1	MVK	10	48	<i>R</i>	99
2	14.4	<i>t</i> -BuOK	25	14.1	MVK	15	75	<i>R</i>	67
3	14.5	H ₂ NK	-78	14.2	MA	7	80	<i>S</i>	83
4	14.4	<i>t</i> -BuOK	-78	14.3	MA	19	80	<i>S</i>	65
5	14.5	H ₂ NK	-78	14.3	MA	9	96	<i>S</i>	63

a. Catalyst turnover Number = (mmol product)/(mmol catalyst complex).

tion were found with the phenylacetic acid derivative **14.3**. The products formed with **14.3** have an epimerizable proton with acidity comparable to that of the methylene protons of the starting material, yet products of significant enantiomeric purity were formed (entries 4 and 5, Table 3). The asymmetric induction realized is strongly dependent upon the reaction temperature, with lower temperatures providing higher selectivity (compare entries 1 and 2, Table 3). In contrast, the choice of base plays only a minor role in determining enantioselectivity. This method should be applicable for the synthesis of either enantiomer of the products as both enantiomers of the catalyst should be available.

When using a valuable catalyst such as **14.4** or **14.5**, an important consideration is catalyst efficiency. The catalyst turnover number (CTN) determines how little catalyst is needed to promote the reaction to completion. In the Cram-Sogah systems, catalyst turnovers as high as 55 were observed, although the highest enantioselectivity occurred with 10 catalyst turnovers. Because of its high molecular weight, a significant mass quantity of the catalyst must be used even with a CTN of 55.

Penades and coworkers (52) have extended the Cram-Sogah approach to crown ethers **15.1-15.4**, derived from carbohydrates. As in the earlier work, these crown ethers were used in the presence of potassium bases. The results of the addition of **15.5-15.7** to methyl acrylate in the presence of these hosts are shown in Table 4 and Scheme 15. With about 5% of crown ether **15.4** and the potassium base, no asymmetric induction was found with **15.6**. Using

Table 4
Catalytic Asymmetric Michael Addition in the Presence of **15.1-15.4** (Scheme 15)

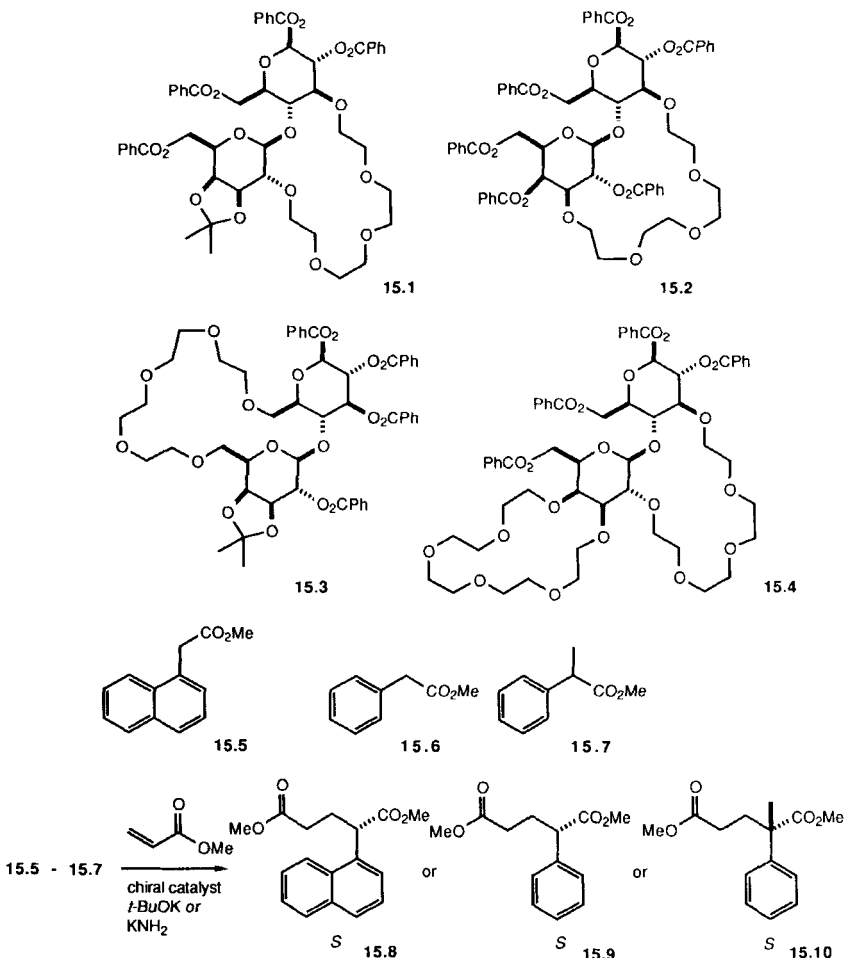
Entry	Enolate	Catalyst	Base ^a	Yield ^b %	ee %
1	15.5	15.1	t-BuOK	58	21
2	15.5	15.2	t-BuOK	45	63
3	15.5	15.3	t-BuOK	84	37
4	15.6	15.1	t-BuOK	67	26
5	15.6	15.2	t-BuOK	73	70
6	15.6	15.3	t-BuOK	98	36
7	15.7	15.1	H ₂ NK	22 ^c	32
8	15.7	15.2	H ₂ NK	65 ^d	16
9	15.7	15.3	H ₂ NK	49 ^c	47

a. Unless noted, reactions were performed at -78 °C.

b. Based on amount of starting material consumed.

c. Reaction performed at -50 °C.

d. Reaction performed at 0 °C.



Scheme 15

similar proportions, the remaining crown ethers resulted in preferential formation of the *S* enantiomer. For substrates **15.5** and **15.6**, the highest enantioselectivities were found with ether **15.2**. With substrate **15.7**, the highest selectivities were found using **15.3** as the complexant.

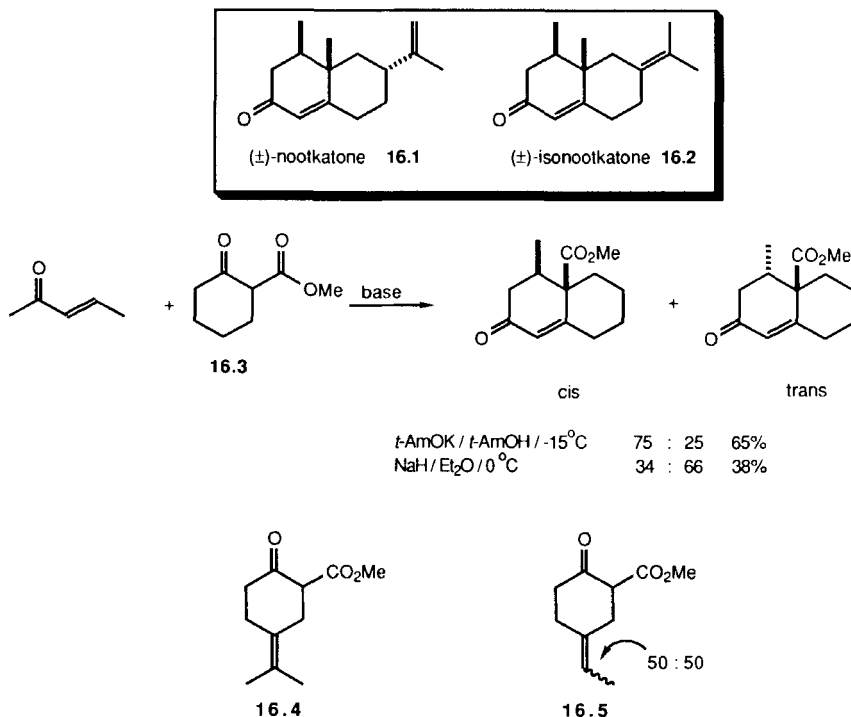
Raguse and Ridley have investigated the addition of indanones to MVK using acyclic, chiral, non-racemic sulfoxide complexants in the presence of potassium *tert*-butoxide (53). Although asymmetric induction was achieved, the enantiomeric excesses obtained are quite low ($\leq 7\%$).

B. Keto Ester Enolates

1. To α,β -Unsaturated Ketones

[P,P] For the synthesis of the sesquiterpenes (\pm)-nootkatone (**16.1**) and (\pm)-isonootkatone (**16.2**), Marshall and coworkers have examined the conjugate addition/cyclization of cyclic β -keto ester **16.3** to *trans*-3-penten-2-one (54, 55). A variety of conditions were examined, including a number of base/solvent combinations (*t*-AmOK/*t*-AmOH, *t*-BuOK/*t*-BuOH, *t*-BuOLi/*t*-BuOH, MeOK/MeOH, MeONa/MeOH, MeONa/DMSO, MeONa/THF, NaH/THF, NaH/Et₂O, and LiH/Et₂O), different ratios of base to keto ester, and a variety of temperatures. The optimal conditions for obtaining either the cis or the trans isomers are shown in Scheme 16.

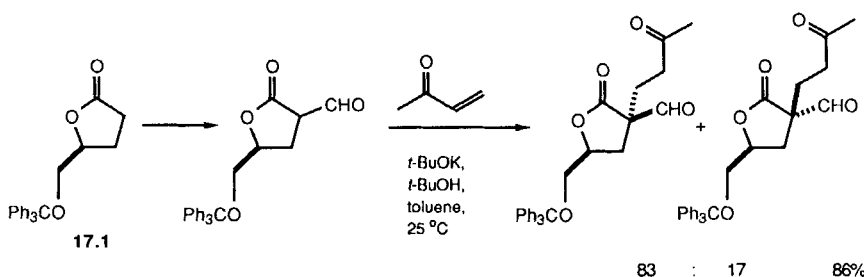
As can be seen in Scheme 16, variation of the reaction conditions results in preferential formation of either the cis or the trans isomers. However, the stereoselectivities attained are low, representing minimal differences in ener-



Scheme 16

gies between the diasteromeric transition states. Application of this technology to the synthesis of **16.1** and **16.2** involved use of the base-catalyzed addition of keto esters **16.4** and **16.5** to *trans*-3-penten-2-one. While the exact isomer ratio for the addition of **16.4** was not reported, a 75:25 (cis/trans) mixture was formed with **16.5** using conditions similar to those described above. The major isomers from **16.4** and **16.5** were converted to **16.2** and **16.1**, respectively.

[P*,N] Koga and coworkers have shown that preferential addition of methyl vinyl ketone occurs on the *Si* face of the formyl derivative of lactone **17.1** (Scheme 17) (56); a 83:17 mixture of isomers was formed in good yield.



Scheme 17

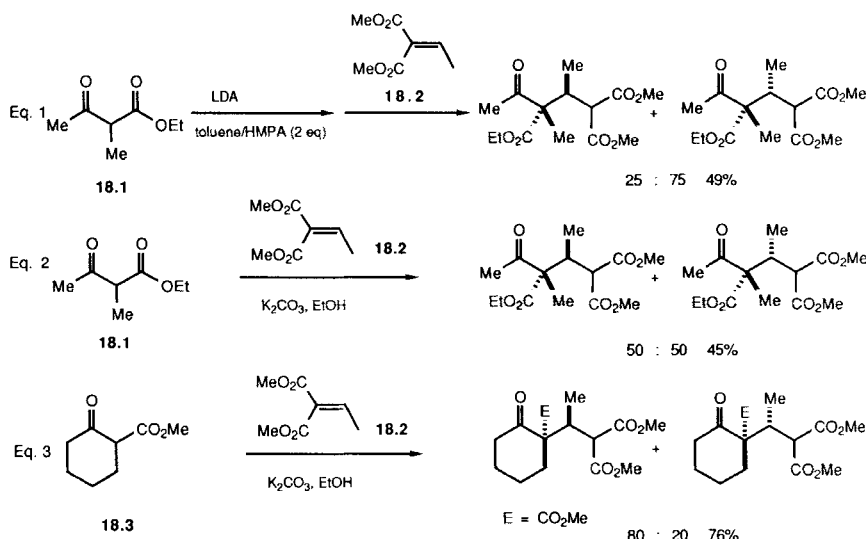
2. To α,β -Unsaturated Diesters

[P,P] In connection with an investigation of the stereochemistry of the addition of vinylogous amides (*vide infra*), Koga and coworkers have also studied the addition of β -keto esters **18.1** and **18.3** to the diactivated diester **18.2** (Scheme 18) (57). Only low levels of stereoselectivity were unobserved, in keeping with Marshall's observations (*vide supra*). A modest base/solvent effect was also noted (compare Eq. 1 with Eq. 2).

C. Vinylogous amides

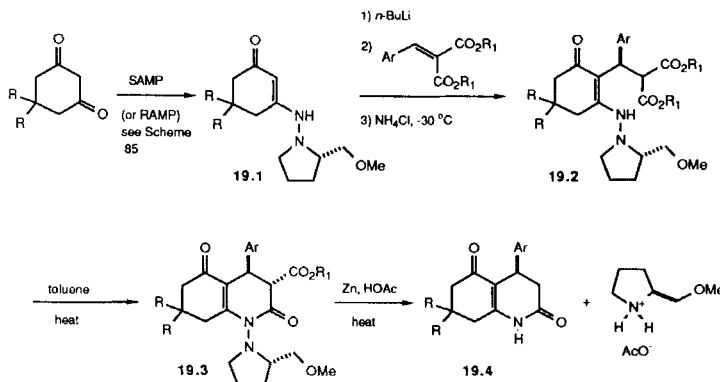
1. To Diactivated Acceptors

[P*,P] Enders and coworkers found that conjugate addition of metallated vinylogous amides **19.1** to diactivated acceptors leads to adducts with very high enantiomeric excess (Scheme 19, Table 5) (58). The high stereoselectivity of this process parallels the results found with non-stabilized hydrazones (*vide infra*). The vinylogous amides were prepared from symmetrical cyclic β -



Scheme 18

diketones and the SAMP and RAMP hydrazines. The initial adducts (**19.2**) were usually not isolated, but instead cyclized to **19.3**. Reduction and decarboxylation of **19.3** leads to tetrahydroquinolinediones **19.4** in moderate overall yields.



Scheme 19

Table 5
Addition of Vinyllogous Hydrazone Amides to α,β -Unsaturated Diesters
(Scheme 19)

Entry	Vinyllogous Amide R	Ar	Yield %	ee ^a %
1	SAMP	Me	Ph	50 >98
2	RAMP	Me	Ph	51 >98
3	SAMP	H	Ph	50 >98
4	SAMP	Me	<i>p</i> -MeO-C ₆ H ₄	52 >98
5	SAMP	H	2,4-Cl ₂ -C ₆ H ₃ ^b	54 >98
6	SAMP	Me	<i>m</i> -NH ₂ -C ₆ H ₄ ^b	57 >98

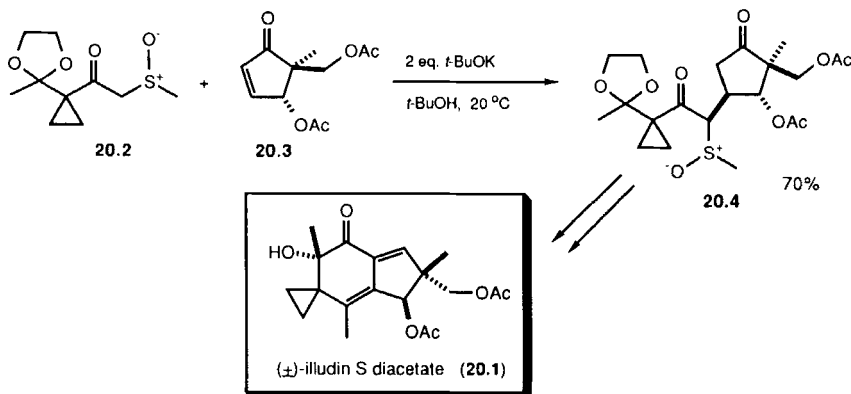
a. The products have the *R* configuration except for entry 2 which has the *S* configuration.

b. The *meta* amino group results from reduction (Zn/HOAc) of a *meta* nitro group.

D. α -Sulfinyl Ketones

1. To α,β -Unsaturated Ketones

[P*,P*] Matsumoto and coworkers, in connection with the synthesis of (\pm)-illudin S diacetate (20.1), have examined the conjugate addition of keto-sulfoxide 20.2 to cyclopentanone 20.3 (Scheme 20) (59). The Michael addition provided 20.4 as a “single adduct.” The trans relationship between the entering nucleophile and the adjacent acetoxy group in 20.4 was established by ¹H NMR spectroscopy. No information was provided about the configura-



Scheme 20

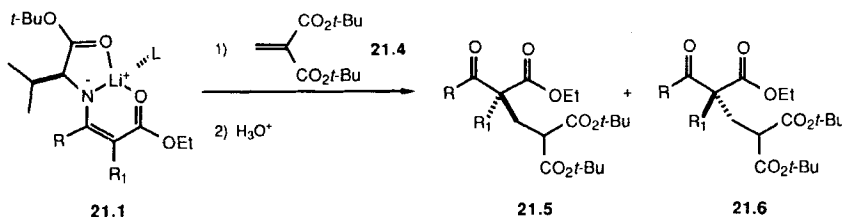
tion of the two side chain stereocenters in **20.4** (α to the carbonyl and at sulfur). However, if **20.4** is truly only one stereoisomer, this reaction must proceed with very high mutual kinetic enantioselection.

E. Vinylogous Carbamates

1. To Alkylidenedemalonates

[P*,N] Koga's research group has reported the addition of valine-derived *N*-monosubstituted vinylogous carbamates of the general structure **21.1** to a variety of acceptors (Scheme 21). Initially, the conjugate addition of **21.2** and **21.3** to di-*tert*-butyl methylenemalonate (**21.4**) was examined (Table 6) (60). As can be seen in Table 6, there is a remarkable solvent effect. For example, in entry 4, using vinylogous carbamate **21.2** in toluene with 4 equivalents of HMPA at -78°C results in the formation of **21.5** and **21.6** in an 86:14 ratio. If, instead, the reaction is performed in THF at -78°C , a 10:90 mixture of enantiomers (**21.5**:**21.6**) is produced. Under optimized conditions, enantioselective excesses between 84–95% were observed (entries 5 and 10 for **21.2**; entries 11 and 13 for **21.3**).

Koga's results have been rationalized by postulating a chelate structure similar to **21.1** as the reactive form of the metallated vinylogous carbamate (Scheme 21). It was suggested that when L is HMPA, the tightly-bound ligand (HMPA) forces the incoming electrophile to approach from the opposite face giving **21.5** as the preferred product. In the presence of THF, the ligand L (THF) is displaced by the incoming electrophile and the reaction proceeds from the face opposite the isopropyl group to yield **21.6**. No attempt was made to explain the lower selectivity when the reaction is performed in tolu-



Cmpd.	R	R_1
21.2	$-\text{CH}_2\text{CH}_2\text{CH}_2\text{CH}_2-$	
21.3	Me	Me

Scheme 21

Table 6
Addition of Valine-Derived Vinylogous Carbamates to 21.4 (Scheme 21)

Entry	Vinylogous Carbamate ^a	R	R ₁	Solvent	Temp °C	Yield %	21.5:21.6	ee %
1	21.2	-CH ₂ CH ₂ CH ₂ CH ₂ -		toluene	-78	59	33:67	33
2	21.2	-CH ₂ CH ₂ CH ₂ CH ₂ -		toluene-HMPA(1 eq)	-78	80	79:21	58
3	21.2	-CH ₂ CH ₂ CH ₂ CH ₂ -		toluene-HMPA(2 eq)	-78	77	84:16	68
4	21.2	-CH ₂ CH ₂ CH ₂ CH ₂ -		toluene-HMPA(4 eq)	-78	86	86:14	72
5	21.2	-CH ₂ CH ₂ CH ₂ CH ₂ -		toluene-HMPA(4 eq)	-95	73	96:4	92
6	21.2	-CH ₂ CH ₂ CH ₂ CH ₂ -		toluene-THF(2 eq)	-78	75	14:86	72
7	21.2	-CH ₂ CH ₂ CH ₂ CH ₂ -		toluene-THF(8 eq)	-78	78	14:86	72
8	21.2	-CH ₂ CH ₂ CH ₂ CH ₂ -		toluene-THF(8 eq)	-95	87	12:88	76
9	21.2	-CH ₂ CH ₂ CH ₂ CH ₂ -		THF	-78	83	10:90	80
10	21.2	-CH ₂ CH ₂ CH ₂ CH ₂ -		THF	-105	86	2.5:97.5	95
11	21.3	Me	Me	toluene-HMPA(4 eq)	-95	82	93.5:6.5	87
12	21.3	Me	Me	toluene-THF(8 eq)	-95	58	17:83	66
13	21.3	Me	Me	THF	-105	86	8:94	84

a. R₂ = ethyl.

ene alone (entry 1, Table 6). In this non-nucleophilic solvent, the enolate may exist as a dimer or higher aggregate, potentially altering the stereochemical outcome.

[P*,P] In a subsequent communication from Koga's laboratory, the base-promoted addition of the valine-derived vinylogous carbamates from ethyl acetoacetate (22.1) to dialkyl alkylidenemalonates was reported (61). The results of this study are summarized in Scheme 22 and Table 7. The reactions were performed by combining the lithiated vinylogous amide 22.2 with 22.3. The initial conjugate addition products were not isolated. Instead, after quenching and hydrolysis, the crude mixture was decarboxylated and treated with diazomethane to provide the corresponding keto esters 22.4. While the

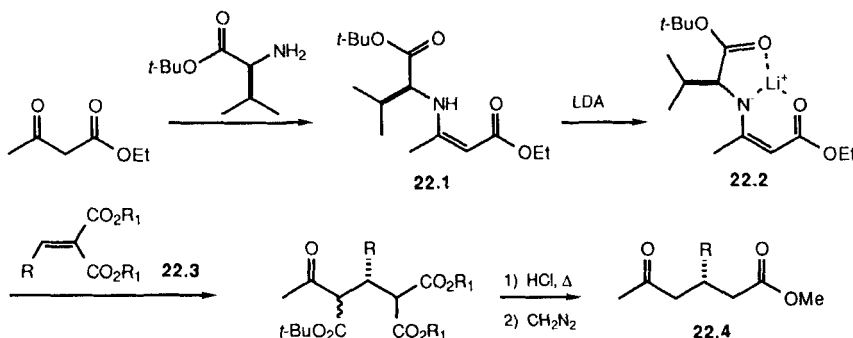


Table 7
Addition of Valine-Derived Vinylogous Carbamates to Prostereogenic, Diactivated Olefins (Scheme 22)

Entry ^a	R	R ₁	Solvent	Yield %	ee ^b %	Kinetic Yield %	Enrichment ^c ee%
1	Ph	Me	toluene	79	82		
<u>2</u>	Ph	Me	toluene-HMPA ^d	88	93		
3	Ph	Me	THF	83	91		
4	Ph	Me	THF-HMPA ^d	43	91		
5	Ph	Et	toluene	85	68		
<u>6</u>	Ph	Et	THF	83	90		
7	Ph	t-Bu	toluene-HMPA ^d	78	55		
8	Ph	t-Bu	THF	68	80		
<u>9</u>	Me	Me	toluene-HMPA ^d	66	56		
10	Me	Me	THF	73	28		
11	Et	Me	toluene-HMPA ^d	67	33	39	55
<u>12</u>	Et	Me	THF	61	37		
13	i-Pr	Me	toluene-HMPA ^d	81	17	30	86
14	i-Pr	Me	THF	74	41		
15	c-Hex	Me	toluene-HMPA ^d	53	22	27	88
<u>16</u>	c-Hex	Me	THF	76	50		

a. The optimal conditions (highest ee's) are underlined.

b. The major enantiomer was the same in all instances.

c. See text.

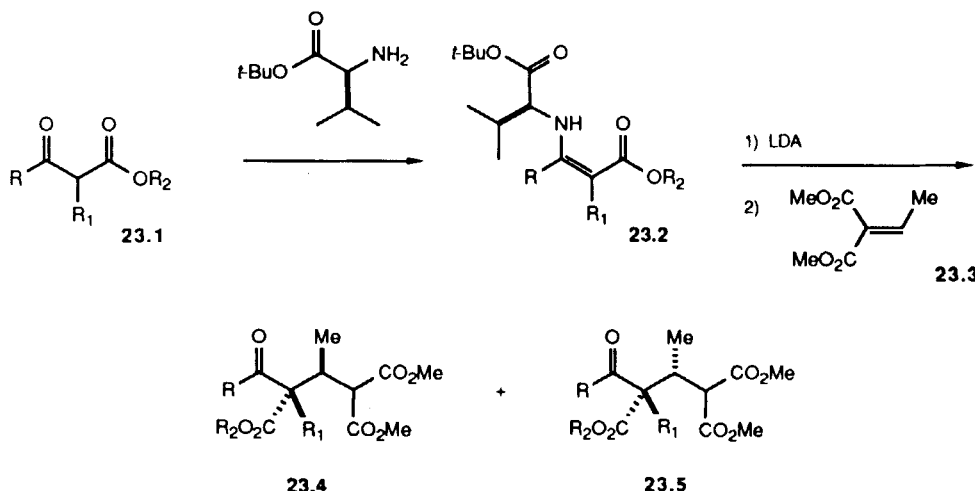
d. Two equivalents of HMPA were used.

optimal choice of solvent for the Michael addition varies from substrate to substrate, the influence of the solvent was not as dramatic as observed in the preceding example.

The influence of the substitution pattern of the acceptor on the stereochemical outcome was systematically explored. By varying R₁ while keeping R as phenyl, it was found that dimethyl and diethyl esters result in products with higher enantiomeric purities than obtained with the corresponding *di-tert*-butyl esters (entries 1–8, Table 7). Changing the substituent at the β -position of the acceptor (R in 22.3, Scheme 22) through the series methyl, ethyl, isopropyl, and cyclohexyl results in differing outcomes depending upon the solvent employed (entries 9–16, Table 7). In toluene/HMPA, the selectivity of the addition roughly *decreases* with increasing steric demand of R. In THF, the stereoselectivity *increases* with increasing steric demand of the R group. Overall, the highest levels of asymmetric induction were found with R as phenyl and R₁ as methyl (93% ee in toluene/HMPA, entry 2).

The enantiomeric purities of the products from entries 11, 13, and 15 are increased, at the expense of chemical yield, by stirring the crude adducts with saturated aqueous NH₄Cl in THF (kinetic enrichment, Table 7), presumably as a result of preferential decomposition of the minor diastereomer (62).

Extending this approach to α -substituted vinylogous carbamates **23.2**, Koga and coworkers found that excellent diastereo- and enantioselectivities are possible (Scheme 23, Table 8). For example, the addition of lithiated **23.2** to ethylenemalonate (**23.3**) under optimal conditions provides a 200:1 mixture of **23.4** to **23.5** in 99% ee (entries 4–6). The stereoselectivity in these cases, unlike the examples above, is relatively insensitive to solvent effects (see entries 1–3).



Scheme 23

Table 8
Addition of Prostereogenic, Valine-Derived Vinylogous Carbamates to
Prostereogenic, Diactivated Olefins (Scheme 23)

Entry	Vinylogous R	Carbamate R ₁	R ₂	Solvent	23.4:23.5	ee %	Yield %
1	Me	Me	Et	THF	97:3	99	54
2	Me	Me	Et	toluene	93:7	a	72
3	Me	Me	Et	toluene/THF(1 eq)	98:2	a	79
4	Me	Me	Et	toluene/HMPA(2 eq)	99.5:0.5	99	94
5	-CH ₂ CH ₂ CH ₂ CH ₂ -	Me		THF	99.5:0.5	99	87
6	-CH ₂ CH ₂ CH ₂ CH ₂ -	Me		THF/HMPA(2 eq)	99.5:0.5	99	86

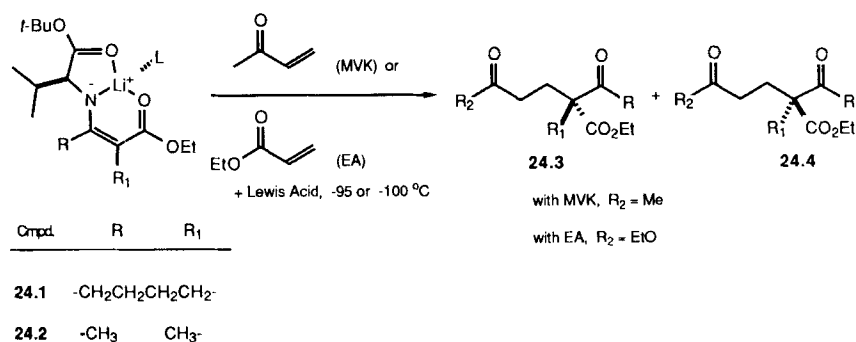
a. Not reported.

Addition of the parent keto esters to the same acceptor is much less selective (see Scheme 18 above). Hence, the amino ester influences both the facial and simple selectivity in this system.

2. To Methyl Vinyl Ketone and Acrylate Esters

[P*,N] Until recently, one of the limitations of Koga's vinylogous carbamate Michael additions has been the need for diactivated acceptors. Using Lewis acid catalysis, Koga's group has now been able to extend the methodology to the singly activated acceptors methyl vinyl ketone (MVK) and ethyl acrylate (EA) (63). The results of this study are summarized in Scheme 24 and Table 9.

The Lewis acids surveyed include LiCl, LiI, $\text{BF}_3 \cdot \text{Et}_2\text{O}$, AlCl_3 , ZnCl_2 , SnCl_4 , TMSCl, and TMSOTf. Of these $\text{BF}_3 \cdot \text{Et}_2\text{O}$, TMSCl, and TMSOTf most efficiently promoted conjugate addition. In reactions that were promoted by TMSCl or TMSOTf, it was necessary to mix the Lewis acid with the acceptor (MVK or EA) prior to the addition of the lithiated vinylogous carbamates 24.1 and 24.2. With $\text{BF}_3 \cdot \text{Et}_2\text{O}$, the Lewis acid was added to the lithiated vinylogous carbamate prior to the addition of MVK or EA. The presence of HMPA necessitated the use of a molar excess of $\text{BF}_3 \cdot \text{Et}_2\text{O}$ over HMPA in order to promote the addition (see entries 5 and 6, Table 9). By modifying the amount and the nature of the Lewis acid used, either enantiomer of the product can be obtained preferentially. For example, use of 2.5 equivalents of trimethylsilyl triflate in toluene/HMPA results in preferential formation of the *R* enantiomer. Using 5 equivalents of trimethylsilyl chloride, the *S* enantiomer is favored (compare entry 7 to entry 8, Table 9). Again, the choice of solvent can dictate the stereochemical outcome. With trimethylsilyl chloride as a promoter, use of THF results in the formation of the *R* enantiomer in good excess (entries 9, 11, 13, 15; Table 9). In toluene/HMPA, the *S*



Scheme 24

Table 9
Lewis Acid-Promoted Addition of Valine-Derived Vinylogous Carbamates to Methyl Vinyl Ketone (MVK) and Ethyl Acrylate (EA) (Scheme 24)

Entry ^a	Donor	Acceptor	Solvent(eq) ^b	Lewis Acid(eq)	24.3:24.4	ee %	Yield %
1	24.1	MVK	THF	none	---	--	trace
2	24.1	MVK	THF	BF ₃ ·Et ₂ O(2)	89.5:10.5	79	90
3	24.1	MVK	THF	TMSOTf(2.5)	88.5:11.5	77	75
4	24.1	MVK	THF	TMSCl(5)	77.5:22.5	55	60
5	24.1	MVK	toluene/HMPA(1)	BF ₃ ·Et ₂ O(2)	84.5:15.5	69	54
6	24.1	MVK	toluene/HMPA(4)	BF ₃ ·Et ₂ O(2)	---	--	trace
7	24.1	MVK	toluene/HMPA(2)	TMSOTf(2.5)	70:30	40	44
8	24.1	MVK	toluene/HMPA(2)	TMSCl(5)	26:74	48	35
9	24.1	MVK	THF	TMSCl(5)	93.5:6.5	87	66
10	24.2	MVK	toluene/HMPA(1)	TMSCl(5)	25:75	50	38
11	24.2	MVK	THF	TMSCl(5)	95:5	90	67
12	24.2	MVK	toluene/HMPA(1)	TMSCl(5)	20:80	60	48
13	24.2	EA	THF	TMSCl(5)	89.5:10.5	79	43
14	24.2	EA	toluene/HMPA(1)	TMSCl(5)	29.5:80.5	41	16
15	24.2	EA	THF	TMSCl(5)	78.5:21.5	57	53
16	24.2	EA	toluene/HMPA(1)	TMSCl(5)	11.5:88.5	77	23

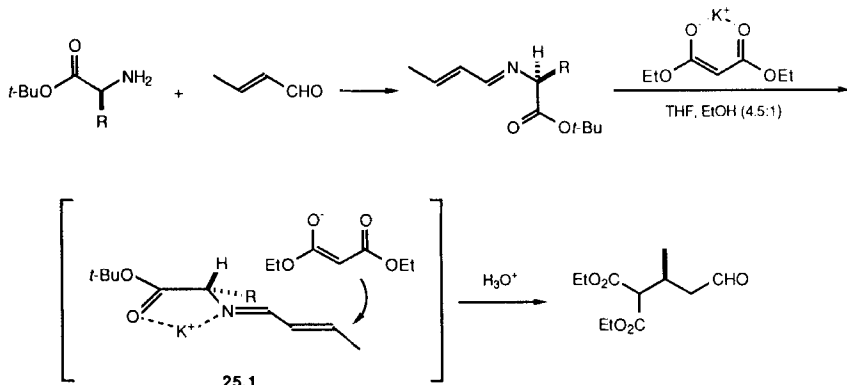
a. Optimized results for a given donor/acceptor combination are in entries 9-16.
 b. All reactions were performed between -95 and -100 °C.

enantiomer is favored, with generally lower selectivity (entries 8, 10, 12, 14, and 16). Superior yields were obtained using the more reactive acceptor MVK rather than EA. Nevertheless, the chemical yields using di-*tert*-butyl methylenemalonate as an acceptor are normally higher than even the Lewis acid-assisted additions to MVK and EA. Similar levels of asymmetric induction were obtained in both the Lewis acid-assisted additions and the unassisted addition to di-*tert*-butyl methylenemalonate.

F. Addition of Diester Anions

1. To Chiral α,β -Unsaturated Imines

[N,P*] Yamada and coworkers have found that diethyl malonate adds to chiral, non-racemic α,β -unsaturated imines with moderate to excellent selectivity (64). The imines used were derived from crotonaldehyde and amino *tert*-butyl esters. The results of this study are summarized in Scheme 25 and Table 10. The excellent selectivity attained using the imine derived from *tert*-butylglycine are particularly encouraging (entry 3, Table 10). Although the amino ester can be recovered after the hydrolysis, some loss of enantiomeric purity is observed. If a chelated transition state such as 25.1 is assumed, the stereochemical outcome can be rationalized by preferential attack of the ma-



Scheme 25

Table 10
Addition of Diethyl Malonate to α,β -Unsaturated Imines (Scheme 25)

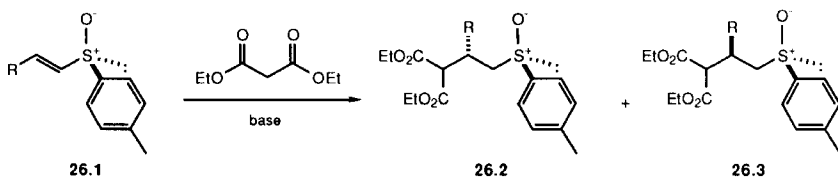
Entry	Amino Ester R	Yield %	ee %
1	i-Pr	54	69
2	i-Bu	49	36
3	t-Bu	48	86 ^a

a. Corrected for the optical purity of the starting amino ester (93.5%).

Ionate from the face opposite the alkyl group. According to this model, larger alkyl groups should lead to greater stereoselectivity, as is observed.

2. To α,β -Unsaturated Sulfoxides

[N,P*] α,β -Unsaturated sulfoxides can add nucleophiles at the β -position (Scheme 26). As the sulfoxide is stereogenic at sulfur (65), nucleophilic addition at a β -prostereogenic center can lead to diastereomers (12). The stereoselectivity of this process has been explored by Tsuchihashi and coworkers for acceptors with β -phenyl substitution (66); acceptors with β -trifluoromethyl groups have been examined by Yamazaki and coworkers (67). The results of this study are summarized in Table 11.



Scheme 26

Table 11
Addition of Diethyl Malonate to α,β -Unsaturated Sulfoxides (Scheme 26)

Entry	Sulfoxide R	Counterion	Solvent	Yield %	26.2:26.3 ^a
1	Ph	Na ⁺	EtOH	87	81:19
2	Ph	K ⁺	EtOH	88	79:21
3	Ph	Li ⁺	3:2 THF:hexanes	63	21:79
4	Ph	Li ⁺	THF	60	22:78
5	Ph	Na ⁺	THF	65	36:64
6	Ph	K ⁺	THF	76	55:45
7	F ₃ C	Li ⁺	THF	95	93:7

a. Measured on the sulfoxide intermediate.

The base and solvent play crucial roles in controlling the facial discrimination in the conjugate addition of diethyl malonate to α,β -unsaturated sulfoxides. With sodium or potassium enolates in ethanol, isomer 26.2 is favored (entries 1 and 2, Table 11). Use of the lithium enolate in THF/hexanes gives chiefly isomer 26.3 with R = Ph (entries 3 and 4). In contrast, addition of diethyl lithiummalonate in THF to 26.1 (R = CF₃) results in preferential formation of 26.2 (entry 7).

3. To α,β -Unsaturated Esters and Nitriles

[N,P*] Abramovitch and coworkers have studied the base-catalyzed reaction of diethyl malonate to the conformationally fixed 4-*tert*-butyl-1-cyano-1-cyclohexene (27.1) (68) and 4-*tert*-butyl-1-carbethoxy-1-cyclohexene (27.2) (69, 70). With 27.2, products with an equatorially orientated malonate group (27.9 and 27.10) were formed preferentially (from 99:1 in toluene to 81:19 in diethyl carbonate). With nitrile 27.1, equatorial products are preferred ((27.5 + 27.6):(27.3 + 27.4) = 96:4 equatorial/axial) in ethanol. However, in toluene, products arising from further reaction of an axially disposed malo-

nate (**27.3** or **27.4**) were produced (9:91 equatorial/“axial derived products”).

On the basis of stereoelectronic considerations, products with an axial disposition of the incoming nucleophile (that is, **27.3**, **27.4**, **27.7**, and **27.8**) should be favored under kinetic conditions (71). “Axial products” are observed for the addition of diethyl malonate to **27.1** in toluene. However, stereoelectronically disfavored equatorial products are formed for the addition of diethyl malonate to **27.1** in ethanol and in the addition of diethyl malonate to **27.2**. The new stereocenter adjacent to the acceptor nitrile or ester was generally formed as a mixture of epimers (for example, **27.5** and **27.6**). Under milder conditions, the axial nitrile (**27.6**) was favored, owing to selective kinetic protonation of the intermediate nitrile-stabilized anion (72). At higher temperatures, **27.6** could be equilibrated to **27.5**. This suggests that **27.6** is the *kinetically* preferred product in ethanol, contrary to the normal stereoelectronic arguments which predict that products from axial attack (**27.3** and **27.4**) should be favored.* The kinetic preference for equatorially disposed products may be the result of the “bulkiness” of the nucleophile under the reaction conditions.

Alder and coworkers have found that base-catalyzed addition of malonates and acetoacetates to **27.11** occurs preferentially from the less hindered exo face (Scheme 27) (73). Notice that this would correspond to equatorial addition of the malonate anion to the activated olefin.

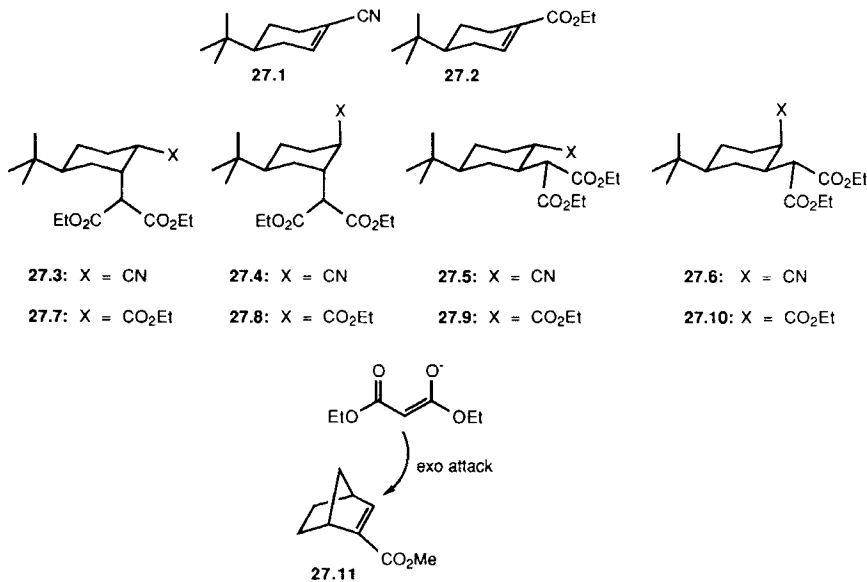
4. To α,β -Unsaturated Ketones

[P*,N] Koga and coworkers have shown that the enolates of derivatives of lactone **28.1** undergo alkylation and Michael additions from the face opposite to the trityl-protected hydroxymethyl group (56). Thus, the Michael addition of **28.2** to methyl vinyl ketone proceeds with good selectivity (Scheme 28). Similar selectivity was obtained with a formyl-activated version of **28.1** (*vide supra*).

5. To Dienones

[N,P*] Several research groups have examined the base-promoted addition of diethyl malonate and diethyl methylmalonate to dienones **29.1** and **29.2** (Scheme 29) (74). In all cases, only products that result from 1,6-addition to the dienone were reported. With **29.2** and the potassium anion of diethyl ma-

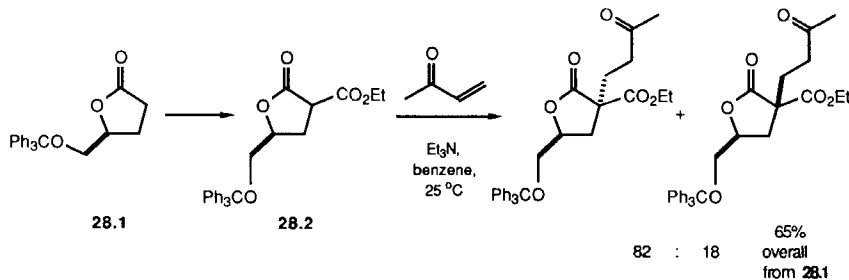
*This statement involves the reasonable assumption that the energies of the transition structures leading from **27.1** and **27.2** to the initial adduct enolates are greater than the energies of the transition structures for the protonation of the resulting adduct enolates.



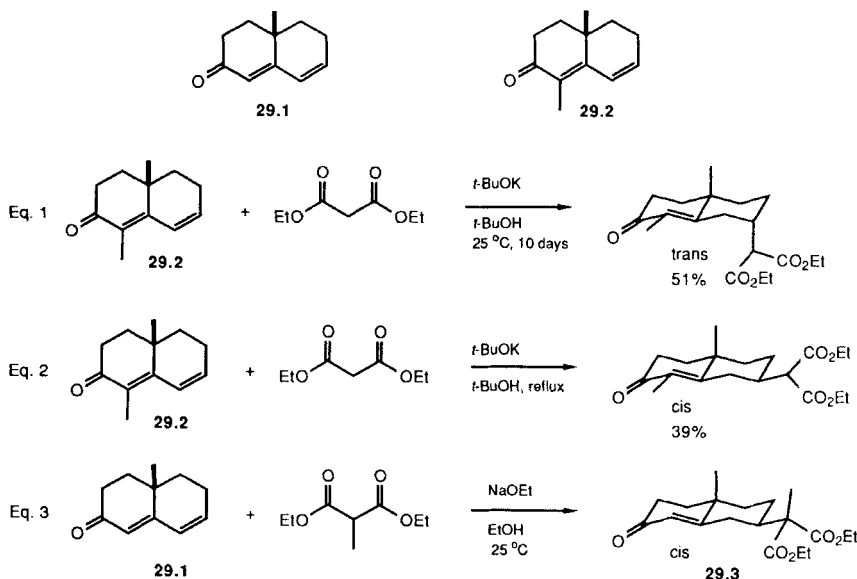
Scheme 27

ionate, the trans isomer is formed predominantly. This result is consistent with stereoelectronically preferred axial attack on **29.2**. Upon refluxing the reaction mixture, the more stable equatorial diastereomer was obtained (Eq. 2). Presumably, the formation of the equatorial isomer occurs as a result of equilibration through a retro-Michael–Michael addition manifold.

The stereochemical behavior of **29.1** and **29.2** in all cases was very similar (Scheme 29). On the other hand, use of the anion of the diethyl methylmalonate with **29.1** resulted in preferential formation of the cis isomer **29.3**.



Scheme 28



Scheme 29

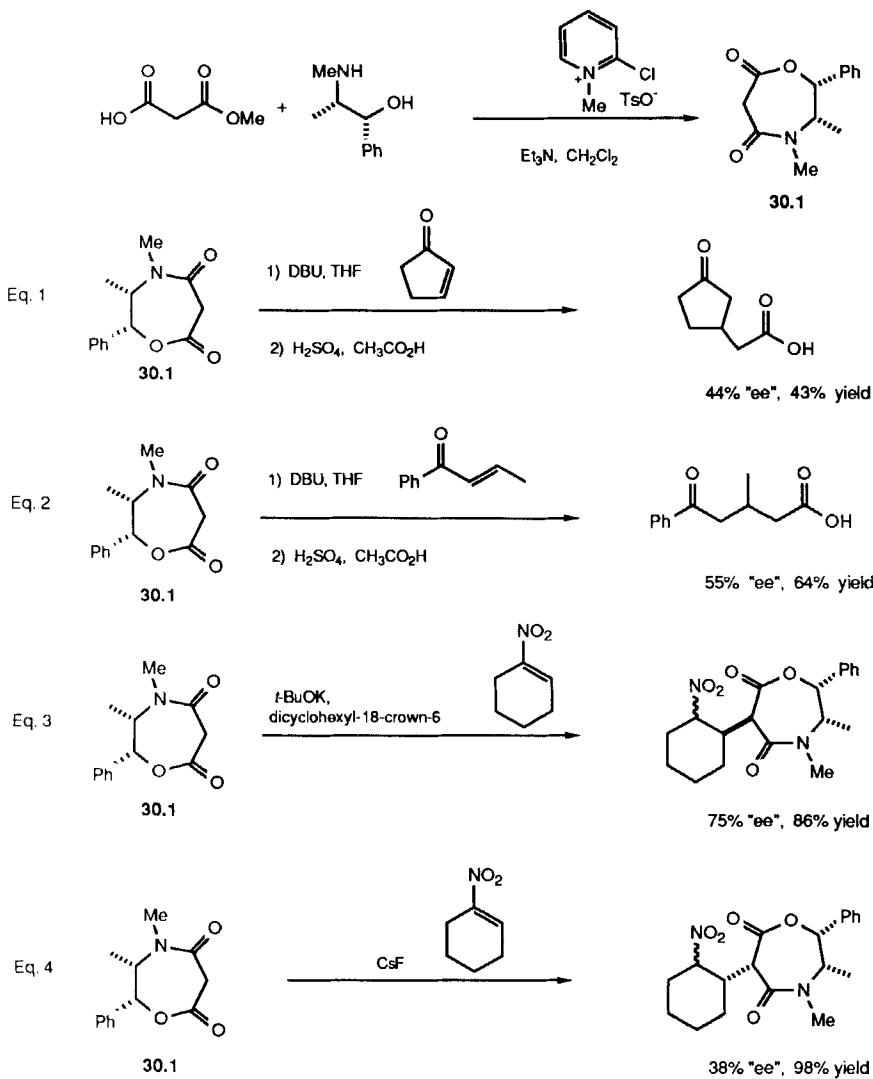
(Eq. 3). No evidence as to whether 29.3 is the result of kinetic or thermodynamic control was adduced. The more bulky nucleophile should exhibit a greater steric preference for equatorial addition. The methyl group should also make equilibration more favorable, both because the malonate group itself has no acidic hydrogens and as a result of the increased steric bulk.

G. Ester-amide Enolates

1. To α - β -Unsaturated Ketones and Nitroolefins

[P*,P] Mukaiyama and coworkers have studied the asymmetric Michael additions of oxazepine 30.1 derived from ephedrine and methyl hydrogen malonate (75). A variety of acceptors (2-cyclopentenone, 1-phenyl-2-butene-1-one, and 1-nitrocyclohexene) were used. The results of this study are summarized in Scheme 30. The nature of the base plays an important role in the stereochemistry of these additions. With enones (Eqs. 1 and 2), increasing selectivity is found along the following series of bases: (least selective), *t*-BuOK with NiCl_2 , Ph_3CLi , *t*-BuOK, *t*-BuOK with dicyclohexyl-18-crown-6, and DBU (1,8-diazabicyclo[5.4.0]undec-7-ene) (most selective). The absolute configurations of the products in Eqs. 1 and 2 were not determined.

The highest selectivities found for the addition of **30.1** to 1-nitrocyclohexene (Eq. 3, Scheme 30) were observed with *t*-BuOK in the presence of dicyclohexyl-18-crown-6 (75% ee) and with CsF/dicyclohexyl-24-crown-8 (71% ee). In the absence of the crown ethers, the products obtained had the opposite configuration, suggesting an interesting dependence of selectivity on the aggregation state. In this instance, employment of CsF results in the highest selectivity (38% ee, Eq. 4).

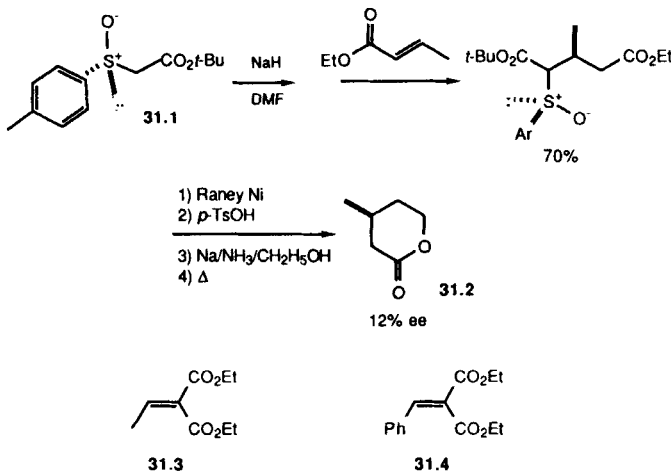


Scheme 30

H. α -Sulfinyl Esters

1. To α,β -Unsaturated Esters and α,β -Unsaturated Diesters

[P*,P] The addition of optically active α -sulfinyl esters to α,β -unsaturated esters has been reported by Matloubi and Solladié (65, 76, 77). The configuration of the major antipode from the addition of 31.1 to ethyl crotonate was assigned by conversion to lactone 31.2, which was formed with 12% ee (Scheme 31). Although the structure of the major isomer was not reported, similar addition of 31.1 to 31.3 resulted in products that, after desulfurization, had 24% ee (Scheme 31). No asymmetric induction occurred in the addition of the anion of 31.1 to 31.4.



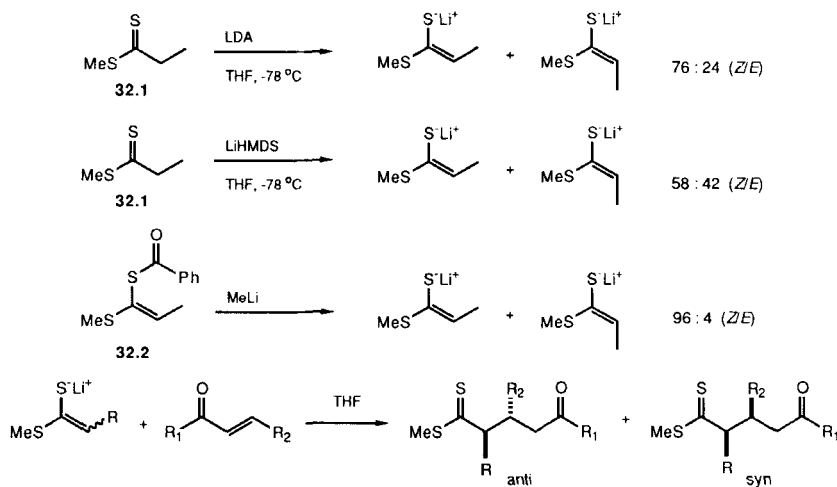
Scheme 31

I. Dithioester Enethiolates

1. To α,β -Unsaturated Ketones

[P,P] Metzner and coworkers have investigated simple diastereoselectivity in the addition of dithioester enethiolates to enones (78). The results from this study are summarized in Scheme 32 and Table 12. Deprotonation of methyl dithiopropionate (32.1) with LDA in THF at -78°C provided a 76:24 (*Z/E*) mixture of enethiolates.* Higher proportions of the *E* enethiolate could be

*In this case, "SLi" is assigned the higher priority in the *E/Z* nomenclature of the enethiolates.



Scheme 32

Table 12
Addition of Dithioester Enethiolates to α,β -Unsaturated Ketones (Scheme 32)

Entry	Enethiolate R	Z:E	α,β -Unsaturated Ketone R ₁	R ₂	Ketone E/Z	Temp. °C	Yield %	Anti:Syn
1	Me	76:24	-CH ₂ CH ₂ -		Z	-40	67	39:61 ^a
2	Me	76:24	-CH ₂ CH ₂ CH ₂ -		Z	-40	70	49:51 ^a
3	Me	76:24	-CH ₂ CH ₂ CH ₂ CH ₂ -		Z	-40	82	50:50 ^a
4	Me	76:24	Ph	Me	E	-70	69	72:28 ^b
5	Me	76:24	Ph	Me	E	20	c	39:61 ^b
6	Me	76:24	Me	Me	E	-50	66	75:25
7	Me	96:4	Me	Me	E	-50	59	92:8
8	Me	58:42	Me	Me	E	-50	85	57:43
9	n-pentyl	85:15	Me	Me	E	-10	76	86:14 ^b
10	CH ₂ =CHCH ₂ -	95:5	Me	Me	E	-5	61	95:5
11	PhCH ₂ -	c	Me	Me	E	-30	57	80:20

a. Identity of major diastereomer not assigned.

b. Identity of major diastereomer not assigned but likely by analogy.

c. Not reported.

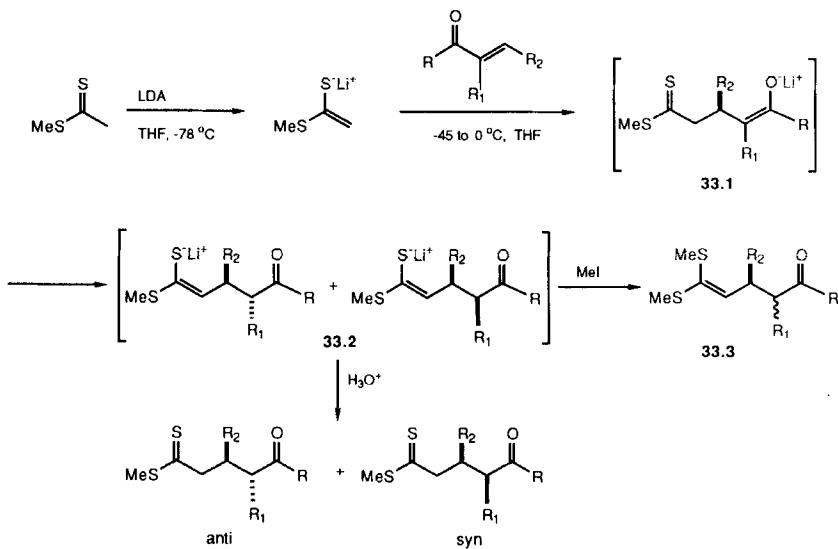
generated by deprotonation of **32.1** with lithium hexamethyldisilylamide (LiHMDS), in contrast with the deprotonation of ketones, where LiHMDS usually gives more of the *Z* isomer than LDA (79). Regeneration of the enethiolate from a purified mixture (96:4 *Z/E*) of benzoyl dithioketene acetals **32.2** with methylolithium allows formation of a 96:4 (*Z/E*) mixture of the enethiolates.

With 2-cycloalkenones, essentially no diastereoselectivity is observed in the

conjugate addition of a 76:24 Z/E mixture of methyl dithiopropionate enethiolates (entries 1–3, Table 12). Addition of an identical mixture of enethiolates to chalcone (entry 4) and 3-penten-2-one (entry 6) at low temperatures provides a mixture of diastereomers where the proportion of the anti diastereomer obtained reflects the amount of Z enolate. At 20°C, a marked change in stereoselectivity is observed (entry 5). In this case, the syn diastereomer is slightly preferred, presumably because of equilibration at the higher temperature.

The data in entries 6–11 reveal a strong correlation between adduct stereochemistry and the enethiolate isomer ratio (Z-anti, E-syn). These results suggest that stereoselectivity is controlled by a kinetic process at low temperatures. The only configuration that was explicitly proved in this study is that of the major anti diastereomer obtained from the addition of the Z enethiolate of 32.1 to 3-penten-2-one (entries 6–8, Table 12). The remaining configurations were assigned by analogy.

Further examples of Michael additions of enethiolates were reported in a later communication by Berrada and Metzner (80). The addition of the lithium enethiolate of methyl dithioacetate to α,β -disubstituted enones results in the formation of two adjacent stereocenters (Scheme 33, Table 13). The stereoselectivity in this process appears to occur in the conversion of intermediate 33.1 to 33.2 through an *intramolecular* proton transfer.



Scheme 33

Table 13
Addition of Dithioacetate Enethiolates to α,β -Substituted α,β -Unsaturated Ketones
(Scheme 33)

Entry	R	Enone R ₁	R ₂	Temp °C	Yield %	Syn:Anti
1	Me	Me	Me	-5	62	76:24
2	t-Bu	Me	Me	0 to 20	64	90:10 ^a
3	Ph	Me	Me	0	81	81:19 ^a
4	Ph	Me	Ph	0	61	85:15 ^a
5	-CH ₂ CH ₂ CH ₂ -		Me	-45	80	>95:5 ^a
6	-CH ₂ (CH ₂) ₂ CH ₂ -		Me	-45	56 ^b	>95:5 ^a
7	-CH ₂ (CH ₂) ₃ CH ₂ -		Me	-25	80	94:6 ^a

a. The stereostructures of the products were not explicitly assigned.

b. Some of the enone (27%) was recovered.

Evidence that proton transfer occurs under the reaction conditions was found by adding methyl iodide to the reaction mixture before quenching. Formation of dimethylthioketene acetals 33.3 indicates the presence of enethiolate 33.2 in solution. This outcome is intriguing in light of the results from the previous study (*vide supra*) where compelling evidence *against* proton transfer was found. Presumably, this is a manifestation of the different substitution patterns of the substrates employed. Chemical correlation with known compounds was used to confirm the structure of the major product in entry 1 (Table 13). The configurations of the remaining compounds were assigned by analogy to entry 1 and should be regarded as tentative. It is to be noted that the stereoselectivity observed in these reactions results from stereoselective enolate protonation and not in the Michael addition itself.

J. Ketone and Aldehyde Enolates

Alkali metal enolates derived from ketones and aldehydes react readily with α,β -unsaturated ketones and more reactive acceptors. In these additions, the geometry of the enolate can determine the stereochemical outcome.

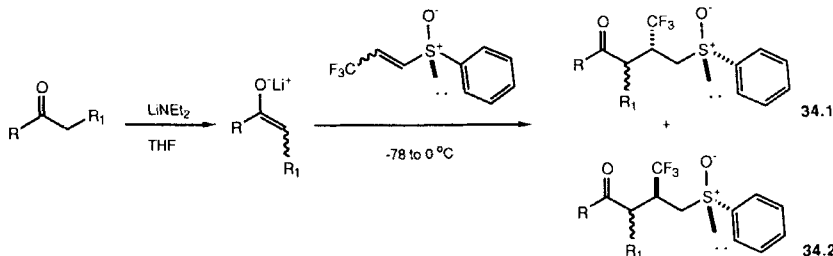
For use in Michael additions, two general methods have been applied for the generation of the requisite enolates. Direct deprotonation of the ketone with a strong base can provide an enolate suitable for conjugate addition. Regiochemical and stereochemical considerations in the deprotonation can limit the utility of this method. However, by altering the base and solvent used, a significant variety of enolates can be formed with good selectivity (8, 31, 81). Three tendencies are worth noting here. First, more bulky alkyl amides under tightly coordinating conditions (lithium and magnesium counter-

ions, ethereal solvents) normally lead to higher percentages of the *E* enolate. Second, ketones with large groups next to the carbonyl usually give high percentages of *Z* enolates, irrespective of the conditions employed. For example, deprotonation of ethyl *tert*-butyl ketone normally gives the *Z* enolate as the only detectable isomer. Third, formation of the *Z* enolate is also favored by the use of weaker bases under more dissociating conditions (sodium or potassium counterions, HMPA/THF). Since the *Z* enolates are frequently more stable than the *E* isomers, equilibration can also be used to obtain them. Alternatively, enolates can be regenerated from the corresponding enol silanes with methylolithium (81b, c). This method allows separation of the *E* and *Z* enol silanes and permits access to enolates that are otherwise not available.

1. To Chiral α,β -Unsaturated Sulfoxides

[N,P*] and [P,P*] Addition of a ketone enolate to a vinyl sulfoxide results in the formation of an anion (pK_a ca. 33) that is significantly less stable than the ketone enolate (pK_a ca. 20). This difference of 13 pK units in anion basicity contributes +12 to +18 kcal/mol to the ΔG_0 of addition (at -78° or 0°C , respectively). Unless some secondary process intervenes, this stability difference usually results in failure of a Michael addition under kinetically controlled, aprotic conditions (*vide supra*). Surprisingly, Yamazaki and coworkers have been able to add lithium enolates of ketones to chiral α,β -unsaturated sulfoxides (65, 67, 82). Although the possibility has not been examined, proton transfer, either inter- or intramolecular from the ketone could serve to drive the reaction. This mechanism is almost certainly operating for the addition of malonates to unsaturated sulfoxides (*vide supra*).

The stereochemical outcome of these reactions is shown in Scheme 34 and Table 14 (12). In all instances, excellent selectivity at the trifluoromethyl substituted stereocenter is observed. As might be expected, the opposite configuration at the trifluoromethyl group is obtained using the *Z* sulfoxide (entry 2).



Scheme 34

Table 14
Addition of Lithium Enolates to Optically Active Unsaturated Sulfoxides
(Scheme 34)

Entry	Sulfoxide <i>E/Z</i> ^a	Ketone R	Enolate R ₁	Yield %	34.1:34.2
1	<i>E</i>	Ph	H	99	97:3
2	<i>Z</i>	Ph	H	92	<1:99
3	<i>E</i>	<i>t</i> -Bu	H	96	>99:1
4	<i>E</i>	Et	Et ^b	86	>99:1 ^c

a. The precise ratio used was not reported.

b. Enolate ratio not reported.

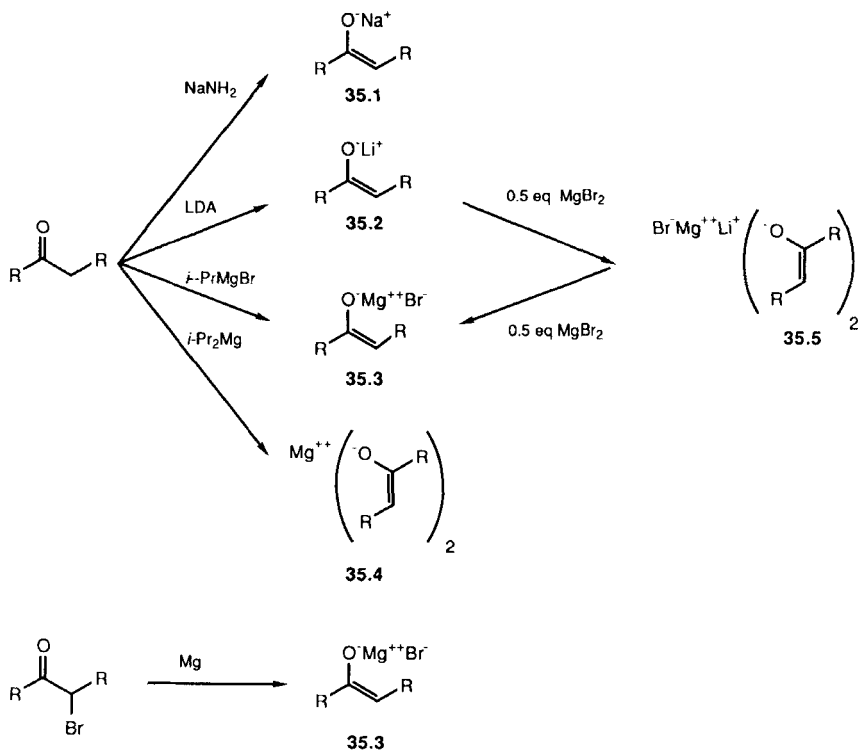
c. A 73:27 mixture of diastereomers with the same configuration at the trifluoromethyl stereocenter was formed.

When the undefined mixture of enolates in entry 4 is used, good facial selectivity at the prosterogenic center of the sulfoxide is observed. However, there is poor control over the relative configuration of the methyl and trifluoromethyl groups.

2. To α,β -Unsaturated Ketones

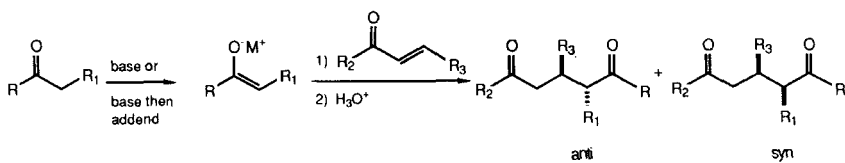
[P,P] The addition of ketone enolates to α,β -unsaturated ketones has been the focus of a physical organic study by Gorrichon-Guigon and coworkers (83). The lithium and sodium enolates (35.1 and 35.2) used were obtained by deprotonation with LDA or NaNH₂. On the other hand, the bromomagnesium enolates (35.3) were prepared by deprotonation of the ketone with isopropylmagnesium bromide or reaction of the α -bromoketone with magnesium (Scheme 35) (84). Magnesium bis-enolates (35.4) are available through deprotonation with diisopropylmagnesium. Alternatively, 35.3 and 35.4 can be obtained by disproportionation reactions. For example, the lithium enolate of the ketone can be transformed into the bromomagnesium enolate (35.3) by treatment with magnesium bromide. By varying the stoichiometry and nature (MgBr₂ or ZnBr₂) of the addend, access to species such as 35.5 with mixed counterions was possible.

The stereochemistry of the Michael additions of several combinations of ketone enolates and α,β -unsaturated ketones has been elucidated (Scheme 36, Table 15) (85, 86). The enolates used are likely to have the *Z* configuration, although this was not explicitly determined. In instances when conditions of apparent kinetic control were employed, the anti diastereomers were obtained selectively. The stereochemistry is virtually independent of the counterion used. At higher temperatures the syn diastereomers are favored, evidently as a result of equilibration (entries 17–19).



Scheme 35

Ketone enolate geometry has a strong effect on the stereochemistry of the conjugate addition to α,β -unsaturated ketones (Scheme 37, Table 16) (87, 88). When the R group is larger than ethyl, the enolate E/Z ratio closely correlates with the syn/anti ratio in the products of addition. With the E enolate of diethyl ketone (entry 11) the correlation breaks down as stereoselectivity is poor and in the opposite sense. A higher proportion of the syn isomer is formed with this enolate in the presence of THF/HMPA (entry 12). Little



Scheme 36

Table 15
Addition of Ketone Enolates to α,β -Unsaturated Ketones (Scheme 36)

Entry	Enolate	Counterion	Unsaturated Ketone	Temp.	Yield %	1,2:1,4	Anti:Syn	
	R	R ₁	M	R ₂	R ₃			
1	<i>i</i> -Bu	<i>i</i> -Pr	MgCl	Ph	Ph	20	65	0:100 ^a 100:0 ^a
2	<i>i</i> -Bu	<i>i</i> -Pr	MgCl	Ph	<i>p</i> - <i>i</i> -PrC ₆ H ₄	b	92	0:100 ^a 100:0 ^a
3	<i>i</i> -Bu	<i>i</i> -Pr	MgCl	Ph	<i>p</i> -ClC ₆ H ₄	b	78	0:100 ^a 100:0 ^a
4	<i>i</i> -Bu	<i>i</i> -Pr	MgCl	Ph	<i>p</i> -MeOC ₆ H ₄	b	78	0:100 ^a 100:0 ^a
5	<i>t</i> -Bu	<i>i</i> -Pr	MgCl	.Ph	<i>p</i> -NO ₂ C ₆ H ₄	b	75	0:100 ^a >75:25 ^c
6	<i>i</i> -Bu	<i>i</i> -Pr	MgCl	<i>p</i> -MeOC ₆ H ₄	Ph	b	68	0:100 ^a 100:0 ^a
7	<i>i</i> -Bu	<i>i</i> -Pr	MgCl	<i>p</i> -ClC ₆ H ₄	Ph	b	66	0:100 ^a 100:0 ^a
8	<i>i</i> -Bu	<i>i</i> -Pr	MgCl	<i>p</i> - <i>i</i> -PrC ₆ H ₄	Ph	b	56	0:100 ^a >75:25 ^c
9	<i>t</i> -Bu	<i>i</i> -Pr	MgCl	<i>p</i> -ClC ₆ H ₄	<i>p</i> -ClC ₆ H ₄	b	72	0:100 ^a 100:0 ^a
10	<i>i</i> -Bu	<i>i</i> -Pr	MgBr	Me	Ph	20 ^e	65	0:100 ^a 100:0 ^a
11	<i>t</i> -Bu	Me	MgCl	Ph	Ph	b	80	0:100 ^a 100:0 ^a
12	<i>t</i> -Bu	Me	MgBr	Ph	Ph	-78 ^e	70	>95:5 ---
13	<i>t</i> -Bu	Me	MgBr	Ph	Ph	-20 ^f	75	50:50 100:0 ^a
14	<i>t</i> -Bu	Me	MgBr	Ph	Ph	20 ^g	100	18:82 100:0 ^a
15	<i>t</i> -Bu	Me	EOMgd	Ph	Ph	-78 ^e	90	25:75 100:0 ^a
16	<i>t</i> -Bu	Me	EOMgd	Ph	Ph	-20 ^h	100	0:100 ^a 100:0 ^a
17	<i>t</i> -Bu	Me	EOMgd	Ph	Ph	20 ^e	100	0:100 ^a 85:15
18	<i>t</i> -Bu	Me	EOMgd	Ph	Ph	20 ^g	100	0:100 ^a 30:70
19	<i>t</i> -Bu	Me	EOMgd	Ph	Ph	20 ⁱ	100	0:100 ^a 15:85
20	<i>t</i> -Bu	Me	Li	Ph	Ph	-78 ^e	55	30:70 100:0 ^a
21	<i>t</i> -Bu	Me	Li	Ph	Ph	-78 ⁱ	75	10:90 100:0 ^a
22	<i>t</i> -Bu	Me	Li	Ph	Ph	20 ^e	90	0:100 ^a 100:0 ^a
23	<i>t</i> -Bu	Me	MgBr	Me	Ph	20 ^e	>90	100:0 ^a ---
24	<i>t</i> -Bu	Me	EOMgd	Me	Ph	0 ^e	70	0:100 ^a 85:15
25	<i>t</i> -Bu	Me	Li	Me	Ph	0 ^j	100	10:90 100:0 ^a
26	<i>t</i> -Bu	Et	MgCl	Ph	Ph	b	80	0:100 ^a 100:0 ^a
27	<i>t</i> -Bu	<i>i</i> -Pr	MgCl	Ph	Ph	b	69	0:100 ^a 100:0 ^a
28	Ph	Me	MgCl	Ph	Ph	b	k	0:100 ^a 100:0 ^a
29	PhCH ₂	Ph	MgCl	Ph	Ph	b	85	0:100 ^a 100:0 ^a

a. Minor isomer not detected (no detection limit given).

b. Not reported, probably room temperature.

c. Exact ratio not reported.

d. Magnesium bisenolate.

e. For 1 minute.

f. For 4 hours.

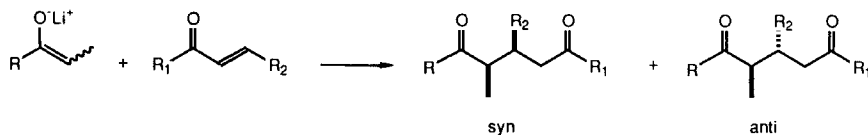
g. For 1 hour.

h. For 5 minutes.

i. For 24 hours.

j. For 2 hours.

k. Not reported.



Scheme 37

Table 16
Addition of *E* and *Z* Enolates from Ketones to α,β -Unsaturated Ketones
(Scheme 37)

Entry	R	Enolate <i>E:Z</i> ^a	Enone <i>R</i> ₁ <i>R</i> ₂	Solvent	Temp. °C	Yield %	Syn:Anti
1	t-Bu	<1:99	t-Bu Ph	THF	-78	70	<1:99
2	Ph	2:98	t-Bu Ph	THF	-78	87	2:98
3	Ph	2:98	t-Bu Ph	THF/HMPA	-78	80	4:96
4	Ph	2:98	Me Me	THF	-78	65	<3:97
5	Ph	2:98	<i>i</i> -Pr Me	THF	-78	63	<3:97
6	Ph	2:98	-(CH ₂) ₃ -	THF	-78	0 ^b	---
7	<i>i</i> -Pr	4:96	t-Bu Ph	THF	-78	88	5:95
8	Et	15:85	t-Bu Ph	THF	-78	78	12:88
9	Ph	87:13	t-Bu Ph	THF	-20	67	83:17
10	<i>i</i> -Pr	90:10	t-Bu Ph	THF	-78	87	90:10
11	Et	81:19	t-Bu Ph	THF	-78	88	39:61
12	Et	81:19	t-Bu Ph	THF/HMPA	-78	98	68:32
13	Me ₃ SiOCMe ₂	<1:99	t-Bu Ph	THF	-10	55	10:90
14	Me ₃ SiOCMe ₂	<1:99	t-Bu Ph	THF	20	67	45:55

a. Determined by treating an aliquot from the reaction mixture with Me₃SiCl followed by capillary GLC analysis.

b. No addition products were isolated.

change in selectivity is observed when THF/HMPA was added to a *Z* enolate prior to the addition of the enone (entry 3).

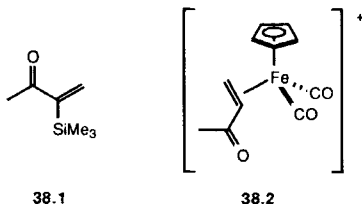
The enolate derived from 2-methyl-2-trimethylsilyloxy-3-pentanone and LDA reacts much slower than the corresponding alkyl enolates (entry 13); at higher temperatures the selectivity drops slightly with this enolate, presumably as a result of equilibration (entry 14). The lowered reactivity could be the result of intramolecular chelation of the lithium counterion of the enolate with the oxygen of the trimethylsilyloxy group. Loss of this stabilization on going to products would be expected to slow the reaction. Even simple, unencumbered enones (*R*₁, *R*₂ = Me; Scheme 37) can be used in the addition (entry 4, Table 16). Cyclic enones (entry 6) could not be coaxed into giving conjugate addition products, however.

3. Robinson Annulations

The Michael addition of the enolates derived from cycloalkanones to α,β -unsaturated ketones has been well studied, mostly in the context of the Robinson annelation (89, 90). Although the stereochemical outcome in many examples is determined by epimerization of stereocenters after the Michael

addition, in some instances stereodifferentiation occurs during the Michael addition (91–94).

Regiochemical problems limit the usefulness of the Robinson annelation of substituted cyclohexanones to methyl vinyl ketone. A potential solution to this problem is the use of a preformed enolate of defined regiochemistry. Unfortunately, with the highly reactive methyl vinyl ketone, only low yields of products are obtained using this methodology (6, 92, 93). A solution to this problem has been developed by Stork and coworkers (95) and by Boeckman (96, 97) who attached a trimethylsilyl group to the α -position of the enone (38.1, Scheme 38). The success of this strategy is probably due to the fact that the trimethylsilyl group shields the carbonyl of the enone, minimizing 1,2-addition and slowing any further addition of this enolate (polymerization). Additionally, the silyl group at the α -position should stabilize the anion produced in the Michael addition, making the kinetically controlled Michael addition more favorable and further reactions less likely.



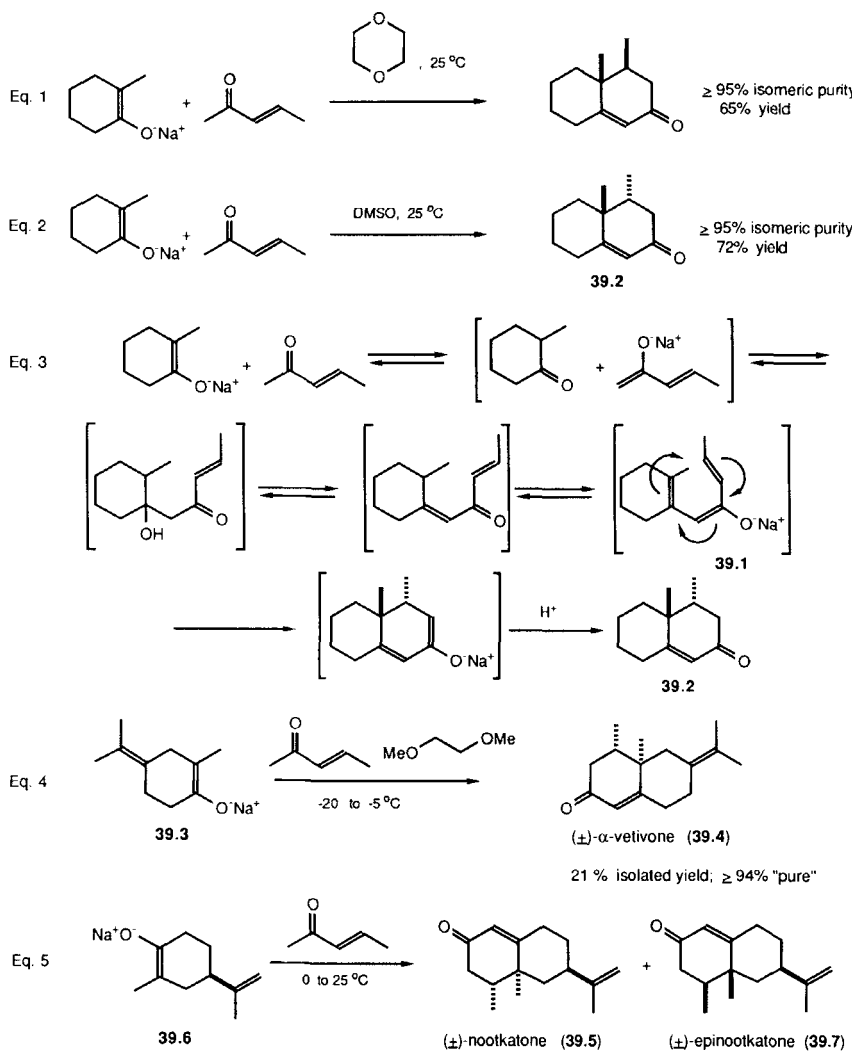
Scheme 38

Another solution to this problem was achieved by Rosan and Rosenblum who precomplexed methyl vinyl ketone with a cationic iron species (38.2, Scheme 38) (98). Addition of a lithium enolate to this species results in a neutral conjugate addition product with a carbon–metal bond. The Robinson annelation is completed by treatment with basic alumina.

[P,P] In the context of the Robinson annelation, some early work was performed with β -keto esters by Marshall and coworkers (see Scheme 16). Although the selectivities observed were generally low, the importance of reaction conditions and particularly solvent was noticed. For the synthesis of many natural products, it is necessary to replace the ester functionality with a methyl group, a transformation that has proven to be troublesome (54). A more direct approach involves the Michael addition/cyclization with a 2-methylcyclohexanone. This possibility has been explored by a number of research groups (*vide infra*) (99).

The Robinson annelation of the sodium enolate of 2-methylcyclohexanone and *trans*-3-penten-2-one has been explored by Scanio and Starrett (Eqs. 1–3, Scheme 39) (100). By changing the solvent, these workers were able to

produce good yields of either the cis or trans isomer. In dioxane, the cis isomer is favored (Eq. 1), whereas the trans isomer is produced in DMSO (Eq. 2). These workers have advanced an intriguing mechanistic proposal to account for the divergent stereochemical outcomes in the different solvents. They have suggested that the cis isomer arises from a stereoselective conjugate addition followed by cyclization. The rationale for the formation of the trans isomer is illustrated in Eq. 3 (Scheme 39). Use of DMSO as solvent



Scheme 39

favors rapid proton transfers. Hence, through a proton transfer/aldol/dehydration/deprotonation sequence, intermediate **39.1** is produced. Intermediate **39.1** then undergoes a thermally-allowed disrotatory cyclization to form the trans isomer **39.2**.

No experimental evidence has been presented to support the foregoing mechanistic proposal. A more direct explanation for the formation of **39.2** is that use of the polar aprotic solvent DMSO strongly affects the stereochemical outcome of the initial conjugate addition. As can be seen in this review, the choice of solvent often has a significant effect on the stereochemistry of the products formed.

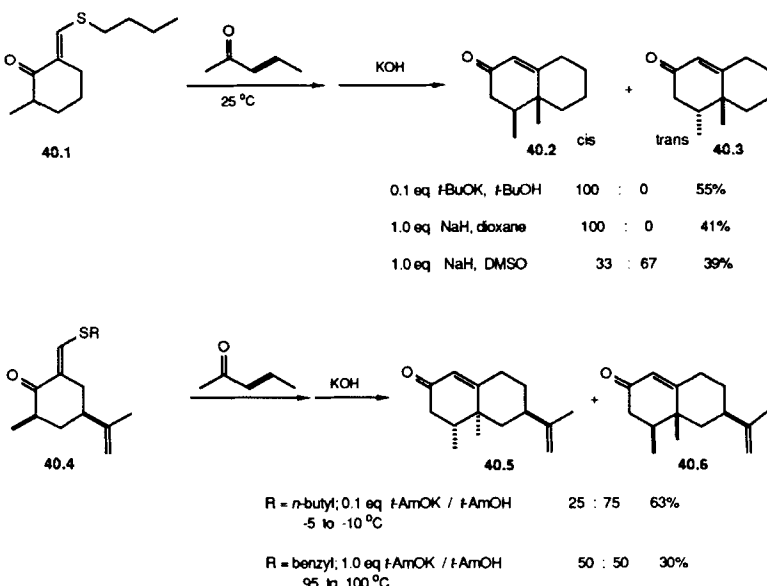
Odom and Pinder found that the sodium enolate **39.3**, when added to *trans*-3-penten-2-one, gives (\pm)- α -vetivone (**39.4**) in low yield (Eq. 4, Scheme 39) (101). The cis isomer is formed with a large preference.

[P*,P] If a substituted cyclohexanone is used in the annelation, the possibility exists for facial discrimination. Some of the first work in this area was performed by Odom and Pinder in connection with the synthesis of (\pm)-nootkatone (**39.5**) (see Eq. 1, Scheme 39). These workers found that the base-catalyzed annelation of **39.6** with *trans*-3-penten-2-one gives **39.5** and **39.7** in approximately a 10:90 ratio in low yield (101, 102). Again, only products with cis methyl groups were found.

The foregoing cyclization reaction was explored in more detail by Gen and coworkers (103). When the reaction is carried out in dimethoxyethane at temperatures between -35 and -5°C , (\pm)-7-epinootkatone (**39.7**) is obtained in 29% yield and greater than 97% isomeric purity (Eq. 5, Scheme 39). McMurry and coworkers improved the yield of the annelation of **39.6** and *trans*-3-penten-2-one to 50% (based on recovered starting material) (104).

In an attempt to enhance the stereochemical preference for (+)-nootkatone, Takagi and coworkers examined annelations of the modified cyclohexanones **40.1** and **40.4** with *trans*-3-penten-2-one (Scheme 40) (105). A two-step procedure (Michael addition followed by base-catalyzed deprotection and closure) was used for the annelation. Initially, the factors governing the control of the relative stereochemistry of the adjacent stereocenters were examined using **40.1** (Scheme 40). In keeping with the observations of Scanio and Starrett, either sodium hydride in dioxane or catalytic *tert*-butoxide in *tert*-butyl alcohol resulted in exclusive formation of the cis isomer **40.2**. Sodium hydride in DMSO does reverse the stereoselectivity of the reaction, but not completely. In this case, the trans/cis ratio is 2:1.

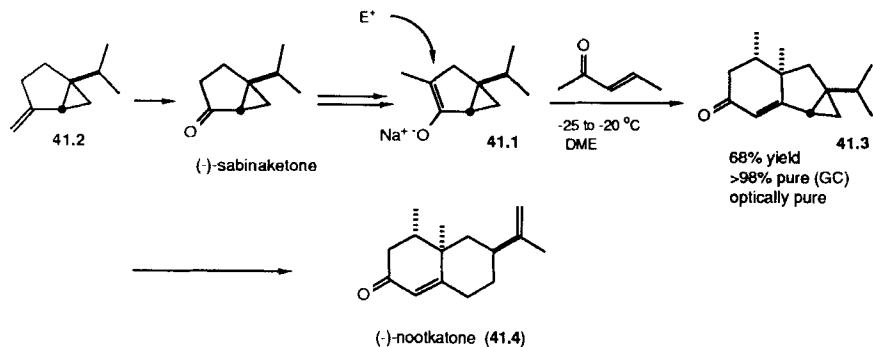
Under similar conditions, little facial selectivity with respect to the preexisting stereocenter was seen with optically active **40.4**. Varying the nature of the thioalkyl blocking group ($\text{R} = n\text{-butyl, sec-butyl, benzyl}$), the base (*t*-BuOK, *t*-AmOK, NaH; catalytic and stoichiometric amounts), and the solvent (*t*-BuOH, *t*-AmOH, dioxane) produces only minor changes in selec-



Scheme 40

tivity. The optimal conditions for obtaining the two diastereomers are shown in Scheme 40. The most important variable appears to be the reaction temperature.

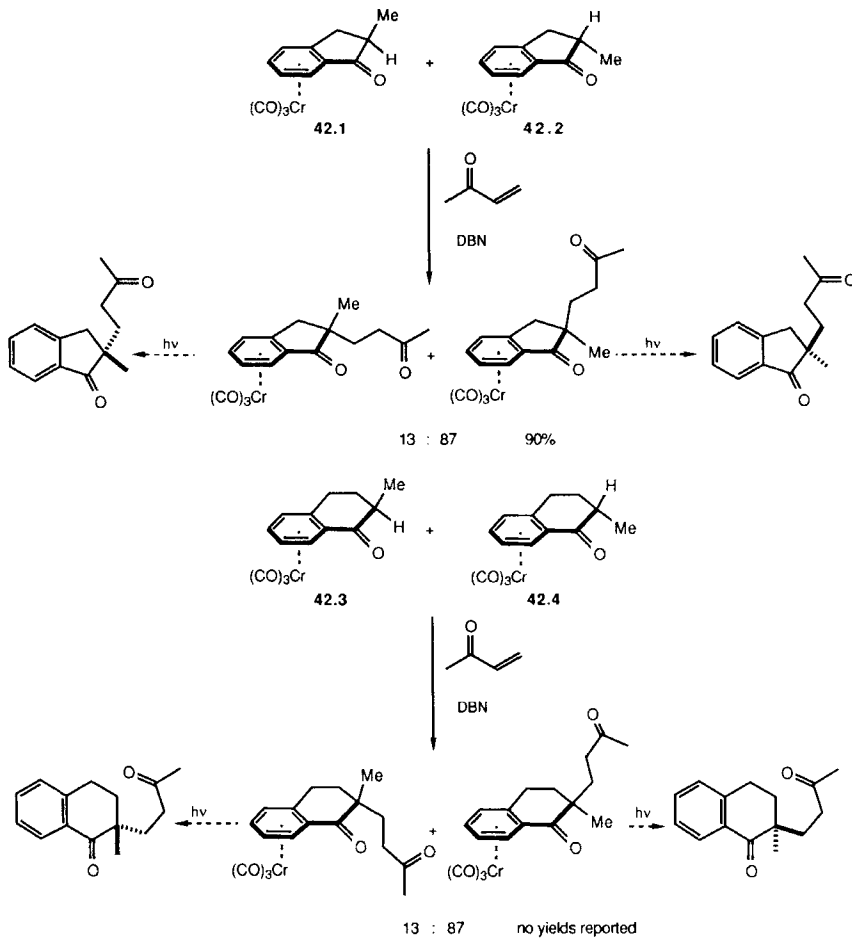
Gen and coworkers have studied a similar cyclization of the sodium enolate derived from *(−)*-sabinaketone (**41.1**, Scheme 41) (106). *(−)*-Sabinaketone is available through direct ozonolysis of *(+)*-sabinene (**41.2**). The cyclopropane ring in enolate **41.1** serves two purposes in the Michael addition. First,



Scheme 41

deprotonation is directed completely away from the 3-membered ring, resulting in preferential formation of one enolate. Second, the electrophile (3-penten-2-one in this example) adds trans to the cyclopropane methylene resulting in high facial selectivity. The major product (**41.3**) was converted by cyclopropane ring opening into (–)-nootkatone (**41.4**).

[P*,N] An interesting approach to asymmetric Michael additions was reported by Meyer and coworkers (107), who have shown that enantiomerically enriched Cr(CO)₃-complexed methylindanones and methyltetralones (108) will give conjugate addition products with methyl vinyl ketone (Scheme 42). The bulky chromium tricarbonyl group blocks attack of one of the faces of

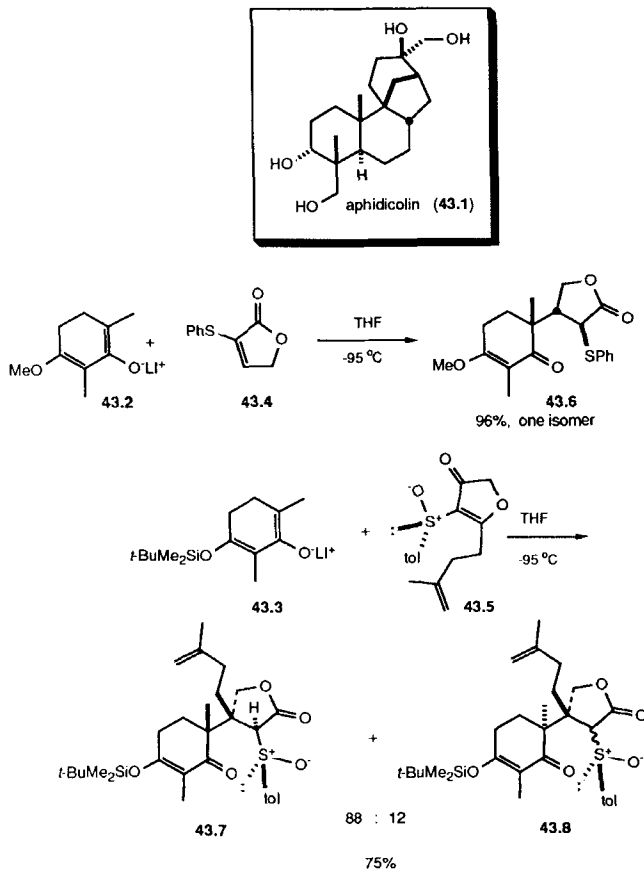


Scheme 42

what would otherwise be a planar enolate. The resulting adducts cannot be directly subjected to the desired cyclization with base because of competing deprotonation of the benzylic protons and subsequent addition of the resulting anion to the side-chain carbonyl group.

4. To α -Sulfinyl Lactones and α -Thiolactones

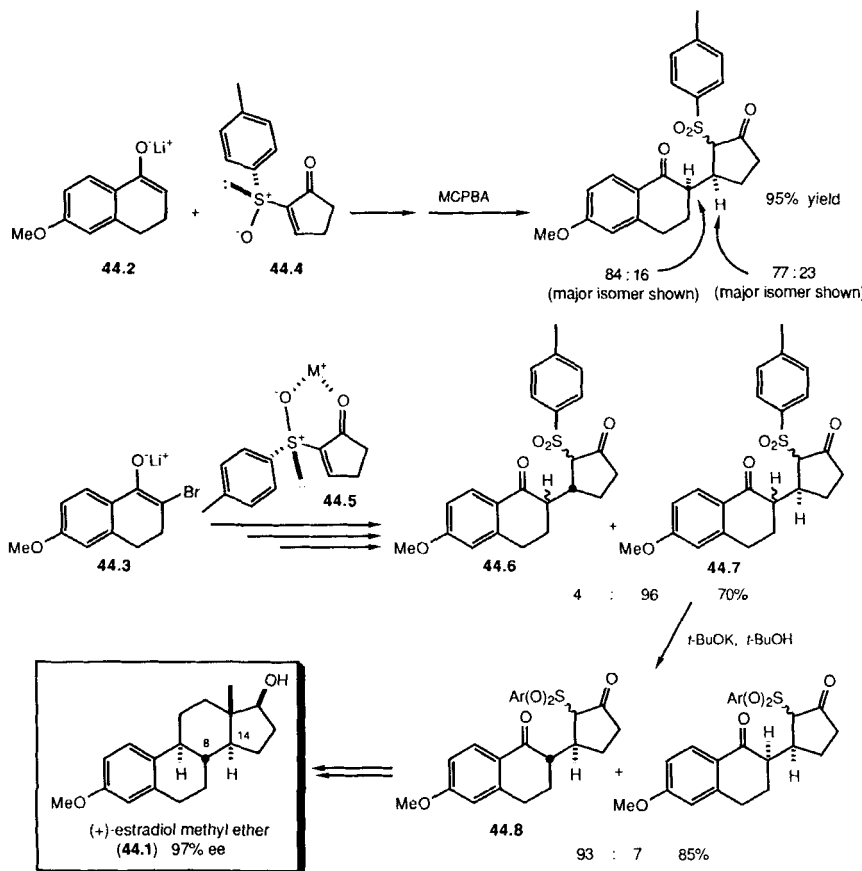
[P,P] and [P,P*] In connection with an enantioselective synthesis of aphidicolin (43.1), Holton and coworkers reported the stereoselective Michael additions of 43.2 and 43.3 to 43.4 (109) and 43.5 (12, 65, 110), respectively (Scheme 43). With 43.2 and 43.4, only one diastereomeric product (43.6) was



Scheme 43

detected, while **43.3** and **43.5** give **43.7** and **43.8** in a ratio of 88:12. The structure of **43.7** was confirmed by conversion to an intermediate of a previous synthesis of aphidicolin.

In their synthesis of (+)-estradiol methyl ether (**44.1**, Scheme 44), Posner and Switzer studied the conjugate addition of lithium enolates **44.2** and **44.3** to optically active 2-sulfinyl-2-cyclopentenones (**44.4** and **44.5**, respectively) (12, 65, 111). Addition of tetralone **44.2** occurs from the top face of **44.4** as depicted in Scheme 44. This result is rationalized by preferential attack away from the *p*-tolyl group in the conformer depicted. Use of the α -bromo-enolate **44.3** and the enantiomeric acceptor **44.5** also results in attack on the *Re* face of the acceptor. It is of note that this corresponds to a reversal of the sense of



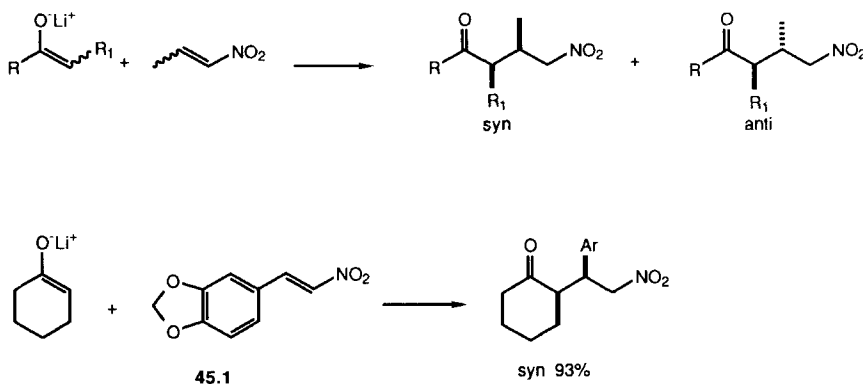
Scheme 44

facial selectivity had the same enantiomer of the acceptor been used. In this case, it is believed that attack of the more substituted enolate occurs away from the *p*-tolyl group in the chelated conformation shown.

The degree of facial selectivity observed with the less substituted enolate **44.2** is lower than with the α -bromoenolate **44.3**. For the synthesis of estradiol methyl ether, **44.3** and **44.5** were used. The sulfoxides of the initial Michael adducts were oxidized and the α -bromides were removed reductively to provide a mixture of isomers **44.6** and **44.7**. Equilibration of the stereocenter in the tetralone provided the desired isomer **44.8** with surprisingly good selectivity. This isomer was carried through to the natural product **44.1**. Overall, the synthesis occurred in 6.3% yield and with an enantiomeric excess of 97%. In this synthesis, the overall stereoselectivity is determined by the strong facial preference of **44.5** that establishes the correct absolute configuration at C-14, and the remarkable equilibration that establishes C-8 in the proper configuration.

5. To Nitroolefins

[P,P] Nitroolefins are excellent Michael acceptors owing to their low propensity for 1,2-addition and the strong anion-stabilizing ability of the nitro group. Seebach and coworkers have studied the addition of lithium enolates from ketones and aldehydes to isomeric *E* and *Z* nitropropenes (112). The results from this survey are shown in Scheme 45 and Table 17. In each pair of reactions shown in Table 17, there is a correlation of nitropropene geometry and adduct stereochemistry. Although the details were not reported, such a correlation is not observed with the lithium enolates of medium- and large-ring ketones and with 1,1,1-triphenyl-2-butanone.



Scheme 45

Table 17
Addition of Lithium Enolates of Aldehydes and Ketones to Nitroolefins
(Scheme 45)

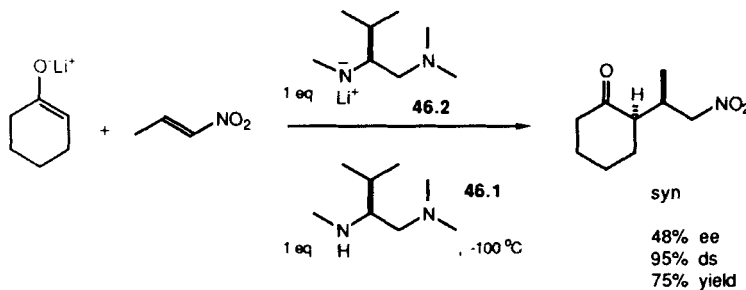
Entry	Enolate		Nitropropene <i>E/Z</i>	Syn:Anti
	R	R ₁		
1	- (CH ₂) ₃ -		<i>E</i>	85:15 ^a
2	- (CH ₂) ₃ -		<i>Z</i>	21:79 ^a
3	- (CH ₂) ₄ -		<i>E</i>	89:11 ^a
4	- (CH ₂) ₄ -		<i>Z</i>	12:88 ^a
5	H	Me	<i>E</i>	84:16 ^b
6	H	Me	<i>E</i>	3:97 ^b
7	H	Me	<i>Z</i>	16:84 ^b
8	H	Me	<i>Z</i>	71:29 ^b

a. Yields were from 60 to 80%.

b. Yields were less than 20%.

The addition of isomeric enolates derived from the enol silanes of propanaldehyde and methylolithium to *E/Z* nitropropenes proceeds in very low yields (<20%, entries 5–8, Table 17). However, in these cases stereochemistry of the Michael addition correlates with the geometry of both the enolate and the nitroolefin. A substituted nitrostyrene (**45.1**, Scheme 45) was also tried. In this case, addition of the lithium enolate of cyclohexanone to the piperonal-derived nitrostyrene **45.1** gives only the syn addition product (113). [N*,P] Conjugate addition of the lithium enolates of some methyl ketones to nitropropene in the presence of a chiral, non-racemic additive has also been reported by Seebach and coworkers (113–115). Very low ($\leq 6\%$) enantioselective excess was found.

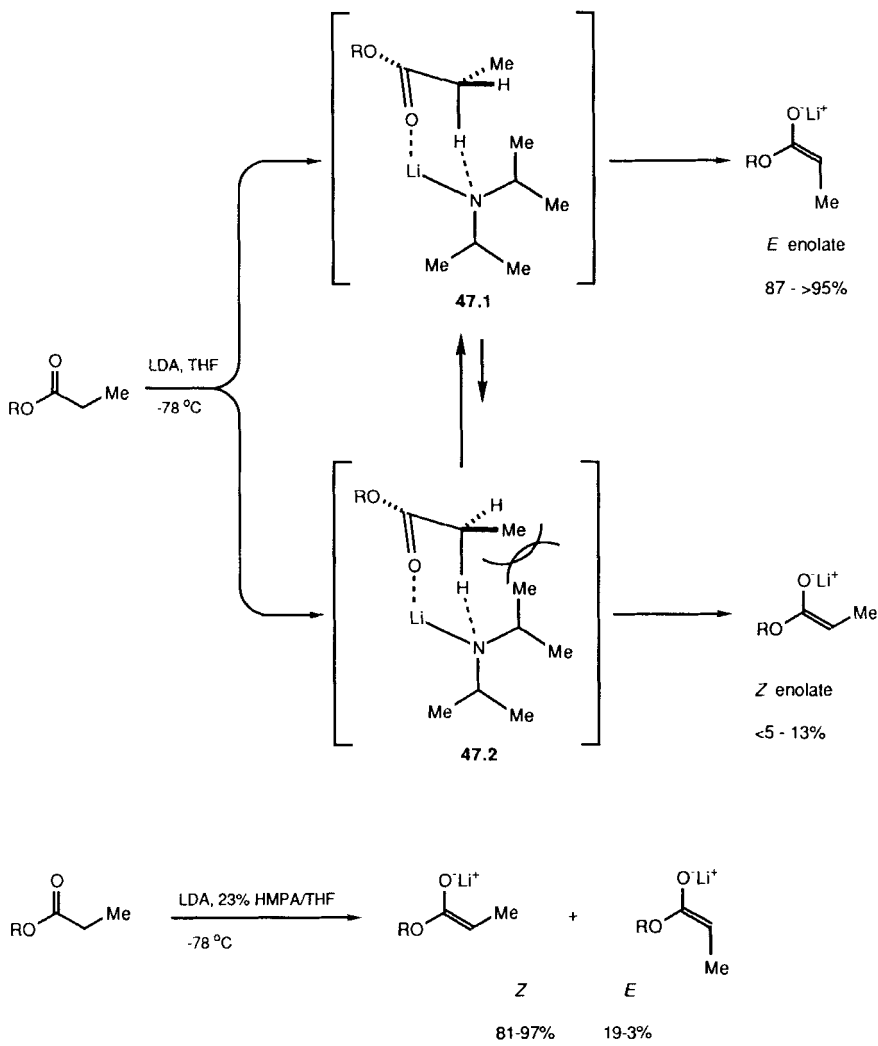
[P*,P] Better success with chiral, non-racemic additives has been achieved in the addition of prosterogenic enolates. Reaction of the lithium enolate of cyclohexanone with nitropropene in the presence of stoichiometric amounts of both amine **46.1** and its corresponding lithium amide (**46.2**) resulted in significant levels of asymmetric induction (Scheme 46) (15, 116).



Scheme 46

K. Ester Enolates

Ireland and coworkers have shown, through subsequent Claisen rearrangement of the allyl esters, that deprotonation of propionate esters with lithium dialkylamides in THF leads to *E* enolates (Scheme 47) (117). This stereochemical assignment was later confirmed by Seebach and coworkers by single-crystal X-ray analysis of the lithium enolate/THF adduct of *tert*-butyl



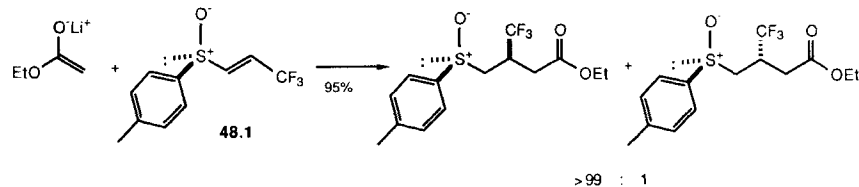
Scheme 47

propionate (116). Depending on the precise conditions used for the deprotonation of the ester, the *E/Z* ratios of the enolates prepared in this manner are from 87:13 to >95:5. A cyclic transition state has been invoked by Ireland to explain the stereochemical outcome. Thus, transition state **47.1** is sterically favored over **47.2** (Scheme 47).

Use of 23% of HMPA in THF as solvent for the deprotonation leads to high percentages of the *Z* enolate. Depending upon the precise conditions used for the deprotonation, between 81 and 97% of the resulting enolate formed has the *Z* configuration. The reasons for the strong solvent effect in the deprotonation process are still a matter of debate (118). Nevertheless, either the *Z* or the *E* enolate can be formed by varying the solvent. Unfortunately, no method has been found for generation of *Z* lithium ester enolates in the absence of HMPA. Because HMPA can influence the stereochemical outcome of the ester enolate Michael addition (*vide infra*), a degree of ambiguity exists when *E* and *Z* enolates are found to give rise to stereochemical differences. Some of this ambiguity can be alleviated by examining the effect on the stereochemical outcome of adding HMPA to the *E* enolate generated in THF.

1. To α,β -Unsaturated Sulfoxides

[N,P*] Addition of the lithium enolate of ethyl acetate to the optically active β -trifluoropropenyl tolyl sulfoxide **48.1** occurs with excellent facial selectivity (>99:1) (Scheme 48) (12, 65, 67, 82), as in the reactions of this substrate with ketone and malonate enolates (*vide supra*).



Scheme 48

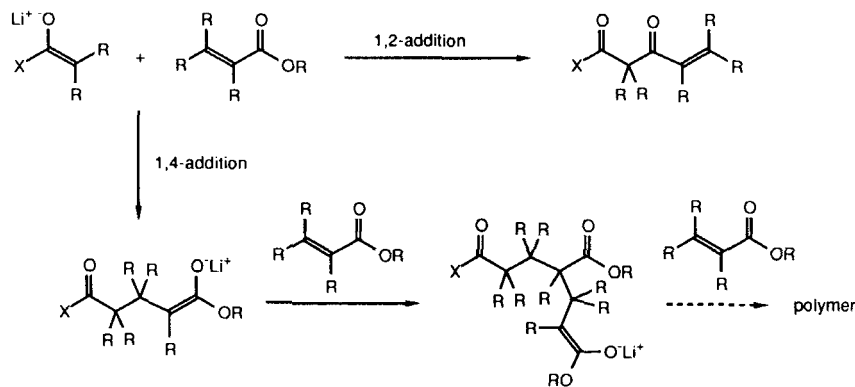
2. To α,β -Unsaturated Esters

Prior to embarking on a study of the kinetically controlled Michael addition of amide and ester enolates to α,β -unsaturated esters, Yamaguchi and co-workers explored the scope of this heretofore infrequently applied reaction (14, 119). As can be seen in Table 18 and Scheme 49, the reaction is dependent on the substitution pattern of both the enolate and enoate and on whether an amide or an ester enolate is used.

Table 18
Reaction of Ester and Amide Enolates with Crotonates

Entry	Lithium Enolate					
1		polymer	polymer	1,4	N.R. ^a	N.R. ^a
2		1,4	1,4	1,4	1,4	N.R. ^a
3		1,4	1,4	1,4	N.R. ^a	N.R. ^a
4		1,4	1,4	1,4	1,4	N.R. ^a
5		1,4	1,4	1,4	1,4	N.R. ^a
6		1,4	b	b	b	b

a. No reaction or 1,2-addition. b. Not examined.



Scheme 49

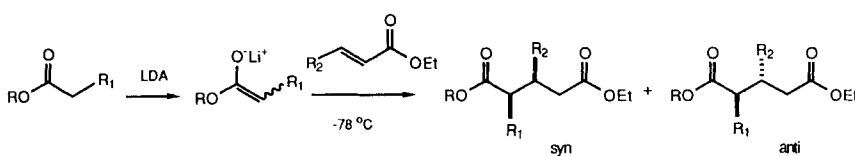
By examining the table, it can be seen that Michael addition (1,4-addition) is favored over Claisen condensation (1,2-addition) in all cases except those in which the activated olefin is trisubstituted. As might be anticipated, the more reactive amide enolates give 1,4-addition in certain instances where 1,4-addition is unfavorable with ester enolates (compare entry 1 with 2 and 3 with 4).

Polymerization limits the scope of the reaction when the acceptor is unsubstituted at the β -position (acrylates and methacrylates) and the enolate formed compares in reactivity to the starting enolate. Thus amides enolates, when added to enoates, are less prone to induce polymerization than ester enolates (Entries 1 and 2, Table 18).

[P,P] The addition of prostereogenic ester enolates to prostereogenic enoates was also studied by Yamaguchi and coworkers (32). The results of this study are summarized in Scheme 50 and Table 19. The Z enolates prepared by deprotonation of ethyl esters in the presence of HMPA give anti diastereomers with high selectivity. Interestingly, if the ethyl ester is deprotonated using LDA in THF (thereby forming the E enolate) followed by the addition of HMPA, subsequent Michael addition gives the anti diastereomers with selectivity approaching that obtained when Z enolate formed in HMPA is used (compare entries 1 and 2, Table 19). In the absence of HMPA, the E enolate from ethyl propionate gives a low preference for the anti diastereomer (entry 3), indicating that, at least with the E enolate, HMPA promotes formation of the anti diastereomer.

Groups R₁ of the enolate and R₂ of the acceptor have little effect on product stereochemistry. If substituent R₂ of the enoate is phenyl or carboethoxy, slightly diminished selectivity results (entries 6, 7, and 11; Table 19).

In THF, the nature of the alkoxy group (RO) of the enolate has a dramatic effect on the stereochemical outcome (compare entries 3 and 13, Table 19). Whereas the ethyl ester gives the anti diastereomer with but modest selectivity, the *tert*-butyl ester gives excellent syn selectivity. Hence, by changing the solvent and the alkoxy group of the enolate, either the anti or the syn diastereomer were obtained with selectivities greater than 95%. Yamaguchi's work further illustrates an important property of the kinetically-controlled Michael addition; in general, *E* lithium enolates give *syn* Michael adducts and *Z* lithium enolates give *anti* adducts. This tendency is amplified by the presence of larger alkoxy groups on the enolate (RO- in Scheme 50).



Scheme 50

Table 19
Addition of Lithium Ester Enolates to α,β -Unsaturated Esters (Scheme 50)

Entry	Ester R	Enolate R ₁	Enolate E/Z	Enoate R ₂	Solvent	Yield ^a %	Anti/Syn ^b
1	Et	Me	Z	Me	THF-hexanes-HMPA ^c	82	>95:5
2	Et	Me	E	Me	THF-hexanes-HMPA ^d	87	90:10
3	Et	Me	E	Me	THF-hexanes	96	76:24
4	Et	Me	Z	n-C ₄ H ₉	THF-hexanes-HMPA ^c	95	>95:5
5	Et	Me	Z	n-C ₇ H ₁₅	THF-hexanes-HMPA ^c	86	>95:5
6	Et	Me	Z	Ph	THF-hexanes-HMPA ^c	85	94:6
7	Et	Me	Z	CO ₂ Et	THF-hexanes-HMPA ^c	62	74:26
8	Et	Et	Z	Me	THF-hexanes-HMPA ^c	87	>95:5
9	Et	Et	Z	n-C ₇ H ₁₅	THF-hexanes-HMPA ^c	83	>95:5
10	Et	Et	Z	Ph	THF-hexanes-HMPA ^c	90	>95:5
11	Et	Et	Z	CO ₂ Et	THF-hexanes-HMPA ^c	62	86:14
12	Et	n-C ₈ H ₁₇	Z	Me	THF-hexanes-HMPA ^c	78	>95:5
13	t-Bu	Me	E	Me	THF-hexanes	84	<5:95
14	t-Bu	Me	E	n-C ₄ H ₉	THF-hexanes	61	<5:95
15	t-Bu	Me	E	n-C ₇ H ₁₅	THF-hexanes	67	<5:95

a. The yield reported is for products which were purified by distillation. Purities obtained (GLC) were from 80 to >95%.

b. Determined by ¹³C NMR.

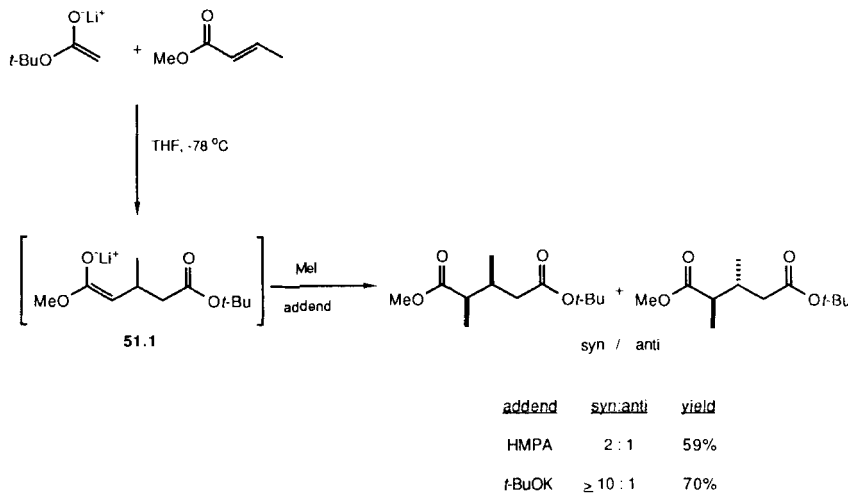
c. 23% HMPA was added to the LDA prior to the addition of the ester.

d. 23% HMPA was added after the deprotonation of the ester.

The kinetically controlled Michael addition of an enolate to an acceptor results in the formation of a new enolate (51.1 in Scheme 51). This enolate is usually protonated in work-up, but it can also be intercepted with other electrophiles (120). Although the initial adduct of *tert*-butyl lithioacetate and methyl crotonate does not react with methyl iodide, addition of either HMPA or potassium *tert*-butoxide results in the formation of alkylated products. With HMPA, a 2:1 (syn/anti) mixture of diastereomers is formed. A 10:1 (syn/anti) mixture is obtained by use of potassium *tert*-butoxide in the methylation step (Scheme 51).

Sequential Michael addition and intramolecular alkylation may be used to prepare ring compounds (Scheme 52, Table 20). For the formation of three-, five-, and six-membered rings, trans products are produced exclusively. The stereochemistry at the exocyclic stereocenter is determined by the initial Michael addition. Again, the presence of HMPA results in anti selectivity in the initial step (entries 3, 6, and 10) whereas syn diastereomers are favored in THF (entries 2, 5, and 9).

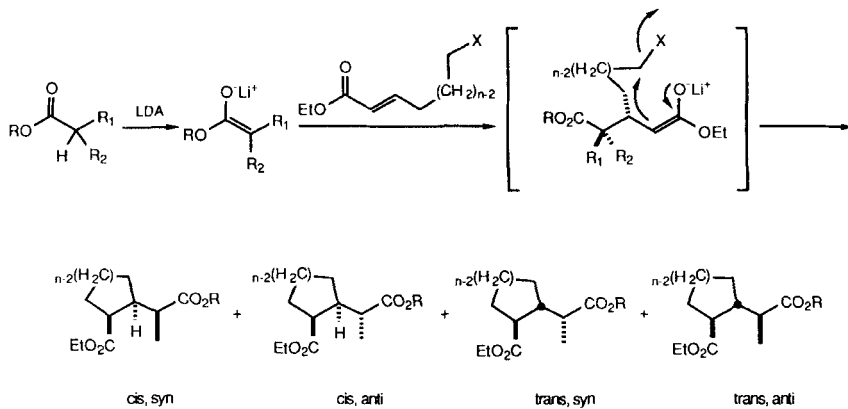
Seven-membered rings form more slowly than the smaller rings; in this case, it is necessary to dilute and warm the reaction mixture (entries 12-14, Table 20). The higher reaction temperatures needed for the 7-exo-tet closure



Scheme 51

apparently allows for concurrent epimerization (120). Use of potassium acetate rather than potassium *tert*-butoxide alleviates this problem and leads to a single isomer (compare entries 12 and 13) (14).

[P*,N] Inouye and coworkers have examined the asymmetric Michael addition/intramolecular alkylation of menthyl α -chloroacetate and menthyl α -chloropropionate to acrylates and methacrylates (121). For example, con-



Scheme 52

Table 20
Sequential Michael Addition/Alkylation of Lithium Ester Enolates and
Halo- α,β -unsaturated Esters (Scheme 52)

Entry	R	Enolate R ₁	Solvent	Enoate n X	Temp. °C	Yield ^a %	Cis:Trans	Anti:Syn
		R ₂						
1	t-Bu	H	H	THF	1	Br	-78	84 ^b
2	t-Bu	H	Me	THF	1	Br	-78	76 ^b
3	t-Bu	Me	H	THF:HMPA	1	Br	-78	89 ^b
4	t-Bu	H	H	THF	3	I	-78	84
5	t-Bu	H	Me	THF	3	I	-78	100
6	t-Bu	Me	H	THF:HMPA	3	I	-78	100
7	Et	Me	Me	THF	3	I	-78	95
8	t-Bu	H	H	THF	4	I	-78	94
9	t-Bu	H	Me	THF	4	I	-78	100
10	t-Bu	Me	H	THF:HMPA	4	I	-78	100
11	Et	Me	Me	THF	4	I	-78	80
12	t-Bu	H	H	THF	5	I	-78 to 0	58 ^c
13	t-Bu	H	H	THF	5	I	-78 to 0	40
14	t-Bu	H	Me	THF	5	I	-78 to 0	60 ^c
								50:50 ^d

a. The yields are for products purified by short-path distillation.

b. The addition of potassium *tert*-butoxide was not needed.

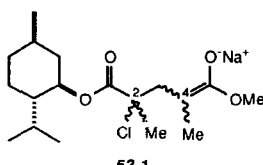
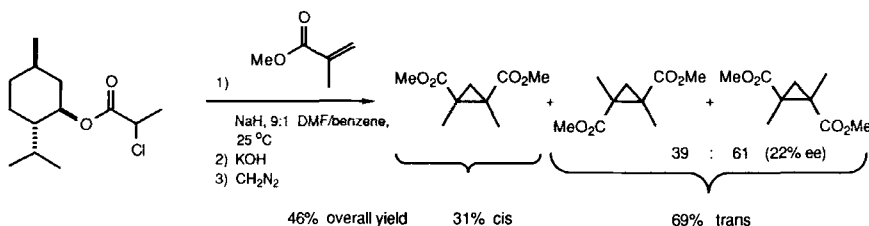
c. Dilution to 0.005 M and warming to 0 °C was necessary.

d. The structural assignment is tentative.

e. Potassium acetate rather than potassium *tert*-butoxide was used.

densation of menthyl α -chloropropionate with methyl methacrylate followed by saponification and esterification results in a 31:69 (cis/trans) mixture of cyclopropanes (Scheme 53). The trans isomer is formed with a 22% enantio-meric excess.

Although only low levels ($\leq 22\%$ ee) of asymmetric induction were found in the resulting 1,2-cyclopropanedioates, an interesting relationship between

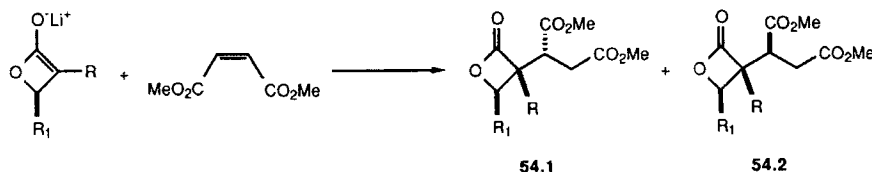


Scheme 53

solvent polarity and the enantiomeric excess was observed. The highest levels of asymmetric induction were obtained in most polar reaction media. In non-polar solvents, a strong preference for the formation of cis cyclopropanes was seen (122). The Inouye results represent an interesting case of facial selectivity in the donor enolate. The intermediate **53.1** has a new stereocenter (C-2) that is presumably established in some diastereomeric excess. The second step, intramolecular alkylation, can preserve this diastereomeric excess or it can "neutralize" it by giving the meso cis isomer. It is not known to what degree the initial enolate formation is stereoselective and how the solvent effect is partitioned among enolate formation, Michael addition, and alkylation.

[P*,P] Mulzer and coworkers have studied the addition of chiral β -lactone enolates to dimethyl maleate (Scheme 54, Table 21) (123). The β -lactone enolate is attacked exclusively from the face opposite the directing alkyl group (R_1), independent of R . Good to excellent syn selectivity was found; the greatest diastereofacial preference was seen with the methyl substituted enolate in entry 4.

In connection with the total synthesis of 7,20-diisocyanojadociane (*vide supra*), Corey and Peterson have described the addition of the *E* lithium enolates derived from menthol, neomenthol, and 8-phenylmenthol propionates (**55.1**, **55.2**, and **55.3**, Scheme 55) to (*E*)- and (*Z*)-methyl crotonates (124). The Michael additions were performed by adding the crotonate to the ester enolate at -100°C . The results from this study are summarized in Table 22.

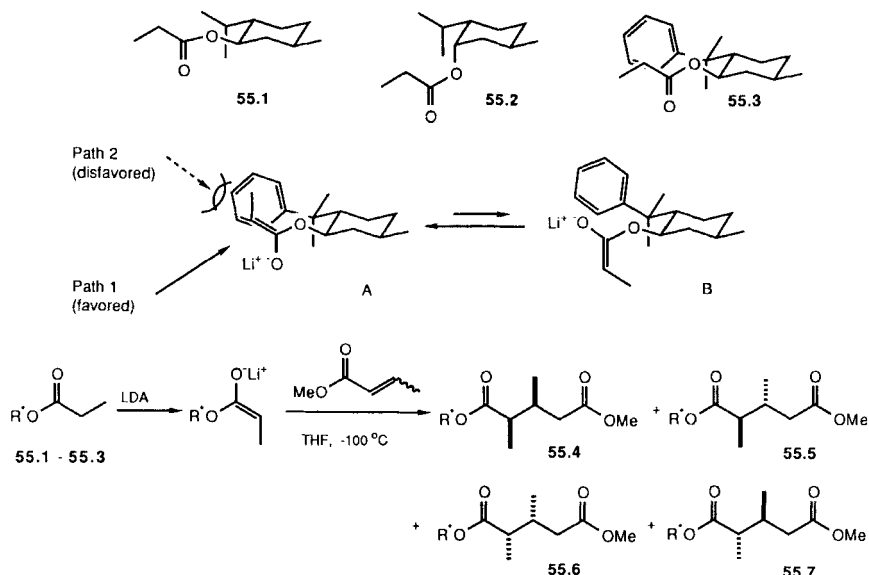


Scheme 54

Table 21
Addition of β -Lactone Enolates to Dimethyl Maleate (Scheme 54)

Entry	Enolate		Yield %	Product 54.1:54.2
	R	R_1		
1	Ph	<i>t</i> -Bu	73	89:11
2	Ph	<i>i</i> -Pr	68	82:18
3	Ph	Me	50	85:15
4	Me	<i>t</i> -Bu	45	100:0 ^a

a. No minor diastereomer could be detected.



Scheme 55

Table 22
Addition of Chiral Propionates to Methyl Crotonates (Scheme 55)

Entry	Ester	Methyl Crotonate	Yield %	(55.4+55.6):(55.5+55.7) ^a	(55.4:55.6)	(55.5:55.7)
1	55.1	<i>E</i>	80	88:12	78:22	b
2	55.2	<i>E</i>	b	80:20	67:33 ^c	50:50
3	55.3	<i>E</i>	75-79	90:10	95:5	b
4	55.3	Z	54	25:75	52:48 ^c	87:13

a. Ratio determined by capillary GLC.

b. Not reported.

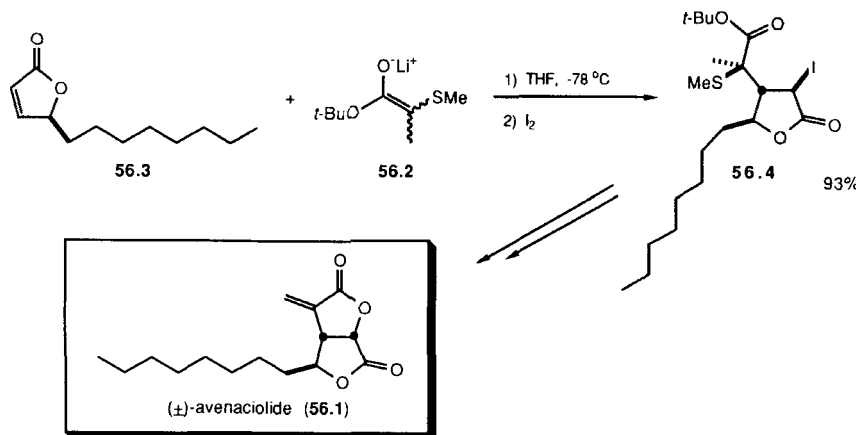
c. Identity of major diastereomer not reported.

The *E* propionate enolates give predominantly the syn diastereomers with (*E*)-methyl crotonate (entries 1–3, Table 22). A trend towards greater simple selectivity is observed in the series: neomenthol (the axial hydroxy isomer of menthol), menthol, 8-phenylmenthol. This variation is probably a manifestation of changes in steric bulk along this series as the selectivity in the addition of *E* ester enolates to α,β -unsaturated esters is strongly dependent on the bulk of the alkoxy group (*vide infra*).

8-Phenylmenthol, although less readily available (125), is by far the most effective auxiliary studied by Corey and Peterson. The diastereofacial selec-

tivity observed is in accord with approach of the acceptor to enolate conformer A via path 1, away from the blocking influence of the dimethylphenyl group (126). Corey and Peterson also examined the stereochemical influence of the double bond geometry of the crotonate (compare entries 3 and 4, Table 22). Whereas the *E* crotonate gives 90% syn adducts, the *Z* crotonate gives 75% of anti adducts.

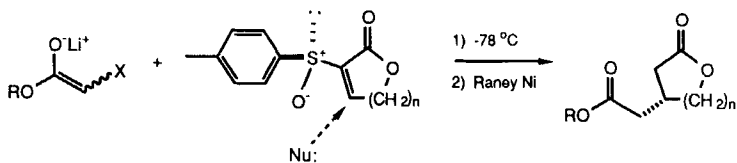
[P,P*] In connection with the synthesis of (\pm)-avenaciolide (56.1), Schlesinger and coworkers have examined the Michael addition of the lithium enolate of *tert*-butyl α -thiomethylpropionate (56.2) to unsaturated lactone 56.3 (Scheme 56) (127). The enolate generated by the conjugate addition was oxidized with iodine to form the iodolactone 56.4 as the only product. Overall, the conversion of 56.3 to 56.1 proceeds in 70% yield.



Scheme 56

3. To α,β -Unsaturated α -Sulfinyl Lactones

[N,P*] and [P,P*] Addition of the lithium enolates of acetates and α -thioarylacetates to optically active α,β -unsaturated α -sulfinyl lactones has been reported by Posner and coworkers (12, 65, 128). By suitable modification of the enolate, excellent enantiomeric excesses were achieved (Scheme 57, Table 23). No information about the simple selectivity with the α -thioaryl esters (entries 3, 4, and 7–9) was provided. The optimum choice of the ester is different for five- and six-membered ring lactones (compare entry 4 with 5 and 8, Table 23). Slightly higher levels of stereochemical differentiation were found with the larger-ring lactone acceptors. The sense of the enantioselectiv-



Scheme 57

Table 23
Addition of Ester Enolates to α,β -Unsaturated- α -Sulfinyl Lactones (Scheme 57)

Entry	R	Enolate X	Lactone n	Yield ^a %	ee ^a %
1	Me	H	1	65	80
2	t-Bu	H	1	82	43
3	Me	PhS	1	100	91
4	MEM ^b	PhS	1	79	78
5	MEM ^b	H	2	62	>96
6	t-Bu	H	2	92	63
7	Me	PhS	2	92	91
8	MEM ^b	PhS	2	94	>96
9	t-Bu	p-MeC ₆ H ₄ S	2	29	88

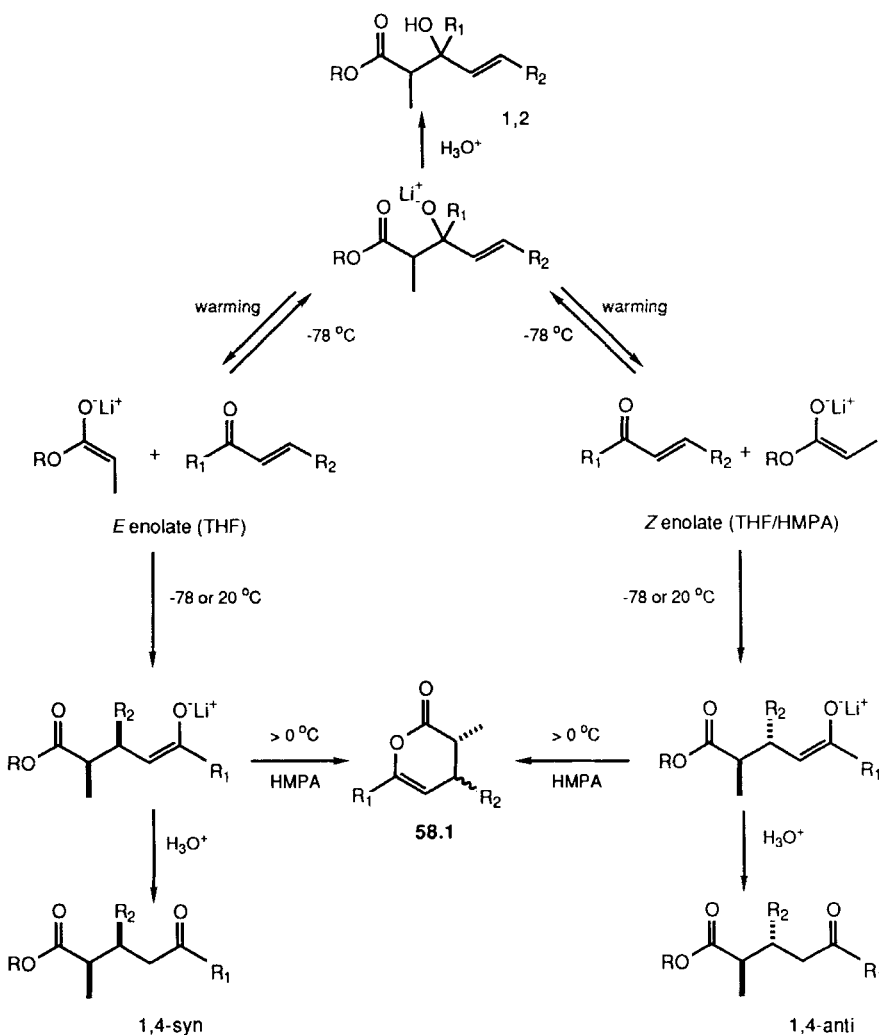
a. For the desulfurized products.

b. Methoxyethyl ester.

ity of the reaction is rationalized by preferential attack on the diastereotopic face of the sulfoxide opposite the aryl group in the conformer depicted (Scheme 57).

4. To α,β -Unsaturated Ketones

[P,P] Addition of the lithium enolates of esters to a variety of α,β -unsaturated ketones has been examined (88) (129). The results of this study are summarized in Scheme 58 and Table 24. With only a few exceptions, the ratio of enolates correlates well with the sense and degree of the stereochemical outcome. The strong correlation between enolate ratio and adduct stereochemistry suggests that *E* enolates give only syn products whereas *Z* enolates provide exclusively the anti adducts. The degree of diastereoselectivity obtained is limited only by the ability to generate enolates in an isomerically homogeneous manner.



Scheme 58

In many instances, 1,2-addition to α,β -unsaturated ketones is merely an inconvenience in the Michael addition. Warming the reaction mixture usually causes equilibration of the initially formed aldolates to the conjugate addition products. The limitation of this strategy for stereoselective Michael additions of ester enolates is adumbrated by the precipitous drop in selectivity found for the room temperature reactions of the *E* lithium enolate of *tert*-

Table 24
Addition of Ester Enolates to α,β -Unsaturated Ketones (Scheme 58)

Entry	Enolate R	Enolate E:Z	Enone R ₁	Enone R ₂	Solvent	Temp. °C.	Yield %	1,2:1,4	syn:anti
1	t-Bu	E ^a	i-Pr	Me	THF	-78	54	85:15	---
2	t-Bu	E ^a	i-Pr	Me	THF	20	68	<3:97	70:30 ^b
3	t-Bu	Z ^a	t-Bu	Me	THF/HMPA	-78	73	<3:97	13:87
4	t-Bu	E ^a	t-Bu	Me	THF	-78	85	<3:97	95:5
5	t-Bu	E ^a	t-Bu	Me	THF/HMPA ^c	-78	89	<3:97	95:5
6	t-Bu	12:88	t-Bu	Et	THF/HMPA	-78	49	<3:97	5:95
7	t-Bu	94:6	t-Bu	Et	THF	-78	86	<3:97	91:9
8	t-Bu	Z ^a	t-Bu	i-Pr	THF/HMPA	-78	88	14:86	7:93
9	t-Bu	E ^a	t-Bu	i-Pr	THF	-78	87	31:69	92:8
10	t-Bu	E ^a	t-Bu	i-Pr	THF	0	73	<3:97	86:14
11	t-Bu	Z ^a	t-Bu	t-Bu	THF/HMPA	-78	0	---	---
12	t-Bu	Z ^a	t-Bu	t-Bu	THF/HMPA	25	25	<3:97	<3:97
13	t-Bu	E ^a	t-Bu	t-Bu	THF	-78	65	>97:3	---
14	t-Bu	E ^a	t-Bu	t-Bu	THF	25	46	<3:97	38:62
15	t-Bu	11:89	t-Bu	Ph	THF/HMPA	-78	88	14:86	7:93
16	t-Bu	11:89	t-Bu	Ph	THF/HMPA	25	76	<3:97	11:89
17	t-Bu	95:5	t-Bu	Ph	THF	-78	95	40:60	94:6
18	t-Bu	95:5	t-Bu	Ph	THF	25	96	<3:97	94:6
19	t-Bu	E ^a	t-Bu	Ph	THF/HMPA ^c	-78	96	30:70	79:21
20	t-Bu	E ^a	mesd	Me	THF	-78	87	<3:97	>95:5
21	Et	Z ^a	mesd	Me	THF/HMPA	-78	65	<3:97	12:88
22	Et	Z ^a	tris ^e	Me	THF/HMPA	-78	65	<3:97	35:65
23	Et	E ^a	mesd	Me	THF	-78	79	<3:97	70:30
24	Et	E ^a	tris ^e	Me	THF	-78	90	<3:97	80:20
25	t-Bu	Z ^a	tris ^e	Me	THF/HMPA	-78	87	<3:97	30:70
26	t-Bu	E ^a	mesd	Me	THF	-78	87	<3:97	>95:5
27	t-Bu	E ^a	tris ^e	Me	THF	-78	85	<3:97	95:5
28	-(CH ₂) ₄ O- ^f	t-Bu	Ph		THF	-78	67	<3:97	50:50

a. Ratio not determined.

b. Structure of diastereomers not assigned.

c. HMPA added to the reaction mixture after formation of the E enolate in THF.

d. 2,4,6-Trimethylphenyl.

e. 2,4,6-Triisopropylphenyl.

f. The lithium enolate of δ -valerolactone was used.

butyl propionate with substrates that give a large percentage of 1,2-addition at low temperature (entries 1-2, 9-10 and 13-14, Table 24). In these cases, the high propensity for 1,2-addition provides a manifold for rapid E/Z equilibration of the enolates via aldol-retroaldol additions (130). Following the Curtin-Hammett principle (131), the stereochemical outcome of the addition process would not be wholly determined by the diastereomeric transition states for a given enolate, but instead by the energy difference between the most stable aldolate and the lowest energy transition states. In these situations, the stereoselectivity drops significantly.

Direct comparison of the results from E and Z enolates is complicated by the presence of HMPA, necessary for the generation of the Z ester enolates. It could be argued that the stereochemical correlation between enolate geome-

try and adduct stereochemistry is a result of the presence of HMPA in the reactions of the *Z* enolates. However, the addition of HMPA to the *E* enolate in THF (entries 4 and 5, 17 and 19; Table 24) results in no significant change in the stereoselectivity of the reaction. The tentative conclusion is that the stereochemical correlation is a function of the enolate geometry and not a result of a solvent effect.

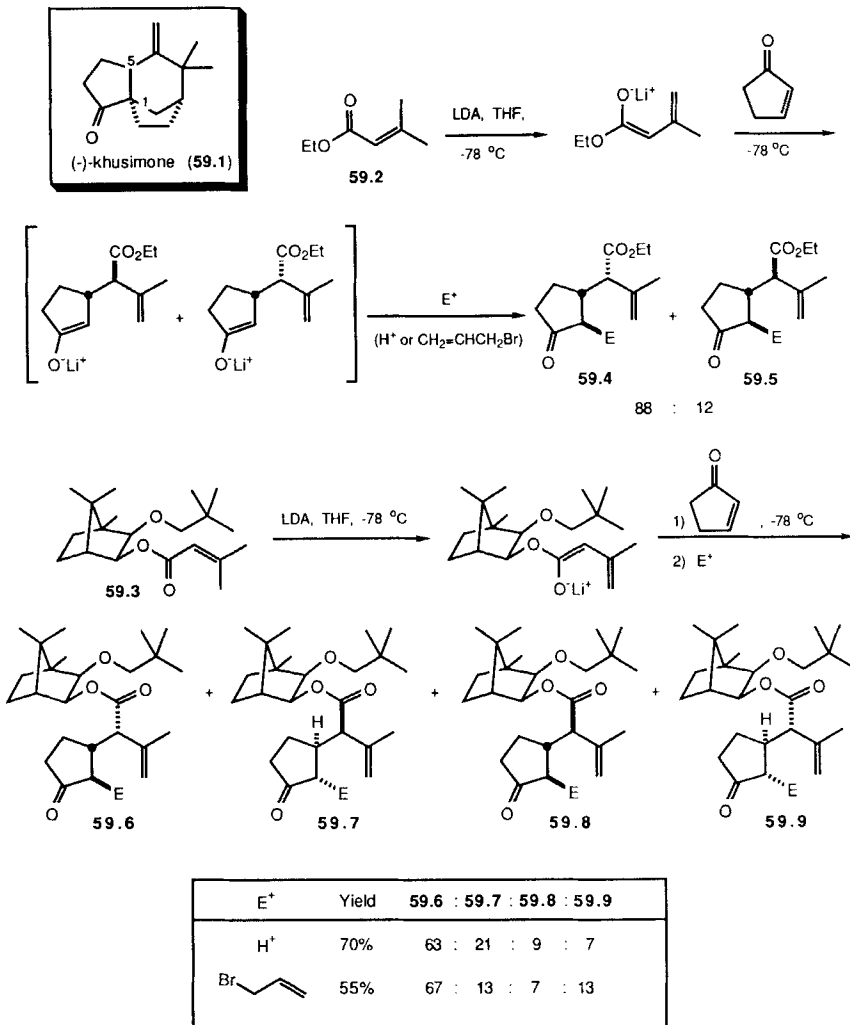
With *tert*-butyl enones ($R_1 = t\text{-Bu}$, Scheme 58, Table 24), HMPA severely retards 1,2-addition. In only one instance (entry 15) is any 1,2-addition product observed in this situation. Additionally, when reaction mixtures that contain HMPA are warmed to room temperature, significant amounts of the enol lactones of the general structure **58.1** are produced. The formation of **58.1** requires that the Michael addition products be *Z* enolates.

With *E* enolates, the stereoselectivities obtained with smaller alkoxy groups (ethyl esters and lactones) are lower than those observed with *tert*-butyl esters (compare entries 23 and 24 with 26 and 27; and entry 28 with 17 and 18, Table 24). To some extent, this drop in selectivity can be overcome by using very large substituents at R_1 of the enone (compare entries 23 and 24).

Trialkylsilyl ketene acetals can be added to α,β -unsaturated ketones under the action of a catalytic amount of tris(dimethylamino)sulfonium difluorotrimethylsiliconate (TASF). The reactive species in these reactions is believed to be an enolate with either a "naked" sulfonium or a pentavalent silicon counterion. This reaction generally is not stereoselective, usually producing a 1:1 mixture of diastereomers (132).

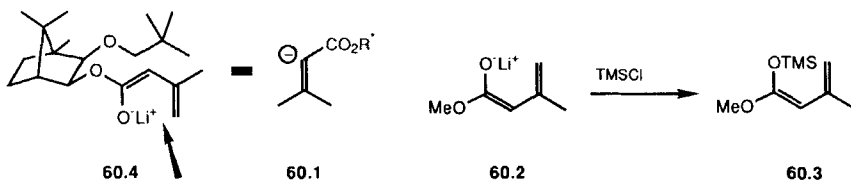
[P,P] and [P*,P] In connection with the synthesis of (−)-khusimone (**59.1**), Oppolzer and coworkers have explored the Michael addition-alkylation of the lithium dienolates derived from senecioates **59.2** and **59.3** to cyclopentenone (Scheme 59) (133). For the purpose of the synthesis, only the configuration of the newly formed stereocenters at C-5 and C-1 (khusimone numbering) is important. The Michael addition of the dienolate of ethyl senecioate (**59.2**) to cyclopentenone provides a mixture of **59.4** and **59.5** (88:12) in 70% yield. Reaction of the enolate formed in the Michael addition with allyl bromide results in exclusive formation of the trans isomers in slightly lower yield (56%).

Facial discrimination was achieved with the dienolate derived from the chiral, non-racemic senecioate **59.3** (Scheme 59). Addition of this dienolate to cyclopentenone followed by rapid protonation produces a 63:21:9:7 mixture of diastereomers (**59.6**:**59.7**:**59.8**:**59.9**) in 70% yield. No change in the stereochemistry occurs on warming the reaction mixture to -20°C for 3 hours. When the enolate product from **59.3** is trapped with allyl bromide, a 67:13:7:13 mixture (**59.6**:**59.7**:**59.8**:**59.9**) of diastereomers is formed in 55% yield (Scheme 59). The difference in stereoselectivity between reactions in which the enolate is protonated and allylated probably results from equili-



Scheme 59

bration or preferential alkylation of some of the diastereomeric enolates. Since the stereocenter adjacent to the ester is unimportant for the subsequent synthesis, both **59.6** and **59.8** could be used for the subsequent synthesis. The structure assignment was confirmed by conversion of **59.6** and **59.8** to (*-*)-khusimone and **59.7** and **59.9** to (*+*)-khusimone. Formally, the dienolate used in the Michael addition in this synthesis is equivalent to vinyl anion **60.1** (Scheme 60).



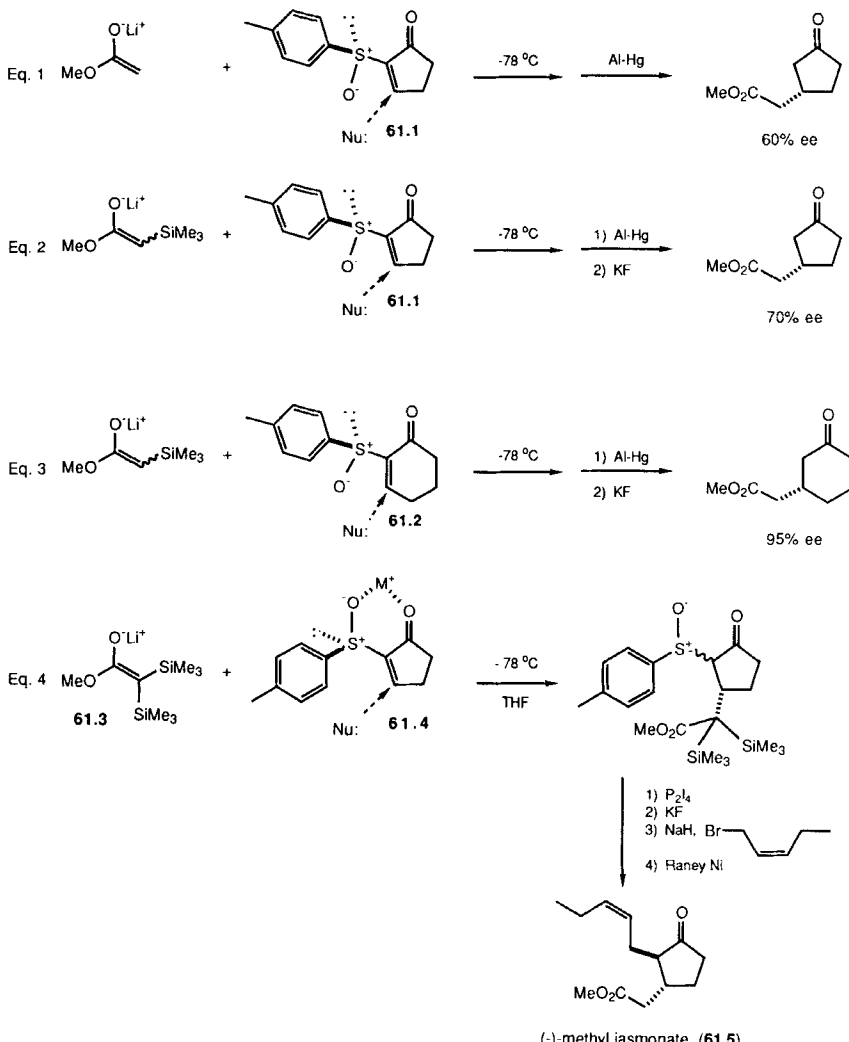
Scheme 60

As part of this study, the stereochemistry of the methyl senecioate enolate **60.2** was assigned (Scheme 60). After trapping enolate **60.2** with trimethylsilyl chloride, difference NOE spectral measurements resulted in assignment of the *Z* configuration to ketene acetal **60.3** (134). Thus, the stereochemical outcome of the Michael addition of dienolate **60.4** to cyclopentenone is consistent with attack avoiding shielding effects of the neopentyloxy group to the *Si* face of the enolate in the conformation shown.

5. To α,β -Unsaturated α -Sulfinylcycloalkanones

[N,P*] and [P,P*] Posner and coworkers found that addition of the lithium enolates of methyl acetate and methyl α -trimethylsilylacetate to enantiomerically pure α,β -unsaturated α -sulfinylcyclopentenone and -cyclohexenone leads, after desulfurization, to a mixture of enantiomeric (3-cycloalkanone)acetic esters (12, 65, 128). In these instances, the major enantiomer results from nucleophilic attack of the enolate away from the *para*-tolyl substituent in Scheme 61 (**61.1** and **61.2**). Improved selectivity was achieved by adding an α -silyl substituent to the ester (compare Eq. 1 with 2 and 3). The stereoselectivity of the reactions is dependent on the ring size of the cycloalkenone used (compare Eqs. 2 and 3, Scheme 61).

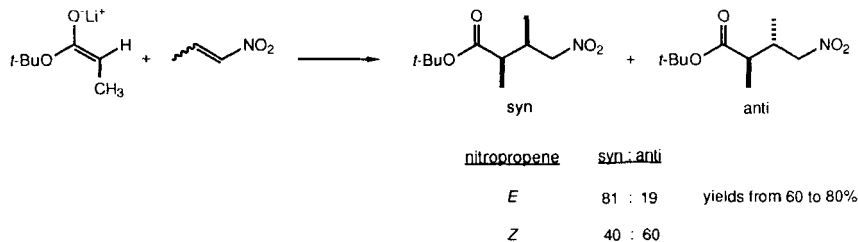
The sense of the stereochemical outcome of the addition of the lithium enolate of methyl α,α -bistrimethylsilylacetate (**61.3**) to **61.4** is reversed relative to the less substituted enolates (Eq. 4, Scheme 61) (135, 136). The effect of the trimethylsilyl groups is striking and mystifying. As seen by comparison of Eqs. 1 and 2, addition of a single trimethylsilyl group results in a moderate enhancement of diastereofacial selectivity in addition to **61.1**. Addition of a second such group causes complete reversal of the diastereofacial preference of the chiral, non-racemic acceptor. It was suggested that the latter reaction proceeds through a chelated form of the acceptor, as shown (**61.4**). Another possibility, however, is that the reaction shown in Eq. 4 is under thermodynamic control. This approach has been applied to an enantioselective synthesis of (−)-methyl jasmonate (**61.5**).



Scheme 61

6. To Nitroolefins

[P,P] Seebach and coworkers found that the stereochemistry of the Michael adducts formed from the *E* lithium enolate of *tert*-butyl propionate and isomeric nitropropenes depends on the geometry of nitropropenes used (112). The results of this study are summarized in Scheme 62. In these examples,



Scheme 62

(*E*)-1-nitropropene shows a modest preference for formation of the syn adduct, but the reaction of (*Z*)-1-nitropropene is essentially stereorandom.

[N*,P] Michael addition of the lithium enolate of *tert*-butyl acetate to nitropropene in the presence of chiral, non-racemic additives was also examined by these workers (113, 114, 115). Although no enantiomeric excesses were reported, the low observed rotation of the product (+0.10°) suggests that little asymmetric induction was achieved.

[P*,P] Calderari and Seebach have studied the Michael addition of the lithium enolates derived from chiral, non-racemic lactones 63.1–63.3 to nitroolefins (137, 138). Lactones 63.1–63.3 are readily available from starting materials in the “chiral pool”. The results of this study are summarized in Scheme 63 and Table 25. The products result from attack of the nitroolefin on the lactone face opposite the *tert*-butyl group. With the exception of the β-nitrostyrene (entry 3), selectivities with (*E*)-1-nitropropene are excellent. After recrystallization, the adducts are obtained in isomerically pure form. As in the [P,P]-type reaction, the *E* nitroolefin shows good stereoselectivity, but the *Z* isomer does not (compare entries 1 and 2, Table 25).

The foregoing approach is also applicable to the amino acid derived esters in Eqs. 1–3 (Scheme 63). The products were obtained with excellent diastereomeric excesses. Unfortunately, none of the stereostructures of these products were assigned. It is believed, however, that reaction of the cyclic enolate occurs on the same face as has been established for other electrophiles. The partial structures are probably as shown in Eqs. 1–3; no information is available about the side-chain stereocenters.

L. Phenylacetonitrile Anion

1. To α,β -Unsaturated Ketones

The addition of phenylacetonitrile to the bicyclic α,β -unsaturated ketones 64.1 (R = H, Me) has been explored by Seyden-Penne and coworkers

Table 25
Addition of Chiral Non-racemic Lactone Enolates to Nitroolefins (Scheme 63)

Entry	Enolate R	Nitroolefin R ₁	Nitroolefin E/Z	Yield %	ds %
1	Me	Me	E	61	93
2	Me	Me	Z	a	65 ^b
3	Me	Ph	E	57	55
4	Me	Me	E	58	93 ^c
5	Me	Et	E	55	92 ^c
6	Me	CH ₂ Br	E	45	>95 ^c
7	Me	H	E	70	>98 ^c
8	Ph	Me	E	40	92
9	CH ₂ CO ₂ Li	Me	E	38	85

a. No yield was reported.

b. The major product has the same configuration as is obtained with the *E* nitroolefin.

c. The enantiomeric lactone was used, hence the product has the opposite configuration.

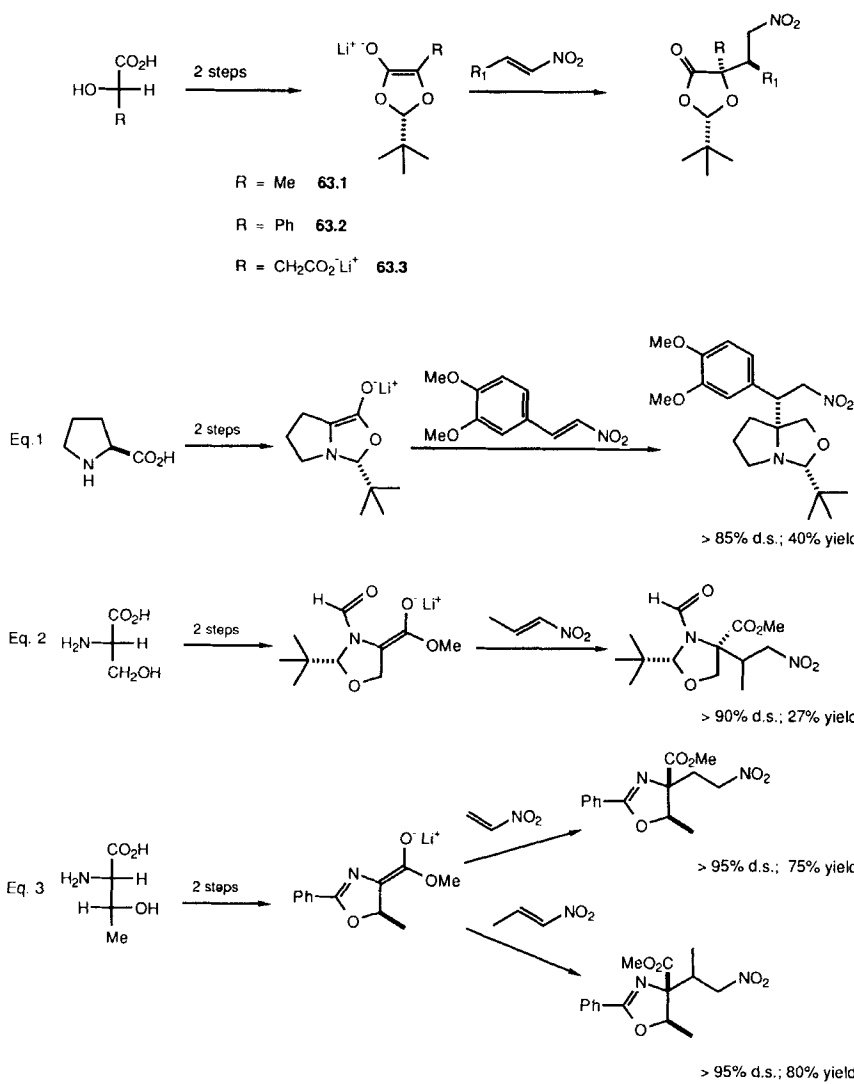
(Scheme 64, Table 26) (139, 140). With **64.1** exclusive formation of cis-fused adducts with little simple selectivity (entries 1 and 2, Table 26) in either THF or THF/HMPA was noted. The cis ring fusion is also obtained from the reaction with 10-methyloctalone **64.1** (R = Me). In this case, only diastereomer **64.2** is formed. When THF/HMPA is used in place of THF as solvent, no addition products are obtained.

M. Vinylogous Carbamates

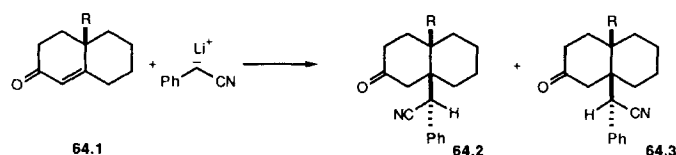
1. To α,β -Unsaturated Esters

[P,P] The Schlessinger group has shown that the enolates of *N,N*-disubstituted vinylogous carbamates are surprisingly selective in aldol-lactonization reactions (141). Recently, these workers have extended their studies to the Michael addition and Michael addition/alkylation reactions of vinylogous carbamates (142). The results of this investigation are summarized in Scheme 65 and Table 27.

Deprotonation of vinylogous carbamates **65.1** and **65.2** had previously been shown to give *Z,E* dienolates (143). Dimethyl maleate reacts with the enolate of methyl ester **65.1** to give 90% of the syn Michael adduct (entry 1, Table 27). With the enolate of *tert*-butyl ester **65.2**, the syn isomer is formed exclusively (entry 2). In both cases, exact stereochemical reversal results from



Scheme 63



Scheme 64

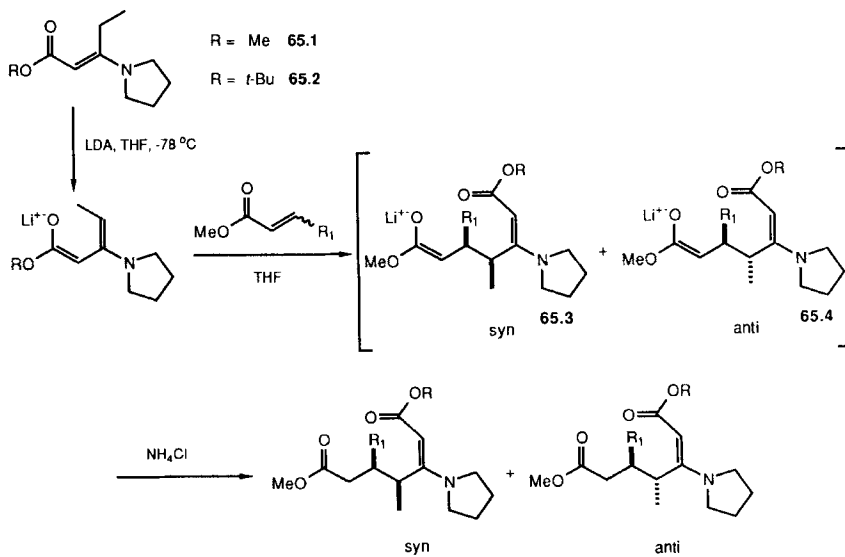
Table 26
Addition of Phenylacetonitrile to Octalones (Scheme 64)

Entry	R	Solvent	Yield %	64.2:64.3
1	H	THF	90	40:60
2	H	THF/HMPA	60	40:60
3	Me	THF	90	100:0
4	Me	THF/HMPA	a	---

a. No addition products were formed.

the use of dimethyl fumarate (entries 3 and 4). Another trans enoate, methyl crotonate, gives solely the anti diastereomer with **65.2** (entry 5).

Attempts to equilibrate the initial adducts **65.3** and **65.4** by warming gives the cyclized products **66.1** and **66.2**, respectively (Eqs. 1 and 2, Scheme 66). Enolates of the general structure **65.4** can also be alkylated with methyl iodide (Eq. 4), yielding anti,anti diastereomers with $\geq 19:1$ selectivity. Methylation of enolate **65.3** is much less selective (70:30 in favor of the syn,anti diastereomer, Eq. 3).

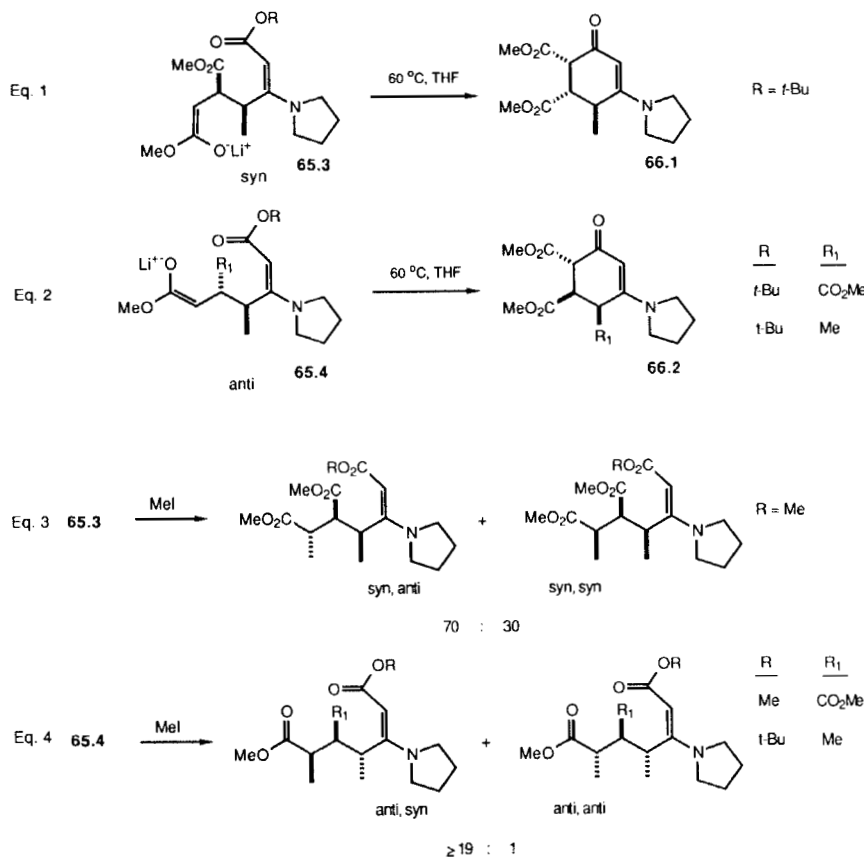


Scheme 65

Table 27
Addition of Lithiated Vinylogous Carbamates to α,β -Unsaturated Esters
(Scheme 65)

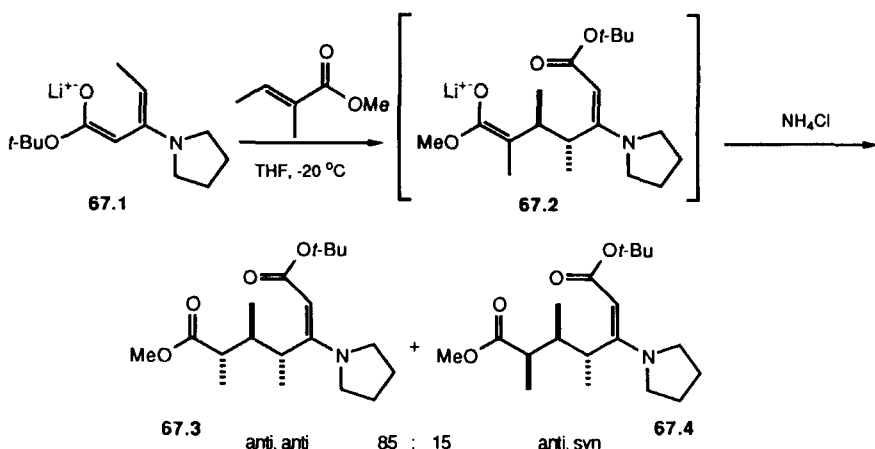
Entry	Vinylogous Carbamate Cmpd.	R	Enoate R ₁	E:Z	Temp. °C	Yield %	anti:syn
1	65.1	Me	CO ₂ Me	0:100	-78	90	10:90
2	65.2	t-Bu	CO ₂ Me	0:100	-78	90	0:100 ^a
3	65.1	Me	CO ₂ Me	100:0	-78	90	90:10
4	65.2	t-Bu	CO ₂ Me	100:0	-78	90	100:0 ^a
5	65.2	t-Bu	Me	100:0	-20	80-85	100:0 ^a

a. The minor diastereomer was not detected.



Scheme 66

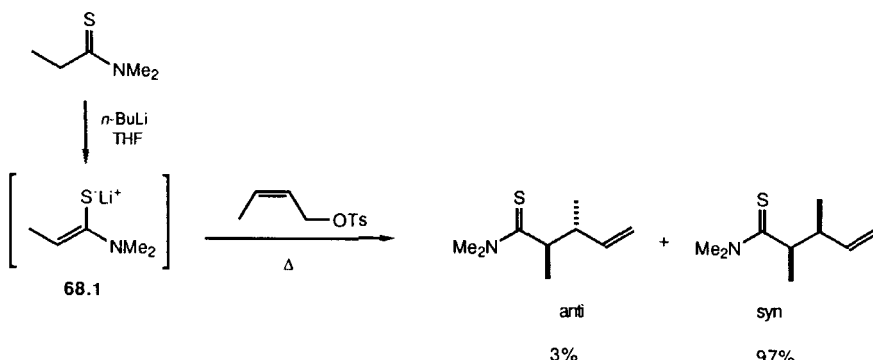
Kinetic protonation of the intermediate enolate formed in the Michael addition is also surprisingly selective. For example, the addition of enolate **67.1** to methyl tiglate occurs with a high degree of anti stereoselectivity to provide enolate **67.2** (Scheme 67). Kinetically controlled protonation of **67.2** with ammonium chloride gives a mixture of **67.3** and **67.4** (85 : 15). Thus the protonation occurs from the same face of the enolate as do the alkylations (Scheme 66), providing an approach to the anti-anti isomer **67.3** (contrast with Scheme 66).



Scheme 67

N. Thioamide Enethiolates

Thioamides are considerably more acidic than the corresponding oxoamides. Deprotonation can be achieved using a variety of bases including alkyl-lithiums, lithium diisopropylamide (LDA), and hexamethyldisilylamides (NaHMDS and KHMDS) at low temperature. The enethiolates of the propionyl thioamides prepared in this manner have the *Z* configuration, analogous to the comparable oxoamides (Scheme 68) (144, 145). The enethiolates isomer ratios from the deprotonation have not yet been directly determined. However, S-alkylation of lithium enethiolate **68.1** with cis crotyl tosylates followed by subsequent Claisen rearrangement results in the formation of stereoisomeric syn and anti diastereomers in a ratio of 97:3, suggesting that the *Z* enethiolate **68.1** is formed with at least 97% selectivity. Because thioamides can be converted to a variety of functional groups (144, 145), they can be viewed as synthetic equivalents of esters, carboxylic acids, or amides.



Scheme 68

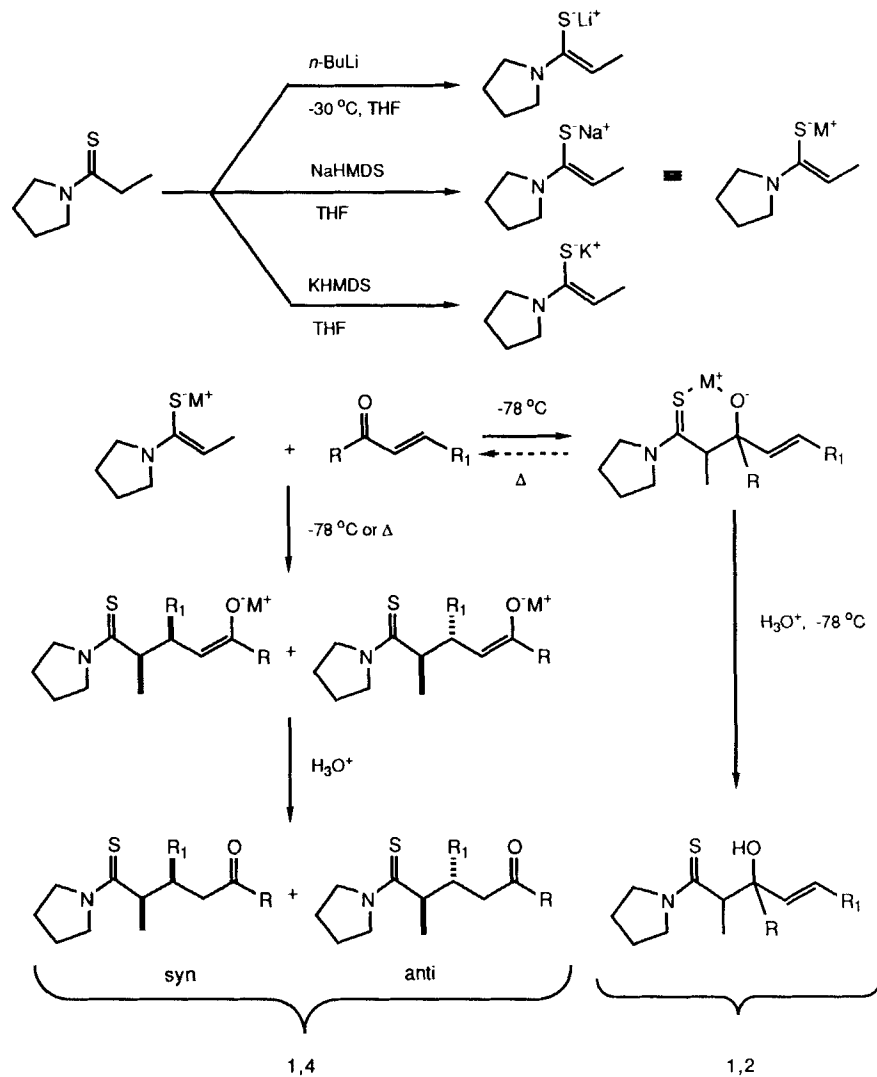
1. To α,β -Unsaturated Ketones

[P,P] The scope and regioselectivity of the addition of thioamide enethiolates to α,β -unsaturated ketones has been explored by Goasdoue et al. (146). Although these workers examined several cases in which the opportunity for diastereoselection exists and tentatively assigned the configurations of the products, the selectivity was not quantified.

Further work in this area has shown that addition of the lithium enethiolate of propionyl thioamides to α,β -unsaturated ketones results in preferential formation of anti diastereomers (Scheme 69, Table 28) (88). The stereoselectivity is dependent on the substituent at the β -position of the acceptor (R_1 , compare entries 3, 6, and 7). The size of the group attached to the enone carbonyl (R) has an effect on stereochemistry; the largest groups give enhanced anti selectivity (compare entries 1, 3, 8, 9).

Comparison of the results from the oxoamide enolates (Scheme 81, Table 35, *vide infra*) with those from thioamide anions (Scheme 69, Table 28) shows two major differences. First, enethiolates show less preference for 1,2-addition, relative to 1,4-addition, than do oxoamide enolates. Second, thioamide enethiolates give 1,4-addition products with significantly greater anti/syn ratios than the oxoamide analogs. Use of sodium and potassium counterions increases the proportion of the anti diastereomer (compare entries 3, 4, and 5, Table 28). The yields in these cases are somewhat lower, probably due to the low solubility of the sodium and potassium enethiolates.

Reactions of the anions of *N*-methyl-2-thiopyrrolidinone with α,β -unsaturated ketones are summarized in Scheme 70 and Table 29. With the lithium enethiolates in THF, additions to simple alkyl enones are essentially unselec-



Scheme 69

tive (entries 2, 4, 5, 12). Acceptors with a very large group (R) attached to the carbonyl give the *syn* adduct nearly exclusively (entries 9 and 10). A similar result is obtained by using sodium or potassium counterions in THF (entries 7 and 8). With the lithium anion in THF/HMPA as solvent, the *anti* diaste-

Table 28
Addition of Propionyl Thioamide Enethiolates to α,β -Unsaturated Ketones
(Scheme 69)

Entry	Enethiolate cation	α -Enones R	α -Enones R ₁	Solvent	Temp. °C	Yield %	1,2:1,4	1,4 syn:anti
1	Li	Me	Me	THF	-78	63 ^a	74:26	17:83
2	Li	Me	Me	THF	25	35	<3:97	25:75
3	Li	t-Bu	Me	THF	-78	77	<3:97	18:82
4	Na	t-Bu	Me	THF	-7	37	<3:97	<5:95
5	K	t-Bu	Me	THF	-7	29	<3:97	<5:95
6	Li	t-Bu	Ph	THF	-78	94	<3:97	<5:95
7	Li	t-Bu	t-Bu	THF	25	61	<3:97	<3:97
8	Li	mes ^b	Me	THF	-78	87	<3:97	<5:95
9	Li	tris ^c	Me	THF	-78	62	<3:97	5:95

a. Two equivalents of the enone were used.

b. 2,4,6-Trimethylphenyl.

c. 2,4,6-Triisopropylphenyl.

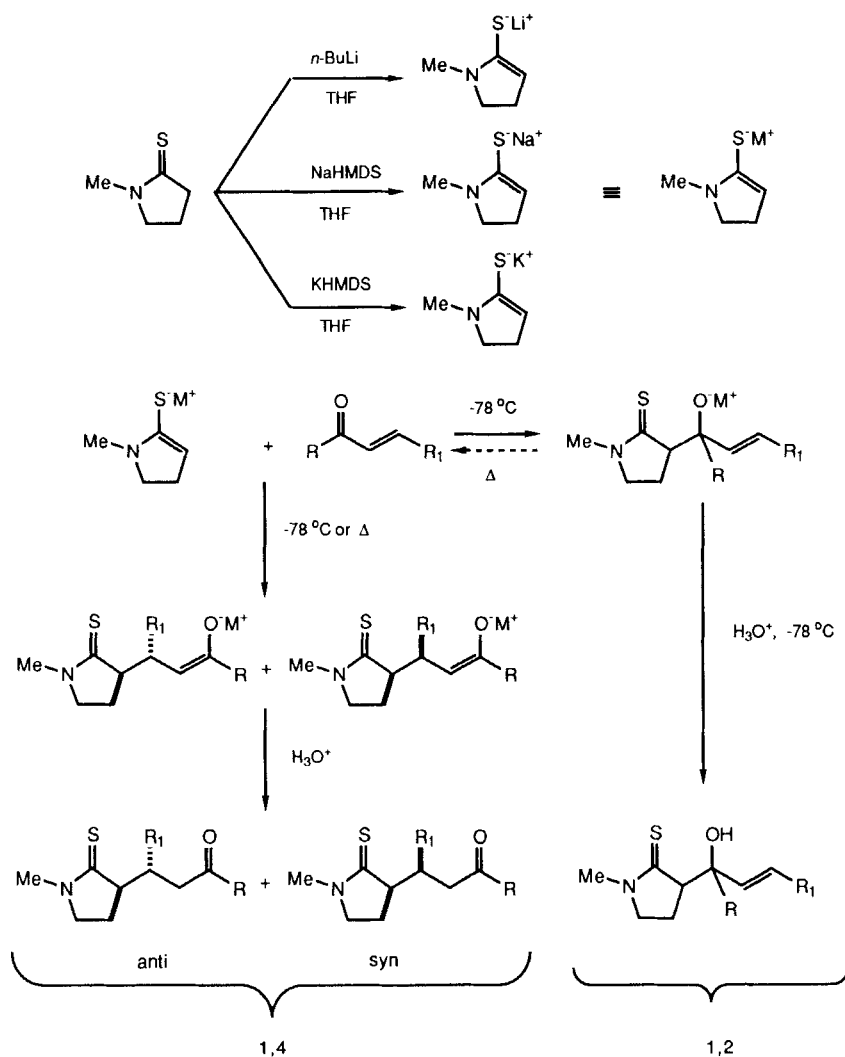
reomer is favored (entries 6 and 11). Hence, by choosing the solvent and counterion, either diastereomer can be favored with simple alkyl enones.

O. Amide Enolates

Enolates are usually generated from amides with a strong base such as LDA. Although a rigorous assignment of the stereochemistry of amide enolates has not been made, Evans and Takacs assigned the stereochemistry of the enolate derived from *N*-propionylpyrrolidine and LDA the Z configuration (147). Their assignment is based on the ¹³C NMR chemical shift of the methyl group (11.7 ppm in THF, consistent with other Z enolates) and on the rationale that allylic strain considerations should strongly favor deprotonation of conformer 71.2 over conformer 71.1 (Scheme 71). Importantly, they were able to observe only one enolate isomer under all conditions employed (equilibration and a variety of bases). This structural assignment has since found support in the stereochemical outcome of alkylation and addition reactions (148).

1. To Cinnamic Acid Dialkylamides

[P,P] The addition of the sodium enolates of *N,N*-disubstituted phenylacetamides to cinnamic acid dialkylamides in a variety of solvents and at different temperatures has been explored by Stefanovsky and Viteva (149-151). Only the results for the addition of *N,N*-(dicyclohexyl)phenylacetamide to *N,N*-(dimethyl)cinnamamide were presented. In THF, ether, and benzene,



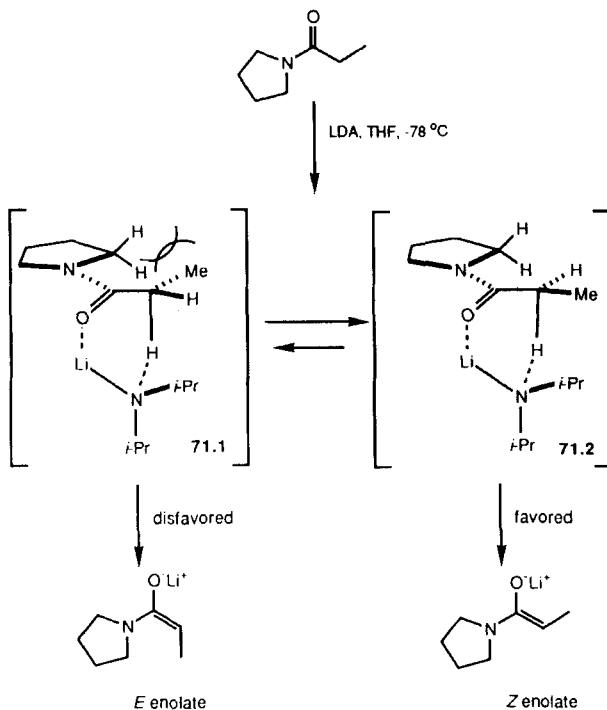
Scheme 70

Table 29
Addition of *N*-Methylthio-2-pyrrolidinone Enethiolates to α,β -Unsaturated Ketones
(Scheme 70)

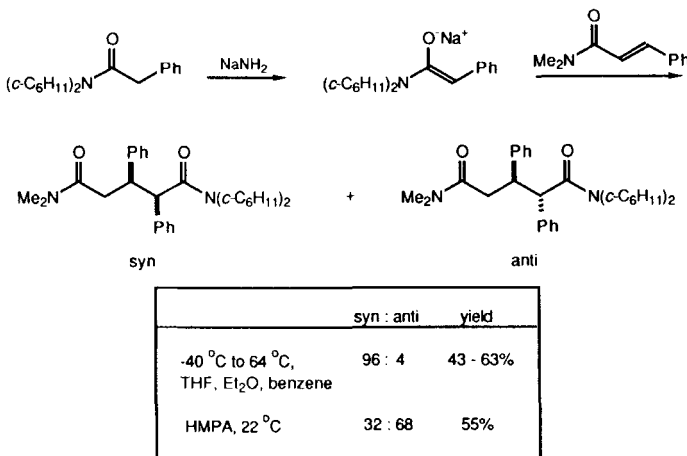
Entry	Enethiolate cation	α -Enone R	α -Enone R_1	Solvent	Temp. °C	Yield %	1,2:1,4	1,4 syn:anti
1	Li	Me	Me	THF	-78	84	95:5	---
2	Li	Me	Me	THF	25	61	<3:97	55:45
3	Li	<i>i</i> -Pr	Me	THF	-78	44	84:16	55:45
4	Li	<i>i</i> -Pr	Me	THF	0	97	<3:97	54:46
5	Li	<i>t</i> -Bu	Me	THF	-78	84	<3:97	60:40
6	Li	<i>t</i> -Bu	Me	THF/HMPA	-78	98	<3:97	15:85
7	Na	<i>t</i> -Bu	Me	THF	-78	74	<3:97	>95:5
8	K	<i>t</i> -Bu	Me	THF	-78	81	<3:97	>95:5
9	Li	mes ^a	Me	THF	-78	67	<3:97	93:7
10	Li	tris ^b	Me	THF	-78	91	<3:97	>95:5
11	Li	tris ^b	Me	THF/HMPA	-78	92	<3:97	35:65
12	Li	<i>t</i> -Bu	<i>i</i> -Pr	THF	-78	67	<3:97	52:48
13	Li	<i>t</i> -Bu	Ph	THF	-78	68	<3:97	95:5

a. 2,4,6-Trimethylphenyl.

b. 2,4,6-Triisopropylphenyl.



Scheme 71



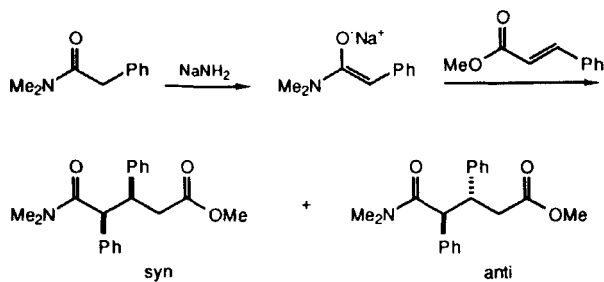
Scheme 72

the syn diastereomers are highly preferred (96:4, Scheme 72). With HMPA as solvent, the selectivity is much lower. The authors were unable to determine whether the ratios represented thermodynamic or kinetic preferences.

2. To α,β -Unsaturated Esters

[P,P] The analogous addition of sodium phenylacetamide enolates to cinnamic acid esters has also been explored by Stefanovsky and Viteva (149, 152, 153). With stoichiometric amounts of base, only the outcome for the addition of *N,N*-(dimethyl)phenylacetamide to methyl cinnamate was reported (Scheme 73, Table 30). At lower temperatures, poor selectivity is observed in ether and THF. Warming the reaction mixture in these solvents or using benzene produces a predominance of the syn diastereomer. The use of HMPA as cosolvent at room temperature results in a slight preference for the anti diastereomer. The stereochemical consequence in ethereal solvents and benzene is consistent with poor kinetic selectivity at low temperatures and good levels of syn selectivity at equilibrium.

The addition of propionamides to crotonates has been extensively explored by Yamaguchi and coworkers (22). The results of this study are summarized in Scheme 74 and Table 31. As can be seen from Table 31, the stereochemistry of the reaction ranges from strongly syn selective (entries 1 and 2) to

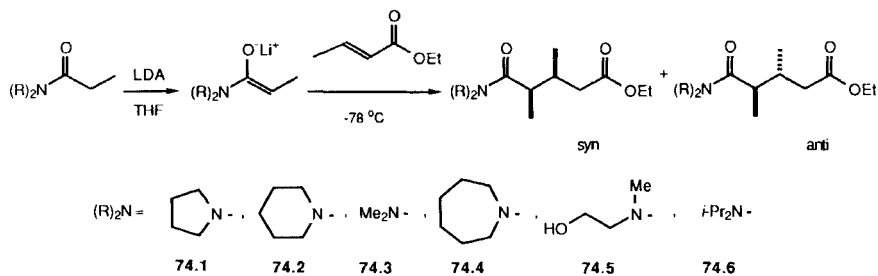


Scheme 73

Table 30
Addition of the Sodium Enolate of *N,N*-(Dimethyl)phenylacetamide to Methyl Cinnamate (Scheme 73)

Entry	Solvent	Temp. °C	Yield %	Syn:Anti
1	THF	-80	55	60:40
2	THF	22	93	94:6
3	Et ₂ O	-40	92	40:60
4	Et ₂ O	22	88	93:7
5	benzene	22	87	91:9
6	HMPA	22	52	30:70

somewhat anti selective (entry 7). A rough trend can be seen from these data where the less sterically hindered amides have a higher propensity to give syn addition products whereas the more hindered amides produce a greater proportion of the anti adducts.



Scheme 74

Table 31
Addition of Propionamides to Ethyl Crotonate (Scheme 74)

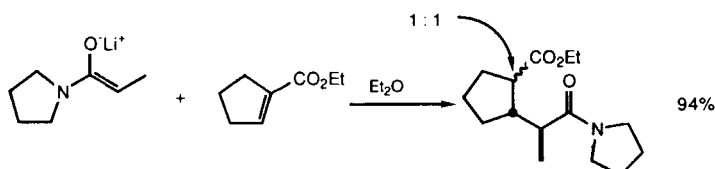
Entry	Amine	Solvent	Yield %	syn:anti ^a
1	74.1	Et ₂ O	86	>95:5
2	74.1	THF	92	95:5
3	74.2	THF	85	75:25
4	74.3	THF	92	67:33
5	74.4	THF	88	50:50
6	74.5	THF	67 ^b	50:50
7	74.6	THF	85	33:67

a. The isomer ratios were determined by ¹³C NMR.

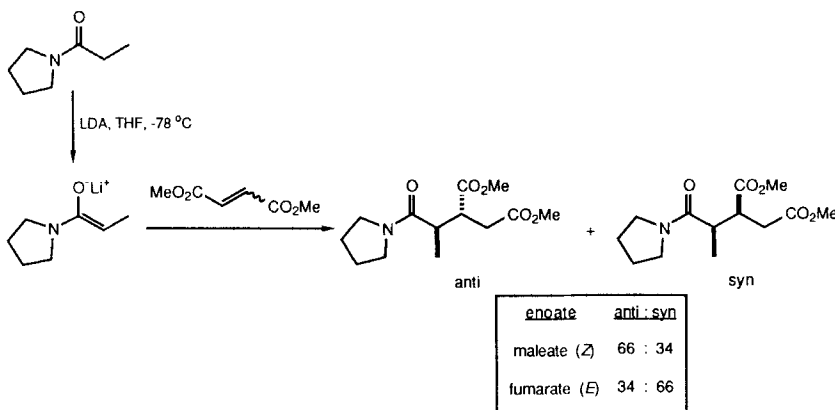
b. Yield of the hydrolyzed diacid.

The configurations of most of the Michael adducts were assigned by an interesting ¹³C NMR correlation. It was observed that the C-3 methyl group of the syn diastereomers have a resonance at δ 15.7±0.3 compared to δ 18.5±0.5 for the anti diastereomers. Although the reference cited (22) does not provide the complete data from which this correlation was established, some of the conjugate addition products of related chiral, non-racemic propionamides were converted into natural products, thereby confirming the assigned configuration of the Michael addition products.

Another example of the addition of a propionamide enolate to an enoate was reported later (14). Upon addition to ethyl 1-cyclopentenecarboxylate, the lithium enolate of *N*-propionylpyrrolidine gives a 1:1 mixture of diastereomers (Scheme 75). The stereoisomers result from stereorandom protonation of the intermediate enolate; the Michael addition appears to occur with very high stereoselectivity.



In connection with their study of the stereochemistry of the Michael addition of vinylogous carbamates (*vide supra*), Schlessinger and coworkers examined the addition of the lithium enolate of *N*-propionylpyrrolidine to dimethyl maleate and fumarate (142). The results of this study are summarized in Scheme 76. Only low levels of stereochemical differentiation were observed



Scheme 76

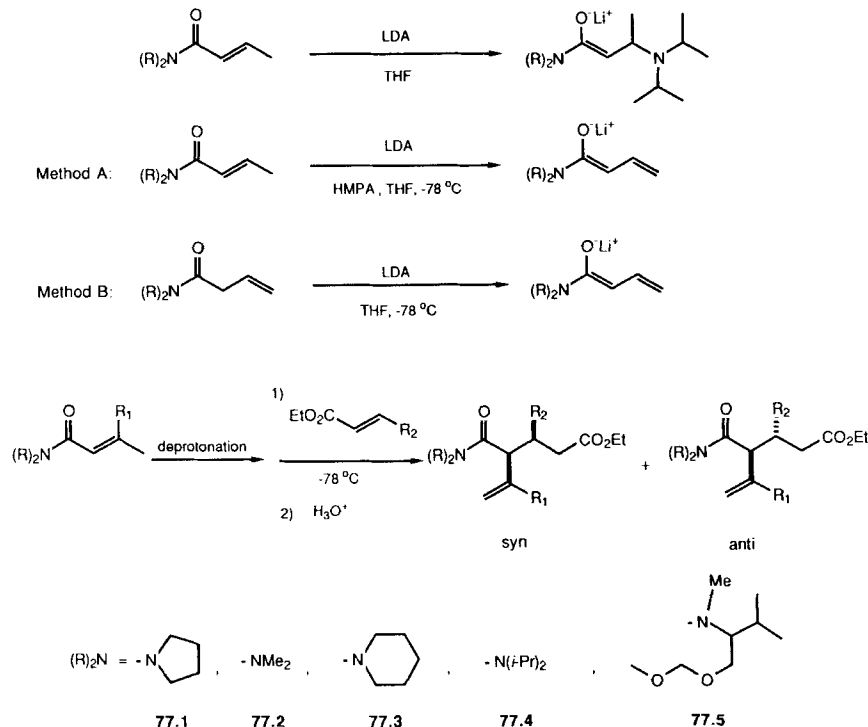
in these examples. Nevertheless, it is interesting to note the reversal in selectivity seen on changing the geometry of the enoate. Also intriguing is the lowered selectivity seen in comparison to the very selective addition of the same amide enolate to ethyl crotonate (*vide supra*).

P. Amide Dienolates

1. To α,β -Unsaturated Esters

Addition of dienolates to α,β -unsaturated esters has been studied by Yamaguchi and coworkers (154). No success was achieved for the addition of unsaturated esters, carboxylic acids, or *N*-monosubstituted amides to enoates. By using the proper conditions, however, the addition of the dienolates derived from *N,N*-disubstituted- α,β -unsaturated amides to enoates was achieved. Attempts to deprotonate *N,N*-disubstituted- α,β -unsaturated amides with LDA in THF resulted in 1,4-addition of the amide base except when a β,β -disubstituted- α,β -unsaturated amide was employed (Scheme 77). Hence, two alternate procedures were utilized for generation of the amide dienolate. The first technique (Method A) involves deprotonation of the α,β -unsaturated amide with LDA in THF/HMPA. The second technique (Method B) avoids the potential conjugate addition of LDA by deprotonating a β,γ -unsaturated amide. Although the geometry of the enolates formed were not determined, it is likely that both procedures give high proportions of the *Z* isomer.

The addition of amide dienolates to a variety of enoates is summarized in Table 32. Two trends may be noted. First, as observed in Yamaguchi's earlier work, more sterically demanding amides give a greater percentage of the anti



Scheme 77

diastereomer. Second, addition of HMPA to the reaction mixture, either before or after deprotonation of the enamide, results in an increase in the proportion of the syn diastereomer.

By optimization of the amine portion of the amide and the solvent employed, either diastereomer can be obtained in reasonable stereoisomeric purity. By using the pyrrolidine amide (77.1), particularly, in THF/HMPA, excellent syn selectivity is achieved (entries 1, 2, 11–17, Table 32). With the valinol-derived amide 77.5 in THF, moderate anti selectivity is possible (entries 9 and 18–20). No information was provided about the facial selectivity of 77.5 (*vide infra*).

Some more complicated examples are shown in Scheme 78 (154, 155). In view of the excellent levels of stereoselection seen in Eqs. 1, 2, 4, and 5, it is likely that deprotonation of the enamides and dienamides provides high proportions of one dienolate (trienolate) stereoisomer in each case. On the basis of comparison with the generation of simpler amide enolates (e.g. Scheme 71), the Z enolate would seem probable in Eqs. 1 and 2. Comparison of the

Table 32
Addition of *N,N*-Disubstituted Amide Dienolates to α,β -Unsaturated Esters
(Scheme 77)

Entry	Enolate R	Enolate R ₁	Method ^a	Enoate R ₂	Yield %	Solvent	syn:anti ^b
1	77.1	H	A	<i>n</i> -C ₇ H ₁₅	65 ^c	THF-HMPA	>95:5
2	77.1	H	B	<i>n</i> -C ₇ H ₁₅	70 ^d	THF	>91:9
3	77.2	H	A	<i>n</i> -C ₇ H ₁₅	68	THF-HMPA	>95:5
4	77.3	H	A	<i>n</i> -C ₇ H ₁₅	82	THF-HMPA	71:29
5	77.3	H	B	<i>n</i> -C ₇ H ₁₅	59	THF	33:67
6	77.4	H	A	<i>n</i> -C ₇ H ₁₅	68	THF-HMPA	50:50
7	77.4	H	B	<i>n</i> -C ₇ H ₁₅	68 ^d	THF	25:75
8	77.5	H	A	<i>n</i> -C ₇ H ₁₅	77	THF-HMPA	80:20 ^e
9	77.5	H	B	<i>n</i> -C ₇ H ₁₅	83	THF	17:83 ^{e,f}
10	77.5	H	B	<i>n</i> -C ₇ H ₁₅	82	THF-HMPA	83:17 ^f
11	77.1	H	A	Me	62 ^c	THF-HMPA	>95:5
12	77.1	H	A	<i>n</i> -C ₄ H ₉	59 ^c	THF-HMPA	>95:5
13	77.1	Me	A	Me	81	THF-HMPA	>95:5
14	77.1	Me	A	<i>n</i> -C ₄ H ₉	84	THF-HMPA	>95:5
15	77.1	Me	A	<i>n</i> -C ₇ H ₁₅	91	THF-HMPA	>95:5
16	77.1	Me	C	<i>n</i> -C ₇ H ₁₅	95	THF	>95:5
17	77.1	Me	A	Ph	87	THF-HMPA	>95:5
18	77.5	H	B	Me	78	THF	20:80
19	77.5	Me	B	<i>n</i> -C ₇ H ₁₅	86	THF	25:75
20	77.5	Me	C	<i>n</i> -C ₇ H ₁₅	67	THF	25:75

a. Method A: LDA in THF/HMPA on the α,β -unsaturated amide.

Method B: LDA in THF on the β,γ -unsaturated amide.

Method C: Deprotonation of the α,β -unsaturated- β,β -disubstituted amide.

b. Determined by ¹³C NMR spectrum of the product.

c. 10% product from reaction at the γ -position of the enolate.

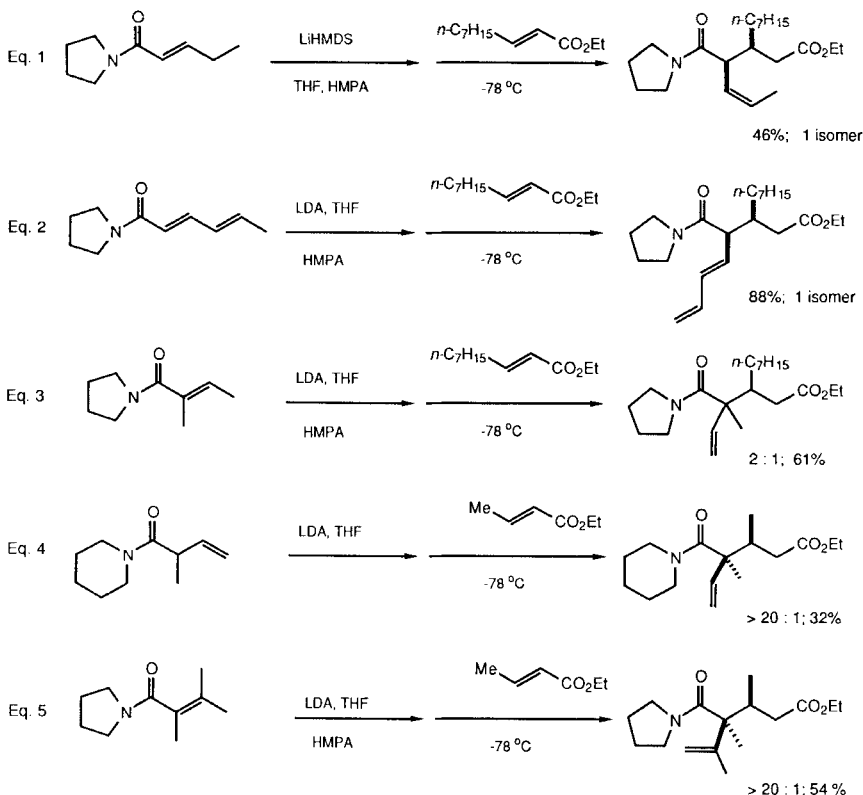
d. A 2:1 mixture of 3-butenamide and 2-butenamide was used.

e. Ratio determined by ¹³C NMR spectrum of lactone derived from Michael adduct (see text).

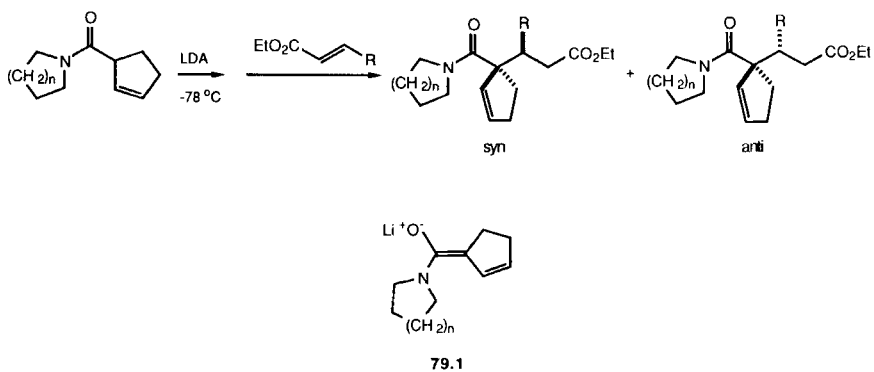
f. Ratio determined on diol from hydrolysis and reduction of the Michael adduct.

results in Eqs. 3 and 4 implies that different enolate ratios result from the deprotonations. In analogy to the senecioate dienolate formation discussed previously (133, 134), it is likely that the Z dienolate is formed in Eq. 5.

Mechanistic considerations aside, the highly diastereoselective formation of adjacent tertiary and quaternary centers is noteworthy (Eqs. 4 and 5, Scheme 78). Some further examples are illustrated in Scheme 79 and Table 33 (155). The anion of 2-cyclopentenecarboxypiperidine gives exceptional syn selectivity in THF (entries 1 and 3). No differentiation was achieved with the pyrrolidine amide dienolates (entries 4 and 5). Again, mechanistic interpretation is hampered by lack of information about the dienolate geometry. Based solely on the stereochemical trends observed, dienolate **79.1** would be expected to be the reactive species.



Scheme 78



Scheme 79

Table 33
Addition of Lithium 1-Cyclopentenecarboxamide Enolates to α,β -Unsaturated Esters (Scheme 79)

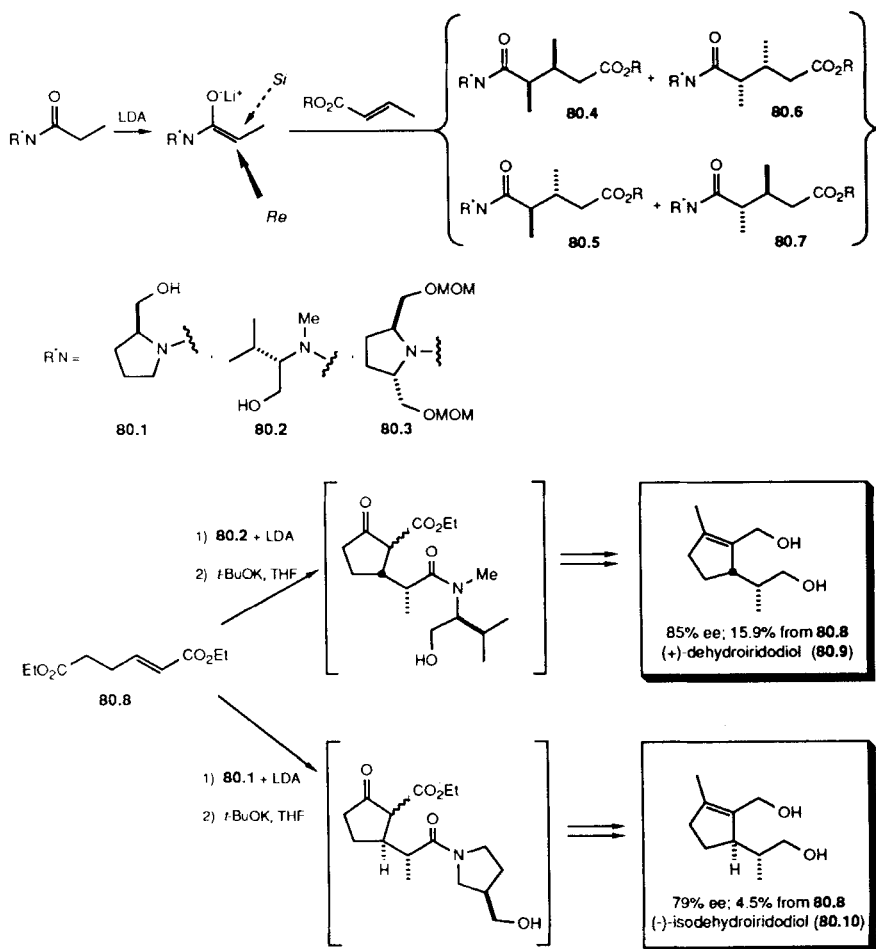
Entry	Enolate n	Enoate R	Solvent	Yield %	syn:anti
1	2	Me	THF	80	>95:5
2	2	Me	THF-HMPA	0	---
3	2	n-C ₇ H ₁₅	THF	80	>95:5
4	1	n-C ₇ H ₁₅	THF	93	50:50
5	1	n-C ₇ H ₁₅	THF-HMPA	61	50:50

[P*,P] The reactions of chiral, non-racemic propionamides **80.1**–**80.3** with crotonates were investigated by Yamaguchi and coworkers (22). The results are summarized in Scheme 80 and Table 34. As observed for achiral amides (*vide supra*), the simple diastereoselectivity correlates with the size of the amine group of the amide. With auxiliaries **80.1** and **80.2**, preferential reaction occurs on the *Si* face of the enolate, leading to **80.4** and **80.5**, respectively. Assignment of absolute configurations to the products of entries 1 and 2 (Table 34) was made by conversion in (+)-dehydroiridodiol (**80.9**) and (–)-isodehydroiridodiol (**80.10**). Starting from enediester **80.8**, sequential Michael addition/Dieckmann condensation with **80.2** leads to **80.9**; **80.1** leads to **80.10** (Scheme 80). The configuration of the major product obtained using **80.3** (**80.5** or **80.7**) was not determined.

2. To α,β -Unsaturated Ketones

[P,P] The conjugate addition of the lithium enolates of *N,N*-disubstituted propionamides has been examined (23, 88). The results from this study are summarized in Scheme 81 and Table 35. Several trends can be observed in these data. As the steric demand of the amino group increases, a greater percentage of anti diastereomer is formed (entries 1, 14, 25, 26). Varying only the alkyl group R₁ of the enone from ethyl to *tert*-butyl results in no significant change in selectivity (entries 3, 5, 7, 14). With extremely large substituents R₁, high anti selectivity is realized (entries 16 and 17). Conjugated aromatic R₁ substituents give moderate syn selectivity (entries 8–13). Higher proportions of the anti diastereomer are formed with increasingly bulky substituents at the β -position of the enone (R₂, entries 14 and 19–24).

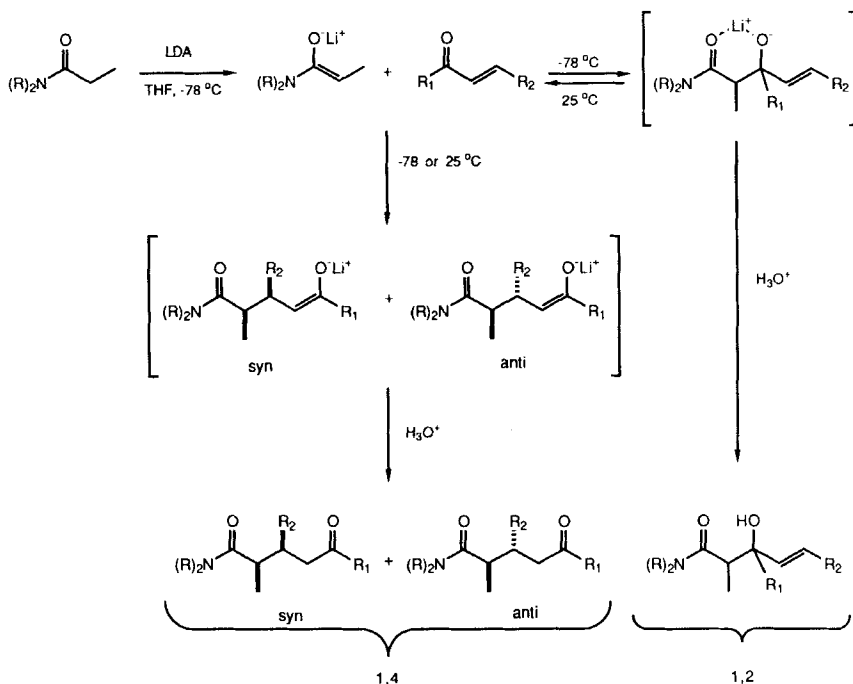
As expected, the percentage of 1,2-addition products at low temperature is dependent upon the relative sizes of R₁ and R₂. By raising the reaction temperature, these adducts are transformed into 1,4-addition products. In contrast to the results from the addition of ester enolates to enones (*vide supra*), the extent of 1,2-addition does not influence the stereochemical outcome.



Scheme 80

Table 34
Addition of Chiral Propionamides to Crotonates (Scheme 80)

Entry	Amide	Crotonate R	Solvent	Yield %	syn:anti	Major Product	ds %
1	80.1	Me	THF	84	88:12	80.4	79
2	80.2	Me	ether-THF	76	9:91	80.5	74
3	80.3	Et	THF	76	6:94	80.5 or 80.7	≥80



Scheme 81

This is probably a result of the higher configurational stability of the *Z* amide enolate.

The effect of HMPA depends upon the substrate used. With the simple dialkyl enone in entry 15 (Table 35), there is no effect. With the extremely hindered acceptor in entry 17, the addition of HMPA leads to a reversal in the selectivity (entry 18).

The *E* enolates of *N,N*-disubstituted amides are not readily available (*vide supra*). To evaluate the effect of enolate geometry on the stereochemical course, the reactions of the lithium enolate of the cyclic amide *N*-methyl-2-pyrrolidinone with α,β -unsaturated ketones have been investigated (Scheme 82, Table 36) (23). With a few exceptions, high proportions of the anti isomer were obtained (Table 36). One exception occurs with a phenyl substituent at the β -position of the enone (R₁) where little differentiation is exhibited (entries 23 and 24). Stereoselection decreases slightly when R is a very large substituent (entries 16 and 17). Use of THF/HMPA as solvent with simple dialkyl acceptors results in a slight shift in the adduct ratios (compare entries 14 and 15). With an extremely bulky substituent attached to the carbonyl, a more pronounced shift is observed (compare entries 17 and 18).

Table 35
Addition of the Lithium Enolates of Propionamides to α,β -Unsaturated Ketones
(Scheme 81)

Entry	Amide ^a R	α -Enones		Solvent	Temp. °C	Yield %	1,2:1,4	1,4 syn:anti
		R ₁	R ₂					
1	Me	t-Bu	Me	THF	-78	72	<3:97	55:45
2	-(CH ₂) ₄ -	Et	Me	THF	-78	78	>97:3	---
3	-(CH ₂) ₄ -	Et	Me	THF	25	26	4:96	43:57
4	-(CH ₂) ₄ -	i-Pr	Me	THF	-78	84	29:71	40:60
5	-(CH ₂) ₄ -	i-Pr	Me	THF	25	85	<3:97	40:60
6	-(CH ₂) ₄ -	c-C ₆ H ₁₁	Me	THF	-78	56	40:60	45:55
7	-(CH ₂) ₄ -	c-C ₆ H ₁₁	Me	THF	25	51	<3:97	45:55
8	-(CH ₂) ₄ -	Ph	Me	THF	-78	92	12:88	87:13
9	-(CH ₂) ₄ -	Ph	Me	THF	25	86	<3:97	85:15
10	-(CH ₂) ₄ -	p-BrC ₆ H ₄	Me	THF	-78	84	50:50	80:20
11	-(CH ₂) ₄ -	p-BrC ₆ H ₄	Me	THF	25	40	<3:97	80:20
12	-(CH ₂) ₄ -	p-MeOC ₆ H ₄	Me	THF	-78	72	35:65	75:25
13	-(CH ₂) ₄ -	p-MeOC ₆ H ₄	Me	THF	25	58	<3:97	75:25
14	-(CH ₂) ₄ -	t-Bu	Me	THF	-78	90	<3:97	45:55
15	-(CH ₂) ₄ -	t-Bu	Me	THF/HMPA	-78	75	<3:97	45:55
16	-(CH ₂) ₄ -	mes ^b	Me	THF	-78	86	<3:97	≤5:95
17	-(CH ₂) ₄ -	tris ^c	Me	THF	-78	85	<3:97	≤9:91
18	-(CH ₂) ₄ -	tris ^c	Me	THF/HMPA	-78	91	<3:97	80:20
19	-(CH ₂) ₄ -	t-Bu	Et	THF	-78	95	<3:97	37:63
20	-(CH ₂) ₄ -	t-Bu	i-Pr	THF	-78	46	7:93	33:67
21	-(CH ₂) ₄ -	t-Bu	i-Pr	THF	25	65	<3:97	27:73
22	-(CH ₂) ₄ -	t-Bu	Ph	THF	25d	69	<3:97	9:91
23	-(CH ₂) ₄ -	t-Bu	t-Bu	THF	-78	70	54:46	<3:97
24	-(CH ₂) ₄ -	t-Bu	t-Bu	THF	25	86	<3:97	<3:97
25	-(CH ₂) ₅ -	t-Bu	Me	THF	-78	98	<3:97	15:85
26	-(CH ₂) ₆ -	t-Bu	Me	THF	-78	87	<3:97	30:70

a. The enolates from the propionyl amides have the Z configuration.

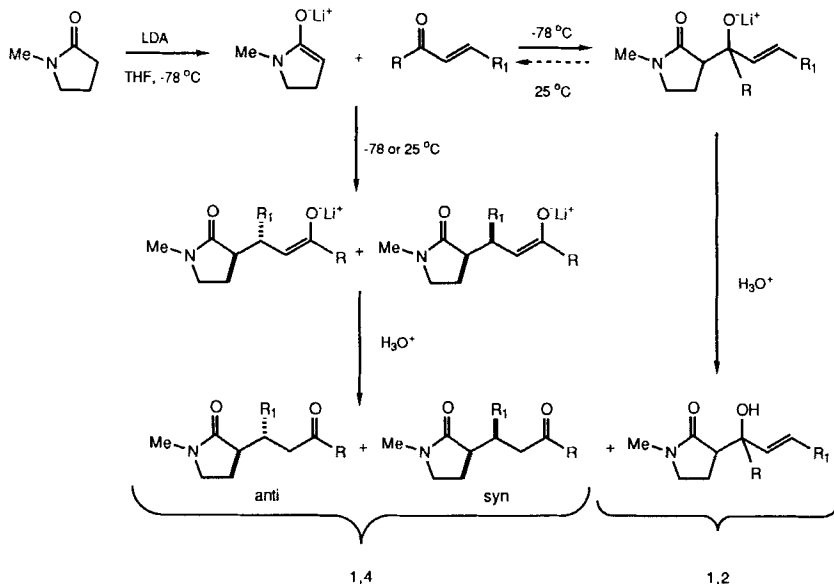
b. 2,4,6-Trimethylphenyl.

c. 2,4,6-Trisopropylphenyl.

d. Control experiments show that no 1,2 addition occurs at -78 °C.

The lactam enolate has a higher propensity for 1,2-addition than the propionamide enolates described previously. This limits the scope of the reaction because substrates that give a large percentage of 1,2-addition are slow to equilibrate to 1,4-adducts (for example see entries 1, 2, and 25, Table 36). However, most of the substrates examined can be effectively transformed to the 1,4-products. At longer reaction times at room temperature, slow changes in the 1,4-adduct ratio occurs. The isomeric stability of the products at low temperature suggests that the selectivity in the process is determined by kinetic factors.

Comparison with the results from the thiolactams is informative. By modifying the counterion, solvent, and/or donor atom (O or S), conjugate addition products having either the syn or anti configuration can be obtained with enolates having the "N-methyl-2-pyrrolidinone" framework with excellent selectivity.



Scheme 82

3. To Nitroolefins

[N*,P] The conjugate addition of the lithium enolate of dimethylacetamide to nitropropene and β -nitrostyrene in the presence of chiral, non-racemic additives has been reported by Seebach and coworkers (113–115). Although asymmetric induction was documented, in no instance was the enantiomeric excess greater than 12%.

Q. Metallated Hydrazones and Imines

Hydrazones and imines are significantly less acidic than the ketones or aldehydes from which they are derived (156–158). Nevertheless, metallation is possible using a strong base such as an alkylmagnesium, an alkylolithium, or LDA (159, 160). The resulting anions are quite reactive and even react with poor electrophiles such as ethylene oxide. Self condensation, either during the deprotonation stage or after reaction with an electrophile, severely limits the utility of aldehyde enolates. These problems can frequently be overcome by using metallated aldimines.

As with ketones, regiochemistry of deprotonation is an issue. Preferential proton abstraction under kinetically controlled conditions normally occurs at

Table 36
Addition of the Lithium Enolate of *N*-Methyl-2-pyrrolidinone to α,β -Unsaturated Ketones (Scheme 82)

Entry	α -Enones		Solvent	Temp. ^a °C	Yield %	1,2:1,4	1,4 syn:anti
	R	R ₁					
1	Et	Me	THF	-78	50	>97:3	---
2	Et	Me	THF	25	60	>97:3	---
3	i-Pr	Me	THF	-78	64	80:20	10:90
4	i-Pr	Me	THF	25	76	50:50	10:90
5	c-C ₆ H ₁₁	Me	THF	-78	93	68:32	10:90
6	c-C ₆ H ₁₁	Me	THF	25	56	20:80	10:90
7	Ph	Me	THF	-78	67	63:37	5:95
8	Ph	Me	THF	25	96	<3:97	5:95
9	p-BrC ₆ H ₄	Me	THF	-78	77	70:30	5:95
10	p-BrC ₆ H ₄	Me	THF	25	90	58:42	5:95
11	p-MeOC ₆ H ₄	Me	THF	-78	49	72:28	10:90
12	p-MeOC ₆ H ₄	Me	THF	25	60	<3:97	10:90
13	t-Bu	Me	THF	-78	72	14:86	10:90
14	t-Bu	Me	THF	25	99	<3:97	10:90
15	t-Bu	Me	THF/HMPA	-78	46	15:85	18:82
16	mes ^b	Me	THF	-78	95	<3:97	30:70
17	tris ^c	Me	THF	-78	83	<3:97	15:85
18	tris ^c	Me	THF/HMPA	-78	92	<3:97	40:60
19	t-Bu	Et	THF	-78	58	31:69	8:92
20	t-Bu	Et	THF	25	87	<3:97	7:93
21	t-Bu	i-Pr	THF	-78	73	57:43	7:93
22	t-Bu	i-Pr	THF	25	62	<3:97	20:80
23	t-Bu	Ph	THF	-78	55	55:45	32:68
24	t-Bu	Ph	THF	25	68	<3:97	40:60
25	t-Bu	t-Bu	THF	-78	60	>97:3	---

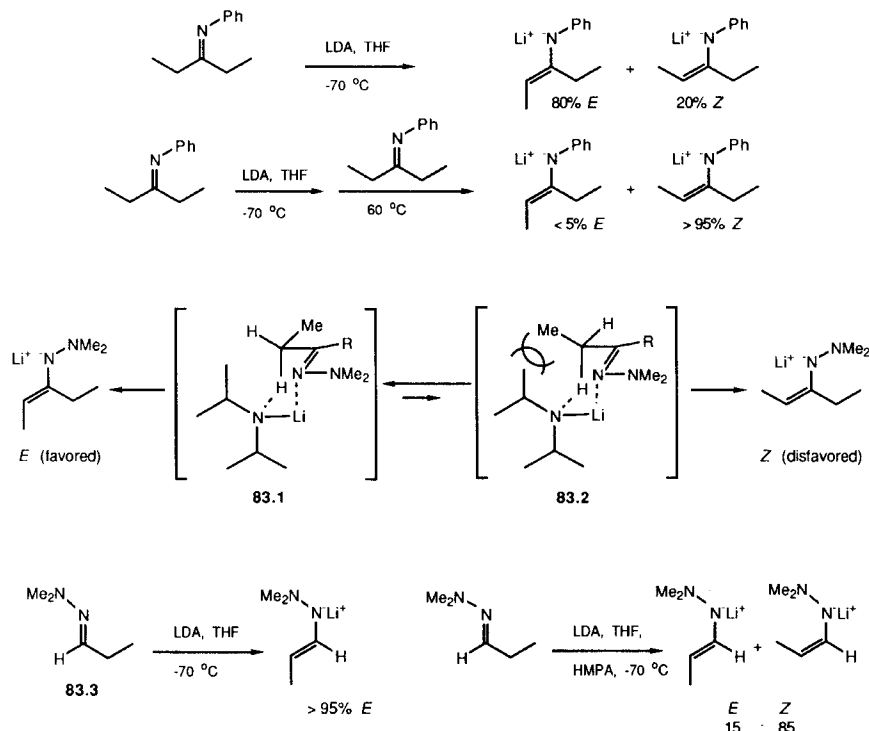
a. Reactions were quenched after 15 min at -78 °C or 1.5-19 hours at 25 °C.

b. 2,4,6-Trimethylphenyl.

c. 2,4,6-Triisopropylphenyl

the less substituted carbon. This propensity can be overcome, at least partially, when an anion-stabilizing group is attached to the more substituted carbon (161).

Azaenolates have substantial double bond character; *E* and *Z* isomers may be formed. For example, deprotonation of the aniline imine of diethyl ketone with LDA in THF at low temperatures results in preferential, but not exclusive, formation of the *E* azaenolate (Scheme 83) (162). Similar results have been found with hydrazones. Localization of the charge on the nitrogen is indicated by the configurational stability of the azaenolates (no change in the isomeric ratio after extended periods at room temperature). In the presence of excess imine at elevated temperatures the thermodynamically favored *Z* isomer is formed. The kinetically controlled *E* selectivity seen in deproto-

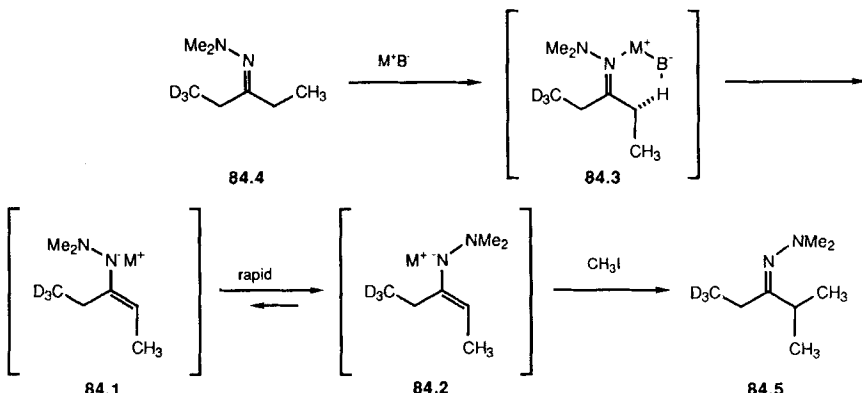


Scheme 83

tion of hydrazones is rationalized in a manner similar to the Ireland hypothesis, wherein deprotonation occurs through a cyclic transition state such as 83.1 (Scheme 83). Transition structure 83.1 is favored over 83.2 as a result of the non-bonding interaction between substituents on the base and the methyl group in 83.2.

As in the deprotonation of ketones and esters, solvent effects are important. With LDA in THF greater than 95% of the *E* azaenolate is produced from propionaldehyde dimethylhydrazone 83.3 (Scheme 83). When HMPA is added to the reaction mixture prior to deprotonation, an excess of the *Z* azaenolate is observed (85:15 *Z/E*) (158).

With hydrazone and imine azaenolates, a further stereochemical issue arises. Because of restricted rotation around the C–N bond, substituents on the nitrogen may be orientated anti or syn with respect to the double bond (84.1 or 84.2, respectively, Scheme 84). With symmetrical hydrazones, deprotonation occurs anti to the dimethylamino substituent. As illustrated elegantly with 84.2 by Jung and Shaw, this directed deprotonation leads directly



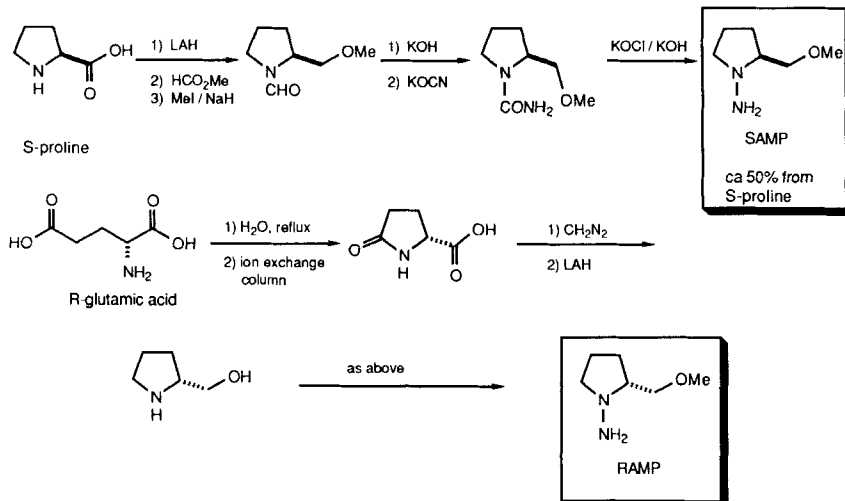
Scheme 84

to 84.1 (163). Rapid equilibration then occurs, resulting in isomerization of 84.1 to 84.2. Preferential attack of the electrophile, in this case methyl iodide, on 84.2 results in the formation of 84.5 with the syn orientation between the new methyl group and the dimethylamino substituent.

Because of their reactivity and stability, metallated hydrazones and imines have played important roles as enolate equivalents in conjugate additions (11, 159, 160). In stereoselective versions, both the orientation of the amino substituent of the hydrazone or imine and the azaenolate geometry can potentially play important roles in the stereochemical outcome of the conjugate additions.

Enders and coworkers have achieved high levels of both diastereomeric and enantiomeric selectivity in the addition of SAMP and RAMP hydrazones to a variety of acceptors. The hydrazones are available from the corresponding hydrazine and ketones or aldehydes. So far, only hydrazones in which the regiochemistry of deprotonation is unambiguous or electronically biased have been studied. The enantiomeric hydrazines (SAMP and RAMP) are available from *S*-proline and *R*-glutamic acid, respectively, by short synthetic sequences (Scheme 85). Thus, either enantiomer of the Michael adducts is obtainable (164).

The Enders hydrazones are deprotonated with LDA at $0^\circ C$ in THF/TMEDA. The structure of the resulting "azaenolate" in solution has not been fully elucidated. However, a methoxy-chelated, carbon-bound or π -allyl lithium species appears most likely (158, 165). After addition of an electrophile, the hydrazone products may be hydrolyzed to reform the carbonyl moiety and regenerate the hydrazine auxiliaries. A number of methods have been developed for this conversion (164). Compared to the mild conditions employed for



Scheme 85

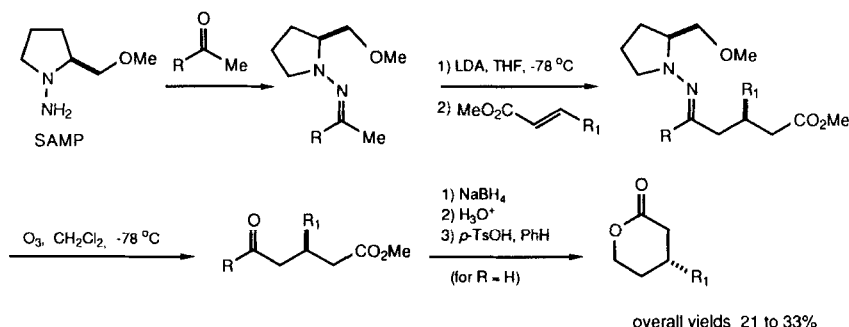
the hydrolysis of dimethylhydrazones (11), cleavage of the SAMP and RAMP auxiliaries commonly requires more drastic conditions. Nevertheless, it has been possible to maintain the stereochemical integrity of the products in the cleavage step.

1. To α,β -Unsaturated Esters

[N*,P] Enders and coworkers have investigated conjugate addition of lithiated SAMP and RAMP hydrazones of acetaldehyde (166) and a series of methyl ketones (167) to methyl enoates. The results of this work are summarized in Scheme 86 and Table 37. In all examples, adducts are obtained with very high enantiomeric excess. After oxidative cleavage of the auxiliary, the oxo esters are obtained in moderate yields. The aldehyde-esters (entries 1–6) can be reduced and cyclized to optically active β -substituted δ -lactones.

[P*,P] In view of the success obtained with hydrazones of methyl ketones and acetaldehyde, the reactions of prostereogenic lithiated hydrazones would be expected to give products with high levels of stereoselectivity. This has indeed proved to be the case. Enders and coworkers have found universally high selectivities for the addition of prostereogenic hydrazones to methyl enoates (Scheme 87, Table 38) (168). In only two examples (entries 6 and 10) were minor stereoisomers detected.

In a later communication, Enders and Rendenbach reported the synthesis of five pheromones **88.1–88.5** isolated from the small forest ant (*Formica po-*



Scheme 86

Table 37
Addition of SAMP and RAMP Hydrazones to α,β -Unsaturated Esters (Scheme 86)

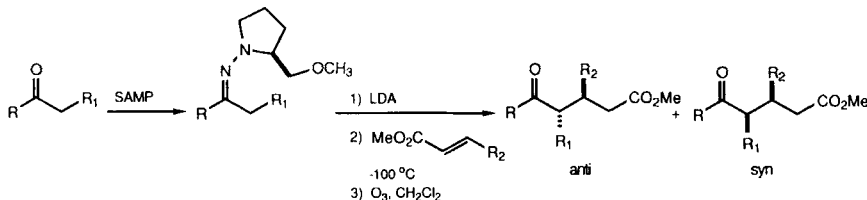
Entry	Hydrazone R	Enoate R ₁	Oxo-esters Yield % ^c	Lactones Yield % ^c	ee ^{a,b} %	
1	SAMP	H	Me	43	33	>96
2	RAMP	H	Me	37	27	>96 ^d
3	SAMP	H	Et	37	25	90
4	SAMP	H	n-Pr	40	28	90
5	SAMP	H	Ph	51	24	>96
6	SAMP	H	p-MeOC ₆ H ₅	30	21	93
7	SAMP	Me	Me	50	--	>96
8	RAMP	Me	Me	61	--	>96 ^d
9	SAMP	Et	Me	45	--	>96
10	SAMP	n-Pr	Me	49	--	>96
11	SAMP	i-Pr	Me	46	--	>96
12	SAMP	n-pentyl	Me	45	--	>96
13	SAMP	n-hexyl	Me	53	--	>99
14	SAMP	Ph	Me	55	--	>96
15	SAMP	Me	Ph	62	--	>96
16	SAMP	Et	Ph	49	--	>96
17	SAMP	n-Pr	Ph	50	--	>96
18	SAMP	n-pentyl	Ph	59	--	>96

a. The ee's were obtained by ¹H NMR using chiral shift reagents.

b. Products have the R configuration unless otherwise indicated.

c. Yields are overall yields from the starting enoate.

d. The RAMP hydrazone was used and the S product is obtained.



Scheme 87

Table 38
Addition of Prostereogenic Lithiated Hydrazones to α,β -Unsaturated Esters
(Scheme 87)

Entry	Hydrazone		Enoate	Yield %	anti:syn ^a	ee ^a %	Config.
	R	R ₁	R ₂				
1	SAMP	H	Me	Me	58	>98:2	>96 SS
2	SAMP	H	Me	Et	59	>98:2	>96 SS
3	RAMP	H	Me	Et	52	>98:2	>96 RR
4	SAMP	H	Et	Ph	38	>98:2	>96 SS
5	SAMP	H	Ph	Ph	38	>98:2	>96 SS
6 ^b	SAMP	Et	Et	Me	45	95:5	92 SS
7	RAMP	Et	Et	Me	40	>98:2	>96 RR
8	SAMP	Ph	Me	Me	45	>98:2	>96 SS
9	SAMP	Ph	Me	Ph	43	100:0	100 SS
10	SAMP	n-Bu	n-Pr	Ph	40	96:4	>96 SS

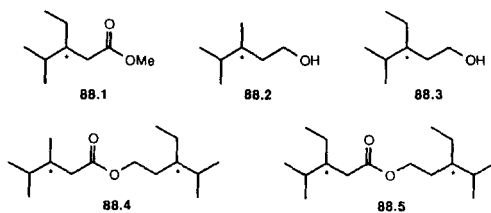
a. Ratio determined by ^1H and ^{13}C NMR using chiral shift reagents.

b. In this entry, HMPA (2 equivalents) replaced TMEDA as cosolvent.

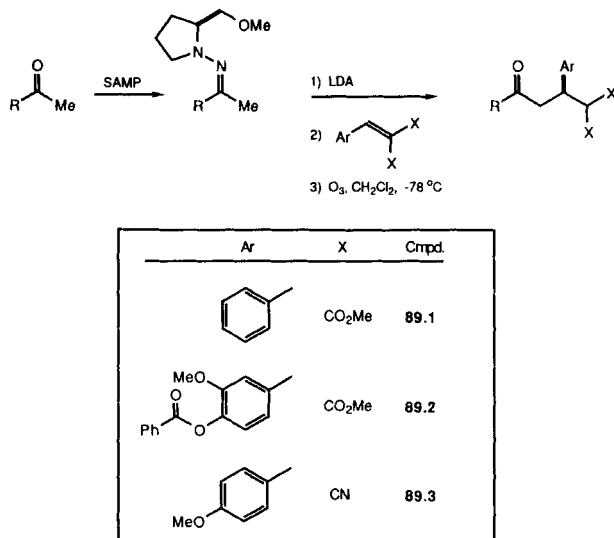
lyctena) and the red wood ant (*F. rufa*, Scheme 88) (169). Because the absolute configuration of these natural products was unknown, it was necessary to prepare both enantiomers of each for the purpose of biological evaluation. The flexibility of the SAMP/RAMP method is epitomized by the ease with which both enantiomers were obtained in each of these synthetic projects.

2. To α,β -Unsaturated Diesters

[N*,P] Addition of the lithiated hydrazones derived from methyl ketones to diactivated styrenes **89.1–89.3** has also been studied by Enders and coworkers (Scheme 89, Table 39) (170). Only one enantiomeric product was detected in all the cases examined. The absolute configuration of the products generated with the diactivated acceptors is the same as with the α,β -unsaturated esters discussed in the previous section.



Scheme 88



Scheme 89

Table 39
Addition of Lithiated Hydrazones to Diactivated Acceptors (Scheme 89)

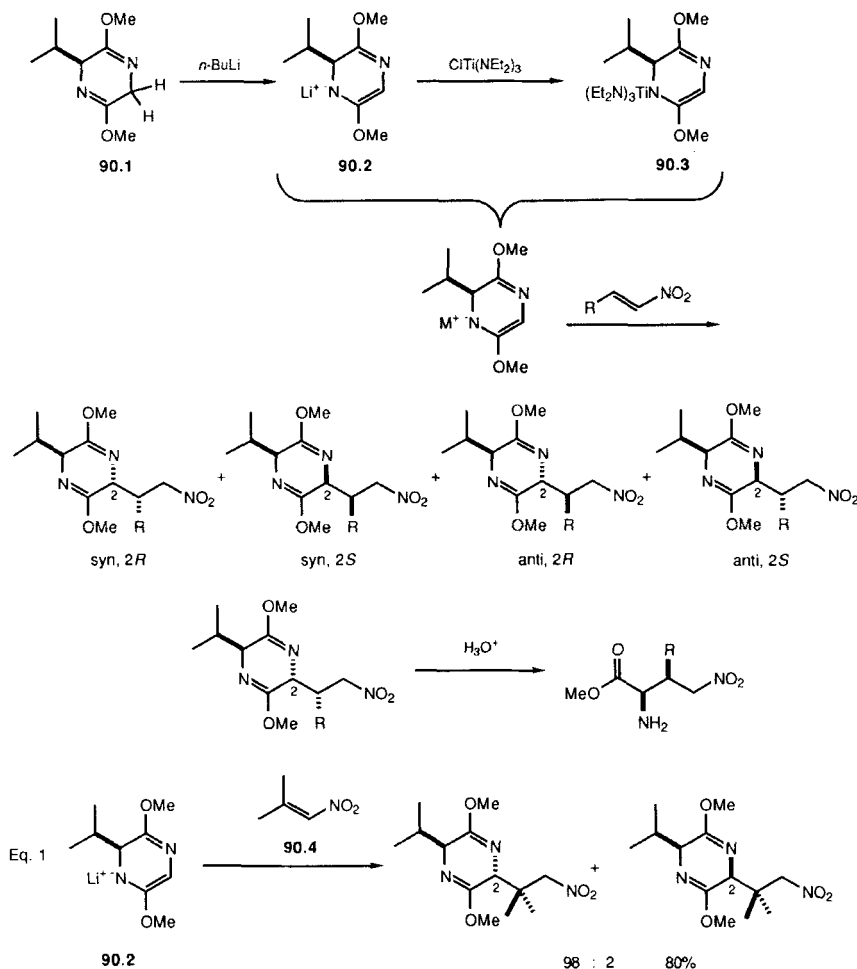
Entry	Hydrazone R	Acceptor X	Yield ^a %	ee ^b %	
1	Me	89.1	CO ₂ Me	72	>95
2	Et	89.1	CO ₂ Me	74	>95
3	Ph	89.1	CO ₂ Me	82	>95
4	Et	89.2	CO ₂ Me	62	>95
5	Ph	89.2	CO ₂ Me	50	>95
6	Ph	89.3	CN	53	>95

a. Overall yield for Michael addition/cleavage sequence.

b. Determined by ¹H NMR using chiral shift reagents.

3. To Nitroolefins

[P*,P] Alkylation of bislactim ether **90.1** (derived from the cyclic dipeptide of valine and glycine) gives α -amino acids with excellent enantioselectivity (171). Conjugate addition of the metallated derivatives of **90.1** to *E* nitroolefins also proceeds with excellent diastereoselection (172). The results of this study are summarized in Scheme 90 and Table 40. Lithium and titanium derivatives of **90.1** (**90.2** and **90.3**) were examined. The lithium derivatives are more reactive and less selective. The enhanced reactivity, however, permits



Scheme 90

Table 40
Addition of the Valine-Derived Bislactim 90.1 to Nitroolefins (Scheme 90)

Entry	Nitroolefin R	Counterion	Yield %	syn:anti	2R:2S
1	Me	Li	81	96:4	86:14
2	Me	(Et ₂ N) ₃ Ti	51	98:2	98:2
3	Ph	Li	78	56:44	83:17
4	Ph	(Et ₂ N) ₃ Ti	57	97:3	97:3
5	Ar ^a	Li	52	55:45	90:10
6	Ar ^a	(Et ₂ N) ₃ Ti	60	99:1	100:0 ^b

a. 3,4-Methylenedioxyphenyl.

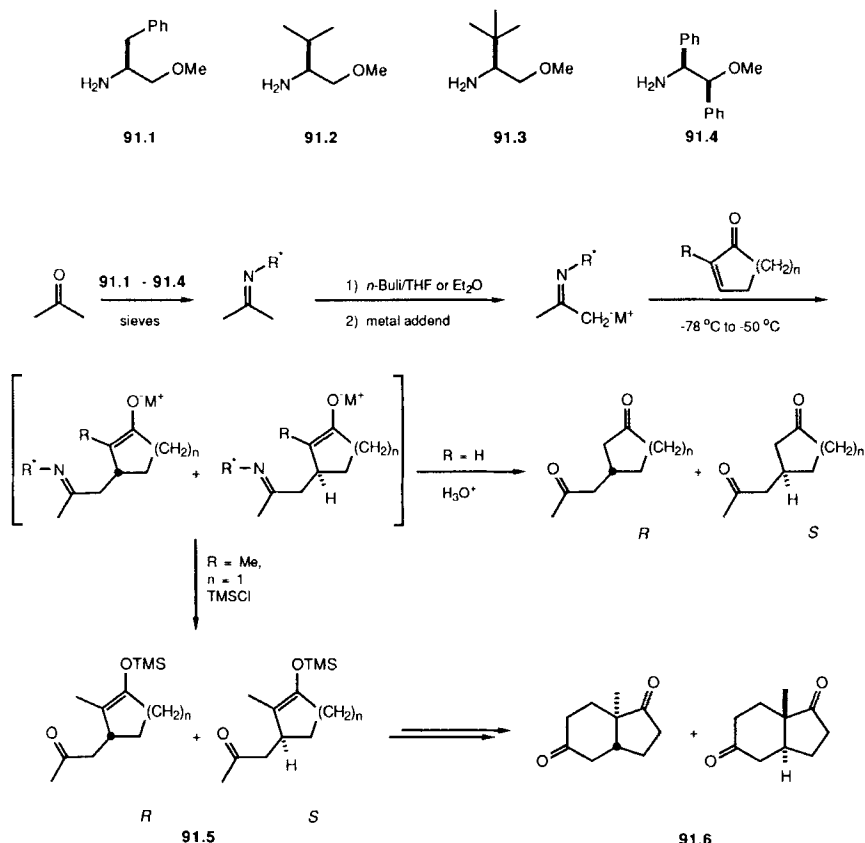
b. The minor diastereomer was not detected.

reaction with the β,β -disubstituted nitroolefin 90.4 with impressive selectivity (Eq. 1). Superior selectivities are obtained with the titanium derivatives (entries 2, 4, and 6); at least 94% of one diastereomer was formed in each case studied. The direction of attack on the metallated heterocycle agrees with the results for alkylations of similar substrates (171). The Michael adducts are hydrolyzed with 0.1 N HCl to the nitro amino ester. Analogous results have been obtained using enoates as acceptors (172b).

4. To α,β -Unsaturated Ketones

[N*,P] K. Yamamoto and his coworkers have reported the addition of metallated imines derived from acetone and amines 91.1-91.4 to cyclic enones (173). Amines 91.1-91.3 are derived from the corresponding amino acids. Amine 91.4 was available from benzoin oxime through catalytic reduction and resolution of the resulting racemic amino alcohol (174). The acceptors used were 2-cyclohexenone, 2-cyclopentenone, and 2-methyl-2-cyclopentenone. The results of this study are summarized in Scheme 91 and Table 41. Of all auxiliaries surveyed, 91.4 was by far the most efficient (entries 11-18). It is also interesting to note that increasing selectivity is observed along the series 91.1, 91.2, 91.3 (entries 1-3, 6-8). The sense of the stereochemical differentiation depends both on the auxiliary and on the substrate (entries 1-10). For example, the methyl group in 2-methyl-2-cyclopentenone results in a reversal in selectivity (compare entries 8 and 9).

Zincates proved to be more selective than the corresponding cuprates (compare entries 11-13 and 16 with entries 14-15 and 17-18). In some instances the zincate is not sufficiently reactive to give an acceptable chemical yield. Addition of an additional equivalent of the zincate increases the yield in



Scheme 91

some of these cases (compare entries 14 and 15). Additionally, zinicates are unreactive towards acyclic enones and gave, with 2-cyclohexenone, small amounts of 1,2-addition. Cuprates and zinicates give comparable selectivities, suggesting a mechanistic similarity.

A degree of variability is seen in these reactions both in yields (entry 1, Table 41) and in selectivity (entries 3 and 4, see footnotes c and e). The apparent non-linearity between the enantiomeric purities of the starting amines and the products between entries 3 and 4, if not an artifact, is intriguing.

With 2-methyl-2-cyclopentenone, the initial adduct of the conjugate addition was trapped with trimethylsilyl chloride to form enol ethers 91.5 (Scheme 91). These enol ethers (91.5) were converted to the enantiomerically enriched

Table 41
Addition of Chiral Metallated Imines to α,β -Unsaturated Ketones (Scheme 91)

Entry	Amine	Acceptor R n	Additive	Solvent	Yield ^a %	Config.	ee %
1	91.1	H 2	CuI	THF	21-41	R	28
2	91.2	H 2	CuI	THF	46	R	29
3	91.3 ^b	H 2	CuI	THF	30	S	44 ^c
4	91.3 ^d	H 2	CuI	THF	31	R	44 ^e
5	91.1	H 2	Cu(I) acetylidedef	THF	16	R	27
6	91.1	H 1	CuI	THF	54	R	17
7	91.2	H 1	CuI	THF	75	S	27
8	91.3 ^d	H 1	CuI	THF	89	R	75 ^e
9	91.3 ^d	Me 1	CuI	THF	9	S	60 ^h
10	91.3 ^b	Me 1	CuI	THF	9	R	62 ^h
11	91.4 ⁱ	H 1	Cu(I) acetylidedef	THF	78	R	78
12	91.4 ^j	H 1	Cu(I) acetylidedef	Et ₂ O	41	S	80
13	91.4 ^j	H 1	Cu(I) acetylidedef	Et ₂ O	56	S	82 ^k
14	91.4 ⁱ	H 1	ZnMe ₂ ^l	THF	26	R	88
15	91.4 ⁱ	H 1	ZnMe ₂ ^l	THF	73	R	92
16	91.4 ^j	H 2	Cu(I) acetylidedef	THF	78	S	71
17	91.4 ^j	H 2	ZnMe ₂ ^l	THF	55	S	82
18	91.4 ^j	H 2	ZnMe ₂ ^l	THF	48	S	88

a. Yields are for purified diketones and are somewhat variable.

b. (S)-91.3 was used.

c. Amine with 80% optical purity was used.

d. (R)-91.3 was used.

e. Amine with 96% optical purity was used.

f. 3-Methoxy-3-methyl-1-butyne was used as dummy ligand.

g. Diketones were not isolated.

h. The optical purity of the starting material was not reported.

i. The (-)-(1*S*,2*R*) enantiomer of the amine was used.

j. The (+)-(1*R*,2*S*) enantiomer of the amine was used.

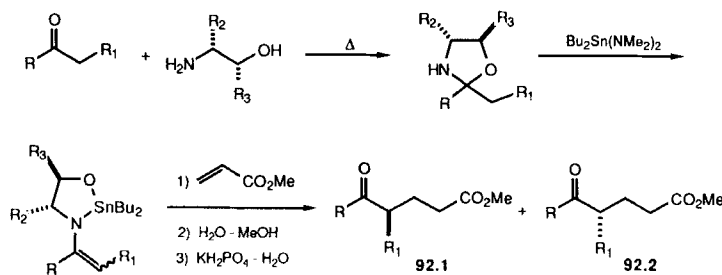
k. TMSCl (1 equiv.) was added with the enone.

l. 2 equivalents of the zincate was used.

trans-hydrindandione 91.6 in 24% overall yield from 2-methyl-2-cyclopentenone.

5. To α,β -Unsaturated Esters

[P*,N] The addition of chiral, non-racemic dibutylstannylated imines to enoates has been reported by de Jeso and coworkers (175). The results of this study are summarized in Scheme 92 and Table 42. Of particular note is the selectivity obtained with the metallated imine derived from cyclohexanone (entry 1). It should be noted, however, that the enantiomeric excesses of the products shown are corrected for the enantiomeric purity of the amino alcohol. Nevertheless, it is clear that good use could be made of this process if enantiomerically pure amino alcohols such as valinol were to be employed.



Scheme 92

Table 42
Addition of Chiral Stannylated Imines to Methyl Acrylate (Scheme 92)

Entry	Ketone R	R_1	Amino R_2	Alcohol R_3	Solvent	Yield %	Temp. °C	92.1:92.2 ^a	ee ^a %
1	$-\text{CH}_2\text{CH}_2\text{CH}_2\text{CH}_2-$		Et	H	benzene	63	60	7:93	86 ^b
2	$-\text{CH}_2\text{CH}_2\text{CH}_2\text{CH}_2\text{CH}_2-$		H	Me	benzene	50	60	63:37	36 ^c
3	H	<i>i</i> -Pr	Et	H	cyclohexane	32	60	34:66	32
4	H	<i>i</i> -Pr	Et	H	pentane	35	20	82:18	64
5	H	Et	Et	H	cyclohexane	43	60	61:49	22
6	H	Et	Et	H	THF	51	0	17:83	66
7	H	Me	Et	H	cyclohexane	11	60	>54:46	>8
8	H	Me	Et	H	pentane	33	20	31:69	37
9	H	Et	Et	H	THF	42	0	59:61	17
10	H	<i>i</i> -Pr	<i>i</i> -Pr	H	cyclohexane	28	60	>54:46	>8
11	H	<i>i</i> -Pr	<i>i</i> -Pr	H	pentane	40	20	37:63	26
12	H	<i>i</i> -Pr	<i>i</i> -Pr	H	THF	58	20	42:58	16
13	H	Et	<i>i</i> -Pr	H	cyclohexane	28	60	63:37	25
14	H	Et	<i>i</i> -Pr	H	pentane	30	20	>54:46	>8
15	H	Me	Et	H	cyclohexane	28	20	46:54	8
16	H	Et	Et	H	cyclohexane	28	20	36:64	28
17	H	<i>i</i> -Pr	Et	H	cyclohexane	33	20	68:32	36
18	H	<i>i</i> -Pr	Et	H	cyclohexane	26	40	44:56	12
19	H	<i>i</i> -Pr	Et	H	cyclohexane	17	0	66:34	31

a. Corrected for the optical purity of the starting amino alcohol.

b. The isolated product obtained had 58% ee.

c. The isolated product had 8% ee.

In general the selectivities and chemical yields obtained with the aldehyde imines are significantly lower than for the cyclohexanone imine (entries 3–19, Table 42). The reversal in selectivity on warming suggests that the reaction may be under thermodynamic control at higher temperatures (compare entries 3 and 4, 7 and 8, 10 and 11).

R. Carboxylic Acid Dianions

[P,P] Prostereogenic enolates derived from carboxylic acids can be added to α,β -unsaturated ketones. Initial 1,2-addition was found to be irreversible. Stereoselectivities in the 1,4-addition reactions are not notable (176).

S. Dithianylidene Anions

1. To α,β -Unsaturated Ketones

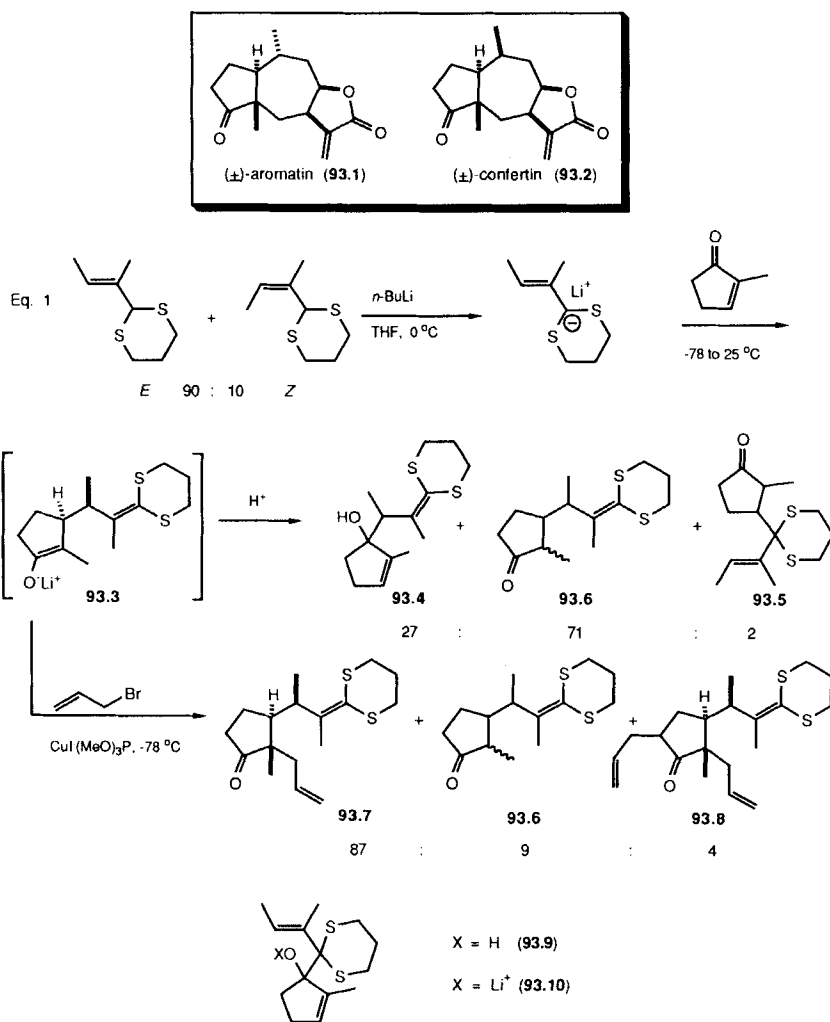
[P,P] In connection with the synthesis of the natural products (\pm)-aromatin (93.1) and (\pm)-confertin (93.2), Ziegler and coworkers have examined the conjugate addition of dithianylidene anions to 2-methyl-2-cyclopentenone (Scheme 93) (177). The dithianylidene anions were generated by lithiating an E/Z mixture of the unsaturated dithianes (Eq. 1). Preferential deprotonation of the E dithiane was observed.

Reaction of the sulfur-stabilized anion with 2-methyl-2-cyclopentenone produces an intermediate enolate that can be either protonated or allylated. The products from the direct protonation revealed that most of the addition occurred in the desired sense to produce 93.6. A significant amount of γ -1,2-addition product (93.4) and a small amount of material coming from conjugate addition at the α -position of the dithiane (93.5) were observed.

For the purpose of the synthesis, the allylated product (93.7) was desired (Scheme 93). Allylation of 93.3 results in preferential formation of 93.7, along with some of the di- and unallylated products 93.8 and 93.6. The desired product (93.7) was obtained in 50% yield in 90% isomeric purity. Two minor isomers are formed (5% each). One of the isomers is epimeric at the exocyclic stereocenter while the other product ensues from allylation of the more hindered face of the cyclopentanone enolate.

Although stereocontrol in the conjugate addition reaction was not required for the subsequent synthesis of 93.1 and 93.2, the simple selectivity in the process is notable. Ozonolysis of the dithioketene acetal yields a ketone. The dithianylidene anion is, therefore, a synthon for the more substituted enolate of ethyl methyl ketone. Overall, the process corresponds to a regio- and stereoselective Michael addition of ethyl methyl ketone to 2-methyl-2-cyclopentenone.

Addition of HMPA or copper(I) iodide to the reaction mixture results in a greater percentage of α -dithiane 1,4-addition products (93.5). For normal alkyl dithianes, addition of HMPA or copper(I) iodide generally leads to a greater proportion of 1,4-addition to α,β -unsaturated ketones (178). One would expect, in the absence of these addends, that α -dithiane 1,2-addition products would be preferred. Indeed, when the reaction mixture is quenched



Scheme 93

at low temperatures, a predominant amount of the α -dithiane 1,2-addition product (**93.9**) is observed. Upon warming, the initial α -1,2-adduct **93.10** is apparently converted to **93.3**, presumably through an anion-accelerated Cope rearrangement (179, 180). Thus, this manifold (1,2-addition/anionic Cope rearrangement) is likely to be the mechanism for stereochemical differentiation in these reactions.

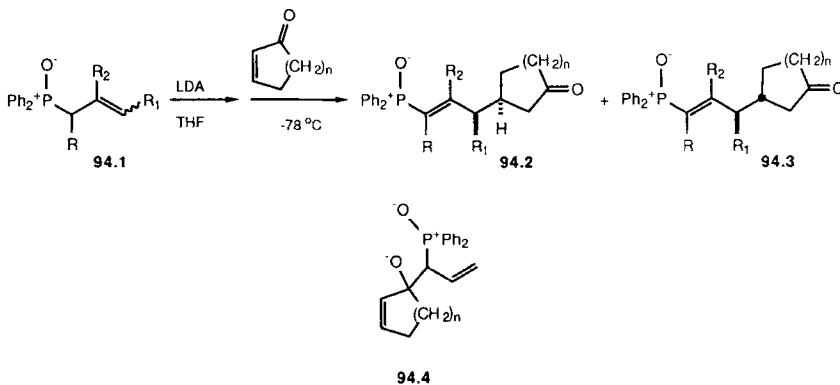
T. Phosphine Oxide Stabilized Allyl Anions

Deprotonation of allylphosphine oxides with a strong base such as LDA, leads to a stabilized allyl anion. On addition of cyclic α,β -unsaturated ketones, preferential reaction occurs by reaction of the γ -position of the allyl anion to the β -position of the acceptor. The vinylphosphine oxide produced in the reaction can be oxidatively cleaved to form a ketone or aldehyde. The allyl phosphine oxide anion is, therefore, an enolate equivalent.

1. To α,β -Unsaturated Ketones

[P,P] Haynes and coworkers have examined the conjugate addition of the stabilized allyl anions from phosphine oxides of the general structure **94.1** to 2-cycloalkenones (181–183, 192); the results are summarized in Scheme 94 and Table 43. A strong correlation between the geometry of the double bond of the starting materials and the stereochemistry of the products has been observed. Use of the *Z* crotylphosphine oxide gives the “syn” product **94.2** (entry 1), while the *E* crotylphosphine oxide gives the “anti” adduct **94.3** (entry 2). Similar stereoselective behavior is manifest by the cyclopentene derivative (entry 3), which gives solely the “syn” adduct.

Haynes' results have been rationalized in terms of a chelated 10-membered transition state. An alternate mechanism involving initial 1,2- α -addition to form **94.4** followed by anion-accelerated Cope rearrangement (180) analogous to Ziegler's mechanism (177, 179) for the addition of dithianyliidene anions to cyclopentenones (*vide supra*) would also seem possible in this case.



Scheme 94

Table 43
Addition of Phosphine Oxide-Stabilized Allyl Anions to Cycloalkenones
(Scheme 94)

Entry	Allyl		Phosphine Oxide	E:Z	Cycloalkenone n	Yield %	94.2:94.3
	R	R ₁					
1	H	Me	H	0:100	1	80	100:0
2	H	Me	H	95:5	2	60	5:95
3	-CH ₂ CH ₂ -		H	0:100	1	63	100:0
4	H	Me	Me	Z ^a	1	93	(94.2) ^b
5	H	Me	Me	E ^a	1	86	(94.3) ^b

a. Exact ratio not reported.

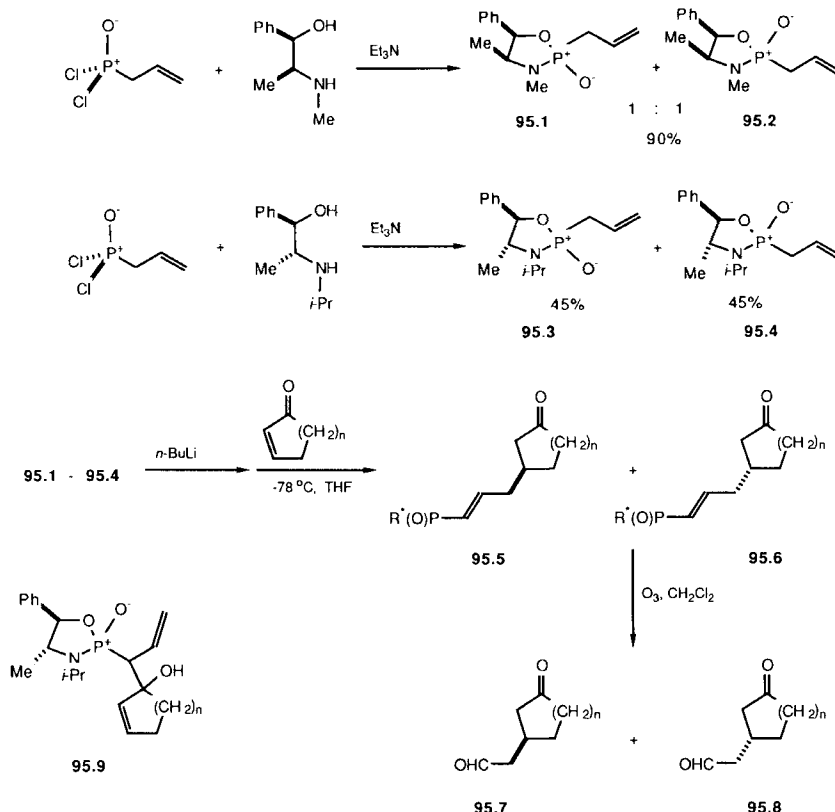
b. "Predominant" product.

However, the low temperatures (-78°C) at which Haynes' reactions are performed, coupled with observations made for the addition of closely related allyl sulfoxides (*vide infra*), make the 1,2- α -addition/anionic Cope rearrangement pathway appear less likely with this system.

[N*,P] By using a chirally modified allylphosphine oxide, Hua and coworkers have achieved asymmetric induction in the conjugate addition of the stabilized allyl anion to cycloalkenones (184). The results of this study are summarized in Scheme 95, Table 44. The chiral, non-racemic phosphine oxides were prepared by reaction of allylphosphonyl dichloride with (-)-ephedrine and (-)-N-isopropylnorpseudoephedrine (Scheme 95). In each case, the amino alcohol complexes were obtained as 1:1 mixtures of isomers. After separation, each isomer was deprotonated with *n*-butyllithium in THF at -78°C , and the cycloalkenone was added. Quench and work-up lead to products 95.5 and 95.6 that result from 1,4- γ addition. Only with the allylphosphonyl anion from 95.4 are any regioisomers obtained from the addition (entries 6 and 7). In these cases, small amounts of the 1,2- α -adducts 95.9 are obtained. Oxidative cleavage of 1,4- γ -adducts with ozone provides keto-aldehydes 95.7 and 95.8 (Scheme 95). At this stage the enantioselectivity of the process was determined.

The level of asymmetric induction in the addition was found to be dependent on both the amino alcohol employed as chiral auxiliary and on the stereochemistry at phosphorus. With the ephedrine-derived substrates 95.1 and 95.2, good enantioselectivities are obtained (entries 1-4, Table 44). The sense of asymmetric induction varies depending on the configuration at phosphorus. For example, 95.1 preferentially leads to the *S* enantiomer 95.7 whereas 95.2 produces 95.8 with similar levels of selectivity.

With the anion from the isopropylamide 95.4, conjugate addition gave lower levels of diastereo- and regioselectivity. On the other hand, the diaste-



Scheme 95

reomeric anion from 95.3 provided exceptional levels of selectivities with all of the cycloalkenones employed (entries 8–10, Table 44).

U. Allyl Sulfoxide Anions

Sulfoxides are attractive components in asymmetric (enantioselective) synthesis because of the ability of the sulfinyl function to stabilize adjacent anions and the potential for stereogenicity at sulfur (65). When a chiral sulfoxide is substituted with an allyl group, deprotonation with a strong base leads to a sulfoxide-stabilized allyl anion capable of potentially asymmetric nucleophilic addition.

Table 44
Addition of Chiral, Phosphorus-Stabilized Allyl Anions to Cycloalkenones
(Scheme 95)

Entry ^a	Nucleophile	Enone n	Yield ^b %	95.7:95.8	ee %
1	<u>95.1</u>	1	65	85:15	70
2	<u>95.1</u>	2	67	87:13	74
3	<u>95.2</u>	1	66	13:87	74
4	<u>95.2</u>	2	68	13.5:86.5	73
5	<u>95.4</u>	1	65	36:64	28
6	<u>95.4</u>	2	48 ^c	36:64	28
7	<u>95.4</u>	3	36 ^d	18:82	64
8	<u>95.3</u>	1	63	99:1	98
9	<u>95.3</u>	2	57	94:6	88
10	<u>95.3</u>	3	58	97.5:2.5	95

a. The optimal conditions are underlined.

b. Overall yield for the keto-aldehyde derived from oxidative cleavage of the initial Michael adduct.

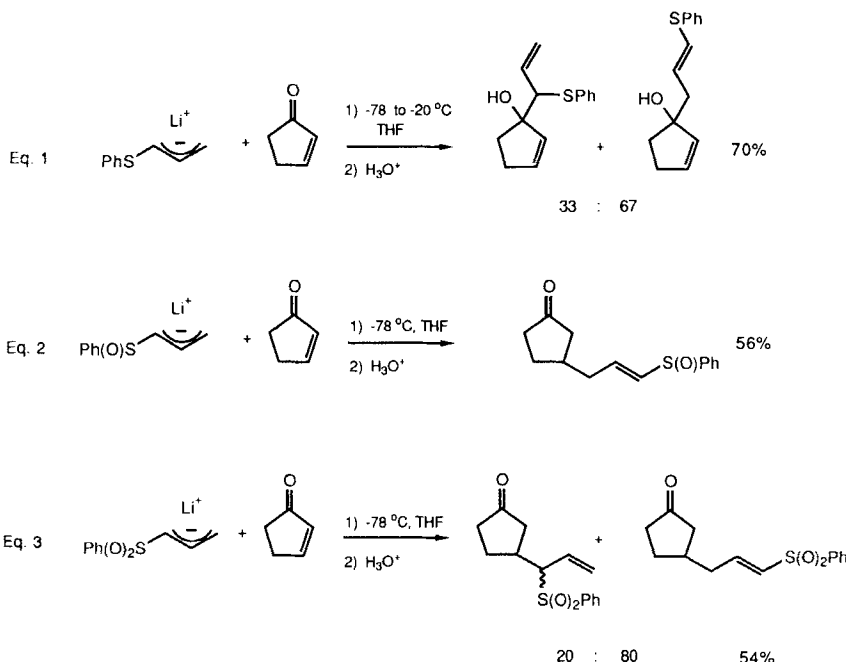
c. 15% 1,2- α -adducts was isolated.

d. 5% 1,2- α -adducts was isolated.

Sulfoxide-stabilized allylic anions have two positions of nucleophilicity, α or γ . If the acceptor has two positions of electrophilicity (for example, an α,β -unsaturated ketone), then four regioisomers are possible in the addition.

Many stabilized allylic anions prefer electrophilic attack adjacent to the anion-sustaining component (*vide supra*) (185). Sulfur-stabilized anions, however, exhibit markedly different regiochemical propensities (at least on addition to cycloalkenones) depending on the oxidation state at sulfur (186-188). For example, the lithium anion of phenyl allyl sulfide in THF gives a mixture of α -1,2- and γ -1,2-addition products (Eq. 1, Scheme 96). On the other hand, the softer phenyl allyl sulfoxide anion in Eq. 2 gives entirely γ -1,4-addition. With the phenyl allyl sulfone anion, mostly the γ -1,4-adducts are formed with some of the α -1,4-products (Eq. 3). If the additions are performed in the presence of HMPA, sulfides, sulfoxides, and sulfones all give a greater proportion of products that result from α -1,4-addition (188).

Enantiomerically enriched allylic sulfoxides can readily racemize through a [2,3] sigmatropic rearrangement (Mislow rearrangement). For allyl *p*-tolyl sulfoxide, racemization occurs at "conveniently measured rates" between 50 and 70°C (189). With the allyl sulfoxide, enantiomeric integrity can be maintained by immediate use after preparation and purification at low tempera-

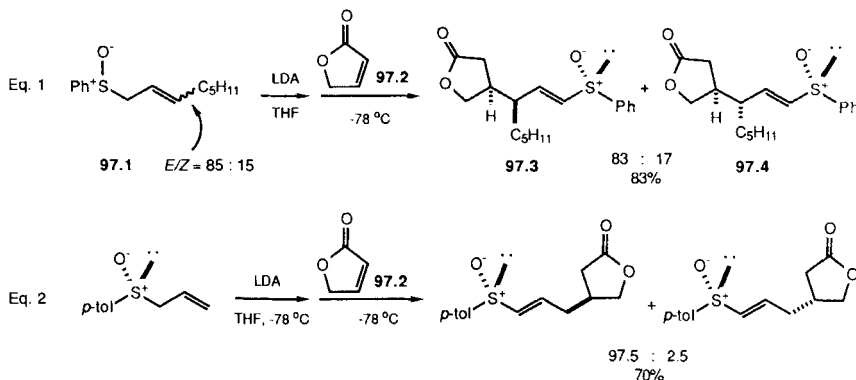


Scheme 96

tures. Crotyl sulfoxides, on the other hand, are more difficult to prepare in an enantiomerically pure form and racemize more readily. Hence, there have been no reports of the conjugate addition of enantiomerically pure crotyl sulfoxides. Haynes, Ridley, and coworkers, however, have recently described an alternative synthesis of allylic sulfoxides that may be applicable to the synthesis of enantiomerically pure crotyl sulfoxides (190).

1. To α,β -Unsaturated Lactones

[P*,P] and [N*,P] Haynes and coworkers have found that the addition of the anion of the racemic allylic sulfoxide **97.1** to furanone **97.2** results in the formation of diastereomers **97.3** and **97.4** (Eq. 1, Scheme 97) (181, 183, 191, 192). Because of the configurational instability of **97.1**, a 85:15 (*E/Z*) mixture of allylic sulfoxides was used, resulting in a 83:17 mixture of **97.3** and **97.4**, which differ only at the relative configuration of the pentyl substituted exocyclic stereocenter. Further work (*vide infra*) strongly suggests that the stereochemistry of this reaction is determined by the geometry of the starting



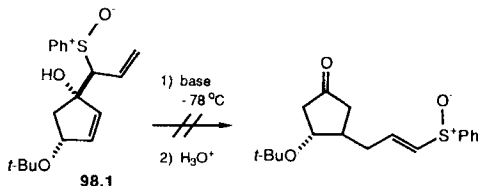
Scheme 97

materials. Hence, it is likely that the *E* isomer of **97.1** leads to the formation of **97.3** while the *Z* isomer of **97.1** provided **97.4**. Importantly, the relative stereochemistry of the lactone stereocenter and the sulfinyl function is the same for both isomers. This suggests that if **97.1** were prepared in a configurationally stable, optically active form, then this protocol should be applicable to the synthesis of optically active substrates.

A similar reaction was reported by Hua and coworkers, who showed that the optically active allyl sulfoxide in Eq. 2 (Scheme 97) gives, on addition to **97.2**, addition products with excellent selectivity (193, 194). In this case, the enantiomeric purity was measured on the desulfurized product, confirming both the asymmetric induction in the reaction and the enantiomeric purity of the starting sulfoxide.

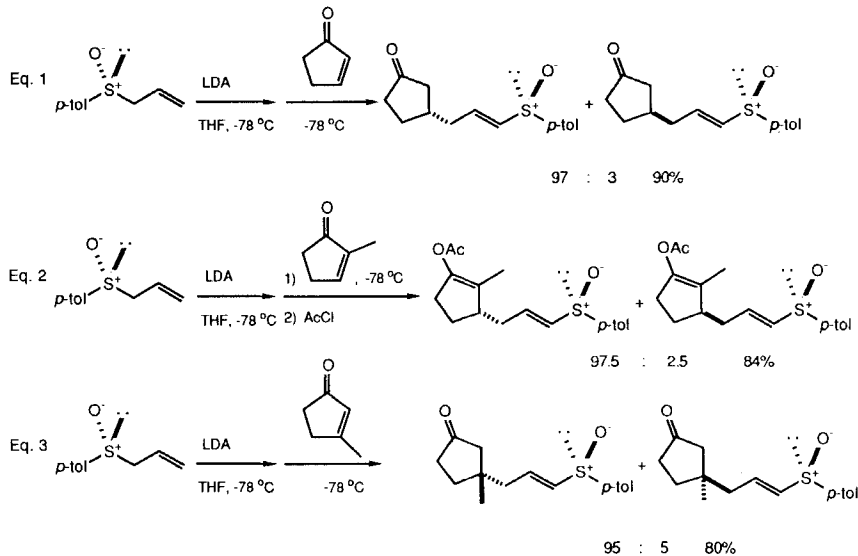
2. To α,β -Unsaturated Ketones

Haynes and coworkers have explored the Michael addition of sulfoxide-stabilized allylic anions to α,β -unsaturated ketones (181–183, 192). As discussed in the preceding section, such anions give products of attack at the β -position of the enone by the γ -carbon of the allylic anion. In contrast to Ziegler's results with dithianyldene anions (177), however, Haynes and coworkers present compelling evidence that, with these substrates, the reaction proceeds through direct conjugate addition. The reaction conditions involved addition of the anion to the acceptor at very low temperature (-78 to -100°C). Cope rearrangement, even the anion-accelerated version, would be expected to be quite slow at these temperatures. Indeed, independently synthesized **98.1** is stable under the reaction conditions employed (Scheme 98).

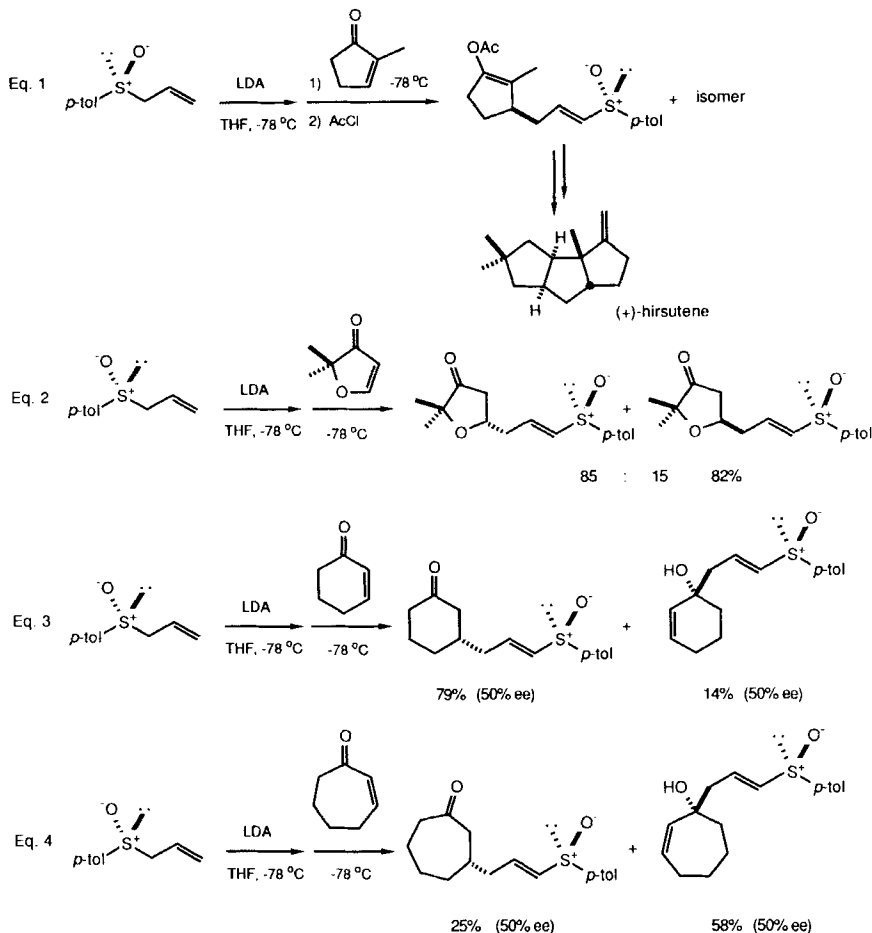


Scheme 98

[N*,P] Hua and coworkers have examined additions to five-membered ring acceptors of optically active allyl sulfoxides (Eqs. 1–3, Scheme 99; Eqs. 1 and 2, Scheme 100) (193, 194). The enantiomeric purities of the products were determined after oxidation of the sulfoxide to the sulfone or reduction to the sulfide. Excellent enantiomeric excesses were achieved in all cases, irrespective of the substitution pattern of the cyclopentenone. The enolate generated in the Michael addition can also be trapped with acetyl chloride (Eq. 2, Scheme 99). This technique was applied, using the enantiomeric sulfoxide, to the synthesis of (+)-hirsutene (Eq. 1, Scheme 100) (195). Addition of the allyl sulfoxide anion to larger ring acceptors results in significantly lower enantioselectivities (Eqs. 3 and 4, Scheme 100) (194). The products obtained in these instances were contaminated with γ -1,2-adducts.



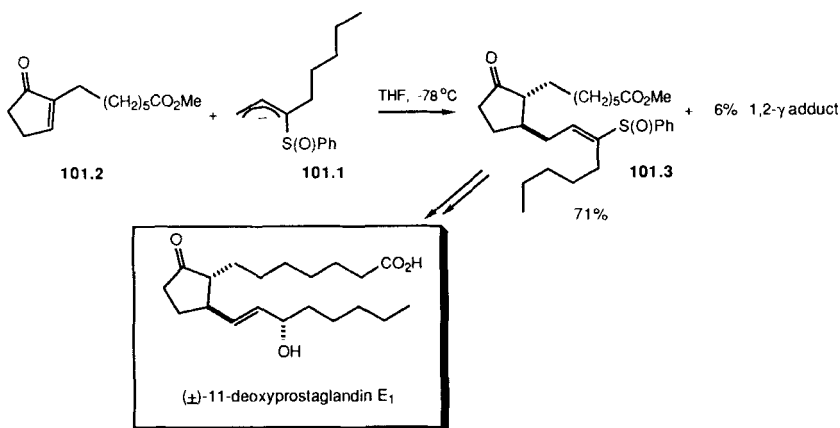
Scheme 99



Scheme 100

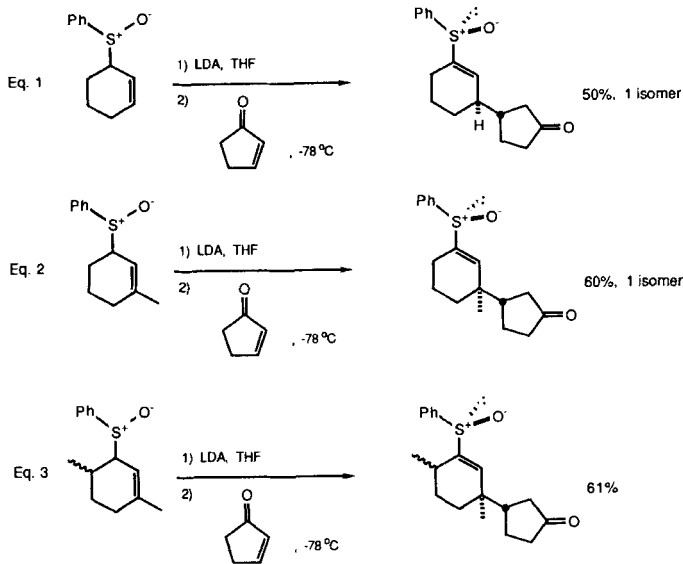
Vasil'eva and coworkers reported the addition of the allylic sulfoxide anion **101.1** to cyclopentenone **101.2** (Scheme 101) (196). The γ -1,4 adduct (**101.3**) was obtained in a "stereochemically homogenous form," accompanied by a small amount of the γ -1,2 regioisomer. No information was provided concerning the relative configuration of the sulfoxide and cyclopentyl stereocenters. The major product (**101.3**) was converted via a short sequence into (\pm) -11-deoxyprostaglandin E₁.

[P*,P] Addition of the anion of racemic cyclic allylic sulfoxides to 2-cyclopentenone proceeds with excellent diastereoselectivity (Scheme 102) (197).



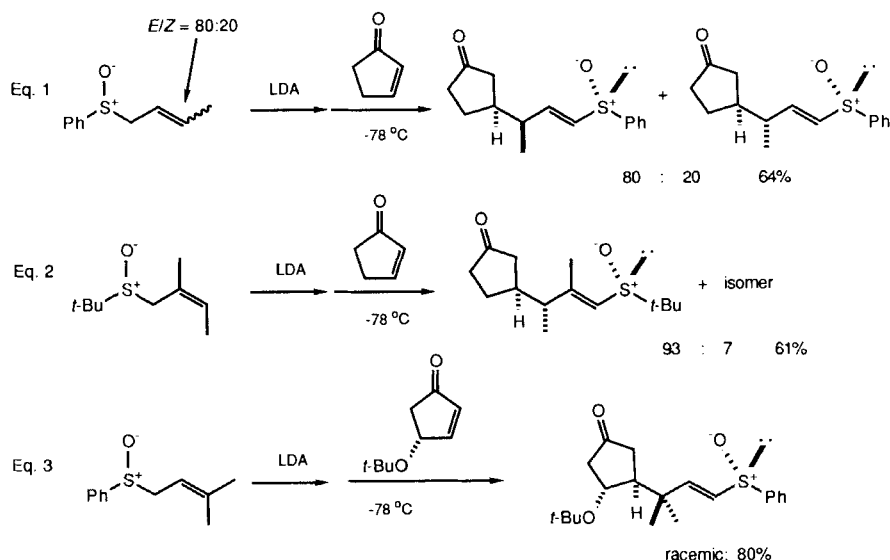
Scheme 101

When β -methylcyclopentenones are used as acceptors, low yields of products with adjacent quaternary centers are obtained ($\leq 15\%$). With the sulfoxide in Eq. 3, the chirality at sulfur overrides any facial direction provided by the methyl group. Although not used with these acceptors, the sulfoxide in Eq. 3 was also prepared in a stereochemically and enantiomerically pure form (*vide infra*).



Scheme 102

In the examples in Eqs. 1 and 2 (Scheme 103), the geometry of the double bond in the racemic allylic sulfoxide determines the relative configuration of the two stereocenters formed in the addition (181–183, 192). Again, the stereochemistry at sulfur appears to be in strong control of the diastereofacial preference of the sulfoxide anion.



Scheme 103

[N*,P*] In Eq. 3 (Scheme 103), the anion of the racemic sulfoxide, when added to racemic 4-*tert*-butoxy-2-cyclopentenone, gives only one diastereomer in 80% yield. This remarkable outcome is a result of mutual kinetic enantioselection (34), that is, one-to-one matching of the enantiomers of two racemates (the sulfoxide and the enone). The *R* enantiomer of the cyclopentenone reacts with the *S* enantiomer of the sulfoxide and the *S* enantiomer of the acceptor reacts with the *R* enantiomer of the nucleophile. In cases of very pronounced mutual kinetic enantioselection, such as that shown in Eq. 3, three conditions must be satisfied:

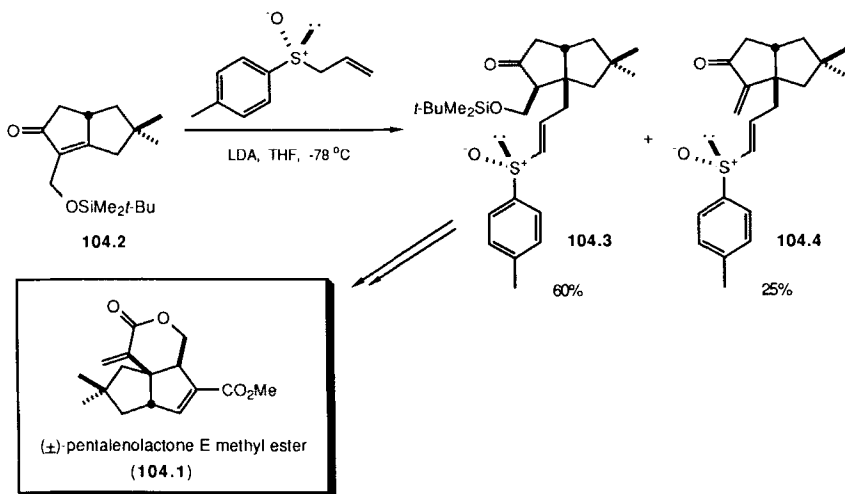
- The donor (the allylic sulfoxide) must have a strong diastereofacial preference with respect to attack by electrophiles;
- The donor and acceptor must combine with a distinct predilection for their relative orientations in the transition states. This situation is manifested with prostereogenic donors and acceptors as simple diastereoselectivity; and

- The acceptor (*4-tert*-butoxy-2-cyclopentenone) must itself exhibit a pronounced facial preference for attack by nucleophiles.

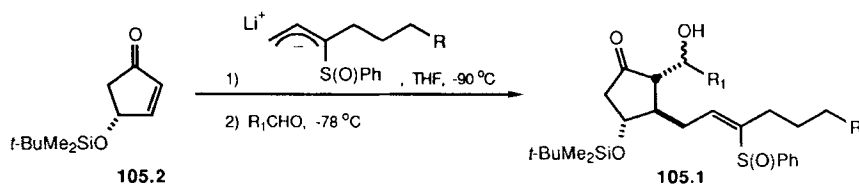
Mutual kinetic enantioselection in this process can be illustrated by examining the fate of one of the enantiomers of the allylic sulfoxide anion. As a result of the strong facial directing influence of the sulfoxide group, only one face of the allylic system is attacked. These systems exhibit a strong orientational inclination in the transition state, as witnessed by the excellent simple selectivity exhibited by each allylic sulfoxide isomer in Eqs. 1–2 (Scheme 103). Hence, the facial propensity of the allylic sulfoxide communicated through the simple selectivity (relative orientational preference) of the systems, results in a compelling propensity for addition to one of the two prosterogenic faces of the cyclopentenone. Now, consider a racemic acceptor, such as *4-tert*-butoxy-2-cyclopentenone, that has a strong preference for adding nucleophiles *trans* to the *tert*-butoxy group. Hence, each enantiomer of the acceptor has a different face (*Si* or *Re*) that is preferentially attacked by nucleophiles. Combining the donor and acceptor, we see that each enantiomer of the allylic sulfoxide has a distinct propensity for adding to either the *Re* or *Si* face of an acceptor while each enantiomer of *4-tert*-butoxy-2-cyclopentenone has a pronounced preference for the addition of nucleophiles to either its *Si* or its *Re* face. The net result is a large inclination for the addition one enantiomer of the allylic sulfoxide to one enantiomer of the *4-tert*-butoxy-2-cyclopentenone.

The use of the foregoing methodology in a synthesis of (\pm)-pentalenolactone *E* methyl ester (**104.1**) has been reported by Hua and coworkers (Scheme 104) (198). Bicyclic enones such as **104.2** add nucleophiles to the convex face, giving the more stable *cis*-fused products. Indeed, addition of the anion of the racemic allyl sulfoxide to the bicyclic enone **104.2** occurs with excellent stereoselectivity providing **104.3** as the only detectable isomer. In this case, the stereocenter adjacent to the carbonyl group is established by a stereoselective protonation. This stereoselectivity is surprising, since bicyclo[3.3.0]octanes usually react at C-2 from the convex, rather than the concave, face. Side product **104.4**, resulting from elimination of the trialkylsilyloxide anion from the enolate formed in the conjugate addition, was also observed. The major product (**104.3**), was converted via a short sequence to **104.1**. Although not important in the pentalenolactone synthesis, the strong facial preference of the sulfoxide anion coupled with the availability of only one face of the acceptor results in mutual kinetic enantioselection and a one-to-one matching of enantiomers of the sulfoxide and the enone is observed.

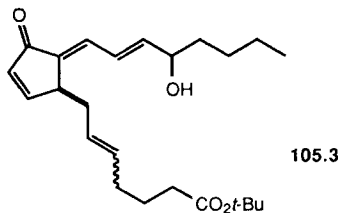
Nokami and coworkers have reported an application of the allylic sulfoxide conjugate addition/mutual kinetic enantioselection process in synthesis of prostaglandin analogues (Scheme 105) (199). The cyclopentanone enolate



Scheme 104



Entry	R	R ₁	Yield
1	-CH ₃	- (CH ₂) ₅ CO ₂ Me	68%
2	-CH ₂ OSiMe ₂ t-Bu	-CH ₂ =CH-CH(OSiMe ₂ t-Bu)(CH ₂) ₃ CH ₃	70%
3	-CO ₂ t-Bu	" "	62%



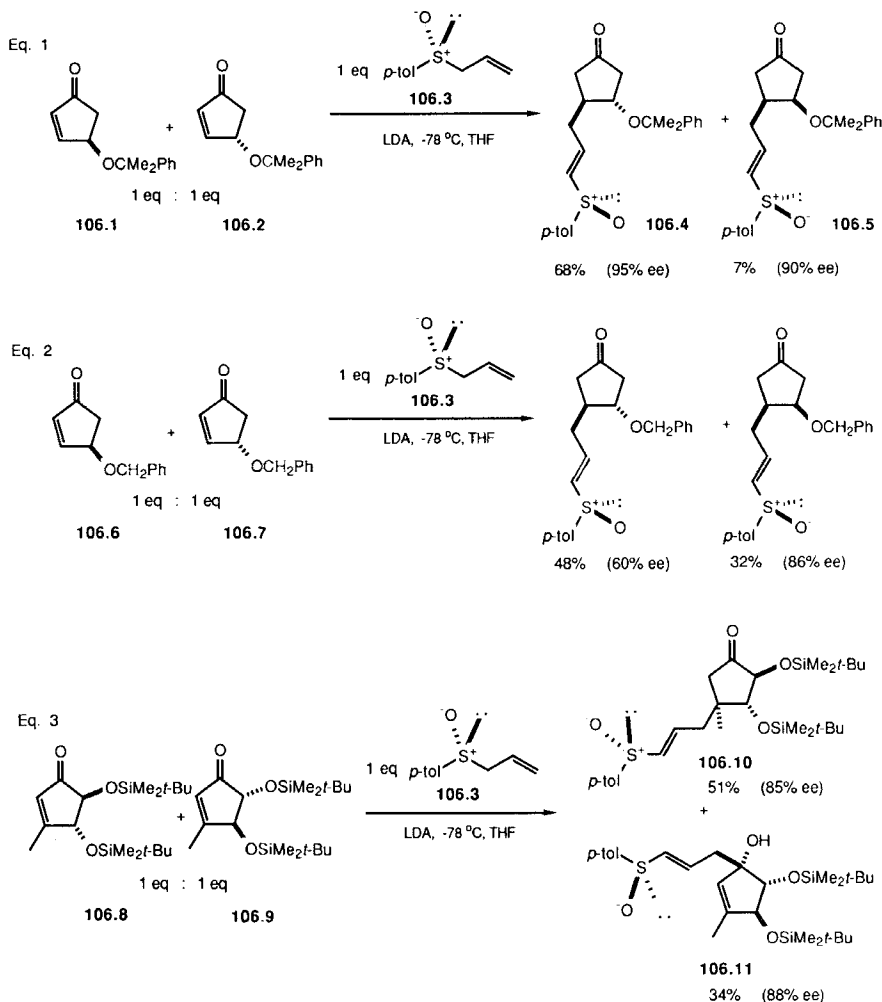
Scheme 105

formed in the Michael addition is trapped with an aldehyde to form adducts of the general structure **105.1**. No details of the simple stereoselectivity of the aldol process were reported. Adduct **105.1**, obtained from two racemic components by mutual kinetic enantioselection (entry 1, Scheme 105), was converted to racemic prostaglandin **105.3**. Mutual kinetic enantioselection is simply a special case of the kinetic resolution phenomenon. Thus, the reaction of 0.5 equivalents of the enantiomerically pure form of either the allylic sulfoxide or the enone, with 1.0 equivalent of a racemic mixture of the other component should result in preferential consumption of one enantiomer of the racemic mixture. In theory, this strategy could be applied to the resolution of either the enone or the allylic sulfoxide. Hence, when optically active cyclopentenone **105.2** was used, prostaglandin **105.3** was obtained with an enantiomeric excess of 75%.

The potential of kinetic resolution in these systems has been explored by Hua and coworkers (193, 194). The acceptors chosen for study were a racemic mixture of cyclopentenones **106.1** and **106.2**, which prefer to add allyl sulfoxide anions on the face trans to the alkoxy group. When the anion of optically active allyl sulfoxide **106.3** is used, preferential formation of adduct **106.4** results (Eq. 1, Scheme 106). A small amount of the cis isomer **106.5** is also formed as a result of nucleophilic attack from the same face as the alkoxy directing group of the acceptor. The enantiomeric purities of the products were determined after oxidation of the sulfoxide to the sulfone or reduction to the sulfide. High levels of enantioselection occur in both adducts (**106.4** and **106.5**). The remaining enone, if isolated, should be enriched in enantiomer **106.1**. With racemic 4-benzyloxy-2-pentenones (**106.6** and **106.7**), little kinetic resolution occurs because the benzyloxy group is not as effective in facial differentiation (Eq. 2).

Kinetic resolution of the racemic mixture of **106.8** and **106.9** with **106.3** provides moderate yields of the resolved product **106.10** with good enantioselectivity (Eq. 3, Scheme 106). Although only one diastereomeric product was detected with the β -substituted acceptor, 34% of the γ -1,2-regiosomer **106.11** was also obtained. This 1,2 adduct (**106.11**) was also obtained in good enantiomeric purity.

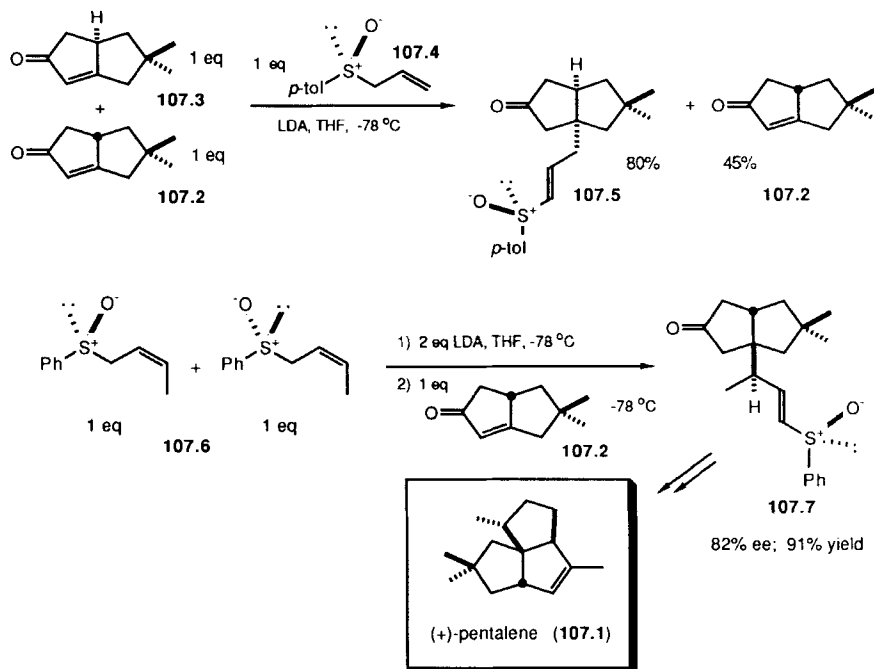
[P*,P*] Hua has applied this methodology in a remarkable synthesis of (+)-pentalene (**107.1**, Scheme 107) (200). Initially, racemic enone **107.2**/**107.3** (2 equivalents) was allowed to react with the anion of **107.4** (1 equivalent), resulting in the preferential formation of **107.5**. From the reaction mixture was recovered **107.2** in optically active form. This enantiomerically pure **107.2** was then allowed to react with two equivalents of the anion of racemic *cis*-crotyl sulfoxide **107.6**. This reaction gives **107.7**, resulting from the preferential addition of one of the enantiomers of sulfoxide **107.6**. The desired ma-



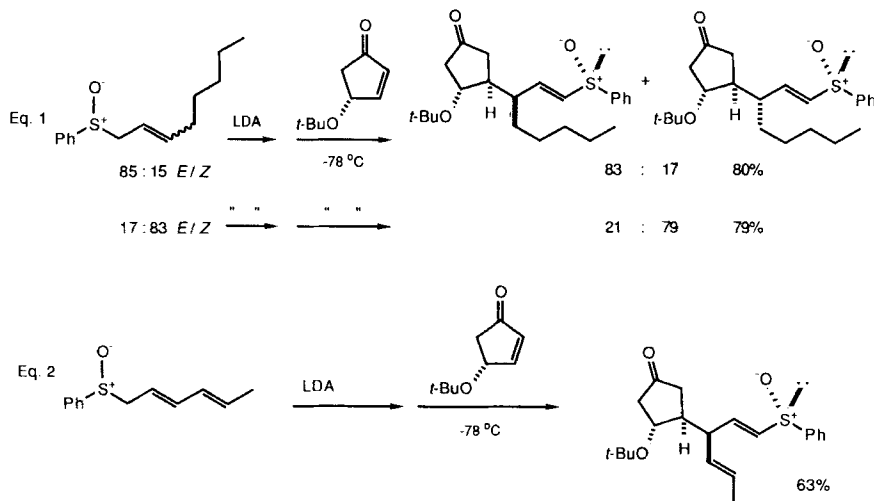
Scheme 106

terial **107.7** was obtained in 91% yield with 82% ee. The enantiomerically enriched sulfoxide **107.7** was converted to (+)-pentalene (**107.1**).

Further examples of mutual kinetic enantioselection are presented in Scheme 108 (181–183). In Eq. 1, the use of mixtures of the *E* and *Z* isomers of the allylic sulfoxides results in the formation of mixtures of isomeric products. However, the ratio of adducts obtained correlates with the sulfoxide



Scheme 107

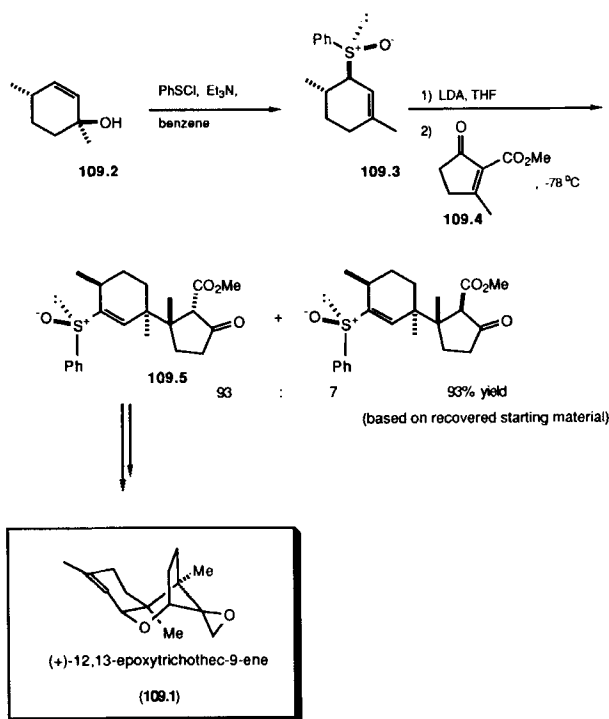


Scheme 108

E/Z isomer ratio. Nevertheless, each enantiomeric component of the racemic material represents a one-to-one combination of donor and acceptor enantiomers. Remarkably, with the *E,E*-dienyl sulfoxide in Eq. 2, only one racemic product out of the 8 possible isomers is obtained. Moreover attack occurs only at the γ -position of the dienyl anion.

3. To α,β -Unsaturated Keto Esters

[P*,P] In connection with the synthesis of (+)-12,13-epoxytrichothec-9-ene (**109.1**), Hua and coworkers have examined the conjugate addition of the anion derived from allylic sulfoxide **109.3** to the diactivated acceptor **109.4** (Scheme 109) (197). The chiral, non-racemic sulfoxide **109.3** was derived from enantiomerically pure allylic alcohol **109.2** by [2,3] sigmatropic rearrangement. This procedure resulted in the formation of the allylic sulfoxide as a single stereoisomer. As mentioned above, reactions of similar sulfoxides



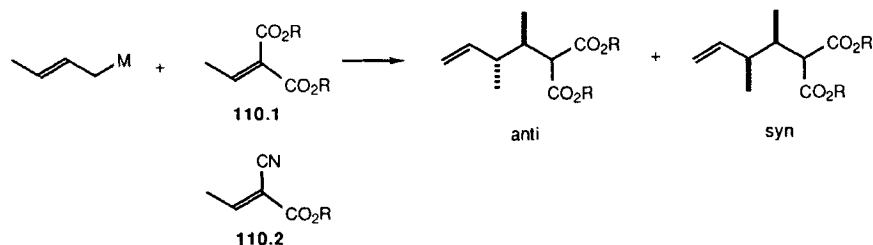
Scheme 109

with 3-methyl-2-cyclopentenone give only low yields of products. To overcome this problem, the diactivated acceptor **109.4** was used. Addition of the anion of **109.3** to **109.4** results in the formation of adjacent quaternary centers with excellent stereoselectivity. The major adduct from the Michael addition was converted to **109.1**.

V. Crotylmetallics

I. To Ethylenemalonates

[P,P] Allylic metal compounds are carbon analogs of enolates and frequently have similar properties. Yamamoto and coworkers have studied the addition of crotyl-metal reagents to ethylenemalonates (**110.1**) and ethyl α -cyanocrotonate (**110.2**) (201, 202). The results of this study are summarized in Scheme 110 and Table 45. Reasonable levels of selectivity are observed when the metal is 9-BBN or $(i\text{-PrO})_3\text{Ti}$ (entries 5 and 8). Interestingly, the



Scheme 110

Table 45
Addition of Crotylmetal Reagents to Dialkyl Ethylenemalonates (Scheme 110)

Entry	Diester R	Metal M	Temp. °C	anti:syn ^a
1	Me	MgCl	-78	60:40
2	Et	MgCl	-78	60:40
3	<i>i</i> -Pr	MgCl	-78	60:40
4	Me	9-BBN ^b	25	80:20
5	Et	9-BBN ^b	25	90:10
6	<i>i</i> -Pr	9-BBN ^b	25	85:15
7	Me	$(i\text{-PrO})_3\text{Ti}$	-78 to 0	75:25
8	Et	$(i\text{-PrO})_3\text{Ti}$	-78 to 0	90:10
9	<i>i</i> -Pr	$(i\text{-PrO})_3\text{Ti}$	-78 to 0	85:15
10	Et	$Cp_2\text{ZrCl}$	0 to 25	80:20

a. Total yields ranged from 80-95%.

b. 9-Borabicyclo[3.3.1]nonan-9-yl.

stereochemical outcome with the dimethyl and diisopropyl esters of **110.1** is inferior to that with the diethyl ester (compare entries 4, 6, 7, and 9 to 5 and 8). With ethyl α -cyanocrotonate (**110.2**) as the acceptor, an 80:20 (anti/syn) mixture of diastereomers is formed with MgCl, $(i\text{-PrO})_3\text{Ti}$, and Cp₂ZrCl as counterions; with 9-BBN, no products are obtained.

W. Stereochemical Trends for Intermolecular Michael Additions

Many variables can affect the stereochemistry of addition of enolates to activated olefins. Often variations of the substrates or the reaction medium do not have a uniform influence on the stereochemical consequence of the reaction. However, several trends may be noted.

- For chiral enolates and acceptors, preferential attack generally occurs from the same face of the enolate as does attack by other electrophiles, particularly alkyl halides.
- Varying the geometry of either the enolate or the double bond of the Michael acceptor can influence the sense of the stereochemical outcome of the addition. Enolates with *E* configuration tend to give, with *E* acceptors, the syn diastereomer. Alternatively, *Z* enolates with *E* acceptors usually give products with the anti configuration. With *Z* acceptors, each enolate tends to give adducts with the opposite configuration; *Z* acceptors with *E* enolates are inclined to generate anti isomers while *Z* enolates and *Z* acceptors prefer syn products. In general, the correlation between enolate and acceptor geometries with the adduct configurations is weaker with the *E* enolates and weaker with the *Z* acceptors.
- Bulky groups on the enolate and on the acceptor tend to reinforce the above trends.
- From the relatively small amount of information available, it appears that both the counterion and the donor atom of the acceptor can have a dramatic effect on the stereochemical outcome of the reaction.
- Use of ethereal, aromatic, or aliphatic solvents has little influence on the stereochemistry of the products. On the other hand, HMPA can dramatically influence the stereochemical result. The sense and degree of the stereoselectivity changes upon use of HMPA are highly variable.

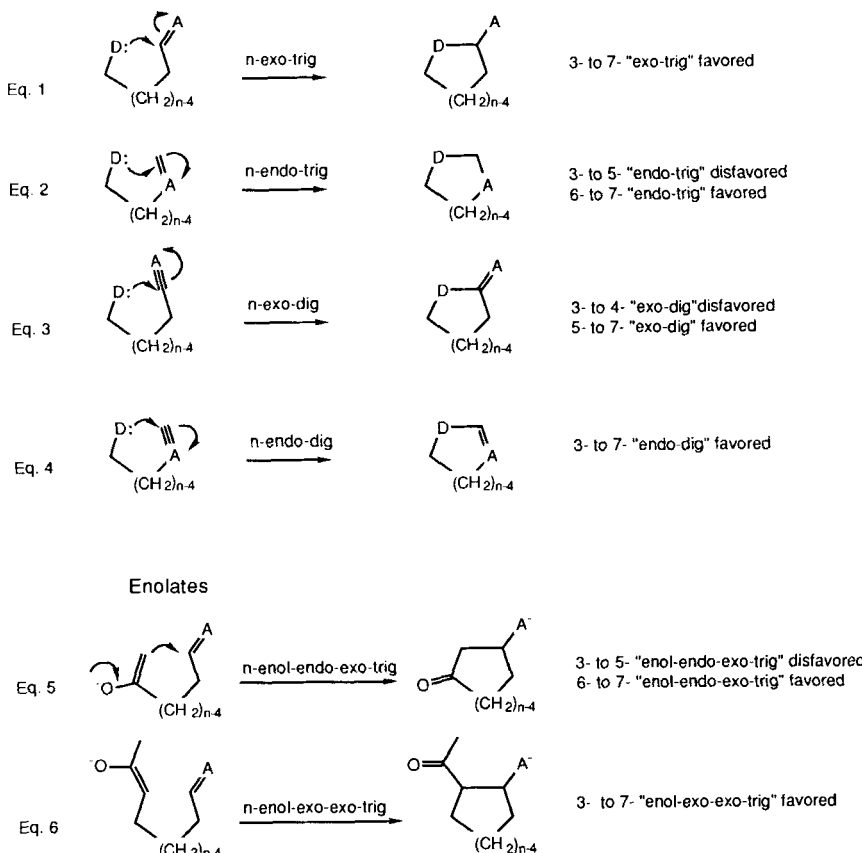
III. INTRAMOLECULAR ENOLATE MICHAEL ADDITIONS

A. Rules for Ring Closure

As might be imagined, intramolecular versions of the Michael addition impose essential conformational constraints in order to achieve sufficient over-

lap between the donor and acceptor portions of the molecule. In particular, the substrate must be able to achieve an arrangement that allows the nucleophilic end of the molecule to overlap adequately with the π -system of the acceptor. Baldwin has analyzed the conformational and stereoelectronic factors that are operative in ring closing reactions and has summarized these requirements in a series of "rules" for ring closures (Scheme 111) (203).

For the intramolecular addition of simple nucleophiles to activated double bonds (trigonal centers or "trig"), the bond being lost (the π -bond of the acceptor olefin) can be either exocyclic or endocyclic relative to the forming ring. The term "exo-trig" is used to describe the former situation where the bond lost is exocyclic (Eq. 1, Scheme 111). When the bond breaking is endo-



Scheme 111

cyclic, the term "endo-trig" is used (Eq. 2). Overlap requirements suggest that formation of three- to five-membered rings with endocyclic bond loss ("3- to 5-endo-trig") should be difficult or disfavored (204). On the other hand, sufficient overlap for the formation of three- to seven-membered rings with exocyclic bond detachment ("3- to 7-exo-trig") or six- and seven-membered rings with endocyclic bond breaking ("6- or 7-endo-trig") can be achieved.

When adding to a triple bond (digonal centers or "dig"), 5- to 7-exo-dig and 3- to 7-endo-dig ring closures are favored (Eqs. 3 and 4, Scheme 111). Closing a three- to four-membered ring onto a triple bond with exocyclic bond breaking (3- to 4-exo-dig) is disfavored.

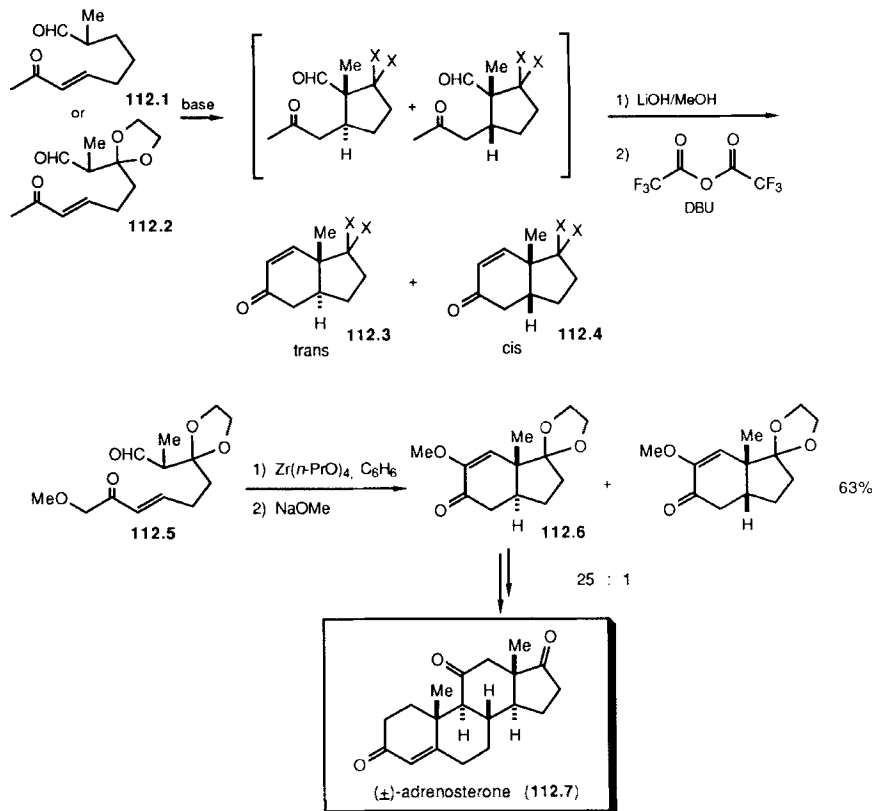
Enolates present similar stereoelectronic constraints. Because of the stereoelectronic requirement for bond forming (namely that electrophiles must approach an enolate's π -system in a manner that allows suitable orbital overlap), the modes of ring formation are restricted. Baldwin and coworkers have examined this arrangement and developed predictive guidelines (Eqs. 5 and 6, Scheme 111) (205).

Experiments and Baldwin's analysis suggest that formation of three- to five-membered rings by attack of an endocyclic enolate on a trigonal center with exocyclic bond breaking should be disfavored (3- to 5-enol-endo-exo trig, Eq. 5, Scheme 111). Although there exist some formal exceptions to this "rule" for intramolecular Michael additions, these usually occur under special circumstances (*vide infra*). Closure of a six- or seven-membered ring between an endocyclic enolate and an exocyclic acceptor is favored (6- or 7-enol-endo-exo trig, Eq. 5). Similarly, closure of a three- to seven-membered ring between an exocyclic enolate onto an exocyclic double bond is favored (3- to 7-enol-exo trig, Eq. 6).

B. Michael Cyclizations

The foregoing discussion suggests that the reaction pathways for intramolecular Michael additions may require profound conformational constraint. As a result, it might be anticipated that good levels of stereoselection can be realized. Indeed, this has proved to be the case.

Stork and coworkers have investigated intramolecular Michael additions of aldehyde enolates to enones (206). The first systems chosen for study were aldehyde-enones **112.1** and **112.2**. After the Michael addition, the initial adducts were cyclized by an aldol/dehydration sequence to form the *trans*- and *cis*-hydrindenones **112.3** and **112.4**. A number of bases were used to cyclize **112.1** and **112.2**; the results of this study are summarized in Scheme 112 and Table 46.



Scheme 112

The stereochemical outcome of the reaction was strongly dependent on the base used in the reaction. The optimal conditions found were $Zr(n\text{-PrO})_4$ in benzene (entries 4 and 10, Table 46). In the absence of more information about the enolate geometry/reactivity, it is premature to advance a meaningful transition state hypothesis. An interesting observation was made by the authors, however. The “tighter” the metal–oxygen bond between the enolate and counterion, the greater proportion of the trans product is formed.

The configurations of the products were assigned by straightforward conversion into known compounds. Further confirmation rested on the conversion of 112.5 into (±)-adrenosterone (112.7) (207). The Michael addition/cyclization of 112.5 into 112.6 proceeded in 63% yield with 96:4 (trans/cis) selectivity (Scheme 112).

Table 46
Base-Promoted Cyclization of 112.1 and 112.2 (Scheme 112)

Entry	Substrate	Base/Solvent	Yield ^a %	trans:cis
1	112.1	KOH/MeOH	b	67:33
2	112.1	NaOMe/MeOH	80	75:25
3	112.1	LiOH/MeOH	b	80:20
4	112.1	<u>Zr(n-PrO)₄/C₆H₆</u>	90	98:2 ^c
5	112.1 ^d	LiOH/MeOH	70	67:33
6	112.2	LiOH/MeOH	b	80:20
7	112.2	Mg(OMe) ₂ /MeOH	b	92:8
8	112.2	Ca(OMe) ₂ /MeOH	b	91:9
9	112.2	Ba(OH) ₂ /MeOH	b	75:25
10	112.2	<u>Zr(n-PrO)₄/C₆H₆</u>	b	96:4 ^c

a. Overall yield of hydrindenones.

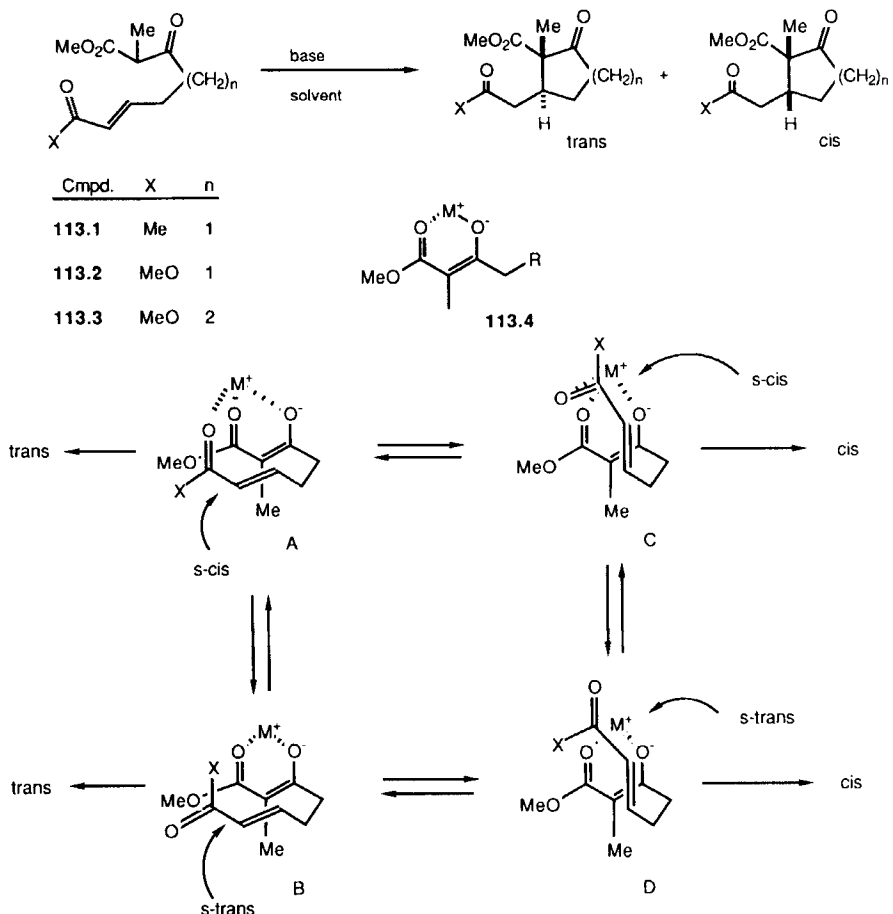
b. The yield was not reported.

c. The optimal conditions (highest selectivity) are underlined.

d. The cis enone of 112.1 was used for cyclization.

In a later communication, Stork and coworkers examined the intramolecular Michael additions of 113.1–113.3 (208). Substrates 113.1–113.3 were cyclized using a variety of bases and solvents. The results of this study are summarized in Scheme 113 and Table 47. Although the selectivity is generally poor in protic solvents (entries 1, 2, 4, and 6), excellent trans selectivity for all substrates is obtained with catalytic amounts of sodium hydride in benzene (entries 3, 5, and 7). After invoking the likely chelate structure 113.4 for the β -keto ester anion (209), examination of Dreiding models reveals that the system has little conformational flexibility. With this rigidity, only four transition states (**A**, **B**, **C**, and **D**, Scheme 113) appear possible. The difference between transition states **A** and **B** and between **C** and **D** is the conformation of the enone (s-cis or s-trans). The stereochemical results are nicely accommodated by the chelated transition state **A** in which the cation is transferred from the enolate to the carbonyl during the course of the reaction. In protic solvents, where the developing charge on the enone carbonyl function can be readily stabilized, transition states **B**, **C**, and **D** could intervene, resulting in the observed lower selectivity.

A similar intramolecular Michael addition was later reported by Hirai et al. (210). Racemic 114.1 is cyclized using sodium methoxide in methanol to provide 114.2 as one isomer (Scheme 114). The structure of this adduct was confirmed by conversion to (\pm)-emetine (114.3). Similarly, when 114.4 is treated with base, 114.5 is formed as the only stereoisomer (211, 212).



Scheme 113

By installing chiral, non-racemic auxiliaries **115.3–115.6** on the β -keto ester, Stork and Saccomano have achieved high levels of asymmetric induction in the intramolecular Michael addition (213). The results of this study are summarized in Table 48 and Scheme 115. Although the trans to cis ratio was not reported, it is presumably high, by analogy to Stork's earlier work (*vide supra*). For a given auxiliary, the nature of the ester of the enoate influences the stereochemical outcome of the reaction. The selectivities obtained with methyl esters are lower than with the corresponding *tert*-butyl esters (entries 1, 3, 5, and 7 versus entries 2, 4, 6, and 8). Of the auxiliaries examined, 8-

Table 47
Base-Promoted Intramolecular Michael Addition of β -Keto Esters 113.1, 113.2,
and 113.3 (Scheme 113)

Entry	Substrate	X	n	Base	Solvent	Yield %	trans:cis ^a
1	113.1	Me	1	<i>t</i> -BuOK	<i>t</i> -BuOH	b	50:50
2	113.1	Me	1	MeONa	MeOH	b	25:75
3	113.1	Me	1	NaH ^c	benzene	90	<u>100:0</u> ^{d,e}
4	113.2	MeO	1	<i>t</i> -BuOK	<i>t</i> -BuOH	b	50:50
5	113.2	MeO	1	NaH ^c	benzene	85	96:4
6	113.3	MeO	2	<i>t</i> -BuOK	<i>t</i> -BuOH	b	50:50
7	113.3	MeO	2	NaH ^c	benzene	88	97:3

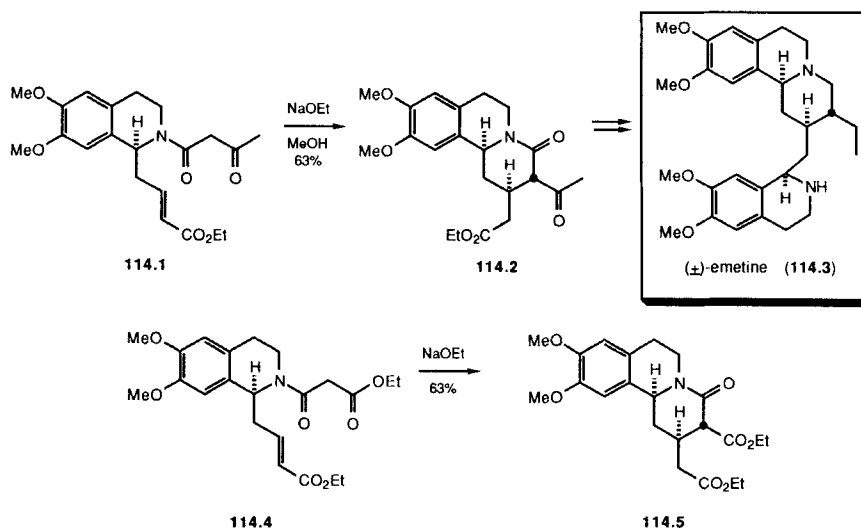
a. Determined by capillary GLC or ^1H NMR.

b. Not reported.

c. A catalytic amount of base was used.

d. The minor isomer was not detected.

e. The optimal conditions (highest selectivity) are underlined.



Scheme 114

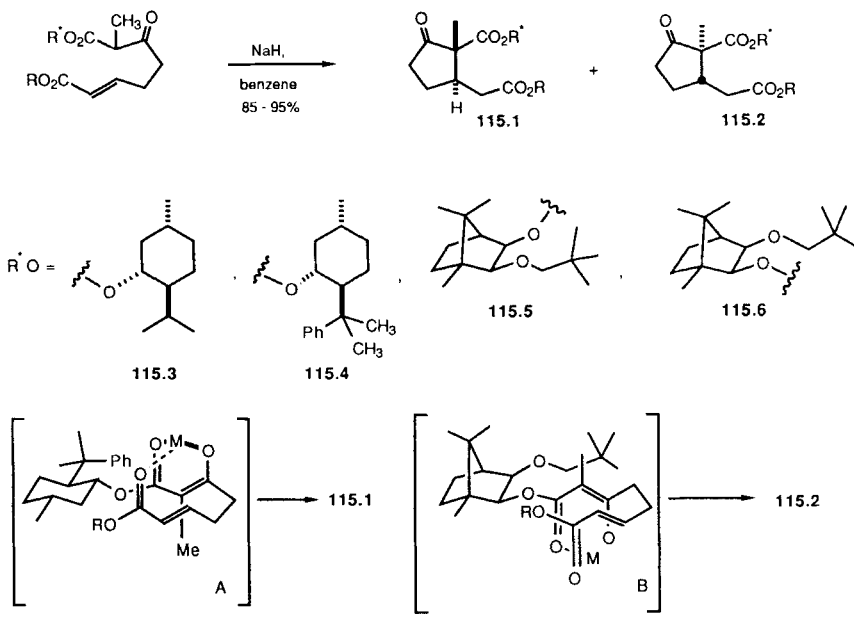
Table 48
Asymmetric Michael Addition of β -Keto Esters (Scheme 115)

Entry	R	R^*	115.1:115.2
1	Me	115.3	69:31 ^a
2	t-Bu	115.3	84:16 ^a
3	Me	115.4	80:20 ^a
4	t-Bu	115.4	92-93:7-8 ^a
5	Me	115.5	77:23 ^b
6	t-Bu	115.5	81:19 ^b
7	Me	115.6	6:94 ^b
8	t-Bu	115.6	<2.5:97.5 ^{b,c}

a. Ratio determined by ^{19}F NMR analysis of the α -methoxy- α -trifluoromethylphenyl acetates prepared from the ketone reduction products.

b. Ratio determined by ^1H NMR.

c. The minor isomer could not be detected.



Scheme 115

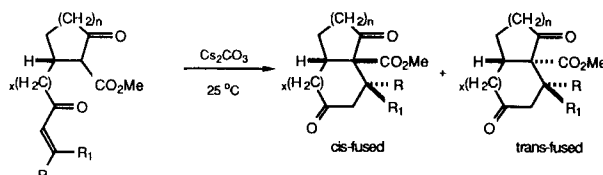
phenylmenthol (**115.4**) (126) and borneol (**115.6**) (214) were found to be the most effective. These results were rationalized by transition states **A** and **B**. With 8-phenylmenthol (**115.4**), transition state **A** is favored, since non-bonded interactions between the ester of the enoate and the dimethylphenyl group are minimized. For borneol ester **115.6**, transition state **B** is favored. In both instances the model transition states predict an increase in selectivity on increasing the size of the R. It is interesting that the stereoselectivity *increases* when the bridgehead methyl group of borneols **115.5** and **115.6** is on the same side as the acceptor portion of the complex (**116.6**). The authors suggest that this methyl group limits the rotational freedom around oxygen of the borneol ester, thus enhancing selectivity. Product **115.2** was converted subsequently into adrenosterone (215).

Deslongchamps and coworkers have explored the intramolecular Michael addition of cyclic β -keto esters to α,β -unsaturated ketones (216). The results of this study are summarized in Scheme 116 and Table 49. As predicted, 5-endo-trig closures fail (entries 1 and 2) (203–205). Reduced yields are also obtained when closing an eight-membered ring ($x = 3$, entries 15 and 16) and when cis α,β -unsaturated ketones are used ($R = H$, $R_1 = Me$; entries 6, 9, and 14).

A number of stereochemical trends can be observed (Table 49). When cyclopentanone- or cyclohexanone-derived β -keto esters ($n = 1, 2$) are used to make a six-membered ring ($x = 1$), the adducts produced have only the cis ring fusion ($n = 1$; entries 3, 5, 6, 10, and 13–15; $n = 2$, $x = 1$: entries 4 and 7–9). The only breakdown in the preference for the generation of cis ring-fused products is seen when seven- and eight-membered rings are created ($n = 2$, $x = 2$ and 3; entries 11, 12, and 16).

When the α,β -unsaturated ketone contains a prostereogenic center, the possibility exists for stereodifferentiation at the newly-established stereocenter. Despite the rigidity of the potential transition states, only low trans diastereoselectivities are generally observed. In most cases, use of the cis enone results in poor yields and even lower selectivities for the generation of this new stereocenter (entries 6 and 9, Table 49).

It is interesting that the best selectivity for the methyl-substituted stereocenter occurs in the creation of the seven-membered ring ($x = 2$, entry 13,



Scheme 116

Table 49
Intramolecular Michael Addition of Cyclic β -Keto Esters (Scheme 116)

Entry	n	Substrate	Solvent	Yield %	Ring Fusion cis:trans	Substituent cis:trans ^a		
	x	R	R ₁					
1	1	0	H	CH ₃ CN	0	---		
2	2	0	Me	H	1:1 THF/DMF	0		
3	1	1	H	H	CH ₃ CN	70	100:0	---
4	2	1	H	H	CH ₃ CN	89	100:0	---
5	1	1	Me	H	CH ₃ CN	71	100:0	29:71 ^b
6	1	1	H	Me	CH ₃ CN	27	100:0	50:50 ^b
7	2	1	Me	H	1:1 THF/DMF	95	100:0	20:80 ^b
8	2	1	Me	H	CH ₃ CN	97	100:0	33:67 ^b
9	2	1	H	Me	CH ₃ CN	27 ^c	100:0	40:60 ^b
10	1	2	H	H	CH ₃ CN	88	100:0	---
11	2	2	H	H	1:1 THF/DMF	40	67:33	---
12	2	2	H	H	CH ₃ CN	57	83:13	---
13	1	2	Me	H	CH ₃ CN	50	100:0	10:90
14	1	2	H	Me	CH ₃ CN	2	100:0	10:90
15	1	3	H	H	CH ₃ CN	14	100:0	---
16	2	3	H	H	CH ₃ CN	25	50:50	---

a. Cis (R = H; R₁ = methyl) or trans (R = methyl; R₁ = H) relative to the adjacent stereocenter.

b. Structure of the minor isomer not given.

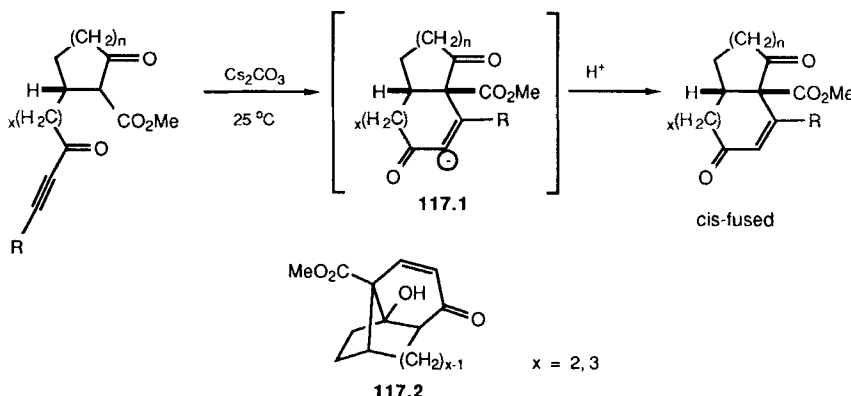
c. Large amounts of the starting material recovered.

Table 49). With this conformationally flexible precursor, the possibility of some manner of chelation between the donor and acceptor portions of the molecule exists.

Acetylenic ketones can also serve as acceptors for intramolecular Michael additions. This possibility has been explored by Deslongchamps and coworkers (217). The results of this study are summarized in Scheme 117 and Table 50. The initial adduct from the Michael addition is apparently the dipole-stabilized vinyl anion 117.1, that either reacts with an internal electrophile or acquires a proton from the reaction medium.

In these cases, the five-endo-dig cyclization occurs in reasonable yield (entry 1, Table 50) (203a). For the generation of seven- and eight-membered rings, addition products of the type 117.2 are formed in low yields ($\leq 13\%$, x = 2 or 3, entry 7). Again, establishment of the cis-fused rings are favored (Table 50).

The intermediate vinyl anions produced in the Michael addition can be trapped with an internal electrophile (Scheme 118) (218). Trapping of the intermediate anion to construct the five-membered ring through displacement of a bromide provides a tricyclic compound in good yield (Eq. 1). Leaving groups other than bromide give greater amounts of products resulting from different modes of alkylation (Eq. 2). Lower yields of the desired tricy-



Scheme 117

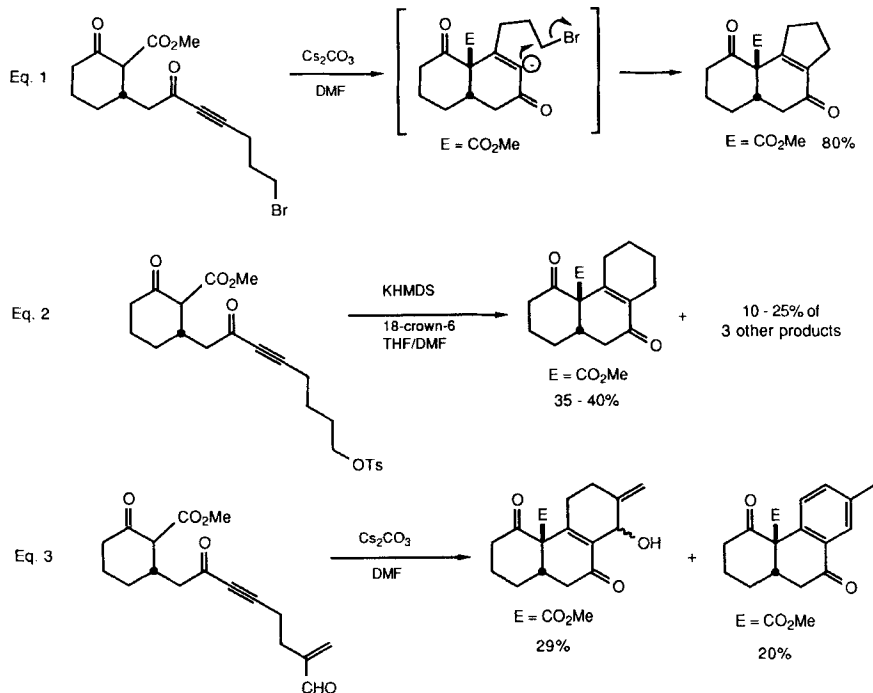
Table 50
Intramolecular Michael Addition of Cyclic β -Keto Esters to Acetylenic Ketones
(Scheme 117)

Entry	n	Substrate x	R	Solvent	Yield %	Ring Fusion <i>cis:trans</i>
1	2	0	Me	1:1 THF/DMF	82	100:0
2	1	1	H	CH ₃ CN	55	100:0
3	1	1	Me	CH ₃ CN	87	100:0
4	2	1	H	1:1 THF/DMF	47	100:0
5	2	1	Me	1:1 THF/DMF	89	100:0
6	2	1	$-(\text{CH}_2)_3\text{OAc}$	1:1 THF/DMF	75	100:0
7	1	2	H	CH ₃ CN	13	100:0

clic compounds are obtained when the vinyl anion is captured internally to assemble a six-membered ring (Eq. 3).

A number of other examples of intramolecular Michael additions are shown in Scheme 119. Again, in all instances when the acceptor portion of the molecule is in a five- or six-membered ring and a five- or six-membered ring is created, the *cis*-fused products are exclusively produced (Eqs. 1 (219), 2 (220), 3 (221–223), 4 and 5 (224)).

The intramolecular Michael additions in Eqs. 1 and 2 (Scheme 119) proceed in a straightforward manner to provide the cyclized materials. Cyclization of substrates of the general structure shown in Eq. 3 leads to the *cis*-fused product or products that result from further transformation of initially generated *cis*-fused Michael adducts. This method has been used to create a *cis*-

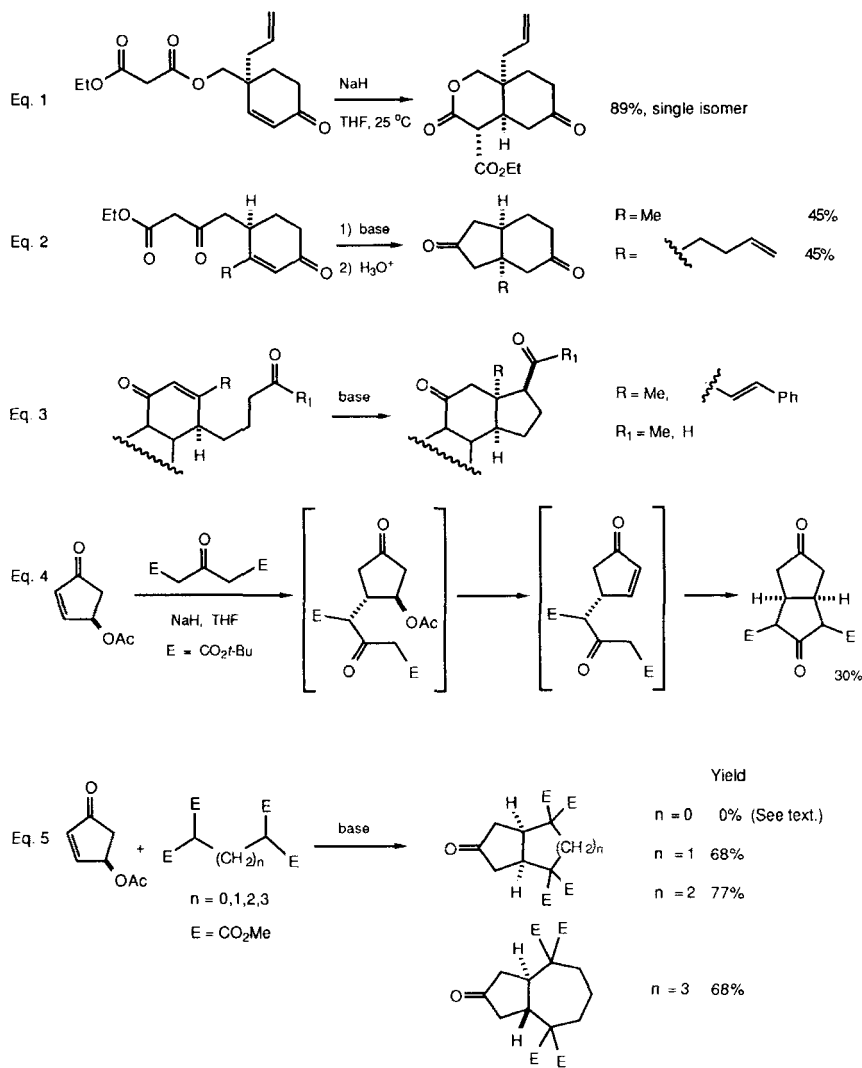


Scheme 118

fused steroidal D ring. In Eqs. 4 and 5, the initial Michael addition is followed by elimination of the acetate anion, regenerating an enone. Further Michael addition results in the construction of the cis-fused products. For the examples given in Eq. 5 (Scheme 119), the reaction does not proceed to completion to form a four-membered ring ($n = 0$). Instead, the products resulting from a single Michael addition followed by elimination of the acetate anion are isolated. For the establishment of five- ($n = 1$), six- ($n = 2$), and seven-membered rings ($n = 3$), this annelation sequence works well. In the case where $n = 3$, the cycloheptane ring-fusion emerges trans.

Kozikowski and coworkers have examined the intramolecular Michael addition shown in Eq. 1 (Scheme 120) for the synthesis of α -cyclopiazonic acid (**120.1**) (225). With the exocyclic acceptor, products in which the ketone and the ester fragments have a trans relationship were obtained.

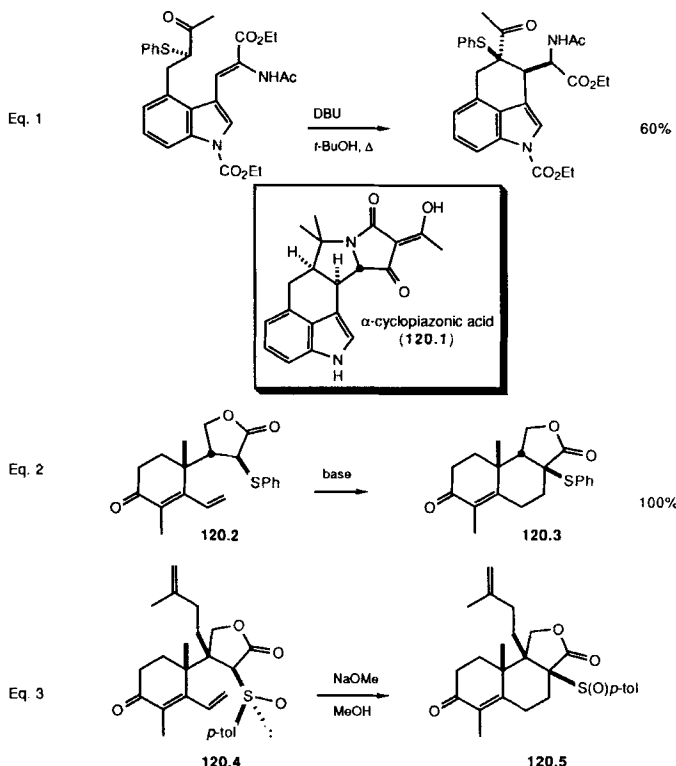
Holton and coworkers have found that **120.2** cyclizes to give only the cis-fused product **120.3** in excellent yield (Eq. 2, Scheme 120) (109). Similarly, **120.4** closes to **120.5** (Eq. 3) (110). The starting materials in both of these



Scheme 119

cases (**120.2** and **120.4**) were prepared by stereoselective Michael additions (*vide supra*).

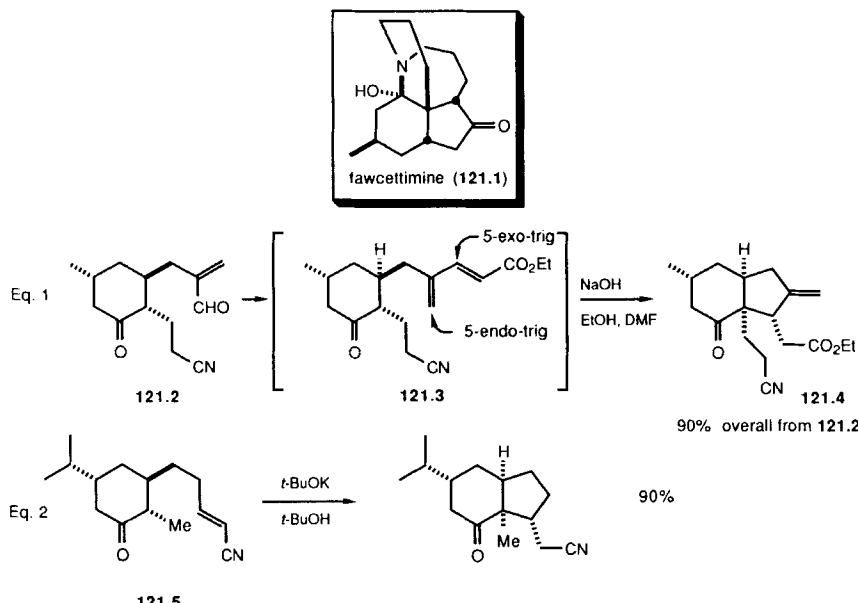
In connection with the synthesis of (\pm)-fawcettimine (**121.1**), the cyclization of **121.3** derived from **121.2** was studied (Eq. 1, Scheme 121) (226). In this instance, reaction can occur through either the 5-endo-trig or 5-exo-trig



Scheme 120

pathways. As predicted by Baldwin's analysis (204), only products from the 5-exo-trig pathway are observed, leading to **121.4**. Product **121.4** was obtained as one stereoisomer. Similarly, the base-promoted cyclization of **121.5** leads exclusively to the cis-fused product (Eq. 2, Scheme 121) (227). Additionally, both cyclizations result in products with the cis orientation between the ethyl acetate or acetonitrile side chain and the ring juncture substituents.

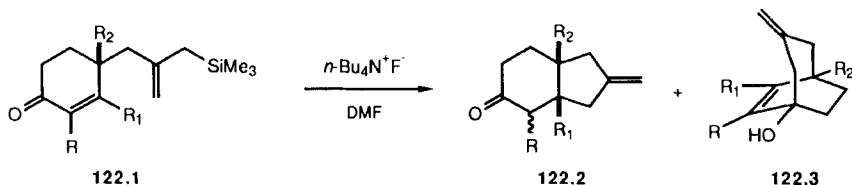
Fluoride-induced intermolecular conjugate additions of allylsilanes to α,β -unsaturated ketones has been studied by Majetich and coworkers (228, 229). The intramolecular version of this reaction has also been explored (230). In all instances examined, the tetra-*n*-butylammonium fluoride-induced ring closure results in exclusive formation of the cis-fused bicyclic system. For example, substrate **122.1** gives the cis-fused 1,4-addition products **122.2** along with the bridged 1,2-adduct **122.3** (Scheme 122, Table 51). Lewis acid catalysis induced only low yields of the conjugate addition products.



Scheme 121

A greater percentage of 1,2-addition products is obtained when the enone is substituted at the β -position (entries 7–9 and 11, Table 51). The 1,2-adducts can potentially be converted to the 1,4-addition products by the anion-accelerated Cope rearrangement. However, subjection of 122.3 addition to such conditions does not result in conversion to 122.2, leading to the conclusion that 122.2 is formed by direct conjugate addition of the allylic anion.

Similar results are obtained with cyclopentenone 123.1 (Scheme 123, Table 52). Again, only cis-fused 1,4-addition products are formed. Fluoride conditions result in 1,4- rather than 1,6-addition to the vinylcyclopentenone in entry 5. The β -vinyl substituent also leads to a larger amount of 1,2-addition.

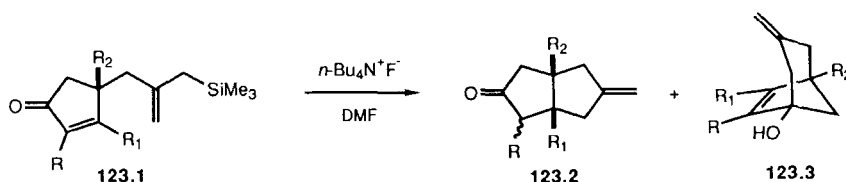


Scheme 122

Table 51
Fluoride-Induced Intramolecular Cyclizations of 122.1 (Scheme 122)

Entry	Substrate			Yields %	
	R	R ₁	R ₂	122.2 ^a	122.3 ^a
1	H	H	H	69	0
2	H	H	Me	63	0
3	H	Me	H	57	0
4	Me	H	Me	55	6
5	H	Me	H	46	0
6	H	Me	Me	65	0
7	Me	Me	H	43	10
8	Me	Me	Me	32	19
9	H	vinyl	Me	45	5
10	H	vinyl	H	11	0
11	Me	vinyl	Me	54	24
12	Me	vinyl	H	0	0

a. Isolated yields.



Scheme 123

Table 52
Fluoride-Induced Intramolecular Cyclizations of 123.1 (Scheme 123)

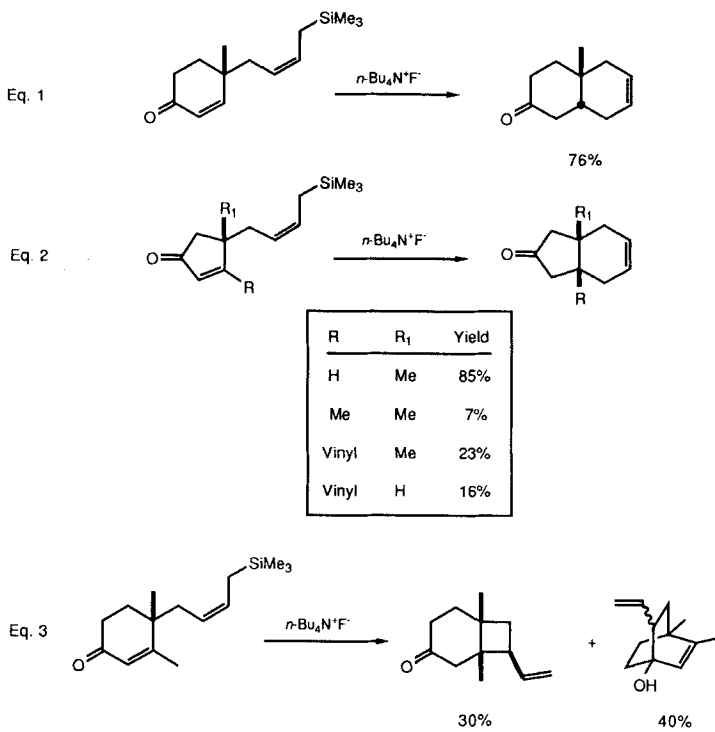
Entry	Substrate			Yields %	
	R	R ₁	R ₂	123.2 ^a	123.3 ^a
1	H	H	H	64	0
2	H	H	Me	55	0
3	Me	H	H	40	4
4	Me	H	Me	40	10
5	H	vinyl	Me	28	33

a. Isolated yields.

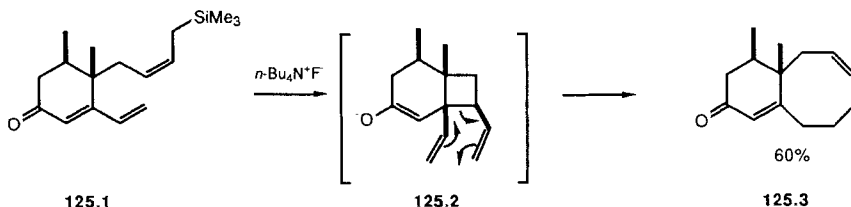
The stereoelectronically preferred cis-fused products are also obtained with the *cis*-crotylsilanes in Eqs. 1 and 2 (Scheme 124). In these cases, cyclization occurs to form the six- rather than the four-membered ring. If the cyclohexenone is substituted with a methyl group at the β -position, then the regiochemistry of the allylsilane addition changes (231, 232); only cyclobutane conjugate addition products are formed, along with the 1,2-addition products (Eq. 3). Note that an additional stereocenter is formed in this example. The only stereoisomer of the cyclobutane detected was one with the vinyl substituent *cis* to the angular methyl groups.

Analogous cyclization of the vinyl derivative **125.1** results in the formation of **125.3** (Scheme 125) (233). Compound **125.3** is formed through the intermediacy of divinylcyclobutane **125.2**, which undergoes enolate-accelerated Cope rearrangement to form **125.3**.

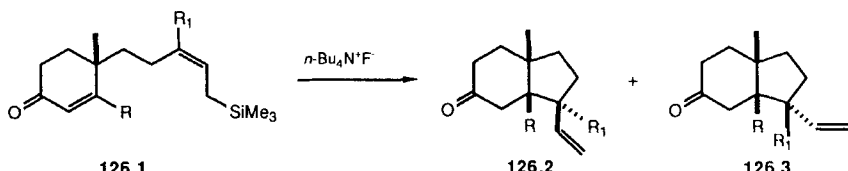
Cyclization of allylsilanes **126.1** results in the generation of an additional stereocenter (Scheme 126, Table 53) (232). Although only *cis*-fused products



Scheme 124



Scheme 125



Scheme 126

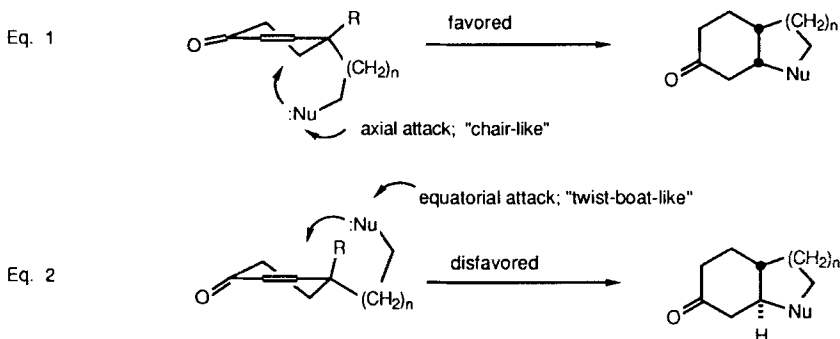
Table 53
Fluoride-Promoted Cyclization of 126.1 (Scheme 126)

Entry	Substrate R	Yield %	126.2:126.3
	R ₁		
1	H	77	50:50
2	H	88	80:20
3	Me	82	86:14
4	Me	70	75:25

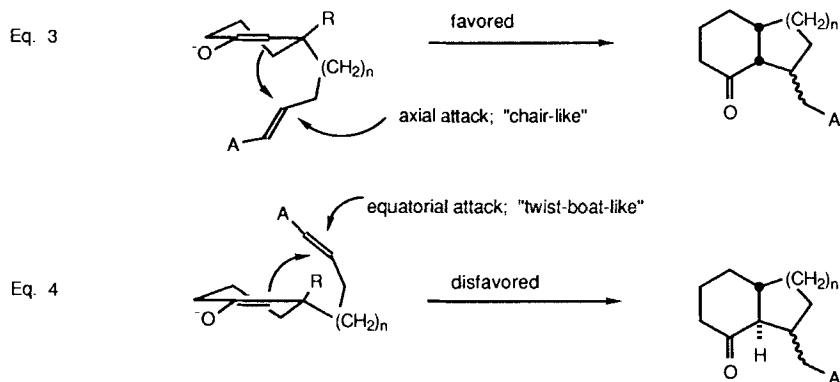
are formed, the stereocenter bearing the vinyl group is created with only moderate selectivity. Lewis acid conditions result, in some cases, in a reversal in the sense of selectivity.

In all of the foregoing examples, nearly exclusive formation of *cis*-fused products is observed when a five- or six-membered ring is formed onto a pre-existing ring. This result is predicted on the basis of stereoelectronic arguments (71). Assuming a chair-like (rather than a twist-boat-like) transition state, incoming nucleophiles prefer to attack the activated olefin from the more "axial" direction, in order to maintain maximum orbital overlap (Eq. 1 favored over Eq. 2, Scheme 127).

Cyclic Acceptors



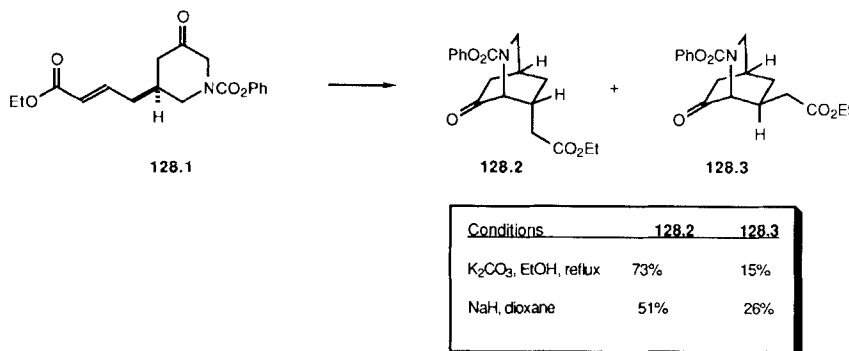
Cyclic Enolates



Scheme 127

Similar arguments apply to the intramolecular addition of cyclic enolates to activated π -systems (Eqs. 3 and 4, Scheme 127). The cis ring fusion in the products results from maintaining the best orbital overlap in the transition state. Thus, when forming a five- or six-membered ring onto a cyclic enolate, cis-fused products are usually preferred.

An intramolecular Michael addition that results in the formation of a bridged system was reported by Hanaoka and coworkers (Scheme 128) (234). Whereas 128.1 did not cyclize to the desired material under acidic conditions, use of basic conditions resulted in the formation of 128.2 and 128.3. The best results are achieved with potassium carbonate in refluxing ethanol. Control

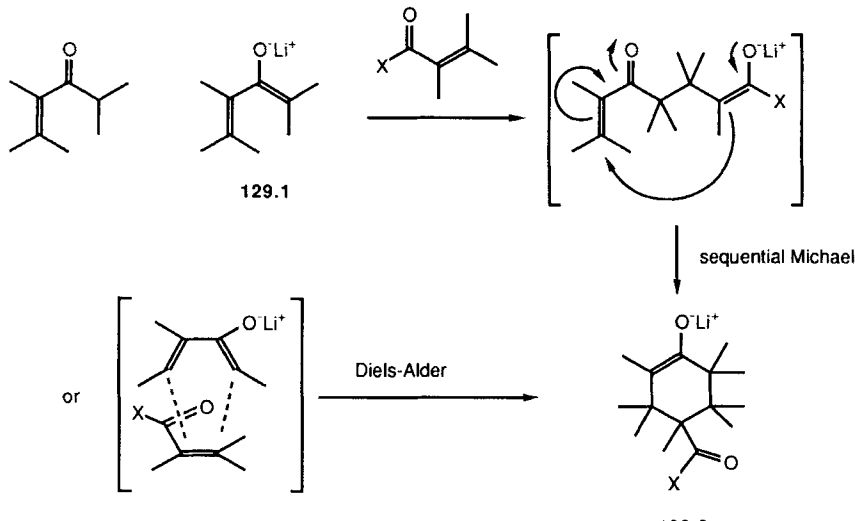


Scheme 128

experiments suggest that the product ratio is determined by kinetic factors. The major product obtained is consistent with some association between the donor and acceptor portions of the substrate in the transition state.

IV. SEQUENTIAL MICHAEL ADDITIONS

Kinetic deprotonation of an α,β -unsaturated ketone typically results in a cross-conjugated dienolate such as 129.1 (Scheme 129). If dienolate 129.1 is



Scheme 129

used in a Michael addition, a new enolate is formed and the α,β -unsaturated ketone is regenerated. At this point, the possibility of an intramolecular conjugate addition of the newly formed enolate to the reestablished α,β -unsaturated ketone exists. If this occurs, a "sequential" Michael addition product (**129.2**) is obtained.

Of course, **129.2** is identical to the product expected from Diels-Alder cycloaddition of **129.1** to the activated olefin. Before considering the stereochemical outcome, the mechanistic issue of "sequential Michael" versus Diels-Alder must be resolved. This topic has been addressed by Lee (235, 236) and also by White and Reusch (237).

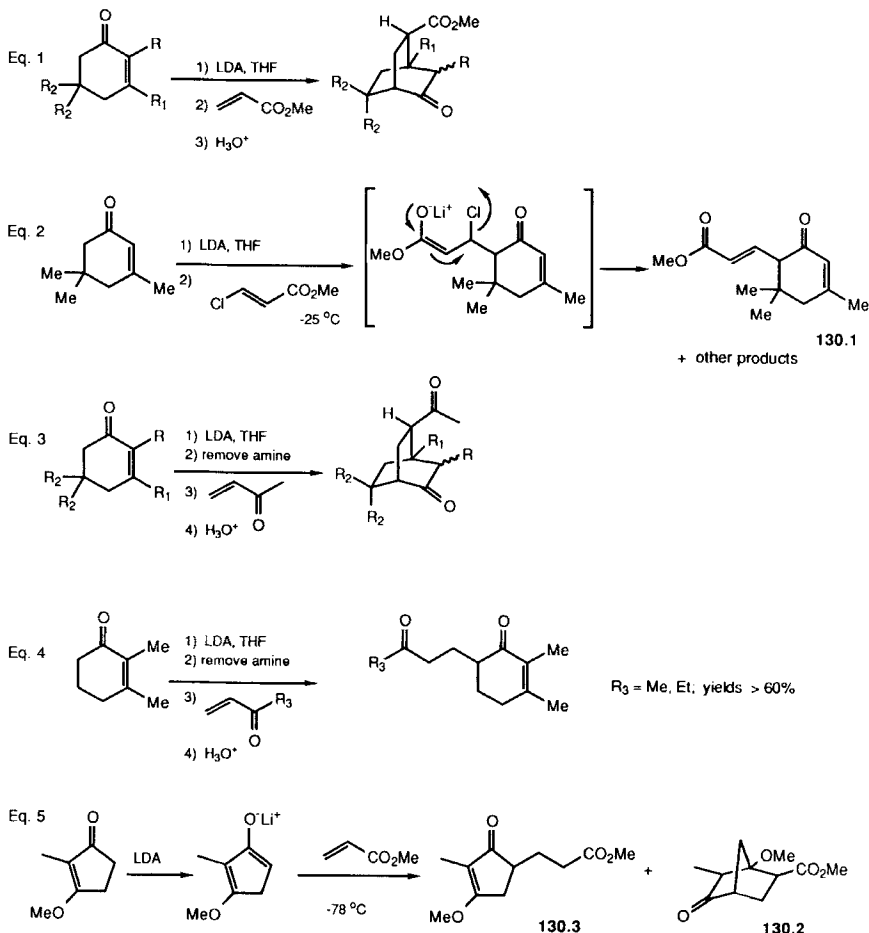
The sequential Michael addition of the dienolates formed from the α,β -unsaturated ketones in Eq. 1 to methyl acrylate occurs efficiently (Scheme 130, Table 54). However, when a similar reaction is attempted between the enone in Eq. 2 and methyl β -chloroacrylate, the product derived from elimination of chloride from the intermediate enolate is obtained. Formation of **130.1** is clearly consistent with the sequential Michael addition mechanism.

Addition of cross-conjugated dienolates to methyl vinyl ketone produces sequential addition products in good yield, provided free amine is removed from the reaction mixture (Eq. 3, Scheme 130, Table 55). With the more substituted dienolate derived from the α,β -unsaturated ketone in Eq. 4, addition to methyl and ethyl vinyl ketones leads to enediones resulting from a single Michael addition (238). Again, this observation provides support for the sequential Michael addition mechanism. In this case, the intramolecular addition is much slower than the initial intermolecular reaction due to increased substitution of the enone.

Schlessinger and coworkers have found that, by careful control of the reaction conditions, a mono-addition adduct can be obtained from the dienolate derived from a vinylogous ester and methyl acrylate (Eq. 5, Scheme 130) (239). Sequential addition is clearly possible in this case, as evidenced by the presence of **130.2** in the product mixture (82:18 **130.3/130.2**). No stereochemical information about **130.2** was reported.

Some additional examples of sequential Michael additions are shown in Scheme 131 (240, 241). A distinct preference for products with a syn relationship between the carbonyls is apparent (see Eqs. 1 (242), 2 (243), 3-8 (244), and 9 (245)). In only one example where an α,β -unsaturated ketone or ester was used as an acceptor has any of the other stereoisomer been detected (Eq. 2). These results strongly suggest chelation of the cation by the carbonyls of the donor and acceptor portions of the molecules in the transition state.

In Eq. 9 (Scheme 131), the configuration of the activated olefin is not retained in the product. Assuming that the reaction is under kinetic control, then some rotation around the "double bond" of the acceptor must occur during the reaction. Additionally, if the ethylthio group is replaced by phenyl-



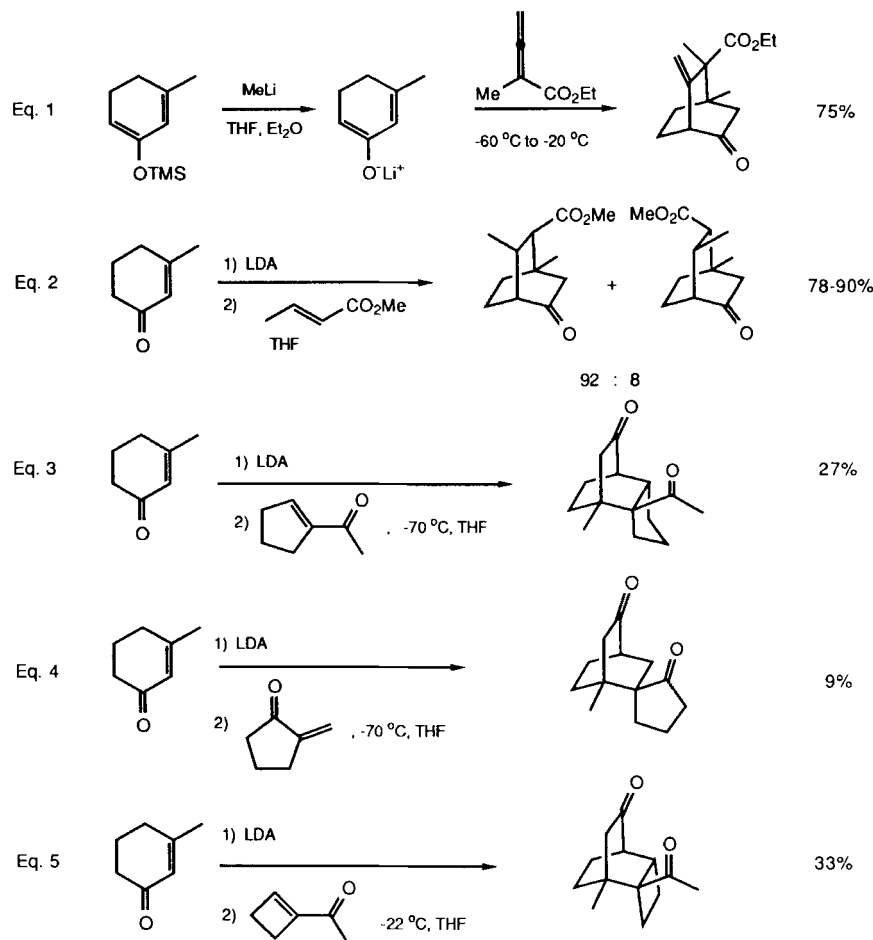
Scheme 130

Table 54
Sequential Michael Addition of Cyclohexenone to Methyl Acrylate
(Scheme 130, Equation 1)

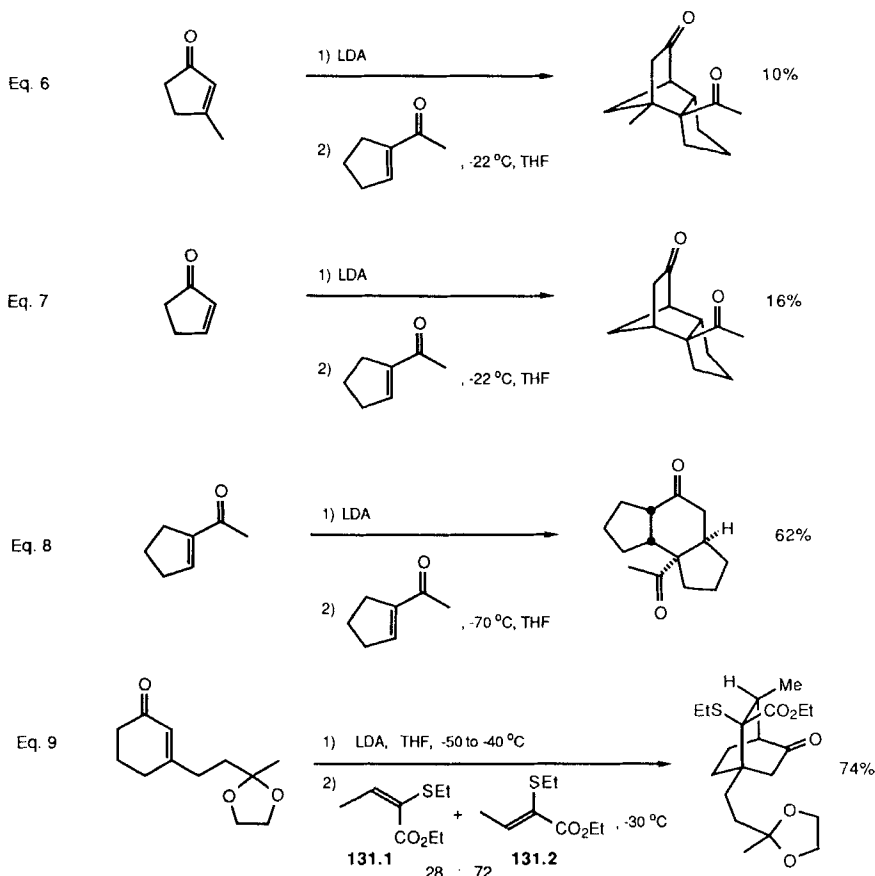
Entry	Cyclohexenone			Yield %
	R	R ₁	R ₂	
1	H	H	H	90
2	Me	H	H	81
3	H	Me	H	98
4	H	Me	Me	98
5	Me	Me	H	98

Table 55
Sequential Michael Addition of Cyclohexenones to Methyl Vinyl Ketone
(Scheme 130, Equation 3)

Entry	Cyclohexenone	Yield %
	R R ₁ R ₂	
1	Me H H	81
2	H Me H	>70
3	Me H Me	>70



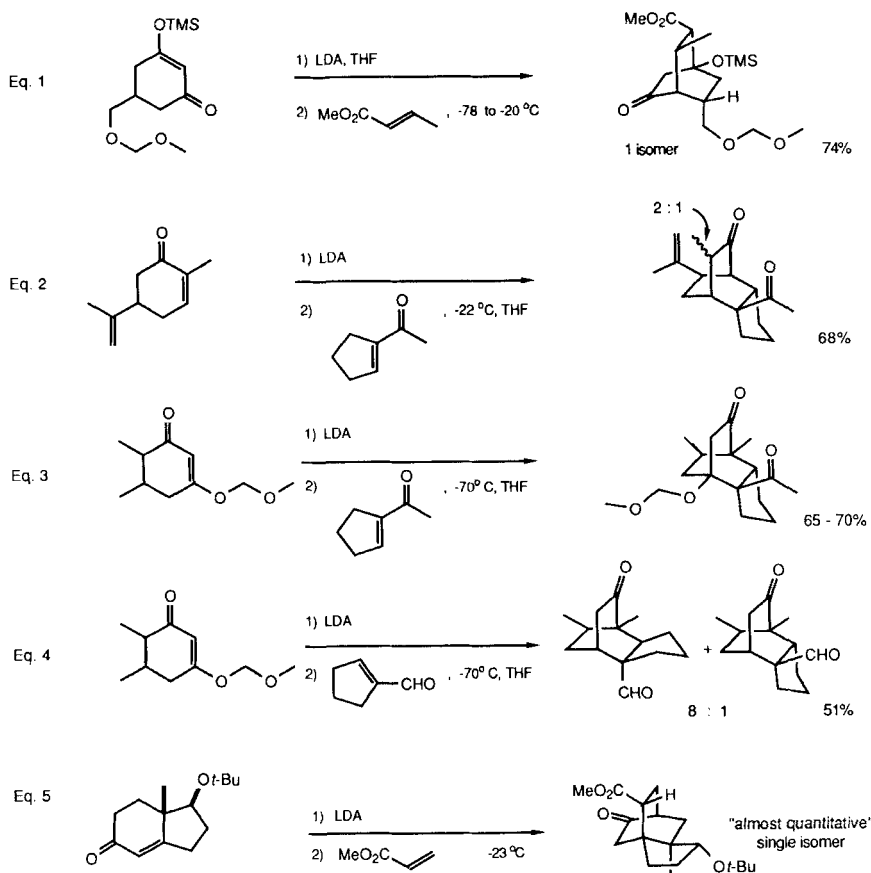
Scheme 131



Scheme 131 (cont.)

thio, the reaction gives only monoaddition products. These observations strongly implicate a stepwise mechanism in which the final addition occurs with some association of the donor and acceptor carbonyls.

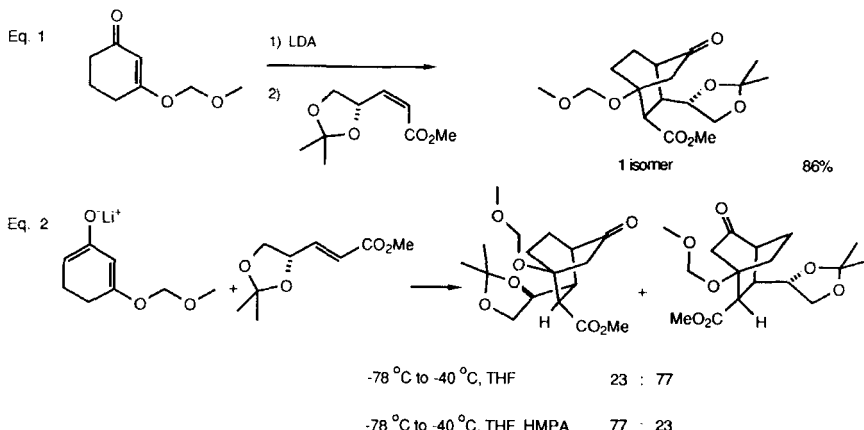
High levels of selectivity with respect to a preexisting stereocenter in either the dienolate or the activated olefin have also been observed (Scheme 132). For example, Roberts and Schlessinger have found that reaction of the dienolate in Eq. 1 with methyl crotonate results a single product (246). Similar stereocontrol was achieved with the substrates in Eqs. 2 and 3 (244). In Eq. 2, the only breakdown in stereoselection results from unselective protonation of



Scheme 132

the enolate formed in the cycloaddition. Interestingly, the exo product is preferred with the cyclopentenecarboxaldehyde in Eq. 4. Usually ketone enolates add 1,2- to α,β -unsaturated aldehydes, making the formation of the sequential addition product in this case unusual. Again, excellent selectivity with respect to the stereocenter in the dienolate was found. In Eq. 5, the dienolate derived from Hajos ketone provides the sequential Michael adduct as one stereoisomer in excellent yield (Scheme 132) (247). Addition occurs from the face opposite the methyl group.

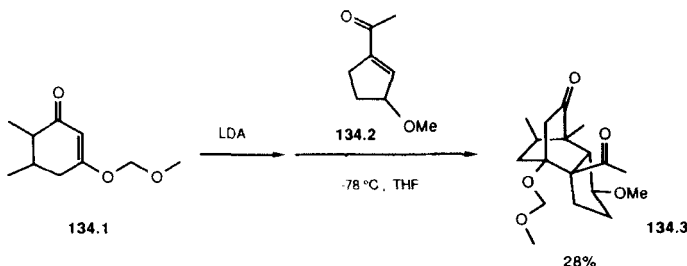
Yamada and coworkers have explored the sequential Michael additions in Eqs. 1 and 2 (Scheme 133) (248). In these cases, the possibility of diastereofa-



Scheme 133

cial selectivity with respect to the acceptor arises. With the *Z* enoate, the sequential Michael addition product is formed as a single diastereomer (Eq. 1). Much lower facial selectivity is observed with the *E* enoate (Eq. 2). Depending on the choice of solvent, a 54% d.e. of either facial diastereomer may be achieved.

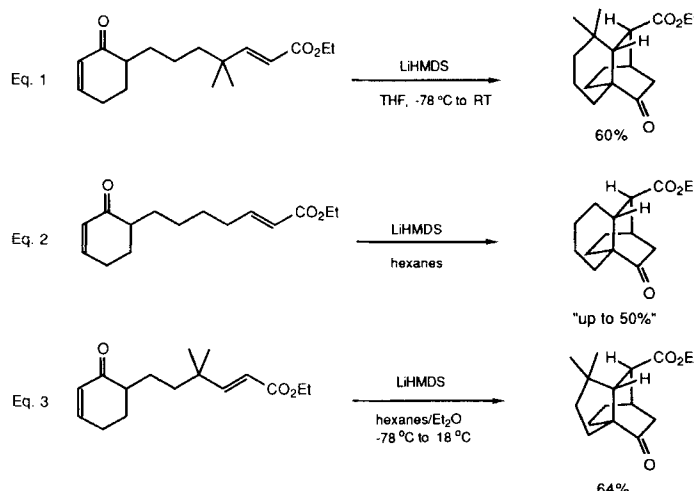
An interesting example of a sequential Michael addition was presented by Gibbons (Scheme 134) (244). In this case, enone 134.2 was combined with the dienolate of 134.1. The methoxy group of 134.2 directs nucleophilic attack to the opposite face of the acceptor to produce trans addition products with good facial discrimination. Coupled with the facial discrimination exhibited by the dienolate of 134.1 (vide supra) and the exceptional endo selectivity, mutual



Scheme 134

kinetic enantioselection should be anticipated. Indeed, the racemic dienolate of **134.1** was combined with the racemic acceptor **134.2** to provide **134.3** as apparently one isomer (although in low yield).

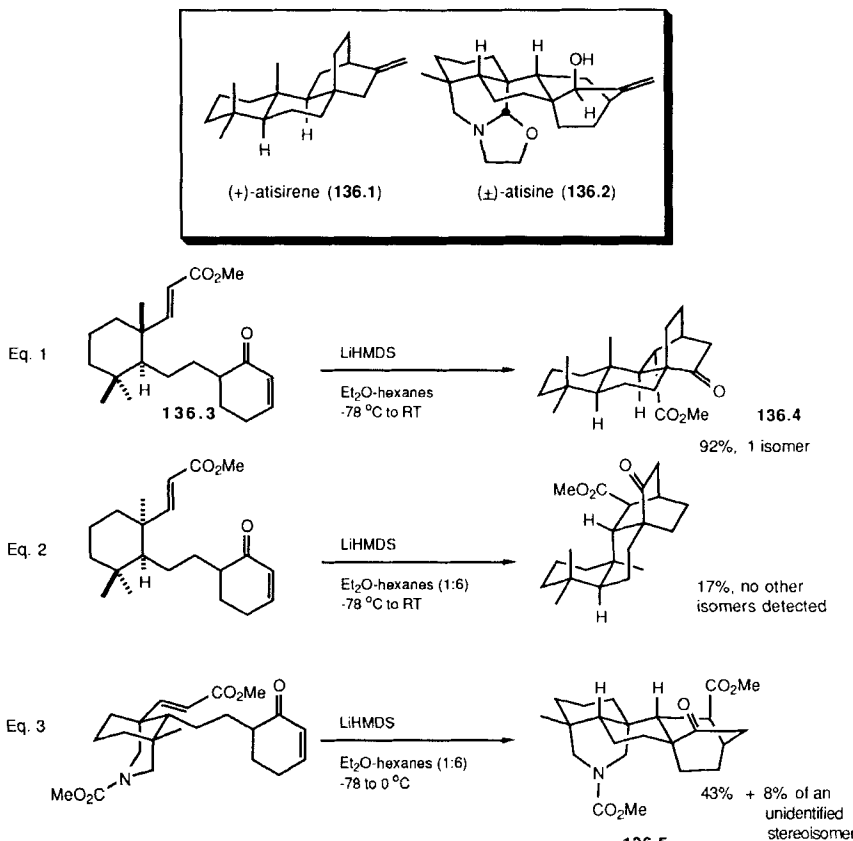
Scheme 135 illustrates several examples that proceed through an intramolecular sequential Michael addition manifold (249). In these cases endo products are predominantly created. Various combinations of lithium amide bases and solvents were explored for the cyclization of the substrate in Eq. 3. Optimal yields are found using lithium hexamethyldisilylamide (LiHMDS) in a combination of ether and hexanes.



Scheme 135

This methodology results in the rapid formation of bridged, polycyclic systems. Hence, it is potentially a powerful weapon for the synthesis of complex natural products. This approach has been extended to the synthesis of (+)-atisirene (**136.1**) (250, 251) and (\pm)-atisine (**136.2**, Scheme 136) (252).

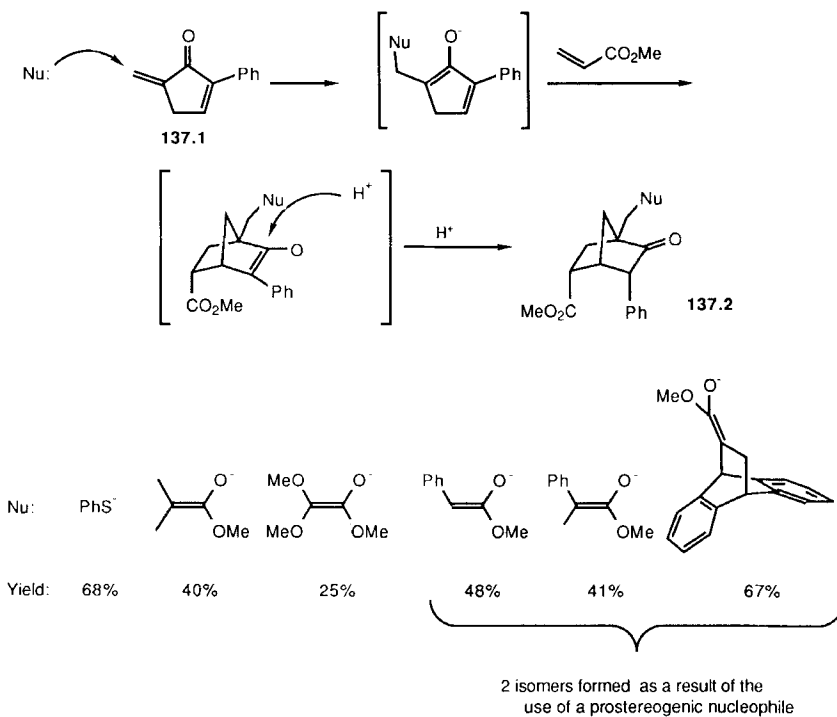
The synthesis of **136.1** utilizes the intramolecular sequential Michael addition of **136.3** derived from optically active Wieland–Miescher ketone (Eq. 1, Scheme 136). The sequential conjugate addition in this case proceeds with excellent endo selectivity and in high yield to form **136.4**. Further elaboration of **136.4** led to an intermediate that had previously been converted to **136.1**, completing the formal total synthesis. In contrast, only low yields of products are obtained in the cyclization of the cis isomer of **136.3** (Eq. 2) (253). Again, however, only one diastereoisomer was detected.



Scheme 136

For the synthesis of (\pm)-atisine, the sequential Michael addition in Eq. 3 (Scheme 136) was performed. A small amount of an as yet unidentified stereoisomer was also formed in the reaction. *This is the only example reported in which a minor diastereoisomer has been detected in the intramolecular version of the sequential Michael addition.* The major product (136.5) was converted to an intermediate in a prior synthesis of 136.2, constituting a formal total synthesis.

A unique entry into the sequential Michael addition manifold has been reported by Thebtaranonth and coworkers (Scheme 137) (254). In this case, conjugate addition of a variety of external nucleophiles to 137.1 initiates the sequential Michael addition sequence with methyl acrylate as the acceptor. The products 137.2 obtained have the endo orientation for both the carbo-methoxy and phenyl groups. Whereas the stereochemistry at the phenyl cen-

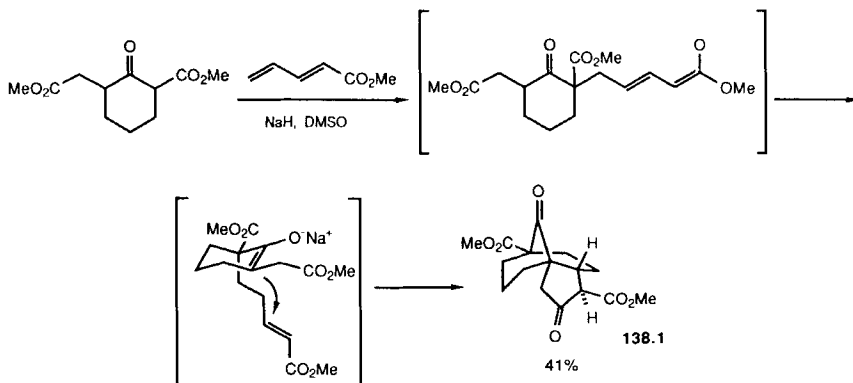


Scheme 137

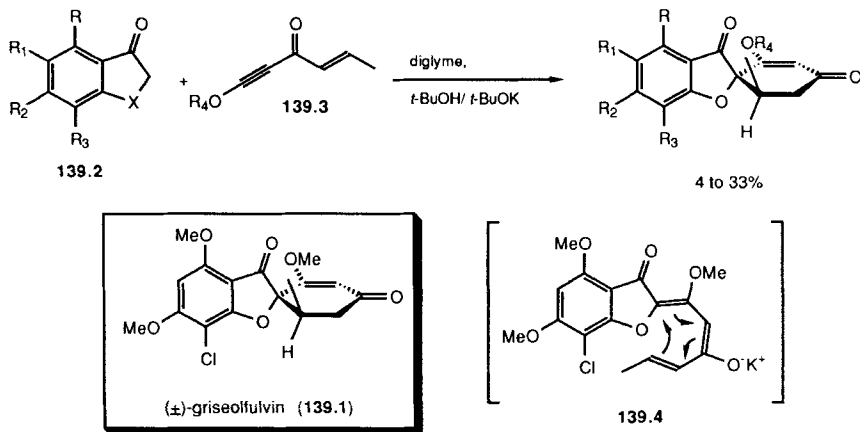
ter is the result of stereoselective protonation, the configuration of the carbo-methoxy group is established in the Michael addition. The stereochemical outcome of the Michael addition is consistent with a chelated transition state.

An example of a sequential Michael addition that does not have the option of proceeding through the “Diels–Alder” type manifold is shown in Scheme 138. In this example, a sequential Michael–Michael–Dieckmann condensation results in the formation of 138.1 (255). Although it is not certain whether the stereochemical outcome of the Michael addition is under kinetic or thermodynamic control, only one isomer of the product 138.1 is detected.

Another stereoselective sequential Michael addition (at least formally) is shown in Scheme 139. These examples were studied in relation to the synthesis of (\pm) -griseofulvin (139.1) (256) and analogs (257). Addition of ketones of the general structure 139.2 ($\text{R}_1, \text{R}_2, \text{R}_3 = \text{H}, \text{MeO}, \text{or Cl}; \text{X} = \text{O}, \text{S}, \text{MeN}$) to enynone 139.3 ($\text{R}_4 = \text{Me}$ or Et) promoted by base gives the griseofulvins in low yields. Although the stereoselectivity of the addition was not quantified, it



Scheme 138



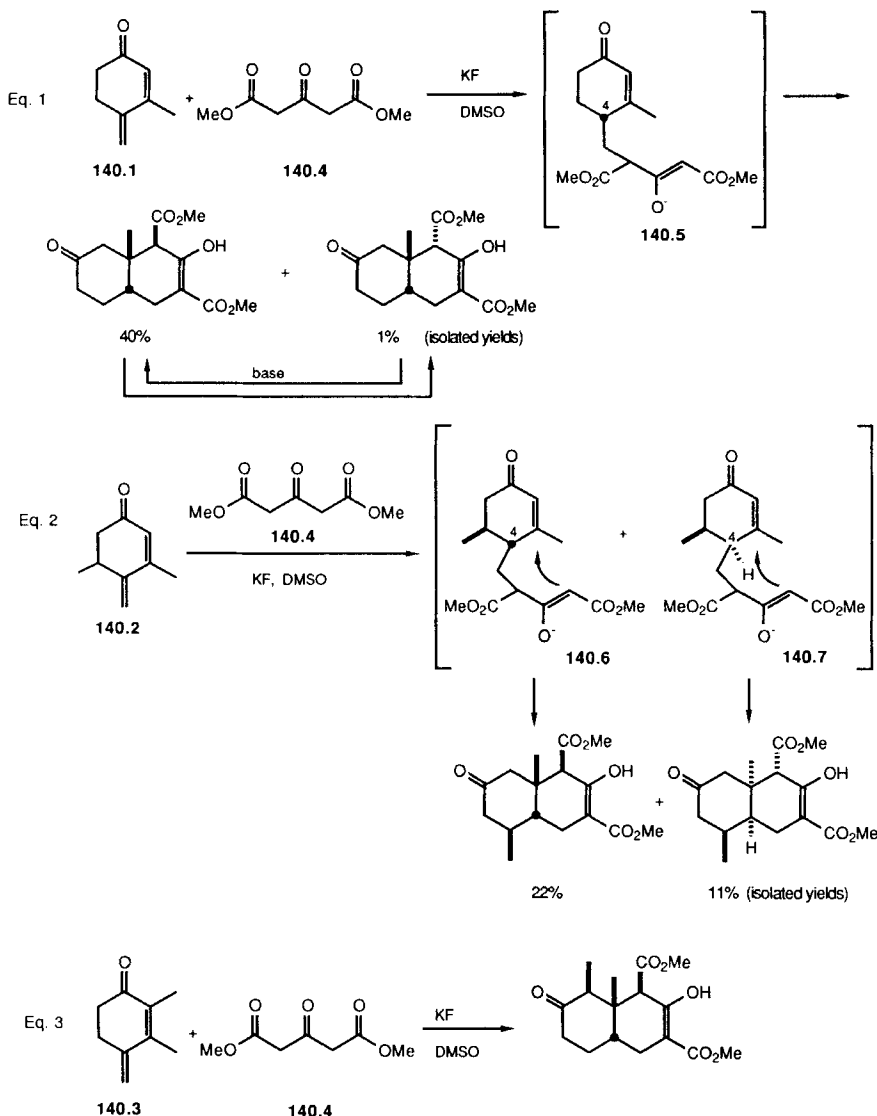
Scheme 139

appears that there is strong preference for the formation of the desired diastereomer.

The mechanism of stereoselection in this case has not been resolved. Acceptor **139.3** can undergo conjugate addition at two positions. If addition occurs first at the acetylenic terminus, stereoselection could be the result of an intramolecular Michael addition. Alternatively, addition to the vinyl terminus of **139.3** would require that stereodifferentiation occurs through preferential cyclization by way of the diastereomeric transition states. Still another possibility has been proposed by Magnus (258). In this proposal, selection occurs as a result of a concerted 6π -electron closure of **139.4**, analogous to

Scanio and Starrett's mechanism for the Robinson annelation in DMSO (*vide supra*) (100).

Another variation of the sequential Michael addition has been presented by Irie and coworkers (Scheme 140) (259). In this approach, the base-cata-



Scheme 140

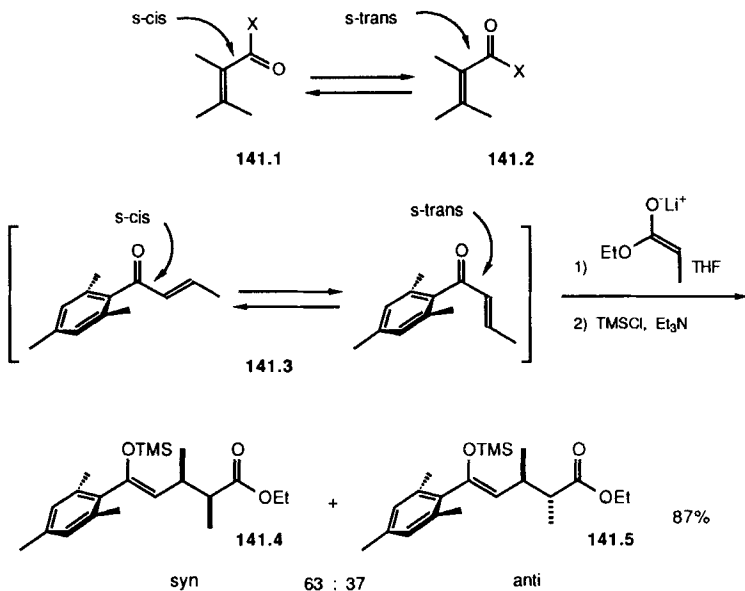
lyzed addition of dimethyl 3-ketoglutamate (**140.4**) to dienones **140.1** and **140.2** was examined. The reaction is believed to proceed through an initial 1,6-addition followed by reconjugation of the enone to form intermediate **140.5**. Closure of **140.5** results exclusively in the formation of cis-fused products, analogous to the observations for intramolecular Michael additions (*vide supra*). With **140.1** and **140.4**, only products that are isomeric at the readily epimerizable carbomethoxy side chain are obtained (Eq. 1).

Low selectivity with respect to a preexisting stereocenter in cyclohexadiene **140.2** is observed in the sequential Michael addition with **140.4** (Eq. 2, Scheme 140). As a result of the large preference for the formation of cis-fused products (*vide supra*), the stereochemical outcome of the second addition is determined by the configuration at C-4 in intermediates **140.6** and **140.7**. The stereochemistry at this center is established by protonation and/or equilibration after the initial 1,6-addition. The more fully substituted dienone **140.3** also gives addition products with **140.4**; however, no details were presented.

V. DISCUSSION OF MODELS

As presented in the foregoing sections of this chapter, excellent levels of simple stereoselection in the Michael addition are possible with a wide variety of components. At this point, consideration will be given to the source of the simple diastereoselection observed. To simplify discussion, the analysis herein will be limited to the addition of enolates to α,β -unsaturated esters and ketones under aprotic conditions. The concepts utilized, however, are generally extendable to a wider variety of donors and acceptors. The model employed shares features proposed by many of the workers in the field.

The first issue that must be confronted is the conformation assumed by acyclic acceptors. With simple substrates, two possibilities exist. Either the s-cis configuration (**141.1**, Scheme 141) or the s-trans orientation is assumed (**141.2**). For the reduction of enones either with L-Selectride or Li/NH₃, Chamberlin and Reich have demonstrated that the geometry of the enolate formed is strongly correlated with the ground state conformation preferred by the acceptor (260). Although this topic has not been fully examined, evidence suggests that this correlation does *not* hold in the case of enolate Michael additions. For example, addition of the *E* lithium enolate of ethyl propionate to the mesitylene derived enone **141.3** gives a mixture of syn and anti addition products (*vide supra*). When the product enolate is trapped with trimethylsilyl chloride, **141.4** and **141.5**, with the Z-configured enol silane, are formed (88). Because of the out-of-plane orientation of the mesityl group in **141.3**, the s-trans conformation should be readily accessible with the enone. Hence,

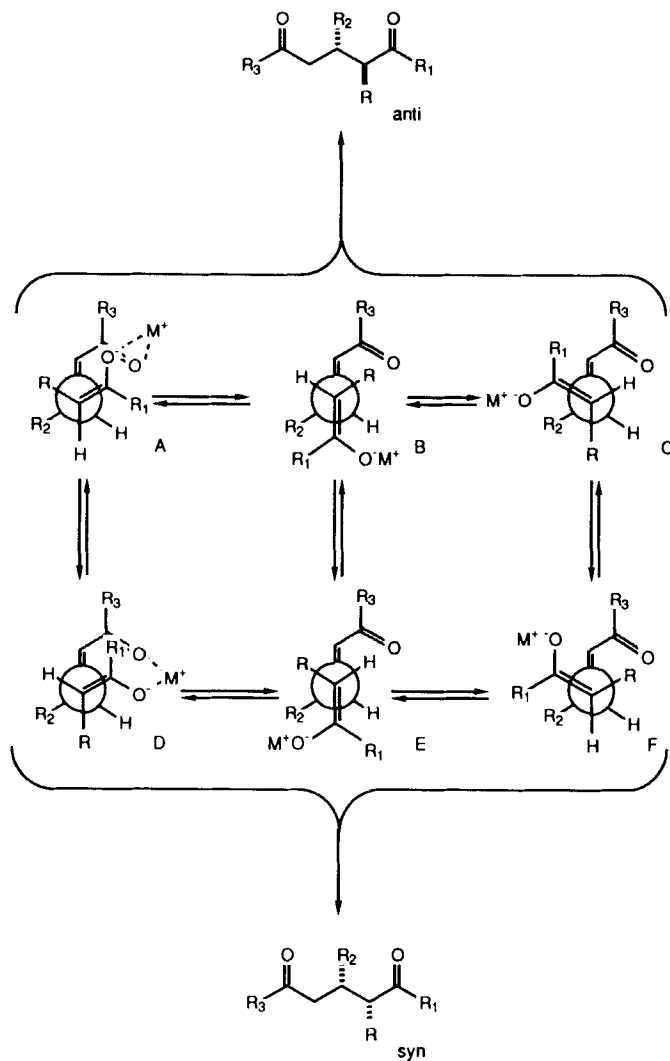


Scheme 141

there seems to be some preference in the Michael addition for the formation of acceptor enolates with the *Z* configuration.

Medium- and small-ring cyclic acceptors cannot achieve the *s-cis* configuration. This, perhaps, is the reason that 2-cyclohexenone fails to give conjugate addition products with the lithium enolate of propiophenone (entry 6, Table 16, Scheme 37).

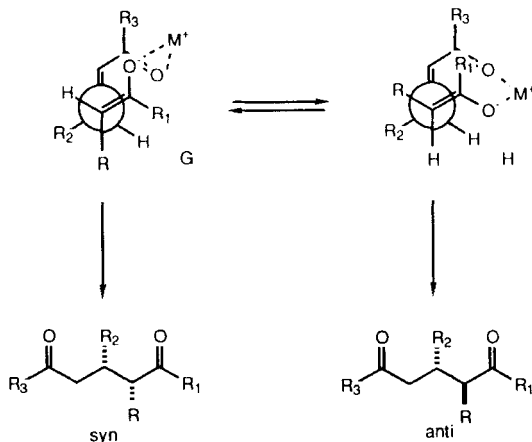
Transition states in which the substituents on the two prostereogenic centers are staggered should minimize unfavorable non-bonding interactions and thus should provide a lower energy pathway. If one starts with the assumption of a staggered transition state, then only the six possible transition states (A-F, Scheme 142) need to be considered for the addition of a *Z* enolate to an *E* acceptor. Of these, only A-C lead to the generally observed anti products (Scheme 142). On the basis of calculations, an open transition state such as B was found to be the sterically preferred configuration for the addition of enamines to acceptors (261, 262). With enolate Michael additions, however, increasing the bulk of R₁ results in higher anti selectivity (*vide supra*). This provides evidence against an “open” transition state because, on comparing B and E, increasing the bulk of R₁ should favor the *syn* diastereomer. Additionally, the results from sequential and intramolecular Michael additions in



Scheme 142

aprotic solvents (*vide supra*) strongly implicate transfer of the metal cation from the enolate to the acceptor in the transition state.

Increasing the bulk of R_1 and R_3 in model transition states A and D predicts that enhanced anti selectivity will be observed. The experimental results (*vide supra*) are consistent with this prediction. Transition state A is generally



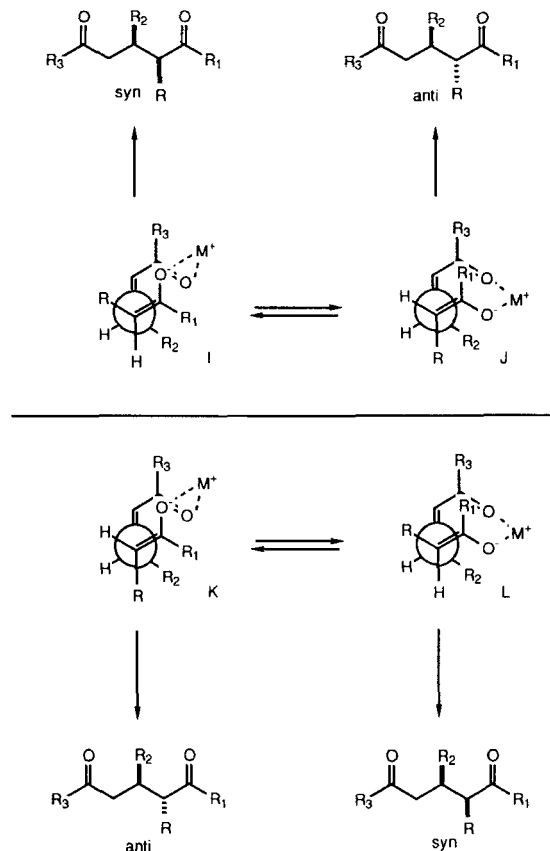
Scheme 143

favored in this addition. When R_1 and R_3 are small, some "leakage" into transition state D can occur, contrary to the prediction of Seebach and Golinski's topological rule where transition state A is intrinsically favored (263). From the data that have been presented, it appears that, in the absence of adverse steric interactions (i.e., very small R_1 and R_3), transition state D is favored, perhaps as a result of a more favorable mode of chelation.

In the reaction of an *E* enolate with an *E* acceptor, analogous staggered chelated transition states G and H are possible (Scheme 143). In this instance, the *syn* diastereomer from G is generally formed preferentially over the *anti* diastereomer from H. Again, with small R_1 and R_3 groups transition state H is favored. This model predicts that increasing the bulk of R_1 or R_3 should result in higher *syn* selectivity, as observed (*vide supra*).

Staggered, chelated transition state models predict that *E* and *Z* acceptors should give opposite stereoselectivity (Scheme 144). For example, transition state I is favored for *Z* enolates and transition state K is favored with *E* enolates. At present, there are insufficient data available to state confidently that transition states J and L are preferred for small R_1 and R_3 .

It must be pointed out that these model transition states predict trends adequately only for a given type of acceptor and donor. Comparison of results for different systems (for example the addition of amide enolates to enones versus the addition of amide enolates to enoates) is difficult. Another loose generalization can be made, however. *Less thermodynamically favorable reactions increase the effective bulk of the substituents, particularly R_1 and R_3 .* This observation is in accord with the "later" transition state expected for a less exothermic reaction.



Scheme 144

This simplified model ignores the pyramidalization of the reacting carbons that must be occurring, at least to some extent, in the transition state. Also not considered is the non-perpendicular approach of the nucleophile along a trajectory analogous to the “Bürgi–Dunitz” angle (264). These considerations are manifest in a difference between the steric priority assigned to the individual substituents of the donor and acceptor.

A difference in the geometry of the chelate ring should also influence the stereochemical outcome (e.g., compare transition states A and D in Scheme 142). Counterions and donor atoms with smaller ionic radii appear to favor the geometry D (Scheme 142), H (Scheme 143), J (Scheme 144), and L (Scheme 144).

Other factors that have been ignored are the role of solvent and the state of aggregation of the metal enolates. In some cases (for instance, HMPA), the role of the solvent is particularly mystifying.

It is interesting to note, however, that for lithium enolates the transition states D, H, J, and L seem to be preferred in the order: ketones (least), esters, amides (most). This order agrees nicely with the order of decreasing degree of aggregation of lithium enolates in ether solution (265). A greater preference for the products from transition states D, H, J, and L is also usually observed in the presence of HMPA.

These considerations aside, this simplified, chelated stereochemical model adequately predicts the trends observed in the intermolecular Michael addition.

For intramolecular and sequential Michael additions, the most important considerations are stereoelectronic and chelation. The stereochemical outcome for the initial step of the sequential Michael addition here is not fully in accord with the proposed model for intermolecular Michael additions. In this case, it is possible that some attractive interaction exists between the cross-conjugated enolate and the acceptor that is not possible with simple aliphatic enolates (secondary orbital overlap?).

VI. CONCLUSIONS

It is apparent from the work described in this chapter that significant progress has been made in elucidating the stereochemical outcome of the Michael addition in the century since its discovery. As a result of the wide variety of substrates that can be employed and the different methods for promoting the reaction, much room exists for further exploration and improvements. A solid foundation has been laid, however, for anticipating and understanding future results.

APPENDIX

In discussing Scheme 11, we used the term "pseudo-simple diastereoselectivity" to describe a stereoselection mechanism that is operative in $[N^*,P]$ and $[P,N^*]$ cases. Since this term has not been used previously in print, it is described here in more detail.

As is explained on page 238 (see Scheme 9), simple diastereoselectivity²⁶⁶ refers to a process in which two new stereocenters are formed. The diastereomeric ratio is governed by the relative orientations of the two reactants as bond formation occurs between two prostereogenic centers. For example, in

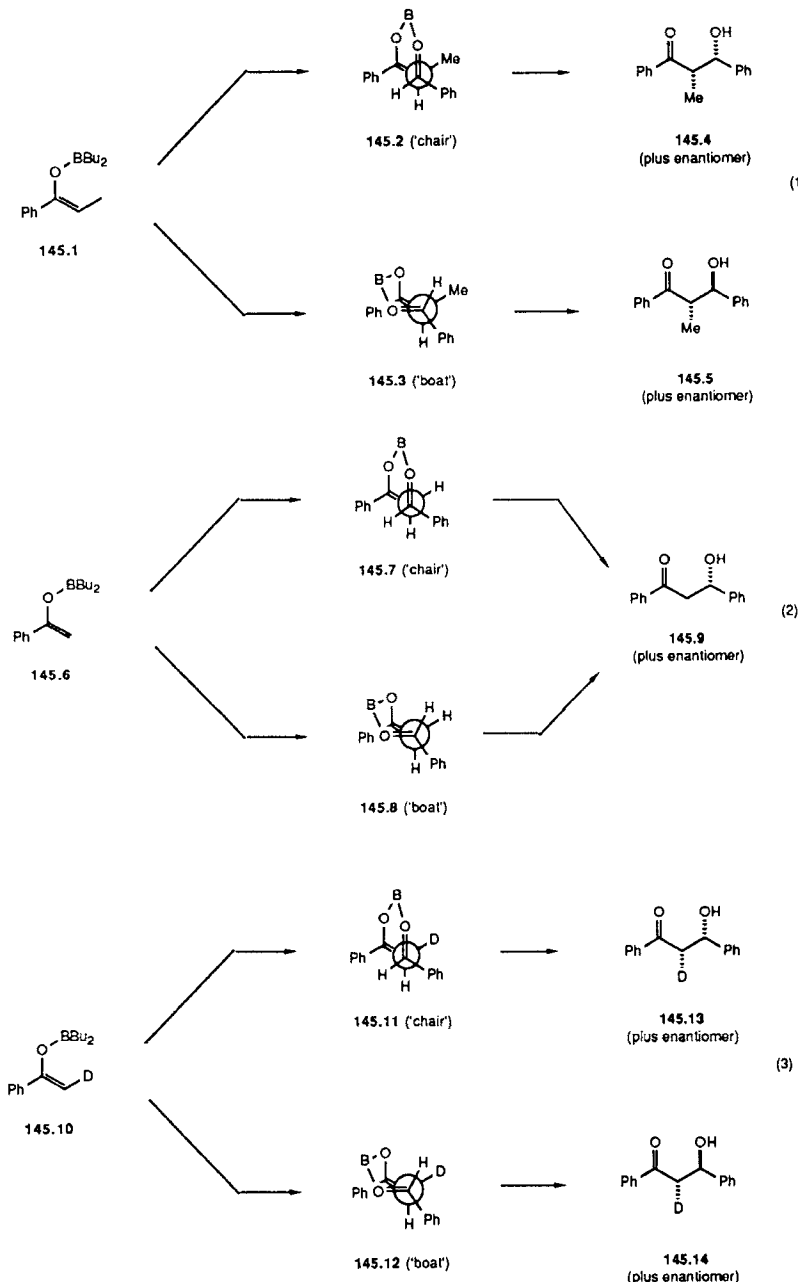
the aldol reaction between the *Z* boron enolate of propiophenone and benzaldehyde, depicted in Scheme 145, equation 1, the syn aldol **145.4** predominates because the chair-like transition state **145.2** is of lower energy than the boat-like transition state **145.3**.*

Now consider the hypothetical reaction in which the acetophenone enolate reacts with benzaldehyde. In this case only one new stereocenter is created and there is no possibility of simple diastereoselectivity (equation 2). Transition state orientations **145.7** and **145.8** are still possible, but there is no experimentally-observable consequence that permits an evaluation of their relative energies. However, if the acetophenone enolate is stereospecifically deuterated at one of the vinylic positions, simple diastereoselection would be apparent from the relative configuration of the deuterium and hydroxy groups (equation 3). The **145.13:145.14** ratio presumably reflects the relative energies of transition states **145.11** and **145.12**. It follows that the **145.7:145.8** ratio in equation 2 is similar to the **145.13:145.14** ratio in equation 3. It is this “invisible” orientational bias that we call “pseudo-simple diastereoselectivity.”

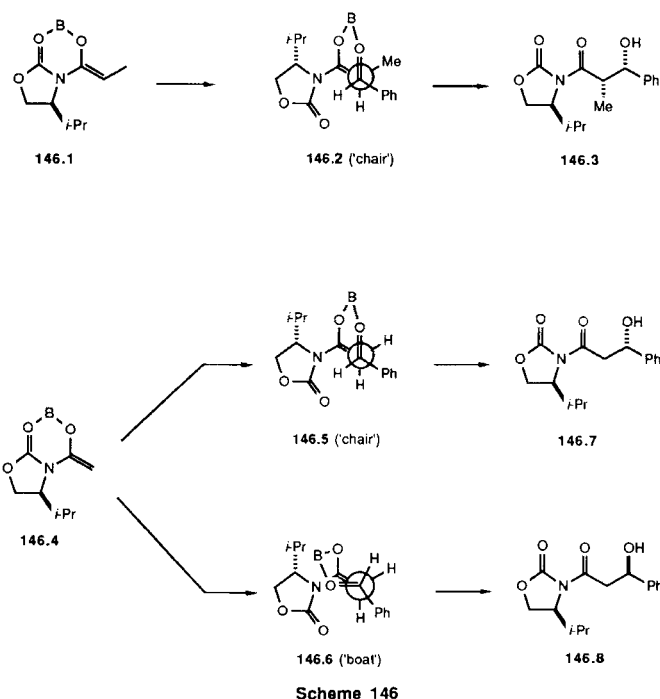
Although pseudo-simple diastereoselectivity leads to no experimentally-observable consequence in a reaction such as that in Scheme 145, equation 2, it is an important mechanism of stereoselection in $[N^*, P]$ and $[P, N^*]$ reactions. This is illustrated by the examples in Scheme 146 (267). The P^* boron enolate **146.1** reacts with benzaldehyde (**P**) to give one of the four possible diastereomeric products, **146.3**, in high yield, presumably *via* the transition state **146.2**. The high stereoselection in this reaction is a result of the high diastereofacial preference of the chiral boron enolate *and* a strong orientational preference of the two reactants. The orientational preference manifests itself in this reaction as a high syn:anti ratio at the two newly-formed stereocenters (e.g., simple diastereoselection).

However, the N^* boron enolate **146.4** reacts with benzaldehyde to give an equimolar mixture of the two diastereomers **146.7** and **146.8**. It is likely that the chiral boron enolate in this case also has a high facial preference, and that the reduced stereoselectivity results from the fact that the two orientations **146.5** and **146.6** are similar in energy. With enolate **146.4**, the lack of orientational preference is not seen as simple diastereoselection, because only one new stereocenter is created. In this case, the low stereoselectivity results from poor pseudo-simple diastereoselectivity. Again, if enolate **146.4** had been stereospecifically deuterated in one of the vinylic positions, the absence of simple diastereoselection would be apparent from the relative configurations of the deuterium and hydroxyl groups in the products.

* In Schemes 145 and 146, the two alkyl ligands on boron are omitted for clarity.



Scheme 145



For high stereoselection to be observed in $[N^*, P]$ and $[P, N^*]$ reactions, it is necessary that *both* the facial preference of the N^* component *and* the pseudo-simple stereoselectivity be high.

ACKNOWLEDGMENTS

The authors would like to thank Mr. A. Ganesan and Mr. Roger Ruggeri for proofreading the manuscript. We also wish to thank Ms. Janet Tamada for her assistance in generating structures with the ChemDraw program. This work was supported by a research grant from the United States Public Health Service (AI15027).

REFERENCES

- Bergman, E. D.; Ginsburg, D.; Pappo, R. *Org. React.* **1959**, *10*, 179–555.
- (a) Komnenos, T. *Liebigs Ann. Chem.* **1883**, *218*, 145–169. (b) Claisen, L. J. *Prakt. Chem.* **1887**, *35*, 413–415.

3. Michael, A. *J. Prakt. Chem.* **1887**, *36*, 113–114.
4. For an interesting discussion of Michael's contributions to organic chemistry, see: Tarbell, D. S.; Tarbell, A. T. *The History of Organic Chemistry in the United States, 1875–1955*; Folio: Nashville, 1986; pp 45–53.
5. (a) Michael, A. *J. Prakt. Chem.* **1887**, *35*, 349–356. (b) Michael, A.; Schulthess, O. *J. Prakt. Chem.* **1892**, *45*, 55–63. (c) Michael, A. *Am. Chem. J.* **1887**, *9*, 112–124. (d) Michael, A. *Chem. Ber.* **1894**, *27*, 2126–2130. (e) Michael, A. *Chem. Ber.* **1900**, *33*, 3731–3769.
6. House, H. O. *Modern Synthetic Reactions*; W. A. Benjamin: Menlo Park, 1972; pp 595–623.
7. Corey, E. J.; Ohno, M.; Mitra, R. B.; Vatakencherry, P. *A. J. Am. Chem. Soc.* **1964**, *86*, 478–485.
8. For example see: Evans, D. A. In *Asymmetric Synthesis*; Morrison, J. D., Ed.; Academic: New York, 1983; Vol. 3, Chapter 1.
9. For example see: House, H. O.; Fischer, W. F. *J. Org. Chem.* **1969**, *34*, 3615–3618.
10. For a review see: Posner, G. H. *Org. React.* **1972**, *19*, Chapter 1.
11. (a) Corey, E. J.; Enders, D. *Tetrahedron Lett.* **1976**, *17*, 3–6. (b) Corey, E. J.; Enders, D. *Tetrahedron Lett.* **1976**, *17*, 11–14. (c) Corey, E. J.; Enders, D. *Chem. Ber.* **1978**, *111*, 1337–1361. (d) Corey, E. J.; Enders, D. *Chem. Ber.* **1978**, *111*, 1362–1383.
12. Posner, G. H. In *Asymmetric Synthesis*; Morrison, J. D., Ed.; Academic: New York, 1983; Vol. 2, Chapter 8.
13. (a) Tomioka, K.; Koga, K. In *Asymmetric Synthesis*; Morrison, J. D., Ed.; Academic: New York, 1983; Vol. 7, Chapter 7. (b) Bartlett, P. A. *Tetrahedron* **1980**, *36*, 2–72. (c) Nógrádi, M. *Stereoselective Synthesis*; Verlag Chemie: Weinheim, 1987.
14. Yamaguchi, M. *Yuki Gosei Kagaku* **1986**, *44*, 405–420. We are indebted to Mr. Ichiro Mori for translating this Japanese-language review.
15. Seebach, D.; Imwinkelried, R.; Weber, T. In *Modern Synthetic Methods 1986*; Scheffold, R., Ed.; Springer Verlag: Berlin; Vol. 4, 1986, pp 125–259.
16. Corey, E. J.; Magriotis, P. A. *J. Am. Chem. Soc.* **1987**, *109*, 287–289.
17. Corey, E. J.; Howe, W. J.; Orf, H. W.; Pensak, D. A.; Peterson, G. *J. Am. Chem. Soc.* **1975**, *97*, 6116–6124.
18. For example see: Binkley, E. S.; Heathcock, C. H. *J. Org. Chem.* **1975**, *40*, 2156–2160.
19. For example see: Deschamps, B.; Anh, N. T.; Seyden-Penne, J. *Tetrahedron Lett.* **1973**, *14*, 527–530.
20. For some leading references see: (a) Kyriakakou, G.; Roux-Schmitt, M. C.; Seyden-Penne, J. *Tetrahedron* **1975**, *31*, 1883–1888. (b) Cossentini, M.; Deschamps, B.; Anh, N. T.; Seyden-Penne, J. *Tetrahedron* **1977**, *33*, 409–412. (c) Deschamps, B.; Seyden-Penne, J. *Tetrahedron* **1977**, *33*, 413–417. (d) Sauvretre, R.; Roux-Schmitt, M.-C.; Seyden-Penne, J. *Tetrahedron* **1978**, *34*, 2135–2140. (e) Roux-Schmitt, M.-C.; Wartski, L.; Seyden-Penne, J. *Synth. Commun.* **1981**, *11*, 85–94. (f) Seuron, N.; Wartski, L.; Seyden-Penne, J. *Tetrahedron Lett.* **1981**, *22*, 2175–2178. (g) Seuron, N.; Seyden-Penne, J. *Tetrahedron* **1984**, *40*, 635–640. (h) Kaiser, E. M.; Knutson, P. L.; McClure, J. R. *Tetrahedron Lett.* **1978**, *19*, 1747–1750. (i) Stork, G.; Maldonado, L. *J. Am. Chem. Soc.* **1974**, *96*, 5273–5274. (j) Wakamatsu, T.; Hobara, S.; Ban, Y. *Heterocycles* **1982**, *19*, 1395–1398. (k) Yamagiwa, S.; Hoshi, N.; Sato, H.; Kosugi, H.; Uda, H. *J. Chem. Soc., Perkin Trans 1* **1978**, 214–224. (l) Seebach, D. *Synthesis* **1969**, 17–36. (m) Ostrowski, P. C.; Kane, V. V. *Tetrahedron Lett.* **1977**, *18*, 3549–3552.

21. See also: Gorrighon-Guigon, L.; Hammerer, S. *Tetrahedron* **1980**, *36*, 631-639.
22. Yamaguchi, M.; Hasebe, K.; Tanaka, S.; Minami, T. *Tetrahedron Lett.* **1986**, *27*, 959-962.
23. Heathcock, C. H.; Henderson, M. A.; Oare, D. A.; Sanner, M. A. *J. Org. Chem.* **1985**, *50*, 3019-3022.
24. Sanner, M. A.; Oare, D. A.; Heathcock, C. H., unpublished results.
25. (a) Bertrand, J.; Cabrol, N.; Gorrighon-Guigon, L.; Maroni-Barnaud, Y. *Tetrahedron Lett.* **1973**, *14*, 4683-4686. (b) Bertrand, J.; Gorrighon, L.; Maroni, P. *Tetrahedron Lett.* **1977**, *18*, 4207-4210.
26. Bertrand, J.; Gorrighon, L.; Maroni, P.; Meyer, R. *Tetrahedron Lett.* **1982**, *23*, 3267-3270.
27. (a) Maruoka, K.; Nomoshita, K.; Yamamoto, H. *Tetrahedron Lett.* **1987**, *28*, 5723-5726. (b) Maruoka, K.; Itoh, T.; Sakurai, M.; Nonoshita, K.; Yamamoto, H. *J. Am. Chem. Soc.* **1988**, *110*, 3588-3597.
28. Eiel, E. *J. Chem. Ed.* **1971**, *48*, 163-167.
29. Masamune, S.; Kaiho, T.; Garvey, D. S. *J. Am. Chem. Soc.* **1982**, *104*, 5521-5523.
30. Masamune, S.; Ali, Sk. A.; Snitman, D. L.; Garvey, D. S. *Angew. Chem. Int. Ed. Engl.* **1980**, *19*, 557-558; *Angew. Chem.* **1980**, *92*, 573-575.
31. Heathcock, C. H. In *Asymmetric Synthesis*; Morrison, J. D., Ed.; Academic: New York, 1983; Vol. 3, Chapter 2.
32. Yamaguchi, M.; Tsukamoto, M.; Tanaka, S.; Hirao, I. *Tetrahedron Lett.* **1984**, *25*, 5661-5664.
33. In this chapter, we utilize terminology suggested by Mislow and Siegel: Mislow, K.; Siegel, J. *J. Am. Chem. Soc.* **1984**, *106*, 3319-3328.
34. (a) Heathcock, C. H.; Pirrung, M. C.; Buse, C. T.; Hagen, J. P.; Young, S. D.; Sohn, J. E. *J. Am. Chem. Soc.* **1979**, *101*, 7076-7077. (b) Heathcock, C. H.; Pirrung, M. C.; Lampe, J.; Buse, C. T.; Young, S. D. *J. Org. Chem.* **1981**, *46*, 2290-2300.
35. Masamune, S.; Choy, W.; Petersen, J. S.; Sita, L. R. *Angew. Chem. Int. Ed. Engl.* **1985**, *24*, 1-30; *Angew. Chem.* **1985**, *97*, 1-31.
36. Heathcock, C. H.; White, C. T.; Morrison, J. J.; VanDerveer, D. *J. Org. Chem.* **1981**, *46*, 1296-1309.
37. Izumi, Y.; Tai, A. *Stereo-differentiating Reactions*; Academic: New York, 1976.
38. Langstrom, B.; Bergson, G. *Acta Chem. Scand.* **1973**, *27*, 3118-3119.
39. For leading references for the closely related studies of the asymmetric Michael addition of nitromethane to chalcone see: (a) Colonna, S.; Hiemstra, H.; Wynberg, H. *J. Chem. Soc. Chem. Commun.* **1978**, 238-239. (b) Colonna, S.; Re, A.; Wynberg, H. *J. Chem. Soc., Perkin Trans 1* **1981**, 547-552. (c) Matsumoto, K.; Uchida, T. *Chem. Lett.* **1981**, 1673-1676.
40. (a) Wynberg, H.; Helder, R. *Tetrahedron Lett.* **1975**, *16*, 4057-4060. (b) Hermann, K.; Wynberg, H. *J. Org. Chem.* **1979**, *44*, 2238-2244. (c) Wynberg, H. *Topics in Stereochemistry*; Eiel, E. L.; Wilen, S. H.; Allinger, N. L.; Eds.; Wiley: New York, 1986; Vol. 16, Chapter 2.
41. While reasonable enantiomeric excesses were found with methyl vinyl ketones, very low selectivity was found for the addition of similar substrates to α,β -unsaturated sulfoximides: Annunziata, R.; Cinquini, M.; Colonna, S. *J. Chem. Soc., Perkin Trans 1* **1980**, 2422-2424.

42. Colonna, S.; Annunziata, R. *Afinidad* **1981**, *38*, 501-502.
43. Hermann, K.; Wynberg, H. *Helv. Chim. Acta* **1977**, *60*, 2208-2212.
44. Hodge, P.; Khoshdel, E.; Waterhouse, J. *J. Chem. Soc., Perkin Trans. I* **1983**, 2205-2209.
45. (a) Kobayashi, N.; Iwai, K. *J. Am. Chem. Soc.* **1978**, *100*, 7071-7022. (b) Kobayashi, N.; Iwai, K. *J. Polym. Sci., Polym. Chem. Ed.* **1980**, *18*, 923-932.
46. For a related study see: Kobayashi, N.; Iwai, K. *Tetrahedron Lett.* **1980**, *21*, 2167-2170.
47. Kobayashi, N.; Iwai, K. *J. Polym. Sci., Polym. Lett. Ed.* **1982**, *20*, 85-90.
48. Brunner, H.; Hammer, B. *Angew. Chem. Int. Ed. Engl.* **1984**, *23*, 312-313; *Angew. Chem.* **1984**, *96*, 305-306.
49. Conn, R. S. E.; Lovell, A. V.; Karady, S.; Weinstock, L. M. *J. Org. Chem.* **1986**, *51*, 4710-4711.
50. For the closely related study of the asymmetric alkylation and formal Robinson annelation of 13.1 see: (a) Bhattacharya, A.; Dolling, U.-H.; Grabowski, E. J. J.; Karady, S.; Ryan, K. M.; Weinstock, L. M. *Angew. Chem. Int. Ed. Engl.* **1986**, *25*, 476-477; *Angew. Chem.* **1986**, *98*, 442-443. (b) Dolling, U.-H.; Davis, P.; Grabowski, E. J. *J. Am. Chem. Soc.* **1984**, *106*, 446-447.
51. Cram, D. J.; Sogah, D. D. *J. Chem. Soc., Chem. Commun.* **1981**, 625-628.
52. Alonso-Lopez, M.; Martin-Lomas, M.; Penades, S. *Tetrahedron Lett.* **1986**, *27*, 3551-3554.
53. Raguse, B.; Ridley, D. D. *Aust. J. Chem.* **1984**, *37*, 2059-2071.
54. (a) Marshall, J. A.; Faubl, H.; Warne Jr., T. M. *Chem. Commun.* **1967**, 753-754. (b) Marshall, J. A.; Ruden, R. A. *Tetrahedron Lett.* **1970**, 1239-1242. (c) Marshall, J. A.; Warne Jr., T. M. *J. Org. Chem.* **1971**, *36*, 178-183.
55. For a related study where preferential addition occurs from one face on a cycloheptanone with a pre-existing stereocenter see: Marshall, J. A.; Partridge, J. J. *Tetrahedron* **1969**, *25*, 2159-2192.
56. (a) Tomioka, K.; Cho, Y.-S.; Sato, F.; Koga, K. *Chem. Lett.* **1981**, 1621-1624. (b) For analogous alkylations of this lactone see: Tomioka, K.; Cho, Y.-S.; Sato, F.; Koga, K. *J. Org. Chem.* **1988**, *53*, 4094-4098.
57. Tomioka, K.; Yasuda, K.; Koga, K. *J. Chem. Soc., Chem. Commun.* **1987**, 1345-1346.
58. Enders, D.; Demir, A. S.; Puff, H.; Franken, S. *Tetrahedron Lett.* **1987**, *28*, 3795-3798.
59. Matsumoto, T.; Shirahama, H.; Ichihara, A.; Shin, H.; Kagawa, S.; Sakan, F.; Miyano, K. *Tetrahedron Lett.* **1971**, 2049-2052.
60. Tomioka, K.; Ando, K.; Yasuda, K.; Koga, K. *Tetrahedron Lett.* **1986**, *27*, 715-716.
61. Tomioka, K.; Yasuda, K.; Koga, K. *Tetrahedron Lett.* **1986**, *27*, 4611-4614.
62. Brandt, J.; Jochum, C.; Ugi, I.; Jochum, P. *Tetrahedron* **1977**, *33*, 1353-1363.
63. Tomioka, K.; Seo, W.; Ando, K.; Koga, K. *Tetrahedron Lett.* **1987**, *28*, 6637-6640.
64. (a) Hashimoto, S.; Komeshima, N.; Yamada, S.; Koga, K. *Tetrahedron Lett.* **1977**, 2907-2908. (b) Hashimoto, S.; Komeshima, N.; Yamada, S.; Koga, K. *Chem. Pharm. Bull.* **1979**, *27*, 2437-2441.
65. For a review of enantioselective synthesis using optically active sulfoxides see: (a) Solladié, G. *Synthesis* **1981**, 185-196. (b) Barbachyn, M. R.; Johnson, C. R. In *Asymmetric Synthesis*; Morrison, J. D., Ed.; Academic: Orlando, Florida; 1984, Vol. 4, Chapter 2. (c) Solladié, G. In *Asymmetric Synthesis*; Morrison, J. D., Ed.; Academic: Orlando, Florida; 1983, Vol. 2, Chapter 6. (d) Mikolajczyk, M.; Dravowicz, J. In *Topics in Stereo-*

- chemistry*; Allinger, N. L.; Eliel, E. L.; Wilen, S. H., Eds.; Wiley: New York, New York; 1982, Vol. 13, 333–468.
66. (a) Tsuchihashi, G.; Mitamura, S.; Inoue, S.; Ogura, K. *Tetrahedron Lett.* **1973**, 323–326.
 (b) Tsuchihashi, G.; Mitamura, S.; Ogura, K. *Tetrahedron Lett.* **1976**, 855–858.
 67. Yamazaki, T.; Ishikawa, N.; Iwatubo, H.; Kitazume, T. *J. Chem. Soc., Chem. Commun.* **1987**, 1340–1342.
 68. (a) Abramovitch, R. A.; Struble, D. L. *Tetrahedron Lett.* **1966**, 289–294. (b) Abramovitch, R. A.; Struble, D. L. *Tetrahedron* **1968**, 24, 357–380.
 69. Abramovitch, R. A.; Singer, S. S.; Rogic, M. M.; Struble, D. L. *J. Org. Chem.* **1975**, 40, 34–41.
 70. For a related study of the Michael addition of thiophenol see: Abramovitch, R. A.; Singer, S. S. *J. Org. Chem.* **1976**, 41, 1712–1717.
 71. Deslongchamps, P. In *Stereoelectronic Effects in Organic Chemistry. Organic Chemistry Series*; Baldwin, J. E., Ed.; Pergamon: Oxford, 1983; pp 209–290.
 72. Zimmerman, H. E. *Acc. Chem. Res.* **1987**, 20, 263.
 73. Alder, K.; Wirtz, H.; Koppelberg, H. *Liebigs Ann. Chem.* **1956**, 601, 138–154.
 74. (a) Yamagita, M.; Inayama, S.; Hirakura, M.; Seki, F. *J. Org. Chem.* **1958**, 23, 690–699 and references therein. (b) Matsui, M.; Toki, K.; Kitamura, S.; Suzuki, Y.; Hamuro, M. *Bull. Chem. Soc. Jpn.* **1954**, 27, 7–10 and references therein. (c) McQuillin, F. *J. Chem. & Ind. (London)* **1954**, 311–312 and references therein. (d) Gunstone, F. D.; Tulloch, A. P. *J. Chem. Soc.* **1955**, 1130–1136. (e) Abe, Y.; Harukawa, T.; Ishikawa, H.; Miki, T.; Sumi, M.; Toga, T. *J. Am. Chem. Soc.* **1956**, 78, 1422–1426. (f) Woodward, R. B.; Yates, P. *Chem. & Ind. (London)* **1954**, 1391–1393. (g) Corey, E. J. *J. Am. Chem. Soc.* **1955**, 77, 1044–1045 and references therein. (h) Ralls, J. W. *J. Am. Chem. Soc.* **1953**, 75, 2123–2125 and references therein.
 75. (a) For addition to α,β -unsaturated ketones see: Mukaiyama, T.; Hirako, Y.; Takeda, T. *Chem. Lett.* **1978**, 461–464. (b) For a correction of the enantioselectivities reported in part a and the addition to 1-nitrocyclohexene see: Takeda, T.; Hoshiko, T.; Mukaiyama, T. *Chem. Lett.* **1981**, 797–800.
 76. Matloubi, F.; Solladié, G. *Tetrahedron Lett.* **1979**, 2141–2144.
 77. For the related addition of a formyl anion equivalent see: (a) Colombo, L.; Gennari, C.; Resnati, G.; Scolastico, C. *Synthesis* **1981**, 74–76. (b) Colombo, L.; Gennari, C.; Resnati, G.; Scolastico, C. *J. Chem. Soc., Perkin Trans 1* **1981**, 1284–1286.
 78. Kpegbé, K.; Metzner, P.; Rakotonirina, R. *Tetrahedron Lett.* **1986**, 27, 1505–1508.
 79. For example see: Heathcock, C. H.; Buse, C. T.; Kleshick, W. A.; Pirrung, M. A.; Sohn, J. E.; Lampe, J. *J. Org. Chem.* **1980**, 45, 1066–1081.
 80. Berrada, S.; Metzner, P. *Tetrahedron Lett.* **1987**, 28, 409–412.
 81. For regiochemical considerations see: (a) d'Angelo, J. *Tetrahedron* **1976**, 32, 2979–2990.
 (b) Stork, G.; Hudrik, P. F. *J. Am. Chem. Soc.* **1968**, 90, 4462–4464, 4464–4465.
 (c) House, H. O.; Czuba, L. J.; Gall, M.; Olmstead, H. D. *J. Org. Chem.* **1969**, 34, 2324–2336.
 82. Yamazaki, T.; Ishikawa, N. *Chem. Lett.* **1985**, 889–892.
 83. (a) Maroni-Barnaud, Y.; Gorrichon-Guigon, L.; Maroni, P.; Bertrand, J. *Tetrahedron Lett.* **1966**, 2243–2248. (b) Maroni-Barnaud, Y.; Gorrichon-Guigon, L.; Maroni, P.; Bertrand, J. *Bull. Chim. Soc. Fr.* **1966**, 3128–3132.
 84. (a) Bertrand, J.; Gorrichon-Guigon, L.; Koudsi, Y.; Perry, M.; Maroni-Bernaud, Y.; Normant, H. *C. R. Acad. Sci. Paris, Ser. C* **1973**, 277, 723–726. (b) Maroni-Barnaud, Y.;

- Bertrand, J.; Ghozland, F.; Gorrlichon-Guigon, L.; Koudsi, Y.; Maroni, P.; Meyer, R. *C. R. Acad. Sci. Paris, Ser. C* **1975**, *280*, 221–224. (c) Meyer, R.; Gorrlichon, L.; Maroni, P. *J. Organomet. Chem.* **1977**, *129*, C7–C10. (d) Bertrand, J.; Gorrlichon, L.; Maroni, P.; Meyer, R.; Viteva, L. *Tetrahedron Lett.* **1982**, *23*, 1901–1904.
85. (a) Gorrlichon-Guigon, L.; Maroni-Barnaud, Y.; Maroni, P. *Bull. Soc. Chim. Fr.* **1972**, 4187–4194. (b) Gorrlichon-Guigon, L.; Maroni-Barnaud, Y. *Bull. Soc. Chim. Fr.* **1973**, 263–270. (c) Bertrand, J.; Gorrlichon, L.; Maroni, P. *Tetrahedron* **1984**, *40*, 4127–4140. (d) Bertrand, J.; Gorrlichon, L.; Maroni, P.; Meyer, R.; personal communication, May, 1985.
86. For structural proofs and NMR correlations see: (a) Gorrlichon-Guigon, L.; Maroni-Barnaud, Y.; Maroni, P. *Bull. Soc. Chim. Fr.* **1970**, 128–130. (b) Gorrlichon-Guigon, L.; Maroni-Barnaud, Y.; Maroni, P. *Bull. Soc. Chim. Fr.* **1970**, 1412–1415.
87. Oare, D. A.; Heathcock, C. H. *Tetrahedron Lett.* **1986**, *27*, 6169–6172.
88. Oare, D. A.; Heathcock, C. H. unpublished results.
89. For reviews of the Robinson annelation see: (a) Jung, M. E. *Tetrahedron* **1976**, *32*, 3–31. (b) Gawley, R. E. *Synthesis* **1976**, 777–794.
90. For a review of the synthesis of polycarbocyclic sesquiterpenes in which stereoselective annelations are discussed see: Vandewalle, M.; De Clercq, P. *Tetrahedron* **1985**, *41*, 1767–1831.
91. For some examples of stereochemical control with respect to a pre-existing stereocenter in a ring see: (a) Ireland, R. E.; Kierstead, R. C. *J. Org. Chem.* **1966**, *31*, 2543–2559. (b) Gardner, J. N.; Anderson, B. A.; Oliveto, E. P. *J. Org. Chem.* **1969**, *34*, 107–112. (c) Halsall, T. G.; Theobald, D. W., Walshaw, K. B. *J. Chem. Soc.* **1964**, 1029–1037. (d) Pinder, A. R.; Williams, R. A. *J. Chem. Soc.* **1963**, 2773–2778. (e) Howe, R.; McQuillin, F. *J. J. Chem. Soc.* **1958**, 1194–1199. (f) Ziegler, F. E.; Hwang, K.-J. *J. Org. Chem.* **1983**, *48*, 3349–3351. (g) Velluz, L.; Valls, J.; Nomine, G. *Angew. Chem. Int. Ed. Engl.* **1965**, *4*, 181–200; *Angew. Chem.* **1965**, *77*, 185–205. (h) Stork, G.; Darling, S. D. *J. Am. Chem. Soc.* **1964**, *86*, 1761–1768. (i) Wenkert, E.; Berges, D. A. *J. Am. Chem. Soc.* **1967**, *89*, 2507–2509. (j) Marshall, J. A.; Fanta, W. J. *J. Org. Chem.* **1964**, *29*, 2501–2505.
92. House, H. O.; Lusch, M. *J. J. Org. Chem.* **1977**, *42*, 183–190.
93. Kretchmer, R. A.; Michelich, E. D.; Waldron, J. *J. J. Org. Chem.* **1972**, *37*, 4483–4485.
94. For a related approach to products with a similar structure that does not use a stereoselective Michael addition see: Hale, R. L.; Zalkow, L. H. *J. J. Org. Chem. Commun.* **1968**, 1249–1250.
95. (a) Stork, G. A.; Ganem, B. *J. Am. Chem. Soc.* **1973**, *95*, 6152–6153. (b) Stork, G. A.; Singh, J. *J. Am. Chem. Soc.* **1974**, *96*, 6181–6182.
96. (a) Boeckman, R. K., Jr. *J. Am. Chem. Soc.* **1973**, *95*, 6867–6869. (b) Boeckman, R. K., Jr. *J. Am. Chem. Soc.* **1974**, *96*, 6179–6181. (c) Boeckman, R. K., Jr.; Blum, D. M.; Arthur, S. D. *J. Am. Chem. Soc.* **1979**, *101*, 5060–5062. In these examples, good stereoselectivity with respect to a pre-existing stereocenter in the cyclohexanone is observed.
97. For a recent enantioselective application of this technology see: (a) Takahashi, T.; Okumoto, H.; Tsuji, J.; Harada, N. *J. Org. Chem.* **1984**, *49*, 948–950. (b) Takahashi, T.; Naito, Y.; Tsuji, J. *J. Am. Chem. Soc.* **1981**, *103*, 5261–5263.
98. Rosan, A.; Rosenblum, M. *J. Org. Chem.* **1975**, *40*, 3621–3622.
99. For a related approach where facial selectivity with respect to a stereocenter in a cyclohexanone is achieved in a Michael addition see: Piers, E.; Kezire, R. J. *Tetrahedron Lett.* **1968**, 583–586.

100. Scanio, C. J. V.; Starrett, R. M. *J. Am. Chem. Soc.* **1971**, *93*, 1539-1540.
101. Odom, H. C.; Pinder, A. R. *J. Chem. Soc., Perkin Trans I* **1972**, 2193-2197.
102. Odom and Pinder initially reported that nootkatone was the major product of this cyclization: Odom, H. C.; Pinder, A. R. *Chem. Commun.* **1969**, 26-27.
103. van der Gen, A.; van de Linde, L. M.; Witteveen, J. G.; Boelens, H. *Recl. Trav. Chim. Pays-Bas* **1971**, *90*, 1034-1044.
104. McMurry, J. E.; Musser, J. H.; Ahmad, M. S.; Blaszczak, L. C. *J. Org. Chem.* **1975**, *40*, 1829-1832.
105. Takagi, Y.; Nakahara, Y.; Matsui, M. *Tetrahedron* **1978**, *34*, 517-521.
106. van der Gen, A.; van der Linde, L. M.; Witteveen, J. G.; Boelens, H. *Recl. Trav. Chim. Pays-Bas* **1971**, *90*, 1045-1054.
107. (a) Jaouen, G.; Meyer, A. *Tetrahedron Lett.* **1976**, 3547-3550. (b) Meyer, A.; Hofer, O. *J. Am. Chem. Soc.* **1980**, *102*, 4410-4414.
108. Jaouen, G.; Meyer, A. *J. Am. Chem. Soc.* **1975**, *97*, 4667-4672.
109. Krafft, M. E.; Kennedy, R. M.; Holton, R. A. *Tetrahedron Lett.* **1986**, *27*, 2087-2090.
110. Holton, R. A.; Kennedy, R. M.; Kim, H.-B.; Krafft, M. E. *J. Am. Chem. Soc.* **1987**, *109*, 1597-1600.
111. Posner, G. H.; Switzer, C. *J. Am. Chem. Soc.* **1986**, *108*, 1239-1244.
112. Haner, R.; Laube, T.; Seebach, D. *Chimia* **1984**, *38*, 255-257.
113. Seebach, D.; Colvin, E. W.; Lehr, F.; Weller, T. *Chimia* **1979**, *33*, 1-18.
114. Seebach, D.; Kalinowski, H.-O.; Bastani, B.; Crass, G.; Daum, H.; Dörr, H.; DuPreez, N. P.; Ehrig, V.; Langer, W.; Nüssler, C.; Oei, H.-A.; Schmidt, M. *Helv. Chim. Acta* **1977**, *60*, 310-325.
115. Langer, W.; Seebach, D. *Helv. Chim. Acta* **1979**, *62*, 1710-1722.
116. Seebach, D. *Proceedings of the Robert A. Welch Foundation Conferences on Chemical Research*, Houston, Texas, Nov. 7-9, 1984, pp 93-145.
117. Ireland, R. E.; Mueller, R. H.; Willard, A. K. *J. Am. Chem. Soc.* **1976**, *98*, 2868-2877, and references therein.
118. For example see: Corey, E. J.; Gross, A. W. *Tetrahedron Lett.* **1984**, *25*, 495-498.
119. Yamaguchi, M.; Tsukamoto, M.; Hirao, I. *Chem. Lett.* **1984**, 375-376.
120. Yamaguchi, M.; Tsukamoto, M.; Hirao, I. *Tetrahedron Lett.* **1985**, *26*, 1723-1726.
121. (a) Inouye, Y.; Inamasu, S.; Ohno, M.; Sugita, T.; Walborsky, H. M. *J. Am. Chem. Soc.* **1961**, *83*, 2962-2963. (b) Inouye, Y.; Inamasu, S.; Horiike, M. *Chem. & Ind.* **1967**, 1293-1294. (c) Inouye, Y.; Inamasu, S.; Horiike, M.; Ohno, M. *Tetrahedron* **1968**, *24*, 2907-2920. (d) For a more recent cyclopropanation using a similar strategy see: Hakam, K.; Thielmann, M.; Thielmann, T.; Winterfeldt, E. *Tetrahedron* **1987**, *43*, 2035-2044.
122. For discussions of the solvent dependence on cis/trans selectivity and asymmetric induction in the Michael addition/cyclopropanations see: (a) McCoy, L. L. *J. Am. Chem. Soc.* **1958**, *80*, 6568-6572. (b) McCoy, L. L. *J. Am. Chem. Soc.* **1960**, *82*, 6416-6417. (c) McCoy, L. L. *J. Am. Chem. Soc.* **1962**, *84*, 2246-2249. (d) McCoy, L. L. *J. Org. Chem. Soc.* **1964**, *29*, 240-241.
123. Mulzer, J.; Chucholowski, A.; Lammer, O.; Jibril, I.; Huttner, G. *J. Chem. Soc., Chem. Commun.* **1983**, 869-71. The structures of the major products in this paper are shown with the incorrect relative configurations (compare the structures in the paper to the ORTEP drawing from the X-ray crystal structure, which shows the correct relative configurations). Mulzer, J. personal communication.

124. Corey, E. J.; Peterson, R. T. *Tetrahedron Lett.* **1985**, *26*, 5025-5028.
125. Ort, O. *Org. Synth.* **1987**, *65*, 203-214.
126. Corey, E. J.; Ensley, H. E. *J. Am. Chem. Soc.* **1975**, *97*, 6908-6909.
127. Herrmann, J. L.; Berger, M. H.; Schlessinger, R. H. *J. Am. Chem. Soc.* **1973**, *95*, 7923.
128. Posner, G. H.; Weitzberg, M.; Hamill, T. G.; Asirvatham, E.; Cun-heng, H.; Clardy, J. *Tetrahedron* **1986**, *42*, 2919-2929.
129. Heathcock, C. H.; Oare, D. A. *J. Org. Chem.* **1985**, *50*, 3022-3024.
130. Fataftah, Z. A.; Kopka, I. E.; Rathke, M. W. *J. Am. Chem. Soc.* **1980**, *102*, 3959-3960.
131. Seeman, J. I. *Chem. Rev.* **1983**, *83*, 83-134.
132. RajanBabu, T. V. *J. Org. Chem.* **1984**, *49*, 2083-2089.
133. Oppolzer, W.; Pitteloud, R.; Bernardinelli, G.; Baettig, K. *Tetrahedron Lett.* **1983**, *24*, 4975-4978.
134. A similar assignment for the stereochemistry of dienolates of allylic senecioates has been made on the basis of the subsequent Claisen rearrangements: (a) Frater, G. *Helv. Chim. Acta* **1975**, *58*, 442-447. (b) Wilson, S. R.; Myers, R. S. *J. Org. Chem.* **1975**, *40*, 3309-3311. There also has been a report that the deprotonation of methyl senecioate with LDA followed by trapping with trimethylsilyl chloride and heating results in a 1:1 mixture of E and Z ketene acetals as a result of equilibration: Casey, C. P.; Jones, H.; Tukada, H. *J. Org. Chem.* **1981**, *46*, 2089-2092.
135. Posner, G. H.; Asirvatham, E. *J. Org. Chem.* **1985**, *50*, 2589-2591.
136. For related work on (-)-methyl jasmonate see: Posner, G. H.; Asirvatham, E.; Ali, S. F. *J. Chem. Soc., Chem. Commun.* **1985**, 542-543.
137. Calderari, G.; Seebach, D. *Helv. Chim. Acta* **1985**, *68*, 1592-1604.
138. For some further examples of the diastereoselective addition of enolates to nitroolefins in which the sense of the selectivity was not defined see: (a) Seebach, D.; Calderari, G.; Knochel, P. *Tetrahedron* **1985**, *41*, 4861-4872. See also reference 113 (b) Fuji, K.; Node, M.; Nagasawa, H.; Naniwa, Y.; Terada, S. *J. Am. Chem. Soc.* **1986**, *108*, 3855-3856. In this example, a β -amino- α,β -unsaturated nitro olefin was used as the acceptor. The products obtained are those from an additional elimination reaction and the diastereocochemical preference for the Michael addition cannot be inferred.
139. (a) Roux-Schmitt, M.-C.; Seyden-Penne, J.; Baddeley, G. V.; Wenkert, E. *Tetrahedron Lett.* **1981**, *22*, 2171-2174. (b) Roux-Schmitt, M.-C.; Seuron, N.; Seyden-Penne, J. *Synthesis* **1983**, 494-497.
140. For a similar study of the addition of cyanohydrins to conformationally fixed cyclohex-enones see: Zervos, M.; Warski, L.; Seyden-Penne, J. *Tetrahedron* **1986**, *42*, 4963-4973.
141. Schlessinger, R. H.; Poss, M. A.; Richardson, S. *J. Am. Chem. Soc.* **1986**, *108*, 3112-3114.
142. Schlessinger, R. H.; Lin, P.; Poss, M.; Springer, J. *Heterocycles* **1987**, *25*, 315-320.
143. Adams, A. D.; Schlessinger, R. H.; Tata, J. R.; Venit, J. J. *J. Org. Chem.* **1986**, *51*, 3068-3079.
144. Tamari, Y.; Harada, T.; Yoshida, Z. *J. Am. Chem. Soc.* **1978**, *100*, 1923-1925 and references therein.
145. (a) Tamari, Y.; Harada, T.; Nishi, S.; Mizutani, M.; Hioki, T.; Yoshida, Z. *J. Am. Chem. Soc.* **1980**, *102*, 7806-7808. (b) Tamari, Y.; Furukawa, Y.; Mizutani, M.; Kitao, O.; Yoshida, Z. *J. Org. Chem.* **1983**, *48*, 3631-3639.
146. (a) Goasdoue, C.; Goasdoue, N.; Gaudemar, M.; Mladenova, M. *J. Organomet. Chem.*

- 1982, 226, 209-215. (b) For a related study of Lewis acid-promoted addition of silyl thioethene acetals to α,β -unsaturated ketones see: Goasdoue, C.; Goasdoue, N.; Gaudemar, M. *Tetrahedron Lett.* 1984, 25, 537-540.
147. Evans, D. A.; Takacs, J. M. *Tetrahedron Lett.* 1980, 21, 4233-4236.
148. Evans, D. A.; Takacs, J. M.; McGee, L. R.; Ennis, M. D.; Mathre, D. J.; Bartroli, J. *Pure Appl. Chem.* 1981, 53, 1109-1127.
149. Stefanovsky, Y. N.; Viteva, L. Z. *Monatsh. Chem.* 1981, 112, 125-128.
150. For additions performed with catalytic amounts of base see: (a) Stefanovsky, Y. N.; Viteva, L. Z. *Monatsh. Chem.* 1980, 111, 1287-1298. (b) Stefanovsky, Y. N.; Viteva, L. *Izv. Otd. Khim. Nauki, Bulg. Akad. Nauk.* 1971, 4, 159-164; *Chem. Abstr.* 1972, 76, 24872f. (c) Stefanovsky, Y. N.; Bozilova, A. G. *Monatsh. Chem.* 1968, 99, 798-803.
151. For a related study see: Stefanovsky, Y. N.; Gospodova, T. *Izv. Khim.* 1982, 14, 336-40; *Chem. Abstr.* 1982, 97, 215154s.
152. Stefanovsky, Y. N.; Viteva, L. *Izv. Otd. Khim. Nauki, Bulg. Akad. Nauk.* 1971, 4, 99-105; *Chem. Abstr.* 1971, 75, 88270v.
153. Viteva, L. Z.; Stefanovsky, Y. N. *Monatsh. Chem.* 1982, 113, 181-190.
154. Yamaguchi, M.; Hamada, M.; Kawasaki, S.; Minami, T. *Chem. Lett.* 1986, 1085-1088.
155. Yamaguchi, M.; Hamada, M.; Nakashima, H.; Minami, T. *Tetrahedron Lett.* 1987, 28, 1785-1786.
156. For a discussion of the use of metallated imines and hydrazones see: Hickmott, P. W. *Tetrahedron* 1982, 38, 3363-3446.
157. For a discussion of the stereochemical aspects of hydrazone and imine alkylations (both with alkyl halides and activated olefins) see: Bergbreiter, D. E.; Newcomb, M. In *Asymmetric Synthesis*; Morrison, J. D., Ed.; Academic: New York, Vol. 2, 1983, Chapter 9.
158. For a discussion of the deprotonation and electrophilic substitution of hydrazones (including SAMP and RAMP hydrazones), along with possibilities for the source of asymmetric induction seen in these reactions see: Davenport, K. G.; Eichenauer, H.; Enders, D.; Newcomb, M.; Bergbreiter, D. E. *J. Am. Chem. Soc.* 1979, 101, 5654-5659.
159. Stork, G.; Dowd, S. R. *J. Am. Chem. Soc.* 1963, 85, 2178-2180.
160. Wittig, G.; Frommeld, H. D.; Suchanek, P. *Angew. Chem. Int. Ed. Engl.* 1963, 2, 683-684; *Angew. Chem.* 1963, 75, 978-979.
161. Kieczykowski, G. R.; Pogonowski, C. S.; Richman, J. E.; Schlessinger, R. H. *J. Org. Chem.* 1977, 42, 175-176.
162. Knorr, R.; Low, P. *J. Am. Chem. Soc.* 1980, 102, 3241-3242.
163. Jung, M. E.; Shaw, T. J. *Tetrahedron Lett.* 1977, 3305-3308.
164. Enders, D.; Fey, P.; Kipphardt, H. *Org. Synth. Synth.* 1987, 65, 173-202.
165. Enders, D. in *Selectivity—A Goal for Synthetic Efficiency*; Bartmann, W.; Trost, B. M., Eds.; Verlag Chemie: Weinheim, 1984; pp 65-86.
166. Enders, D.; Redenbach, B. E. M. *Chem. Ber.* 1987, 120, 1223-1227.
167. Enders, D.; Papadopoulos, K. *Tetrahedron Lett.* 1983, 24, 4967-4970.
168. Enders, D.; Papadopoulos, K.; Redenbach, B. E. M. *Tetrahedron Lett.* 1986, 27, 3491-3494.
169. Enders, D.; Redenbach, B. E. M. *Tetrahedron* 1986, 42, 2235-2242.
170. Enders, D.; Demir, A. S.; Redenbach, B. E. M. *Chem. Ber.* 1987, 120, 1731-1735.
171. Schöllkopf, U.; Groth, U.; Deng, C. *Angew. Chem. Int. Ed. Engl.* 1981, 20, 798-799; *Angew. Chem.* 1981, 93, 793-795.

172. (a) Schöllkopf, U.; Kühnle, W.; Egert, E.; Dyrbusch, M. *Angew. Chem. Int. Ed. Engl.* **1987**, *26*, 480–482; *Angew. Chem.* **1987**, *99*, 480–482. (b) For a recent example of the addition of **90.2** to enoates see: Schöllkopf, U.; Schröder, J. *Liebigs Ann. Chem.* **1988**, 87–92.
173. (a) Yamamoto, K.; Iijima, M.; Ogimura, Y. *Tetrahedron Lett.* **1982**, *23*, 3711–3714. (b) Yamamoto, K.; Iijima, M.; Ogimura, Y.; Tsuji, J. *Tetrahedron Lett.* **1984**, *25*, 2813–2816. (c) Yamamoto, K.; Kanoh, M.; Yamamoto, N.; Tsuji, J. *Tetrahedron Lett.* **1987**, *28*, 6347–6350.
174. Saigo, K.; Ogawa, S.; Kikuchi, S.; Kasahara, A.; Nohira, H. *Bull. Chem. Soc. Jpn.* **1982**, *55*, 1568–1573.
175. (a) de Jeso, B.; Pommier, J.-C. *Tetrahedron Lett.* **1980**, *21*, 4511–4514. (b) Nebout, B.; de Jeso, B.; Pommier, J.-C. *J. Chem. Soc., Chem. Commun.* **1985**, 504–505.
176. (a) Mulzer, J.; Hartz, G.; Kuhl, U.; Bruntrup, G. *Tetrahedron Lett.* **1978**, 2949–2952. (b) We have also observed low levels of diastereoselection for the Michael additions: Oare, D. A.; Heathcock, C. H. unpublished results.
177. (a) Ziegler, F. E.; Tam, C. C. *Tetrahedron Lett.* **1979**, *20*, 4717–4720. (b) Ziegler, F. E.; Fang, J. *J. Org. Chem.* **1981**, *46*, 825–827. (c) Ziegler, F. E.; Fang, J.; Tam, C. C. *J. Am. Chem. Soc.* **1982**, *104*, 7174–7181.
178. Brown, C. A.; Yamichi, A. *J. Chem. Soc., Chem. Commun.* **1979**, 100.
179. Ziegler, F. E.; Chakraborty, U. R.; Wester, R. T. *Tetrahedron Lett.* **1982**, *23*, 3237–3240.
180. Evans, D. A.; Golob, A. M. *J. Am. Chem. Soc.* **1975**, *97*, 4765–4766.
181. Binns, M. R.; Haynes, R. K.; Katsifis, A. A. *Tetrahedron Lett.* **1985**, *26*, 1565–1568.
182. Binns, M. R.; Chai, O. L.; Haynes, R. K.; Katsifis, A. A.; Schober, P. A.; Vonwiller, S. C. *Tetrahedron Lett.* **1985**, *26*, 1569–1572.
183. For recent full papers on this subject see: (a) Binns, M. R.; Haynes, R. K.; Katsifis, A. G.; Schober, P. A.; Vonwiller, S. C. *J. Am. Chem. Soc.* **1988**, *110*, 5411–5423. (b) Haynes, R. K.; Katsifis, A. G.; Vonwiller, S. C.; Hambley, T. W. *J. Am. Chem. Soc.* **1988**, *110*, 5423–5433.
184. Hua, D. H.; Chan-Yu-King, R.; McKie, J. A.; Myer, L. *J. Am. Chem. Soc.* **1987**, *109*, 5026–5029.
185. Gompper, R.; Wagner, H.-U. *Angew. Chem. Int. Ed. Engl.* **1976**, *15*, 321–333; *Angew. Chem.* **1976**, *88*, 389–401.
186. (a) Vasil'eva, L. L.; Mel'nikova, V. I.; Pivnitskii, K. K. *J. Org. Chem., USSR (Engl. Transl.)* **1983**, *19*, 581–582; *Zh. Org. Khim.* **1983**, *19*, 661–662. (b) Vasil'eva, L. L.; Mel'nikova, V. I.; Gainullina, É. T.; Pivnitskii, K. K. *J. Org. Chem., USSR (Engl. Transl.)* **1983**, *19*, 835–843; *Zh. Org. Khim.* **1983**, *19*, 941–951 and references therein. (c) Vasil'eva, L. L.; Mel'nikova, V. I.; Pivnitskii, K. K. *Zh. Org. Khim.* **1984**, *20*, 690–704; *Chem. Abstr.* **1984**, *101*, 170928e.
187. (a) Kraus, G. A.; Frazier, K. *Synth. Commun.* **1978**, *8*, 483–486. (b) Nokami, J.; Ono, T.; Iwao, A.; Wakabayashi, S. *Bull. Chem. Soc. Jpn.* **1982**, *55*, 3043–3044 and references therein.
188. (a) Binns, M. R.; Haynes, R. K.; Houston, T. L.; Jackson, W. R. *Tetrahedron Lett.* **1980**, *21*, 573–576. (b) Binns, M. R.; Haynes, R. K.; Houston, T. L.; Jackson, W. R. *Aust. J. Chem.* **1981**, *34*, 2465–2467. (c) Binns, M. R.; Haynes, R. K. *J. Org. Chem.* **1981**, *46*, 3790–3795. (d) Hirama, M. *Tetrahedron Lett.* **1981**, *22*, 1905–1908 and references therein.
189. Bickart, P.; Carson, F. W.; Jacobus, J.; Miller, E. G.; Mislow, K. *J. Am. Chem. Soc.* **1968**, *90*, 4869–4876.

190. Goodridge, R. J.; Hambley, T. W.; Haynes, R. K.; Ridley, D. D. *J. Org. Chem.* **1988**, *53*, 2881-2889.
191. Binns, M. R.; Haynes, R. K.; Katsifis, A. A. *Tetrahedron Lett.* **1985**, *26*, 1569-1571.
192. Haynes, R. K.; Katsifis, A. G. *J. Chem. Soc., Chem. Commun.* **1987**, 340-342.
193. Hua, D. H.; Sinai-Zingde, G.; Venkataraman, S. *J. Am. Chem. Soc.* **1985**, *107*, 4088-4090.
194. Hua, D.; Venkataraman, S.; Coulter, M. J.; Sinai-Zingde, G. *J. Org. Chem.* **1987**, *52*, 719-728.
195. See also: Hua, D. H.; Venkataraman, R. A.; Ostrander, R. A.; Sinai, G.-Z.; McCann, P. J.; Coulter, M. J.; Xu, M. R. *J. Org. Chem.* **1988**, *53*, 507-515.
196. Vasil'eva, L. L.; Mel'nikova, V. I.; Pivinitskii, K. K. *J. Gen. Chem. USSR (Engl. Transl.)* **1983**, *52*, 2346-2347; *Zh. Obshch. Khim.* **1983**, *52*, 2651-2652.
197. Hua, D. H.; Venkataraman, S.; Chan-Yu-King, R.; Paukstelis, J. V. *J. Am. Chem. Soc.* **1988**, *110*, 4741-4748.
198. Hua, D. H.; Coulter, M. J.; Badejo, I. *Tetrahedron Lett.* **1987**, *28*, 5465-5468.
199. Nokami, J.; Ono, T.; Wakabayashi, S. *Tetrahedron Lett.* **1985**, *26*, 1985-1988.
200. Hua, D. H. *J. Am. Chem. Soc.* **1986**, *108*, 3835-3837.
201. Yamamoto, Y.; Nishii, S.; Maruyama, K. *J. Chem. Soc., Chem. Commun.* **1985**, 386-388.
202. Yamamoto, Y.; Nishi, S. *J. Org. Chem.* **1988**, *53*, 3597-3603.
203. For a discussion of Baldwin's rules for ring closure see: (a) Baldwin, J. E. *J. Chem. Soc., Chem. Commun.* **1976**, 734-736. (b) Baldwin, J. E. *J. Chem. Soc., Chem. Commun.* **1976**, 738-741. (c) Baldwin, J. E.; Thomas, R. C.; Kruse, L. L.; Silberman, L. *J. Org. Chem.* **1977**, *42*, 3846-3852.
204. For a discussion of Baldwin's rules with respect to "five-endo-trigonal" closures see: (a) Baldwin, J. E.; Cutting, J.; Dupont, W.; Kruse, L.; Silberman, L.; Thomas, R. C. *J. Chem. Soc., Chem. Commun.* **1976**, 736-738. (b) Anselme, J.-P. *Tetrahedron Lett.* **1977**, 3615-3618. (c) Fountain, K. R.; Gerhardt, G. *Tetrahedron Lett.* **1978**, 3985-3986.
205. For a discussion of Baldwin's rule's with respect to intramolecular reaction of enolates see: (a) Baldwin, J. E.; Kruse, L. I. *J. Chem. Soc., Chem. Commun.* **1977**, 233-235. (b) Baldwin, J. E.; Lusch, K. J. *Tetrahedron* **1982**, *38*, 2939-2947.
206. Stork, G.; Shiner, C. S.; Winkler, J. D. *J. Am. Chem. Soc.* **1982**, *104*, 310-312.
207. Stork, G.; Winkler, J. D.; Shiner, C. S. *J. Am. Chem. Soc.* **1982**, *104*, 3767-3768.
208. Stork, G.; Winkler, J. D.; Saccamano, N. A. *Tetrahedron Lett.* **1983**, *24*, 465-468.
209. Jackman, L. M.; Lange, B. C. *Tetrahedron* **1977**, *33*, 2737-2769, and references therein.
210. Hirai, Y.; Hagiwara, A.; Yamazaki, T. *Heterocycles* **1986**, *24*, 571-574.
211. Hirai, Y.; Hagiwara, A.; Terada, T.; Yamazaki, T. *Chem. Lett.* **1987**, 2417-2418.
212. (a) For a similar approach where the base-promoted cyclization products underwent further condensation see: Massiot, G.; Mulamba, T. *J. Chem. Soc., Chem. Commun.* **1984**, 715-716. (b) For recent applications of intramolecular Michael additions towards the synthesis of forskolin see: Koft, E. R.; Kotnis, A. S.; Broadbent, T. A. *Tetrahedron Lett.* **1987**, *28*, 2799-2800 and Li, T.; Wu, Y. *Tetrahedron Lett.* **1988**, *29*, 4039-4040.
213. Stork, G.; Saccamano, N. A. *Nouv. J. Chim.* **1986**, *10*, 677-679.
214. Oppolzer, W.; Chapuis, C.; Dao, G.; Reichlin, D.; Godel, T. *Tetrahedron Lett.* **1982**, *23*, 4781-4784.
215. Stork, G.; Saccamano, N. A. *Tetrahedron Lett.* **1987**, *28*, 2087-2090.

216. Berthiaume, G.; Lavallée, J.-F.; Deslongchamps, P. *Tetrahedron Lett.* **1986**, *27*, 5451–5454.
217. Lavallée, J.-F.; Berthiaume, G.; Deslongchamps, P. *Tetrahedron Lett.* **1986**, *27*, 5455–5458.
218. Lavallée, J.-F.; Deslongchamps, P. *Tetrahedron Lett.* **1987**, *28*, 3457–3458.
219. Isobe, M.; Iio, H.; Kawai, T.; Goto, T. *Tetrahedron Lett.* **1977**, *18*, 703–706.
220. (a) Stork, G.; Taber, D. F.; Marx, M. *Tetrahedron Lett.* **1978**, *19*, 2445–2448. (b) Stork, G.; Boeckmann, Jr., R. K.; Taber, D. F.; Still, W. C.; Singh, J. *J. Am. Chem. Soc.* **1979**, *101*, 7107–7109.
221. Johnson, W. S.; Shulman, S.; Williamson, K. L.; Pappo, R. *J. Org. Chem.* **1962**, *27*, 2015–2018.
222. Yamada, K.; Aratani, M.; Hayakawa, Y.; Nakamura, H.; Nagase, H.; Hirata, Y. *J. Org. Chem.* **1971**, *36*, 3653–3656.
223. Barton, D. H. R.; Campos-Neves, A. S.; Scott, A. *I. J. Chem. Soc.* **1957**, 2698–2706.
224. Harre, M.; Winterfeldt, E. *Chem. Ber.* **1982**, *115*, 1437–1447.
225. Kozikowski, A. P.; Greco, M. N.; Springer, J. P. *J. Am. Chem. Soc.* **1984**, *106*, 6873–6874.
226. Heathcock, C. H.; Smith, K. M.; Blumenkopf, T. A. *J. Am. Chem. Soc.* **1986**, *108*, 5022–5024.
227. Brattesani, D. N.; Heathcock, C. H. *J. Org. Chem.* **1975**, *40*, 2165–2170.
228. (a) Majetich, G.; Casares, A. M.; Chapman, D.; Behnke, M. *Tetrahedron Lett.* **1983**, *24*, 1909–1912. (b) Majetich, G.; Casares, A.; Chapman, D.; Behnke, M. *J. Org. Chem.* **1986**, *51*, 1745–1753.
229. For a recent review of this subject see: Schinzer, D. *Synthesis* **1988**, 263–273.
230. (a) Majetich, G.; Desmond, R.; Casares, A. M. *Tetrahedron Lett.* **1983**, *24*, 1913–1916. (b) Majetich, G.; Hull, K.; Defauw, J.; Desmond, R. *Tetrahedron Lett.* **1985**, *26*, 2747–2750. (c) Majetich, G.; Desmond, R. W.; Soria, J. *J. Org. Chem.* **1986**, *51*, 1753–1769.
231. Majetich, G.; Hull, K.; Defauw, J.; Shawe, T. *Tetrahedron Lett.* **1985**, *26*, 2755–2758.
232. Majetich, G.; Defauw, J.; Hull, K.; Shawe, T. *Tetrahedron Lett.* **1985**, *26*, 4711–4714.
233. Majetich, G.; Hull, K. *Tetrahedron Lett.* **1988**, *29*, 2773–2776.
234. Imanishi, T.; Yagi, N.; Hanaoka, M. *Chem. Pharm. Bull.* **1985**, *33*, 4202–4211.
235. Lee, R. A. *Tetrahedron Lett.* **1973**, 3333–3336.
236. Similar observations about the stepwise nature of the reaction have been made by Ban and coworkers: Ohnuma, T.; Oishi, T.; Ban, Y. *J. Chem. Soc., Chem. Commun.* **1973**, 301–302.
237. White, K. B.; Reusch, W. *Tetrahedron* **1978**, *34*, 2439–2443. For an application of this technology towards the synthesis of natural products see: Spitzner, D. *Tetrahedron Lett.* **1978**, 3349–3350.
238. For another example of isolation of mono-addition products see: Hagiwara, H.; Nakayama, K.; Uda, H. *Bull. Chem. Soc. Jpn.* **1975**, *48*, 3769–3770. Although the possibility of stereochemical differentiation occurs with the substrates studied in this reference, no mention of the stereochemical outcome was given.
239. Quesada, M. L.; Schlessinger, R. H.; Parsons, W. H. *J. Org. Chem.* **1978**, *43*, 3968–3970.
240. For some additional examples of formal tandem Michael additions where no stereochemical insight can be gained see: (a) Bellamy, A. *J. J. Chem. Soc. (B)* **1969**, 449–455. (b) Wiemann, J.; Bobic-Korejzl, L.; Allamamagny, Y. *C. R. Acad. Sc. Paris* **1969**, 2037–

2039. (c) Brown, H. L.; Buchanan, G. L.; Cameron, A. F.; Ferguson, G. *J. Chem. Soc., Chem. Commun.* **1987**, 399-400. (d) Elizarova, A. N. *J. Gen. Chem. USSR* **1964**, *34*, 3251-3256; *Zh. Obshch. Khim.* **1964**, *34*, 3205-3212.
241. For related studies see: (a) Hagiwara, H.; Uda, H.; Kodama, T. *J. Chem. Soc., Perkin Trans I* **1980**, 963-977. (b) Hagiwara, H.; Kodama, T.; Kosugi, H.; Uda, H. *J. Chem. Soc., Chem. Commun.* **1976**, 413.
242. (a) Spitzner, D. *Angew. Chem. Int. Ed. Engl.* **1982**, *21*, 636-637; *Angew. Chem.* **1982**, *94*, 639. For a closely related example where the subsequent alkylation strongly supports the initial generation of the endo product see: (b) Spitzner, D.; Engler, A.; Liese, T.; Splettstoerber, G.; de Meijere, A. *Angew. Chem. Suppl.* **1982**, 1722-1729. (c) Hagiwara, H.; Kodama, T.; Kosugi, H.; Uda, H. *J. Chem. Soc., Chem. Commun.* **1976**, 413.
243. (a) Spitzner, D.; Engler, A. *Org. Synth.* **1987**, *66*, 37-42. (b) For a similar cycloaddition to ethyl sorbate see: Nagaoka, H.; Kobayashi, K.; Matsui, T.; Yamada, Y. *Tetrahedron Lett.* **1987**, *28*, 2021-2024.
244. Gibbons, E. G. *J. Org. Chem.* **1980**, *45*, 1540-1541.
245. Hagiwara, H.; Uda, H. *J. Chem. Soc., Perkin Trans I* **1986**, 629-632.
246. Roberts, M. R.; Schlessinger, R. H. *J. Am. Chem. Soc.* **1981**, *103*, 724-725.
247. Weber, W.; Spitzner, D.; Kraus, W. *J. Chem. Soc., Chem. Commun.* **1980**, 1212-1213.
248. Nagaoka, H.; Kobayashi, K.; Okamura, T.; Yamada, Y. *Tetrahedron Lett.* **1987**, *28*, 6641-6644.
249. (a) Ihara, M.; Toyota, M.; Fukumoto, K.; Kametani, T. *Tetrahedron Lett.* **1984**, *25*, 2167-2170. (b) Ihara, M.; Toyota, M.; Abe, M.; Ishida, Y.; Fukumoto, K. *J. Chem. Soc., Perkin Trans. I* **1986**, 1543-1549. (c) Ihara, M.; Ishida, Y.; Abe, M.; Toyota, M.; Fukumoto, K.; Kametani, T. *J. Chem. Soc., Perkin Trans. I* **1988**, 1155-1163.
250. Ihara, M.; Toyota, M.; Fukumoto, K.; Kametani, T. *J. Chem. Soc., Perkin Trans. I* **1986**, 2151-2161.
251. For closely related application to the synthesis of atisiran-15-one see: Ihara, M.; Toyota, M.; Fukumoto, K.; Kametani, T. *Tetrahedron Lett.* **1985**, *26*, 1537-1540.
252. Ihara, M.; Suzuki, M.; Fukumoto, K.; Kametani, T.; Kabuto, C. *J. Am. Chem. Soc.* **1988**, *110*, 1963-1964.
253. Ihara, M.; Toyota, M.; Fukumoto, K.; Kametani, T. *Tetrahedron Lett.* **1984**, *25*, 3235-3238.
254. Thanupran, C.; Thebtaranonth, C.; Thebtaranonth, Y. *Tetrahedron Lett.* **1986**, *27*, 2295-2298.
255. Danishefsky, S.; Hatch, W. E.; Sax, M.; Abola, E.; Pletcher, J. *J. Am. Chem. Soc.* **1973**, *95*, 2410-2411.
256. (a) Stork, G.; Tomasz, M. *J. Am. Chem. Soc.* **1962**, *64*, 310-312. (b) Stork, G.; Tomasz, M. *J. Am. Chem. Soc.* **1964**, *86*, 471-478.
257. Mulholland, T. P. C.; Honeywood, R. I. W.; Preston, H. D.; Rosevear, D. T. *J. Chem. Soc.* **1965**, 4939-4953.
258. Magnus, P. *Nouv. J. Chim.* **1978**, *2*, 555-557.
259. Irie, H.; Katakaka, J.; Mizuno, Y.; Ueda, S.; Taga, T.; Osaki, K. *J. Chem. Soc., Chem. Commun.* **1978**, 717-718.
260. Chamberlin, A. R.; Reich, S. H. *J. Am. Chem. Soc.* **1985**, *107*, 1440-1441.
261. Sevin, A.; Tortajada, J.; Pfau, M. *J. Org. Chem.* **1986**, *51*, 2671-2675.
262. For a discussion of open-extended versus closed chelated transition states for the addition

- of phenyllithium to α,β -unsaturated ketones see: Ignatova-Avramova, E. P.; Pojarlieff, I. G. *J. Chem. Soc., Perkin Trans. 2* **1986**, 69-73.
263. Seebach, D.; Golinski, J. *Helv. Chim. Acta* **1981**, *64*, 1413-1423.
264. (a) Bürgi, H. B.; Dunitz, J. D.; Shefter, E. *J. Am. Chem. Soc.* **1973**, *95*, 5065-5067.
(b) Bürgi, H. B.; Lehn, J. M.; Wipff, G. *J. Am. Chem. Soc.* **1974**, *96*, 1956-1957. (c) Bürgi, H. B.; Dunitz, J. D.; Lehn, J. M.; Wipff, G. *Tetrahedron* **1974**, *30*, 1563-1572. (d) Bürgi, H. B.; Dunitz, J. D. *Acc. Chem. Res.* **1983**, *16*, 153-161.
265. Bauer, W.; Laube, T.; Seebach, D. *Chem. Ber.* **1985**, *118*(2), 764.
266. Heathcock, C. H.; White, C. T.; Morrison, J. J.; VanDerveer, D. *J. Org. Chem.* **1981**, *46*, 1296-1309.
267. Evans, D. A.; Nelson, J. V.; Taber, T. R. *Topics in Stereochemistry*; Allinger, N. L.; Eliel, E. L.; Wilen, S. H. Eds.; Wiley: New York, 1982; Vol. 13, Chapter 1.

SUBJECT INDEX

- Acceptor conformation, 386
Acceptor geometry-adduct stereochemical correlation, 282, 292, 355
Acetoacetate decarboxylase, 196
stereospecificity, 133, 158
Acetophenone, chemical shift tensors in, 39
 (\pm) -Acetoxy cyclopentanes, 105
 (\pm) -1-Acetoxy-2,3-dichloropropane, 94
 (\pm) - $(4R^*,5S)$ -4-Acetoxy-4-methyl-5-allyl-2-cyclopenten-1-one, 109
 (\pm) -5-Acetoxymethyl-3-*tert*-butyl-oxazolidin-2-one, 96
 (\pm) - $(4R^*,5S^*)$ -4-Acetoxy-4-methyl-5-substituted-2-cyclopenten-1-one, 109
 (S) -2-Acetoxy-3- α -naphthoxypropionitrile, 96
 (\pm) -3-Acetoxy-4-oxo- β -ionone, 104
 (\pm) -*O*-Acetylallethrolone, 107
 (\pm) -Acetylenic acetates, 112, 113
Acholeplasma, 177
Aconitase, 189
cis-Aconitate decarboxylase, 189
Active site, global chirality, 142
Acyclic α,β -unsaturated alcohols, resolution, 110
Acyclic alcohols, resolution, 94
 (\pm) -2-Acyloxy-3-chloropropyl *p*-toluenesulfonate, 94
Adaptive traits, 127, 129
1,2-Addition, 232, 319, 369
1,6-Addition, 386
Addition-elimination reactions, stereospecificity of enzymatic, 188
S-Adenosylmethionine decarboxylase, 140
Adenylosuccinase, 189
Adrenosterone, 363
 (\pm) -Adrenosterone, 358
Alcaligenes sp. lipase, 107
Aldehyde dehydrogenase, 178
iron-dependent, 184
site directed mutagenesis, 182
Aldehyde dehydrogenases, stereospecificity, 184
Aldehyde reductases, 172
Alkaline phosphatase, 130
p-Alkoxybenzoic acids, 27
Alkylcyclohexyl acetates, 102
Alkyl diazoacetates, 214
 (\pm) -Allenic esters, 115
Allethrin, 106
Allethrolone, 106
 $(+)$ -*(S)*-Allethrolone, 107
Allylic sulfoxides, isomeric stability, 341
(S)-2-Allyl-3-methyl-4-hydroxycyclopenten-1-one, 109
Allyl sulfoxide anions, regiochemistry of the addition of, 340
Amidases, 86
Amide dienolates, generation, 315
stereochemistry, 316
Amides, stereochemistry of deprotonation, 309
Amino acid decarboxylases, 137
Amino acid dehydrogenases, 186
Amino acids by enantioselective hydrogenation, 212
Amino acid transaminases, 147
DL- α -Amino- ϵ -caprolactam, 91
 α -Amino- ϵ -caprolactamase, *L*-specific, 91
5-Aminolevulinate synthase, stereospecificity, 157
DL-2-Aminothiazoline-4-carboxylic acid, 92
Anion-accelerated Cope rearrangement, 337, 338, 369
Aphidicolin, 280
Archaeabacteria, 168, 179, 180
Arginine decarboxylase, 140
Arginosuccinase, 189
Aromatic shift tensors in β -quinol (1,4-hydroxybenzene), 36
 (\pm) -Aromatin, 336
Arthrobacter lipase, 107
Aspartame, synthesis, 213
Aspartate ammonia lyase, 189
Aspartate β -decarboxylase, stereospecificity, 160

- Aspartate- β -semialdehyde dehydrogenase, 178
Aspergillus niger lipase, 99
 Asymmetric Michael additions, catalytic, 242, 245
 Asymmetric synthesis, *see* Enantioselective synthesis
 Asymmetric transformations, second-order, 90
 L-ATC hydrolase, 92
 ATC racemase, 92
 ATC, *see* DL-2-Aminothiazoline-4-carboxylic acid
 (\pm)-Atisine, 381, 382
 (+)-Atisirene, 381
 Atomic orbitals, gauge invariant, 9
 ATPases, 148
 ATPases, stereospecificity, 54
 historical models, 155
 (\pm)-Avenaciolide, 293
 Axial attack, 261
 Baldwin rules, 356
 Bimolecular reaction, substrate types, 239
 (*S*)-BINAP, 218
 Biocatalytic resolution:
 irreversible case, 64
 reversible case, 72
 Borneol, 363
 Bromomagnesium enolates, 271
 Bürgi-Dunitz trajectory, 390
 1,3-Butadiene, ^{13}C shielding components in, 53
n-Butane, ^{13}C shielding components in, 53
cis- and *trans*-Butene powder spectra, 30
 tert-Butyl hydroperoxide, 216
 ^{13}C -5-Bacteriorhodopsin (bR) in membranes, shielding tensors in, 48
 ^{13}C Shielding components, in 1,3-butadiene and *n*-butane, 53
 ^{13}C Shielding tensors, in polysubstituted methoxybenzenes, 40
Candida cylindracea lipase, 89, 104, 116, 118, 119
 Canonical molecular orbitals (MOs), 9
 Captopril, 80
 N-Carbamoyl-L-amino acids, 91
 Carbanion stability, 190
 Carbocation stability, 190
 Carbonyl principal shift values in glycine, 45
 Carbonyl reductase, 172
 (\pm)-Carboxylic acids, resolution, 112
 Carboxylic carbon shielding tensors, 37
cis-cis-Carboxymuconate, 190
 Carboxymuconic acid cyclase, stereospecificity, 189
 β -Carboxymuconolactone, 190
 γ -Carboxymuconolactone, 190
 (\pm)-*cis*-Carveol, 106
 Catalytic binding domain, in dehydrogenases, 168
 Chair-like transition states, 372
 Chelated transition states, 359, 375, 387
 Chelation, 364
 Chemical process, 210
 economic factors, 210
 Chemical shielding, quantum mechanical formulation, 5,
 calculation by *ab initio* methods, 8
 Chemical shielding tensor, *see also* Shielding tensor
 crystal packing effects, 49
 diamagnetic and paramagnetic bond contributions, 49
 diamagnetic term, 6
 paramagnetic contribution to, 6
 Chemical shift tensors in acetophenone, 39
 Chiral, non-racemic crown ethers, 247, 248
 Chiral, non-racemic sulfoxide complexants, 249
 Chiral compounds, non-racemic, synthesis, 210
 Chirally-ligated copper catalysts, 214
 Chiral phosphines, 212
 Chloral, 220
 3-Chloro-2-methyl-1-propanol, 97
 (\pm)-3-Chloro-2-methylpropyl propionate, 97
 (+)-(R)-2-(*p*-Chlorophenoxy)propionic acid, 89
 (\pm)-2-(*p*-Chlorophenoxy)propionic acid, 87
 Chorismate mutase, 131
 newly evolved, 168
 Chrysanthemic acid, 113
 Chymotrypsin, 78
 stereospecificity, 133
 Cilastatin, 215
 Cinchona alkaloids, 242, 245
 Cinnamyl alcohol dehydrogenase, 164
 (*R*)- and (*S*)-Citramalic acid, synthesis, 220
 (*R*)-Citronellal, 219
 Claisen condensation, 233, 287
 stereospecificity of enzymatic, 193

- Claisen rearrangement, 284, 306
 Compactin, 80
 (\pm)-Confertin, 336
 Consecutive kinetic resolution system, 84
 Conservation of stereospecificity in dehydrogenases, 166
 Conserved trait, 128
 Convergent evolution, 128, 179, 181
 Conversion, 70
 Cope rearrangement, anion accelerated, 337, 343, 389
 Corey lactone, synthesis, 220
 Counterion and regiochemistry of nucleophilic attack, 235
 CP, *see* Cross polarization (CP) experiments
 $\text{Cr}(\text{CO})_3$ -Methylindanone complexes, 279
 $\text{Cr}(\text{CO})_3$ -Methyltetralone complexes, 279
 Cross polarization (CP) experiments, 13
 Cryptic stereospecificity, 128, 129
 Crystal packing effects, on chemical shielding tensors, 49
 Crystal packing forces, 27
 Curtin-Hammett principle, 296
 Cyanohydrins, 96
 α -Cyano-3-phenoxybenzyl alcohol, 107, 110
 Cyclic alcohols, resolution, 102
 Cyclic allylic alcohols, resolution, 105
 (\pm)-*trans*-Cycloalkane-1,2-diol diacetate, 84
 $(S)(+)$ -2,5-Cycloheptadienecarboxylic acid, 116
 Cyclohexanols, α -substituted, 118
 (\pm)-2-Cyclohexenol, 105
 (\pm)-*trans*-4-Cyclopentene-1,3-diol diacetate, 84
 α -Cyclopiazonic acid, 366
 Cypermethrin, 111
L-Cysteine, 92
 Cytidine diphosphate dideoxyhexose synthetase, 196
- Decarboxylase stereospecificity:
 functional model for, 157
 historical models for, 145
 Decoupling, high power, 12
 Dehydrogenases, 162
 Dehydrogenase stereospecificity:
 functional models for, 172
 historical models for, 166
 (+)-Dehydroiridiodiol, 319
 Dehydroquinate dehydratase, 189
 Dehydroquinate synthase, 189
- Deletion-replacement, in protein evolution, 168
 (\pm)-11-Deoxyprostaglandin E₁, 345
 Descending staircase internal thermodynamics, 186
 2,2'-Diacetoxy-1,1'-binaphthyl, 83
 1,2-Diacetoxyp propane derivatives, 3-substituted, 94
 Dialkylzinc, 224
 Diamagnetic and paramagnetic bond contributions, 10
 Diamagnetic term, *see* Chemical shielding tensor
 Diaminopimelate decarboxylase, 140, 142, 146
 Diastereofacial selectivity, 239
 Diastereomeric transition states, 87, 198
 Diastereoselectivity, pseudo-simple, 391
 Dienolate stereochemistry, 299
 Diethylgeranylamine, 218
 (S,S) -Diethyl tartrate, 216
 Digonal centers or "dig", 357
 Dihydrofolate reductases, 178, 179, 181
 stereospecificity, 133
 Dihydropyrimidinase, 91
 1,4-Dihydroxybenzene, *see* β -Quinol
 7,20-Diisocyanoacociane, 291
 synthesis, 230
 Diisopinocampheylborane, 220
 1,4-Dimethoxybenzene, 40
 $(-)(1R,2R,4R)$ -2,4-Dimethyl-1-cyclohexanol, 104
 (\pm) -*t*-2,*t*-4-Dimethyl-*r*-1-cyclohexanol, 103
 3,6-Dimethyloctanol, synthesis, 220
 Dinucleotide binding domains, 178
 in dehydrogenases, 168
 DIPAMP, 212
 Dipolar dephasing experiment, 13
 Dipolar spectroscopy, 24
 two-dimensional technique, 24
 $(7R, 8S)$ -Disparlure, synthesis, 216
 Disrotatory cyclization, 277
 Divergent evolution of stereospecificity, 132
 Domain shuffling, 167
L-DOPA, synthesis, 212
 Double asymmetric synthesis, 241
 Double stereodifferentiation, 242
- Ectocarpene, 116
 Effect of the peptide secondary structure on the principal shift values, 45

- 6 π -Electron closure, 384
 Electronic effects on shielding components, 41
 Electronic Hamiltonian, 5
 (\pm)-Emetine, 359
 Enantiomer excess:
 of product fraction, 70
 of remaining substrate, 70
 Enantiomer ratio (E value), 65, 70, 76
 Enantioselective 2 + 2 cycloaddition reactions, 220
 Enantioselective cyclopropanation, 214
 Enantioselective epoxidation:
 of allylic alcohols, 216
 catalytic, 216
 Enantioselective hydroboration, 220
 Enantioselective hydrogenation:
 amino acids by, 212
 phenylalanine by, 213
 Enantioselective olefin isomerization, 218
 Enantioselective synthesis, economic factors, 210
 large scale, criteria for, 211
 ligand-accelerated, 223
 Enantioselectivity, 65, 94
 strategies for improving, 75
 Endo-dig, 357, 364
 Endo-trig, 357
 5-Endo-trig, 363
 Enolase, 189
 Enolate, preformed, 232
 Enolate-accelerated Cope rearrangement, 371
 Enolate-adduct stereochemical correlation, 272, 283, 287, 294, 338, 355
 Enolate equilibration, 296
 Enolate formed in Michael addition, stereochemistry, 386
 Enolate trapping, 344
 Enone, conformation, 359
 Enoyl-CoA hydratase, 189
 Enoyl-CoA reductase, 178
 stereochemical diversity, 193
 Enzymatic behavior:
 functional models, 134
 historical models, 134
 Enzymatic enantio-convergent transformation, 93
 Enzymatic hydrolysis, of racemic axially-disymmetric diacetates, 82
 Enzymatic stereospecificity, correlations in, 164
 Enzyme-phosphoryl intermediates, 154, 155
 Epichlorohydrin, 94
 (\pm)-7-Epinootkatone, 277
 Epoxidation of (Z)-2-tridecen-1-ol, 216
 (+)-12,13-Epoxytrichothec-9-ene, 353
 Equatorial attack, 261
 Equilibrium constant, 72, 86
 Erythronolide A, 99
 Esterification, 72, 87
 (+)-Estradiol methyl ether, 281
 Ethanol dehydrogenases, 143, 167, 170, 175, 177, 178, 198
 Ethyl (S)-2,2-dimethylcyclopropane-carboxylate, synthesis, 215
 7,7-(Ethylenedioxy)-bicyclo[3.3.0]octane-3-one, 85
 1-Ethynyl-2-methyl-2-penten-1-ol, 107, 112
 Eubacteria, 168, 179, 180
 Eukaryotes, 168, 179, 180
 Evolution, 129
 Evolutionary conservation, 132
 Evolutionary "cost", 152
 Evolutionary optimality, kinetic criteria, 143
 Exo-dig, 357
 7-Exo-tet closure, 288
 Exo-trig, 356
 E/Z nomenclature, 236
 E/Z nomenclature for enethiolates, 268
 Fast reacting enantiomer, 75
 Fatty acid synthetase, 189
 stereospecificity, 193
 (\pm)-Fawcettimine, 367
 Fenvalerate, 110
 Fitting techniques, 21
 Flavin-dependent dehydrogenases, stereo specificity, 184
 Flurbiprofen, 116
 L-Fucose dehydrogenase, 179, 184
 Fumarase, 131, 189
 Functional models, 128
 criteria for tests, 175
 for decarboxylase stereospecificity, 157
 for dehydrogenase stereospecificity, 172
 for enzymatic behavior, 134
 formalism, 177
 for phosphotransferase stereospecificity, 153

- Functional trait, 128
 2-Furylcarbinols, 108

 β -Galactosidase, newly evolved, 168
 Gauge, selection, 7
 Gauge invariant atomic orbitals (GIAO), formulation, 9
 Gauge method, individual, for localized orbitals (IGLO), 9
 GIAO, *see* Gauge invariant atomic orbitals (GIAO)
 Global chirality of an active state, 142
 Glucose dehydrogenase, 170, 177, 178, 181
 D-Glucose dehydrogenase, 179, 184
 Glucose-6-phosphatase, stereospecificity, 154
 Glucose-6-phosphate dehydrogenase, 177
 Glutamate decarboxylase, 138
 Glutamate dehydrogenase, 175
 Glutathione reductase, 173, 177
 Glyceraldehyde-3-phosphate dehydrogenases, 167, 175, 178
 (*R*)- and (*S*)-Glycidol, synthesis, 216
 Glycidol esters, 78
 (*R*)-Glycidyl butyrate, synthesis, 218
 Glycine, carbonyl principal shift values in, 45
 (\pm)-Griseofulvin, 383

 Hajos ketone, 379
 Hemiacetal dehydrogenases, 183
 High power decoupling, 12
 (+)-Hirsutene, 344
 Histidine ammonia lyase, 189
 Histidine decarboxylases, 138
 Historical models, 128
 - for ATPase stereospecificity, 155
 - for decarboxylase stereospecificity, 145
 - for dehydrogenase stereospecificity, 166, 170, 177
 - for enzymatic behavior, 134
 HMG-CoA, *see* Hydroxymethylglutaryl-CoA
 Homologous enzymes, 131, 145
 Homology, 128
 Hydantoins, 5-substituted, 90
 Hydrazones, cleavage, 326
 - stereochemistry of the deprotonation, 323*trans*-Hydrindandione, 334
cis- and *trans*-Hydrindenones, 357
 (\pm)-*trans*-1-Hydroxy-2-acetoxyhexane, 105
 3-Hydroxybutyrate dehydrogenases, 168, 169

 3-Hydroxybutyryl CoA dehydrogenases, 173
 (*S*)-2-Hydroxy-3-chloropropyl *p*-toluenesulfonate, 94
 Hydroxycitronellal, synthesis, 220
 4-Hydroxycyclopentenones, 2-substituted, 108
 β -Hydroxydecanoylthioester dehydratase, 189
 3-Hydroxy-3-methylalkanoic acid esters, 78
 (*S*)-5-Hydroxymethyl-3-alkyloxazolin-2-one, 96
 Hydroxymethylglutaryl-CoA (HMG-CoA), 177
 3-Hydroxy-3-methylglutaryl coenzyme A (HMG-CoA) reductases, 179, 180
 - inhibitor, 80
 4-Hydroxy-3-methyl-2-propargyl-2-cyclopentenone, 107
 3-Hydroxy-4-oxo- β -ionone, 104
 3-Hydroxysteroid dehydrogenase, 174
 20-Hydroxysteroid dehydrogenase, 174
 21-Hydroxysteroid dehydrogenase, 174

 Ibuprofen, 116
 IGLO, *see* Individual gauge for localized orbitals (IGLO), method
 (\pm)-Illudin S diacetate, 253
 Imines, stereochemistry of the deprotonation, 323
 Imipenem, 214
 Individual gauge for localized orbitals (IGLO), method, 9
 Intermolecular force equation, 82
 Intramolecular proton transfer, 268
 Intramolecular sequential Michael addition, 381
 Ionic radius of the counterion, 390
 Ireland hypothesis, 325
 Isocitrate dehydrogenase, 175
 ($-$)-Isodehydroiridiodiol, 319
cis-trans Isomerization in retinal derivatives, 47
 (\pm)-Isonootkatone, 250
 ($-$)-Isopulegol, 103
 (\pm)-Isopulegyl acetate, 103

 Ketene, 220
 β -Ketoacid decarboxylases, 139, 156
 Ketone enolates, generation, from enol silanes, 270
 Ketoprofen, 116

- Ketoprostaglandin reductase, 172
 (-)-Ketorolac, 93
 (-)-Khusimone, 297
 Kinetic control, 64
 Kinetic isotope effect, 67
 Kinetic parameter, 73
 Kinetic resolution, 241, 350
 lipase catalyzed, 100
 Kinetic resolution system, consecutive, 84
- Lactaldehyde reductase, 176
 Lactate dehydrogenases, 173, 178, 181
 stereospecificity, 165
 D-Lactate dehydrogenases, 179
 L-Lactate dehydrogenases, 179, 180
 Lewis acid conditions, 372
 Lipase AL (*A. chromobacter sp.*), 97
 Lipase-catalyzed esterification, 87
 Lipase-catalyzed kinetic resolution, 100
 Lipase PL 266 (*Alcaligenes sp.*), 97
 Lipases, 86, 96
 Lipid-water interface, 89
 Lipoprotein lipase (LPL), 94, 97
 of *P. aeruginosa*, 97
 Liquid crystals, use, to measure shift tensors, 26
 Liver alcohol dehydrogenase, 170, 175
 Localized orbital/local origin (LORG),
 method, 9
 Localized orbitals, 10
 Locally enantiomeric transition states, 141,
 198
 LORG, see Localized orbital/local origin
 (LORG), method
 LPL, see Lipoprotein lipase
 L-Lysine, synthesis, 91
 Lysine decarboxylase, 140, 146
- MAD, see Methylaluminum bis(2,6-di-*tert*-butyl-4-methylphenoxide) (MAD)
 Magic angle spinning (MAS), 13
 Magnesium bis-enolates, 271
 Malate dehydrogenases (MDH), 167, 168,
 173, 179, 180, 181
 stereospecificity, 165
 Malease, 189
 (*R*)- and (*S*)-Malic acid, synthesis, 220
 D-Mannitol, 94
 MAS, see Magic angle spinning (MAS)
 MAT, see Methylaluminum bis(2,4,6-tri-*tert*-butylphenoxide) (MAT)
- MDH, *see* Malate dehydrogenases (MDH)
 Menthol, 292
 (-)-Menthol, 103
 (\pm)-Menthol, 119
 L-Menthol, synthesis, 218
 Menthyl laurate, 89
 Menthyl propionate, 291
 (\pm)-Menthyl succinate, 103
 1-[*(2S)*-3-Mercapto-2-methylpropionyl]-L-proline, *see* Captopril
 Metal-dependent alcohol dehydrogenases,
 177, 181
 Metal ions:
 in dehydrogenases, 184
 in enzymatic reactions, 172
 Metals in enzymatic reactions, 143
 Methoxybenzenes, methyl shifts in, 41
 Methoxycitronellal, synthesis, 220
 Methylaluminum bis(2,4,6-tri-*tert*-butylphenoxide) (MAT), 235
 Methylaluminum bis(2,6-di-*tert*-butyl-4-methylphenoxide) (MAD), 235
 (\pm)-Methyl (*RS*)-3-arylothio-2-methyl-propionate, 80
 α -Methyarylacetic acids, 116
 Methylglutaconyl-CoA hydratase, 189
 (*R*)- and (*S*)-Methylglycidol, synthesis, 216
 Methyl (+)-(1*R*,2*R*,3*S*,5*S*)-3-hydroxy-7,7-(ethylenedioxy)bicyclo[3.3.0]octane-2-carboxylate, 85
 (-)-Methyl jasmonate, 299
 Methylmalonyl CoA mutase, 196
 (\pm)-Methyl 2-methyl-3-acetoxypropionate derivatives, *syn* and *anti*, 99
 Methyl (2*RS*)-3-oxo-7,7-(ethylenedioxy)bicyclo[3.3.0]octane-2-carboxylate, 85
 (\pm)-Methyl phenyllactate derivatives, 78
 Methyl shifts in methoxybenzenes, 41
 Mevaldate reductase, 172
 Mevinolin, 80
 Michael addition:
 Baldwin rules in, 356, 368
 catalytic and enantioselective, 242, 245
 competing 1,2-addition in, 229, 232
 development, 229
 driving force, 232
 equatorial addition, 262
 kinetic enrichment, 256
 Lewis acid assisted, 232, 235
 Lewis acid catalysis, 258, 368

- menthol ester, 230
nomenclature, 236
 8-phenylmenthol ester, 230
 polymerization, 229, 232, 275, 287
 proton transfer, 232
 stereochemistry of enolate formed, 386
 stereoelectronic considerations, 262,
 263, 356
 use of catalytic amounts of base, 229, 232,
 242
- Michael addition-alkylation, 288, 289, 297,
 302, 304, 336, 364
- Michael addition-Dieckmann condensation,
 319
- Michaelis-Menten kinetics, 65, 86
- Michael-Michael-Dieckmann condensation,
 383
- Microbial lipases, 86, 95, 97, 111
- Mislow rearrangement, 341
- Molecular conformations in the solid state,
 freezing, 26
- Molecular sieves, 216
- cis-cis*-Muconate cycloisomerase, 189
- Muconolactone, 190
- Mucor miehei* lipase, 80, 120
- Mutual kinetic enantioselection, 241, 254,
 347, 348, 351, 380
- N** and **N***, *see* Nonprostereogenic centers
- N**, **N**, substrate type in bimolecular reactions,
 239
- N***, **N**, substrate type in bimolecular
 reactions, 239
- N**, **N***, substrate type in bimolecular
 reactions, 239
- N***, **N***, substrate type in bimolecular
 reactions, 241
- N**, **P**, substrate type in bimolecular reactions,
 239
- N***, **P**, substrate type in bimolecular
 reactions, 239, 283, 301, 323, 329, 332,
 339, 342, 344
- N**, **P***, substrate type in bimolecular
 reactions, 239, 259-261, 262, 270, 285,
 293, 299
- N***, **P***, substrate type in bimolecular
 reactions, 241, 347
- Naphthalene, packing effects on the shielding
 tensors, 43
- Naproxen, 116
- Neomenthol, 292
- Neomenthyl propionate, 291
- Neutral drift, 128, 130
- Nitrate reductase, 164
- Nitrite reductase, 164
- Nonprostereogenic centers (**N** and **N***), 239
- (*-*)-Nootkatone, 279
- (*+*)-Nootkatone, 277
- (\pm)-Nootkatone, 250, 277
- (*-*)-endo-Norbornenyl acetate, 104
- (*+*)-endo-Norneo, 104
- Nucleophilic attack, counterion and
 regiochemistry of, 235
- Nucleoside phosphotransferase, 150
- OAD, *see* Oxaloacetate decarboxylase
- (\pm)-2-Octanol, 120
- Oleic acid dehydratase, 189
- Open transition state, 387
- Orcinol hydroxylase, stereospecificity, 133
- Orientation of the PAS in the sample
 frame, 15
- Ornithine decarboxylase, 140
- Ortho effects on shielding components, 41
- Oxaloacetate decarboxylase, 161
- DL-2-Oxazolidine-4-carboxylic acid, 92
- Oxazolidinone nucleus, 97
- P**, **N**, substrate type in bimolecular reactions,
 239
- P***, **N**, substrate type in bimolecular
 reactions, 239, 242, 251, 254, 258, 262,
 279, 289, 334
- P**, **N***, substrate type in bimolecular
 reactions, 239
- P***, **N***, substrate type in bimolecular
 reactions, 241
- P** and **P***, *see* Prostereogenic centers
- P**, **P**, substrate type in bimolecular reactions,
 239, 250, 251, 266, 271, 275, 280, 282,
 287, 294, 297, 300, 302, 307, 309, 319,
 336, 338, 354
- P***, **P**, substrate type in bimolecular
 reactions, 239, 251, 255, 264, 266, 277,
 291, 297, 301, 319, 331, 342, 345, 353
- P**, **P***, substrate type in bimolecular
 reactions, 239, 270, 280, 283, 293, 299
- P***, **P***, substrate type in bimolecular
 reactions, 241, 253
- Packing effects on the shielding tensors of
 naphthalene, 52
- Pancreatin, 97

- Paramagnetic contribution, *see* Chemical shielding tensor
 Partition coefficient, 117
 PAS, *see* Principal Axis System (PAS)
 (+)-Pentalene, 350
 (\pm)-Pentalenolactone *E* methyl ester, 348
 Phenoxybenzaldehyde, 111
 Phenylalanine ammonia lyase, 189
 8-Phenylmenthol, 292, 363
 8-Phenylmenthol ester, 230
 8-Phenylmenthyl propionate, 291
 Pheromone synthesis, 216
 Phosphodiesterases, stereospecificity, 154
 Phosphoryl-enzyme intermediate, 148
 Phosphoryl transferases, 148
 Phosphotransferases, stereospecificity, 148
 functional model, 153
 Physiological substrates, of dehydrogenases, 174, 177
 Pig liver esterase (PLE), 78, 84, 105, 115
 PLE, *see* Pig liver esterase
 PNPNP, 213
 Polymer attached alkaloid, 245
 Polysubstituted methoxybenzenes, ^{13}C
 shielding tensors in, 40
 Porcine pancreas lipase (PPL), 78, 99, 119
 Powder pattern, break points, 21
 Powder spectra, 18
 break points in, 21
 of *cis*- and *trans*-butenes, 30
 two dimensional experiments, 22
 PPL, *see* Porcine pancreas lipase (PPL)
 Prediction of enantioselectivity, 82
 Principal axes for the $^{13}\text{CH}_2$ shift tensors, 32
 Principal Axis System (PAS), 15
 (*S*)-(-)-Propranolol, 96
 Prostaglandin analogues, 348
 Prostaglandin intermediates, synthesis, 220
 Prostereogenic centers (**P** and **P***), 239
 Proteases, 86
 Protein sequence comparison, 131
 Protocatechuate synthase, 189
Pseudomonas fluorescens lipase, 105
Pseudomonas sp. lipase, 107
 Pseudo-simple diastereoselectivity, 239, 391
 Pyrethrin-I, 106
 Pyrethroid alcohol, 107
 Pyrethroid insecticides, 215
 Pyridoxal phosphate, 138, 197
 Pyromellitic acid dihydrate (PMDH), 37
 5-Pyrophosphomevalonate decarboxylase, 189
 Pyruvyl residue, 138
 Quinidine, 220
 Quinine, 220
 β -Quinol(1,4-dihydroxybenzene), aromatic
 shift tensors, 36
 Racemization, *in situ*, 90
 Radical intermediates in dehydrogenases, 197
 RAMP hydrazine, 252, 327
 RAMP hydrazone, 326, 327
 Random phase approximation (RPA), 11
 Rate constants, 72
 Re-citrate synthase, 143
 Recycling of product, 77
 Regiochemistry:
 of addition of allyl sulfoxide anions, 340
 of nucleophilic attack, 233
 ^{13}C NMR chemical shift in, 235
 all-trans-Retinal, 47
 Retinal derivatives, *cis-trans*-isomerization
 in, 47
 6-s-trans-all-trans-Retinoic acid, 47
 Retro-Michael addition, 232, 263
 Retrosynthetic strategy, 230
 Ribitol dehydrogenase, 170, 178
 Ring closure, rules, 355
 Robinson annelations, 274, 385
 Rotational pattern for single crystals, 16
 RPA, *see* Random phase approximation
 Rules for ring closure, 355
 Ruthenium-based catalysts, 214
 S-Adenosylmethionine decarboxylase, 140
 (-)-Sabinaketone, 278
 (+)-Sabinene, 278
 SAMP hydrazine, 252, 327
 SAMP hydrazone, 326, 327
 Schiff's base, 138, 141, 156
 Scope of ester-enolate Michael additions, 285
 Secondary alcohols, synthesis, 224
 Secondary orbital overlap, 391
 L-Serine, 92
 Serine hydroxymethylase, 138
 Shielding, isotropic value, 5

- Shielding tensor(s), *see also* Chemical Shielding tensor
- Shielding tensor(s), *see also* Chemical shielding tensor
- of carboxylic carbons, 37
 - ^{13}C -5-bacteriorhodops in (bR) in membranes, 49
 - $^{13}\text{CH}_2$, effect of the CCX angle on, 32
 - crystal packing effects on, 49
 - methyl, paramagnetic bond contributions to, 44
 - of naphthalene, 52
 - non-symmetric part, 4
 - principal axes, 5
 - principal values, 5
 - σ , 4
 - symmetric and antisymmetric parts, 5
 - trace of, 5
- Shift tensors, measurement with liquid crystals, 26
- principal axes for the $^{13}\text{CH}_2$, 32
 - in pyromellitic acid dihydrate (PMDH), 37
 - from single crystal experiments, 14
- Shift values, principal, effect of the peptide secondary structure on, 45
- Si*-citrate synthases, 143
- Sidebands, analysis, 21
- σ , *see* Shielding tensor(s)
- [2,3] Sigmatropic rearrangement, 341, 353
- Simple diastereoselectivity, 238, 239, 391
- Simple selectivity, 242, 348
- Single crystals, two dimensional technique, 16
- Single crystal spectrum, 15
- Slow reacting enantiomer, 75
- Solid phase NMR, assignment problems, 27
- Solid state, molecular conformations in, freezing, 26
- Solvent polarity, 117
- Sorbitol dehydrogenase, 170
- Stereochemical infidelity, 196
- Stereochemistry of deprotonation:
- of amides, 309
 - of dithio esters, 266
 - of hydrazones, 323
 - of imines, 323
 - of thioamides, 306
 - of vinylogous carbamates, 302
- Stereochemistry of enolate formed in Michael addition, 386
- Stereochemistry of ester enolates, 284
- Stereochemistry of ketone enolates, 269
- Stereoelectronic considerations, 356, 372, 391
- in Michael additions, 262, 263
- Stereoelectronic hypotheses, 139
- Stereoelectronic theory:
- in addition-elimination reactions, 188
 - of dehydrogenases, 172
- Stereoselective processes, 237
- Stereoselective protonation, 306, 348, 383
- Stereoselective reaction, combination of components, 241
- Stereospecificity, of acetoacetate
- decarboxylase, 133
 - of chymotrypsin, 133
 - cryptic, 129
 - of dihydrofolate reductase, 133
 - divergent evolution, 132
 - of orcinol hydroxylase, 133
- Steroidal D ring, 366
- Strategies for improving enantioselectivity, 75
- Streptomyces griseus*, protease, 93
- Structural analysis in highly reactive compounds, 33
- Structural assignments, 242
- Substituent effect concepts, 40
- α -Substituted cyclohexanols, 118
- 2-Substituted-4-hydroxy-cyclopentenones, 108
- Substrate specificity:
- divergence, 170
 - divergent evolution, 181
- (+)-(S)-Sulcatol, 119
- Suprofen, 116
- Syn/anti convention, 236
- Synthesis of L-DOPA, 212
- Tetrahydroquinolinolinediones, 252
- Thermodynamic control, 67
- Thermodynamic parameter, 73, 86
- Thienamycin, 214
- Tight-binding MO theory, 45
- Titanium isopropoxide, 216
- Topological rule, 389
- (*R*)-3-Tosyloxy-1,2-propanediol, 94
- Transesterification, 72
- Transhydrogenase, 186
- stereospecificity, 153
- Transition states, free energy difference of diastereomeric, 67

- chair-like, 372
chelated, 359, 375, 387
Transition state theory, 67
Trichloroacetone, 220
endo-Tricyclodecadienones, 115
Trigonal centers or "trig", 356
1,2,3-Trimethoxybenzene, 40
1,3,5-Trimethoxybenzene, 40
 α -Trimethylsilyl enones, 275
Twist-boat-like transition states, 372
Two dimensional experiments in powder patterns, 22
Two dimensional technique, in single crystals, 16
for dipolar spectra, 24
Tyrosine decarboxylase, 138
- Van Slyke kinetics, 65
Variable-angle sample spinning (VASS), 22
VASS, *see* Variable-angle sample spinning
Vector potential, 6
(\pm)- α -Vetivone, 277
Vinyllogous carbamates, stereochemistry of deprotonation, 302
- Wieland-Miescher ketone, 381
Wilkinson's homogeneous catalyst, 212
- Xenobiotic ketone reductase, 172
- Zincates, 332

CUMULATIVE INDEX

	VOL.	PAGE
Absolute Configuration of Chiral Molecules, Crystals as Probes for the Direct Assignment of (<i>Addadi, Berkovitch-Yellin, Weissbuch, Lahav, and Leiserowitz</i>)	16	1
Absolute Configuration of Planar and Axially Dissymmetric Molecules (<i>Krow</i>)	5	31
Absolute Stereochemistry of Chelate Complexes (<i>Saito</i>)	10	95
Acetylenes, Stereochemistry of Electrophilic Additions (<i>Fahay</i>)	3	237
Aldol Condensations, Stereoselective (<i>Evans, Nelson and Taber</i>)	13	1
Alkaloids, Asymmetric Catalysis by (<i>Wynberg</i>)	16	87
Aluminum Hydrides and Tricoordinate Aluminum Reagents, Asymmetric Reductions with Chiral Complex (<i>Haubenstock</i>)	14	231
Analogy Model, Stereochemical (<i>Ugi and Ruch</i>)	4	99
Asymmetric Catalysis by Alkaloids (<i>Wynberg</i>)	16	87
Asymmetric Reductions with Chiral Complex Aluminum Hydrides and Tricoordinate Aluminum Reagents (<i>Haubenstock</i>)	14	231
Asymmetric Synthesis, New Approaches in (<i>Kagan and Fiaud</i>)	10	175
Asymmetric Synthesis Mediated by Transition Metal Complexes (<i>Bosnich and Fryzuk</i>)	12	119
Atomic Inversion, Pyramidal (<i>Lambert</i>)	6	19
Atropisomerism, Recent Advances in (<i>Oki</i>)	14	1
Axially and Planar Dissymmetric Molecules, Absolute Configuration of (<i>Krow</i>)	5	31
Barriers, Conformational, and Interconversion Pathways in Some Small Ring Molecules (<i>Malloy, Bauman, and Carreira</i>)	11	97
Barton, D. H. R., and Hassel, O.-Fundamental Contributions to Conformational Analysis (<i>Barton, Hassel</i>)	6	1
Bicyclic Compounds, Walk Rearrangements in [n.1.0] (<i>Klarner</i>)	15	1
Carbene Additions to Olefins, Stereochemistry of (<i>Closs</i>)	3	193
Carbenes, Structure of (<i>Closs</i>)	3	193
sp ² -sp ³ Carbon-Carbon Single Bonds, Rotational Isomerism about (<i>Karabatsos and Fenoglio</i>)	5	167
Carbonium Ions, Simple, the Electronic Structure and Stereochemistry of (<i>Buss, Schleyer and Allen</i>)	7	253
Chelate Complexes, Absolute Stereochemistry of (<i>Saito</i>)	10	95
¹³ C Chemical Shifts in Aliphatic Molecular Systems, Substituent Effects on. Dependence on Constitution and Stereochemistry (<i>Duddeck</i>)	16	219
Chirality, On Factoring Stereoisomerism and (<i>Hirschmann and Hanson</i>)	14	183
Chirality Due to the Presence of Hydrogen Isotopes at Noncyclic Positions (<i>Arigoni and Eliel</i>)	4	127
Chiral Crown Ethers (<i>Stoddart</i>)	17	207

	VOL.	PAGE
Chiral Homogeneity in Nature, Origins of (<i>Bonner</i>)	18	1
Chiral Lanthanide Shift Reagents (<i>Sullivan</i>)	10	287
Chiral Monolayers at the Air-Water Interface (<i>Stewart and Arnett</i>)	13	195
Chiral Organic Molecules with High Symmetry, The Synthesis and Stereochemistry of (<i>Nakazaki</i>)	15	199
Chiral Organosulfur Compounds (<i>Mikolajczyk and Drabowicz</i>)	13	333
Chiral Solvating Agents, in NMR (<i>Pirkle and Hoover</i>)	13	263
Classical Stereochemistry, The Foundations of (<i>Mason</i>)	9	1
Conformational Analysis, Applications of the Lanthanide-induced Shift Technique in (<i>Hofer</i>)	9	111
Conformational Analysis, The Fundamental Contributions of D. H. R. Barton and O. Hassell (<i>Barton, Hassel</i>)	6	1
Conformational Analysis of Intramolecular Hydrogen-Bonded Compounds in Dilute Solution by Infrared Spectroscopy (<i>Aaron</i>)	11	1
Conformational Analysis of Six-membered Rings (<i>Kellie and Riddell</i>)	8	225
Conformational Analysis of Steric Effects in Metal Chelates (<i>Buckingham and Sargeson</i>)	6	219
Conformational Analysis and Torsion Angles (<i>Bucourt</i>)	8	159
Conformational Barriers and Interconversion Pathways in Some Small Ring Molecules (<i>Malloy, Bauman and Carreira</i>)	11	97
Conformational Changes, Determination of Associated Energy by Ultrasonic Absorption and Vibrational Spectroscopy (<i>Wyn-Jones and Pethrick</i>)	5	205
Conformational Changes by Rotation about sp^2-sp^3 Carbon-Carbon Single Bonds (<i>Karabatsos and Fenoglio</i>)	5	167
Conformational Energies, Table of (<i>Hirsch</i>)	1	199
Conformational Interconversion Mechanisms, Multi-step (<i>Dale</i>)	9	199
Conformations of 5-Membered Rings (<i>Fuchs</i>)	10	1
Conjugated Cyclohexenones, Kinetic 1,2 Addition of Anions to, Steric Course of (<i>Toromanoff</i>)	2	157
Crystals as Probes for the Direct Assignment of Absolute Configuration of Chiral Molecules, A Link Between Macroscopic Phenomena and Molecular Chirality (<i>Addadi, Berkovitch-Yellin, Weissbuch, Lahav, and Leiserowitz</i>)	16	1
Crystal Structures of Steroids (<i>Duax, Weeks and Rohrer</i>)	9	271
Cyclobutane and Heterocyclic Analogs, Stereochemistry of (<i>Moriarty</i>)	8	271
Cyclohexyl Radicals, and Vinylic, The Stereochemistry of (<i>Simamura</i>)	4	1
Double Bonds, Fast Isomerization about (<i>Kalinowski and Kessler</i>)	7	295
Electronic Structure and Stereochemistry of Simple Carbonium Ions, (<i>Buss, Schleyer and Allen</i>)	7	253
Electrophilic Additions to Olefins and Acetylenes, Stereochemistry of (<i>Fahey</i>)	3	237
Enantioselective Synthesis of Non-Racemic Chiral Molecules on an Industrial Scale (<i>Scott</i>)	19	209
Enantioselective Synthesis of Organic Compounds with Optically Active Transition Metal Catalysts in Substoichiometric Quantities (<i>Brunner</i>)	18	129
Enzymatic Reactions, Stereochemistry of, by Use of Hydrogen Isotopes (<i>Argoni and Eliel</i>)	4	127

	VOL.	PAGE
1,2-Epoxides, Stereochemistry Aspects of the Synthesis of (<i>Berti</i>)	7	93
EPR, in Stereochemistry of Nitroxides (<i>Janzen</i>)	6	177
Ethylenes, Static and Dynamic Stereochemistry of Push-Pull and Strained (<i>Sandström</i>)	14	83
Five-Membered Rings, Conformations of (<i>Fuchs</i>)	10	1
Foundations of Classical Stereochemistry (<i>Mason</i>)	9	1
Geometry and Conformational Properties of Some Five- and Six- Membered Heterocyclic Compounds Containing Oxygen or Sulfur (<i>Romers, Altona, Buys and Havinga</i>)	4	39
Hassel, O. and Barton, D. H. R.-Fundamental Contributions to Conformational Analysis (<i>Hassel, Barton</i>)	6	1
Helix Models, of Optical Activity (<i>Brewster</i>)	2	1
Heterocyclic Compounds, Five- and Six-Membered, Containing Oxygen or Sulfur, Geometry and Conformational Properties of (<i>Romers, Altona, Buys and Havinga</i>)	4	39
Heterocyclic Four-Membered Rings, Stereochemistry of (<i>Moriarty</i>)	8	271
Heterotopism (<i>Mislow and Raban</i>)	1	1
Hydrogen-Bonded Compounds, Intramolecular, in Dilute Solution, Conformational Analysis of, by Infrared Spectroscopy (<i>Aaron</i>)	11	1
Hydrogen Isotopes at Noncyclic Positions, Chirality Due to the Presence of (<i>Arigoni and Eliel</i>)	4	127
Infrared Spectroscopy, Conformational Analysis of Intramolecular Hydrogen-Bonded Compounds in Dilute Solution by (<i>Aaron</i>)	11	1
Intramolecular Hydrogen-Bonded Compounds, in Dilute Solution, Conformational Analysis of, by Infrared Spectroscopy (<i>Aaron</i>)	11	1
Intramolecular Rate Processes (<i>Binsch</i>)	3	97
Inversion, Atomic, Pyramidal (<i>Lambert</i>)	6	19
Isomerization, Fast, About Double Bonds (<i>Kalinowski and Kessler</i>)	7	295
Ketones, Cyclic and Bicyclic, Reduction of, by Complex Metal Hydrides (<i>Boone and Ashby</i>)	11	53
Kinetic Resolution (<i>Kagan and Fiaud</i>)	18	249
Lanthanide-induced Shift Technique—Applications in Conformational Analysis (<i>Hofer</i>)	9	111
Lanthanide Shift Reagents, Chiral (<i>Sullivan</i>)	10	287
Mass Spectrometry and the Stereochemistry of Organic Molecules (<i>Green</i>)	9	35
Metal Chelates, Conformational Analysis and Steric Effects in (<i>Buckingham and Sargeson</i>)	6	219
Metal Hydrides, Complex, Reduction of Cyclic and Bicyclic Ketones by (<i>Boone and Ashby</i>)	11	53
Metallocenes, Stereochemistry of (<i>Schlogl</i>)	1	39
Metal Nitrosyls, Structures of (<i>Feltham and Enemark</i>)	12	155
Molecular Mechanics Calculations—Application to Organic Chemistry (<i>Osawa and Musso</i>)	13	117

	VOL.	PAGE
Molecular Structure and Carbon-13 Chemical Shielding Tensors Obtained from Nuclear Magnetic Resonance (<i>Facelli and Grant</i>)	19	1
Monolayers, Chiral, at the Air-Water Interface (<i>Stewart and Arnett</i>)	13	195
Multi-step Conformational Interconversion Mechanisms (<i>Dale</i>)	9	199
Nitroxides, Stereochemistry of (<i>Janzen</i>)	6	177
Non-Chair Conformations of Six-Membered Rings (<i>Kellie and Riddell</i>)	8	225
Nuclear Magnetic Resonance, ¹³ C Chemical Shifts in Aliphatic Molecular Systems, Substituent Effects on. Dependence on Constitution and Stereochemistry (<i>Duddeck</i>)	16	219
Nuclear Magnetic Resonance Chiral Lanthanide Shift Reagents (<i>Sullivan</i>)	10	287
Nuclear Magnetic Resonance, ¹³ C Stereochemical Aspects of (<i>Wilson and Stothers</i>)	8	1
Nuclear Magnetic Resonance, Chiral Solvating Agents in (<i>Pirkle and Hoover</i>)	13	263
Nuclear Magnetic Resonance, for Study of Intra-Molecular Rate Processes (<i>Binsch</i>)	3	97
Nuclear Overhauser Effect, Some Chemical Applications of (<i>Bell and Saunders</i>)	7	1
Olefins, Stereochemistry of Carbene Additions to (<i>Closs</i>)	3	193
Olefins, Stereochemistry of Electrophilic Additions to (<i>Fahey</i>)	3	237
Optical Activity, Helix Models of (<i>Brewster</i>)	2	1
Optical Circular Dichroism, Recent Applications in Organic Chemistry (<i>Crabbé</i>)	1	93
Optical Purity, Modern Methods for the Determination of (<i>Raban and Mislow</i>)	2	199
Optical Rotatory Dispersion, Recent Applications in Organic Chemistry (<i>Crabbé</i>)	1	93
Organic Solid-State, Stereochemistry and Reactions (<i>Green, Arad-Yellin, and Cohen</i>)	16	131
Organosulfur Compounds, Chiral (<i>Mikolajczyk and Drabowicz</i>)	13	333
Origins of Chiral Homogeneity in Nature (<i>Bonner</i>)	18	1
Overhauser Effect, Nuclear, Some Chemical Applications of (<i>Bell and Saunders</i>)	7	1
Phosphorus Chemistry, Stereochemical Aspects of (<i>Gallagher and Jenkins</i>)	3	1
Phosphorus-containing Cyclohexanes, Stereochemical Aspects of (<i>Maryanoff, Hutchins and Maryanoff</i>)	11	186
Piperidines, Quaternization Stereochemistry of (<i>McKenna</i>)	5	275
Planar and Axially Dissymmetric Molecules, Absolute Configuration of (<i>Krow</i>)	5	31
Polymer Stereochemistry, Concepts of (<i>Goodman</i>)	2	73
Polypeptide Stereochemistry (<i>Goodman, Verdini, Choi and Masuda</i>)	5	69
Pyramidal Atomic Inversion (<i>Lambert</i>)	6	19
Quaternization of Piperidines, Stereochemistry of (<i>McKenna</i>)	5	75

	VOL.	PAGE
Radical Pair Reactions, Stereochemical Aspects of (<i>Porter and Krebs</i>)	18	97
Radicals, Cyclohexyl and Vinylic, The Stereochemistry of (<i>Simamura</i>)	4	1
Reduction, of Cyclic and Bicyclic Ketones by Complex Metal Hydrides (<i>Boone and Ashby</i>)	11	53
Resolution of Enantiomers via Biocatalysis (<i>Sih and Wu</i>)	19	63
Resolving Agents and Resolutions in Organic Chemistry (<i>Wilen</i>)	6	107
Rotational Isomerism about sp^2-sp^1 Carbon-Carbon Single Bonds (<i>Karabatsos and Fenoglio</i>)	5	167
Silicon, Stereochemistry at (<i>Corriu, Guérin, and Moreau</i>)	15	43
Solid State Reactions, Organic, Stereochemistry (<i>Green, Arad-Yellin and Cohen</i>)	16	131
Small Ring Molecules, Conformational Barriers and Interconversion Pathways in Some (<i>Malloy, Bauman and Carreira</i>)	11	97
Stereochemical Aspects of ^{13}C Nmr Spectroscopy (<i>Wilson and Stothers</i>) ..	8	1
Stereochemical Aspects of Phosphorus-containing Cyclohexanes (<i>Maryanoff, Hutchins and Maryanoff</i>)	11	186
Stereochemical Aspects of Radical Pair Reactions (<i>Porter and Krebs</i>) ..	18	97
Stereochemical Aspects of Vibrational Optical Activity (<i>Freedman and Nafie</i>)	17	113
Stereochemical Nomenclature and Notation in Inorganic Chemistry (<i>Sloan</i>)	12	1
Stereochemistry, Classical, The Foundations of (<i>Mason</i>)	9	1
Stereochemistry, Dynamic, A Mathematical Theory of (<i>Ugi and Ruch</i>) ..	4	99
Stereochemistry of the Base-Promoted Michael Addition Reaction (<i>Oare and Heathcock</i>)	19	227
Stereochemistry of Biological Reactions at Protoprochiral Centers (<i>Floss, Tsai, and Woodard</i>)	15	253
Stereochemistry of Chelate Complexes (<i>Saito</i>)	10	95
Stereochemistry of Cyclobutane and Heterocyclic Analogs (<i>Moriarty</i>)	8	271
Stereochemistry of Germanium and Tin Compounds (<i>Gieden</i>)	12	217
Stereochemistry of Linear Macromolecules (<i>Farina</i>)	17	1
Stereochemistry of Nitroxides (<i>Janzen</i>)	6	177
Stereochemistry of Organic Molecules, and Mass Spectrometry (<i>Green</i>) ..	9	35
Stereochemistry of Push-Pull and Strained Ethylenes, Static and Dynamic (<i>Sandström</i>)	14	83
Stereochemistry of Reactions of Transition Metal-Carbon Sigma Bonds (<i>Flood</i>)	12	37
Stereochemistry at Silicon (<i>Corriu, Guérin, and Moreau</i>)	15	43
Stereochemistry of Transition Metal Carbonyl Clusters (<i>Johnson and Benfield</i>)	12	253
Stereoisomeric Relationships, of Groups in Molecules (<i>Mislow and Raban</i>)	1	1
Stereoisomerism, On Factoring Chirality and (<i>Hirschmann and Hanson</i>)	14	183
Stereoselective Aldol Condensations (<i>Evans, Nelson and Taber</i>)	13	1
Stereospecificity in Enzymology: Its Place in Evolution (<i>Benner, Glasfeld and Piccirilli</i>)	19	127
Steroids, Crystal Structures of (<i>Duax, Weeks and Rohrer</i>)	9	271
Structures, Crystal, of Steroids (<i>Duax, Weeks and Rohrer</i>)	9	271

	VOL.	PAGE
Torsion Angle Concept in Conformational Analysis (<i>Bucourt</i>)	8	159
Ultrasonic Absorption and Vibrational Spectroscopy Use of, to Determine the Energies Associated with Conformational Changes (<i>Wyn-Jones and Pethrick</i>)	5	205
Vibrational Optical Activity, Stereochemical Aspects of (<i>Freedman and Nafie</i>)	17	113
Vibrational Spectroscopy and Ultrasonic Absorption, Use of, to Determine the Energies Associated with Conformational Changes (<i>Wyn-Jones and Pethrick</i>)	5	205
Vinylic Radicals, and Cyclohexyl, The Stereochemistry of (<i>Simamura</i>) ..	4	1
Wittig Reaction, Stereochemistry of (<i>Schlosser</i>)	5	1